WORLD METEOROLOGICAL ORGANIZATION

INSTRUMENTS AND OBSERVING METHODS

REPORT No. 57

PAPERS PRESENTED

AT THE

WMO TECHNICAL CONFERENCE ON

INSTRUMENTS AND METHODS OF OBSERVATION

(TECO-94)

Geneva, Switzerland, 28 February - 2 March 1994

WMO/TD - No. 588

02-SH16
C.2

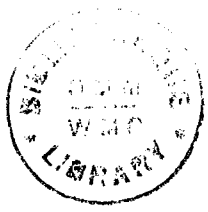

NOTE

The designations employed and the presentation of material in this publication do not imply the expression of any opinion whatsoever on the part of the Secretariat of the World Meteorological organization concerning the legal status of any country, territory, city or area, or of its authorities, or concerning the delimitation of its frontiers or boundaries.

This report has been produced without editorial revision by the WMO Secretariat. it is not an official WMO publication and its distribution in this form does not imply endorsement by the Organization of the ideas expressed.

KS D:\MISC-COL\M-PUB-57.PAC\5 January 1994 12:25pm

IOM 57
TD 588
c. 2

Page

TABLE OF CONTENTS

Page

III. ENVIRONMENTAL MEASUREMENTS

IV. RADIATION MEASUREMENTS

V. QUALITY ASSURANCE

Page

VI. REMOTE SENSING

POSTER PRESENTATION

APPENDICES

****

FOREWORD

Scientific lectures and discussions formed an integral part of sessions of the WMO Commission for Instruments and Methods of Observations since the first WMO CIMO session (Toronto, 1953). The growing interest in these lectures conducted CIMO-V (Versailles, 1969) to recommend the organization of technical conferences on instruments and methods of observation. Since 1970 some ten technical conferences have been organized by CIMO with steadily increasing success showing the state of the art in meteorological measuring technology.

The present CIMO technical conference, TECO-94, will take place during the CIMO-XI session in Geneva, providing the opportunity for all CIMO delegates to participate in the conference. It will further allow for the simultaneous interpretation of several presentations into the six working languages as requested by delegates at CIMO-X (Brussels, 1989). Moreover, this timing allows views and suggestions emanating therefrom to be considered by CIMO-XI.

The International Organizing Committee, composed of Dr. A. Van Gysegem (Scientific Director of TECO-94) and Mr. M. Rochas (France), has been responsible for specifying the themes and contents of sessions and for selecting the papers.

The Conference reflects the diversity of CIMO activities and covers new directions and operational experience in the field of surface, radiation, upper-air, radiation and environmental measurements, remote sensing and quality assurance. A scan of presented papers shows the progress in development and improvement of measuring capabilities as well as the application of these capabilities to improve the quality and compatibility of measurements and to better respond to the evolution in observational needs and requirements of WMO Programmes and of National Meteorological and Hydrological Services.

This report contains the papers to be presented at the Conference and is being issued prior to it, so as to enable the participants to study them beforehand. It will place the papers on permanent record, making them available to a much wider audience than the participants at the Conference. I hope that all readers of this report will find the contents useful and informative and that the Conference will provide opportunities to discuss new ideas and to learn from the experience of others.

I wish to express my deep gratitude to all authors of papers, the International and Local WMO Organizing Committees and to the Secretary-General of WMO for all efforts and resources devoted to planning and holding TECO-94.

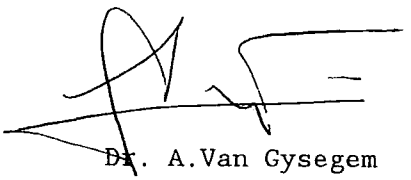

Dr. A.Van Gysegem

Vice-president of CIMO
Scientific Director of TECO-94

OVERVIEW PAPERS

CONDITIONS, REQUIREMENTS AND NEEDS FOR OUTDOOR MEASUREMENTS IN DEVELOPING COUNTRIES: THE CASE OF AGROMETEOROLOGY AND AGROCLIMATOLOGY

C.J. STIGTER
TRADITIONAL TECHNIQUES OF MICROCLIMATE IMPROVEMENT (TTMI)*)
PROJECT, CO-ORDINATED AT WAGENINGEN AGRICULTURAL UNIVERSITY,
THE NETHERLANDS

EXTENDED ABSTRACT

This will be a somewhat unusual keynote address for a Technical Conference on Instruments and Methods of Observation. The starting point is not equipment results, improvements, accuracies and a new equipment progress strategy, but their virtual absence in the developing non-industrialized world.

It is an accepted fact, also within WMO, that nowadays routine measurements and observations have in many places in Africa, Latin America and a number of Asian countries severely deteriorated. National Weather Services can't cope with the necessary networks, even new challenges apart, due to lack of funds for equipment replacement for maintenance and repair, for transport, for appropriate training, for increased salaries and status to be awarded to equipment expertise and observers within their measurement departments.

Data sets long enough to detect increased climate variability or other changes in the local environment are often non-existent, or with large gaps, badly quality controlled or otherwise without the necessary indications of the conditions under which they were obtained. Requests for data from within the economically active parts of society remain limited for many reasons. A group of reasons has to do with non-availability of special data sets.

Agrometeorology/climatology shares this malaise and for specific agrometeorological measurements and observations even less money is available. However, routine measurements and observations are of only limited use without added value in derived products for agricultural applications. Due to the occurrence of new environmental hazards, there are also needs in agricultural meteorology for additional environmental data.

---

*) The TTMI-Project has Units at the Physics Department, University of Dar es Salaam, Tanzania; the Department of Meteorology, University of Nairobi, Kenya; the Department of Environmental Sciences and Natural Resources, University of Gezira, Wad Medani, Sudan; and the Department of Geography, Ahmadu Bello University, Zaria, Nigeria. The TTMI-Project, bilaterally funded by the Environment Programme and the Research Focal Programme of the Directorate General for International Collaboration of the Netherlands Government (DGIS), has also many affiliations with national and international agricultural research and education organizations that operate in Africa and India.

A matter of wrong priorities? Yes, but the problems are even structural in other aspects, such as in an actually deteriorating environment or economy or both. In the sixties there was at least a debate in the Western world on priority applications of scientific efforts and their role in society. Can the developing non-industrialized world afford such a debate at present?

Will UNCED be a turning point? Resources depending, that could be the case. By all means another, partly complementary structure of organizing environmental monitoring and impact assessment is necessary. What could be a policy/strategy proposal for this approach?

Let us limit ourselves here to agrometeorology/climatology. With better definitions of the most urgent specific needs for routine and derived data, such an initial approach could come from parts of a wider GCOS or GTOS system, with strong country based components. What and who defines the additional data sets? How are they distributed?

With a better tuning of initially the simplest weather and agrometeorological forecasting techniques to the most pressing needs of different farming communities, such as in the West African pilot protects (WMO/FAO) or in Moisture Availability Index technique applications (FAO/WMO) or related to other priority environmental risk factors (UNEP/TTMI), another more needed information pattern would be covered. From those needs and cost/benefit ratio calculations, the actual need for the presently ailing routine and derived data systems could be better determined and their collection and use better justified.

Finally, there is a high need for the collection of location specific problem oriented data sets. Obtainment of the latter will be illustrated from a more sophisticated instrumentation level down to the level of development of specific low-cost equipment. Some conditions and requirements will be given.

The above approaches cannot be implemented at each level through one organization or via one source of funds. It is here that complementarity of WMO, FAO, UNEP, UNESCO, CGIAR-institutes, local Research Organizations and Universities and bilaterally supported programmes comes in, as far as such programmes deal with environmental hazards and risk factors with agrometeorological components, in the limitation adopted here.

Complementarity in programmes means, however, also common or at least overlapping interests in the service to farming communities of all levels of affordable and environment friendly inputs, in all kinds of farming systems, in all parts of the developing world.

This paper wants to make the point that quantitative monitoring of the environment has its well defined role in this context in agrometeorology and agroclimatology. However, if present trends prevail, this will remain beyond reach in the actual world.

HOMOGENEITY OF DATA AND THE CLIMATE RECORD

Dr. Kenneth D. Hadeen and Dr. Nathaniel B. Guttman
National Climatic Data Center
National Oceanic and Atmospheric Administration
Asheville, NC, USA

1. INTRODUCTION

We live in an age of rapidly advancing technology. Inevitably, changes and improvements in observing systems become part of maturing environmental programs. These changes include variations in spatial and temporal sampling, processing algorithms, quality assurance procedures, instrumentation, instrumental accuracy and precision, and representativeness of measurements. Sometimes these changes can seriously impact the interpretation of data and products derived from the measurements, particularly for trend analyses.

Climate researchers are being forced to focus more and more on the homogeneity of data sets they are using to correctly quantify changes in the state of the environment. It is not possible to quantify changes to the long-term reference data bases without spending time to determine the potential biases in the data. As the environmental science community starts to use data for climate uses from new observing instruments like automated surface and remote observing systems, the potential problem of non-compatibility of data from the new observational systems with past observations gets much worse.

Reliable data with adequate quality to address the multitude of environmental problems and issues are fundamental to the understanding of the earth system as well as to the prediction of future events. Data collected in the past and present are used to understand oceanographic and atmospheric processes, to develop prediction techniques, to assess short- and long-term changes in the environment, and to understand the effects of human activities on the environment. Data collected in the future will also be used for these and other purposes. Homogeneity of data records is therefore critical.

2. THE IDEAL WORLD

In an ideal world, the attributes of a successful monitoring system include the delivery of timely and relevant data and information with adequate temporal and spatial resolution. In addition, the data from the system will be of sufficient quality and would also maintain continuity with previous observations. The system would evolve with changes in technology and focus such that there are minimal impacts on the data quality and homogeneity of past, present and future measurements. A sound data management system is necessary to fulfill these requirements.

Also, in the ideal world measurements of an environmental variable are made with respect to a specific problem or goal of interest. The appropriate temporal and

spatial scales of the measurements, the accuracy, precision, continuity and overall quality of the measurements are determined to meet the defined goals of the system. Data bases are assembled over time, and because new observing systems are often operated simultaneously with old systems, much is known about the calibration and validation between new and old sensors.

Data are periodically reanalyzed to take advantage of new algorithms and/or new understanding of science. Metadata, or information about data, are vital for linking old measurements with new data into homogeneous data bases. Metadata relates to all the information necessary to interpret measurements, including, but not limited to, instrumental characteristics (e.g., calibration, sensor response, sensor sensitivity), sensor location, site changes, observation times, processing procedures, data transmission procedures, and data summarization or averaging methodology.

Complete information about a data base allows the analyst to make the necessary scientific and statistical adjustments to the measurements so that the old and new observations can be linked with a high degree of confidence.

3. THE REAL WORLD

In contrast with the ideal world, the real world is quite different. More often than not, observational data are used to study phenomena and solve problems that have very little connection with the purpose for which the data were originally collected, processed or summarized. Proper scientific decisions and judgments pertaining to the use of the data therefore heavily depend upon a precise knowledge of all the information about the data; i.e., the metadata. Unfortunately, documentation about data often is lacking or incomplete.

Without adequate metadata, the analyst can only assume characteristics about the sensors, instrument citing, processing methodologies, etc. Adjusting data to compensate for biases, calibration errors, sensor moves, and other artificial changes so that homogeneous data sets can be constructed can be imprecise and may lead to erroneous analytical and scientific conclusions.

4. EXAMPLES OF PRACTICAL PROBLEMS

In the late 1980's the National Weather Service replaced liquid-in-glass maximum and minimum thermometers in wooden Cotton Region Shelters with thermistor-based sensors housed in plastic shelters. Analyses by Quayle et al. (1991) showed that a mean daily maximum temperature change of -0.4C, (Figure 1a), a mean daily minimum change of +0.3C, (Figure 1b), and a change in average temperature of -0.1C resulted from the new instrumentation. The change of -0.7C, (Figure 1c), in daily temperature range is particularly significant for climate change studies that use this element as an independent variable. The artificial shift, however, can be adjusted to construct homogeneous data bases since it appears as a sharp discontinuity on a time series graph and also because there exists adequate documentation (metadata) about the instrument changes.

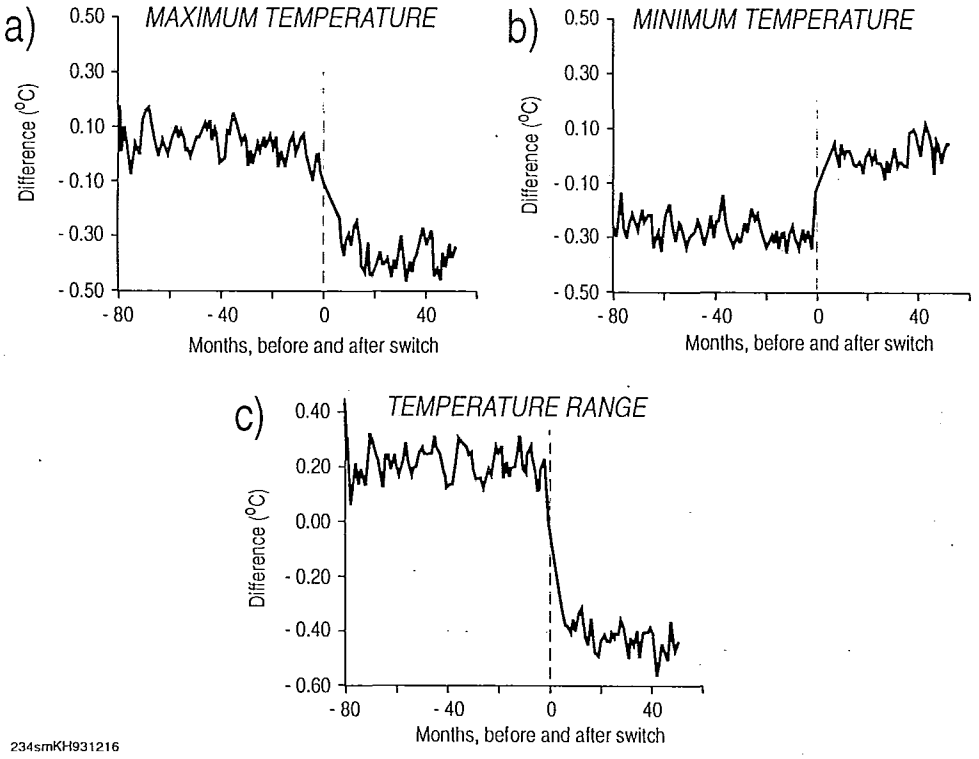

Figure 1. Estimated Bias Introduced by New Sensors in NOAA's 6000-Station Cooperative Network

---

Another study by Easterling et al. (1993) examined the effects on the climate record of switching from an HO50 series hygrometer first to an HO60 series and then to an H083 series instrument. The average effect of the switch to the HO60 series was to slightly increase both the monthly maximum and minimum temperatures (Figure 2). The switch to the HO83 instrument, however, caused an increase in monthly maximum temperatures, but a decrease in the monthly minimum temperatures . The changes were not as sharply delineated as those noted above by Quayle et al. (op. cit), so that data adjustments are difficult to make with confidence.

Karl et al. (1986) showed the importance of standardizing the time of observation of maximum and minimum temperatures. They found that when the observation changes from late afternoon to near sunrise, biases greater than 2 degrees C. can occur. From a data user's view, (Figure 3), spatial and temporal analyses of climate and climate change must be concerned with adjusting the data for the time of observation bias. The adjustments can only be made with a high degree of confidence if the appropriate metadata are available to the analyst.

Continuity and gauging problems with precipitation measurements are well known, especially for snow that often blows over or out of the gauge. According to Golubev and Groisman (1992), precipitation undercatch caused by wind on unshielded gages can be substantial, and when records from shielded gauges are combined with records from unshielded gauges, the result is an inhomogeneous long-term precipitation

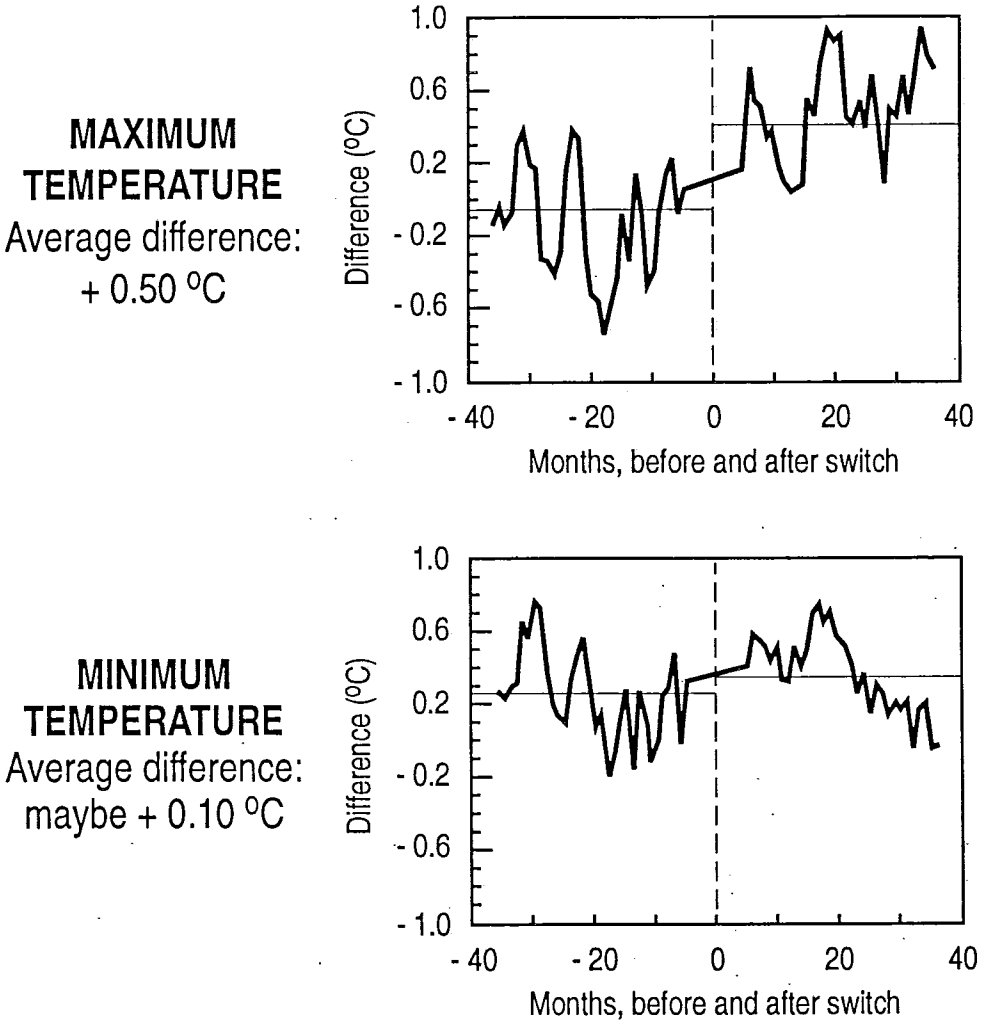

Figure 2. Effects of Changing Instruments from HO60 Series to HO83 Series

---

time series. Use of these data by scientists studying climate change could be misleading. Many different types of gauges are used throughout the world. The precipitation homogeneity discontinuity caused by using different gauges over the last hundred years is shown in Figure 4.

Monitoring of oceanic surface conditions was examined by Quayle (1974). Suspecting that climatological studies derived from transient ship observations was biased toward good weather conditions, he compared fixed Ocean Weather Station (OWS) site data with ship observations. He found that wave heights, precipitation and visibilities reported by OWSs were uniformly higher those from the transient ships, indicating that the ship observations are biased. Quayle concluded that the bias is probably relatively unimportant when dealing with routine climatological records, but could be important when concerned with extremes.

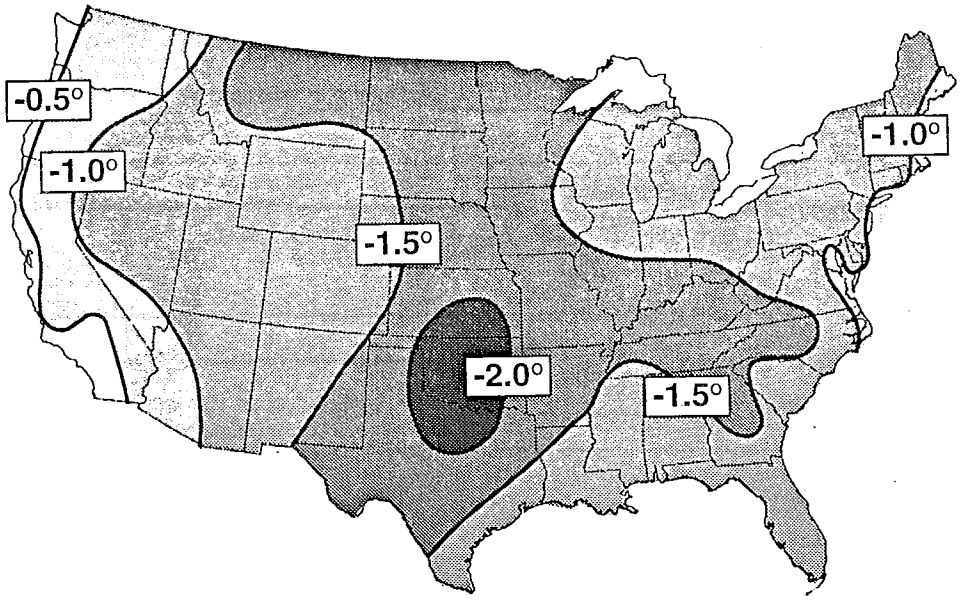

Figure 3. Change in the Average March Temperatures (°C) Resulting from Changing the Time of Observation from 5 P.M. to 7 A.M. Local Time.

The use of satellite data for monitoring environmental conditions poses a different set of potential biases in the data. These vary from change in instruments with each series of satellites, changes in orbital characteristics during the life cycle of the satellite causing time and space changes in the observation during the day, to changes in sensitivity of individual sensors and the algorithms used in deriving geophysical parameters. External factors like change in aerosols in the space between the satellite and the feature being observed can cause biases in the data. An example of the changes in sea surface temperature before and after the eruption of Mt. Pinatubo is shown in Figure 5.

5. IMPACTS

The examples above are only a few of the hundreds that could be given to show the data problems that face the analyst. Homogeneity of data in time and space is rarely inherent in the data used by researchers to advance the state of science, to assess the effects of the environment on human endeavors, to assess the effects of human endeavor on the environment, and to predict future environmental states. Coupled with the lack of homogeneity is the often incomplete metadata about the measurements.

The result of this usual state of affairs is that the analyst must resort to making many assumptions when using the data. Redundancy in measurements by dense station networks and different observing systems and use of multiple variables to test climatic hypotheses can be employed. For example, tropospheric temperatures can be monitored by land stations, radiosondes and satellites. Oceanic temperatures from ships (day vs.

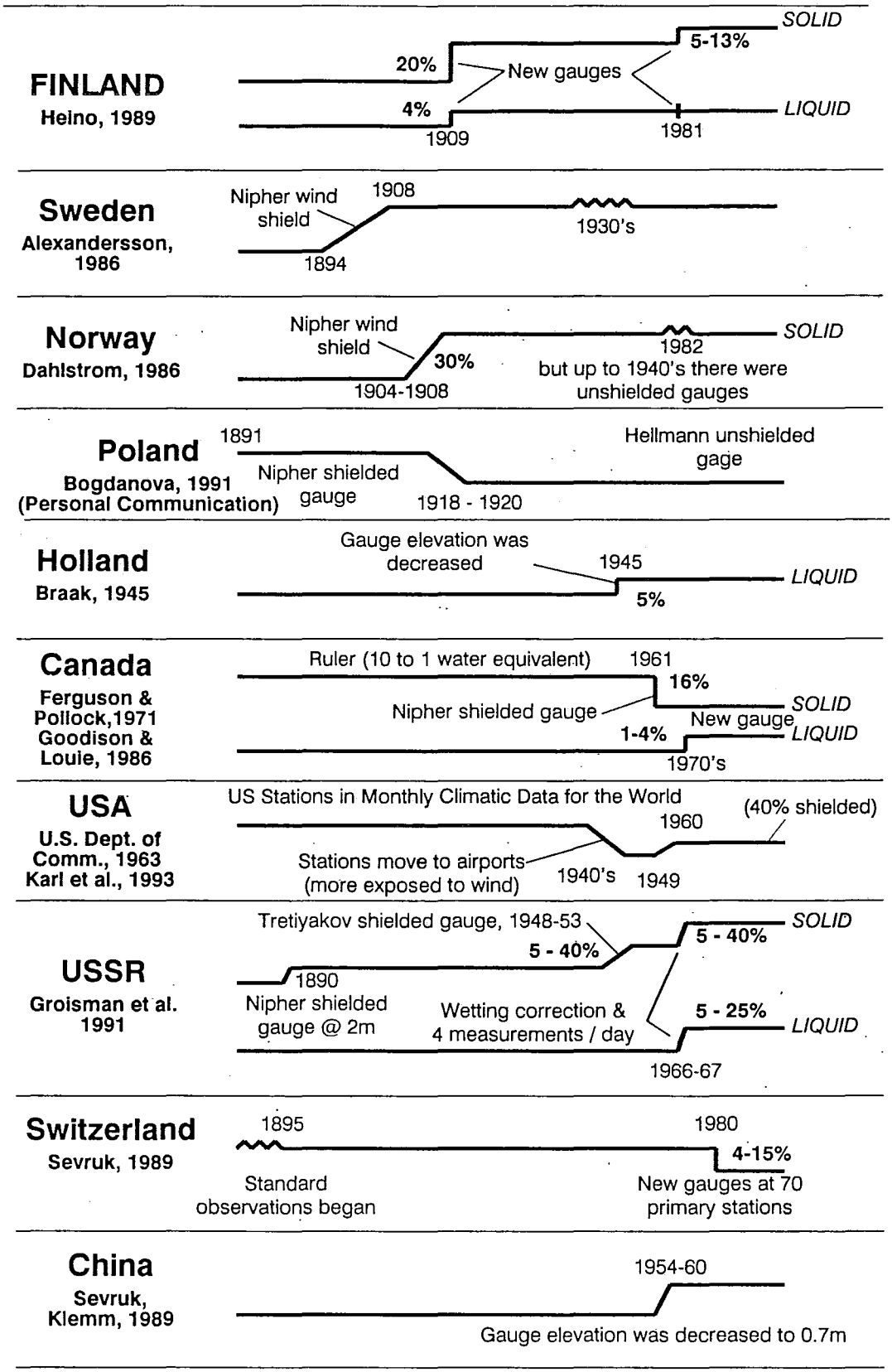

Figure 4. Precipitation Homogeneity Discontinuities in the Last 100 Years

night, sea vs. air, voluntary vs. oceanographic) and islands/coastal areas can independently reinforce or bring into question conclusions for one or more of the data sets. In addition, the analyst must also use other sophisticated methodologies to arrive at conclusions. Even with modern computer technology, extensive time and financial resources are often needed to construct an adequate homogeneous record upon which to base an analysis.

Two examples illustrate the situation. First, in the preparation of the U.S. Historical Climate Network data base (Karl et al., 1990), hundreds of hours were spent in examining both manually and by machine the station history records to identify non-climatic factors that could compromise data homogeneity, and in developing adjustment routines for known and suspected (unverified because of inadequate metadata) inhomogeneities. Second, for the preparation of a risk-based drought atlas for the U.S. (Guttman, 1993; Guttman et al., 1993), extensive resources were committed to developing statistical procedures and then to processing algorithms so that spatial homogeneity of precipitation data could be assumed with reasonable confidence.

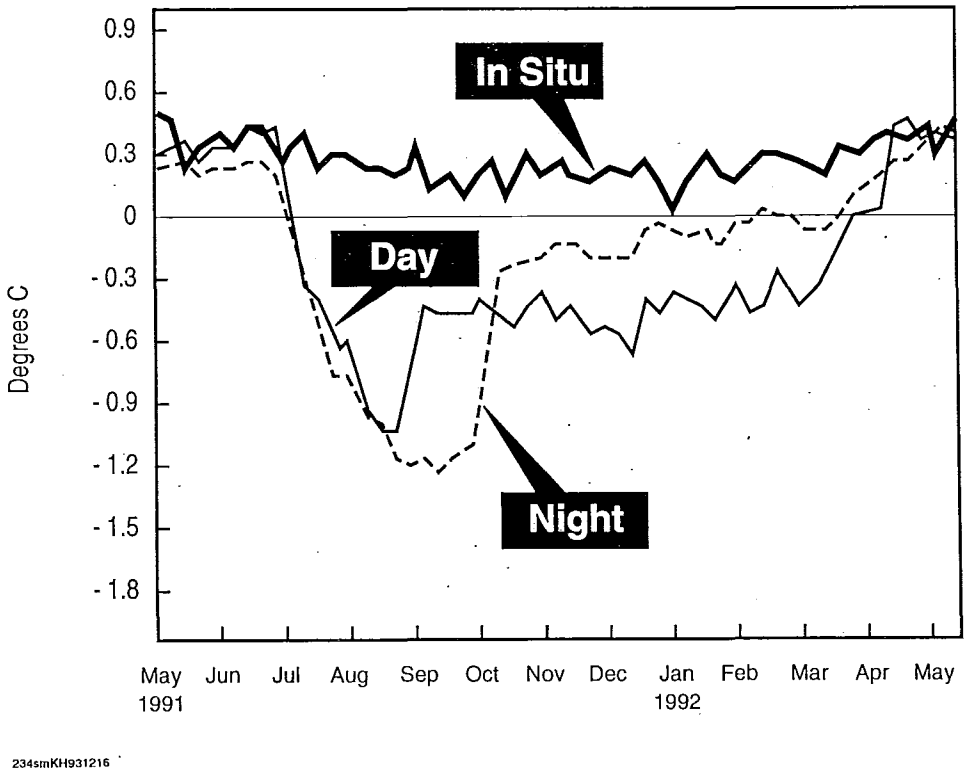

Figure 5. Global Ocean In-Situ and AVHRR-Derived Anomalies of SST Prior and Subsequent to the Eruption of Mt. Pinatubo (from Reynolds, 1993).

6. RECOMMENDATIONS

Responsibility for providing and using data is a shared responsibility between the data collector and the researcher. Paraphrasing Karl et al. (1993) and Guttman (1991), the current situation could be improved if:

a) Standard procedures were established for collecting overlapping measurements for all significant changes made in instrumentation, observing practices, and sensor citing;

b) Detailed documentation were made available of the procedures, rationale, testing, assumptions, and known problems involved in the construction of the data set from the measurements;

c) Routine assessments were made of ongoing calibration, maintenance, or homogeneity problems for the purpose of taking corrective actions when necessary; and

d) Open communication channels between the data collector and the researcher were established to provide feedback mechanisms for recognizing data problems, the correction or at least the documentation of problems, and the improvement of or addition to documentation to meet initially unforeseen user requirements.

Recognizing that data are often used for purposes other than those for which the data were collected, these four recommendations would have the effect of providing enough metadata to a data user to enable manipulation, amalgamation and summarization of the data with minimal assumptions regarding data quality and homogeneity.

Improvements to the monitoring systems and data management systems must be more than one nation's commitment. An international organization such as the WMO should take the leadership position and build the cornerstones as recommended above for projects such as Global Climate Change Detection, Global Climate Observing System, and Global Oceanographic Observing System.

7. REFERENCES

Easterling, D.R., R.G. Quayle and P.Y. Hughes, 1993: The effects of thermometer changes on the temperature record of U.S. first-order stations, *Proc. 8th Symp. on Meteor. Observations and Instrumentation*, Anaheim, CA, Amer. Meteor. Soc.

Golubev, V.S., P.Ya. Groisman and R.G. Quayle, 1992: An evaluation of the United States standard 8-in nonrecording raingage at the Valdai Polygon, Russia, *J. Atmos. Oceanic Tech.*, **9**, 624-629.

Guttman, N.B., 1993: The use of L-moments in the determination of regional precipitation climates. *J. Clim.*, **6**, 2309-2325.

Guttman, N.B., 1991: Using secondary data sources, *Clim. Change*, **18**, 95-105.

Guttman, N.B., J.R.M. Hosking and J.R. Wallis, 1993: Regional precipitation quintal values for the continental U.S. computed from L-moments. *J. Clim.*, **6**, 2326-2340.

Karl, T.R., R.G. Quayle and P.Ya. Groisman, 1993: Detecting climate variations and change: new challenges for observing and data management systems, *J. Clim.*, **6**, 1481-1494.

Karl, T.R., C.N. Williams, F.T. Quinlan and T.A. Boden, 1990: United States Historical Climatology Network (HCN) serial temperature and precipitation data, *ORNL/CDIAC-30 NDP-019/R1*, Oak Ridge Nat. Lab., Oak Ridge, TN.

Karl, T.R., C.N. Williams, Jr., P.J. Young and W.M. Wendland, 1986: A model to estimate the time of observation bias associated with monthly mean maximum, minimum and mean temperatures for the United States, *J. Clim. Appl. Meteor.*, **25**, 145-160.

Quayle, R.G., 1974: A climatic comparison of Ocean Weather Stations and transient ship records, *Mariners Wea. Log*, **18**, 307-311.

Quayle, R.G., D.R. Easterling, T.R. Karl and P.Y. Hughes, 1991: Effects of recent thermometer changes in the Cooperative Station Network, *Bull. Amer. Meteor. Soc.*, **72**, 1718-1723.

Reynolds, R.W., 1993: An improved real-time global sea surface temperature analysis. *J. Clim. Appl. Meteor.*,**6**, 114-119.

Session I

SURFACE MEASUREMENTS

WMO SOLID PRECIPITATION MEASUREMENT INTERCOMPARISON: PRELIMINARY RESULTS

B.E. Goodison, Atmospheric Environment Service, Downsview, Canada
E. Elomaa, Finnish Meteorological Institute, Helsinki, Finland
V. Golubev, State Hydrological Institute, St. Petersberg, Russia
T. Gunther, Deutscher Wetterdienst, ZHEA Berlin, Germany
B. Sevruk, Swiss Federal Institute of Technology, ETH, Switzerland

INTRODUCTION

The WMO Solid Precipitation Measurement Intercomparison was initiated in 1985 after approval by CIMO-IX. The goal of the study was to assess national methods of measuring solid precipitation against methods whose accuracy and reliability were known, including past and current procedures, automated systems and new methods of observation. Countries which participated, operated the reference standard and have submitted complete data summaries for analysis were: Canada, China, Croatia (originally Yugoslavia), Denmark, Finland, Germany (originally German Democratic Republic), Japan, Norway, Russia (originally USSR), Sweden and the United States. Other countries collecting and submitting comparative data for at least one winter included Bulgaria, India, Romania and Slovakia (originally Czechoslovakia), and the United Kingdom.

The Intercomparison was designed to: determine wind related errors in national methods of measuring solid precipitation, including consideration of wetting and evaporative losses; derive standard methods for correcting solid precipitation measurements; and, introduce a reference method of solid precipitation measurement for general use to calibrate any type of precipitation gauge. The experiment, conducted by Members at sites selected in their own country, ran for the winters of 1986/87 through 1992/93.

SUMMARY OF SYSTEMATIC ERRORS

Reference Method for Snowfall Measurement: After reviewing all possible methods (bush shield, double fence shield, forest clearing, snow boards, dual gauge approach) the octagonal vertical double-fence shield (with manual Tretyakov gauge) was designated as the Intercomparison Reference (DFIR) (WMO/CIMO, 1985; Goodison et al., 1989). An artificial shield was selected since natural bush sheltering would not be available in all climatic regions. The DFIR is a secondary standard. Errors in measurement using the DFIR and correction procedures are given in Golubev (1986) and WMO/CIMO (1992). Initial results from the experiment are given in WMO/CIMO (1992), Aaltonen et al. (1993), Gunther (1993) and Metcalfe and Goodison (1993). Errors in solid precipitation measurement were quantified for over 20 different gauge and shield combinations.

Wetting and Evaporative Losses: Evaporation and wetting losses from manual gauges contribute significantly to the undermeasurement of solid precipitation. Aaltonen et al. (1993) reported on the comprehensive Finnish assessment of evaporation losses; average daily losses varied by gauge type and time of year. Losses in April of over 0.8 mm/day were measured in some gauges. Average losses for winter periods, ranging from 0.1-0.2mm/day, were much less than during summer periods.

Wetting loss varies by precipitation type, gauge type and the number of times the gauge is emptied. Average wetting loss can be up to 0.2mm per observation. At some Canadian synoptic stations, wetting loss was calculated to be 15-20% of measured winter precipitation (Metcalfe and Goodison, 1993).

Wind Speed: For most precipitation gauges, wind speed is the most important environmental factor contributing to the undermeasurement of solid precipitation. Deviations from the DFIR measurement varied by gauge type and precipitation type. All of the results will be given in the final intercomparison report. Some results are summarized below to emphasize the magnitude and variability between gauge types (and shielding) and precipitation type in the undermeasurement of solid precipitation.

Valdai, Russia was the only site where the DFIR was compared to gauges sited in bushes (cut to gauge height), the latter deemed to provide the best estimate of "ground true". Table 1 compares precipitation totals for November 1991 to March 1992 for the DFIR, the bush gauge and some of the other gauges operated at Valdai.

Table 1: Precipitation totals (rain and snow) measured by different gauges at Valdai, Russia,November 1991-March 1992 (WMO/CIMO, 1992)

Gauge type	Total Precip.(mm)	% of bush total
Tretyakov in bushes	367	100
DFIR (Tretyakov)	339	92
DFIR (Canadian Nipher)	342	93
Canadian Nipher shielded	314	86
Tretyakov	258	70
8" USA Alter shielded	273	75
8" USA unshielded	208	57

The measurements show the need to correct the DFIR to the "ground true" value of the bush gauge to account for the effect of wind and other environmental factors (e.g. temperature). Methods to correct the DFIR were developed and applied (WMO/CIMO, 1992; Yang et al.,1993) before comparing the catch of national gauges to the DFIR. Finland conducted the most extensive comparison of gauge types and shielding at a single site (8 manual, 3 autogauge types). Table 2 shows the average percentage catch for selected gauges (allowing for wetting loss) compared to the corrected DFIR. Gauge catch decreased with increasing wind speed for all gauges, with the relationship varying by gauge type, shielding, precipitation type and, in some instances, air temperature. Shielded gauges caught more than their unshielded counterparts. As well, Table 3 shows the results reported in WMO/CIMO (1992) and Gunther (1993) for the unshielded German Hellmann gauge and the Tretyakov shielded gauge compared to the DFIR, clearly showing an increasing loss with increasing wind speed and, for the same wind speed, a higher undermeasurement during snow than for rain or mixed precipitation.

Each country is preparing an analysis of the data from its sites for its national gauge. A comprehensive analysis of measurements for the same gauge tested in different countries is also being done. Figure 1 shows the regression of gauge catch ratio (gauge/DFIR) as a function of wind speed for Hellmann gauge data from Croatia, Finland, Germany and Russia. The combined results are very similar to those in Table 3 and reported by Gunther, 1993.

Table 2: Average gauge catch (%) compared to DFIR (corrected to bush value) for snowfall at Jokioinen, Finland, 1987-1993.

Gauge	Catch(%)	Gauge	Catch(%)
DFIR	100	Danish Hellmann (unshielded)	48
Canadian Nipher Shielded	82	Hungarian Hellmann (unshielded)	46
Tretyakov(shielded)	74	Geonor (weighing, Alter shield)	62
Tretyakov (unshielded)	46	Tipping Bucket (heated)	62
Swedish	69	Wild (shielded)	57
Norwegian	66	Wild (unshielded)	40

Table 3: Gauge catch as a percent of DFIR as a function of wind speed and precipitation type for Tretyakov and unshielded German Hellmann gauges, Harzgerode, Germany, December-March 1986-1992.

Wind speed m/s	TRET/DFIR(%) snow	mixed	rain	HELL/DFIR(%) snow	mixed	rain
1.1-2.0	86	85	92	68	80	94
2.1-3.0	71	76	91	56	69	91
3.1-4.0	49	62	90	42	57	89
4.1-5.0	49	52	88	26	46	86
5.1-20.0	33	56	83	22	50	87

Figure 1: Ratio of gauge catch to DFIR as a function of wind speed for the unshielded Hellmann gauge for snow only for all sites.

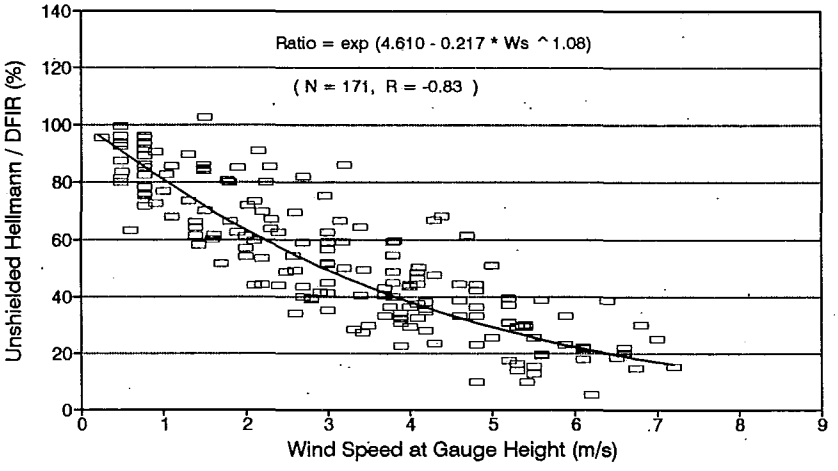

CORRECTION PROCEDURES FOR PRECIPITATION GAUGE MEASUREMENTS

Archived data: Procedures are now being tested to correct historical national gauge measurements for wind, wetting and evaporative losses. Wind speed at gauge height is required; it can be measured or derived using a mean wind speed reduction procedure. This is site dependent; estimation will require a good knowledge of the station and gauge location, hence, a good metadata record. Wetting loss is cumulative and depending on the number of times the gauge is emptied, it can become a very large value for the year. Canada has conducted preliminary tests in applying correction procedures on its digital archive data. Figure 2 shows the result of correcting the Dease Lake synoptic station annual snowfall precipitation as measured by the Canadian standard methods of snowfall measurement (ruler and Nipher gauge) and by the DFIR

operated at the site for 1987/88-1990/91. Average winds at this station are less than $3ms^{-1}$; hence the Nipher gauge showed only a 5-10% undercatch compared to the DFIR, whereas ruler measurements, using a density of $100kgm^{-3}$, overestimated precipitation by as much as 20%. Metcalfe and Goodison (1993) showed that by applying corrections to gauge measurements for wind, wetting loss and trace precipitation (assigning a non-zero value), and to ruler measurements for variations in regional fresh snowfall density, the corrected values were within a few percent of the corrected DFIR (C/DFIR). Figure 3 shows initial results comparing corrected and uncorrected Canadian Nipher gauge data for Resolute, NWT for 1963-1992, applying corrections for wind, wetting loss and trace precipitation to archived data. For some years the corrected values are double the measured, and published, totals.

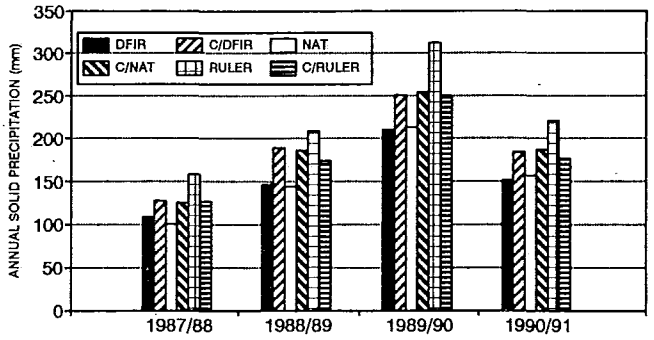

Figure 2: Annual measured and corrected snowfall precipitation for Dease Lake, Canada for DFIR, Nipher(NAT) and ruler measurement.

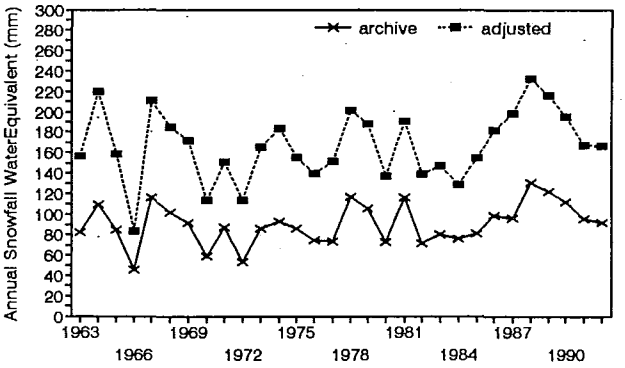

Figure 3: Archived and corrected annual snowfall precipitation at Resolute,Canada for Nipher gauge

Automatic Precipitation Gauges: Correction curves for automatic gauges for wind induced errors were derived. Additional problems were identified, but the intercomparison was not designed to resolve some of these. Heated gauges, including heated tipping bucket gauges were tested. Finland and Germany reported a large undercatch by unshielded heated gauges, caused by wind and evaporation of melting snow (Aaltonen et al., 1993; Gunther, 1993). Aaltonen et al. (1993) reported that the performance of heated tipping buckets was very poor and that they cannot be recommended for winter time precipitation measurement in Finland.

Weighing gauges were assessed in Canada, Finland, and the USA. Operational problems included wet snow or freezing rain sticking to the inside of the orifice of the gauge and not falling into the bucket to be weighed until some time later (adversely affecting accurate timing of the precipitation event), gauges catching blowing snow, differentiation of the type of precipitation and wind induced oscillation of the weighing mechanism. These problems affect real-time interpretation and use of the data as well as the application of an appropriate procedure to correct the measurement for systematic errors. Continuing assessment of automatic precipitation gauges, their performance during all weather conditions and refinement of correction procedures is required.

CONCLUSIONS AND RECOMMENDATIONS

The goal and objectives of the experiment were successfully achieved. Data from all experiment sites confirm that solid precipitation measurements must be corrected for wetting loss (for

volumetric measurements), evaporation loss and undercatch due to wind speed before one can estimate precipitation at ground level.

Recommendations on the measurement and correction of solid precipitation submitted for consideration at CIMO-XI included:

* the DFIR be accepted as a secondary standard for solid precipitation measurement; on-going assessment of it as a standard is recommended;

*methods developed from this intercomparison for correcting systematic errors in precipitation measurement that are available for different types of gauges and for different types of precipitation and various time intervals should be adopted and applied to current and archived data;

*both measured and corrected precipitation data should be reported and archived;

*trace precipitation should be treated as a non-zero event;

*gauges should be shielded either naturally (e.g., forest clearing) or artificially (e.g., Alter, Canadian Nipher type, Tretyakov) to minimize the adverse effect of wind speed;

*use of heated tipping-bucket gauges for winter precipitation measurement should be carefully assessed; their usefulness is severely limited in regions where temperatures fall below 0°C for prolonged periods of time; and,

*additional wind speed measurements be taken at the level of the gauge orifice in order to correct for wind-induced errors.

REFERENCES

Aaltonen, Ari, Esko Elomaa, Asko Tuominen and Perti Valkovuori, 1993: Measurement of precipitation. In, Proc. Symp. on Precipitation and Evaporation (ed. B. Sevruk and M. Lapin), Vol.1, Bratislava, Slovakia, 20-24 September 1993, 42-46.

Golubev, V., 1986: On the Problem of Standard Conditions for Precipitation Gauge Installation. In, Proc. Int. Workshop on the Correction of Precipitation Measurements, WMO/TD No. 104, Geneva, 57-59.

Goodison, B.E., B. Sevruk and S. Klemm, 1989: WMO Solid Precipitation Measurement Intercomparison: Objectives, Methodology and Analysis. In, Atmospheric Deposition (Proc. Baltimore Symp., May 1989), IAHS Pub. No. 179, IAHS Press, Wallingford, U.K., 57-64.

Gunther, Th., 1993: German participation in the WMO Solid Precipitation Intercomparison: Final results. In, Proc. Symp. on Precipitation and Evaporation (ed. B. Sevruk and M. Lapin), Vol.1, Bratislava, Slovakia, 20-24 September 1993, 93-102.

Metcalfe, J.R. and B.E. Goodison, 1993: Correction of Canadian winter precipitation data. In, Proc. Eighth Symp. on Meteorological Observations and Instrumentation. 17-22 January, 1993, Anaheim, Calif. AMS, Boston, 338-343.

WMO/CIMO, 1985: International Organizing Committee for the WMO Solid Precipitation Measurement Intercomparison, Final Report of the First Session, WMO, Geneva, 31pp.+ Appendices.

WMO/CIMO, 1992: International Organizing Committee for the WMO Solid Precipitation Measurement Intercomparison, Final Report of the Sixth Session, Toronto, Canada. WMO, Geneva, 14pp + 24 Appendices.

Yang, D., J.R. Metcalfe, B.E. Goodison and E. Mekis, 1993: Evaluation of DFIR accuracy at Valdai WMO Intercomparison site. Proc. Eastern Snow Conf. 50th Meeting, Quebec City, Canada, June 8-10, 1993 (in press).

INTERCOMPARAISON OMM D'INSTRUMENTS DE MESURE DE VENT

par P.GREGOIRE et G.OUALID

METEO-FRANCE

SETIM BP 202 78195 Trappes CEDEX

FRANCE

1. INTRODUCTION :

Suite à la recommandation de la CIMO X, portant sur une Intercomparaison de capteurs de mesure de vent, l'Institut Suisse de Météorologie (ISM) et Météo-France ont présenté leurs candidatures et proposé un site de montagne afin de couvrir la plus large gamme de vitesses de vent et de conditions climatiques.

La station du Mont Aigoual (altitude 1567m) située dans le massif des Cévennes (France) a été retenue comme site pour accueillir l'Intercomparaison OMM. Les conditions climatiques sont telles qu'on y observe des vents pouvant atteindre 60 m/s et des givrages très importants en période hivernale, en été les conditions orageuses y sont très fréquentes.

Suite à l'appel à participation, douze pays ont mis à disposition des organisateurs 26 capteurs basés sur des principes différents tels que : coupelles-drapeau, turbine-drapeau, hélice-drapeau, sonic, pression différentielle , film chaud. Parmi ces capteurs, seuls
L'intercomparaison qui a débuté en juillet 1992 s'est terminée en septembre 1993

2. LES OBJECTIFS DE L'INTERCOMPARAISON :

Le Comité International d'Organisation définit les objectifs suivants :
- évaluer, dans un environnement de type montagne, les caractéristiques dynamiques des capteurs soumis à des conditions de vent fort et givrage important. Des périodes distinctes (été, hiver) sont envisagées afin de tenir compte des caractéristiques de capteurs retenus.
- déterminer, en termes de fiabilité, les matériels adaptés à un environnement de type montagne notamment en période hivernale.
- effectuer des propositions éventuelles pour des futurs développements
- analyser et publier les résultats sous forme d'un rapport OMM/CIMO.

3 L' ORGANISATION DE L'INTERCOMPARAISON

3.1 LE SITE :

La station météorologique du Mont Aigoual, est équipée de deux tours orientées nord-sud, de 10 m de hauteur et séparées d'environ 28 m. Elles ont été aménagées pour recevoir de 16 (hiver) à 20 capteurs(été).
Le Comité a confié l'organisation de cette intercomparaison à Météo-France, avec l'Institut Suisse de Météorologie comme partenaire principal.
Météo-France est chargée de toute l'infrastructure, assistance et mise en route opérationnelle, de plus elle assurera l'archivage et le traitement des données. L'I.S.M. se chargera de l'acquisition des données primaires et des données météorologiques (matériels et logiciels).

3.2. LES CAPTEURS :

Etant donné le nombre limité d'emplacements disponibles, le Comité International d'Organisation a décidé d'accueillir en priorité les instruments de mesure de vent utilisés dans les réseaux d'exploitation. Exceptionnellement et en fonction des places disponibles, d'autres capteurs pourront être acceptés.
Il a été décidé que les instruments seraient classés en deux groupes d'utilisation, un groupe "tout an"(supportant tout type de temps y compris de sévère givrage) et un groupe "été" (sans givrage).
On trouvera en annexe la liste des Pays participant avec le type de matériel présenté et son principe de mesure. Les quatre principes de base pour les anémomètres sont représentés
- coupelle, hélice ou turbine
- ultrasonique .
- Pitot (pression différentielle)
- film chaud

3.3 LES ANEMOMETRES DE "REFERENCE"

Il n'existe pas à proprement parler de référence métrologique pour la mesure du vent en extérieur. Suite à la réunion du CIO, l'ISM a proposé d'installer deux anémomètres soniques commercialisés par la société MESA .
Comme référence de travail, l'Angleterre a fourni des anémomètres, utilisant le principe de Pitot, commercialisés par la société Smith Industrie qui ont posé quelques problèmes. Ces capteurs ont été remplacés par deux anémomètres, mis à notre disposition par l'ISM, utilisant le même principe et commercialisés par la société Campbell.
Il a été admis que les deux tours équipant le site de mesure seront vraisemblablement soumis à des champs de vent de caractéristiques différentes. La tour sud serait soumis à des vents soumis à des fluctuations dues à une vitesse de vent vertical turbulente. Il sera, donc, nécessaire d'équiper chacune des deux tours d'instruments "tout an" identiques .

4 L'INSTALLATION :

La réception des capteurs s'étale sur la période de mai à juin 92. Les essais en soufflerie, prévus fin mai sur 2 PITOTS et 3 ULTRASONICS , posent quelques problèmes lors de l'acquisition des données. Ces résultats seront confirmés lors de l'installation des capteurs sur le site.
L'installation s'effectue très laborieusement sur le site du MONT-AIGOUAL, la documentation accompagnant certains capteurs étant très succincte
L'ISM installe ses équipements :
L'acquisition des données issues des capteurs est effectuée par des stations CAMPBELL CR 10 montées en réseau et pilotées par PC. Ces données brutes 1s sont archivées et traitées pour calculer des "valeurs moyennes 10 mn" ainsi que différents paramètres tels que V moy, V min, V max, déviation standard,Vz etc....
Les données METEO sont également archivées sur le PC ISM.

METEO-FRANCE installe les capteurs et met en place son réseau PC Novell Netware 2.2 assurant la liaison entre les différents PC locaux (mesures, archivages, traitement) et celui du SETIM. Les données 1s et 10mn sont archivées sur disques optiques numériques. De plus chaque jour, les fichiers 10mn sont transféré par modem vers le SETIM pour le suivi opérationnel journalier et stockés pour analyses et traitements. Les fichiers 1s seront récupérés sur disques optiques par expédition de courrier au SETIM.
Sur le site, un technicien assure le suivi de qualité des données des capteurs ainsi que la maintenance éventuelle de l'ensemble de l'opération. Il alimente le carnet de bord journalier par toute intervention d'assistance, de maintenance ou toute observation de phénomène particulier.

5. LES OBJECTIFS D'ANALYSES DES RESULTATS :

On peut définir les grandes lignes de l'analyse finale en supposant que l'on puisse utiliser "une référence" ce qui n'est pas acquit à l'examen des premiers résultats disponibles :

6.2.Etude métrologique :

- évaluer l'erreur de capteur entre eux ou par rapport à une référence dans des conditions "idéales" à savoir T > 0, pas de précipitation, pas de givrage,
- quantifier pour chaque capteur l'erreur par rapport à la référence selon des classées de types de temps définis ainsi
  Classe de vitesse FF ms^{-1} :
  0 - 4, 4 - 8, 8 - 12, 12 - 18, 18 - 25, 25 - 50
  Givrage :
  absence , présence
  Précipitation :
  absence , présence
- éventuellement, l' influence de la vitesse verticale du vent sur les capteurs à coupelles dans les conditions "idéales",
- quantifier l'erreur des pointes maximales par rapport à la référence dans les conditions "idéales",
- évaluer l'erreur en direction par rapport à la référence dans le cas général, puis selon la force du vent de "référence",
- réaliser une classification par type des capteurs,

6.2 Etude de la fiabilité :

- étude au cas par cas pour les pannes franches,

- étude en fonction des types de temps (capteur sonique et pluie, capteur à coupelles et givrage).

Ces objectifs ne sont en aucun cas exhaustifs, et pourront être reconsidérés et/ou complétés au fur et à mesure de l'étude en cours.

6 LES PREMIERS RESULTATS :

A l'heure où est rédigé cet article, on peut donner quelques résultats préliminaire de l'étude en cours.

6.1 Période HIVER :

En période de fort givrage tous les capteurs ont givré exceptés le CAMPBELL, le SMITHS et le LAUMONIER. Les capteurs THIES , FRIEDRICH, YOUNG, KRONEIS, continue de fonctionner mais les valeurs fournies tendent vers zéro . Les capteurs sonic ou film chaud IRDAM et MESA, fournissent des valeurs aberrantes. Tous les autres capteurs présents sont bloqués : LAMBRECHT, BELFORT, VALCOM, VAISALA.

L'étude de fiabilité est en cours.

L'étude métrologique des capteurs s'avère très délicate étant donné le comportement des capteurs en cette période.

6.2. PERIODE ETE :

Nous avons choisi d'utiliser comme référence un capteur fictif fournissant des données égales à la médiane de celles des capteurs présents en éliminant certains capteurs qui majorent manifestement le vent moyen ou qui fournissent trop de valeurs aberrantes .

PYLONE NORD:

L'étude des moyennes calculées sur la vitesse moyenne, vitesse maximale et écart type de la vitesse, fait apparaître différents groupes:

- Groupe 1 : MESA, KRONEIS, DEGREANE, KNMI, SHILTKNECHT, YOUNG, VECTOR,

- Groupe 2 : LAUMONIER, THIES, CAMPBELL,

- SMITH

- SOLENT (UK)

Le groupe 1 est globalement très homogène. Néanmoins, le MESA et le VECTOR présentent des moyennes de vent maximal plus grandes. Le groupe 2 est plus dispersé. Les moyennes de vent moyen et de vent maximal sont plus fortes que celles du groupe 1 . Par contre les moyennes d'écart-types sont comparables.
Le SMITH et le SOLENT sont très différents des groupes 1 et 2.
Le SMITH présente des problèmes de dérive dans le temps et le SOLENT est influencé par humidité relative.

Les graphes de l'écart-type en fonction du vent moyen et les histogrammes du vent moyen et maximal donnent une idée (à confirmer) sur le seuil de démarrage des anémomètres :

Une classification hiérarchique effectuée sur les capteur du pylône nord confirme les groupes cités ci-dessus avec le meilleur accord pour les vents moyens entre le KNMI et le DEGREANE

Vent moyen minimal détecté			
0-0,5 m/s	0,5-1 m/s	1-1,5 m/s	1,5-2 m/s
DEGREANE	KNMI	THIES	SOLENT
KRONEIS	CAMPBELL		LAUMONIER
SCHILTK.	MESA		SMITH
YOUNG	VECTOR		

PYLONE SUD :
L'étude est en cours.

7. CONCLUSION :

L'Intercomparaison OMM de capteurs de mesure de vent au Mont Aigoual a suscité l'intérêt de nombreux industriels et utilisateurs pour une connaissance plus approfondie du comportement des capteur dans un environnement sévère de type montagne(vents forts, conditions orageuses, givrage sévère).

Même si l'étude n'est pas terminée, on peut se faire une idée sur le comportement de chaque type d'anémomètres : par exemple, les capteurs à film chaud ont montré leurs limites de fonctionnement dans un environnement perturbé. En période de givrage, seuls les anémomètres conçus spécifiquement pour cet environnement, fonctionnent correctement.

Par contre, cette comparaison a déjà apporté quelques informations intéressantes :
- au niveau des techniques d'interfaçage des capteurs. Il semble urgent de normaliser le support physique et les protocoles de dialogue avec les capteurs numériques.

- au niveau des installations des capteurs. Certains, devront être "durcis" pour une utilisation en réseau, dans des conditions réelles d'exploitation.

- au niveau de l'étude des nouveaux principes. Les résultats sont tout à fait encourageant pour les capteurs utilisant le principe de Pitot. Il s'est avéré, quand il est correctement réalisé, parfaitement bien adapté pour les conditions sévères de montagne : il réalise des mesures précises par vent fort et le fait qu'il soit compact permet d'effectuer aisément son dégivrage.

Les organisateurs de cette intercomparaison espèrent fortement que ce travail apportera de nombreuses information utilisables.

ANNEXE : LES CAPTEURS :

Liste des capteurs ayant participé en partie ou en totalité à l'intercomparaison:

T.A = TOUTE L'ANNEE ET. = ETE

PAYS	TYPE	CONSTRUCTEUR	PRINCIPE	E.T.A/ET.
ALLEMAGNE	SK565/SK566	A.THIES	COUP/DRAP	T.A
AUTRICHE	263 PR	KRONEIS	COUP/DRAP	T.A
CANADA	78D	VALCOM	COUP/DRAP	T.A
DANEMARK	4031 / 4121	FRIEDRICHS	COUP/DRAP	T.A
FRANCE 2	MONTAGNE	LAUMONIER	TURBINE	T.A
KENYA	WAD 21S	VAISALA	COUP/DRAP	T.A
SUISSE.	WNT-METEO	MESA	ULTRASONIC	T.A
SUISSE.1	PTA1-1001	CAMPBELL	PITOT	T.A
SUISSE.3	THER AN..	COSSONAY	FILM CHAUD	T.A
SUISSE 4	MT 20 DHS	IRDAM	FILM CHAUD	T.A
SUISSE 6	14512	LAMBRECHT	COUP/DRAP	T.A
U.K. REF	ORTHOGONAL	SMITHS IND.	PITOT	T.A
U.S.A. 1	M 2000 D.	BELFORT	COUP/DRAP	T.A
U.S.A. 3	05103 WIND	YOUNG COMP.	HEL/DRAP	T.A
U.S.A.4	MODEL 8600	SUTRON CORP.	FILM CHAUD	T.A
FRANCE 1	DEOLIA 92	DEGREANE	COUP/DRAP	E.T.
FRANCE 3	ULTRASONIC	SOLENT .	SONIC	E.T.
JAPON	FF-8A	KOSHIN DENKI	HELICE	E.T
PAYS BAS	01-002/-003	K.N.M.I.	COUP/DRAP	E.T.
SUISSE.2	566.2.52	SCHILTKNECHT	COUP/DRA	ET.
SUISSE.5	ONZ	METEO LABOR	HEL/DRAP	E.T
U.K.1	A100H/W200P	VECTOR .	COUP/DRAP	E.T.
U.K 2	ULTRASONIC	SOLENT.	SONIC	E.T.

AN INTERCOMPARISON TO DETERMINE THE PERFORMANCE CHARACTERISTICS OF SOME CURRENT WIND SENSORS

D B Hatton, D W Jones, A P Scott

Meteorological Office, United Kingdom

1. Introduction

In 1991 the UK Meteorological Office commenced a field trial of a selection of wind sensors. Jones et al 1992 described the site layout and data collection for the first two phases of the trial (1). The periods of data collection have subsequently been extended through 1992/3 in order to increase the number of different makes and models of instruments under investigation.

Brief details of all the sensors used in the trials are shown in table 1.

TABLE 1

Manufacturer	Model	Output	Tower
Belfort Instrument	2000 rotating cup and vane	digital - serial	10
Casella	speed - rotating cup direction - vane	digital frequency analogue potentiometer	13
Didcot	DWD 105 rotating cup DWD 205 vane	digital frequency analogue potentiometer	9
Gill Instruments Ltd	Solent 3-axis met. logging ultrasonic anemometer	analogue voltages	9
Gill Instruments Ltd	Solent 3-axis standard (4Hz) ultrasonic anemometer	digital - serial	12
Kaijo Denki	WA 200 3-axis ultrasonic anemometer	analogue voltages	9
R W Munro Ltd	IM 206 (lightweight) - IM 204 anemometer - IM 205 windvane	analogue voltages from frequency to dc converter syncro to dc converter	7
R W Munro Ltd	IM 146 anemometer	analogue voltage from frequency to dc converter	7
R W Munro Ltd	IM 2000 rotating cup & vane	digital - serial	11
Obsermet	OMC 165 rotating cup & vane	digital - serial	10
Penny & Giles	WS 2000 aerodynamic propeller and vane	digital - serial	9
Qualimetrics	Model 2102 skyvane propeller and vane	speed - analogue voltage direction - potentiometer	8
Qualimetrics	2031 micro anemometer 2020 micro vane	analogue dc voltage analogue potentiometer	10
Thies Clima	4.3302.22.000 rotating cup 4.3121.22.000 vane	analogue current loops from interface unit	11
Vaisala	WAA15 rotating cup WAV15 vane	serial - digital from WAT15 interface	12
Vector Instruments	A100 rotating cup anemometer W200P/M vane	analogue voltages	7 to 13
R M Young	05103 propeller & vane	analogue voltages from 05603 interface	8

Seven separate towers were used to support the sensors and each tower was fitted with separate Vector Instruments (VI) A100 anemometers and W200P/M wind vanes. These act as relative reference instruments to remove any spatial variability that may occur at the site. They are relatively small lightweight sensors with no obvious shortcomings, and have some limited operational use within the Meteorological Office. The sensors under test were exposed alongside these.

2. Data analysis

One of the difficulties of showing results from a multi-instrument trial of wind sensors is how to present the data in a concise form.

Two instruments that are separated spatially on a tower will frequently indicate different instantaneous measurements of wind speed. Various statistical analysis methods are therefore necessary in order to demonstrate the instruments' overall performance.

The main method of determining relative performance has been by comparing data from a large sample of 10 minute mean winds, using scatter plot and linear regression analysis. Similar comparison analysis has also been performed for the maximum 3 second gust in the 10 minute period, and scatter plots have been produced for each instrument, comparing the 10 minute mean wind speed with the maximum 3 second gust in that period. Space precludes the inclusion of all in this paper, but examples are given in figures 1 to 6. Due to the nature of the site, the upper range of mean wind speeds is about 20 knots.

The linear regression analysis has been performed on the data for each instrument pair (x_i, y_i), and an equation for the best fit straight line through all the data points has been calculated in the form $y = mx + c$ where m is the slope of the line.

In order to see how good the linear relationship is, it is necessary to examine how well the regression line fits the data points. For this the correlation coefficient r, calculated from the relationship

$$r = \frac{\sum (x_i - \bar{x})(y_i - \bar{y})}{\sqrt{\{[\sum (x_1 - \bar{x})^2][\sum (y_1 - \bar{y})^2]\}}}$$

has been computed.

The value of r can lie between +1 and -1, depending upon whether the correlation is positive or negative, and high or low. r^2 provides a coefficient of determination to show how well the data fit the line. It can vary between 0 and +1, where a low value shows a poor fit and a value close to 1 shows that the data points fit the line well.

All of the comparative readings can be influenced by the fact that one or both anemometers may have stopped measuring at low wind speeds, because they have finite start speeds. This is clear from the scatter plots (see example at figure 1) and so for the regression analysis in this paper, the data have been selected for periods with a mean wind speed greater than 4 knots. It must be remembered that for some instruments, although these data appear to be good, there may be anomalies in the sub 4 knot data. For example, one of the instruments which had a pulse output was prone to occasional noise on the output which manifested itself as a low windspeed value mainly less than 4 knots.

Table 2 provides a brief summary of the results using data from approximately 2000 ten minute periods, and lists the instruments according to make and tower identification. Against each pair of instruments are shown the values of r^2 and m from the linear regression analyses for 10 minute mean speeds, 3 second gusts, and gust ratios for each individual instrument. In order to demonstrate the statistical agreement that can be expected between two identical instruments, the first line of data in Table 2 shows two Vector Instruments anemometers side by side on tower 10.

3. Results

The operational units for measurement of wind speed in the United Kingdom is knots, and the results have been analysed using these units, (1.943 knots is equal to 1 metre per second).

a) 10 minute mean wind speeds

The first two columns of data in table 2 show the results of comparing 10 minute mean wind speeds recorded by two instruments on the same tower. Nine instruments have very good agreement with their VI anemometer, shown by values of $r^2 = 0.99$. Values < 0.97 have been shaded as they show that there was considerable scatter in the results.

FF > 4 knots only

TABLE 2

	speed 10 min. mean		gust 3 second		gust ratio instrument		gust ratio ref. Vector	
	r^2	m	r^2	m	r^2	m	r^2	m
Vector 10 vs Vector A100	0.99	1.00	0.99	1.00	0.82	1.90	0.82	1.93
Vector 7 vs Munro IM 146 (Mk2)	0.97	1.14	0.93	1.11	0.89	1.63	0.90	1.66
Vector 7 vs Munro IM 204 (Mk4) test 1	0.98	1.08	0.94	0.98	0.86	1.57	0.87	1.70
Vector 7 vs Munro IM 204 (Mk4) test 2	0.93	1.21	0.86	1.17	0.84	1.61	0.90	1.66
Vector 8 vs Young's 05103 test 1	0.97	0.94	0.98	0.96	0.84	1.85	0.86	1.84
Vector 8 vs Young's 05103 test 2	0.99	1.01	0.99	1.03	0.87	1.89	0.88	1.87
Vector 8 vs Qualimetrics skyvane 2102	0.94	0.97	0.97	0.97	0.85	1.81	0.88	1.87
Vector 9 vs Gill Inst. Solent analogue	0.99	0.95	0.96	0.96	0.84	2.01	0.86	1.98
Vector 9 vs Kaijo Denki WA 200	0.99	0.94	0.97	0.96	0.84	2.02	0.86	1.98
Vector 9 vs Penny & Giles WS 2000	0.93	1.01	0.87	0.92	0.58	1.81	0.89	1.92
Vector 9 vs Didcot DWD 105/205	0.44	1.25	0.23	1.16	0.80	2.33	0.89	1.92
Vector 10 vs Obsermet OMC 165	0.98	0.98	0.98	1.01	0.83	1.81	0.78	1.71
Vector 10 vs Qualimetrics micro-anemo	0.99	1.01	0.99	0.99	0.88	1.89	0.88	1.92
Vector 10 vs Belfort model 2000	0.99	0.98	0.97	1.00	0.89	2.01	0.88	1.92
Vector 11 vs Thies Clima	0.99	1.08	0.94	1.02	0.84	1.74	0.87	1.81
Vector 11 vs Munro IM 2000	0.93	0.99	0.96	1.01	0.92	1.84	0.91	1.82
Vector 12 vs Vaisala WA 15	0.99	0.98	0.97	0.92	0.79	1.75	0.78	1.84
Vector 12 vs Gill Inst. Solent digital	0.97	0.94	0.94	1.01	0.91	2.03	0.92	1.92
Vector 13 vs Casella	0.99	0.93	0.97	0.97	0.88	2.03	0.87	1.93

Figure 2 shows the scatterplot of the Munro IM 204 (r^2= 0.93) and its reference VI anemometer and Figure 1 shows a scatterplot of the two VI A100 sensors (r^2= 0.99), to illustrate the differences in the scatter likely from two identical sensors.

All sensors were calibrated in a wind tunnel prior to deployment and the values shown are corrected to within 2% where the wind tunnel calibration shows this to be necessary. It will be noted that the values of m differ quite significantly from 1 in some instances. Where they correspond to a low (shaded) value for r^2this can be attributed to the poor fit of the line. However, for other occasions a different explanation is necessary.

Take for example the Thies Clima anemometer which has a value of r^2= 0.99 but a value of m = 1.08. The scatterplot figure 3 shows that the instrument is tending to read higher at increased speeds under dynamic conditions, possibly due to overspeeding of the cups, relative to the VI A100. Conversely, the Gill Solent (figure 4) and the Kaijo Denki both have slopes less than 1. These instruments are ultrasonic anemometers and have no moving parts, implying that the VI A100 may itself have some overspeeding of the cups under dynamic conditions. These effects are not apparent during steady state wind tunnel calibrations.

The results from the three propeller anemometers (Youngs, Penny & Giles and Qualimetrics) are not conclusive, since the only good fit (r^2 > 0.97) was obtained with the Youngs 05103. Data from two periods of testing are shown, and one has a value of m = 0.94, and the other m = 1.01. There is thus some evidence that the propeller anemometer is less susceptible to overspeeding, but the fact that it may have to change direction before it can fully respond to changes in wind speed may cause it to under read anyway.

b) 3 second gusts

Data columns 3 and 4 in table 2 show the values for r^2 and m for comparisons of the measurement of the maximum 3 second gust in each 10 minute period. There is more scatter than for the 10 minute mean data, and values of $r^2$are noticeably lower. In view of the values obtained by intercomparison with the ultrasonic anemometers, r^2> 0.95 has been considered acceptable, and lower values are shaded. The dynamic response of the instrument would be expected to have more influence on the scatter of the values for gust measurements and the table generally shows this to be true. Values of m are broadly similar to the mean speed data.

c) Gust ratios

The gust ratio of the instrument under test and the VI relative reference can be calculated independently for each tower, and a linear regression curve of maximum gust on 10 minute mean wind calculated for both. The slope m will give a value for the gust ratio, and r^2 will again show how well the data fit the line over the range of speeds. Table 2 data columns 5 to 8 show the results. The gust ratio data will be much more variable than the mean wind and gust correlations, as the gust ratio will vary spatially, and with wind direction. The scatter plots shown in figures 5 and 6 show the typical variability in the relationship. Generally, the gust ratio derived from these plots is fairly constant when the mean wind speed exceeds 4 knots. This may not necessarily hold true for mean wind speeds in excess of 20 knots.

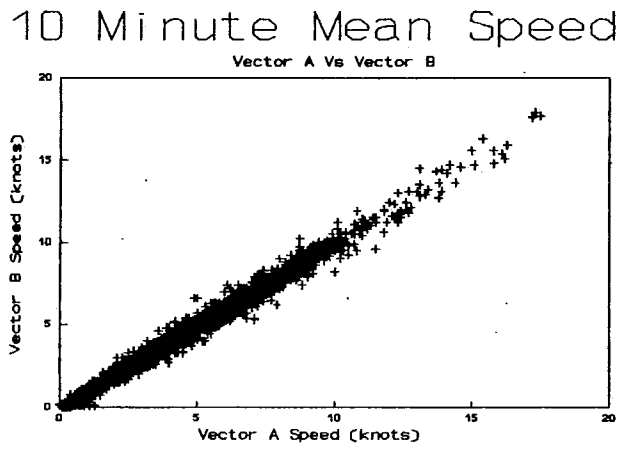

Figure 1

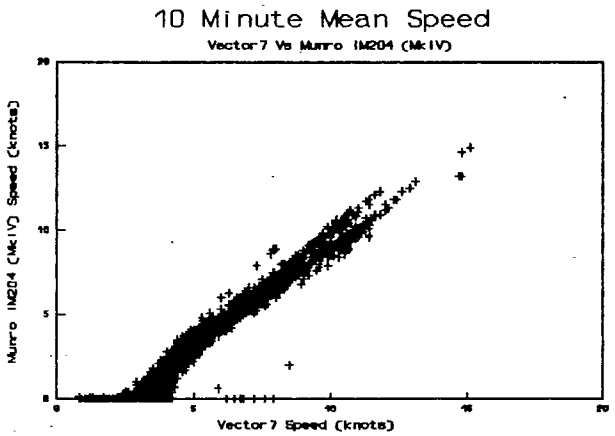

Figure 2

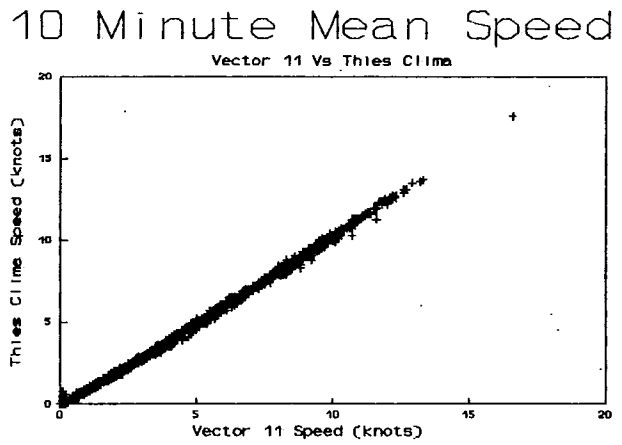

Figure 3

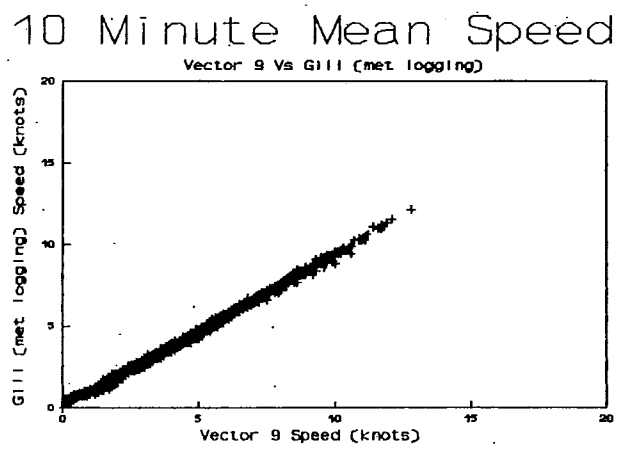

Figure 4

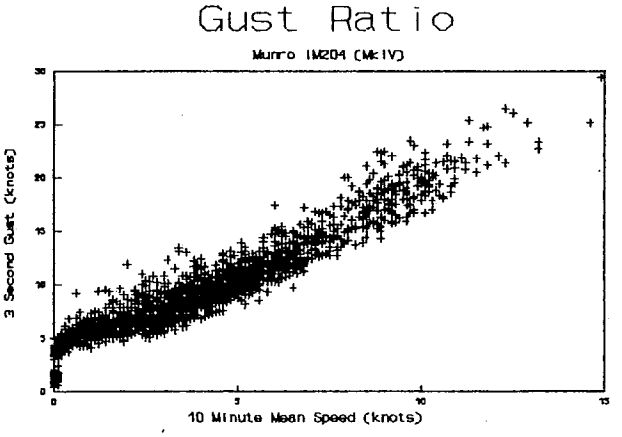

Figure 5

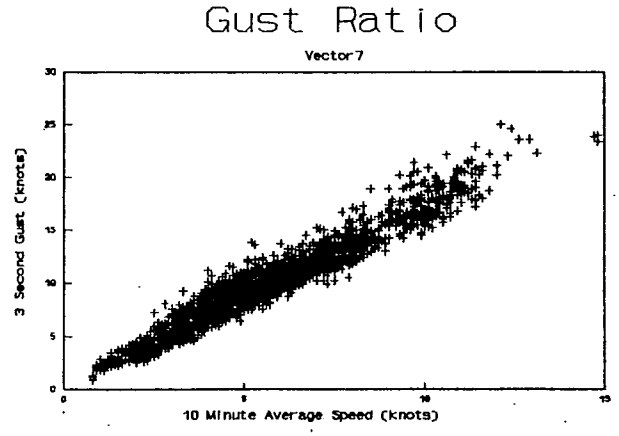

Figure 6

Instrument gust ratios are not directly dependant upon comparison with another instrument. In table 2 there is a large variation in gust ratio values for different instruments on different towers, but in most cases where good correlations have been shown for mean winds and gusts, the values of r^2 and m for the instrument gust ratio and the corresponding Vector are also in good agreement (within 5%).

4. Anemometer and wind vane features

When considering a wind system for long term operational use, many factors other than purely dynamic response may affect the choice. These include the materials used in construction and the susceptibility to corrosion of all parts including fixing screws, the rating of bearings and friction effects, the mechanical integrity, sealing and general robustness.

The weight will be important when considering the ease and arrangement of mounting, and the selection of masts to support instrumentation.

The dimensions of the instrument will affect its ability to fit into a wind tunnel and therefore have direct affect on the cost and choice of calibration facility. The moment of inertia of moving parts may affect dynamic performance.

Maintenance requirements, spares, servicing, mechanical interchangeability and conformity of calibrations will all contribute towards the overall cost of a system.

Electrical requirements must also be considered. These include power at the mast, electrical inputs and outputs, signal processing and conditioning, methods for transmission of data to displays or loggers and isolation and protection against lightning surge damage.

The ability of sensors to stand alone and support different output requirements, or to integrate into existing data collection and/or display systems may be important.

The quality of the data output will be affected by the speed and direction resolution, (pulses per revolution, volts per knot, degrees per bit, ohm, volt, etc). If the output data are processed after sampling, then details of the raw data sampling period, filtering and smoothing must be considered. The algorithms used to derive the raw and processed speed and direction values must be known and acceptable.

In order to faithfully measure gusts the ability to sample outputs frequently to obtain a true 3 second (or other period) value is essential. It is beyond the scope of this paper to analyse each instrument in this trial against all these factors.

5. Conclusions

Wind measuring instruments fall into two main groups, those that make very simple measurements, such as a pulse count, voltage or resistance change, and those with electronic processing, often microprocessor controlled, to produce a scaled output. The cost differential can be considerable, and it is often not clear what advantages a more expensive system offers in terms of the actual wind speed and direction measurement. The instruments with electronic processing may be simpler to interface to modern displays and loggers, but a more cost efficient path may sometimes incorporate simple displays with a separate output interface unit.

The instruments used in the trials also group according to their measuring performance. Many of them produce very similar measurements over the wind speed range 0 to 20 knots, but a small number give cause for concern. The highlighted boxes in table 2 show instruments for which the data are not consistent with the majority.

The measurements in table 2 show that there is a need to test instruments under dynamic conditions in order to establish their true performance characteristics. For this, a windy site is not as important as a site with a high gust ratio, which will amplify dynamic effects.

Reference

1: D W Jones, D B Hatton, D A Jenkins and A P Scott; 'A Field Intercomparison of some Wind Sensors'; WMO, Instrument and Observing Methods Report no. 49, TECO-92, May 1992.

The WMO Present Weather Sensors - System Intercomparison

Michel Leroy
METEO-FRANCE/SETIM France

Roger Van Cauwenberghe
Atmospheric Environment Service, Canada

1. Introduction

The forty second session of the Executive Council approved in Resolution 6 a "WMO Comparison of Automated Present Weather Sensors/Systems".

Canada and France were candidates for the organization of the intercomparison in Canada and in France.

2. The First Session of the International Organization Committee

During December 1992, the International Organizing Committee (IOC), made up of representatives from the United Kingdom, United States, CAeM, Canada, France, Holland and WMO held its first session at SETIM in Paris. They worked out the basis for the realization of this intercomparison and determined the objectives.

2.1 Objectives of the Intercomparison

The IOC agreed that a clear statement of objectives should be prepared for the intercomparison. Considering the wide range of capabilities of present weather sensors and the difficulties of reference measurements, it was decided to limit the intercomparison to code groups 00 and 40-98 for Code 4680. Code 4680 is the new code for observations from automatic weather stations.

Code 00 is for no significant weather. Codes 40 to 98 represent precipitation in various forms including thunderstorms. The code is designed to be used by automatic weather stations of different capabilities so that there are code groups for presence or absence of precipitation, as well as types of precipitation without a rate or amount. The code also allows for the normal report from full capability automatic weather station.

The main objectives agreed to were:

- To record the highest level output from each sensor or system;
- To make and record visual estimates of present weather plus where possible, reference measurements, precipitation intensity and other meteorological variables;
- To analyze the data in order to investigate the performance of the instruments' ability to identify different weather classes;
- To assemble information on the operational aspects of the instruments entered into the intercomparison;
- To evaluate and publish the results of these analysis.

The OC recognised that many of the more sophisticated sensors provided diagnostic status information within their output messages which when analyzed by the manufacturer in conjunction with the visual and meteorological data should permit the manufacturer to improve the operational sensor algorithms. It was therefore agreed that this data should also be recorded and made available to the manufacturer on request.

The OC agreed that these analyses would enable guidance to be given on the advantages and disadvantages of the different physical principles used by the instruments under different conditions and assist Members in developing and improving operational practises for the use of these types of instruments.

The inclusion of a statement on different factors in the final report, such as routine maintenance and calibration, electrical and mechanical reliability, as well as the use of the different output messages and displays, was considered important when choosing operational instruments.

2.2 Locations of Intercomparison

CANADA proposed the St. John's, Newfoundland site. This site offers unique severe conditions:

A large number of storms track through the area each year, bringing a variety of wind driven liquid, freezing and frozen precipitation.

The means per year are:

217 days with precipitation occurance (≥ 0.2 mm)
48 days with precipitation occurance (≥ 10 mm)
38 days with freezing precipitation occurance

Total rain amount of 1157 mm.
Total snow amount of 359 mm.
Average wind speed of 24.3 km/hr.

FRANCE proposed the site of Trappes, located near Paris. This site was thought complementary to St. John's, offering less extreme perturbations, representative of temperate climatic countries. The means per year are:

170 days with precipitation occurrence (≥ 0.1 mm)
113 days with daily precipitation amount higher than 1 mm
44 days with daily precipitation amount higher than 5 mm
15 days with daily precipitation amount higher than 10 mm

Total precipitation amount of 640 mm.

The mean precipitation rate is therefore quite low.

Snow events are scarce (mean of 18 days/year) and light.

The OC considered that these two complementary sites will allow to cover a large range of meteorological situations in different conditions.

2.2.1 Instruments

Selection of instruments:

Priority in the intercomparison was be given to

1) Sensors/systems which classify precipitation in"liquid/freezing/frozen" and eventually subgroups of those.

2) Sensor/systems which make precipitation judgements (yes/no).

3) Sensors/systems which measure instantaneous rate of precipitation not using catchment.

4) Sensors employing catchment techniques only would normally be considered in other intercomparison tests.

2.2.2 Comparison Reference

There is no comparison reference for present weather. It was agreed; therefore, that a human observer should be given preference to deliver the reference data for the distinction of the present weather code figures of the WMO Code 4680. In addition to the regular observation, both host countries will provide other observers who will be able to deliver detailed high frequency reports during periods of interest of at least 5 hours per week on average. These detailed observing periods can be "clinic observation," occurrence, nature and intensity of hydrometeors being noted every minute. This observer will be equipped with aids of all types, including rods for measuring ice thickness and a camera for recording unusual events, such as ice and snow on sensors.

In addition to the observer data, other instruments will be available to assist with measurements of intensity of precipitation, and accumulation of precipitation. This would include a pit gauge in snow free periods, as well as shielded snow gauges in the winter time.

2.2.3 Complementary Meteorological Data

In addition to the comparison reference data, a wide range of supplementary data will be available, including air temperature, dew point temperature, snow depth, wind speed and direction at sensor height, visibility and sunshine duration.

2.3 Organization of the Intercomparison

The intercomparison will be run at two different locations. The first part of the project will begin in St. John's in December, 1993 and carry on for 12 months with a possible extension to 18 months. The second phase will commence at SETIM in the autumn of 1994 and carry on for at least six months.

The organization of the intercomparison will be shared by France and Canada, with each country being responsible for there own site facilities. This includes the provision of mounting pads and towers, wiring, power, reference sensors, reference observations, data acquisition equipment including software, communications and archiving of data.

3. The Intercomparison

3.1 The Canadian Project

Following the announcement of the intercomparison by the WMO, 7 countries proposed 11 types of sensors following the priority selection criteria. Since some manufacturers sent only one sensor, there are 17 sensors in the intercomparison. See table 1 for the list of sensors.

Access to the test site is difficult during severe weather events so that extra evidence of blockage of sensors with ice and snow will be available via the use of a video camera with tilt, pan and zoom capability. The system will also give extra confirmation of obstructions to vision and other conditions.

This is a unique opportunity given the broad array of sensors under test and the weather conditions at St. John's (frequent storms with different types of precipitation, and often mixed precipitation, often with strong winds). Canada will therefore make every attempt to maximize the reference measurements of precipitation type and intensity, both by having the observer make extra measurements such as estimating particle size diameters and by employing unconventional instrumentation such as the ASCME (Airborne Snow Concentration Measuring Equipment). The ASCME is a snow sampling device on a rotating arm which provides a mass concentration per cubic meter. (Ref 1.)

A personal computer with digital, analog, counter and communications option boards was programmed to archive the data from the sensors under test for the intercomparison, as well as the reference data and the other sensors and systems under test. There are more than 45 sensors and systems logged at the site. Data is communicated daily to Toronto, a distance of 2000 km, where graphing of results and quality control is immediately performed. Problems are noted and action is decided on a daily basis.

3.2 The French Project

The French test site has the advantage of being directly located at the SETIM, the Service for Meteorological Instrumentation of METEO-FRANCE.

An operational observing station (surface and upper-air) is also located at the same site.

All the facilities are therefore available on site: conventional instruments, operational observations, data acquisition systems, computer for data analysis and staff. The instruments will be directly under visual control.

A small computer network will be used for data acquisition. Standard data acquisition system and software will be used for sensors with analog output and fixed and simple digital output. Experience has shown that a system such as this has limits, especially concerning serial line management. In this case, specific software will be written to handle specific output, the principle being to adapt the acquisition system to the sensors and not the contrary.

All the data will be recorded on optical disks. Common format will be used, thus allowing exchange of large amount of data between the two test sites.

It was agreed that the main part of data analysis will be conducted by the French team. This team has just worked on the WMO wind intercomparison data analysis. The methods to be used will still have to be discussed and adjusted in details with the OC.

3.3 Data Analysis

The primary output of the intercomparison of present weather sensors will be presented on contingency tables and correlation matrices based on weather classes according to the Present Weather Code 4680. Past national comparisons have shown that start and end of precipitation events are sometimes difficult to define, even by a human observer, especially during light precipitations. Contingency matrices are therefore perturbated when taking in account all one minute data. Specific analysis will have to be conducted with the notion of occurrence of event on a period of time. There will also be classification of performance of sensors in different types of conditions, such as wind, snow, ice accretion etc.

This will also be an opportunity to discover how non-catchment gauges perform in various conditions, so that a large portion of the analysis will deal with this aspect of these sensors.

4. Conclusions

Present weather sensors are only now coming into service in some countries. These sensors, while new, are one of the key sensors to a complete and viable automation plan. This intercomparison will not only define the state of the art, but will provide valuable information to manufacturers so that they can develop improved products.

5. Acknowledgements

The authors wish to thank Klaus Shultze of the WMO and Wynn Jones of the UK Met Office for their guidance at the International Organizing Committee meeting in SETIM and in making the intercomparison possible.

References:

1. Lacombe, J., "Technique for Measuring the Mass Concentration of Falling Snow," SPIE Proceedings 414, p. 17, 1983.

CANADA

1. POSS, Andrew Canada Inc. (two sensors) Bistatic Microwave (10GHz) Doppler Radar which measures the fall velocity of precipitation particles. Classifies precipitation type and calculates precipitation rate.

2. CAPMON, Meteorological Instruments Co. (two sensors)
Precipitation conductivity grid.

FINLAND

1. FD12P, Vaisala Oy (two sensors) Combination of optical (infra red) forward scatter sensor and capacitive grid. Classifies precipitation type, measures visibility and calculates precipitation rate.

FRANCE

1. SCHUBERT, SETIM (one sensor) Bistatic Microwave (35 GHZ) Doppler Radar which measures the fall velocity of precipitation particles. Classifies precipitation type and calculates precipitation rate.

GERMANY

1. RS85, G.K. Walter Eigenbrodt (two sensors) Precipitation conductivity grid.

2. IRSS88, G.K. Walter Eigenbrodt (two sensors) Optical (infra red) sensor to sense precipitation occurrence, provides an estimate of precipitation intensity.

SWEDEN

1. OPVD, Sten LÖfving Optical Sensors (one sensor) Optical (infra red) backscatter sensor. Measures visibility and raw information (does not classify) about precipitation type and intensity.

UNITED KINGDOM

1. 875C, Rosemount Ltd. (two sensors)
Latent heat sensor. Detects solid precipitation.

UNITED STATES

1. OWI-240 LEDWI, Scientific Technology Inc. (two sensors) Optical (infra red) sensor. Classifies precipitation type and measures precipitation rate.

2. 872E1, Rosemount Aerospace Inc. (two sensors) Vibrating ice accretion detector. Detects freezing precipitation occurrence, calculates accretion rate.

3. PW 402B, HSS Inc. (two sensors) Optical (infra red) forwardscatter and backscatter sensor. Classifies precipitation type, calculates precipitation rate and measures visibility.

TABLE 1 The sensors participating in the first phase of the intercomparison in St. John's, Canada.

WINTER 92/93 PRESENT WEATHER SENSOR FIELD TRIAL

A Stepek, D W Jones and D B Hatton.
Meteorological Office, United Kingdom

1. INTRODUCTION

This paper will compare the measurements of seven Present Weather instruments with professional observers' descriptions of precipitation (ie snow, rain or drizzle), and the absence of precipitation. It will also compare liquid precipitation intensity measurements from four of these instruments with data from a collection gauge. An intercomparison of visibility measurements (available from two of the optical devices) is also made.
The 7 instruments, and the abbreviations used to represent them in TABLE 1, are :-
1. NE1 - Vaisala O.Y. Rain Detector DRD 11A (northeasterly orientation)
2. SW1 - Vaisala O.Y. Rain Detector DRD 11A (southwesterly orientation)
3. SW2 - Vaisala O.Y. Precipitation Detector DPD 12A (southwesterly orientation)
4. ORG - Scientific Technology Inc. Optical Rain Gauge ORG-700
5. HSS - HSS Inc. Present Weather Sensor PW-402
6. LED - Scientific Technology Inc. LEDWI OWI-220 (enhanced sensitivity software)
7. VAIS - Vaisala O.Y. Present Weather Sensor FD 12P

The site for the trial was the Meteorological Office's Eskdalemuir Observatory (W.M.O. Station Number 03162) in southern Scotland ($55^0$19'N, $03^0$12'W, 240m A.M.S.L.). All the instruments, except the LEDWI, were installed on 13/12/92 and the trial ended on 1/4/93. The Ledwi was installed on 11/2/93.

2. PRECIPITATION TYPE IDENTIFICATION RESULTS

TABLE 1 compares the instruments with Meteorological Office staff's observations of precipitation and dry weather. For this particular analysis, the instruments' identification of the form of precipitation was considered to be correct even if the intensity classification did not match that reported by the observer.

HUMAN OBSERVATION		PRECIPITATION(PPN) DETECTED(%)							PPN IDENTIFIED (%)		
PPN TYPE	NO. MINS	PPN DETECTORS			OPTICAL SENSORS				OPTICAL SENSORS		
		NE1	SW1	SW2	ORG	HSS	LED	VAIS	HSS	LED	VAIS
SNOW LIGHT	1047	58	44	18	60	71	90	90	60	63	30
SNOW M/H	144	93	94	70	99	98	99	100	98	96	65
RAIN LIGHT	782	88	93	76	79	93	88	98	14	43	42
RAIN M/H	1713	100	100	100	100	100	100	100	87	95	97
DRIZ LIGHT	732	32	52	17	22	23	15	56	2	8	51
DRIZ M/H	236	83	90	56	69	39	36	96	12	12	93
NO PPN	17030	0.4	0.5	0.1	0.1	0.5	4.9	2.2	99	95	98

TABLE 1 : OBSERVATIONS OF PRECIPITATION TYPE 12/2/93-31/3/93

The abbreviations used are :-
NO.MINS - Number of minutes of precipitation of that type
LIGHT - Light precipitation intensity (<0.5mm/h for rain and snow)
M/H - Moderate and heavy precipitation intensities
DRIZ - Drizzle (liquid precipitation with drop diameters < 0.5mm).

3. DISCUSSION OF PRECIPITATION TYPE IDENTIFICATION RESULTS

The more recently developed Vaisala Rain Detectors (DRD 11A) are clearly an improvement (17% more precipitation detected irrespective of type) on the DPD 12A that they were designed to replace. Furthermore, they are at least as good at detecting liquid precipitation as the optical sensors and therefore represent a significant cost saving if detection of liquid precipitation is the sole requirement. However, orientation affects their performance in all precipitation except for moderate and heavy snow and rain. Furthermore, NE1 detects more light snow than SW1, but less drizzle and light rain. For 85% of the time that light snow was observed the 10 metre wind was either from the northeasterly sector of the compass or less than 5 knots in strength. There is thus some evidence that the Rain Detector performs better when the sloping sensing surface faces into the oncoming wind.

Although the Vaisala Present Weather Sensor FD 12P detects precipitation more frequently than any of the other sensors, it is often incorrect when identifying snow. In addition to the optical sensor this instrument incorporates two DRD 11A Rain Detectors, facing in opposite directions. This appears to provide a level of performance in liquid precipitation better than that achieved by the other instruments. However, it is sometimes oversensitive and may detect precipitation when the observer does not.

All the instruments had problems with false alarms to varying degrees, but since Meteorological Office observers are not infallible, their "no precipitation" observations may include short periods of unnoticed light precipitation which the instruments manage to detect. The rate of false alarms from the instruments may therefore be lower than TABLE 1 suggests. The operational Snowdon rain gauge and tilting syphon rain recorder measurements gave no indication that the observers were ever wrong, but wetting losses can account for that. Since the LEDWI and the FD 12P had the highest false alarm rates, the times when they detected precipitation simultaneously were examined - this represented 0.5% of the time that the observers classified as "no precipitation". One would expect an observer to have greatest difficulty during the hours of darkness. This is in fact borne out by the data since 88% of the joint LEDWI/FD 12P precipitation reports occurred in darkness (1900-0700 UTC). Ten suspect periods, with joint LEDWI/FD 12P precipitation reports separated by no more than two or three minutes, were discovered. There was further evidence of precipitation from the other instruments during seven of these suspect periods. The false alarm rates of TABLE 1 were therefore reassessed accepting the uncertainty of the human observation during the suspect periods. The precipitation detection rates for the NO PPN category fell by 0.3% for the HSS, by 0.5% for both the LEDWI and the FD 12P, and by less than 0.1% for the other instruments.

The LEDWI was tested in an earlier (unreported) trial at Eskdalemuir during winter 91/92 and it detected none of the drizzle observed that winter. By February 1993 a software revision (Version 3.50 18/5/92) had been incorporated to increase sensitivity by a factor of five. This has successfully improved drizzle detection and identification rates without increasing the false alarm rate, but the LEDWI still misses two-thirds of the drizzle that the observer sees. The LEDWI and the HSS performance was very similar in snow identification, but the LEDWI detected 20% more light snow than the HSS, and their snow identification performance was about 30% better than the FD 12P. In rain identification the LEDWI and the FD 12P

performance was similar for moderate and heavy rates, but the FD 12P detected 10% more when the intensity was light.

Results from an earlier period of this trial (in December and January, before the LEDWI was installed) indicated that the HSS correctly identified 57%, and the FD 12P 73%, of the light rain reported by the observers. For both instruments, the apparent poorer precipitation identification performance reported in TABLE 1 corresponded to an increase in the frequency of drizzle messages produced during periods when the observer was reporting light rain. Furthermore, average precipitation rates and visibilities were both lower in February and March confirming the possibility that there was more drizzle, mixed in with the rain in this period (shown in TABLE 1), than the observations of light rain indicate. Also a higher proportion of the observations were made in darkness during this period. The difficulties of observing light precipitation during the hours of darkness might also explain the FD 12P's higher detection rate (94%) for light drizzle in the earlier period. In December and January 96% of the light drizzle observations were made in the early morning (0000-0400 UTC), in contrast to 25% in February and March. Confining the analysis of the February and March data to 0000-0400 UTC improves the detection rate, bringing it into closer (within 10%) agreement with the December and January rate. This is a specific example of a problem relevant to both human observers and to instrument designers; the intensity thresholds for the different types of precipitation, especially mixed precipitation, are often ill defined and may vary internationally.

The earlier trials (described in reference 1) and the subsequent trial of winter 91/92 showed the LEDWI performance was consistently poor in drizzle. Furthermore, the new model (OWI-220), first tested in 91/92, produced more false alarms than the old one. Data from the two Rain Detectors (DRD 11A) were used in conjunction with the LEDWI (OWI-220) data to demonstrate how instrument performance can be improved (retrospectively) in drizzle and no precipitation conditions. The resulting change in performance reduces the false alarm rate to 0.5% and improves the drizzle detection (53% of light, 91% of moderate and heavy) and identification (46% and 67% respectively) rates. Light rain detection was improved by 1%, but light snow was detected 4% less often. Performance in moderate and heavy rain and snow was unaffected. The algorithm applied to the data was :-

1. LEDWI messages of "no precipitation" were changed to drizzle if either of the Rain Detectors detected precipitation.

2. LEDWI messages of any form of precipitation were changed to "no precipitation" if both the rain detectors indicated "no precipitation"; provided that visibility was better than 26km or air temperature was higher than 3^0C, as measured by the HSS.

This temperature condition preserves the LEDWI's light snow reports (90% of which were correct) that would otherwise be changed to no precipitation. The requirement for good visibility gives greater confidence in the "no precipitation" classification and enables the correction of some of the low temperature LEDWI false alarms. The performance of the HSS can also be improved with additional Rain Detector information, but the problem of incorrectly identifying light rain as drizzle would remain. The values of the temperature and visibility thresholds were chosen to optimise the performance results for this particular dataset; applying the algorithm to real time data may produce different results and further refinement would almost certainly be required. However, this example does show the potential benefit of combining multi sensor data in this way.

4. LIQUID PRECIPITATION INTENSITY RESULTS

The one minute average liquid precipitation rates from the four optical instruments were compared with measurements from a Thies Clima Gmbh Ombrometer HP and best fit straight line relationships were produced by the method of least squares. The Ombrometer HP is a precipitation gauge that was installed in a Turf Wall Pit to reduce wind induced errors. The precipitation collected by the Ombrometer passes through a constricting nozzle which is designed to produce drops of equal volume (equivalent to 0.005mm of water) that are counted as they fall through a beam of light. The drops fall into a tipping bucket which produces an independent measure of the precipitation amount. The linear relationships are summarised in TABLE 2 where X represents the one minute average rates derived from the Ombrometer's drop counter (resolution of 0.3 mm/h). Ombrometer rates of 0.0 and 0.3 mm/h were not considered because wetting losses are known to reduce the amount of precipitation collected by gauges. The maximum rate considered was 6.3 mm/h and 995 one minute averages were used in the analysis.

INSTRUMENT	EQUATION	CORRELATION COEFFICIENT	STANDARD ERROR OF Y ESTIMATE
LEDWI	Y = 1.29X-0.05	0.936	0.50 mm/h
HSS	Y = 1.05X-0.05	0.896	0.55 mm/h
ORG	Y = 1.00X-0.09	0.962	0.30 mm/h
FD 12P	Y = 0.50X+0.45	0.799	0.39 mm/h

TABLE 2 : PRECIPITATION INTENSITY RELATIONSHIPS (X=OMBROMETER)

Comparing the results in TABLE 2 with those from previous trials (see reference 1) shows that the calibrations of the LEDWI and the HSS have remained substantially the same, whilst the ORG has changed significantly. The FD 12P underestimates all but the lightest intensities and conforms less well to a linear relationship with the Ombrometer HP, than the other optical instruments. The FD 12P tends to level off in higher intensities, because the integral Rain Detector (DRD 11A) surfaces reach a limiting 'wetness' condition.

5. VISIBILITY RESULTS

An intercomparison of one minute mean visibility measurements, in low visibility conditions, from the HSS and the Vaisala FD 12P was made and a scatter plot is shown in FIGURE 1. A linear regression analysis was carried out for measurements made when the mean was under 600 metres and there was no indication of precipitation from any of the instruments or from the observer. The FD 12P visibilities (Y, in metres) were related to those of the HSS (X, in metres) by the following equation :-

$$Y = 1.106X + 46m$$

with a correlation coefficient of 0.90 and standard error of the Y estimate of 58 metres. The FD 12P was 25% higher than the HSS on average. At higher visibilities the relationship was less clear and less reliable. Seven observations, made by Meteorological Office staff, from 100 to 500 metres, were on average 270 metres lower than the FD 12P's measurements and 200 metres lower than those of the HSS. However, the observation could also be higher (by 400 metres) and lower (by 1000 metres) at times when the two instrument measurements were within 20 metres of each other. Such large differences demonstrate the problem of the representativeness of any assessment of visibility due to it's spatial variability.

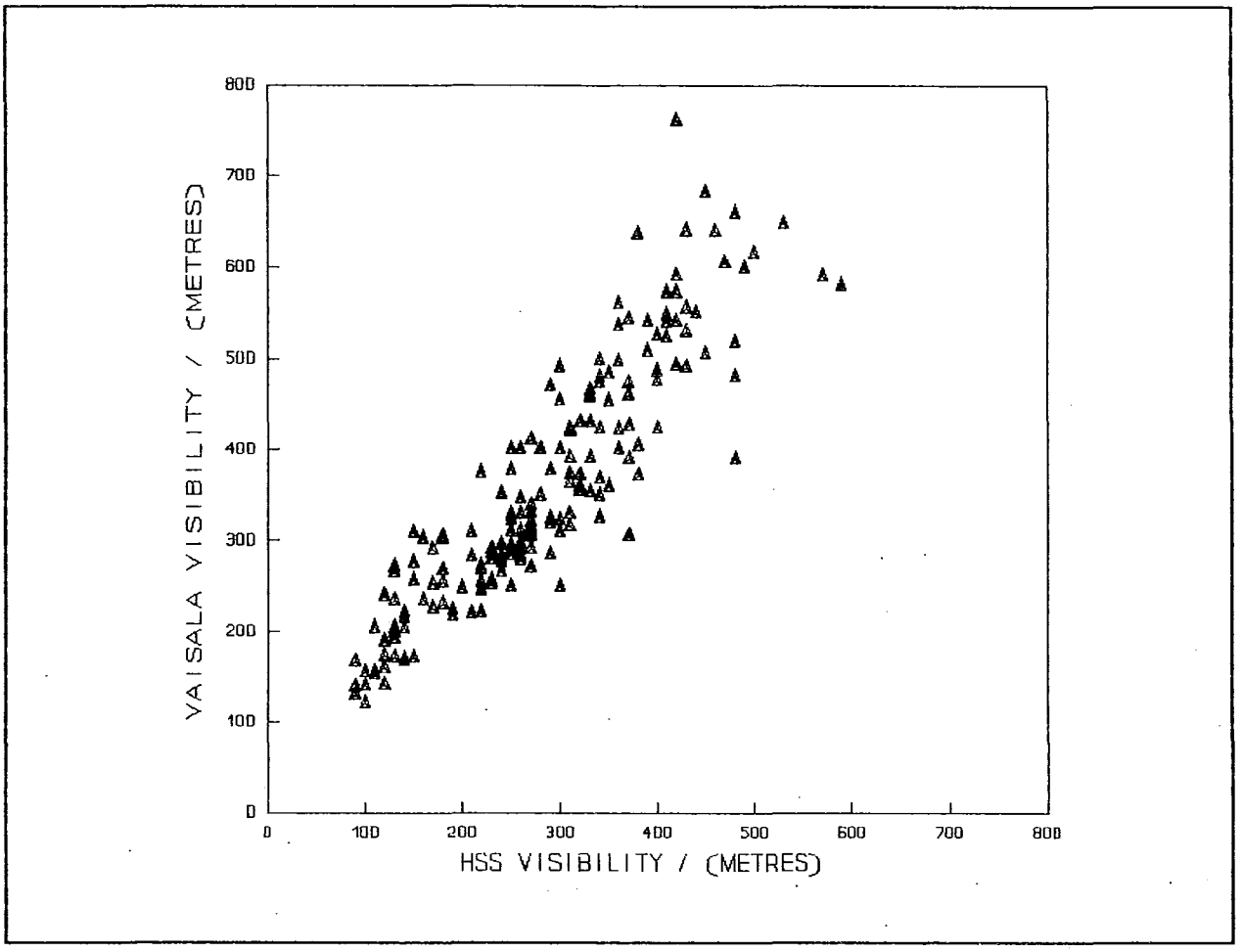

FIGURE 1 : ONE MINUTE MEAN VISIBILITY MEASUREMENTS

6. CONCLUSIONS

Overall, no one instrument performs well at all measurements. The Vaisala Rain Detector DRD 11A performance in liquid precipitation was at least as good as that of the more expensive optical instruments. The Vaisala FD 12P is the most sensitive of the instruments in the trial, with the highest rates of drizzle detection and identification, but it's measurements of liquid precipitation rate are often lower than those of the other optical instruments and are half those measured by wind-shielded collection gauges. The intercomparison of the visibility measurements, below 600 metres, from the FD 12P and the HSS revealed that they were linearly related and the FD 12P was consistently higher (25% on average). Neither showed good agreement with the human observer, but the HSS was closer on average. Despite new software, the LEDWI still misses much of the observed drizzle, but when it's data are used in conjunction with data from two Vaisala Rain Detectors DRD 11A, the combination produces the best overall performance in correctly identifying snow, rain, drizzle and no precipitation.

7. REFERENCES

1. Field Trials of Some Present Weather Sensors - A. Stepek, D.W. Jones and D.B. Hatton. W.M.O. Instruments and Observing Methods Report No. 49, TECO-92, May 1992.

A Comparison of two Present Weather Systems with Human Observations

Jitze P. van der Meulen
Royal Netherlands Meteorological Institute,
de Bilt, Netherlands

Abstract

In March 1993 an instrument comparison is started with two Present Weather sensors (HSS PW402B and Vaisala FD12P). Data output (in $w_a w_a$ or NWS-code) is compared with the wwW_1W_2 codes reported by operational observers at the same location.
In this paper the results will be presented. Especially differences between the reported ww and $w_a w_a$ codes will be discussed.

1. Introduction.

In order to get experienced with automatic present weather observing systems KNMI has selected two systems for test purposes:

1) HSS, model PW 402b, and
2) Vaisala, model FD 12P.

These instruments are selected because both type and amount of precipitation and visibility is reported. This feature is relevant, since precipitation and visibility should be used selecting an appropriate present weather code.

At present however, there are no systems on the market which will report on the following items in combination with type and amount of precipitation and visibility:

- state of the sky; development of clouds
- discrimination between smoke, dust, sand, water particles
- thunderstorm/lightning
- tornado.

Today, WMO has defined two types of present weather codes:

1) Group $7wwW_1W_2$, code tables 4677 (and 4561):
   ww-present weather reported from manned weather station
2) Group $7w_aw_aW_{a1}W_{a2}$, code tables 4680 (and 4531):
   w_aw_a - present weather reported from an automatic weather station.

Although both code tables are largely comparable with regard to the structure, there are significant differences.

The present weather codes reported from manned stations (table 4677) are typically split in a number of sections, and with subsections:

ww = 00-49: No precipitation at the time of observation.
- ww = 00-19: No precipitation, fog, dust/sandstorms, drifting or blowing snow, etc.
- ww = 20-29: Precipitation, fog, etc. during the preceding hour, but not at the time of observation.
- ww = 30-39: dust storm, sandstorm, drifting or blowing snow.
- ww = 40-49: Fog or ice fog at the time of observation.

ww = 50-99: Precipitation at the station at the time of observation.
- ww = 50 .. 59 : drizzle
- ww = 60 .. 69 : rain
- ww = 70 .. 79 : solid precipitation
- ww = 80 .. 89 : showery precipitation.

The present weather codes reported from an automatic weather station (table 4680) are largely split into classes:

w_aw_a = 00 - 19: Many items, like "no significant weather", state of the sky, cloud forming/dissolving,

haze or smoke, mist, diamond dust, etc. (Since low code numbers have low priority, this codes are often overruled by codes with $w_aw_a > 19$)

w_aw_a = 20 - 26: precipitation, fog thunderstorm during preceding hour but not at the time of observation
w_aw_a = 27 - 29: blowing or drifting snow or sand
w_aw_a = 30 - 35: fog
w_aw_a = 40 - 48: precipitation
w_aw_a = 50 - 58: drizzle
w_aw_a = 60 - 68: rain
w_aw_a = 70 - 76: snow and ice pellets
w_aw_a = 80 - 87: showers or intermittent precipitation
w_aw_a = 90 - 99: thunderstorm and tornado

An important issue for the w_aw_a code is the fact choices can be made, depending an the quality or possibilities of the techniques involved in the measurements system. For instance in cases with continuous rain, moderate and not freezing, a manned station may only report: ww = 63. An automatic station may report:

w_aw_a = 40: precipitation, or
w_aw_a = 43: moderate liquid precipitation, or
w_aw_a = 60: rain, or,
w_aw_a = 62: rain, not freezing, moderate.

In fact, the reported w_aw_a code will depend on the capability of a system to discriminate between types of present weather and in a detailness up to a certain extend.

Because of those typical differences it is difficult to compare the results from an automatic observing system with the ww-reports from a manned station. Moreover one should omit comparisons with ww-reports in which items are incorporated like "state of the sky", "smoke/dust/sand", "thunderstorm/lightning" or "tornados" or issues like "precipitation within sight, but not at the station" (present weather near to a station).
Another problem a present weather system is to discriminate between freezing and not-freezing precipitation: Temperature (air and wet bulb) may offer some help to be able to indicate any "freezing" phenomenon, but the accuracy is rather doubtful. Furthermore the ww-codes discriminate between "continuous" and "intermittent" within the ww = 50 - 79 group. Concerning the w_aw_a code, intermittent rain or snow are possibilities with a code number > 80 and mixed together with rain or snow showers. Consequently the sequence of priorities (higher code numbers overrule lower numbers) is different for both code tables.

Moreover the number of reports from the present weather systems as well as the quality control (and calibration) are limited. For instance, the HSS provides only the NWS present weather code (P+, L-, S, etc.) together with Fog or Haze. To discriminate between "slight", "moderate" or "heavy" both system are capable to measure the precipitation intensity. However, there are no objective procedures provided to calibrate the systems.

One should take into account that phenomena without precipitation will result in w_aw_a = 00 ("no significant weather"), whereas the manned station may report any type of weather not related to precipitation.
In a previous paper [1] such type of analysis is done already. In this paper the output of the HSS was compared with the NWS type reports, provided by the manned station on site. For this test only hourly reports of ww codes are available. Therefore it is only useful to perform analysis of the acquired present weather data on a rather simple manner.

2. Station characteristics

To get a brief impression of ww codes reported by the station, a frequency distribution is shown by fig. 1. In this figure the number of reported ww codes is presented, relative to the total amount of hourly reported ww codes (inclusive ww = 'no significant weather'). Obviously, the range ww = 01 - 29 is very popular. Notice however that this code is within the range reserved for "no precipitation at the time of observation ". Consequently, analysis of w_aw_a data is not very useful here: Although the discrimination between classes of precipitation intensity is subject to discussion, it was found that the data, received during the past hour both systems, did not give reason to

---

[1] van der Meulen, J.P. (1992): "Present Weather Observing Systems: One year of experience and comparison with human observations", in: Instruments and Observing Methods Report No. 49 (WMO/TD - No. 462), pp. 300

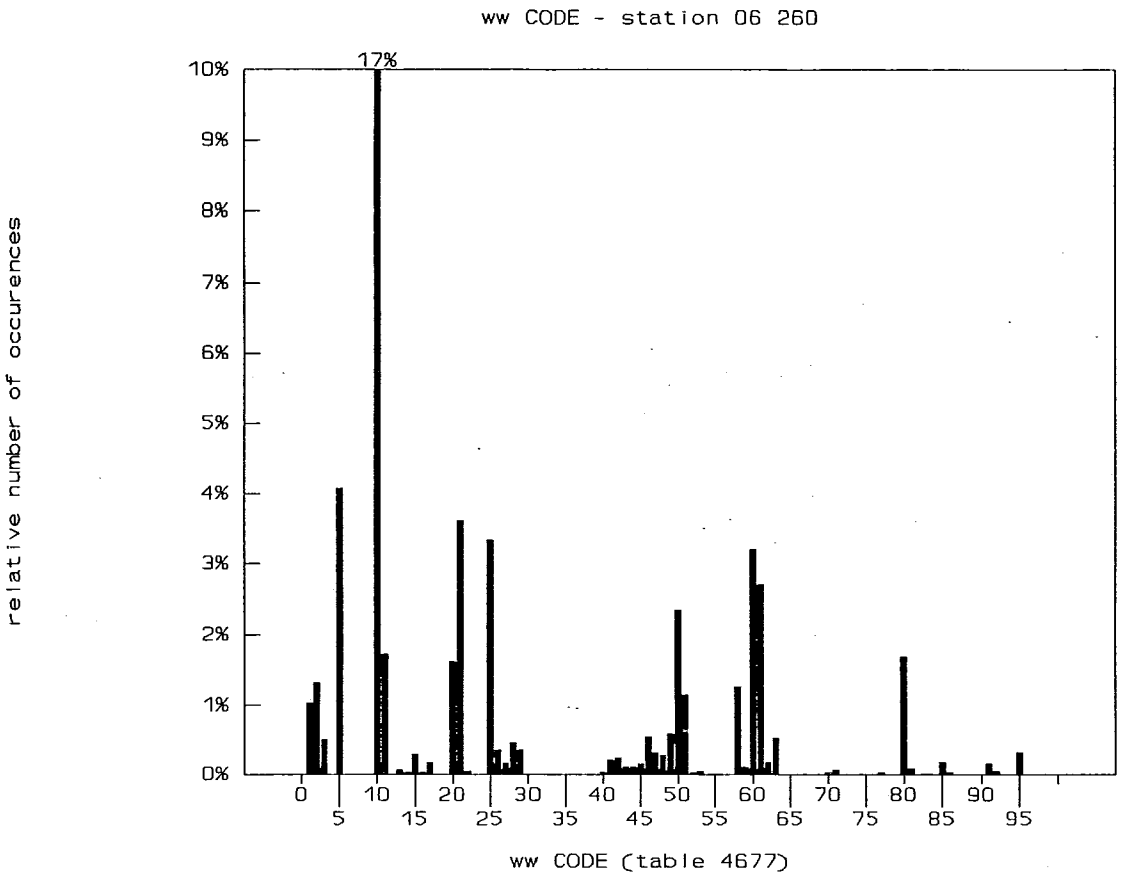

Fig. 1, frequency distribution of the reported ww-codes

any conflict at all with respect to such ww code.

Other popular ww codes are the tenfolds: ww = 50, ww = 60, ww = 80 (precipitation, not freezing if liquid, intermittent and slight). It is clear that in most cases we have "slight/intermittent"; may be most of the weather phenomena are accordingly, or the observer is not very sure and prefers a code, which looks most acceptable. Furthermore the observer discriminates between "continuous" and "intermittent". This issue is relevant since ww is reported once an hour only. Automatic observing systems, however, are capable to report once or several times each minute. Data transmitted by these systems yield real time information about the current type and intensity of precipitation. Of course, form the history of these data and a well defined algorithm it is possible to distinguish "continuous" and "intermittent", but since "intermittent" is incorporated in group $w_a w_a$ = 80 .. 89 ("showers and intermittent precipitation", analysis by intercomparing ww and $w_a w_a$ is hazardous in cases when the observer reports "intermittent precipitation".

3. data output of the automatic systems

Both tested systems have a rather different output format and protocol:

1) HSS 4026:
   + visibility/extinction;
   + fog/haze/clear;
   + NWS code: NP, P, L, R, S (with intensity indicators "+" = heavy or "-" = slight, to distinguish from moderate)
   - no $w_a w_a w_{a1} w_{a2}$ code
   + data output: ASCII text, RS 422/RS232
   + instruments status control: yes;

2) Vaisala FD12P:
+ visibility;
+ present weather (text format, related to $w_a w_a$)
+ $w_a w_a$ code (limited set: non-observable parameters excluded)
+ NWS-code: C, P, L, R, S, IP, H, IC, SG, SP, ZL, ZR (with intensity indicators "+" = heavy or "-" = slight to distinguish from moderate)
+ data output: ASCII text, RS 422/RS232
+ instrument status control: yes

The most significant difference between both systems is the capability of the Vaisala system to produce $w_a w_a$ code. Although this is a major benefit of a stand alone system, data acquiring and processing computer systems connected to the present weather sensors may also produce $w_a w_a$ codes, based on real time data and history. As a consequence analysis of data should focus on the basis of the weather phenomena:

(1) type of precipitation: "drizzle", "rain", "solid precipitation"
(2) precipitation intensity: "slight", "moderate", "heavy".

Note that WMO has not expressed clear statements or definitions concerning "slight", "moderate" or "heavy" and it is up to the local authorities to define the appropriate ranges (which will depend on the local climate).

Another feature of Vaisala's FD12P is the capability to distinguish between several types of solid precipitation: Snow, ice pellets/sleet, hail, ice crystals, snow grains, snow pellets, freezing drizzle and freezing rain. All those phenomena are reported by HSS simply by: "S" (solid precipitation). However, none of the systems have the possibility to report "blowing snow".

4. Data acquisition and analyses

Both present weather observing systems are installed at the meteorological station De Bilt, Netherlands (WMO, no. 06 260). All data and status messages are collected within an 1 minute time interval. As a consequence it is possible to compare every hour the ww code, reported by station 06 260 with 60 data outputs from both systems. It is pointed out already, that only simple comparisons are useful (e.g discrimination between drizzle, rain, snow). Reports with 'no precipitation' but with Fog (ww = 40 - 49), Mist (ww = 10) or Haze (ww = 05) are kept outside the analysis since those depend on visibility measurements only. Regular calibration of the visibility data output from both systems, performed according to procedures documented by the manufactures, have demonstrated that both systems meet the accuracy requirements necessary for distinguishing fog, mist or haze.
From the beginning of the test until the writing of this paper (March - November 1993) there was only one hour during with a substantial amount of snow has been fallen (with positive results of both instruments). As a consequence the analysis will be restricted to liquid precipitation only.

The following table will give a brief overview of the relative distribution of the reported ww-code for the different groups:

ww = -, no significant weather:	47%
ww = 00 - 49, no precipitation at the station at the time of observation:	39%
ww = 50 - 59, drizzle:	5%
ww = 60 - 69, rain:	7%
ww = 70 - 71, solid precipitation	0%
ww = 80 - 99, showery precipitation, or precipitation with current or recent thunderstorm:	2%

For the dataset with ww = 'no significant weather', both instruments reported in almost all cases: no precipitation or clear:

HSS PW402b :	99,6%	(No Precipitation)
Vaisala FD12P:	99,5%	(Clear)

For the dataset with ww = 00 - 49 both systems should report no precipitation at the time of observation.
We found:

HSS PW402b :	98,8%	(No Precipitation)
Vaisala FD12P:	98,2%	(Clear)

However a significant decrease of correlation was found, in case we focused on the dataset with ww = 20 - 29 (precipitation during preceding hour):

HSS PW402b : 93,4% (No Precipitation)
Vaisala FD12P: 89,6%. (Clear)

It is expected that differences in sampling periods and response times between systems and observer will cause a "deviation rate" of approximately 10%.

To analyze the dataset for which the observing systems should report any kind of precipitation (reported ww = 50 - 79) we had to restrict to a limited number (or a range) of reported ww codes, *i.e.* which are reported frequently enough (the number of 100 is token as a minimum).
Taken these constraints into account, the following sub-datasets are chosen, and with the following results:

1) ww = 50 - 59, drizzle; results:

	no precipitation	drizzle slight	drizzle moderate	drizzle heavy	precipit. slight	precipit. moderate	rain slight	rain moderate	rain heavy
HSS PW 402b	64%	-	-	-	11%	1%	22%	2%	-
Vaisala FD12P	35%	23%	14%	0,5%	-	-	26%	1,5%	-

2) ww = 60 - 61, rain - slight; results:

	no precipitation	drizzle slight	drizzle moderate	drizzle heavy	precipit. slight	precipit. moderate	rain slight	rain moderate	rain heavy
HSS PW 402b	24%	-	-	-	15%	2%	51%	6%	1%
Vaisala FD12P	8%	11%	3%	-	1%	-	73%	5%	-

3) ww = 80 - 81, rain - showers (slight/moderate); results:

	no precipitation	drizzle slight	drizzle moderate	drizzle heavy	precipit. slight	precipit. moderate	rain slight	rain moderate	rain heavy
HSS PW 402b	58%	-	-	-	8%	2%	26%	5%	1%
Vaisala FD12P	20%	6%	2%	-	-	-	67%	4%	1%

Because the number of occurrences of all other ww-codes is too low (10 or less) it has no sense to evaluate datasets related to these codes.

5. Conclusions

Since the start of the comparison only a few periods with snow are reported. Therefore these conclusions are only based on liquid precipitation only.

Good correlation is found between ww-reports and automatic present weather observing systems if we restrict us to detection of precipitation only. However, a significant lower degree of correlation is found for cases when drizzle or rain-slight is reported by the manned station. After intercomparing both instruments, the Vaisala FD12P demonstrated a better performance for these types of precipitation.

The Vaisala FD12P has a much more extensive range of possibilities to report types of solid precipitation than the HSS PW 4026 has. Moreover the Vaisala FD12P is the only system capable to transmit $w_a w_a$-codes.

A PRESENT WEATHER SENSOR FIELD TEST AND INTERCOMPARISON

Tage Andersson[1], Srećko Bandalo[1], Esko Elomaa[2], Ture Hovberg[1] and Pertti Valkovuori[2]

[1] Swedish Meteorological and Hydrological Institute
[2] Finnish Meteorological Institute

1. Introduction

The aim of the study was to test how present weather sensors (PW) perform under routine operations in observing synoptic weather and in continuous weather monitoring in the climate of the Nordic Countries, where low temperatures and snow, including sticking snow at temperatures close to 0 °C, are frequent. As to the manual synoptic observations, *ww* (present weather), *VV* (visibility) and *RR* (accumulated precipitation during 6 hours periods) are treated.

The test was run from February 10 to June 28, 1993, at the Meteorological Observatory in Jokioinen, the south-western Finland (60°49'N, 23°30'E).

Three types of instruments were used:
1) The ScTI OWI-240 LEDWI (Light Emitting Diode Weather Identifier), manufactured by the Scientific Technology Incorporated, Rockville, MD.
2) The HSS PW 402B-125, manufactured by the HSS, Bedford, Mass.
3) The weather sensor FD 12P, manufactured by the Vaisala Oy, Helsinki, Finland.

The LEDWI and HSS sensors were connected to a PC logging system, polling the sensors every minute. Before storing the messages on the hard disc, a code conversion from the internal instrument codes into WMO 4680-code and a METAR-like code was performed. The FD12P readings were recorded at 15 sec intervals by a separate PC system, and the *ww* information was coded in a WMO 4680-like code.

Manual synoptic observations were made by experienced observers of the Observatory every 3rd hour. Continuous weather monitoring was made with a time resolution of 5 minutes all day, according to the WMO synoptic code for manual observations (WMO,1988). Precipitation was compared to the reference gauge of the WMO Solid Precipitation Measurement Intercomparison, a Tretyakov gauge, and to a Geonor gauge in a Valdai double fence, corrected for losses due to the wind. The weather conditions during the test period were as follows:

Weather	Minutes	%
- no significant	146 827	71
- mist/fog	16 342	8
- drizzle	3 095	2
- rain	10 074	5
- rain and snow (mixed)	4 019	2
- snow	24 929	12

2. Verification methods

The PW data were compared with both the 3-hourly manual synoptic observations and the continuous ones. For the comparison with the 3-hourly synoptic observations an observation period is defined as the 10 minute preceding the synoptic hour. For these periods the arithmetic mean of the visibility measurements and the most common of the *ww* codes from the automated observations were extracted. These quantities were considered as the PW-sensor observations and compared to the manual synoptic ones. The manual observations give 6 hours accumulated precipitation. Therefore corresponding PW-sensor quantities were computed and compared with the manual measurements.

3. Results and discussions

The results will be given in the form of *contingency tables,* giving frequencies of events under given conditions, and certain statistics, mainly the *coefficient of correlation.*

3.1 Comparisons using 3-hourly synoptic observations

Table 1 shows the coefficient of correlation between the automatic and the manual observation. We must note that these statistics depend upon the scaling of the parameters. For visibility, *VV,* the observations are scaled after the WMO code table 4377, the fine scale. For the 6-hours' accumulated precipitation, *RR*, a logarithmic scale (mm) is used, and for the present weather, *ww*, a special scale, see Bandalo et al (1993). A correlation figure must be interpreted with caution, especially when there is no 'natural' scaling, as for the *ww*. Nevertheless, we feel that the correlation coefficient is instructive here. Since we measure the same quantity at the same spot and time, with two different methods, a correlation coefficient close to 1.0 should emerge if both methods are good. Evidently,

Table 1. Coefficients of correlation between manual and automatic observations. VV = visibility, RR = 6 hours' accumulated precipitation (logarithmic scale), ww=present weather. Jokioinen, Feb. 10 - Jun. 28, 1993.

EVENT	*LEDWI*	*HSS*	*FD 12P*
VV	-	*0.89*	*0.90*
RR	*0.60*	*0.88*	*0.89*
ww	*0.62*	*0.65*	*0.73*

only the visibility and the accumulated precipitation observations show correlation coefficients as high as about 0.9. While this value perhaps may be regarded as satisfactory for the visibility, it is low for the accumulated precipitation (also, remember that a logarithmic scale is used for the latter).

Table 2 shows that the HSS and the FD 12P underestimate the precipitation frequency, while the LEDWI overestimates it considerably. We suspect that the latter is due to some fault in the LEDWI individual used; for long periods it did monotonously give the same precipitation rate. Consequently the LEDWI has the by far highest proportion of 'NOT DEFINED' precipitation. As to specified precipitation, also the LEDWI shows lower frequencies than the manual observations. Since the HSS and the FD 12P underestimate the precipitation frequencies, they overestimate the frequency of 'CLEAR'. With its large frequency of 'NOT DEFINED' the LEDWI has a much too low 'CLEAR'.

Table 2. Frequencies of weather observations, %. The column PR gives all types of precipitation, including 'NOT DEFINED'. ND = not defined, SN = snow, RA = rain, DZ = drizzle, CL = clear, MANU = manual observation. Jokioinen, Feb. 10 - Jun. 28, 1993.

	MANU	*LEDWI*	*HSS*	*FD 12P*
PR	***19***	*34*	*12*	*15*
ND	*--*	*25*	*3.6*	*3.4*
SN	***12***	*4.6*	*7.3*	*6.3*
RA	***5.7***	*4.0*	*1.3*	*3.9*
DZ	***1.5***	*0.2*	*0.1*	*0.9*
CL	***81***	*66*	*88*	*86*

Tables 2 and 3 indicate remarkably low frequencies of detecting drizzle, but also fairly low ones for detecting other kinds of precipitation, the maximum frequency hardly surpassing 60 %.

Table 3. Frequencies, %, of detecting a specified event that occurred. Jokioinen, Feb. 10 - Jun.28 , 1993.

EVENT	*LEDWI*	*HSS*	*FD 12P*
SNOW	*39*	*48*	*52*
RAIN	*59*	*17*	*61*
DRIZZLE	*6*	*6*	*18*
CLEAR	*76*	*99*	*99*

As important as a high frequency of detecting an event is a low frequency of indicating an event when it does not occur, i. e. a low false larm risk. Excluding the 'DRIZZLE' row in Table 4, the 'DRIZZLE' indications being very few, the FD 12P evidently has the lowest risks of false larms.

Table 4. Risk for false larm, %, i. e. giving an event that did not occur. NOT D. gives the risk that 'CLEAR' occurred when the instrument recorded 'NOT DEFINED PRECIPITATION'. Jokioinen, Feb. 10 - Jun. 28, 1993.

EVENT	*LEDWI*	*HSS*	*FD 12P*
NOT D.	*73*	*8*	*14*
SNOW	*0*	*22*	*3*
RAIN	*16*	*29*	*10*
DRIZZLE	*50*[1]	*0*[2]	*70*
CLEAR	*7*	*8*	*6*

[1] *2 observations,* [2] *1 observation*

3.2 Comparisons using continuous observations

During the test period 'continuous' recordings were made at intervals as follows : FD12P 15 sec, HSS and LEDWI 1 min, manual observations of present weather 5 min, Geonor accumulated precipitation 10 min. For a closer examination of the nature of the precipitation events, percentiles of precipitation rate are presented in Table 5. Noteworthy are the high frequencies of very low rates. Thus, according to the Geonor, more than 15% of the rates were below 0.01 mm/h. It also seems obvious that the LEDWI overestimates the intensity values through the whole scale.

Table 5. Percentiles of precipitation rate, mm/h, hourly means, during observed precipitation events. REF = Geonor in Valdai double fence, corrected for losses with Golubev's equation (WMO,1992). Jokioinen, Feb. 10 - Jun. 28, 1993.

	15	*30*	*45*	*60*	*75*	*90*
REF	***.00***	***.04***	***.11***	***.27***	***.50***	***.82***
FD 12P	*.02*	*.05*	*.11*	*.24*	*.49*	*.90*
HSS	*.01*	*.03*	*.06*	*.14*	*.32*	*.76*
LEDWI	*.10*	*.15*	*.28*	*.56*	*.98*	*1.97*

When the PW precipitation type records were compared to the continuous manual observations, results very similar to those of Tables 3 and 4 emerged. Most often the observer and the PW disagreed when the precipitation rate was very low. This was very pronounced in some cases when snowfall was observed for several hours by the observer, but the reference gauge did not accumulate even 0.01 mm. Thus, also conventional precipitation gauges have their limitations. We therefore sorted out the cases with precipitation rate greater than or equal to 0.01 mm/h. The use of only these values resulted in the frequencies of detection shown in Table 6. Compared to Table 3 this is a substantial improvement. The rather bad 'RAIN' figures for the HSS are caused by some rain showers in June, which were mostly reported as 'SNOW'.

Tables 7 and 8 give the accumulated precipitation. Although the FD 12P had a reasonably good figure for the total, it grossly underestimated the solid precipitation.

Table 6. Frequencies of detecting a specified event that occurred (provided a precipitation rate greater than or equal to 0.01 mm/hr according to the Geonor). E = same precipitation type, D = another precipitation type, N = clear, n = number of cases. Jokioinen, Feb. 10 - Jun. 28, 1993.

	SNOW			RAIN			DRIZZLE		
	E	D	N	E	D	N	E	D	N
FD 12P	93	7	-	91	9	-	50	50	-
HSS	91	6	3	15	65	20	17	83	-
LEDWI	81	16	3	73	9	19	-	83	17
	n = 179			n = 158			n = 6		

Table 7. Accumulated precipitation (water equivalent), mm. REF. = Geonor in Valdai double fence corrected with Golubev's eq., STAND. = Tretyakov gauge with wind shield. Jokioinen, Feb. 10. - Jun. 28. 1993.

	REF.	STAND.	FD12P	HSS	LEDWI
mm	148.20	130.50	132.15	94.07	417.23

Table 8. Accumulated precipitation in % of the reference values. Jokioinen, Feb. 10 - Jun. 28, 1993

	SOLID	LIQUID	TOTAL
FD 12P	70	102	89
HSS	88	61	64
LEDWI	287	150	281

4. Conclusions

The two instruments giving visibility, the HSS and the FD 12P, produce visibilities which correspond fairly well with those of manual observations. As to accumulated precipitation and present weather, the instruments tested here show a definitely positive ability, though it is doubtful if this is high enough to replace the traditional manual observations. It must be remembered that the manual present weather observation, following a scheme that has been developed to suit a human observer, must be extremely difficult to replace with quantitative measurements. As an example, the observer and the PW often disagreed during very light precipitation. Also, it is obvious that several *ww* figures will never be recorded with these instruments, as for instance distant events and thunder. On the other hand, information from radars, satellites and lightning location systems will be used together with automatic ground observations, and the total system will offer the meteorologists a lot of new information.

References:

Bandalo, S., T. Andersson and T. Hovberg, 1993: Three present-weather sensors and manual synoptic observations - a field test. To be published in *SMHI Reports: Meteorology and Climatology.*

World Meteorological Organization, 1988. Manual on Codes. *Vol. 1, International Codes, Part A - Alphanumerical Codes, 1988 Ed., WMO - No. 306.*

World Meteorological Organisation, 1992. International Organizing Committee for the WMO solid precipitation Measurement Intercomparison, Sixth session, Final report. *Toronto Canada, 1992.*

UN RADAR DOPPLER BISTATIQUE POUR LA DETERMINATION DU TEMPS PRESENT

J. DUVERNOY, J.L. GAUMET
METEO-FRANCE
SETIM / Recherche et Développement
Trappes, France

C. GLOAGUEN, J. LAVERGNAT, J.Y. DELAHAYE
Centre de Recherches en Physique de l'Environnement
CNET-CNRS
Issy les Moulineaux, France

I. INTRODUCTION

Le remplacement quasi systématique des observateurs humains par des systèmes d'observation restreints la nuit ou dans des sites isolés est à l'origine d'un manque de données pour certains aspects de la prévision et du renseignement aux usagers. En effet, les stations automatiques ne sont pas capables d'effectuer le tour d'horizon à la place de l'observateur et en particulier de déterminer le temps présent.

Pour palier à ces manquements, la Direction de Météo-France a décidé de s'engager dans la voie de l'automatisation totale de l'observation météorologique de surface. Le projet correspondant, qui est un objectif prioritaire de METEO-FRANCE, consiste à définir, réaliser et installer les capteurs et dispositifs permettant d'automatiser intégralement le réseau français. Il a été appelé SOLFEGE pour Système d'Observation Locale Favorisant l'Exploitation des paramètres GEophysiques (Pilon, 1989). Le futur réseau devra fournir tous les paramètres actuellement observés automatiquement ou manuellement. Les premiers efforts porteront donc sur l'automatisation du temps présent, c'est-à-dire essentiellement l'identification du type d'hydrométéore (pluie, neige, grêle...).

Dans le cadre de ce projet, Météo-France a engagé plusieurs actions de recherche pour l'étude de l'interaction des ondes électromagnétiques avec les hydrométéores avec comme objectif prioritaire d'aboutir à la réalisation d'un instrument fiable pour la reconnaissance des hydrométéores précipitants. Deux configurations ont été étudiées. Le premier prototype est conçu à partir d'un radar monostatique du commerce. Il a permis de prouver la faisabilité de la mesure et d'ébaucher les algorithmes de reconnaissance (Duvernoy et al, 1992). La deuxième configuration a été réalisée à la demande de Météo-France par les laboratoires du CRPE (Lavergnat et al, 1993). Cette version bistatique ou diffusomètre se rapproche du POSS (Precipitation Occurrence Sensor System), capteur développé au Canada par Sheppard (1990) possédant des caractéristiques différentes (Tableau 1).

II. INSTRUMENTATION

A. Configuration

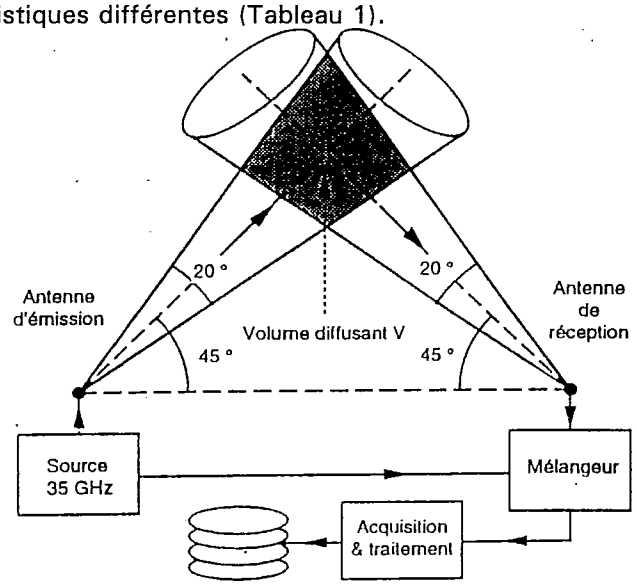

Figure 1 : Schéma synoptique du radar

Le synoptique de fonctionnement est présenté dans la figure 1. Pour la réalisation de la première maquette de laboratoire, de plus grandes précautions ont été prises. Ainsi l'émetteur est constitué de plusieurs sous-parties qui sont :

* un oscillateur local de type diode Gunn verrouillée électroniquement en phase qui fournit une fréquence intermédiaire très stable de 17,5 GHz.

* un doubleur de fréquence pour permettre l'émission à 35 GHz

* un séparateur qui prélève la moitié de la puissance pour d'une part, alimenter l'antenne d'émission et d'autre part, fournir l'onde utilisée par le mélangeur.

Les deux antennes utilisées sont des cornets dont les dimensions ont été calculées de manière à assurer la formation d'un faisceau d'ouverture 20 degrés.

Du fait de la fréquence utilisée, les ondes émise et reçue sont véhiculées entre les antennes et les parties actives par des guides d'onde rigides pour les parties internes et semi-rigides pour les parties externes.

L'onde reçue est mélangée à la fréquence d'émission. La combinaison des deux est ensuite mise en forme par un amplificateur faible bruit.

B. Caractéristiques techniques

Caractéristiques	Diffusomètre	POSS
Fréquence	35 GHz	10,525GHz
Puissance	9 dBm	20 dBm
Distance antennes	1 m	0,45 m
Ouverture antenne	20 °	52 °
Angle d'élévation	45 °	70 °
Amplification	40 dB	84 dB
Bande passante	30 Hz <-> 3kHz	35 Hz <-> 1 kHz

Tableau 1 : Comparaison des caractéristiques des radars Doppler bistatiques français et canadien.

III. METHODOLOGIE

A. Traitement du signal

La méthode repose sur le phénomène de rétrodiffusion des ondes électromagnétiques sur les phases condensées de l'eau. Le décalage en fréquence dû à l'effet Doppler (Eq. 1) est utilisé pour déterminer le spectre de vitesse d'une population de gouttes. Les précipitations observées sont constituées d'un ensemble de particules de tailles et donc de vitesses diverses qui peut être considéré comme une distribution continue. La répartition de la puissance reçue par le radar dépend directement de cette distribution en vitesse des diffuseurs contenus dans le volume exploré ainsi que de certaines caractéristiques du radar. Cette répartition en fonction de la fréquence s'appelle la puissance fréquentielle ou plus communément le spectre de puissance. La densité spectrale correspondante servira à déterminer d'une part, la distribution des particules d'hydrométéores et d'autre part, la nature de la précipitation.

$$f_d = \frac{2V}{c} f_o \qquad [1]$$

où f_o est la fréquence d'émission
f_d est le décalage Doppler

Pour des vitesses de chute de précipitation jusqu'à 30 m/s, l'acquisition des signaux doit se faire à 10 kHz. Les données acquises sont ensuite pondérées par une fenêtre de Hamming avant d'être transposées dans le plan des fréquences par une Transformée de Fourier Discrète.

Une sommation incohérente de 32 spectres de puissance permet d'améliorer le rapport signal sur bruit et fournit une meilleure estimation du spectre de vitesse des particules. (Figure 2).

Une transposition de l'échelle linéaire en échelle logarithmique (dBm) est effectuée avant l'extraction des paramètres utiles (puissance, vitesse moyenne et largeur de spectre).

D'après des études radars précédemment menées (Atlas, 1973), la puissance diffusée latéralement par les particules d'hydrométéores est proportionnelle à D^6 (où D est le diamètre de la particule) et au nombre d'hydrométéores N(D) dans le volume diffusant.

La forme des spectres obtenus en fin de traitement est donc caractéristique de la précipitation. La figure 2 présente 3 spectres correspondant à des situations météorologiques stables avec des observations de neige, bruine et pluie.

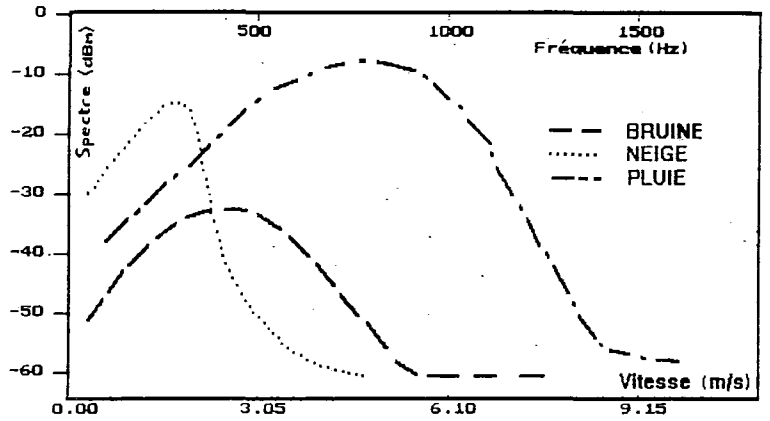

Figure 2 : Spectres Doppler typiques
pour des situations de neige, bruine et pluie.

B. Algorithme de reconnaissance

Le radar Doppler utilisé fournit une estimation de la distribution de vitesse des hydrométéores par la mesure du décalage en fréquence. Avec la relation de Gunn et Kinzer (1949), cette mesure peut être traduite en terme de diamètre de particules..

L'algorithme de reconnaissance a été établi après une première période d'apprentissage avec un premier jeu de données. Celles-ci ont permis de définir des seuils qui ont ensuite été testés en grandeur nature lors d'une campagne d'essais.

Les critères retenus sont résumés dans le tableau 2 suivant :

Critères (m/s)		Temps présent
Vitesse V	Largeur L	
9,15 < V	- - -	Grêle
V < 9,15	L < 0,56	Neige
V < 9,15	0,56 < L < 0,85	Bruine
V < 9,15	0,85 < L	Pluie

Tableau 2 : Critères de reconnaissance

Le critère de détection est assuré par un test de niveau du rapport signal sur bruit. En effet celui-ci augmente considérablement lors de la présence d'une précipitation.

Après différentes recherches, le meilleur critère pour la reconnaissance s'est avéré être la largeur spectrale, estimée par le calcul de l'écart-type. Ceci est visible sur la figure 2 qui montre des spectres typiques.

IV. COMPARAISONS DES OBSERVATIONS DE TEMPS PRESENT

A. Conditions expérimentales

Une campagne d'évaluation a été menée pendant l'hiver 92 pour déterminer la capacité des radars à détecter et identifier le type de temps présent par rapport à un observateur humain servant de référence.

Lors de cette expérimentation, deux types de comparaisons ont été effectués. Le premier concerne les données brutes, c'est à dire les spectres de vitesse des particules. Ces spectres de vitesse ont été comparés à ceux fournis par un spectropluviomètre optique (Hauser, 1981) figure 3. Le deuxième type de comparaison porte sur les messages de temps présent, ou données élaborées. Pour assurer un synchronisme entre les différents systèmes, toutes les données élaborées transitent par un concentrateur de données.

B. Spectres de vitesse

Lors d'une campagne d'évaluation, les deux radars ont pu être comparés au spectropluviomètre optique. Les distributions obtenues avec le spectropluviomètre ont été traitées de manière à être rapprochées à celles obtenues par les radars.

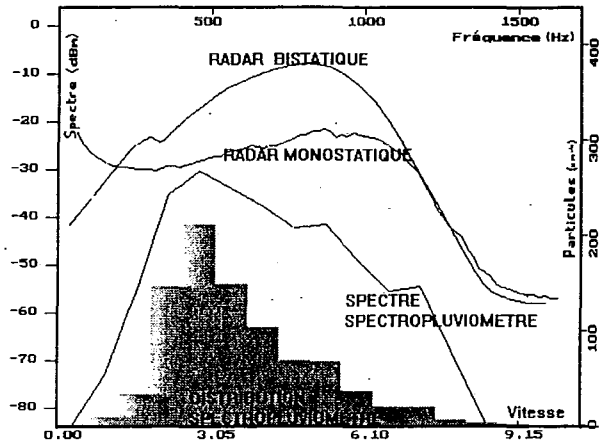

Figure 3 : Comparaisons entre les spectres de vitesse des radars mono et bistatique, et les données du spectropluviomètre lors d'un épisode pluvieux.

C. Messages de temps présent

Les messages de temps présent, délivrés chaque minute, ont été comparés à l'observation humaine. Les résultats sont résumés dans le tableau 3 suivant :

Observateur humain	Radars							
	Clair		Bruine		Pluie		Neige	
	mono	bi	mono	bi	mono	bi	mono	bi
Clair (80mn)	99	99	1	0	0	1	0	0
Bruine (165mn)	7	0	2	0	39	16	52	84
Pluie (609mn)	1	0	3	0	96	96	0	5
Neige (689mn)	1	0	5	0	20	5	74	95

Tableau 3 : Scores (exprimés en %) obtenus en comparant les radars mono- et bistatique avec un observateur humain (1543 minutes)

Les résultats obtenus par les deux radars en présence de pluie ou de neige sont excellents et tout à fait comparables. Le léger avantage de la version bistatique semble lié au fait que celui-ci est moins sensible aux variations de son environnement immédiat (arbre, passage du personnel de maintenance...), et qu'il bénéficie d'un volume d'échantillonnage constant.

Par contre l'observation de la bruine pose problème quant à son identification.

V. CONCLUSION

Au vu des résultats, il est possible d'affirmer que la faisabilité d'un nouveau capteur de temps présent à partir d'un radar Doppler est démontrée. L'avantage de cette technique réside dans sa grande sensibilité et sa capacité à travailler aussi bien le jour que la nuit et même par brouillard.

Le taux de non détection, tous hydrométéores confondus, pour le radar bistatique est inférieur à 0,2% ce qui en fait le capteur le plus sensible. Cet excellent score est conforté par le taux de fausses alarmes qui est inférieur à 1%.

De même, son aptitude à la caractérisation est excellente en ce qui concerne la séparation entre phase liquide (bruine et pluie) et solide (neige). La reconnaissance de la bruine est mal appréhendée. Cela peut s'expliquer par le fait que les cas de bruine ont été peu nombreux et que la frontière entre les paramètres Doppler pour la bruine et la pluie faible est souvent assez floue. Même un observateur humain expérimenté doit parfois utiliser d'autres paramètres tels que le type de nuage pour caractériser véritablement la bruine.

Enfin, il faut noter que les brouillards, pour lesquels la vitesse de sédimentation est de quelques centimètres par seconde, ne sont pas détectables.

Au regard des performances obtenus, METEO-FRANCE a décidé en Juillet 93 de retenir cet instrument pour son futur réseau d'observation automatique. Son industrialisation est engagée et les premiers prototypes industriels seront disponibles au cours de l'année 1994.

De plus, le prototype de laboratoire participera à l'intercomparaison de capteurs de temps présent organisée par l'OMM, qui se déroulera à Terre-Neuve au Canada puis à Trappes en France en 1994-95.

VI. BIBLIOGRAPHIE

Atlas D., R.C. Srivastava and R.S. Sekhon, 1973 : Doppler Radar characteristics of precipitations at vertical incidence. *Review of Geophysics and Space Physics Vol. 11, 1-35.*

Duvernoy J., J.L. Gaumet and M. Gilet, 1992 : Caractérisation du temps présent au moyen d'un radar Doppler pointé verticalement. *Organisation Météorologique Mondiale TECO-92 11-15 Mai 1992, Vienne, Autriche, p305-309.*

Gunn R. and G.D. Kinzer, 1949 : The terminal velocity of fall water droplets in stagnant air. *J. Meteorol., 15, 243-248.*

Hauser D. and P. Amayenc, 1981 : A new method for deducing hydrometeor-size distributions and vertical air motions from Doppler radar measurements at vertical incidence. *J. Appl. Meteor., 20, 547-555.*

Lavergnat J., C. Gloaguen, J.Y. Delahaye, J.Duvernoy and J.L. Gaumet, 1993 : Radar Doppler bistatique pour l'observation automatique du temps présent. *MTT Workshop, Les applications nouvelles en Hyperfréquence, 21-22 Novembre 1993, La Baule, France.*

Pilon J., 1989 : Vers l'automatisation complète de l'observation météorologique de surface : le projet SOLFEGE. *4th WMO Technical Conference on Instruments and Methods of Observation, Report N°35, 101-104.*

Sheppard B.E., 1990 : Measurement of raindrop size distributions using a small Doppler radar. *J. Atmos. Oceanic Technol., 7, 255-268.*

SAMOS

A STATE OF THE ART OBSERVING SYSTEM

D W Jones, A M Wright, B A Whiten
Meteorological Office, United Kingdom

1. INTRODUCTION

The Meteorological Office's Semi Automatic Meteorological Observing System, SAMOS, is a computer aided system designed to automate the measurements from conventional sensors and allow an observer to interact and expand on the data in real time and use his or her judgement to complete an observation. The encoding and transmission of meteorological messages is also automated. In the absence of an observer a reduced report containing only automatic data is transmitted.

2. BACKGROUND

There is no doubt that the rapid development in microprocessor technology has had a significant effect on meteorological sensor and observing system design. However the basic architecture around which these observing systems are built has for the large part changed very little. They are frequently still based on central, dedicated data acquisition and processing units collecting raw data and distributing processed data via multiple dedicated ports arranged in a star configuration. Painting (1985) listed the following drawbacks to such system design:

i. Difficult to accommodate changes in sensor types, sensor processing requirements or additional sensors.
ii. Complex software requirement to accommodate redundant sensors or other duplicate components, usually resulting in severely limited capability in this respect.
iii. Software changes are often not possible to implement without specialist equipment.
iv. High cost overhead if used at a fraction of design capability.
v. Complex fault diagnosis and difficult field repair since often there is much interaction between software/ hardware modules.
vi. Complex cable and connector systems - a serious reliability problem.
vii. Limited output capability.

Despite some improvement due to more widespread use of software controlled systems many of these disadvantages are still present in today's systems. Painting (1985) also describes a new observing system based on a series of independent modules. These were made up of a series of integrated intelligent sensors, 'standard' commercially available data processing and display units and local area networks for data collection and dissemination. One of the ideas behind this proposed system was that any of the modules could be replaced, changed or upgraded without impacting on the rest of the system. The design could develop gradually and was not linked totally to any one manufacturer. Since the inception of the project, SAMOS has followed this modular design philosophy.

3. SAMOS DEVELOPMENT

Sparks and Wright (1991) have described the initial design of SAMOS. A schematic of this is shown in Fig 1, and as of December 1993 there are 38 such systems in full operational use within the Meteorological Office's observing network.

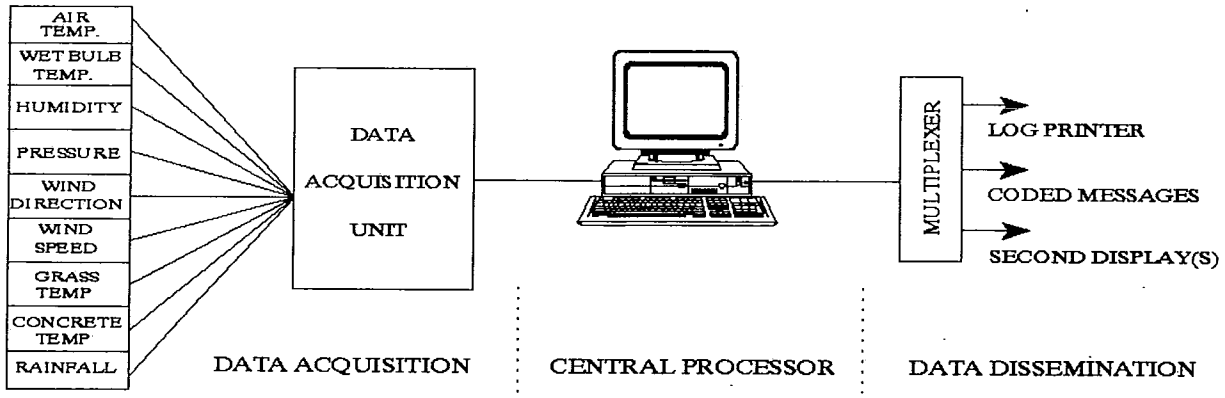

Figure 1 SAMOS 1 Schematic Diagram

It is clear from Fig. 1 that this system readily breaks down into three functional modules:

3.i Central processor.
3.ii Data acquisition.
3.iii Data dissemination.

3.i The central processor - the heart of SAMOS - was selected to be an IBM or compatible PC-AT with a minimum specification (see Sparks and Wright). The major functions performed by this computer are shown in Figure 2, where it will be seen that this also serves as the observer's display and system interaction interface.

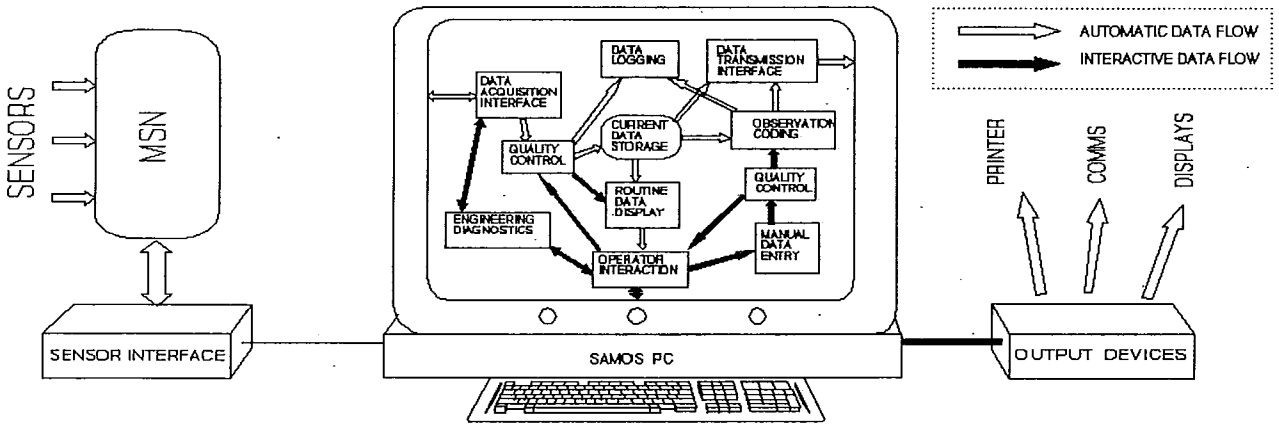

Figure 2 SAMOS Data Processing Software

The effectiveness of this interface has the greatest impact on the operational meteorologist; the software must be user friendly and robust if he is to have confidence in the system overall. Considerable attention has therefore been given to the design of the individual software modules and to system testing before introduction into operational use. Although Fig. 2 shows SAMOS configured for networked intelligent sensors on the data input side, the computer and its functions are in fact identical with those described by Sparks and Wright and fully interchangeable; the SAMOS central processor is independent of the data source. Data are received in sensible units (e.g. deg. celsius) and given a unique channel number to identify the data type. The list of data types is extensive and includes variables likely to be automated in the future. It also allows for sensor duplication.

3.ii The data acquisition system selected for the design given in Fig. 1 was the CR10 data logger produced by Campbell Scientific. This is an intelligent unit, with all data capture being under software control. It has the advantage that it can accept a number of analogue and simple digital signal inputs and perform raw

data conversion into scientific values; it is also able to do some data processing and compute period averages, extremes and totals, for example. However, as with most dedicated logging systems the number of inputs is limited and some sensors may still require additional interfaces. Also it is not easily interfaced with modern sensors, such as laser ceilometers, which produce serial digital data. The use of this logger module did, however, permit the rapid development of a basic SAMOS, with the main development effort being channeled into the processing software described in 3.i above.

3.iii Data dissemination is currently through a proprietary multiplexer, with data routeing being controlled by the central SAMOS software.

4. SAMOS 2 DEVELOPMENT

The reader will have seen that the *data acquisition function* for the SAMOS described in Fig 1 is still essentially a 'starred', dedicated system, with most of the disadvantages discussed by Painting. To overcome these limitations and extend the scope and number of sensors that can be used, the SAMOS 2 is based on a series of intelligent sensors and a Meteorological Sensor Network. A schematic for this is shown in Figure 4.

4.i Meteorological Sensor Network (MSN). Many designs of Local Area Networks (LAN's) already exist (cf Ethernet, IBM Token Ring, Localnet...). These permit easy connection between two or more system users, or enable multiple users to use common shared facilities. They are, however, mostly designed for high speed, high volume, high reliability data transmission. To implement them it is necessary to follow their predefined architecture and protocols, with consequential penalties of high cost due to over specification, in most cases. The transmission requirements for meteorological data are rarely very demanding; most data are averaged, update rates are relatively low and 100% data collection is unlikely to be a requirement for most variables. Provided critical key data can be identified if corrupt, and retransmitted or retrieved on demand, it is acceptable if, for example, an occasional 1 minute temperature value is missed. A higher data rate is required for some sensors,e.g. wind, but even here 4Hz samples of speed and direction transmitted once per second are adequate for most applications, and the data volume on a network will still be low.

The design of Meteorological Sensor Network (MSN) implemented in SAMOS 2, see Figure 3, is based on widely available, inexpensive, RS485 devices. Data transmission over distances up to 1Km are easily achieved using low cost twisted pair cable.

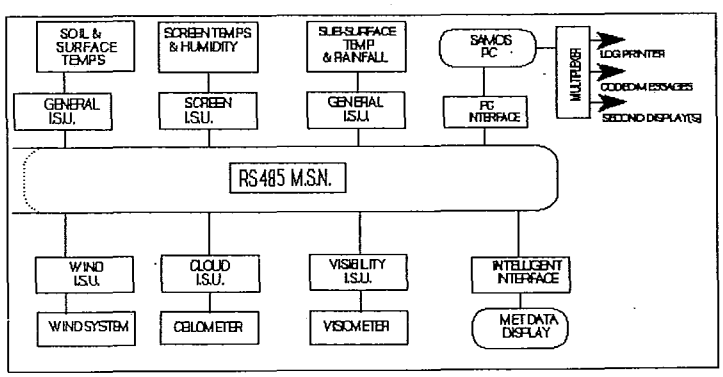

Figure 3 SAMOS 2 Schematic Diagram

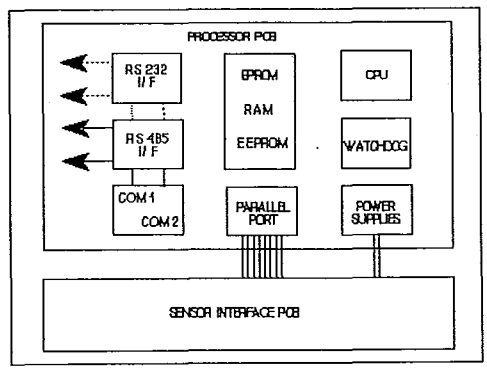

Figure 4 ISU Schematic Diagram

The majority of data on the MSN are 'unsolicited', i.e. they are transmitted by each individual device without being requested. All data packets are available to, and readily decoded and used by, any device on the network. A multiple access protocol has been developed which has a low software overhead but gives good reliability and acceptable transmission latency (timeliness). Each device monitors

the network for a random period before transmitting, and will only transmit if it remains clear for that period. Although a 'multidrop' standard, RS485 does not readily allow collision detection by transmitting devices. The protocol that has been developed allows any device to detect corrupt data and request a repeat transmission. All recently sent packets will then be retransmitted. No transmission order is imposed on the MSN, even on initial power up; the devices determine their own transmission sequence without a separate network controller.

There is also provision in the protocol for requesting data. This is used when diagnostic information is required and can be used to enhance transmission reliability by requesting any missing data if these are critical. Data can be requested by channel (i.e. data type) without reference to the source device or sensor(s). This increases flexibility, allowing the exchange of an intelligent sensor unit for a different type with the fact of the exchange being transparent to the rest of the system. Data may also be requested from a specific intelligent sensor unit.

Data packets on the network are readable ASCII characters. Each is labelled with the source sensor and its unique data 'channel' indicator (e.g. time,air temperature, rainfall in past hour,..); the data is in sensible units (e.g. deg. celsius). The protocol is symmetric so failure of one unit will not affect the network operation. A degree of data loss is acceptable for most variables (e.g. an occasional single sample), so long as the data are reliably identified as corrupt. The protocol uses a 16 bit cyclic redundancy check on each short package to ensure a high level of reliability. In practice less than 1% of data packets are lost, even with a heavily loaded system.

4.ii Intelligent Sensor Unit, (ISU). A schematic of an ISU is shown in figure 4 and Table 1 lists the ISU's which have been designed to date, together with the sensors used and the derived or processed data that are generated.

ISU TYPE	VARIABLE	SENSOR USED	ISU GENERATED DATA
GENERAL PURPOSE: CONFIGURED AS SCREEN ISU	DRY BULB TEMPERATURE	PLATINUM RESISTANCE THERMOMETERS	1 MINUTE MEAN VALUES FOR ALL VARIABLES. MAXIMUM AIR TEMP 06-18,09-21,21-09 UTC. MINIMUM AIR TEMP 00-06,09-21,21-09 UTC.
	WET BULB TEMPERATURE		
	HUMIDITY	VAISALA HMP35A OR ROTRONIC MP340	
GENERAL PURPOSE: CONFIGURED AS SOIL AND SURFACE ISU	GRASS TEMPERATURE	PLATINUM RESISTANCE THERMOMETERS	1 MINUTE MEAN VALUES FOR ALL VARIABLES. THE MINIMUM VALUE FOR GRASS AND CONCRETE TEMPERATURE BETWEEN 21-09 UTC.
	CONCRETE TEMPERATURE		
	100CM SOIL TEMPERATURE		
	30CM SOIL TEMPERATURE		
GENERAL PURPOSE: CONFIGURED AS SOIL AND RAINFALL ISU	10CM SOIL TEMPERATURE		1 MINUTE MEAN VALUE.
	RAINFALL	TIPPING BUCKET (0.2 MM PER TIP)	TOTAL RAINFALL THIS HOUR PERIOD TOTALS: 06-12,06-18,18-24 18-06,09-21,21-09 & 09-09 UTC.
PRESURE ISU	PRESSURE	SOLATRON VIBRATING CYLINDER TYPE 7881	1 MINUTE MEAN AS READ PRESSURE. 3 & 24 HOUR PRESSURE CHANGE. 3 HOUR PRESSURE TENDENCY CHARACTERISTIC. MASTER REAL TIME CLOCK.
WIND ISU	WIND DIRECTION	MUNRO Mk4 WIND SYSTEM	DIRn. 4 Hz RAW DATA TRANSMITTED ONCE PER SECOND. SPEED 2,10 & 60 MINUTE PERIOD VALUES. GUST MAXIMUM GUST IN LAST 10 MINUTES AND LAST HOUR. TIME OF MAXIMUM GUST IN LAST HOUR.
	WIND SPEED		
GENERAL PURPOSE: CONFIGURED AS WIND ISU	WIND DIRECTION	VECTOR INSTRUMENTS WIND SYSTEM (A1000R / W200)	
	WIND SPEED		
CLOUD ISU	CLOUD	TRANSTECHNOLOGY MODEL 7013C	HEIGHT AND AMOUNT OF UP TO 5 CLOUD LAYERS.
VISIBILITY ISU	VISIBILITY	BELFORT MODEL 6210	1 MINUTE MEAN VALUE.

Table 1

Most ISU's contain two Printed Circuit Boards; all have an identical processor PCB based on an NEC V25 microcontroller. This emulates a PC and is programmed in Turbo Pascal. The processor PCB also contains the RS485 and RS 232 interfaces and is the power source for the second PCB, the dedicated sensor interface.

It would have been possible to design SAMOS 2 around an individual ISU for each separate sensor. However, most meteorological observing enclosures have clusters of identical or, at least similar, sensors. (e.g. a Stevenson radiation screen will contain dry and wet bulb thermometers and a solid state hygrometer, and soil thermometers are usually grouped in one small area. It was therefore decided to design a general purpose interface that can be easily configured using links and/or software selection. This ISU can accept up to four inputs, configured individually either to measure resistance or analogue voltage. It also has a pulse counting or frequency measuring capability. The individual configurations and current applications for this ISU are given in table 1. Specific interfaces have been developed for the Munro wind instruments currently in operational use in the Meteorological Office, and the Solartron vibrating cylinder pressure transducer; this interface also provides a time standard for the other ISU's on the network.

The cloud and visibility ISU's use only the processor PCB's. They take the RS 232 data output directly from the ceilometer or visiometer, process these data further and then retransmit via the RS 485 MSN.

Since the processor PCB is built to emulate a PC, software development skills are readily available and standard or existing software modules can be easily adapted or imported. This minimises learning curves and simplifies software development and maintenance overheads. A standard set of serial drivers have been written allowing new ISU software to be developed quickly.

5. FUTURE DEVELOPMENTS

One development which will be implemented will be a LAN for data dissemination. This will significantly increase flexibility over the multiplexer currently in use.

Although each sensor has access to and is capable of interpreting data from other sensors there is minimal use of this facility at present. It does, however, offer considerable scope for improving the performance of sensors which are themselves affected by the weather (e.g. ceilometers in rain, fog, snow), and the development of present weather algorithms based on data from multiple sensors. Also when introducing new sensors or other devices to the observing network it will be possible to evaluate them in a live situation, and compare them with existing practices, before introducing them operationally.

This design of observing system also lends itself to a high degree of remote monitoring for engineering maintenance. By the use of an MSN interface and standard telephone modems an engineer can monitor data without recourse to, or affecting the local observer or other user. He can access detailed ISU diagnostic information and flag a suspect or defective device, or select a 'hot' spare.

The SAMOS 2 design has overcome the restrictions on system expansion described in section 2; the possibilities for future application and expansion are extensive.

6. REFERENCES

Sparks W. R. and Wright A. M. 1991: The Meteorological Office Semi Automatic Observing System. The American Meteorological Society 4th International Conference on Aviation Weather Systems, 1991, pp 359-364.

Painting D.J. 1985: A New Automatic Observing System. WMO Technical Conference on Instruments and Methods Of Observation (TECIMO), 8-12 July 1985, pp 193-196.

THE APPLICATION AND TEST OF THE VIBRATING CYLINDER BAROMETER

Yao Bin, Zhu Lekun
China Meteorological Administration

1. General

Vibrating cylinder barometers have been used widely for measuring atmospheric pressure in automatic weather stations. But it is the first time to take pressure caliberation as a standard instead of the double tube mercurial manometer by using precise vibrating cylinder barometer. We have done some studies and have made progress.

All kinds of the vibrating cylinder barometers, including high accuracy vibrating cylinder barometer, standard vibrating cylinder barometer and common vibrating cylinder barometer could be manufactured in China. We determined the Model XEY02 which is more econamical with accuracy 0.3 hPa for testing sample . In this paper, the application and test of the vibrating cylinder barometer are introduced as follows.

2. Result and Analysis of Testing

In order to find out whether the Model XEY02 vibrating cylinder barometers could meet the requirement of caliberation , we tested three sets of them numbered separately as No. 032, No. 034 and No. 035. Moreover we selected two sets of other vibrating cylinder barometers with high accuracy (±0.1 hPa) as standard instruments which standard indication had been set up. The testing items include: ① Caliberation of the indication and linear analysis; ② Imitative test for altitude; ③ Test of temperature-affected; ④ Statistics for annual change of indication; ⑤ Comparison of the vibrating cylinder barometers with double tube mercurial manometer. We also examined the affection by humidity.

①. Caliberation of the indication and linear analysis

The test was conducted in the range 1050hPa to 600hPa. In order to adjust pressure freely, two precise vibrating cylinder barometers were connected with

three sets of tested vibrating cylinder barometers . Pressure points were caliberated at interval of 50hPa. Each point was taken reciprocating caliberation for three times and its average value was evaluated . The deviations at all testing points were less than 0.13 hPa , and the Max. difference of deviation for each tested barometer was also within 0.2 hPa. Shown in fig. 1. P: Caliberation pressure, ΔP: deviation.

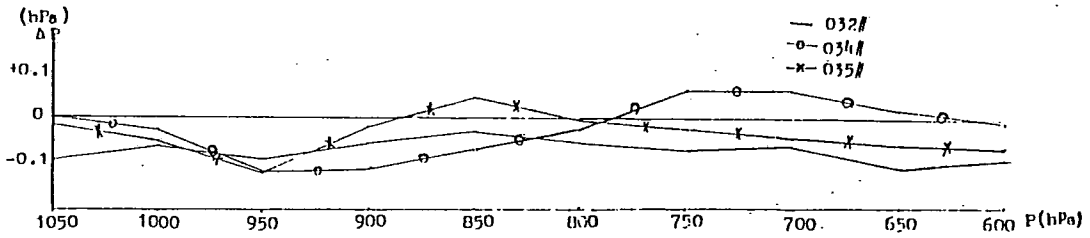

Fig. 1 Caliberation Curve of Indications

②Imitative test for altitude

In order to find out the change of indication at different pressure points, we compared the indication of the XEY02 vibrating cylinder barometers inside and outside the pressure chamber ranging 1050 to 650 hPa

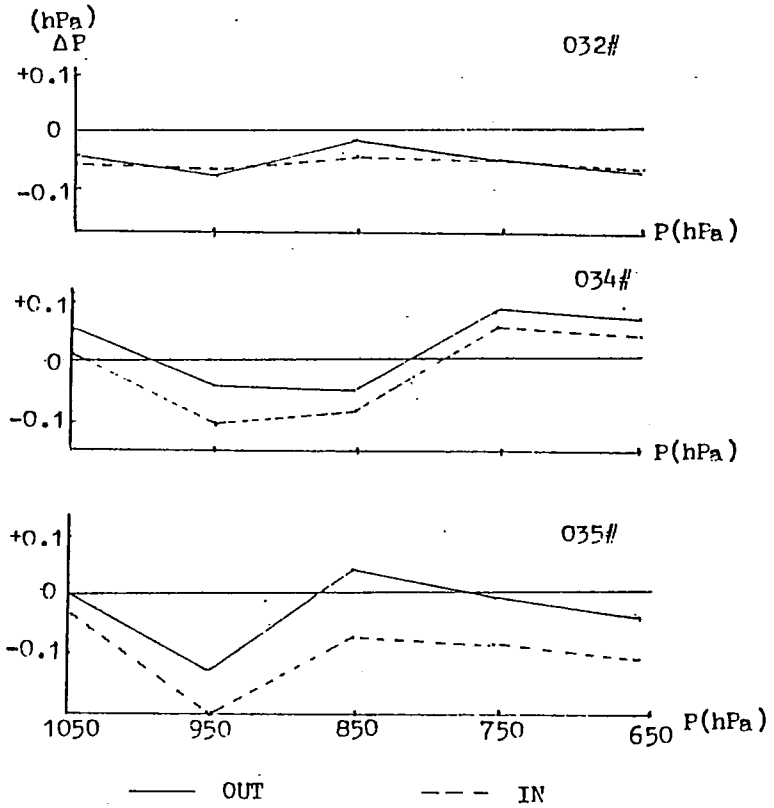

Fig. 2 Curve of Imitative Test for Altitude

at interval of 100hPa. The testing results were same inside and outside, most of deviations were less than 0.1hPa. Shown in fig. 2. With a view confirming the results, the vibrating cylinder barometers and a standard mercurial manometer were compared at the plateau with an elevation of 1500 and 2300 meters. The deviations were still within 0.1～0.2 hPa. (Remarks: We used the formula recommended by WMO to calculate the station pressure.)

③. Test of temperature-affected

Before the vibrating cylinder barometers are delivered to user, they were made temperature correct to reduce the temperature affection but it is not completed. According to the testing result, the temperature affection are still kept. Shown in fig. 3. (No. 32 barometer was not tested in this time). So the vibrating cylinder barometers should better be uesed in the same temperature condition as caliberation.

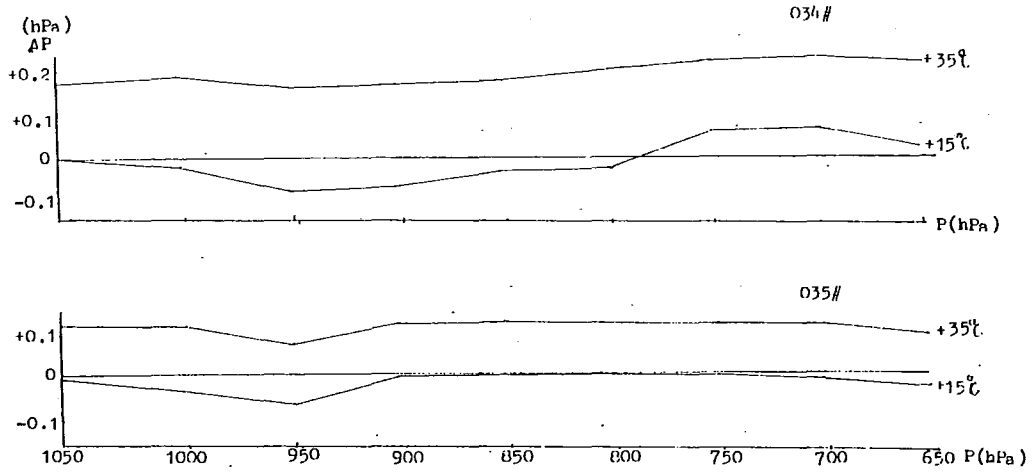

Fig. 3 Curve of Test of Temperature-Affected

④. Statistics of annual change of indication

The indications were re-caliberated after one year. We compared with the indications in the different time to find out the deviations at all pressure points. Shown in fig. 4. The No. 32 barometer had little deviations , the Max. deviation was only 0.05 hPa , and the No. 34 and No. 35 barometer had some systematical deviations with average value of 0.22hPa, but the systematical deviations could be deleted by revising.

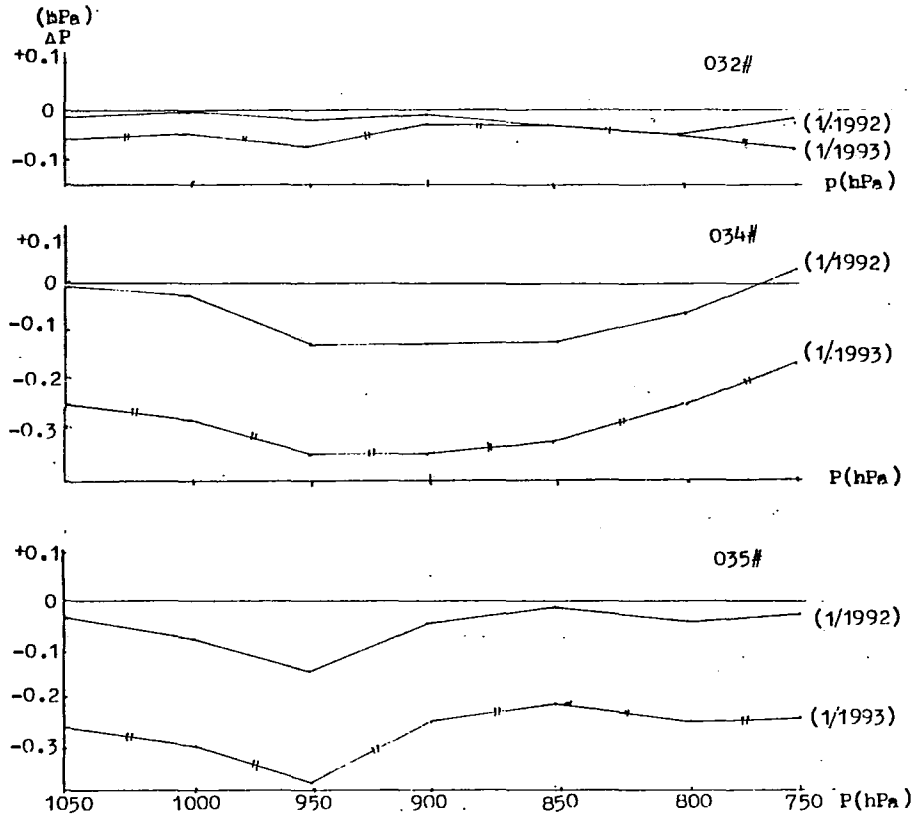

Fig. 4 Curve of Annual Change of Indication

⑤. Comparison between the vibrating cylinder barometers and double tube mercurial manometer

We compared the vibrating cylinder barometers and the double tube mercurail manometer as a standard in the range 1050 to 600hPa. Most of the devations were within 0.1 hPa , only one or two of deviations was 0.15 hPa (including the reading error of the double tube mercurial manometer). Shown in fig. 5.

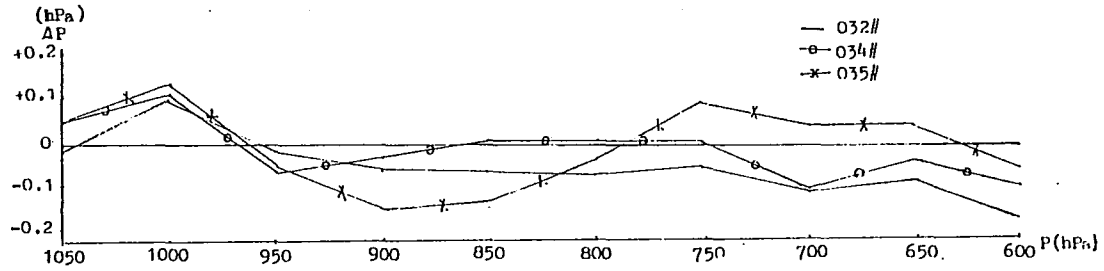

Fig. 5 Comparison Curve

In addition , we also conducted a test of humidity-affected . The high humidity could affect the indication, but it was difficult to calculate quantitatively. So it was nessesary to install a reducing moisture device on the vibrating cylinder barometers.

After test mentioned above, we thought the vibrating cylinder barometers as an ideal instrument with high accuracy , good linear, high sensitivity , and its deviations were systematical, easy to revise. It can be used for replacing the double tube mercurial manometer.

3. Application

Because the satisfied result is in keeping with using the double tube mercurial manometer , the vibrating cylinder barometers can be used for pressure caliberation as a standard.

It is not only convenient, but also easy to operate . It has many features with the reduction of the reading and adjusting error, improvement of the calculation accuracy and no mercurial polution.

By using a computer and RS-232 interface , The vibrating cylinder barometer can compose an auto-control system for caliberating the aneriod barometer (or barogragh). Shown the new pressure caliberation equipment in fig. 6.

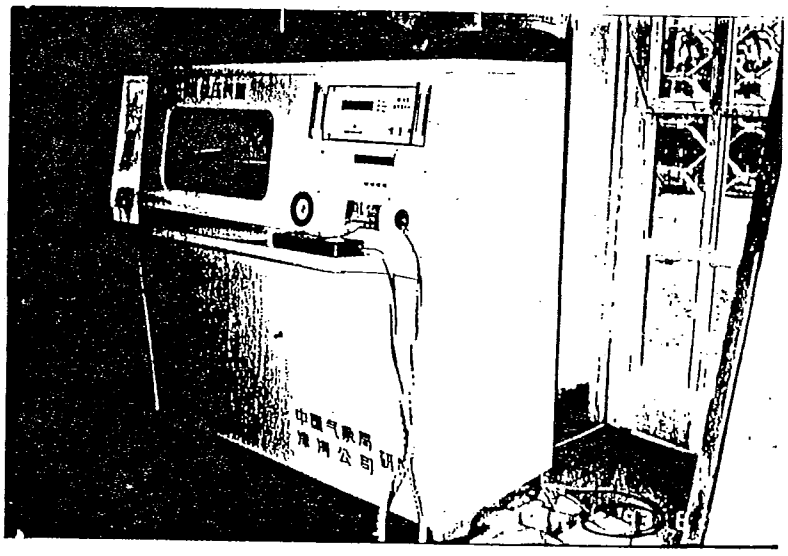

Fig. 6 A New Pressure Caliberation Equipment

Besieds, we are going to use the vibrating cylinder barometers to replace single tube mercurial barometer for caliberating the pressure sensor of radiosonde. At the present time, the test are underway.

Using the vibrating cylinder barometers to measure pressure in meteorological stations will have a good future.

TRANSDUCERS AND SENSORS FOR TEMPERATURE HUMIDITY, RAINFALL, WIND, PRESSURE AND LEAF WETNESS MEASUREMENTS

G. M. MUCHEMI

KENYA

1.0 INTRODUCTION

A transducer is a device that converts a measured variable to an electrical signal that varies with the changes in measured variable or quantity being measured. The transducer output signal can be indicated directly by an electrical measuring instrument or can be transmitted to a distant indicating instrument or recorder. The measured variable is said to be telemetered. The telemetering means can be a pair of wires or a radio link, or a satellite link.

2.0 TYPES OF TRANSDUCERS AVAILABLE

2.1.0 Transducers for measurement of Temperature, Humidity, Wind, pressure and leaf wetness fall under any of the following types.

(a) Movable contact transducers
(b) Capacitive transducers
(c) Inductive transducers
(d) Resistive transducers
(e) Photo electric transducers
(f) Piezo electric transducers

2.1.1 Movable contact transducers consist of a resistive element and a movable contact. The displacement of the contact by the measured variable causes changes in resistance between terminals of the element. A Potentiometer is a good example. A voltage or current proportional to the changes in the variable is generated.

2.1.2. Capacitive transducers change the capacitance of a variable capacitor either directly or indirectly. Changes in capacitance may be due to changes in distance between plates or due to change in dielectric composition or due to change in area of the plates. Pressure and humidity are transduced through these types of devices. Capacitive transducers have very short lead wires and are connected via an A.C. bridge, or an oscillator to indicating meters.

2.1.3 Inductive transducers are either self-generating or passive. The self-generating types generate a voltage or current due to cutting of magnetic flux, while passive types require an external source of power. The cup-generator wind speed sensor and synchromotor for direction sensor are good examples of these types of -transducers. Also in pressure measurement a linear variable differential transformer (LVDT) (passive type) is being used to convert capsule variations to an electrical signal.

2.1.4 Resistive transducers change their ohmic resistance to an electrical current with the measured variable. In this category Resistance thermometers and thermistors are used for monitoring termperature changes. Humidity sensors using lithium chloride and the sulphonated polystyrene rod fall under this category. An alternating current is used to avoid polarization of ions. The Guide (reference

1) recommended the use of Resistance thermometers and thermistor. Their principles of operation are explained in paragraph 4.3.0.

2.1.5 Photoelectric transducers fall into three categories:_

(a) The photo voltaic effect transducers cause the generation of a potential between two electrodes when one of them is illuminated.

(b) The photo conductive effect transducers cause electrical resistance of a material to change in response to variations in illumination.

(c) The photoemissive transducers cause emission of charged particles in form of light from a material when subjected to illumination. A current is generated.

Vaisala Wind Sensor utilise photo-conductive transducers to generate a grey code in the case of direction sensor and a frequency in the case of speed sensor.

2.1.6 Piezoelectric tranducers utilize the piezoelectric characteristics of crystalline material and ceramic materials to generate an electric signal with varying frequency proportional to the force acting on the material. Crystalline material used are quartz and tourmaline. Ceramic type are made from polarized polycrystalline barium titanate. Pressure can be measured with piezoelectric transducers directly.

3.0 MEASUREMENT

3.1 Temperature is measured with resistance thermometers and thermistors. The resistance of pure metals increases proportionally with the temperature changes as shown in equation (I)

$$R_T = R_O \quad (1 + aT + bT^2 + CT^3 + ...) \quad ..... \quad (I)$$

Where R_O = Resistance of reference temperature 0°c ohms.

R_T = Resistance at temperature T, ohms

a = temperature coefficient of resistance ohm/ohm at around 0°c.

b, and c = temperature coefficients calculated on the bases of two or more known temperature points.

The Guide ref. 1, allows the equation (I) to be limited to the first three terms, that is:

$$R_T = R_O \quad (1 + aT + bT^2)$$

The resistance temperature relationship in thermistor thermometer is:

$$R_T = R_O \text{ Exp. } B \left(\frac{1}{T} - \frac{1}{T_O} \right)$$

Where R_o = resistance value at reference temperature, T_o °K, ohms.

R_T = resistance at temperature T ohms.

B = constant over temperature range dependent on Manufacturing process and construction characteristics given as:

B = E/K where E = Electron volt energy level

K = Boltzmann's constant (8.625×10^{-5} eV/K)

The temperature coefficient a, of thermistor is given by:-

$$a = \frac{1}{R_O} \quad \frac{dR_O}{dT_O} = -b/T^2$$

3.2 HUMIDITY

Relative Humidity sensors include the Vaisala humicap, the lambrecht hair and potentiometer system, the Dunmore and the pope sensors.

Dunmore sensor consist of bifilar wound inert wire grid on an insulator coated with lithium chloride. This type of sensor cannot go full scale, but can be used at a limited interval.

The pope Sensor utilizes sulphonated polystyrene rod. A bifilar wire grid is wound on to the rod. The sensor has a range of 15% to 99% relative humidity.

The sulphonation of the longer polystyrene molecules with concentrated sulphuric acid results in highly mobile sulphate radical $(SO_4)^{-2}$ in presence of hydrogen ions. The mobility of SO_4^{-2} ions which migrate to take on hydrogen ions from the vapour molecules change the resistivity of the sensor as function of relative humidity.

3.3. RAINFALL MEASUREMENT

The most widespread rainfall transducer is the tipping bucket. A metal container divided into 2 compartments is balanced in unstable equilibrium about the horizontal axis along the dividing line. In normal operation the bucket rests on a stop preventing it from complete tip. The water collected in upper bucket makes its centre of mass to move outward so that at some calibrated amount it overcomes the moments due to lower bucket and eventually tips over. The axis carries with it a magnet which operates a proximity switch each time a tip occurs, resulting into an electrical pulse. This pulse controls either a relay to actuate recording system or an electronic circuit driving a electro-maechanical counter, or transmitter or microprocessor.

3.4.1. WIND SPEED

Conventional cup or propeller anemometers produce analogue signal with a limited number producing frequency. The analogue signal can be converted to digital through analogue to digital converters. However due to losses involved frequency generating types such as that of Vaisala Ward 21 speed sensor is very ideal for Automatic Station.

3.4.2. WIND DIRECTION

Similarly Vaisala Ward 21 direction Sensor which uses shaft or grey code to produce a direction indicating code for all 360° at interval 5° should be recommended for us in automatic stations.

3.5.0 PRESSURE TRANSDUCERS

4.3.5.1. The capsule continues to be the most suitable sensing element for pressure changes. A variety of possible transducers for pressure are now available. Lambrecht use pressure capsule to vary a resistive transducers while cascella uses piezo electric pressure sensor directly. Linear variable differential transformer (LVDT) can also be used with the capsule. Capacitive pressure transducers have also been reported where the capacitance is varied with capsule variations with pressure. The best zero calibration of pressure transducers shall continue to be 1000 hpa. Table shows comparative accuracy.

TRANSDUCER	ACCURACY/ SENSITIVITY	SENSOR	LINEARITY
Capacitive	0.2 hpa.	Capsule	Non-linear
Piezoelectric	0.2 hpa.	Crystal	Non-liner
Linear variable Differential Transformer (LVDT)	0.002 hpa	Capsule	Linear
Frequency Change	0.05 hpa	Resonant Crystal	Non-Linear
Strain Gauge	0.2 hpa.	Capsule or Diaphragm	Linear

The accuracy rating in this table include Linearity, hysteresis and repeatability. All sensors are robust.

Non-linearity in these transducers and temperature dependency if any are overcome through use of micro- processors incooperated in transmitting unit.

3.6.0 LEAF WETNESS SENSORS

Humidity sensors can also be used to detect leaf wetness, because under leavy conditions there is more water molecules in form of vapour than in free air way. One sensor that can easily be adapted for this purpose uses resistive principle.

A two thin foil grid stamped on plastic forma to form an interlaced pattern but without actual contact between them and coated with a hygroscopic salt such as lithium chloride is used. Lithium chloride absorb moisture causing a electrical conduction between grids.

The readout units will normally indicate either dry, wet or very wet.

4.0 WMO Accuracy requirement for Automatic Weather Stations for Synoptic meteorology.

Air Temperature ± 1°c

Sea Temperature ± 1°c

Humidity	not given
Atmospheric Pressure	± 1.0 hpa over land ± 2.0 hpa over sea
Wind Direction	± 20°
Wind Speed	± 2M/S below 2M/S ± 20% above 20M/S
Rainfall	± .5mm below 5mm overland ± 10% above 5mm overland.

REFERENCES

1. Guide to Meteorological Instruments and methods of observation (5th edition, WMO - No - 8)

2. Transducer measurements, 2nd Edition, Kenneth Aurther, Tektronix.

3. Process instruments and controls handbook (3rd Edition) Douglas M. Considine and Glenn D. Considine.

LOW-DRIFT THERMISTORS FOR MEASURING AIR TEMPERATURE

Bert Heusinkveld, Rushdi M. M. El-kilani, Willy Hillen, Teun Jansen, Dick Welgraven.

Wageningen Agricultural University, Department of Meteorology, Duivendaal 2, NL-6701 AP Wageningen, The Netherlands.

INTRODUCTION

In micrometeorological studies at the earth's surface, temperature gradients can be used to gain knowledge about the energy balance terms. For these measurements, it is important to measure temperature differences within 0.02°C. Recently, new thermistor types have been introduced. These new types have a glass or an epoxy coating which improves long term stability.
Both thermistor types have been evaluated. In this paper, we will use stability as a criteria for selecting glass coated thermistors for our measurements. We will also suggest a measuring procedure to enhance the signal to noise ratio and show a set up in the field designed to reduce radiation errors.

CALIBRATION AND SELECTION

Three glass and three epoxy coated thermistors were calibrated by comparison with a standard platinum resistance thermometer. The calibration equipment has an absolute accuracy of 0.04K. The calibration was done twice with a period of 2 month in between. This to check the stability in time of the thermistor. At present, the Steinhart Hart relationship (eq. 1), has wide industry acceptance as the most useful equation for precise thermistor R-T computation. The Steinhart-Hart equation is an empirical third degree polynomial expression.

$$\frac{1}{T} = A + B \cdot \ln(R) + C \cdot (\ln(R))^3 \qquad \textbf{(1)}$$

Where T temperature (K), R resistance of thermistor in Ω, A,B and C are calibration coefficients. The exactness of the fit is excellent from -30 to +70°C. Only at the temperature extremes, there is a deviation of less than 20 mK. The thermistors used here, are more sensitive than PT100 temperature sensors (more than 10 times better), this can improve signal to noise ratio. The calibrated thermistors, glass coated and epoxy coated, have a typical resistance of 10×10^3 Ohm at 25°C (33×10^3 Ohm at 0°C). The glass coated thermistor has a diameter of 1.4 mm while the epoxy coated one has a diameter of 2.4 mm. Figure 1 and 2 show the difference between the first and second calibration for glass coated and epoxy coated respectively.

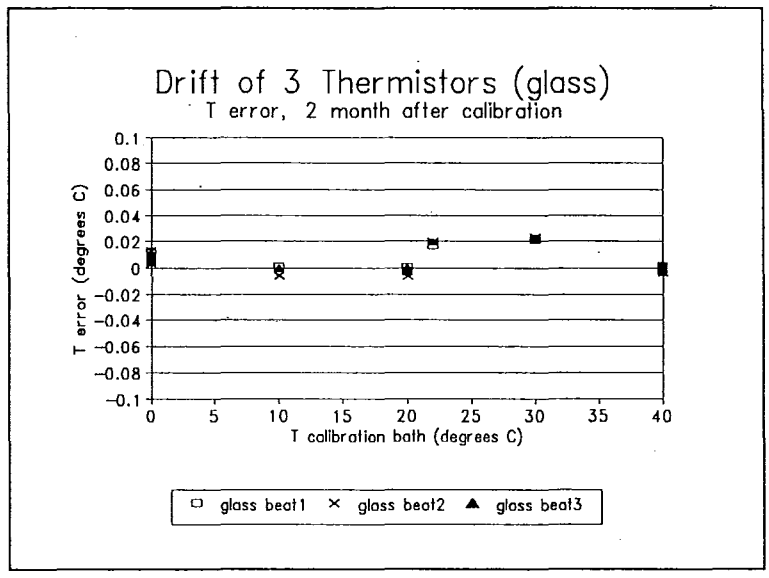

Figure 1 Stability of glass coated thermistors

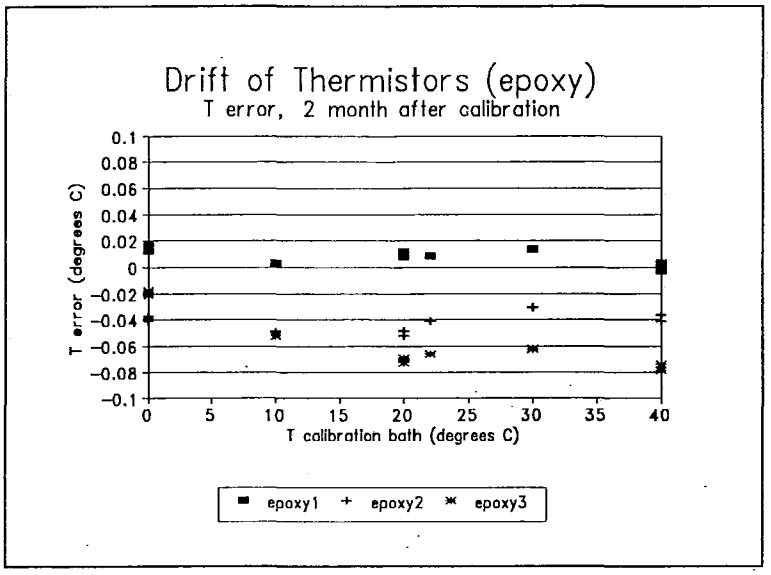

Figure 2 Stability of epoxy coated thermistors

Comparison of these two figures shows that the stability of glass coated thermistors is much better. There were no change of the temperature measured with the glass coated thermistor compared to deviation range of more than 0.02..-0.08°K for the epoxy coated thermistor. There were also no dispersion of the measuring error for the three glass coated ones. It seems to us that the glass coated thermistors are much better to use since they have much better time stability and a minimal standard deviation.

EXCESS TEMPERATURE AND TIME CONSTANT OF THERMISTORS

To use a thermistor in measuring temperature, an excitation current must be applied to measure its resistance. This current would itself heat the thermistor, thus producing what is called self heat. The resulting increase in temperature is called excess temperature. The maximum allowable energy dissipation (I^2R) is calculated by using the energy equation of the sensor (eq. 2).

$$\rho_s c_s V \frac{dT_s}{dt} = xQA_{radiation} + I^2R - \rho_{air} c_{p\,air} \alpha (T_s - T_{air}) A_h \qquad (2)$$

Where: rho_s c_s is the volumetric heat capacity of the sensor in J m^{-3} k^{-1}, V is the volume of the sensor in m^{-3}, x is the radiation absorbtion coefficient of the sensor (-), Q is the incident radiation in W m^{-2}, $A_{radiation}$ is the sensor area effective for radiation exchange, I is the measurement current (Ampere), R resistance of thermistor (Ω), T_s temperature of sensor, rho_{air} $c_{p\,air}$ is the volumetric heat capacity of the air (constant pressure) in J m^{-3} K^{-1}, T_{air} temperature, A_h sensor area effective for heat transfer and α in m s^{-1} is the boundary layer conductance given by equation 3.

$$\alpha = \frac{D_H Nusselt}{d} \qquad (3)$$

Where: D_H thermal diffusivity (m^2s^{-1}), d is characteristic dimension (m).

Nusselt number is a function of Reynolds number, shape of the sensor and the convection regime (forced or free). A complete list of these functions are given in Monteith 1990.

Assuming a steady state solution, a maximum allowable excess temperature of 0.01K and a ventilation rate of 4 m/s would allow us a maximum dissipation of 16μW. At this low dissipation, a constant in time applied current would become very low with corresponding low signal to noise ratio. A varying in time application

of the measuring signal would allow us to apply a much higher current during a short interval of time (the measuring time), while keeping the average power dissipation the same. The whole measuring cycle will include an application period which is dependant on the datalogger used and a relaxation period in which we apply no current at all. In our case, an application period of 0.1 second and a relaxation period of 0.9 seconds was used. This leads to one hertz frequency of measurement. Increasing the frequency of measurement by two while keeping the average power dissipation constant would lead to a decrease of I^2 by half. This would lead to a decrease in the signal to noise ratio by a $\sqrt{½}$ while we will have a double number of measurements. This would improve our estimations of the mean temperature gradients. An application of a I^2 higher than the maximum averaged I^2 would lead to a higher signal to noise ratio. If the period of application is much less than the time constant of the sensor, there would be no problem. The time constant of the sensor (τ) is given by eq. (4).

$$\tau = \frac{\rho_{sensor} c_{sensor} V_{volume}}{A_h \rho_{air} c_{air} \alpha} \qquad (4)$$

Four m/s ventilation speed gives a time constant of two seconds for the glass coated thermistor. A numerical solution of this problem is shown in figure 3.

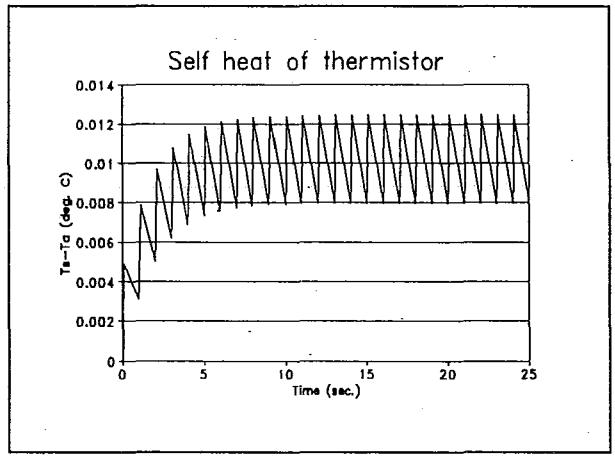

Figure 3 Self heat of thermistor, ventilated at 4 m/s, measurement time is 0.1 seconds, measurement frequency is 1 Hz. for a varied in time current with a maximum excess temperature of 0.01K.

This last figure shows that excess temperature is less than 0.01K while the applied I^2 was 10 times higher than the current allowed for maximum power dissipation in the case of continuous application. This would increase the signal to noise ratio by a factor $\sqrt{10}$ while keeping the average power dissipation within our determined limit. It is to be noticed that there are some dispersion of the temperature of the sensor around 1 Hertz frequency. The datalogger averages the signal during the time of application, in this case 0.1 second, so it averages during each positive slope of this curve, this removes the peaks in figure 3.

LAY-OUT IN THE FIELD

In eq. 2, the first term on the right represents the effect of radiation interception by the sensor on its temperature. Radiation can cause high (T_s-T_a) differences. Suppose Q is 100 W m^{-2} on a glass coated thermistor with an absorbtion coefficient x of 0.5, ventilated at V=4 m s^{-1}, this will give an excess temperature of 0.12K. This difference is much higher than our allowable 0.01K limit. To reduce our radiation error, the set up in the field must give as good protection as possible from radiation.

Active ventilation usually removes any remaining error to a level accepted by WMO accuracy. Figure 3 shows a design which is well protected from radiation. The effect of Q on T_s-T_a is dependant on ventilation rate of the sensor. The isolation foam at the bottom of this design has to be cut away, this prevents air entering the tube from pre heating.

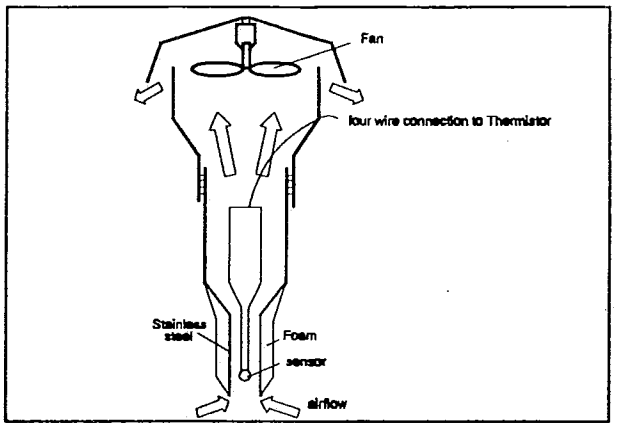

Figure 3 Active ventilated radiation shielded thermistor

One could think that placing a radiation shield below the entrance of the tube would reduce radiation intercepted by the sensor, but this does not work, because the shield is heated by radiation absorbtion and raises T_a before entering the tube. In a configuration to measure gradients, a bottom plate would also make T_s-T_a dependant on windspeed (causing overestimation of the gradient). The radiation load can be quite high especially above bare soil (high albedo). For the set-up shown in figure 3, T_s-T_a, is dependant on ventilation speed, it is therefore important to keep the ventilation speed equal for all sensors in a gradient measurement.

REFERENCES

Monteith J.L.:1990, 'Principles of Environmental Physics'

Wise J.A., 'Stability of glass-encapsulated disc-type thermistors', National Institute of Standards and Technology, Maryland 20899, American Institute of Physics

METEOROLOGICAL MEASUREMENTS IN EXTREME CONDITIONS

Kai Inha, Vaisala Oy, Finland

INTRODUCTION

Instrumentation used in the Meteorological Services today must meet demanding specifications while instrumentation spreads to unmanned sites, ships, lighthouses, masts and isolated areas. Yet resources and budgets typically stay the same or decrease. Life Cycle Cost becomes very important. It is totally different a situation, if one has to maintain and monitor couple of station, versus a nationwide network based on tens or even hundreds of installation sites. When this becomes a reality, questions like: What software version was at that site?; Has that station failed, or has it just run out of battery power?; Should someone go there, or can we update the system software via a modem connection? - become important.

Many of these stations are installed to sites where it is possible to visit only couple times per year, if weather is favourable. Again, overall reliability becomes a key question. The automatic data collection system may be alive, but the configuration, that was loaded into it, fails to run. Why and when? Then we have EMI, ESD, vibrations and corrosion.

HOW TO SOLVE THESE QUESTIONS

Vaisala has faced these questions, when we operate globally having various installations from surface ships to Antarctica and deserts. Keeping all the mentioned questions in our mind, Vaisala came with a new generation Weather Station, the MILOS 500. We listened our customers and collected information during one year before we started to create the product. Let me explain phase by phase the most important properties of this product, specifications that make it reliable and cost effective system from laboratory to oceans away.

MILOS 500 AUTOMATIC WEATHER STATION

POWER SUPPLY SECTION

One of the basic demands is the ability to accept directly a set of solar panels or a convenient wind generator without the need of having an external battery charger or voltage regulator. Eliminating this part extends the system efficiency and reliability. MILOS 500 power supply section, which is totally floating, accepts anything from 10.5V DC to 80V DC. You may have two different sources connected simultaneously and external battery setups, if needed. All

these run under the software control in MILOS 500. If You have a remote connection, it is possible to read the battery net current, temperature, remaining capacity, external currents and voltages. There is one independent real-time process, that handles only the power system. All the mentioned parameters can be found from the MILOS 500 database. For what purpose?

When the system is installed days or even months away from maintenance people, it extremely important to have local intelligence, that may, per Your configuration, shut off power consuming sensors, cut heaters, reduce transmission rates and create special message based on power supply conditions. Having this information appended to the received messages, You can correctly plan the possible maintenance actions, and save.

Life cycle of the system batteries may be a huge problem. It is extremely important to treat the batteries correctly, or the usable life-time may drop from years to months, even weeks in extreme conditions. MILOS 500 hardware and software make no compromises. Under software control the station performs all the required phases, namely:

* Start Charging: Find the optimum current and voltage combination from the solar panel or generator for example.
* Bulk charge: Charge at full power, if battery's temperature is within limits.
* Over Charge: Go up to 120%, depending on programmed battery capacity and temperature.
* Float Charge: Adjust the battery set net current to zero and adjust the float voltage as propriety to the battery type and capacity.
* As programmed, periodically stop from charging, calculate the battery capacity based on the disharge slope and report the remaining capacity. Start from beginning.

Does it have to be that complicated? YES. At remote site, where system must survive in freezing conditions, where sun may not show up for weeks, it is worth of big money to maximize the power system reliability.

Could You do this all with a low-cost data logger? How about a PC-based system? Hardly. In MILOS 500 system it becomes as standard without extra cost.

HOUSING AND MECHANICS

Housing is very important part of the installation. Standard MILOS500 outdoor enclosure is of stainless steel. It is not the only choice. It can also be of glass fiber or even plastics, if required. What is important, is that the housing is not a fixed part of the data collection system.

SHOCK AND VIBRATION RESISTANCE

One of the extreme installation sites is an icebreaker deck on the Baltic sea. Temperature is low but shocks and vibration levels are tremendous. You may

come close to this on high broadcasting mast installations, where falling ice and continuous vibration hits the installation. To jump away from the Meteorological Field, how about mounting a station onto a huge marine diesel engine. MILOS 500 is used in all these applications successfully. What makes the difference?

The difference lies in the printed circuit design and mechanics. All the printed circuit boards are relatively small in size. They slide into their slots, and are fixed with captive screws. All screws on the boards have been glued in or otherwise captive.

MILOS 500 printed circuit boards are extremely compact and dense. These multilayer boards have high density surface mounted components, that use no sockets. Jumpers are not used, nor high profile components. Finally, almost all the boards are dip coated, which glues all the components firmly. System withstands corrosion and is able to run even if moisture is found over the boards.

MAINTENANCE

It is important to have a system, where all the key elements can be replaced in couple of minutes without a need of reconnecting cable ends or removing shadowing objects. In MILOS 500 system, all the boards having active electronics, can be replaced literally in seconds. You may even have powers connected. All cables have removable connectors that withstand severe vibration.

FLASH memories are modern way of storing data, allow for secure configuration and convenient software update. All the memory devices containing calibration values, board serial numbers and customer configurations, are kept in a non-volatile memory system. Even if You have to pull all the boards out and replace all the batteries, you do not lose Your setups or configurations. Even the data can be logged and saved into the PCMCIA standard FLASH memories. This is a very rare and reliable concept.

EMI, ESD AND TRANSIENT PROTECTION

One of the most important objectives of the MILOS 500 system design has been tight EMI (ElecroMagnetic Interference) and EMC (ElectroMagnetic Compability) specifications. Because the station can be mounted onto a same mast with some radio transmitting antennas, where sensors may be in the EMI field, it is not exaggeration to demand meeting of some MIL- and SISPR-standards. A low cost data logger, which has little or no internal shielding, may influence with other systems, or show wrong values in strong EMI- field. This means external shielding components, bigger boxes and lot of on-site testing. Most of the PC board- and data logger manufacturers do not specify EMI levels for their systems. For safety, it is important to ask for EMI, ESD (ElectroStatic Discharge) and Transient Burst test reports for the systems used outdoors close to any antenna or sensitive system. Failing to do this, may become a nightmare.

MILOS 500 printed circuit boards consume as little power as possible, typically around one watt for the whole station. Multilayer (4 to 8) printed circuit boards have a solid ground layer, which effectively reduce the transmitted noise. Finally metal rack for surface mounted circuit boards with on-board filters make the unit both immune to ambient EMI, as well as quiet. Third party test data is also available for several setups.

MILOS 500 systems with Power Supply board, CPU board, Sensor Interface board and Mother board make the minimum system. Figure 1. show the emission levels, when measured per MIL-STD-461/462. Sensors and power cables were connected. No ambient case was on. System was operating normally.

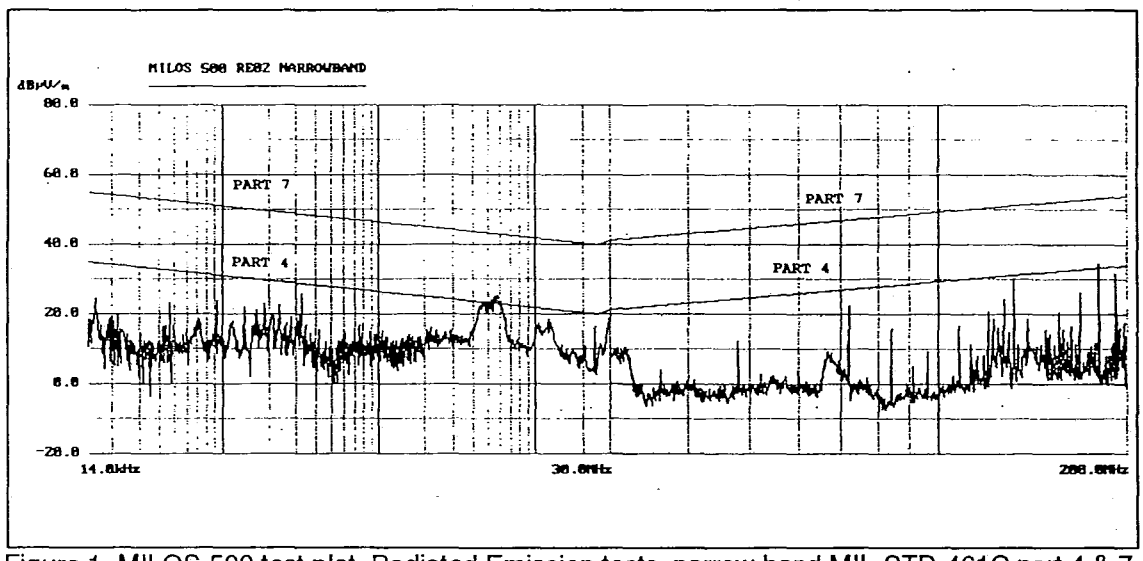

Figure 1. MILOS 500 test plot. Radiated Emission tests, narrow-band MIL-STD-461C part 4 & 7.

SELF DIAGNOSTIC

Self diagnostic and remote diagnostic features are valuable part of MILOS 500 system. All the station modules have their own EEPROM memory for possible fail information. If the system software detects something being wrong in some of the modules, it writes the FAIL code with time and date stamp onto the board memory. It is then possible to detect the cause of failure more easily.

All the serial numbers, calibration data and fail-codes may be read remotely, if a two-way communication link exists. Software also includes a SERVICE program, which can be switched active remotely. The whole system setup can be checked using this feature.

REAL TIME DIAGNOSTICS PROGRAM

There is one valuable feature, which typically is missing from the previous Automatic Weather Stations of this size. It is the real-time diagnostic program module, which can be activated to any of the four serial ports. Using this tool, user may look at the operations of the real-time database. All the incoming

results from the sensors, values used by the mathematics module, results, messages, status's can be monitored in real time without slowing down the system. All the database items can be monitored. Formats may be of BYTE, REAL, STRING or UNFORMATTED / BINARY.

This software also allows for starting and blocking any of the some 30 individual processes that run in the MILOS 500. If mathematics module does not operate properly, it can be blocked, tested and released, while all the other operations still continue. It is possible to see how serial messages come in, how variables are isolated, how data is passed via the module and stored into the database and how SYNOP code is transmitted to the satellite transmitter, for example.

CONFIGURATION OF THE STATION

MILOS 500 can be used for variety of applications. The YourWay configuration program, that runs on a PC, is used to define the configuration. Then it is loaded into the MILOS station using a direct connection or a MILOS500 internal modem. New parameter files may be loaded into FLASH memory system as parameter files. They can be then activated or just stored for future use. Loading operation does not disturb normal operations of the station. Many of the new program features can even be started without need of resetting or stopping of the on going measurements.

When new software modules are loaded in, the diagnostic system monitors the behavior of the new modules loaded. If some problem occur, six last error codes along with a time stamp are stored into the system memory. If new parameters create a bad problem, the diagnostic's system blocks the faulty modules, and rest of the system continues normally, if only possible.

CONCLUTION

MILOS 500 with all the mentioned properties is a new generation system for demanding applications. It consumes little power, being ideal for remote sites that rely on batteries and solar panels. However it has extremely flexible software system having some 500 kBytes of compiled C-code and a true real-time-operating system. Lot of intelligence is put on power supply section, which is vital. Lightning and EMC issues are covered. Mechanics is made to withstand conditions no man could take. MTBF calculations are available.

Vaisala believes, that it is time for reliable automation. There is lot to do with more accurate and more intelligent sensors, and we work hard on that, too. MILOS 500 is ready for those future sensors, Vaisala's and others. MILOS 500 is step towards open system architecture and offers tools for customizing.

Mobile Measuring Equipment (MME)

Josef Lutmayr
Instrumentenamt München (Instrument Office Munich)
Deutscher Wetterdienst (German Meteorological Service), Germany

Introduction

There is a long tradition for mobile environmental measuring in Deutscher Wetterdienst (DWD). The first trucks for these measurements were installed in the mid-seventies. Meanwhile there are four Mobile Measurement Units (MMU) who use the Mobile Measuring Equipment (MME). These MMUs are spread over Germany.
During the last about two years, a new MMU was established and therefore a new MME was built up.

In this paper I want to show the task of the MMUs, the resulting requirements for MME and the realization of it. Especially we pay attention on two vehicles and on the so-called 'temporary stations', which have been build up in Instrumentenamt München (IAM), see the pictures at the end of this paper. Finally I will point out further possibilities of development.

Origin and tasks of MMU

According to the growing sense for environmental problems, it has arisen considerable legislation, which caused many tasks for DWD as a federal institution and as a neutral testifier. In it, there are a variety of tasks for the MMUs. The main categories will be shown here:

- Country and regional planning
  e. g. State and changes of the climate
- Planning and testification of sites
  . industry
  . power stations
  . waste disposal sites
  . sewage plants
- Planning of traffic
  . roads
  . airports
  . railways
  . Water-channels
- Planning of towns and buildings
  . land utilization
  . redevelopment (Sanierung)
- Smog-warning service
- Science
  . International campaigns, e.g. UNESCO: 'Man and Biosphere'
  . cooperation with research institutions, universities and foreign meteorologic services
- Public-relations
  To show the work to public and to potential customers
- Additional tasks
  . substitution for cases of breakdowns,
  e. g. aerological station
  . comparing measurings of different systems
  . support of special measuring-networks, health resortclimatology(Kurort-Klimatologie)

From these categories come out many tasks that induce a lot of requirements to the MME.

Requirements to a MME

Under response of the Central Office (CO) and in collaboration with the users and the builders a conception of MMUs was developed which contents a nominal conception of the MME.
First I will show this conception and afterwards I will present the resulting requirements.

The main-task of the MME is the collection of meteorological, climatological measuring data of relevance. Such as horizontal and vertical profiles of the parameters temperature (T), relative humidity (rh), air-pressure (p) and wind. The horizontal profiles are from special interest at the near earth. These tasks should often be done outside at special places and should be sometimes combined with further parameters like precipitation, special weak winds, radiation or temperatures in the earth. The duration of measurings is very different. They can last some hours and sometimes some years.

To fulfill these tasks, some work had to be done, such as figuring out the measuring equipment with possibilities of its installation and transportation, the accommodation and transportation of staff, the keeping and transportation of required materials and tools. A set of vehicles, each of them with special tasks, has been defined. Contrary to earlier realisations, in which big trucks did keep the measurement equipment, now smaller vehicles have been suggested because of their higher agility. In detail the suggested vehicles have been:

- Profil-Bus (PB)
- Multipurpose-Bus (MB)
- Mobile windfinder-radar
- Car
- Camping-trailer
- Trailer for transportations

Requirements in Detail

Preliminary remark:
During the phases of design and realization of the MME, the requirements have been refined and extended. Therefore, changes in the schedule had been necessary. Apart of technical requirements it was necessary to finish the work in shortest possible time and with a good economic result under conditions of public service.

Profile-Bus (PB)

The so-called PB was destined for getting horizontal profiles of the parameters T, rh, and p. The ranges of the parameters had to meet the meteorological circumstances in Germany. A multitude of requirements had to be fulfilled, from which I will present the most important here:

- Continuous acquisition and storage of the parameters T, rh and p at the near earth, half metre to 2 metres
- coordination of measuring-data with the position
- easy and ergonomic possibilities of configuration the system
- a reliable, cheap and commonly used storage medium
- good data-monitoring
- a working place for a person
- using of DWD-standards in instrumentation and sensors, as far as possible
- installation of a reliable power-supply
- telephone, extra heating and refrigerator-box
- warning facility for measuring at public roads and licence for doing it
- free space for transportation of external used sensor equipment, portable instruments, tools and power generator
- occasional use as a receiver station for aerological ascents

Multipurpose-Bus (MB)

The MB was mainly destined for being a carrier of an aerological ground-station, a basis for balloon ascents included. It should be possible to get vertical profiles of the parameters T, rh, p and the wind. For exact measurings of balloon-positions, the radar-equipment had been suggested.
Here I will show the most important requirements to MB:

- The commonly in DWD used aerological system should be used as far as possible
- installation of an additional working place
- installation of a reliable power-supply
- telephone, extra heating and refrigerator-box
- free space for transportation of all equipment for balloon ascents, some materials like balloons, gas, radiosondes, radar-reflectors and additional tools
- use for transportation of additional staff-members
- occasional transportation of some TS

Equipment for temporary, stationary measuring (TS)

The TS are destined for temporary limited measuring, which normally last from some hours to some years. Generally such measurings have to be done at sites where no connections to public power-supply are possible. Necessarily the need of maintanance for TS should be a minimum. Therefore the handling should be easy and they should have many possibilities of configurations. The most interesting physical parameters are:

- T
- rh
- wind (speed, direction; Scalar and vectorial averaging), special weakwind measuring

Further parameters should be included if necessary, like precipitation, radiation or air-pressure.
The common height of measuring is 2 metres and for wind also 10 metres. Actually there is growing interest in measuring the gradients of T and rh. Therefore, the additional heights of 1/2 metre and 10 metres are required for these parameters.

Realisations

Profil-Bus

All requirements have been regarded for realisation and they have been mostly fulfilled.
Essential details now will be reported.
The basis of all installations is a bus-vehicle of the typ VW T4 Kombi.
The sensor-equipment for T are electrical platinum resistors of the typ Pt 100. They are also used in two electrical psychrometers that serve for measuring rh. Additionally a capacitive hygrometer-sensor is installed for purposes of control and of quicker response. The parameter p is destined with the aid of an electrical pressure metre.
The data acquisition and storage will be done by a comfortable datalogger-system, which is controlled by a ruggidized industry-laptop-PC. The storage medium are 3 1/2" floppy disks. They have the advantage of being readable at nearly all PC-computers and so the data-transfer for further utilizations is easy. The laptop-PC is of the same type as the PC of the aerological station, which is installed at MB. In cases of a breakdown they could be exchanged. Some facts produce comfort in data-aquisition. Such things are: Easy possibilities of configuration the system in dialogue, checking the measuring-data to plausibility-limits or the graphical display of data on demand.
The datalogger is able for acquisition of a rich variety of digital and analog signals and it could be extended to a maximum of 64 channels.
The localisation of measuring data happens with the aid of a tachometer-pulse-system, which turned out as economical and practical. The use of a GP-system was discussed. As a high resolution ($< \pm$ 10 m) was required, only a differential-GP-system was thought to be able to fulfill these requirements. The relation of advantage and costs was not convincing.

An additional power-supply for measuring-equipment is based on 12 volts dc. The sources are an extra onboard-generator, a portable generator for 230 volts and the possibility of a connection to the public power supply.
For an occasional use as a receiver station for radiosondes, an adequate antenna was installed. After exchanging the PC-systems of PM and MB or after extension the laptop-PC such a use is possible.

Multipurpose-Bus

The requirements have found a far degree of realization.
The basis of the installations is a bus of the typ Mercedes 310 D, which turned out as an economic solution with good logistical infrastructure. The MB was formed to fulfill the requirements of measuring and also these of transportation people and materials. Beside of the driver, there are three additional places for persons and also possibilities of transportation some TS. The main equipment for measuring vertical profiles, is a PC ground station that consists of a portable industrial laptop-PC including an integrated UHF-receiver, a so-called SPU-card and a softwaresystem. Additionally a reading facility for punched paper tapes, an external omnidirectional antenna and a ground check set for recalibration the sensors (T, rh) of radiosondes is necessary. The laptop is installed in a drawer of a 19" rack and can be activated easily. For the purpose of balloon ascents, there are integrated things like filling facility, metre for gasvolumina, the gas helium and some balloons, radiosondes and radar-reflectors.

The measuring of balloon position in the free atmosphere can be done with the radar equipment, an additional vehicle of MME, or with the aid of two optical theodolites.

Balloon ascents in series, which can last for many hours, cause high demands to the power supply. The power supply of MB consists of three circuits and is based on 12 volts dc. One of it is selectable for measuring purposes only. The sources of this board net are: The light-dynamo, a photovoltaic facility with its collectors on the roof of the MB, connection to external 230 V power supply and a portable emergency generator.
There are some further remarkable installations, like extra heating, refrigerator box, two additional working tables, and a portable telephone.
The transportation capacity for TS includes places for installation tools. Further there is a case with an emergency set of nonelectric instruments consisting of a thermometer, a mechanical anemometer and a sling psychrometer.

Temporary Stations

In the centre of data acquisition is a datalogger (DL) with five channels. The storage medium is a magnetic card. The DL normally works on 12 V accumulators for a typical time of one month. It is configurable in dialogue and it can fulfill the requirements mostly. It is possible to select many different intervals of measuring and everaging and you can choose different sets of sensors. For example it is feasible to measure vectorial and scalar wind and also the parameters T and rh. Alternatively the use of instruments for measuring precipitation and air pressure is possible and also the measuring of gradients of maximum 5 temperatures. If required the number of channels could be extended. Restrictions exist at low temperatures. Because of the capacity of battery , the heating of sensors (wind, precipitation) is not possible and has to be installed separately if required.
What sensors do we use?

For measuring **rh** we use a capacitive sensor and for temperature we have resistor-thermometers of typ Pt 100. These sensors are installed in radiation protective shelters. Windspeed is gotten by an cup anemometer and the wind direction is measured by an windvane with potentiometer scan.

There are some strained ten-metre telescopic masts in use and some two-metre poles.

Future Possibilities

New technical possibilities, changes in requirements and economic facts will influence the MME. I will hint some points of interest:

- For TS: Support of power supply by photovoltaic facilities

- Required improvements for PM:
  . Sensors with low time constants could enable faster driving-speed.
  E.g. optical rh measurements (Lyman Alpha, photoacoustical methods, ...), thermistors,

  . Better accuracy for rh at low temperatures.
  E.g. optical methods and dewpoint hygrometers together

  . extended tasks like measuring the state of road surfaces
  e.g. IR-measurings

- Further requirements can result from environmental measurings like pollution gases or dusts in stationary or mobile way.

- The use of radio-theodolites instead of radar seems to be cheaper if not too many balloon rises are necessary.

- Measuring of vertical wind- and air-temperature profiles with SODAR or LIDAR

Profil-Bus

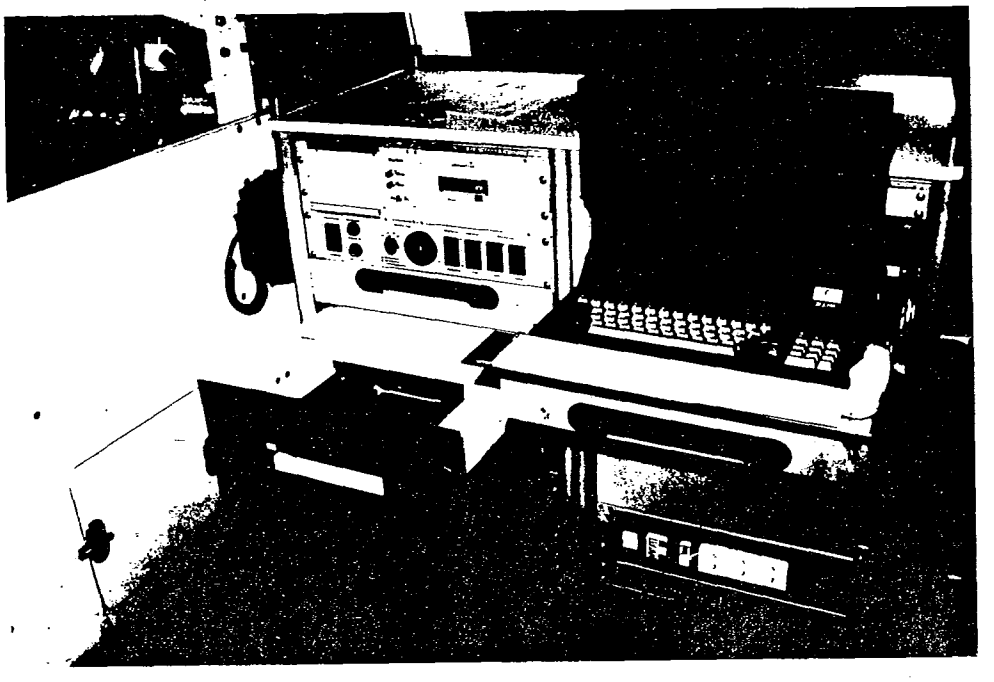

Data-Acquisition

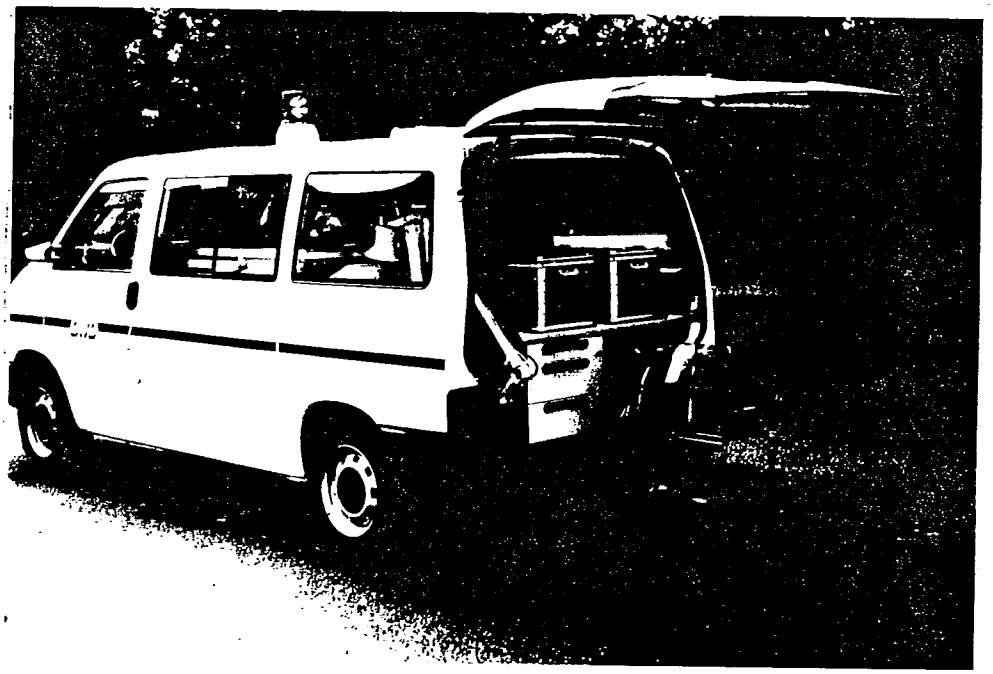

Profilbus

Multipurpose-Bus

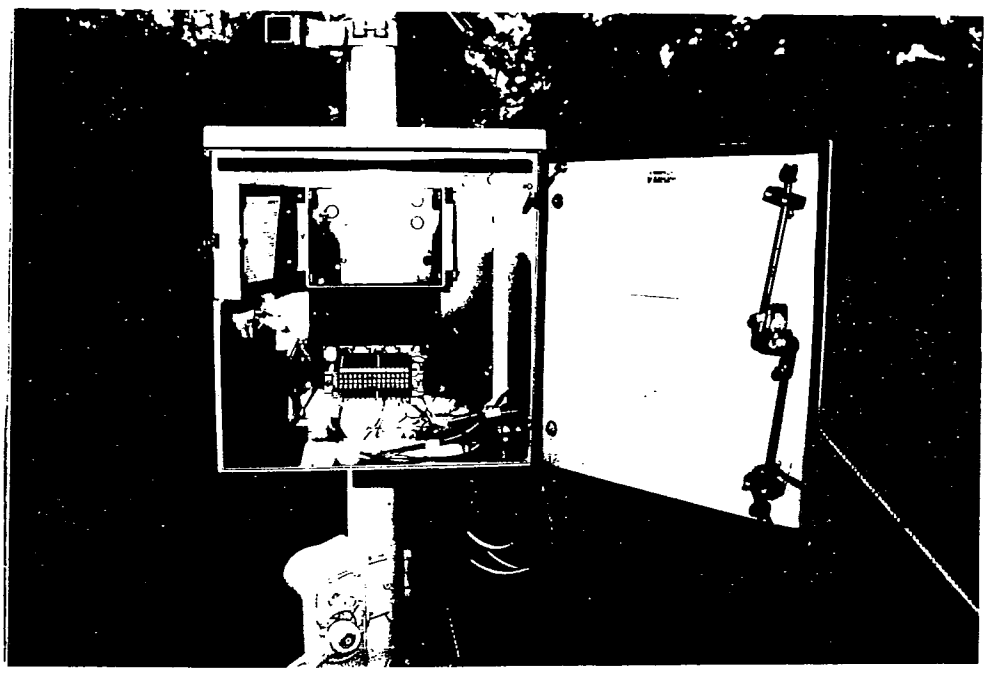

Temporary Station
(Datalogger)

NEW SHIP RAIN GAGE

L. Hasse, M. Großklaus and K. Uhlig
Institut für Meereskunde, Kiel, Germany

Introduction

Measurements of precipitation at sea are an important part of the WCRP and GAW. Life on earth crucially despends on water supply. The hydrological cycle is intimately linked with almost all aspects of climatic change. Precipitation at sea forms by far the strongest branch of the hydrological cycle. Yet, undisturbed precipitation measurements at sea, except from a few stations at small islands, are practically not existent. We hope that in future numerical weather forecast models and satellite remote sensing methods will provide improved precipitation estimates for the world oceans. However, precipitation estimates from weather forecast models and satellite remote sensing algorithms urgently need ground truth at sea, as do ground based remote sensing methods, e.g. seaward looking radars.

The present note deals with a specialised mechanical ship rain gage that was developed at Institut für Meereskunde Kiel in order to overcome the difficulties for rain measurements at sea from moving ships. Our contribution today is an update of earlier reports that we have delivered at other WMO meetings. We believe that now, after a number of years of tests and improvements and after two years of routine use, the ship rain gage reliably can be used at other ships. To my opinion, the time has come to introduce ship rain gages at voluntary observing ships.

Conventional rain collecting instruments fail when used at buoys or ships. The problem stems from the rather high flow velocities around rain gages at ships, that may result from addition of wind and ship velocities. This yields to two sources of biases:

(i) The flow around the ships superstructure may induce spurios vertical velocities and enhanced or reduced speeds at the location of the equipment, leading to under- or overcatch.

(ii) The flow around the raingage for most conventional types of raingages tends to carry the rain above the orifice of the gage, leading to a wind speed dependent undercatch.

Of these two sources of error the first one is easier to deal with. The effect of flow distortion from the ships superstructure can be alleviated somewhat by suitable siting of the instrument, say above the flying bridge, where the flow might be expected to be nearly horizontal (Austin and Geotis, 1980). Also, the measurement technique could make the instrument less susceptible to high speeds and to local up-/or downdrafts.

Basic principle

Our ship rain gage is designed to enable rain fall measurements from moving ship where relative wind speeds of 10 to 20 m/sec are not uncommon. The high relative flow velocities may carry the rain almost horizontally over the ship. We have therefore fitted the instrument with a lateral collecting surface. By measuring the amount of water collected at the side, a correction for the wind speed effect is possible. It is evident that the local relative wind speed at the site of the instrument needs to be measured simultaneously.

The lateral collecting surface measures liquid water content in the volume of air that is formed by the cross-section of the gage and the local relative windspeed. From the liquid water content of the air, the rainfall rate can be estimated by assuming a raindrop size distribuion. The horizontal orifice measures rainfall like any landbased conventional raingage. We have taken care to reduce the wind induced errors by an improved aerodynamic design. From the informations of the two collecting surfaces, considering local flow velocity, the rain fall rate can be determined.

Technical realisation

In our design, the horizontal orifice of a conventional raingage has been supplemented by a cylindrical lateral collecting surface (figure 1) . The water amount from both surfaces is collected separately, and measured by forming and counting drops of calibrated size. The aerodynamic shape of the instrument was designed to reduce the undercatch resulting from flow distortion by the gage itself. Specially, the upper part, that forms the horizontal orifice, roughly corresponds to the champagne bowl design recommended by Folland (1988) but has a more slender shape and less wind resistance.

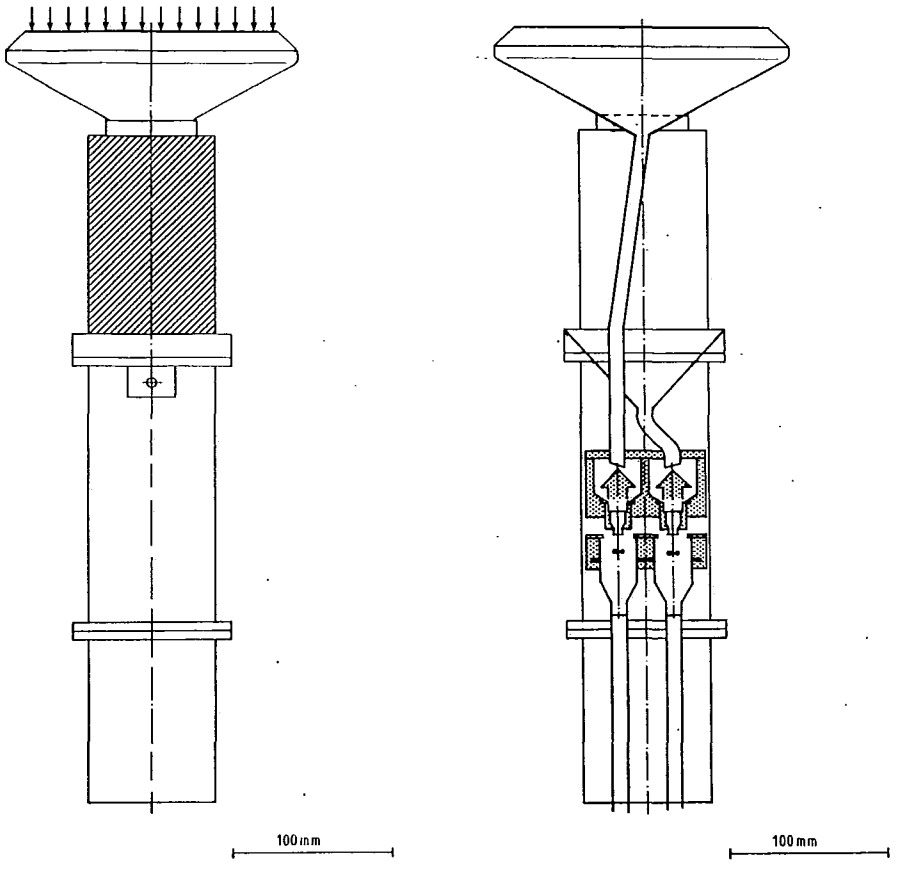

Figure 1 Side view and vertical cross-section of the ship rain gage
Rain is collected at the horizontal orifice (arrows) and at the lateral collector (shaded). There are 5 vertical T-bars at the circumference of the lateral collector that hinder rain water to wander around the cylinder and be blown off in lee (not shown in the diagram). Horizontal sampling area is 200 cm^2, and lateral sampling cross-section 106.6 cm^2. Total length is 48.5 cm and weight 4.0 kg

Calibration

The calibration of the ship rain gage depends on the flow around the instrument. Even with the improved aerodynamic shape, some wind influence on the catch with the horizontal collector is expected (Sevruk, 1989), and an empirical calibration is necessary. The catch of the liquid water content at the side also depends on the aerodynamics of flow around the cylinder. Its effective cross-sectional area needs not equal the geometric cross-section. Hence, we calibrate the ship raingage in the field in natural rain. Calibration is obtained in situ by simultaneous measurements with an optical disdrometer by steaming the ship in the wind. An example of such measurements is given in figure 2. The correlation appears to be rather good. There is some unevitable scatter due to different sampling characteristics: According to our experience, the scatter is mainly due to the sampling variability of the optical disdrometer: Its active cross-section is by a factor of four smaller than that of the ship rain gage. When we assume that the unexplained error variance is distributed 4:1 between disdrometer and ship raingage, we arrive at an sampling error of roughly 7% for short term averages (8 minutes). Hourly or daily totals will be considerably more stable. The in field calibration also allowed to check the performance of the upper and sideward collection separately. It was found that at low wind speeds the measurements by the upper orifice are more accurate, while at higher relative wind speeds the lateral collection performs better. Hence, we use one or the other collecting surface according to wind speed with a linear transition between 9 m/s and 11 m/s. It may be mentioned that the drop forming devices are rather linear and agree with each other up to a rain intensity of about 60 mm/h. For higher rain rates calibration is possible, but behaviour of individual drop formers differs.

Results

Comparisons of the ship rain gage have been conducted both at sea against ship borne optical disdrometers and at land against standard meteorological rain gages. The intercomparison at land has been made at the test site of the Deutscher Wetterdienst at Harzgerode. There the ship raingage was mounted such that the horizontal orifice was at 1 m height above the ground. The same height was used with the standard Hellmann type recording rain gage of the weather service. Additionally, a Hellmann rain gage in a pit, with its orifice level with the surrounding ground, was used.

Hellmann rain gage	**ship rain gage**	**pit rain gage**
1 m	1 m	ground level
459 mm	494 mm	498 mm
92.2 %	99.2 %	100 %

Table 1: Comparison of rain gages at the precipitation test site of Deutscher Wetterdienst Harzgerode, January through November 1993. The intercomparison is based on daily averages, cases with solid precipitation are excluded. Since the mean wind speeds measured at 1 m height rarely exceeded 5 m/s, only the measurements from the upper, horizontal orifice are considered.

Our design of the upper part of the instrument is very similar to the shape of a precipitation gage, that independently has been developed by Wiesinger (1993) for alpine use. Hence, our results are perhaps somewhat more gerneral than expected from the title of this lecture. With regard to the deployment of the gage at a ship it is worth noting that the measurement of the liquid water content at the side is independent of local up- or downdrafts. The catch by the horizontal orifice can be influenced by local up-/or downdrafts, depending on the drop-size distribution. This requires to place the instrument above the superstructure of the ship in order to minimize influence of local ship induced velocities. In order to deal with ship roll motions in a seastate, the instrument is suspended to swing freely around an axis parallel to the ship's long axis.

The instrument output provides counts of calibrated drops from the top and from the side. Typically, these are recorded together with the counts of a cup anemometer (and auxiliary data like date, time, position of ship) on a PC. Basic recording time unit is 2 minutes. For this time, rainfall rates are calculated for the top and the side separately and a corrected rain fall rate is obtained as a wind speed dependent weighted average.

Optical disdrometer

For calibration of the ship raingage we use optical disdrometers that have been built at our laboratory. The principle of operation is light extinction. Each drop passing through the active volume results in a reduction of light proportional to its cross-sectional area. Minimal detectable size of droplets is 0.32 mm. Each drop is measured separately and recorded with a resolution of 0.05 mm diameter to form a droplet size spectrum. The rain rate is determined from the droplet spectra by assuming terminal fall velocity of the drops according to their size. Our optical disdrometer uses a cylindric active volume, that is hold perpendicular to the local flow direction by aid of a wind vane. The cylindrical form makes the measurement independent of the incidence angle of the rain drops. Hence, local up- and downdrafts do not influence the measurements. The sensitivity of the optical volume can be calibrated quite accurately, hence the disdrometer can be used to calibrate the ship rain gage under natural conditions.

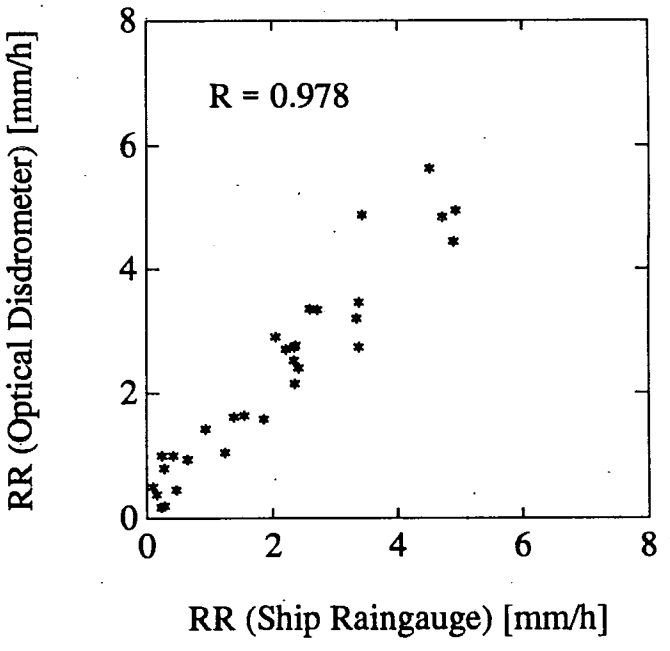

Figure 2: Calibration of ship rain gage against optical disdrometer from a cruise with R.V. ALKOR.
Time interval is 8 minutes. The scatter is mainly due to sampling characteristics of the optical disdrometer and reduces with longer averaging times.

It is anticipated that under windy conditions the standing Hellmann will experience some undercatch as a result of flow distortion, and that the measurements in the pit can be used as a reference. The results of the intercomparison of the earlier version of the ship raingage were given in Hasse et al (1993), they showed a surprisingly good agreement of our instrument with the pit raingage. The intercomparisons obtained during 1993 at Harzgerode are given in table 1. Unfortunately, situations of higher wind speeds with rain are rare, even at the exposed site of Harzgerode (in the Harz mountains, station height about 440 m). It shows that the ship rain gage compares well with the pit measured rain amount, better than the standard "Hellmann" does. Because of the moderate wind speeds, the comparison pertains to the upper, horizontal collector only.

Conclusion

We have shown the feasibility to measure rain at moving ship with a specialised ship rain gage. Calibration is obtained by use of optical disdrometer in natural rain. An intercomparison at land showed improved performance of the ship rain gage compared to standard rain gages, due to improved aerodynamic design.

Our ship rain gage has now successfully operated at R.V. METEOR for two years. We feel assured that we can recommend this ship rain gage to WMO for introduction to operational use at ships.

Acknowledgement

We thank the Deutsche Forschungsgemeinschaft for funding the development of the ship rain gage and the optical disdrometer as a contribution to WOCE. The Deutscher Wetterdienst kindly hosted our ship rain gage at its site in Harzgerode and provided the intercomparison data. The work of station manager Rönsch is appreciated. Also, we thank the personnel of the Deutscher Wetterdienst at R.V. METEOR who care for the operation of the ship rain gage.

References

Folland, C.K., 1988: Numerical models of the raingage exposure problem, field experiments and an improved collector design. Q.J.R.Meteorol. Soc. 114, pp 1485 - 1516.

Hasse, L., Großklaus, M., Isemer H.-J. and K. Uhlig, 1992: New instrumentation for measurement of precipitation at sea. In: Instruments and observing methods, Report No. 49, Geneva. WMO-TD - No. 462, pp 195 - 198.

Hasse, L., Großklaus, M. and K. Uhlig, 1993: Measurement of precipitation at sea. In: B. Sevruk and M. Lapin (eds.): Precipitation measurement and quality control. Slovak Hydromet. Inst., Bratislava, and ETH, Zürich, pp 36-41.

Sevruk, B., 1989: Precipitation measurement. WMO/LAHS/ETH Workshop on precipitation measurement, St. Moritz, Dec. 1989. ETH Zürich, pp 584.

Wiesinger, T., 1993: Improved design of precipitation gages based on aerodynamic principles. In: B. Sevruk and M. Lapin (eds.): Precipitation measurement and quality control. Slovak Hydromet. Inst., Bratislava, and ETH, Zürich, pp 143 - 147.

A STREAMLINED COLLECTOR FOR PRECIPITATION (ASCOP)

Thomas WIESINGER and Werner KRONEIS

KRONEIS, manufacturer of meteorological equipment
Iglaseegasse 30-32, A-1190 Vienna, Austria

Introduction

Conventional precipitation gages with a cylindrical shape are a barrier in the wind field and cause the air flow to separate from the rim, to alter its direction and to accelerate as it passes over the opening (Sevruk et al., 1989). The consequence of this aerodynamic blockage is a deficiency in catch, because the trajectories of hydrometeors are deflected away from the opening. The problem increases in severity as windspeed increases and as the falling speed of the precipitation decreases. Thus, undercollection is greatest at high windspeeds, and for snow and fine rain as opposed to larger sized raindrops.

The aerodynamic performance of exposed precipitation collectors depends on their relative depth, the ratio of depth to radius (aspect ratio), the size and shape of the rim (Sevruk et al., 1989) and upon other details of their shape. Reducing the depth of the collector reduces the displacement and acceleration of the flow over the opening, by reducing the aerodynamic blockage caused by the collector (Hall et al., 1992). If a precipitation collector is to make use of reduced depth in order to improve the flow characteristics over the opening, it must be quite shallow. The aspect ratio would need to be below 0.25 and preferably below 0.1 (meaning: for a 20 cm diameter collector, the depth should be below 10 cm, preferably below 4 cm). The aspect ratio of ASCOP is 0.66, compared to 3.79 of the Austrian standard gage (Paar AP 23).

The precipitation collectors presented here are instruments for the measurement of all forms of precipitation with collector and container separated in order to reduce the aerodynamic blockage of the collector. By applying the principles of an airfoil or wing design, it is possible to redistribute the disturbance between the upper and lower surfaces of the collector, thus minimizing those over the opening. Acceleration takes place under the collector (there must be an acceleration associated with the barrier in the airflow) and the flow field remains almost unaffected above the opening. The goal is that the trajectories of snowflakes above the opening are not altered by the existence of the gage.

Materials and Methods

The design of a perfect precipitation collector must consider several criteria. It must be capable of collecting and storing snow at least until it has melted. The orifice opening must be a defined, effective size and must have special aerodynamic characteristics, these being small vertical

displacement and acceleration of the wind flow over the opening. The separation of the boundary layer on the collector surface should be horizontal across the opening. A wind-driven circulating flow in the collector must be eliminated and the collector must be as shallow as possible.

The last design feature is based upon aerodynamic considerations and is associated with practical difficulties (e.g. ineffective drainage and limited storage capacity). Thus, deeper collectors are preferred for practical reasons although their aerodynamic performance is not as good.

The design of the collectors was based upon flow simulation of ideal inviscid flow over a Karman - Trefftz airfoil profile (Wiesinger 1993a). In any real fluid, viscosity is present which produces boundary layers, turbulence and separation. Often, however, in the majority of the flow field, viscous effects are small and the flow can be modelled as inviscid, assuming ideal flow. For shapes such as airfoils which are rounded and not too thick, inviscid analysis typically yields very accurate predictions of the velocity field and surface pressure.

The design of ASCOP is also based on investigations and experiences made with similar prototypes (Wiesinger 1993a,b) in Japan. Improvements were made with the installation of the heating device, the use of other materials such as carbon fibre and aluminum instead of polyacetal and wood. Moreover the orifice area has been reduced to 200 cm^2, because experiences from field testing in Japan did not reveal any significant differences in performance between collectors with sizes between 250 and 750cm^2.

ASCOP is being manufactured as both, a heated winter version with overflow drainage system that keeps a heated water bath with a constant level inside the collector, as well as a summer version without water bath which drains via a funnel and tube into a container. The two versions can be exchanged very simply. The water bath inside the container improves the aerodynamic performance, prevents collected snow of being blown out and reduces evaporation which usually occurs when funnels are heated. This evaporation amount can be in the order of 20% of collected snow. A thin layer of oil prevents evaporation of the collected precipitation. We use LV/SM 1036 (manufactured by the Austrian ÖMV) which is a synthetic ester with a density of 0.83 g/ml (at +15°C), a point of congelation of -60°C and viscosities of 130 and 600 centistokes at 0°C and -20°C, respectively. 600 centistokes (at -20°C) corresponds to the state of a standard transmission oil at room temperature.

As can be seen from the figures (1 and 2) the ratio of collector height to its radius has a considerable effect on the flow field. With deeper collectors, the velocity above the collector is lower than the free-stream and the velocity gradients around the collector are larger as opposed to a shallower collector. With decelerated flow over the orifice the collector might actually collect more snow per area than is actually accumulating. Likewise the angle of attack influences the distribution of flow speeds. For a collector which has a ratio of height / radius equal 0.510 the flow speed above the center of the orfice is 0.8 when the angle of attack is zero (horizontal flow). It is 0.61 when the flow comes from 10 degrees below the horizontal and 0.97 when it comes 10 degrees from above the horizontal plane (Wiesinger 1993b).

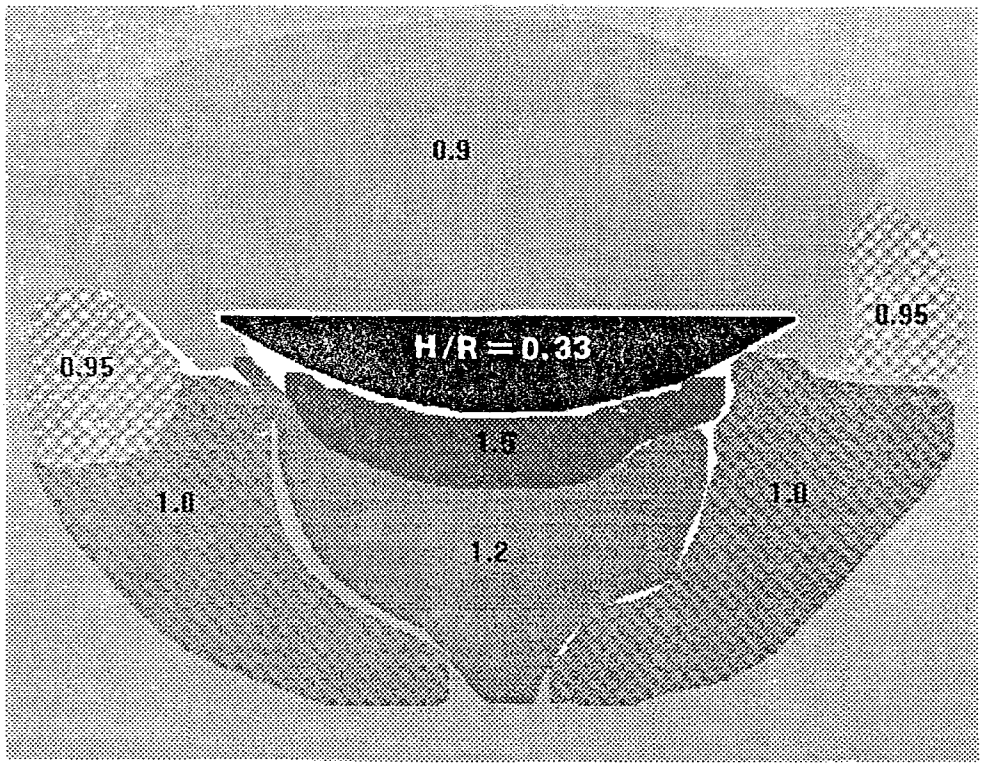

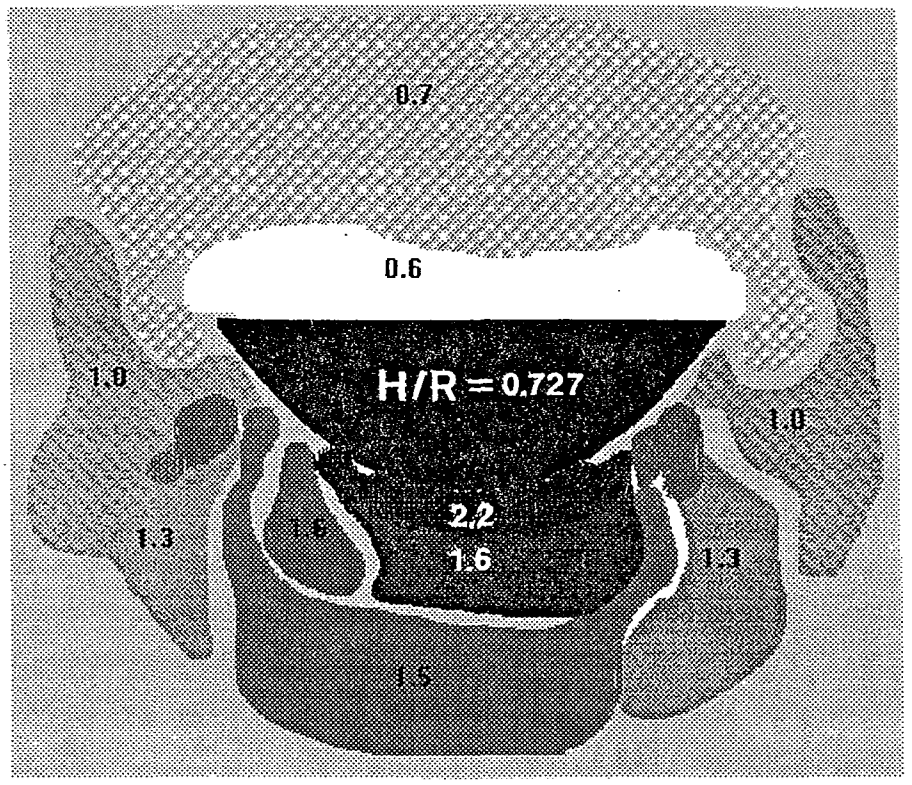

Fig. 1 and 2: Velocity distribution of the airflow along 2 Karman Trefftz airfoil profiles which have a similar shape as the ASCOP. The simulation is made for ideal inviscid flow. The angle of attack is zero (horizontal flow) and the velocity of the free stream is 1.0. H/R is the collector height / radius of collector. The hatched areas show different classes of flow speed, where darker areas stand for faster flow and light areas for decelerated flow. The collector itself is drawn as a black bowl.

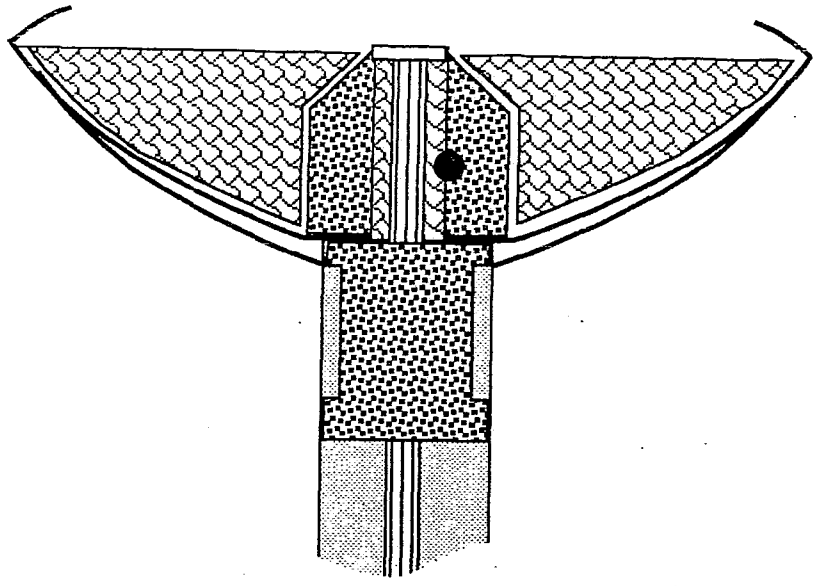

Fig.3: Cross sectional view of ASCOP-winter. The collector is filled with water which is protected against evaporation by a thin layer of oil. The overflow-heater unit in its center prevents oil from flowing down and prevents the drainage system from obstruction by contamination, and it heats the liquid when the temperature gets close to freezing. A Teflon tube drains liquid from the collector when precipitation is added. The liquid is collected in a container which rests on electronic weighing scales.

Results

Streamlined precipitation collectors are less affected by wind than gages with a cylindrical shape. They show a catch much closer to that of the references which are protected against wind than common gages of cylindrical shape.

The predecessor model of ASCOP-winter showed 98% of the catch (mostly snowfall) as compared to the Double Fence International Reference gage, whereas the Japanese standard gage for winter operation (shielded Yokogawa B-071) measured only 78%. The ASCOP-summer (a model with 250 cm^2 orifice area) was set up at 3.5 m elevation and was compared to a ground level gage (reference, collected 100%) and to the Japanese standard gage for summer operation (Yokogawa B 011). The latter measured 87% whereas the ASCOP measured 98%, although being installed in a layer with significantly higher windspeeds (Wiesinger 1993a).

The overflow-heater unit (see Fig.3) is capable of keeping the water bath liquid down to -25°C at a windspeed of 4 m/s with relatively low power consumption.

The evaporation protecting oil (LV/SM 1036) does not evaporate by itself and prevents evaporation of water over 100 days at room temperatures between 30 and 50°C completely.

Conclusions

The gages of aerodynamical superior performance (ASCOP) can be automated and combined with any system of measurement, but only accurate and reliable systems are appropriate. The simplest way is the collection of water in a sealed container that is weighed. With this method evaporation losses are very small and the instrumentation for the collection of rain is comparatively cheap. Thus, this "low tech" instrument is useful for studies on the aerial distribution of rainfall where many accurate gages at a low cost are required. The use of high performance weighing scales appears to be the most reliable method, if a continous data set is needed.

The ASCOP-winter is not as simple as the ASCOP-summer since it needs a power line for the melting of the snow. If electricity is available, the instrument serves well as a collector of rain and snow, even at windy sites. However, the careful selection of a site for precipitation measurement, which is representative and not extremely wind exposed, is still required.

Perspectives for the near Future

We are going to set up three test- and evaluation sites in the Austrian Alps. The sites are sheltered, open and extremely wind exposed, respectively. The performance of ASCOP will be compared to the Austrian standard gage (Paar, AP 23, 500 cm^2 orifice area) as well as to snow water equivalent measurements from the snow board and other prototypes (including a version of ASCOP-winter that does not require power line).

Acknowledgements

We are grateful for the financial support by the "Fonds zur Förderung der gewerblichen Wirtschaft" of Austria.

References

Hall, J.D., Irwin, J.G., Stone, B.H. and Upton, S.L.(1992): Aerodynamic considerations in precipitation collector design. National Measurement System Symposium, Airborne Pollutants Measurement, March 17-18, 1992, Warren Spring Lab., Stevenage, U.K.

Sevruk, B., Hertig, J.-A. and Spiess, R. (1989): The effect of precipitation gauge orifice rim on the wind field deformation as investigated in a wind tunnel. Atmospheric Environment, Vol. 25 A, No. 7. p.1173-1181.

Wiesinger, T. (1993a): Improved design of precipitation gages based on aerodynamic principles. in: Precipitation Measurement & Quality Control, Sevruk, B. & Lapin, M. eds., Proc. of the Int. Symposium on Precipitation and Evaporation, Bratislava 1993, Vol.1, p.143-147.

Wiesinger, T. (1993b): Accurate measurement of snowfall - development of two innovative precipitation gages based on the analysis of existing errors. Dissertation, University of Vienna, Institute of Meteorology and Geophysics, 230pp.

WMO (1985): International Organizing Committee for WMO Solid Precipitation Measurement Intercomparison, 1st Session, Norrköping, 16-20 Dec. 1985, Final Report, 32pp.

EXPERIENCE WITH AUTOMATED METEOROLOGICAL MEASUREMENTS IN SLOVAKIA

Branislav Gajar, Elena Nieplová,
Dušan Jakubík, Ján Danč
Slovak Hydrometeorological Institute,
Bratislava, Slovakia

1. Introduction

Growing requirements for exact, high-quality and frequent meteorological information and requirements for information from unsettled locations led to development of many automatic weather systems (AWS).The development of its own automatic system started in the Slovak Hydrometeorological Institute in the 1980s. This system is still in operation for continual measurement of solar radiation. The main deficiency of this period was the fact that due to the isolation of our country s economy the advanced technologies could not be utilized in the development. Adaptation of the AHS (automatic hydrological system) for meteorological purposes was a further attempt done in this field.

Almost independent from the measuring systems the process of checking, processing, coding and storing of data has been automated.

At the beginning of the 1990s the work has been started on the connection of both systems and on the creation of automatic system for data measurement, checking, reports preparation, telecommunication, data presentation and storing.

2. Architecture of System

Automatic measurement system, which at present is in the experimental operation in the Slovak Hydrometeorological Institute s network, allows automatic measurement of some meteorological parameters and additional data not currently observed by the AWS can be entered via PC keyboard.

The system consists of the data logger (ESC 8800E), which is also equipped with software for mathematical and statistical processing of measured parameters. The data are transmitted from the data logger to PC at observer s work-station through the RS 232 serial port. Sensor of atmospheric pressure is connected with PC also through a serial port. Data logger has 16 differential analog programmable ports, the raingauge entry, 8 digital ports, the 32 kB RAM, the 64 kB ROM, the battery backup of clock and memory and two RS323 ports.

The following sensors of meteorological parameters are connected to the datalogger:

a) air temperature, soil temperature - the NTC linear thermistors, extent of measuremnt -40°C - +60°C, accuracy 0.1°C
b) relative air-humidity - capacity sensor, extent of measurement 0 - 100%, accuracy ± 2%
c) precipitation - tipping bucket raingauge, heated orifice 500 m^2, resolution 0.1 mm
d) wind speed and direction - extent of measurement: wind speed 0-60 m/s, direction 0-360°
e) sunshine duration - based on photoelectric principle, heated, output parameter TTL, sensitivity threshold 120 W/m^2
f) measurement of the height of water level in evaporation pan, resolution 0.3 mm, extent 142 mm
g) air-pressure - extent 500-1060 hPa, accuracy ± 0.3 hPa

All elements have the same sampling program of 2 s. The parameters of sensors and both the sampling and data processing programs have been made to comply with the requirements for AWS [1]. Measured data are processed by PC software at the observer s work-station at various time levels:

A) 1-minute processing and calculations
   mean values - air temperature, relative air humidity, water vapor pressure, dew-point temperature, air pressure, soil temperature at depths of 5,10,20,50 cm
   sums - precipitation

B) 10-minute processing and calculations
   mean values - wind speed arithmetic and vector average
   - wind direction vector average
   extreme values - maximum and minimum value of gusty wind direction
   - limit values of variable wind direction for the last 10 minutes

C) hourly processing and calculations
   mean values - air and soil temperatures, relative air humidity
   sums - precipitation, sunshine duration, evaporation from water level
   extreme values - maximum wind gust for the last hour

D) further processing

- maximum wind gust for the last 6 hours and for the period 07-07 of local mean time
- extreme values of minute averages of air and soil temperatures for the periods 06-18 UTC, 18-06 UTC, 07-21 and 21-07 local mean time
- sunshine duration per day

- sum of precipitation for the periods 06-18 UTC, 18-06 UTC, 07-07 of local mean time
- evaporation from water level for 07-07 of local mean time

3. Data Control and Processing

Primarily the limits check of input data is carried out:
- air-temperature within the range from -45°C to + 45°C
- relative humidity within the range from 0 to 100%
- wind direction from 0 to 360°
- wind speed:
  gust not exceeding 80m/s
  2-minute average not exceeding 70m/s
  10-minute average not exceeding 60 m/s
- air pressure within the range from (950-0.125H)hPa to (1060-0.125H) hPa, H is elevation of barometer in m
- evaporation within the range 0-20 mm
- precipitation - sums for above mentioned periods not exceeding 350 mm
- soil temperature:
  at 5 cm depth from -20.0°C to + 45°C
  at 10 cm depth from -15.0°C to + 35°C
  at 20 cm depth from -15.0°C to + 30°C
  at 50 cm depth from -7.0°C to + 25°C

Further quality control is carried out during reports and tables making - tests of identification and completeness, internal consistency tests, tolerance tests.

Data files of minute and hourly values created from measured and processed data are stored at observer s work-station PC. In weekly intervals they are transferred on a floppy disk and in monthly intervals they are sent for further processing into central SHMI data bank.

From the data measured and processed by automatic system and also from data manually observed and keying into PC meteorological reports SYNOP, INTER (internal weather reports), CLIMAT, METAR conforming to international guidelines are created. After consistency control and/or correction of report it is transmitted to NTC.

4. Operation of Meteorological Stations

At present 8 AWS are in operation. Their installation at manned meteorological stations allows to add data not measured by AWS (cloudiness, visibility etc.). In case of failure automatic measuring can be replaced by manual measurement. Simultaneous comparison of measurements can be done too. The site for AWS was chosen so as to provide minimum vegetation and building s influence on sensors.

Comparison measurements are carried out at 2 stations located in different orographic conditions. Manual

measurements are done simultaneously with measurements at automatic station in climatological terms:

- extreme air temperatures at 21 and 07 local mean time
- air humidity, air pressure, wind speed and direction, soil temperatures at 07, 14 and 21 local mean time
- precipitation and evaporation for the last day (07-07 local mean time)

Simultaneously with comparison measurements reliability and failure rate of system is being monitored. Preliminary results have not been evaluated for meantime.

At present SHMI experts develop new software for integrated observer s work-station with the following main functions:

- management of automated meteorological and other environmental quality data systems measurement
- measurements, processing, quality control, decision-making and meteorological reports coding
- manual measurements processing - communication with NTC and other measuring points
- presentation of information including graphics
- distribution of received information

5. Conclusion

Automatic measurement and data processing systems have contributed to the extension of information from meteorological stations and improved quality of reports from the stations. With configuration designing, station installation, software designing, sensors testing, failures removing and measurement comparison, technical and science workers of our Institute obtained unique experience and knowledge, which can be used at present and also in the future with measurement network automation.

Literature:

[1] Guide to Meteorological Instruments and Methods of Observation, Fifth edition, WMO-No 8, 1983.
[2] A.Van Gysegem: Guidelines for Standartization of Automatic Weather Stations, WMO, Instruments and Observation Methods Report No. 49, WMO TD-No.462, 1992.

Session II

UPPER-AIR MEASUREMENTS

COMPARISON OF POTENTIAL REFERENCE RADIOSONDE OBSERVATIONS -RESULTS FROM PREFRS -92

J. NASH
Meteorological Office, Bracknell, Berks, U.K.

1. Introduction

The PREFRS 92 radiosonde test was hosted by the U.K. Meteorological Office, at Crawley (WMO Station No. 03 774) for three weeks from 16 February until 6 March 1992. The test was performed under an agreed memorandum of understanding between the U.K. Meteorological Office , NASA, GSFC (USA) and the Swiss Meteorological Institute, Payerne. Fieldwork teams were headed by F. Schmidlin (NASA) and B. Hoegger (Payerne). V.Antikainen (Finland) checked that Vaisala radiosondes were being deployed to the standards expected by the manufacturer. G.Illey (Met. Office) managed the practical aspects of the test. S. Kurnosenko , Central Aerological Observatory, Russia developed the data checking and processing software . This paper presents a very brief overview of the temperature comparison results from PREFRS 92

The purpose of PREFRS was to compare measurements by four radiosonde systems that have good potential as "working" temperature reference radiosondes. Here, a "working" temperature reference will be taken as a radiosonde cheap enough to be used regularly in routine operations , as well as for comparisons and development tests. Experience in radiosonde development, suggests that common operational use is extremely useful, if not essential, to ensure that the radiosondes work reliably in as wide as possible range of weather conditions. The associated ground system should be small and portable, so that the reference can be deployed within a national network or in any region around the world, as required. Ideally , the" working reference" should measure temperature at all pressures from the surface to at least 10 hPa with a reproducibility of better than 0.1 °C (1 s.d.) and with systematic errors less than 0.3°C, stable to 0.1°C in all conditions for groups of 10 flights or more. If different types of "working" reference radiosonde were flown together in radiosonde comparisons, measurements might not agree to ± 0.1 °C , but systematic differences should be stable from one group of 10 tests flights to the next, to better than 0.2 °C.

2. Potential Reference Radiosondes

The Crawley site was chosen for the PREFRS test so that measurements could be compared with those by the U.K. RS3 radiosonde [helical tungsten wire temperature sensor, wire diameter 13 μm]. RS3 observations were designated MK3 in Figs. 1 to 3 . The four potential "working " reference radiosondes examined in PREFRS 92 were:-

- the Vaisala RS-80 radiosonde[aluminised thermocapacitative temperature sensor]. This was operated using the operational PC-CORA ground system at Crawley. All radiosondes were subjected to pre-flight ground checks as recommended by Vaisala. RS80 data were designated MK4 for standard output using the V86 radiation correction scheme and RAW(MK4) when the temperatures were processed without any radiation corrections.
- the Meteolabor SRS-400 from Switzerland [1], [Cu-Const. thermocouple temperature sensors , 0.05 mm diameter]. No radiation corrections were applied to daytime or night-time observations. Following PREFRS, the relationship between observed emf and temperature difference in the SRS-400 thermocouple channels was modified to take account of stray micro voltages . This new relationship was based on laboratory investigations by Meteolabor completed later in 1992,. The data from the SRS-400 were subsequently reprocessed to produce the SWI3 data set used here.
- two versions of "three thermistor" technique radiosondes implemented by NASA [3] [VIZ rod thermistor temperature sensors (size used operationally in the USA) with coatings applied by NASA staff]. In one version , the thermistors were flown on a modified AIR Intellisonde, operating at 1680 MHz, and in the other , the thermistors were flown on a modified VIZ Microsonde II body . White rod thermistor measurements, similar to those used in operational VIZ observations were designated AR1 and VZ1 for AIR and VIZ respectively, with corrected "three thermistor" measurements designated AR2 and VZ2 respectively.

3. Test Procedures and data processing

The test flights (77 in total) were performed in similar fashion to the WMO Radiosonde Comparisons. All systems had automated ground stations, but software deficiencies corrupted the sample timings in some systems. Times were checked by matching significant structure in temperature and relative humidity profiles at 2s resolution, see Fig 1(a). Samples at 1 minute intervals, see Fig. 1(b) and (c), were then edited and

anomalies from ground processing removed (e.g. errors from interpolation during signal loss). The temperature differences presented in Figs. 2 and 3 were then computed from the remaining data .

4. Overall results

Average temperature differences from "3 thermistor" measurements and associated standard deviations are shown in Fig. 2 for pressure layers from 900 hPa to 7 hPa.
At night AR2 and VZ2 agreed within 0.1 °C , and MK3 and MK4 did not differ by more than ± 0.3 °C from the average of AR2 and VZ2 at all pressures. The standard deviations were compatible with "working reference" performance for AR2, VZ2, MK3 and MK4. [Note:- Following the PREFRS test, the design of the connecting wires to the SRS-400 sensor was modified to reduce spurious micro voltages. After this modification, tests in Switzerland in late 1992 found night-time SRS-400 temperatures were offset relative to RS80 measurements by about -0.5 °C at 100 hPa , similar to those of the MK3 in PREFRS.]

However, AR2 and VZ2 measurements in the day differed by more than 0.1°C at pressures lower than 40 hPa with standard deviations also becoming larger than ideal at about the same pressure. Further work is required to optimise the three thermistor technique during the day. AR2 was chosen as the preferred reference for daytime conditions. It was judged that heat conduction to the VIZ temperature sensor from the plastic outrigger used (uncorrected by the three thermistor technique) was probably larger than the heat conduction from the metal outrigger to the AIR sensor. Use of AR2 as a reference produces a plausible linear increase in SWI3 solar heating error with height, namely from about 0.2°Cat 500 hPa to about 1 °C at 14 hPa.

Stratospheric temperature showed little variation throughout PREFRS, but the upper cloud conditions varied considerably from day to day and produced significant variation in the upwelling infrared flux. The influence of cloud cover on night-time VZ1 and AR1 and on all daytime measurements can be judged from Fig. 3 . The average temperature differences for different daytime cloud categories are summarised in Table 1. Night-time 3 thermistor measurements were only made in clear conditions on one flight. The bias of AR1 and VZ1 relative to the other data was similar to that for the medium /low cloud category in Fig.. 2. Thick cirrus produced substantial cooling of AR1 and VZ1, at least 0.4°C on average at night, at pressures lower than 300 hPa. Details of an individual flight are shown in Fig. 1(c), where AR1 and VZ1 measurements cooled by about 0.5 °C relative to the other radiosondes, starting at about a temperature of -40°C in the cloud (minute 24). Cirrus also produced cooling of at least 0.3°C in AR1 and VZ1 daytime observations at the same levels.

Layer hPa	Radiosonde type	Day, clear ΔT (K)	Day, medium level ΔT (K)	Day, cirrus ΔT (K)	Night All ΔT (K)
100-30	MK4-AR2	0.11	0.32	0.28	0.24
100-30	SWI-AR2	0.92	1.13	1.05	0.31
100-30	VZ2-AR2	0.13	0.06	0.11	0.03
100-30	VZ1-VZ2	0.59	0.49	0.22	-0.22
100-30	AR1-AR2	0.64	0.60	0.30	-0.12
30-10	MK4-AR2	0.25	0.65	0.35	0.29
30-10	SWI-AR2	1.22	1.56	1.23	0.41
30-10	VZ2-AR2	0.30	0.31	0.21	0.05
30-10	VZ1-VZ2	0.76	0.47	0.27	-0.47
30-10	AR1-AR2	0.81	0.69	0.27	-0.22

Table 1 Temperature differences with respect to "3 thermistor" temperature measurements, categorised according to daytime cloud cover:- clear, medium level cloud, or cirrus.

5. Conclusions

It is concluded that PREFRS provided useful insights into the performance of several potential reference radiosondes and into the influence of clouds on radiation errors. Improvements to some radiosonde systems have already been implemented . Several radiosonde types have good potential as "working references" at night , but further work is required to improve the compatibility of daytime references.

References

1. B. Hoegger, et.al, 1989, TECIMO-IV, WMO Instr. and Obs. Methods Report No. 35, p197-202.
2. J. Nash, 1992, TECO-92, WMO Instr. and Obs. Methods Report No 49, pp 134-138.
3. F. J. Schmidlin, 1992, TECO-92, WMO Instr. and Obs. Methods Report No 49, pp 129-133.

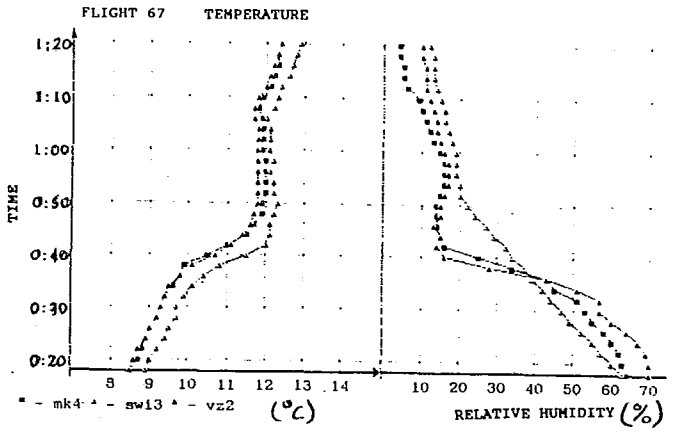

Figure 1[a]

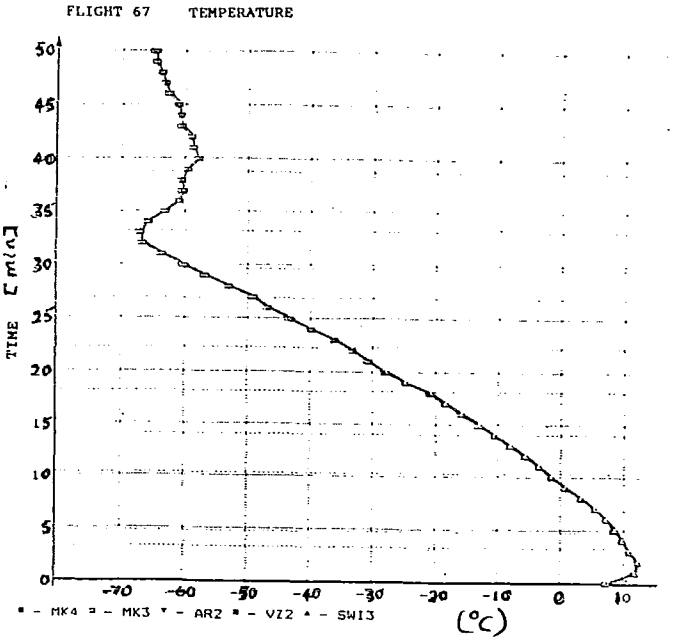

Figure 1[b]

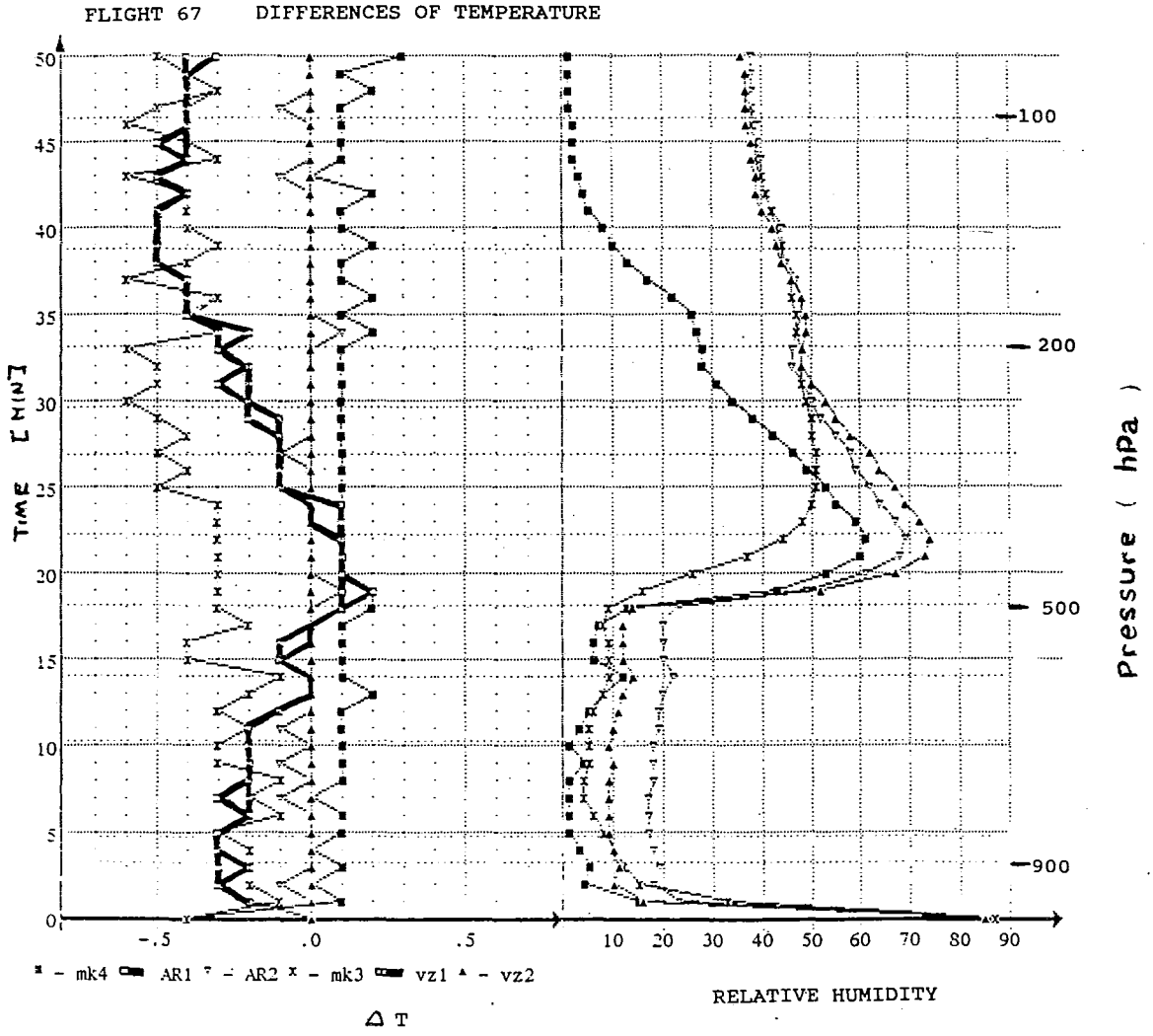

Figure 1[c]

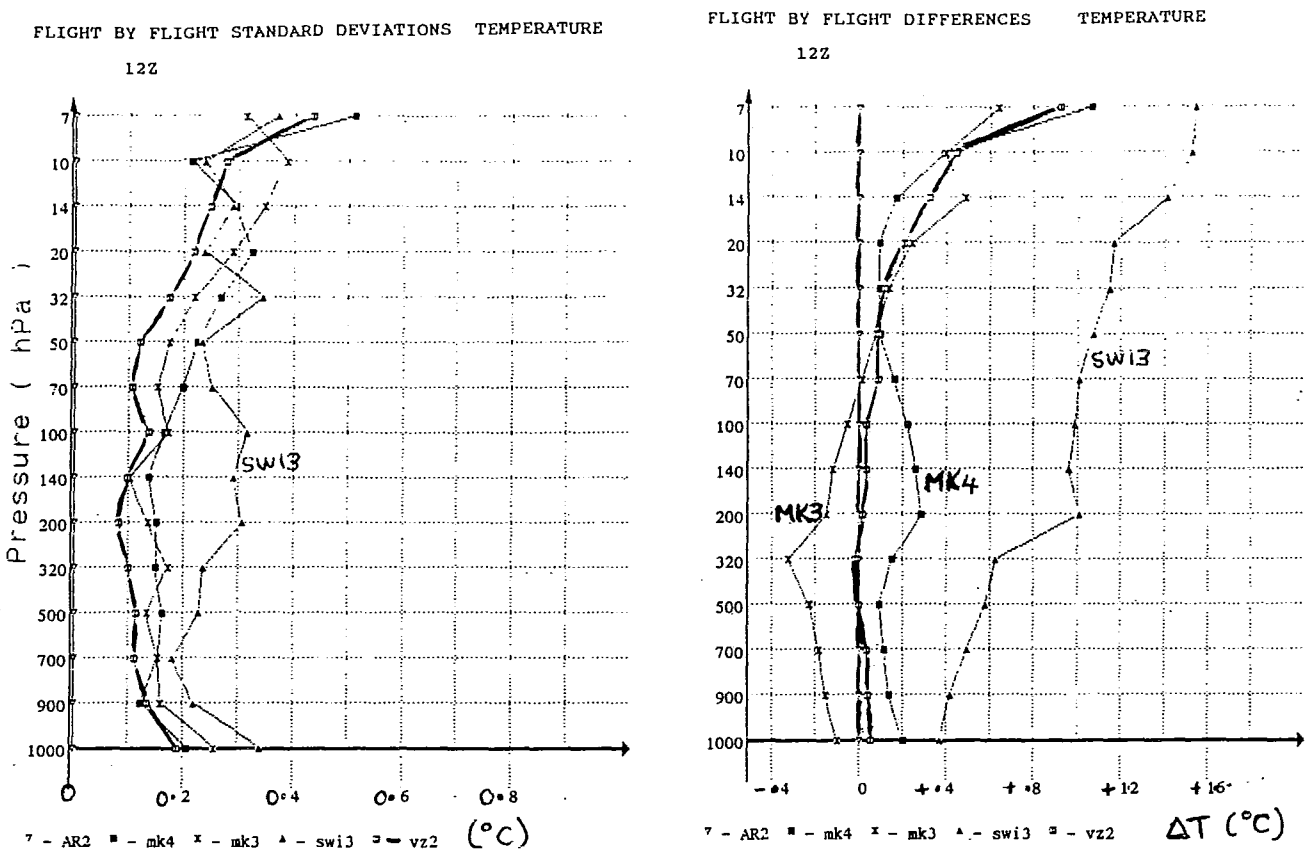

SUMMARY DAY

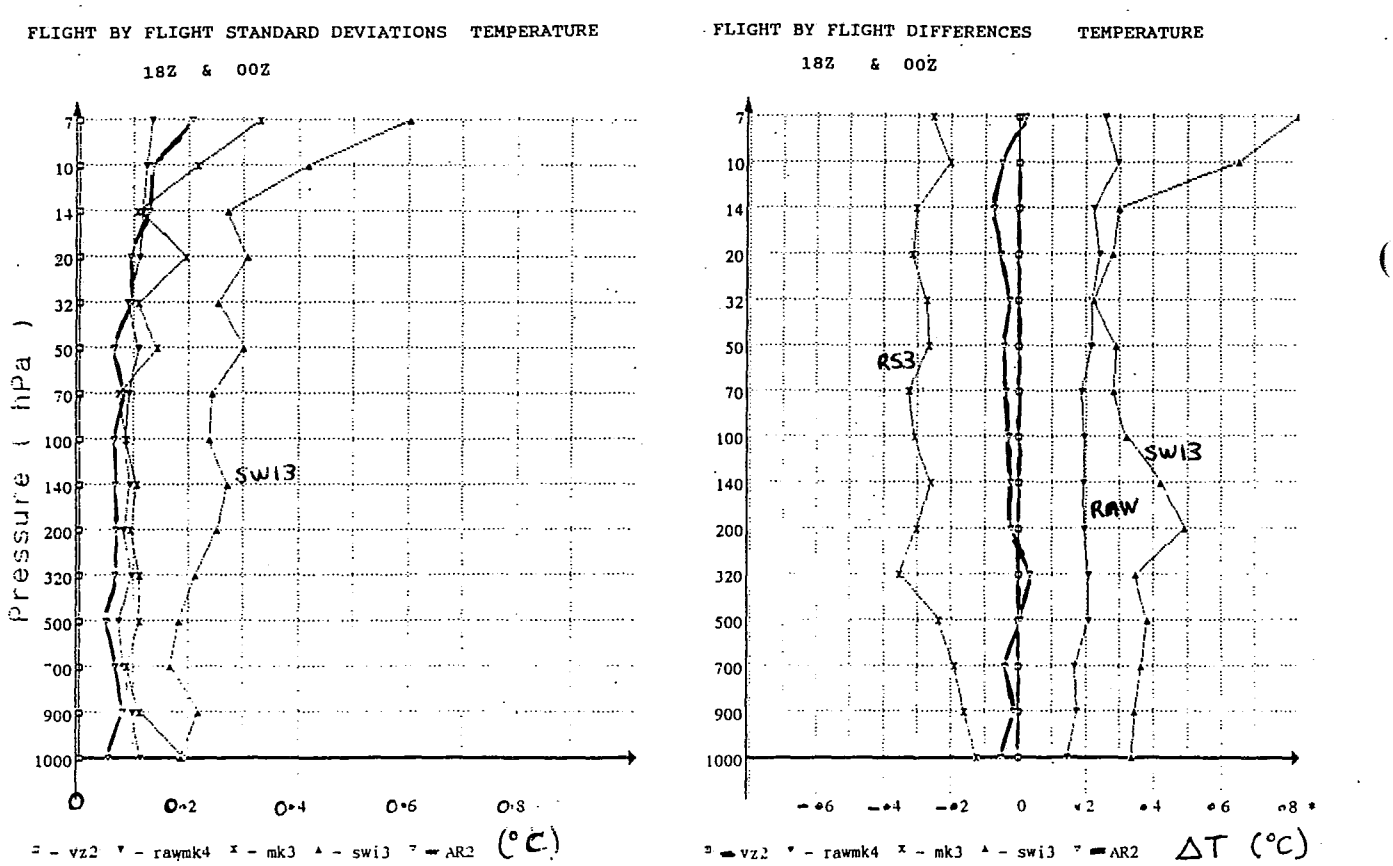

SUMMARY NIGHT

Figure 2

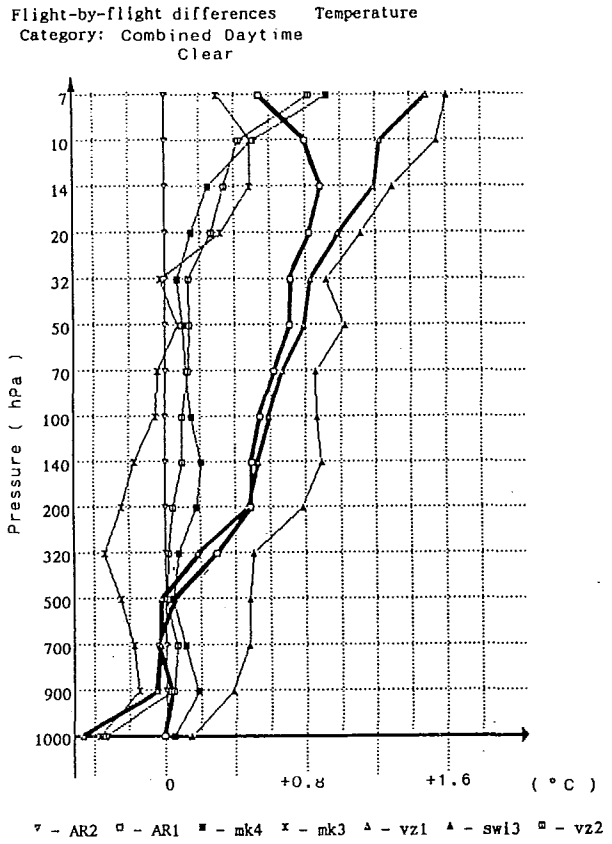
Flight-by-flight differences Temperature
Category: Combined Daytime
Clear
Pressure (hPa)
7
10
14
20
32
50
70
100
140
200
320
500
700
900
1000
0
+0.8
+1.6
(°C)
▽ - AR2 □ - AR1 ■ - mk4 ✕ - mk3 △ - vz1 ▲ - swi3 ⊡ - vz2

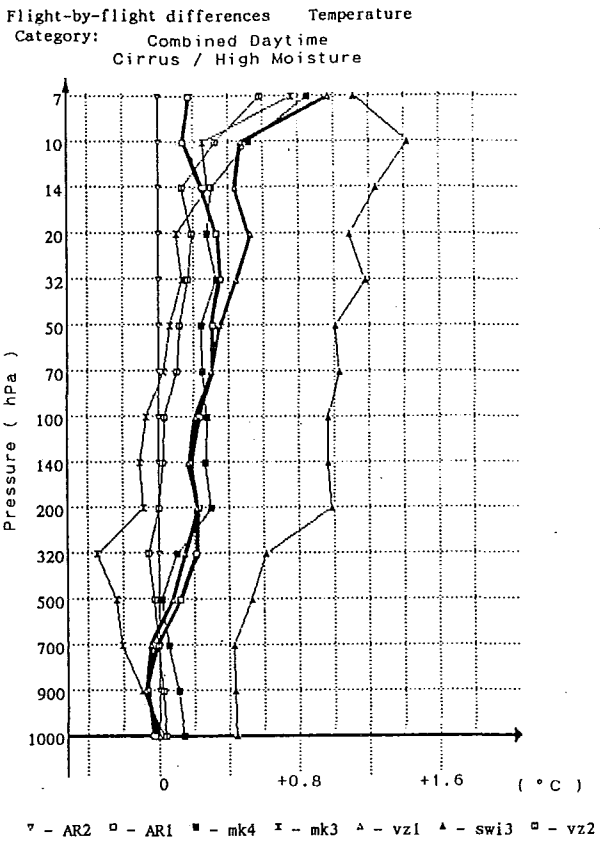
Flight-by-flight differences Temperature
Category: Combined Daytime
Cirrus / High Moisture
Pressure (hPa)
7
10
14
20
32
50
70
100
140
200
320
500
700
900
1000
0
+0.8
+1.6
(°C)
▽ - AR2 □ - AR1 ■ - mk4 ✕ - mk3 △ - vz1 ▲ - swi3 ⊡ - vz2

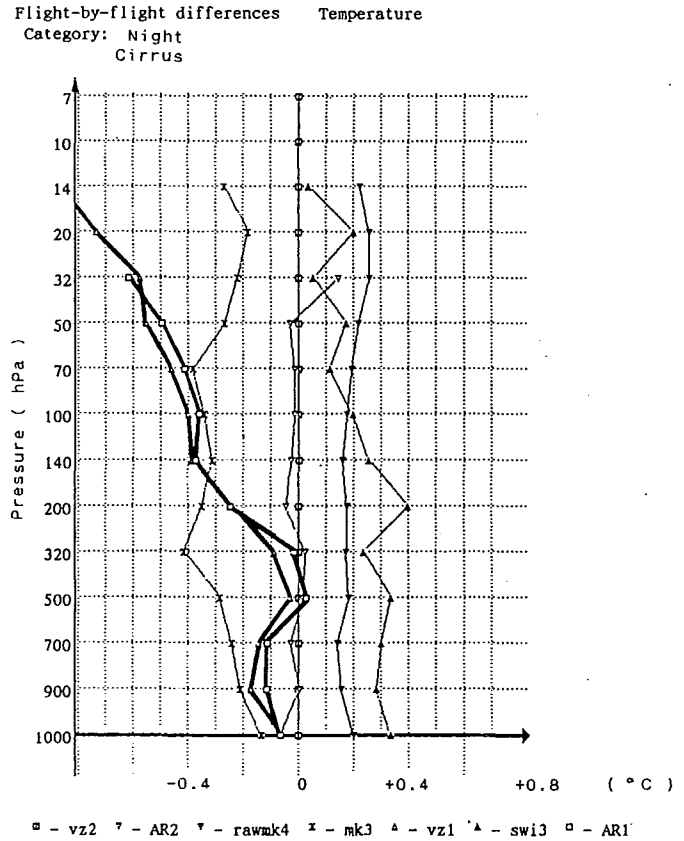
Flight-by-flight differences Temperature
Category: Night
Cirrus
Pressure (hPa)
7
10
14
20
32
50
70
100
140
200
320
500
700
900
1000
-0.4
0
+0.4
+0.8
(°C)
⊡ - vz2 ▽ - AR2 ▼ - rawmk4 ✕ - mk3 △ - vz1 ▲ - swi3 □ - AR1

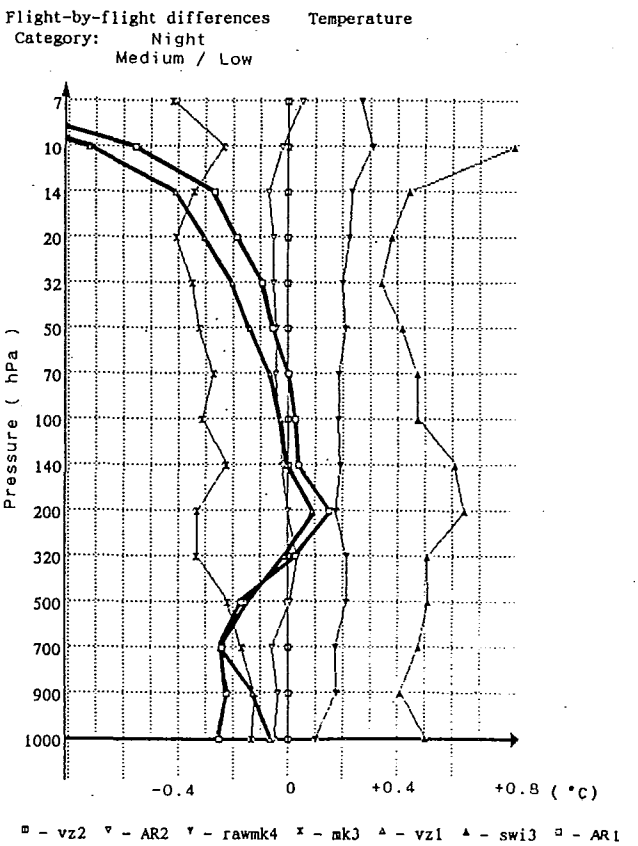
Flight-by-flight differences Temperature
Category: Night
Medium / Low
Pressure (hPa)
7
10
14
20
32
50
70
100
140
200
320
500
700
900
1000
-0.4
0
+0.4
+0.8 (°C)
⊡ - vz2 ▽ - AR2 ▼ - rawmk4 ✕ - mk3 △ - vz1 ▲ - swi3 □ - AR1

Figure 3

THE DIFFERENCE IN OBSERVED TEMPERATURES FROM RADIOSONDES SUSPENDED 10M & 40M BENEATH A 1400G BALLOON.

J B Elms, J Nash, G Williams
Meteorological Office Bracknell

1. Introduction.

In order to improve the quality of radiosonde observations and their impact on numerical weather forecasts and climatological studies, major trials were conducted in the last decade to define the systematic biases between simultaneous measurements of temperature and geopotential heights. [1, 2]. The results of such Trials have enabled corrections to be applied either to the radiosonde design, radiosonde calibration procedure or ground station software. Advice has also been provided to users on the characteristic observation differences between the various systems.

Differences in radiosonde station practices may also provide further variations in systematic errors from one national network to another even when the same type of radiosonde is used in routine operations. One operational practice that may be critical is the amount of suspension used between the balloon and the radiosonde .WMO guidance in the CIMO Guide [3] suggests that the radiosondes should be suspended 40m below the balloon. The tests on which this recommendation was based have not been identified. However, in many national networks suspensions as short as 5 or 10m are in common use, or were used in the past. Previous investigations into the balloon wake effect by Vaisala in 1964/65 (refs. [4] & [5]), suggested that even with radiosondes suspended 40 or 60m below the balloon, heating from the balloon wake was significant at pressures lower than 70 hPa. Vaisala's measurements were produced using a single radiosonde with operational and reference sensor, with the radiosonde suspended at different lengths below the balloon on different days. The method was strongly dependent on the reference sensor and a knowledge of its radiation errors in daylight conditions. The method also relied on evaluating day/night differences from individual soundings made over several weeks. Vaisala's results were not particularly consistent, even at pressures higher than 30 hPa where the radiosondes tested at 25 and 45 m under the balloon identified less balloon wake heating on average than radiosondes tested at 15 and 65 m under the balloon.

Thus, in order that future CIMO guidance on radiosonde suspension length should be supported by test results , it was decided to identify the differences in temperature observed by two radiosondes of similar type , one suspended close to the balloon and the other at the recommended 40m below the balloon. The U.K. Meteorological Office Upper Air Trials Team initiated these experiments in 1991 at Crawley (WMO No. 03 774), using two Vaisala RS80 radiosondes suspended at different heights from the same rig. The tests were subsequently moved to Hemsby (WMO No. 03 496) in 1993 , following closure of Crawley towards the end of 1992 .

2. Test Flight Procedures

Vaisala Loran RS80-15L radiosondes were used for the tests as this enabled operational winds to be recorded without using a radar reflector which may have disturbed the balloon wake. The top radiosonde was suspended either 5 or 10m below a 1400g TOTEX CR balloon . A small parachute with hoop spreader was also attached to the balloon. A measured length of string ensured that the lower radiosonde was deployed at 40m below the balloon. The tests were performed on days when the surface winds were relatively calm. This enabled the rig to be launched with the required suspension length without endangering the deployment of the lower radiosonde.

The Vaisala radiosonde signals were processed by independent PC-CORA systems using exactly the same software. Raw pressure, temperature and humidity measurements were used to produce edited data archives at 2s intervals from which operational messages were derived.. Both raw and edited data were archived for further analysis off-line. Pre flight ground checks were performed using the same ground check set and mercury in glass thermometer. The two systems were connected to the same start button at the balloon shed . This was pressed to initialise the flight at the moment the lower radiosonde left the ground.

After burst the 2 radiosondes were monitored on descent to obtain comparison data until signal fade near the surface.

4. Elimination of temperature differences other than those from the balloon wake

4.1 .Radiosonde signal quality

The radiosonde signal reception was usually very good during ascent and only a few small sections of data had to be flagged as unusable. On some occasions, psychrometric cooling of the temperature sensors occurred when the radiosondes emerged into dry air after wetting or icing in cloud .The data from these parts of the flights were excluded.

The quality of the radiosonde data during descent varied a great deal, since this depended to a large extent on the time taken for effective deployment of the parachute. On a limited number of occasions , radiosondes were damaged during

balloon burst, on others the parachute failed to deploy effectively in the lower stratosphere and it was clear that the radiosondes were falling in a different orientation relative to the sun than during the radiosonde ascent at the same level. The procedure for determining balloon wake heating as recommended in the CIMO guide is to compute the difference between temperatures immediately before and after burst.This would have given wrong values for balloon wake heating,since in daylight the temperatures measured by Vaisala radiosondes increased on average following burst, probably due to an increase in the effective solar heating cross section of the sensor and outrigger as the radiosonde tumbled following burst.

4.2 Differences in radiosonde calibration.

The WMO Radiosonde Comparisons have demonstrated that the reproducibility of temperature measurements by the Vaisala RS80 radiosonde is better than or equal to 0.2 °C at all but the lowest pressure levels (standard deviation) [1, 2]. Under normal circumstances it is relatively unusual for pairs of Vaisala RS80 radiosondes flown together at the same height to consistently indicate temperatures differing by more than 0.4 °C. However, in some of the early tests at Crawley a limited number of radiosondes were flown from a delivery with batch calibration errors . These radiosondes produced differences larger than 0.4 °C when compared with standard radiosondes in some Crawley flights. The original plan had been to identify calibration differences by comparing the temperatures measured by the two radiosondes during descent. However, this did not prove very successful because the parachute only deployed sufficiently to reduce the rate of descent to about 8 $m.s^{-1}$ at pressures higher than about 200 hPa. Without adequate deployment of the parachute the motion of the radiosondes during descent was unstable and temperature differences between the radiosondes at the same height fluctuated with much larger amplitude than during ascent.

When the test was moved to Hemsby in 1993, the Vaisala Loran radiosonde pairs were always chosen from the same cartons of 10 radiosondes and it was checked that the radiosondes had been calibrated during the same calibration run at the factory. Consequently, the standard deviation of the temperature differences between pairs of radiosondes in the troposphere where balloon wake effects were expected to be small was reduced from about 0.23° C for a mixture of day and night flights at Crawley to 0.17° C for a similar number of daytime flights at Hemsby.

4.3 Differences in timing of the measurements at a given height.

The statistical processing software package used required that observations at a given height should have identical times. As both flights were initiated at the same time, the lower radiosonde had later times into flight for a given height than the upper radiosonde. The rates of ascent of the flight rig were computed for 1 minute time intervals updated at 2s intervals through the flight. The rate of ascent was then used to reduce the times of the data samples of the lower radiosonde so that the times into flight to a given height were as close as possible for both radiosondes.. Values for the lower radiosonde were then interpolated linearly in time to produce a set of observations with the same times as the upper radiosonde.

Plots of 2s data samples for daytime and nighttime flights after timing has been adjusted can be seen in Figs. 1 and 2.

4.4 The orientation of the radiosondes relative to the sun

In daytime observations, the radiosondes rotate relative to the sun during ascent. As the Vaisala temperature sensor is deployed to one side of the axis of rotation of the radiosonde, the cross section of solar absorption of the sensor and its support varies as the radiosonde rotates. This produces short term variations in comparisons between two daytime Vaisala RS80 observations that are absent from comparisons in night-time conditions, as seen in Fig. 1 and 2 and also found in earlier tests in the U.K. with both radiosondes flown at the same level.

In order to reduce the impact of the variations due to rotation of the radiosondes, comparisons between the upper and lower radiosondes were based on one minute averages of temperature differences (i.e. averages of 30 differences at 2s intervals).

5. Statistical Analysis.

75 twin flights were flown altogether of which seven were not included in the statistics due to problems with one or other of the radiosonde systems. Average temperature differences and pressures were computed for each minute of the test flights. The statistical software package, provided by S. Kurnosenko of the Central Aerological Observatory, Russia for the WMO Radiosonde Comparison tests [2], was then used to produce mean temperature differences and associated standard deviations for data samples grouped in the predetermined pressure layers used for the WMO Comparisons.

The ascents made with the upper radiosonde suspended 10 m below the balloon were categorised according to mean solar elevations as follows ("sunset" = 0 to 15 degrees, "medium " = 15 to 40 degrees, "high " = above 40 degrees) .

6. Results

Mean temperature difference (lower radiosonde (40m) minus upper radiosonde (10m)) and associated standard deviations for respective pressure levels are presented in Fig. 3 for dark conditions and in Figs 4 to 6 for the three daytime categories. Results from a further set of ascents at "high" and "medium" elevations with the upper radiosonde suspended only **5m** below the balloon are superimposed as dashed lines on Figs. 4 and 5. The plots show that:-

- . Mean temperature differences between the 2 radiosondes were close to zero at the surface. This confirmed the adequacy of the pre-flight radiosonde ground checks.
- .At night , there was no significant evidence of cooling of the upper radiosonde from the balloon wake, Fig. 3.
- In daytime, positive trends in the upper radiosonde observations were found in all 3 categories at pressures lower than 30 hPa. This is considered to be caused by heating of the upper radiosonde by the balloon wake. The magnitude of the differences at pressures lower than 20 hPa does not show a strong dependence on solar elevation, but the number of test flights reaching these levels was too small to reach definitive conclusions at this time.
- . The positive trend in the upper radiosonde observations appeared to start at 50 hPa for the sunset flights whereas it did not commence until about 30hPa for the higher solar elevations. .
- The standard deviations of the results from each of the categories was generally 0.2 °C or less, except in the "medium" and "sunset" categories where the values increased to 0.4 °C at pressures lower than 30 hPa.
- With the upper radiosonde at 5m below the balloon, the positive trend in upper radiosonde temperatures appeared to start between 70 hPa and 50 hPa , rather than at 30 hPa for the 10m radiosondes. The positive bias in the upper radiosonde was higher than for the 10m radiosondes at pressures less than 20 hPa with magnitude increasing to approximately 1°C at 10 hPa, but again the data set at upper levels is currently too small to draw strong conclusions.

7. Conclusions

7.1 These tests have demonstrated that using Vaisala RS80 radiosondes the temperatures obtained with a radiosonde on a 10 m suspension and a 40m suspension at night will not differ significantly. This might not be the case if a radiosonde was used with a temperature sensor with high emissivity in the infrared, since the balloon might influence the infrared heat exchange of the upper radiosonde. Here, the balloon diameter expanded from about 1.5m on launch to about 7m at 10 hPa . The circumference of the balloon at 10 hPa would then subtend an angles of about 45 degrees relative to the suspension for a 5m sonde ,about 28 degrees for a 10m sonde and about 9 degrees for a 40m sonde.

7.2 In daytime test flights , the balloon wake did not cause a significant difference in temperature (> 0.2 °C) between radiosondes at 10m and 40 m until pressures lower than 20 hPa .With the upper radiosonde at 5m below the balloon significant temperature differences were again only found below 30 to 20 hPa.

7.3 The results from these tests suggest that the temperature bias between the upper and lower radiosondes was similar or slightly lower at high solar elevations than at low or medium elevations. An analysis of operational day/night temperature differences for various stratospheric pressure levels before and after balloon suspension length was changed from 7 to 15 metres in Japan [6] inferred a gradual increase in balloon wake heating as solar elevation decreased from about 60° to 20. Currently, we have insufficient measurements at low pressures to detect this trend.

8. Recommendation

Suspension lengths of less than 10m should be avoided if best quality radiosonde temperature observations are required at pressures lower than 50 hPa. A suspension length of 40m is probably longer than necessary for most routine operational radiosonde observations . Additional tests need to be performed to decide whether a suspension length of 20 to 30m is most suitable for good quality temperature observations to pressures as low as 10 hPa.

9. References.

1. Instruments and Observing Methods Report No30.WMO Intern. RS Comparison Phases 1&2 - Nash,Schmidlin 1987
2.Instruments and Observing Methods Report No 40 .WMO International RS Comparison Ph. 3 -Ivanov,Kats et al. 1991
3.WMO Guide to Met Instruments and Methods of Observation 5th Edition No 8 page 13.20
4 An Analysis of the Radiation Error Appearing in Temperature Measurements Made With Radiosondes. - V.Vaisala 1964 Ann. Acad. Scient. Fennicae,A. VI.158 & Mitt. Papers Met Inst. Univ. Helsinki No 103
5. Observations Concerning the Daily Variation of the Temperature & Balloon Effect on the Temperature Measurement at High Altitudes. - V Vaisala Vaisala News 1965 No 28
6.Influence of Solar Radiation On Temperature Measurement Before And After The Change Of The Length Of Suspension Used For The Japanese Radiosonde Observation.- Suzuki & Asahi. Journal of Met. Research . Vol 30 ,93-97

10. Acknowledgements.

T Oakley and G Iley (Upper Air Trials Team) who organised the original trials at Crawley., S. Kurnosenko , Central Aerological Observatory, Russia for the processing software. The operational staff of Crawley and Hemsby stations

Figure 1

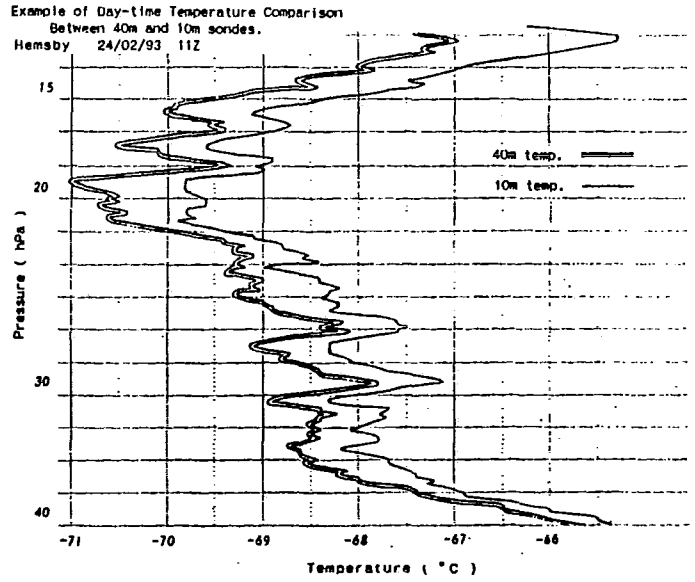

Figure 2

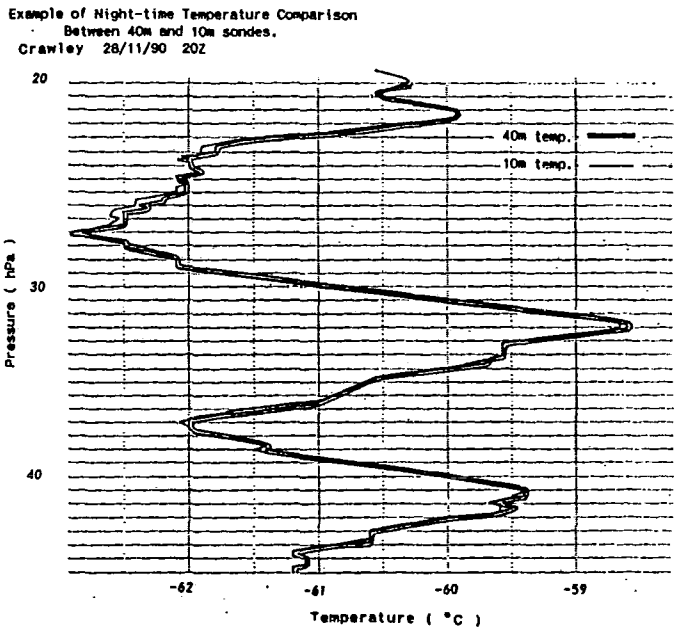

Figure 3a

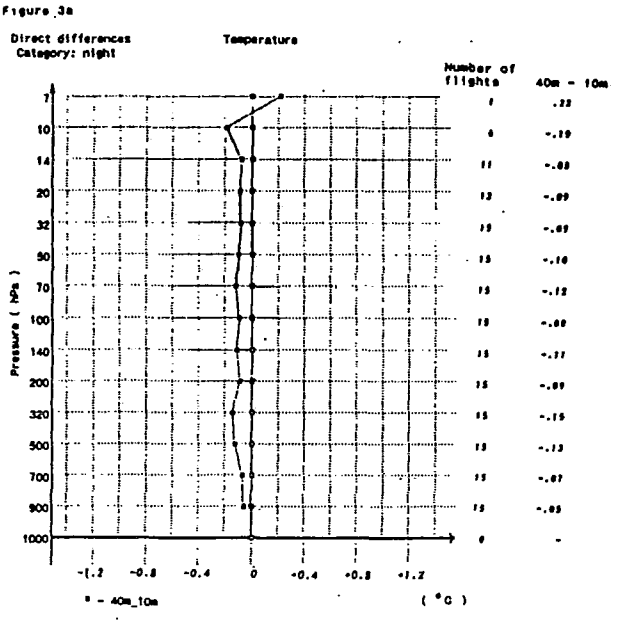

Figure 3b

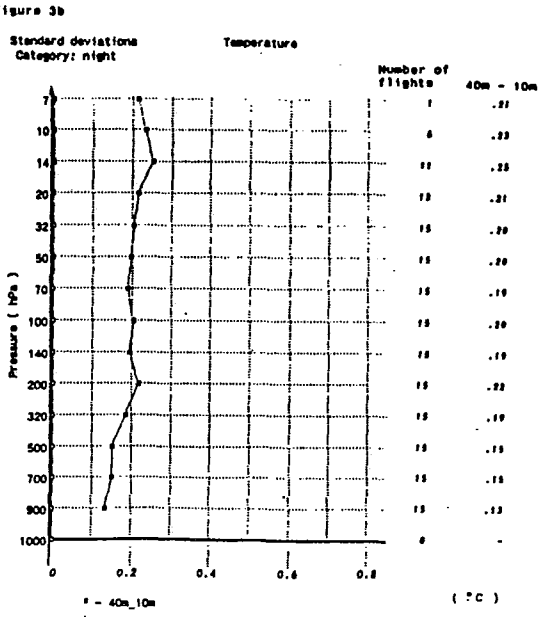

Figure 4a

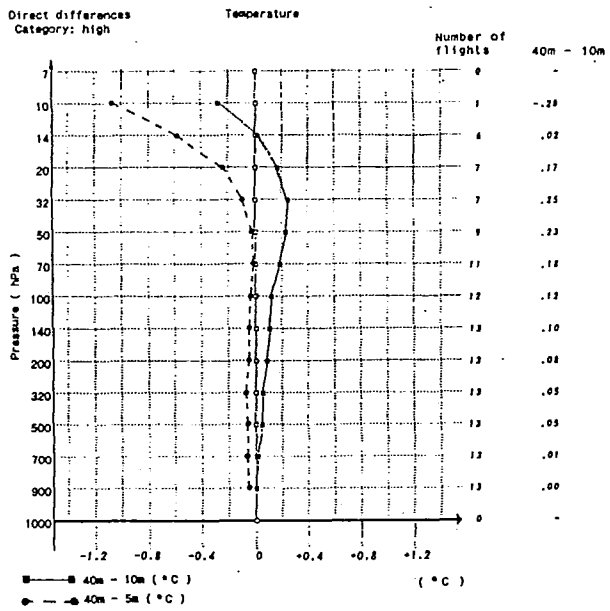

Figure 4b

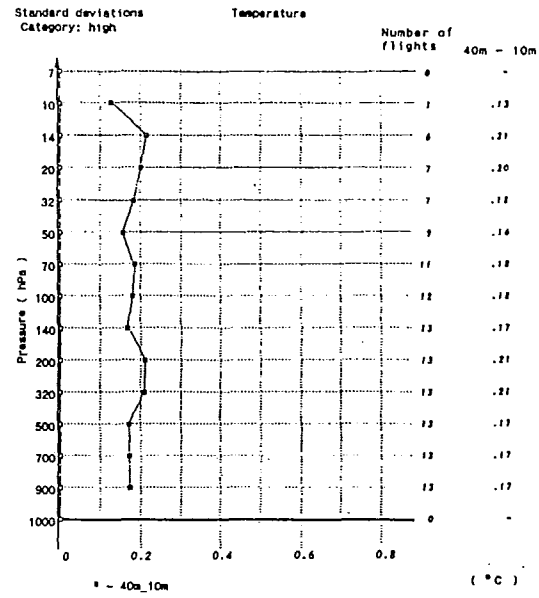

Figure 5a

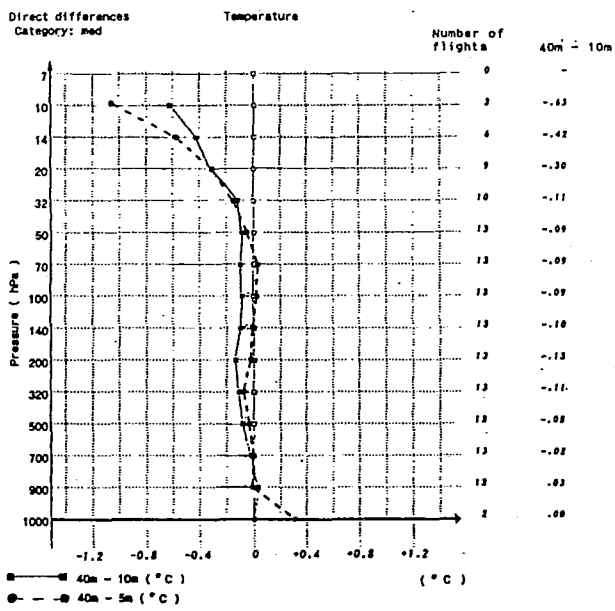

Figure 5b

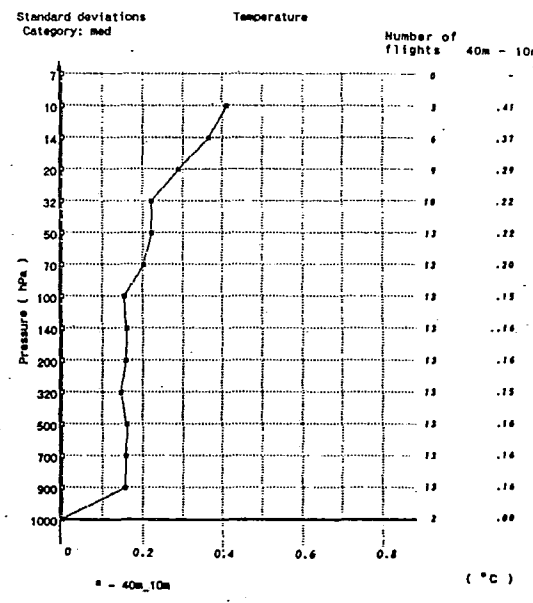

Figure 6a

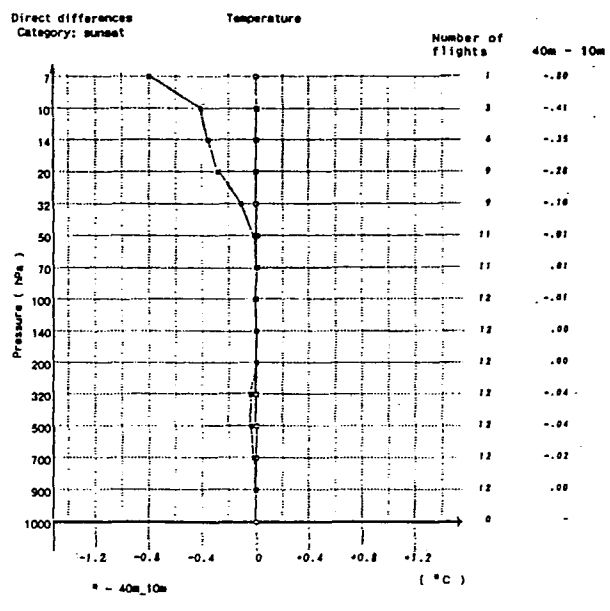

Figure 6b

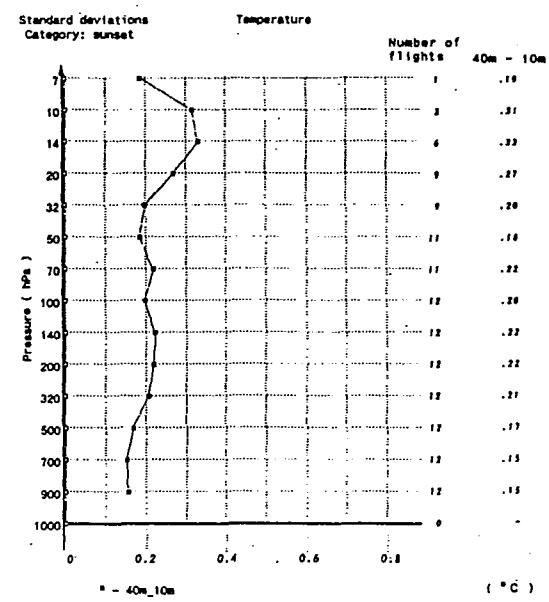

EFFECTS OF CHANGES IN RADIOSONDE INSTRUMENTS AND PRACTICES ON CLIMATOLOGICAL UPPER-AIR TEMPERATURE RECORDS

Dian J. Gaffen

National Oceanic and Atmospheric Administration
Air Resources Laboratory
1315 East West Hwy., Silver Spring, Maryland USA

1. INTRODUCTION

Climate models predict that increases in atmospheric greenhouse gases will cause tropospheric warming and stratospheric cooling. To detect these changes, we require long-term measurements of upper-air temperature. Although satellite measurements are beginning to be used to create such datasets, currently the only multi-decadal upper-air temperature dataset is the global radiosonde archive. However, over the past half century, radiosonde technology and observing practices have changed, and if the data are to be used for climate change detection, we should know to what extent they are affected by the changes.

During the intercessional period since CIMO-X, a study was undertaken to ascertain what changes have been made in radiosonde instruments and observing practices in WMO member nations since about the late 1950's (Gaffen 1993). This paper combines the historical information collected in that study with monthly mean ("Climat Temp") radiosonde reports from the National Center for Atmospheric Research, to determine whether the changes in instruments and practices had a noticeable effect on the climatological temperature data.

Examples are shown of the effects of (1) instrument changes, (2) changes in radiation corrections, and (3) changes in the length of the cord between the balloon and radiosonde. Examples are also shown of temperature data discontinuities whose causes are not known. The general approach is to compare the historical information with time series of monthly mean upper-air temperature. If a large, abrupt data discontinuity is coincident with a radiosonde change, if no other explanation is found, and, where applicable, if similar discontinuities are found at stations with similar radiosonde changes, the discontinuity is attributed to the radiosonde change.

2. CHANGES IN RADIOSONDE TYPE

Hong Kong 200 mb temperature anomalies (deviations of monthly mean temperatures from long-term monthly means) for 1950-90 (Fig. 1) seem to be affected by at least two major changes in radiosonde type. A chronology of sonde types used at the Royal Observatory Hong Kong is: 1949-69 British Kew Mark IIB, 1969-74 Finnish Väisälä model RS13, 1975-80 Väisälä RS18, 1981-83 Väisälä RS21, 1984-present Väisälä RS80. With the 1969 switch from Kew to Väisälä sondes, simultaneous abrupt temperature increases were recorded at all pressure levels, and the magnitude increases with altitude. At 200 mb, temperature anomalies increased 1.0°C (Fig. 1).

These changes are consistent with the results of direct comparisons of the two radiosondes (Apps 1971) made by flying them together on the same balloon in a series of tests during 1969. The Väisälä sonde gave higher temperature readings than the Kew; the difference at 200 hPa was 1°C, with larger differences at higher altitude and smaller ones at lower altitude. The agreement of the test results with the climatological data analysis is testament to the value of direct comparisons in assessing the likely effects of an instrument change.

The 1980 change from the Väisälä RS18, with a bimetal ring temperature sensor, to the RS21, with a similar sensor but mounted in a duct (Huovila and Tuominen 1990), is associated with an 0.7°C 200 mb temperature drop (Fig. 1). The changes in the Väisälä sondes are not unique to

Hong Kong; Väisälä sondes are now used at a majority of stations in Africa, Australia, Europe, and South America (Parker and Cox, unpublished manuscript). Over time, improvements in Väisälä temperature sensor time lags (Fig. 2a), among other things, have probably influenced the data.

To determine the potential effect of improvements in sensor response time, a finite difference numerical simulation of each Väisälä sonde type ascending through the U.S. Standard atmosphere was made, assuming a constant 6.6 m s^{-1} ascent rate. The simulated errors, the differences between the simulated and Standard Atmosphere temperature profiles (Fig. 2b), are positive in the troposphere and negative in the stratosphere. Most important, the bias decreases with each successive sonde model.

The implied trend in 500 mb temperature is a 0.5°C cooling, no change in the tropopause layer (because the temperature profile changes slowly), and 0.04°C, and 0.44°C warmings at 50 and 10 mb, respectively. It should be emphasized that these sensor changes did not occur in isolation; rather, they were generally accompanied by other design and data reduction changes.

3. CHANGES IN RADIATION CORRECTIONS

Solar and infrared radiation can cause errors in radiosonde temperature measurements. Since the 1950's many nations have made corrections for solar radiation effects in their data. Changes in radiation correction usually accompany changes in sonde types, and the effects of the two changes are not easily separated. Sometimes, radiation corrections have been improved for a given sonde type, as was recently done for the Väisälä RS80 radiosonde. Modifications in correction schemes are usually small and therefore difficult to detect in data records.

On the other hand, the initial introduction of radiation corrections can have a dramatic effect. A good example is the Scrase (1956) corrections for British Kew radiosondes. These were implemented at Hong Kong in 1956, and seemed to have had the effect of reducing mean 200 mb temperature by about 1.7°C (Figs. 1 and 3). The effect is smaller at lower altitude, consistent with the increase in the magnitude of the corrections with decreasing pressure (Scrase 1956). Comparable temperature drops are evident in the data from Valentia, Ireland (Fig. 3), where Kew sondes were also used.

4. CHANGES IN WAKE EFFECTS

Radiosonde balloons leave a wake of perturbed air below them as they ascend. If the instrument package is in the wake, measurements will not represent ambient conditions. In Japan, in 1968, recommended radiosonde train length was increased from 7 to 15 m. The result was a drop in monthly mean temperature of a few tenths of a degree (Fig. 4), probably due to a decrease in daytime values (Suzuki and Asahi 1978).

5. DISCONTINUITIES WITH UNKNOWN CAUSES

Unfortunately, historical information is not available for all countries operating radiosonde stations. Nevertheless, it is likely that some changes have been made at almost all stations that have been operating for several decades. Some temperature time series show abrupt discontinuities that suggest the sort of changes in instruments and practices shown above. Two examples are Tahiti, Society Islands, and Niamey, Niger (Fig. 5). Both stations exhibit 100 mb temperature drops of a few degrees in 1976, and there is another larger drop at Niamey in 1965. It seems possible that both stations used the same observing systems, which might explain the coincidence of the 1976 discontinuities.

6. CONCLUSION

The examples given above show the type of data discontinuities found in the global radiosonde data archive. In general, the discontinuities increase with altitude, partly because early difficulties associated with sensor time lag and radiation error, which are most problematic at high altitude, have been partially rectified in modern radiosondes. In most cases, these effects are such as to suggest a spurious cooling of the upper troposphere and stratosphere. Because interannual variability in temperature increases with latitude, data discontinuities are more easily detected in the tropics.

Radiosonde data have been used by Angell (1988), Hense et al. (1988), and Oort and Liu (1993) to estimate temperature trends. In general, these investigators have found stratospheric cooling and tropospheric warming trends with magnitudes on the order of 0.1°C per decade. However, we have seen that some of the archived data contain discontinuities associated with changes in instruments and observing practices of between several tenths and several degrees Celsius. It is quite probable that temperature trends computed using radiosonde data from the past several decades are influenced by data inhomogeneities. For example, of the 63 stations in Angell's (1988) global network, 43% of them have obvious discontinuities in stratospheric temperature records since 1958, the start of his analyses. Since most of these suggest a spurious temperature drop, it is likely that estimates of stratospheric cooling are too high. This problem seems to be most pronounced in the tropical and Southern Hemisphere stations in the network.

As time goes on, more changes will be made to the global upper-air observing network. Ensuring the long-term continuity and homogeneity of the data is not, in general, among the priority goals of national weather services' upper-air programs. At the very least, however, the changes made in radiosondes and observing practices must be recorded, centrally compiled, and made public if upper-air data are to be of any value in detecting climate change.

7. REFERENCES

Angell, J.K., 1988: Variations and trends in tropospheric and stratospheric global temperatures, 1958-87. J. Climate, 1, 1296-1313.

Apps, R.F., 1971: Comparison between the results obtained with the new MK IIB and the Väisälä RS13 radiosondes under operational conditions in Hong Kong, Royal Observatory Technical Note No. 31, Hong Kong, 11 pp.

Gaffen, D.J., 1993: Historical changes in radiosonde instruments and practices, WMO/TD-No. 541, Instruments and Observing Methods Report No. 50, World Meteorological Organization, Geneva, 123 pp.

Hense, A., P. Krahe, and H. Flohn, 1988: Recent fluctuations of tropospheric temperature and water vapour content in the tropics. Meteorol. Atmos. Phys., 38, 215-227.

Huovila, S., and A. Tuominen, 1990: On the influence of radiosonde lag errors on upper-air climatological data in Finland 1951-1988. Meteorological Publications No. 14, Finnish Meteorological Institute, Helsinki, 29 pp.

Oort, A.H., and H. Liu, 1993: Upper-air temperature trends over the globe, 1958-1989. J. Climate, 6, 292-307.

Scrase, F.J., 1956: Application of radiation and lag corrections to temperatures measured with Meteorological Office radiosonde. Meteorol. Mag., 1005(85), 65-78.

Suzuki, S., and M. Asahi, 1978: Influence of solar radiation on the temperature measurement before and after the change of the length of suspension used for the Japanese radiosonde observation. J. Met. Soc. Japan, 56, 61-64.

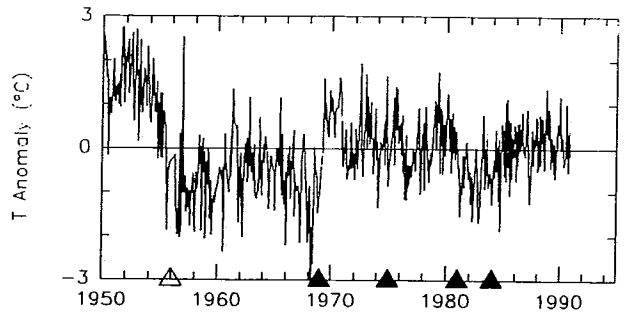

Fig. 1 Time series of 200 mb monthly temperature anomalies at Hong Kong. Marks on horizontal axis show dates of changes in instruments (▲) or radiation corrections (△).

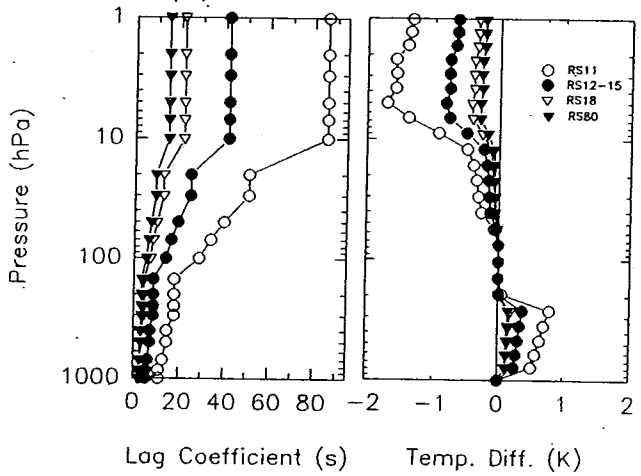

Fig. 2 a (left): Temperature sensor time lags for different Väisälä radiosonde models (Huovila and Tuominen 1990). b (right): Simulated error in measurements of Standard Atmosphere temperature profile due to sensor lags.

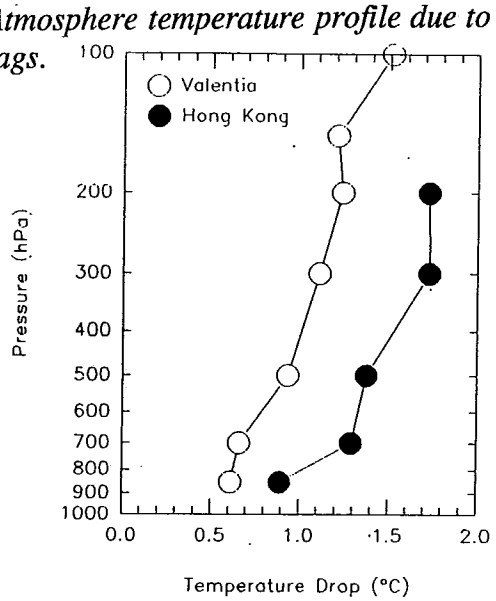

Fig. 3 Temperature drops at Valentia, Ireland, and Hong Kong associated with 1956 introduction of radiation corrections for British radiosondes.

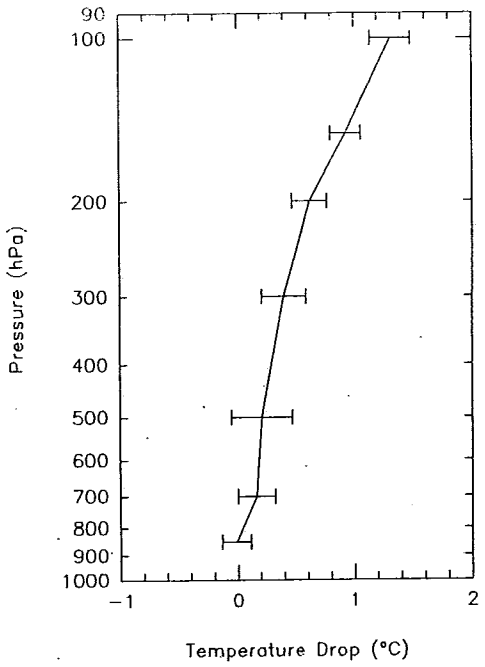

Fig. 4 Average and standard deviation, over 13 Japanese stations, of temperature drops associated with 1968 lengthening of radiosonde trains.

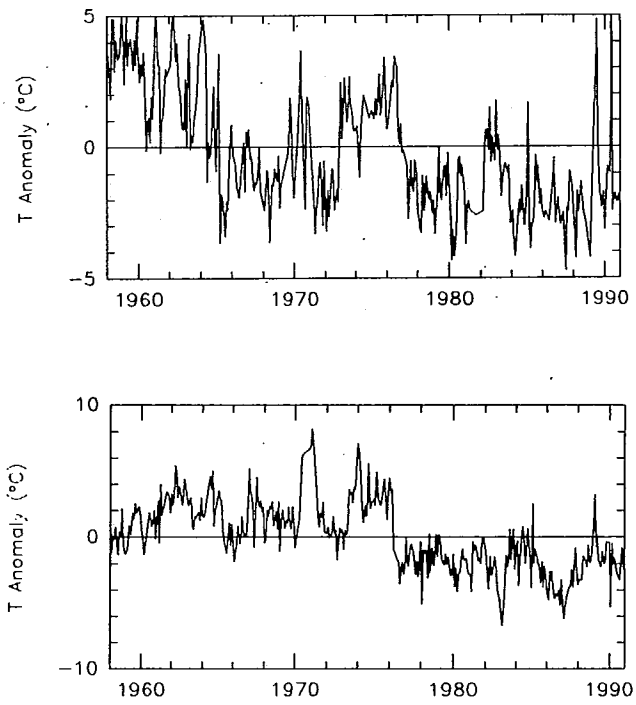

Fig. 5 100 mb temperature anomalies at Niamey, Niger (top) and Tahiti, Society Islands (bottom).

Spectral Analysis of Upper-Air Wind Profiles

Robert Olsen

U.S. Army Research Laboratory
White Sands Missile Range, New Mexico 88002, USA

Prasan Chintawongvanich

Physical Science Laboratory, New Mexico State University
Las Cruces, New Mexico 88003, USA

1. INTRODUCTION

A number of systems utilizing the track of balloon-borne sensors for measurements of upper-air atmospheric parameters have recently been developed. With the introduction of these systems, it has become necessary to determine experimentally the capabilities of measurement precision and vertical resolution, relative to one another. Detailed wind profiles are required in assessing the performance of rocket vehicles. They are also important in determining the transport and diffusion of airborne materials, as well as in other areas of atmospheric research studies. This paper addresses the issue of wind measurement capability of various upper-air systems. The study highlighted the method of spectral analysis used to evaluate the performance of upper-air wind sensors [Olsen and Chintawongvanich, 1990]. The evaluation was made by analyzing and comparing sets of wind data obtained from field tests conducted at White Sands Missile Range (WSMR), New Mexico, and at Cape Canaveral, Florida. Wind data from a series of upper-air sounding involving four ground station radio direction finding (RDF) tracking systems were used for the study.

2. INSTRUMENTATION

Four ground station RDF tracking systems were deployed for the study. These upper-air systems are: (1) ground based radio theodolite, (2) WF-100 radar, (3) FPS-16 radar/Jimsphere system, and (4) MPS-39 radar/Jimsphere system.

The radio theodolite uses a 1680 MHz balloon-borne radiosonde and is tracked automatically by a phased array antenna. Wind data are sampled at a maximum rate of 0.5 samples per second. The WF-100 is a moderate precision X-band monopulse tracking radar, capable of measuring balloon's position coordinates at 1.5 s intervals from near the surface to about 10 km. Data reduction process converts the measurements from spherical to Cartesian coordinates and performs a 10-point non-overlapped low-pass filtering. In this study, the WF-100 radar tracked the balloon which carried the radiosonde. Thus, a comparison of wind profiles between the theodolite and WF-100 systems can be made directly. The FPS-16 is a high-precision C-band monopulse tracking radar with a loop gain of 221 dB. It is designed to measure balloon positions at 0.1 s intervals from near the surface to about 20 km. Finally, the MPS-39 is a high-precision C-band phased array radar designed to track up to 10 targets simultaneously. The MPS-39 has a loop gain of 237 dB. It is capable of measuring multiple balloon positions, each at 0.1 s intervals from near the surface to an altitude of 30 km. Data reduction for both the FPS-16 and MPS-39 are performed by a processing unit that edits the 0.1-second radar measurements for wild points and smoothes the data over 6-second non-overlapping intervals resulting in an output data rate of 1/6 samples per second. The FPS-16 and MPS-39 radars track a common 2-m diameter Jimsphere balloon, a rigid roughened sphere constructed of 0.5 mil aluminized mylar. The rigidity is provided by maintaining an internal overpressure of 5 mb, controlled by two pressure relief valves. There are 398 conical roughness elements on the balloon surface to control vortex shedding, thereby reducing the amplitude and spectral bandwidth of aerodynamically induced balloon motions.

3. EXPERIMENTATION

The experiment was carried out in two parts. For each part, a series of 12 balloon flights were made resulting in a total of 24 sets of vertical wind speed profiles. Part one was conducted during October-December, 1991 at the U.S. Army Research Laboratory (ARL), WSMR. The radio theodolite and

WF-100 radar were deployed for the test. Part two of the experiment involves a comparison between the two high-precision radars, the FPS-16 and MPS-39. Upper-air wind speed profiles obtained from the Patrick AFB research facility, Cape Canaveral during September 1992-May 1993 were utilized for the study.

There are several factors affecting the quality of upper-air wind measurements. For example, the azimuth and elevation angles become increasingly difficult to resolve as the balloon drifted further upward resulting in lower signal-to-noise ratio (S/N), and the pressure sensor becomes non-linear over low pressure ranges making high-altitude measurements unreliable. In order to isolate these factors from the comparison, wind data used for the analysis are limited to three height ranges as follows: (a) 0 to 6 km, (b) 6 to 12 km, and (c) 12 to 18 km. For part one of the experiment, the comparison is limited to those measurements in the 0 to 6 km height range, since both the theodolite and WF-100 radar systems have an operating range of just below 10 km. In part two, which involves the high-power, high-precision FPS-16 and MPS-39 radars, wind measurements from all three height ranges are included in the comparison.

4. DATA ANALYSIS AND RESULTS

Vertical wind speed profiles from all 24 comparison flights were used for the analyses. Wind profiles depicted in Fig. 1 are typical of the radio theodolite and WF-100 comparison (part one), which compares wind speed at three averaging intervals: (a) 15-second, (b) 30-second, and (c) 60-second. For an averaged rise rate of 5 m/s, these averaging intervals are equivalent to vertical resolutions of 75, 150, and 300 m. Root-mean-square (RMS) of wind speed differences between the two systems over the 6 km range are: 2.6, 2.0, and 1.5 m/s for the 15-, 30-, and 60-second data, respectively. Figure 2 shows a sample of wind profiles of the FPS-16 and MPS-39 comparison (part two) at the three height ranges: (a) 0-6, (b) 6-12, and (c) 12-18 km. The oscillations observed at lower altitude, with an averaged wavelength of 90 m, are aerodynamically induced motions that trend to reduce the accuracy of sensing the true wind [Susko, 1987]. Values of the RMS of wind speed differences between the two systems are: 0.4, 0.5, and 0.4 m/s for the height ranges 0-6, 6-12, and 12-18 km, respectively.

Time-domain analysis is often useful in comparing differences in the measurements between the systems under investigation to that of a reference system. However, in the situation where the ground truth is not available, results of the comparison would merely be a measure of the differences among themselves. In this study, a method of spectral analysis in frequency domain is used to evaluate the performance of the sensors in absolute terms. Information about noise component and other characteristics response of the sensors are determined. Conversion of the reference frame from spatial coordinates to frequency scales was made using Taylor's hypothesis, $\kappa - 2\pi f/R$. Here κ is wave number, f is sampling frequency, and R is the averaged balloon rise rate. Figure 3 shows the resulting auto-spectra of the theodolite (solid line) and WF-100 (dotted line), and the co-spectrum (heavy dotted line) of the comparison. These spectra were determined from averaging individual spectra over the 12 comparison flights in part one. Similarly, the averages of 12 comparison flights in part two yielded the auto- and co-spectra for the three height ranges. Figure 4 shows the spectra of the FPS-16 (solid line) and MPS-39 (dotted line) for the 6-12 km range.

Wind measurements obtained from all upper-air systems are mainly composed of wind signal and incoherent noise. In light of this analysis, using the superposition theory, the auto-spectrum of wind measurements from each system converges the spectrum of actual wind plus incoherent noise. The co-spectrum, however, converges to the averaged wind signals presented in the systems under testing. This is because the incoherent noise in one system is uncorrelated to that of the other. The noise spectrum in the co-spectral estimates is thus cancelled to zero. The departure of the auto-spectra from the co-spectrum, observed in Figs. 3 and 4, represents the errors of the measurements. The absolute RMS of measurement errors, error(κ), at a specific wave number (i.e., wavelength or vertical resolution) of interest is obtained from the following expression:

$$\text{error}(\kappa) = [(\text{spec}(\kappa) - \text{cospec}(\kappa)) * \kappa]^{1/2} \qquad (1)$$

where spec(κ) and cospec(κ) are the auto- and co-spectral densities at wave number κ.

Coherency defines a ratio of the co-spectrum squared to the product of the auto-spectra. When the noise levels in the two systems are similar, the coherency can be approximated by the ratio of signal to signal plus noise squared. This analysis is given in the following equations:

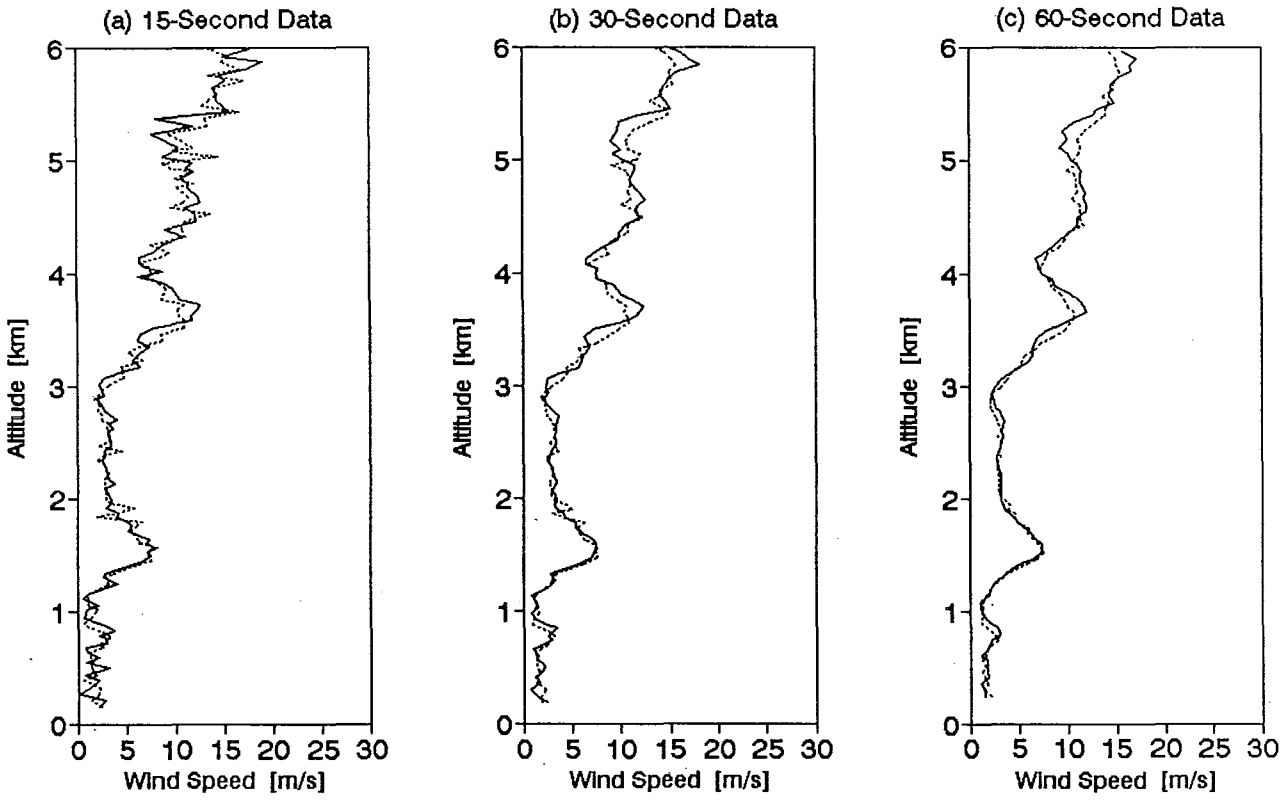

Figure 1. Wind speed profiles of the theodolite (solid) and WF-100 (dotted) over range 0-6 km: (a) 15-sec, (b) 30-sec, and (c) 60-sec averages. 5 Dec 1991, 2011 GMT.

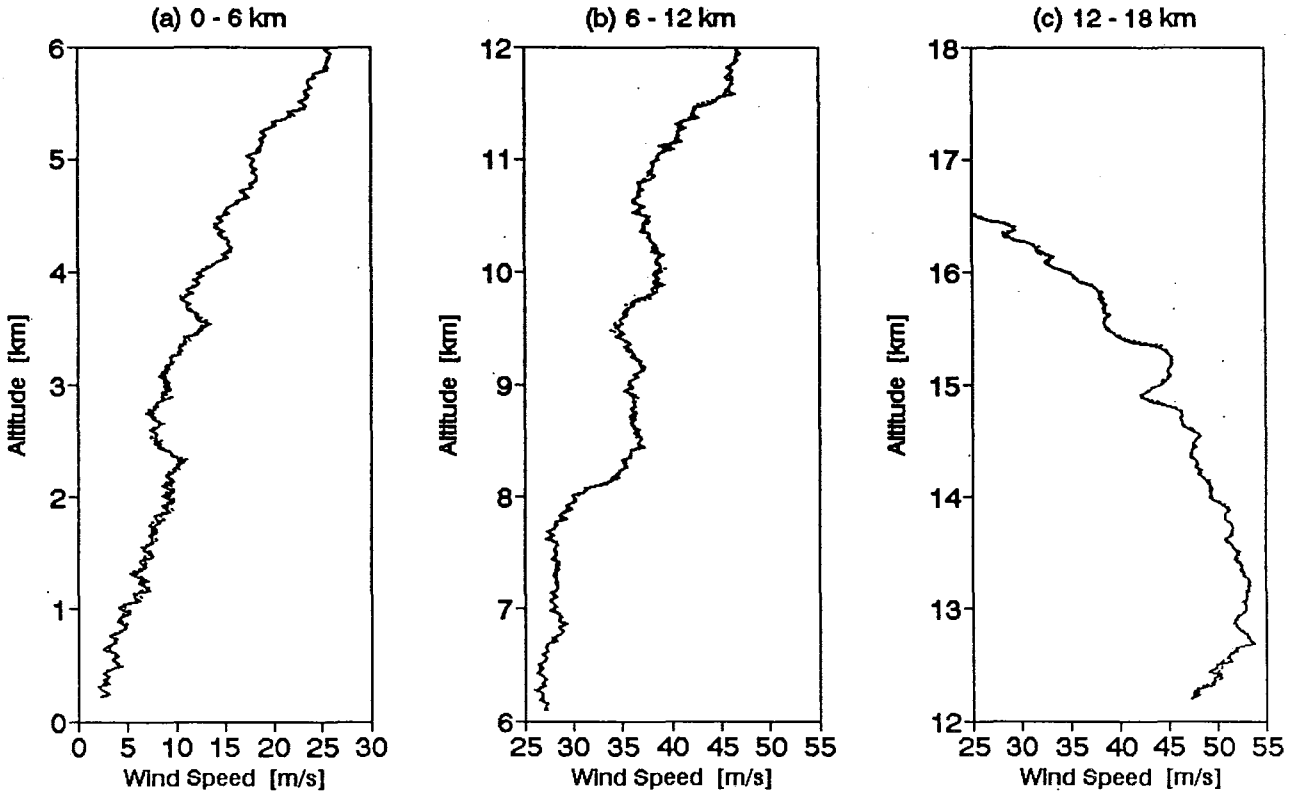

Figure 2. 6-second averaged wind speed profiles of FPS-16 (solid) and MPS-39 (dotted): (a) 0-6 km, (b) 6-12 km, and (c) 12-18 km. 31 May 1993, 1900 GMT.

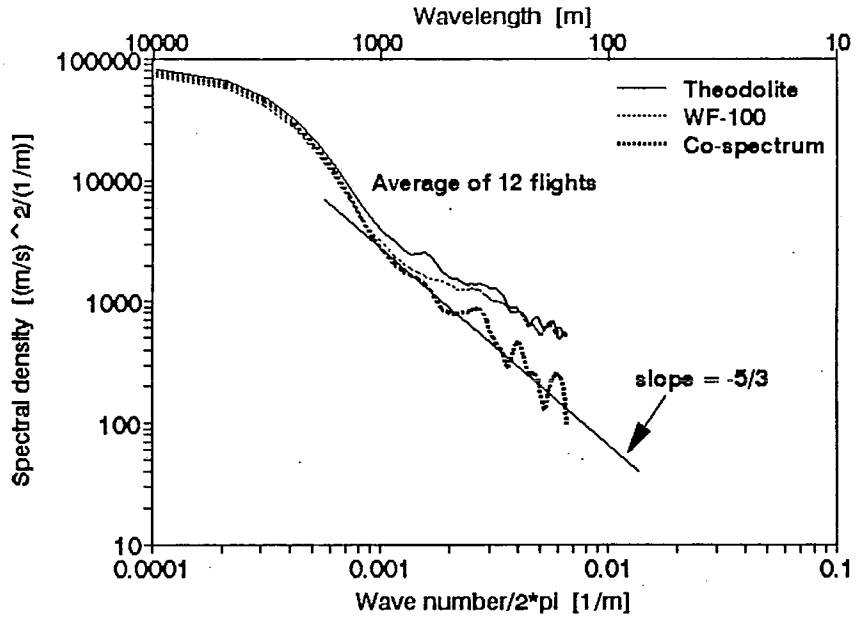

Figure 3. Averaged wind speed profile spectra of theodolite and WF-100

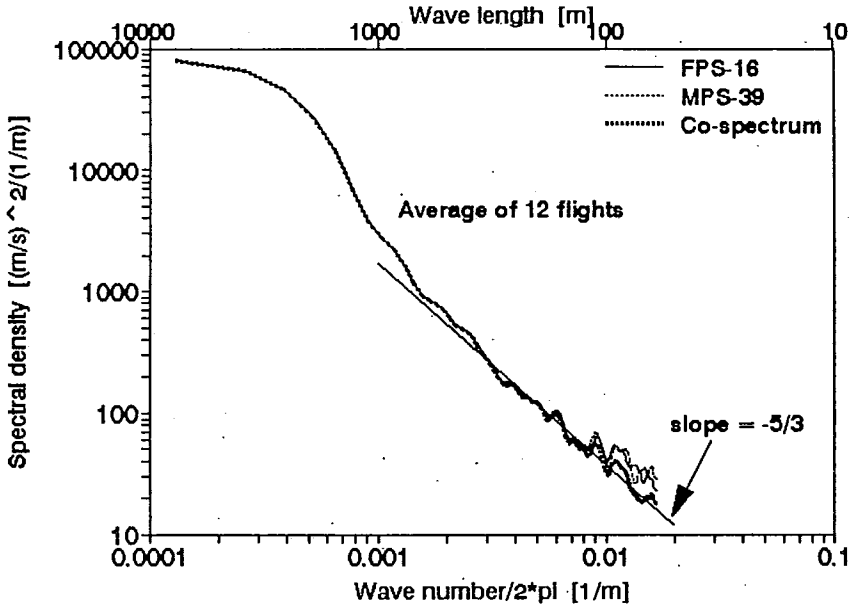

Figure 4. Averaged wind speed profile spectra of FPS-16 and MPS-39

Table 1. RMS of measurement errors of the theodolite and WF-100

System	Vertical resolution (m)	S/N	RMS error (m/s)
AIR	150	< 0.1	1.8
WF-100	150	< 0.1	1.7
AIR	300	~ 1	1.5
WF-100	300	~ 1	1.4
AIR	600	> 2	1.3
WF-100	600	> 2	0.8

Table 2. RMS of measurement errors of FPS-16 and MPS-39

System	Vertical resolution (m)	S/N			RMS error (m/s)		
		0-6 km	6-12 km	12-18 km	0-6 km	6-12 km	12-18 km
FPS-16	60	1	1	2	0.40	0.46	0.30
MPS-39	60	1	1	2	0.36	0.50	0.30
FPS-16	150	5	14	10	0.21	0.19	0.20
MPS-39	150	5	14	10	0.20	0.18	0.21
FPS-16	300	30	60	30	0.07	0.10	0.17
MPS-39	300	30	60	30	0.05	0.10	0.20

$$\text{coherency}(\kappa) = \frac{\text{cospec}(\kappa)^2}{\text{spec}_1(\kappa) * \text{spec}_2(\kappa)} = \frac{[\text{signal}_{12}(\kappa)]^2}{[\text{signal}_1(\kappa) + \text{noise}_1] * [\text{signal}_2(\kappa) + \text{noise}_2]} \quad (2)$$

assuming: $\text{noise}_1 \approx \text{noise}_2$, $\text{signal}_1(\kappa) \approx \text{signal}_2(\kappa) \approx \text{signal}_{12}(\kappa)$,

$$\text{coherency}(\kappa) \approx \left[\frac{\text{signal}(\kappa)}{\text{signal}(\kappa) + \text{noise}(\kappa)} \right]^2 \quad (3)$$

Equation (3) provides a mean to quantify coherency of the measurements in terms of S/N, thereby making it possible to express measurement errors as a function S/N. For example, using Eq. (3), a S/N ratio of 1:1 corresponds to a coherency of 0.25.

Using the criteria developed above, the RMS errors of wind speed measurements were computed. The results are tabulated in Table 1 for the radio theodolite and WF-100 comparison (part one) and in Table 2 for the FPS-16 and MPS-39 comparison (part two). At a vertical resolution of 150 m, measurements of the theodolite and WF-100 are mostly noise (S/N < 0.1) and the RMS of measurement errors are relatively large: 1.8 m/s (theodolite) and 1.7 m/s (WF-100). At a vertical resolution of 600 m, however, the signal-to-noise ratio is significantly higher (S/N > 2) and the RMS errors are lower: 1.3 m/s (theodolite) and 0.8 m/s (WF-100). For the comparison of the two high-resolution radars, the RMS errors for the three height ranges span from approximately 0.5 m/s at a vertical resolution of 60 m to about 0.1 m/s at a vertical resolution of 300 m. The performance of the two high-precision radars is also indicated by the quality of signal-to-noise ratio, which in all cases ranges from a low of 1 to a high of greater than 10.

5. CONCLUDING REMARKS

A method of spectral analysis has been successfully deployed to evaluate the four upper-air systems: the theodolite, WF-100, FPS-16, and MPS-39. Results of the study show that the WF-100 performs slightly better than the theodolite. However, reliable measurements from both systems cannot be expected for wavelengths smaller than 300 m where the signal-to-noise ratio drops below unity. The FPS-16 and MPS-39 systems, on the other hand, are far superior in measurement precision and range capabilities. These high resolution radars are shown to have a measurement precision of better than 0.5 m/s at a vertical resolution of 60 m over the 0 to 18 km range.

The advantage of the spectral method lies in the use of co-spectrum for referencing, because the noise components in the co-spectral estimates are incoherently cancelled to zero. The co-spectrum thus represents averaged wind signals detected by the sensors under testing. This feature greatly facilitates the onset identification of noise components in the auto-spectrum. The RMS of measurement error, at a wavelength of interest, is simply determined from the difference in the energy levels between the auto- and co-spectrum. In addition, spectral characteristics of wind turbulence in the inertial subrange is known to follow the -5/3 law [Kaimal, 1988]. This property provides a natural reference for checking on the co-spectrum itself. In this study, the -5/3 slope is found over the region with wavelengths smaller than about 1000 m, corresponding to sizes of the turbulence typically found in the troposphere.

6. REFERENCES

Kaimal, J. C., 1988: The Atmospheric Boundary Layer - Its Structure and Measurement, Lecture Notes, NOAA, Wave Propagation Laboratory, Boulder, CO.

Olsen, R., and P. Chintawongvanich, 1990: Spectral Analysis of Upper Air Wind Profiles, Preprint Volume, 2nd Symposium on Lower Tropospheric Profiling, Boulder, CO.

Susko, M., 1987: Analysis of the Bivariate Parameter Wind Differences between Jimsphere and Windsonde, NASA Tech. Memo. 4014, 72 pp.

STUDIES ON IMPROVING HUMIDITY MEASUREMENT IN RADIOSONDES

Veijo Antikainen and Ari Paukkunen
Vaisala Oy, UAD, Box 26, 00421 Helsinki, Finland

1. Introduction

Although the requirements and needs for the accuracy of humidity measurement in radiosonde are not relatively as demanding as the ones for the other sensors, the design and construction of humidity sensor that guarantees error free and good performance in all conditions can be much more challenging than is the case with other sensors. There exist several conflicting requirements. Protection of the sensor against rain and solar radiation is needed. This has often been solved by using a duct or cap in current radiosonde designs. The use of the duct can produce harmful effects caused by wetness in the duct originated from residual water of rain.The use of a cup can produce poor ventilation under the cup and increase the lag of the sensor and the relatively massive size of the sensor can produce thermal lag.The conduction of heat from the body of the radiosonde or the sensor boom can cause a difference between the sensor and the ambient temperature.Water condensation or ice formation can take place on the surface or the close surroundings of the sensor.

The other group of unfavorable effects can originate from the properties of the sensor itself. Such as long term stability, hysteresis, short term drift and temperature dependence belong to this category.

The improvement of design and construction of the humidity sensor of Vaisala Radiosonde has been continued in order to eliminate or minimize the unfavorable effects mentioned above. Vaisala HUMICAP humidity sensor is a capacitive thin film sensor. The change of the thin film material (H-polymer) has improved both long- and short term stability of the sensor and thereby improved accuracy is achieved. The size of the sensor has been reduced to a third of the current one (0.4 mm x 1.5 mm x 4 mm) in order to minimize the thermal effects. This gives also a possibility for the elimination of the rain cap and at the same time for the improvement of the ventilation and lag. The pulse heating of the sensor or some kind of external heating seems to be solution to the icing problems.(pat. pend.).

2. Sources of unfavorable effects in humidity measurements

2.1 Direct rain.

Sensors must be protected by some way against direct exposure to rain. This is generally made in most existing radiosondes by using a duct or cup. Vaisala has made successfully tests with the sensor treated specially to make it water repellent.(1). All sensors used in current Vaisala radiosondes are treated this way.

2.2 Solar radiation and long wave radiation.

The same protection as used for rain protection is generally used to eliminate radiation effects. In Vaisala radiosonde a highly reflecting aluminized cap is used. Aluminium has also good properties as to the long wave radiation properties. (Low emission for infrared.) However, as already mentioned both duct and cup has some undesirable properties: residual water in the duct and reduced ventilation in the cup. Therefore the ideal sensor for humidity is the one that does not need any radiation shield. That means that the sensor must be so small as possible. Vaisala has made tests with the sensor, which is only 0.2 mm x 1 mm x 4 mm. The error without cup in troposphere due to solar radiation seems to be less than 2 % RH.

2.3 Long term stability and drift in high humidity.

This is the property of the material used to sense (generally to absorb) humidity. Vaisala has developed a new polymer (H-polymer) which has excellent long term stability and extremely low drift also in high humidity The sensor has been tested in NIST (The National Institution of Standards and Technology) in U.S.A. The results are presented in table 1.

2.4 Calibration error and temperature dependence.

Each sensor of Vaisala radiosondes is individually calibrated against internationally traceable references. The temperature dependence has been determined for the sensor design and correction coefficients are delivered together with individual calibration coefficients. The temperature dependence correction calculations are made by the software of the ground equipment.

2.5 Humidity lag.

This is the property of both the sensing material as well as the principle of the sensor. Vaisala has traditionally used a capacitive measuring principle. The humidity sensor is a capacitive thin film on a glass substrate (Humicap). The relative humidity dependent dielectric between the capacitance plates is a polymer. Humidity penetrates through the porous surface electrode to the polymer. The polymer characteristics are the most important factors affecting the sensor behavior, such as stability, hysteresis, humidity time response, and temperature dependence.The thickness of polymer layer is the dominating factor of the time response up to certain thickness. After that the dominating factor is porosity of the surface electrode. The mechanical size of the sensor and the capacitance limitations of measuring electronics gives a certain limit for the thickness of the polymer film.The thickness of the film in the new sensor is now only 0.5 micron. In addition Vaisala has developed a special (patent appl.) method for the vacuum deposition of the thin film surface electrode so that the time response can have been minimized. At 1000 hPa and 20°C with ventilation 6 m/s humidity time response is less than 1 sec(fig .1)

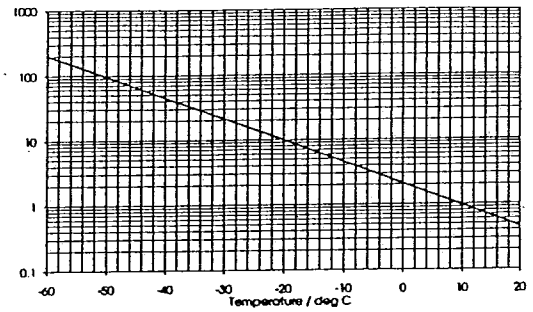

FIGURE 1 : HUMIDITY TIME RESPONSE OF H-POLYMER HUMICAP

	Average differences: NIST reference - H-humicap					
Temperarure	HUMIDITY LEVEL %rh					
deg C	15	30	45	60	75	98
25	-1.5	-0.8	0.5	0.7	1.5	3.7
5	-1.4	-1.2	-0.7	-0.2	0.2	0.1
-2	-1.4	-1.1	-0.7	-0.2	0.3	-0.4
-20	-1.1	-0.5	-0.7	0.1	0.6	1.9
-40	-1.4	-0.5	0.3	1.4	2.2	

TABLE 1 : H-HUMICAP TEST RESULTS AT NIST

2.6 Thermal lag.

To minimize thermal lag, the small size of the sensor is again very welcome. Also heat conduction from the sensor boom or radiosonde body should be minimized. The small size of the new Vaisala humidity sensor improves essentially these factors. Thermal time response is presented in figure 4.

2.7 Water condensation and icing on the surface of the sensor or surfaces nearby.

Together with The University of Helsinki theoretical and experimental research was made to clarify the nature of the condensation and ice formation on the sensor and surrounding nearby. (2)

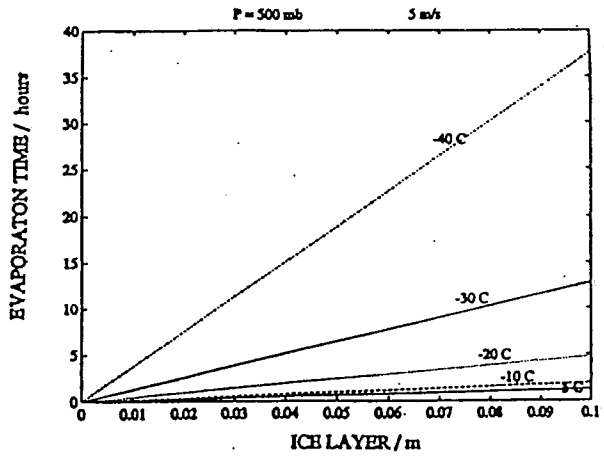

FIGURE 2: EVAPORATION TIME AS A FUNCTION OF ICE LAYER

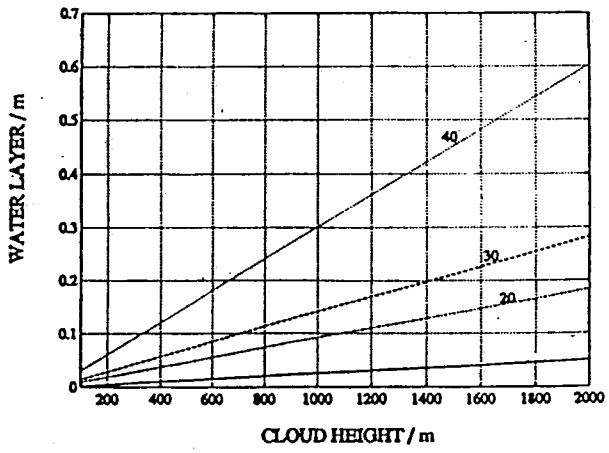

FIGURE 3 : WATER LAYER WHEN DROPLET DENSITY IS 100 /ccm, AVERAGE DROPLET DIAMETERS 40,30,20 µm AND ONE MIXED COMBINATION, ASCENT RATE 5 m/s

The occurrence frequency of these phenomena is highly dependent on the weather type. It happens mainly in heavy clouds. Rain promotes its occurrence. It is clearly indicated by high humidity readings well above tropopause. Formation of ice on the sensor may happen when super cooled water drops hit the sensor or

when water vapor condensates on a surface. Condensation of ice is a minor phenomena (2,3). The amount of super saturation and number of active CCN (cloud condensation nuclei) mainly define the variation of drop diameters. The number of droplets depends greatly on cloud type (20.....1100 pcs/ccm). Droplet diameter range is 10...100 µm. At temperatures below 0 °C formation of ice starts to happen. Generally super cooled and liquid water is still present down to -30 °C. Impaction directly perpendicularly to the surface of the sensor and to the boom was applied (2,4,5) for approximation of impaction distance. Finally the thickness of formed water film on sensors was estimated taking the water film to be a function of cloud thickness. Above the cloud ice and water begin to evaporate. Evaporating time was estimated (fig 2). Cloud having height more than 400 meters may produce so much of water and ice (fig 3), that the sensor does not have time enough to recover during the rest of the sounding. According to the impaction theory all surfaces are also good traps for droplets. Small surfaces as such accelerates the evaporation and prevents formation of ice and water film. Again the small size of the sensor is a great advantage.

The already mentioned water repellent treatment helps in these phenomena but in some extreme conditions it does not always have the desired effect.
May be the only way to solve the problem is to have some kind of heating of the sensor. One way is to heat the sensor and then measure the temperature of the sensor and thereafter to make the correction calculations needed. Another way is to heat the sensor for a moment and then let it recover from the heating, make a measurement and then heat again and so on. We have in Vaisala made several kinds of experiments and tests with heated sensors. The most attractive and most promising is the method where sensor is heated with very short electric pulse of only a few milliseconds (0.3... 5 ms) just after the humidity measurement has been done. After having waited for the time when other sensors and references are being measured, i.e. about 1.3 seconds the humidity is again measured and just after this a heating pulse is again sent to the humidity sensor. The heating element has been integrated on the same small glass substrate as the sensor itself by using the same thin film technology (fig. 4 and 5). The small size of the sensor again helps the heating and recovering of the sensor system. Unfortunately, as the theory shows, sometimes the thickness of the ice layer can be so thick that the energy of the heating pulse will not be sufficient to evaporate the ice.

Therefore we have made tests using two separate sensors in the same radiosonde. While one sensor is being heated and is recovering another (already recovered) sensor is connected to the measuring electronics. (fig. 8)

3 Sensor heating engineering.

In order to optimize the heating parameters and methods to be used and the construction of the integrated heated sensor the heating phenomena were studied carefully before a sensor for heating was specified. A model for the heat transfer characteristics was developed using the following formulas.

Heat transfer equation (6,7) for this case is
$m\, c\, dT/dt = h_c A_s (T_a - T) + Q_r + Q_h + Q_c$, ,where
m = body mass , c = specific heat of the sensor T = temperature of the sensor ,t= time , h_c = convective heat transfer coefficient , A_s = surface area, T_a= ambient air temperature , Q_h = electrical heating in sensor
$Q_r = \varepsilon R + \gamma S - \delta \varepsilon A_s T^4$, radiative heat flux , where
R= infrared radiation power , ε = emissivity for infrared radiation , γ = solar absorptivity, S = solar radiation power, δ = Stefan-Bolzman constant. $Q_c = \alpha A_c (T_a - T)$ = conductive heat flux ,where α = heat conduction , and A_c area perpendicular to heath flux,
Thermal time constant τ can be expressed
$\tau = \rho V c / h_c A_s$, where ρ = density of the sensor, c = specific heat of the sensor, m = mass of the sensor, V = volume of the sensor, A_s = surface area, h_c = convective heat transfer coefficient = Nu k / d, Nu = Nusselt number, d = width of the sensor,
Depending on geometry and boundary conditions h_c can be calculated (6,7).
For the humidity sensor
$Nu = 0.66\, Re^{1/2}\, Pr^{1/3}$
Reynolds number (Re) is a function of pressure and Prandtl number (Pr) is a function of temperature.
$Re = v\, d\, / \nu$
ν = kinematic viscosity of air, v = flow rate of air,

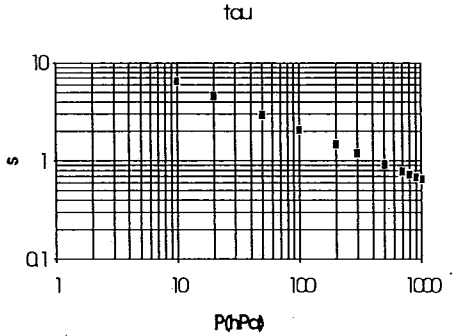

FIGURE :4 TERMAL TIME RESPONSE OF PULSE HEATED SENSOR

Pressure dependence of thermal time response can be calculated. For the sensor having characteristic dimension.1.5 mm , the dependence is shown in figure 4. In normal use humidity time response dominate. If heat pulses are fast and heat remains only on the surface until it is removed by convection, the dominant time constant would be thermal.Temperature profile in sensor body can be determined after some simplifications. This leads typically to very small heating areas, heating times below 1 ms and power below 5 W.
Vaisala INTERCAP construction is favorable for integration of a heating element. Electrical disturbances are minimized. Surface electrode in figure 6 is also a heating element. In another version (fig.6) a heating resistor is placed on the substrate covering as large area as possible of it. Size of the sensor was minimized from 4x4x0.4 mm to 1.5x4x0.4 mm . A heated protection cap is shown as an example of continuous external heating arrangements (fig. 7). Temperature measurement of humidity sensor is needed.

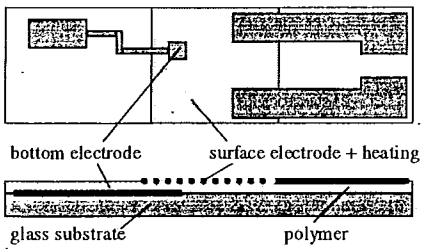

FIGURE 5 : CONSTRUCTION OF SURFACE HEATED HUMICAP

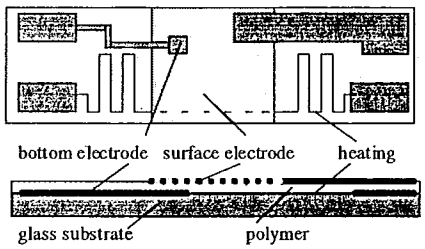

FIGURE 6 : CONSTRUCTION OF BOTTOM HEATED HUMICAP

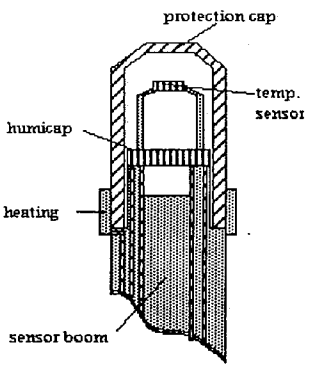

FIGURE 7 : CONSTRUCTION OF EXTERNAL HEATING

4. Test soundings

In spite of all laboratory testing and engineering, the most effective way to test sensors is to carry out real soundings. This is especially true if condensation phenomena are discussed. More than 100 twin flights have been done using different kind of constructions of the sensor and heating parameters. The lack of suitable weather conditions have has delayed the schedule of the research work.
All solutions are technically working, but there are large differences in accuracy and in preventing condensation problem. The main problem is to get a fast sensor, which can be used with high heating power . In figure 8. there is an example of a sounding where two heated sensors are used. While one is being heated and waiting for recovery, another is used for measurement. The time constant of the sensor system can be calculated from soundings, and it can be used to determine proper timings between heating periods.
In figure 9 is an example of sounding with a pulse heated H-humicap sensor. Some soundings have been done with heating resistance integrated with the protecting cap of the sensor. Also with this arrangement positive results were achieved. An additional temperature measurement is needed for humidity sensor when heating is on all the time. This solution is very sensitive to ventilation of the sensor and temperature measurements may still cause problems.
The major reason for slow recovery after heating is the humidity lag . It is obvious that thermal lag may be fast , but polymer recovery after heating depends on the humidity lag constant. This is very true in cold, and will limit heating frequency to a great extent. Heating frequency or heating power must be controlled by temperature. This makes it possible to heat as much as needed in clouds and then reduce heating to avoid errors caused by a slow time constant in cold.

5. Discussions and conclusions.

The small size of the sensor, new H-polymer, increased ventilation and heating of the sensor seem to reduce remarkably the unfavorable phenomena in humidity measurements in radiosondes.

According to the developed model for icing of the sensor a cloud of thickness of 2 km may generate such a thick ice layer that the recovery by free evaporation will not be possible. Therefore heating is needed and even then the icing may take place in very bad weather conditions.

Some heating applications seems to prevent condensation. Many more soundings in various weather conditions must be done to verify the final solution . At the same time much attention must be paid to the complete sensor

boom design to avoid heat conduction problems. Radiation errors must be minimized and defined . Thermal lag is planed to become sufficiently low. The condensation problem can be avoided, but sensors lags and tolerance of high heating power will guide the direction of the solution. Excellent stability of the H-Humicap sensor makes it possible to carry out accurate and reproducible measurements.
The research work still continues for the construction of the sensor and the boom and the determination of parameters.

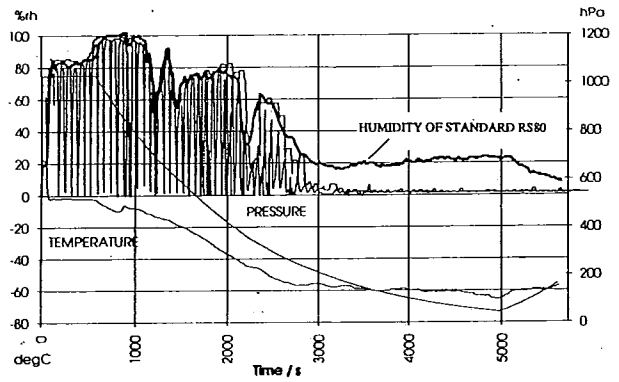

FIGURE 8 : SOUNDING WITH TWO (IN TURN) HEATED SENSOR . HUMIDITY OF STANDARD RS 80, HUMIDITY OF ONE HEATED SENSOR AND COMBINED HUMIDITY OF TWO HEATED SENSOR ARE SHOWN

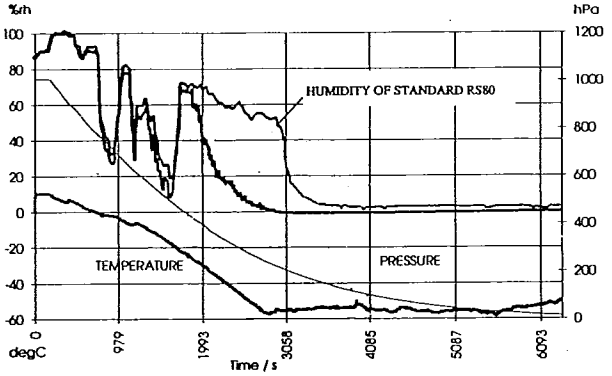

FIGURE 8 : A SOUNDING WITH PULSE HEATING

References:

1.V. Antikainen , V. Hyvönen : Radiosonde Performance in Rain and Clouds. WMO/TD-No.50 ,1985
2. Pekka Korhonen : Research on Icing Phenomena of RS80 Boom (Private report made for Vaisala Oy) Helsinki University ,Department of Physics.
3 . L. Makkonen : Analysis of rotating Multicylinder Data in Measuring Cloud droplet Size and liquid water Content. J. of Atmos. and Oce.Techn.,Vol 9 ,1992.
4. W.C. Hinds . Aerosol Technology : Properties , Behavior and Measurement of Airborne Particles ,1992
5. R.C. Flagan and J.H. Steinfeld : Fundamentals of Air Pollution Engineering,1988.
6. F. P. Incorporate and D. P. De Witt : Fundamentals ofHeat and Mass Transfer. 1990
7. Jacob : Heat Transfer, vol.1,2 ,1959.

THERMISTOR CORRECTIONS: THE NASA MODEL VS MULTI-THERMISTOR CORRECTIONS

F. J. Schmidlin

NASA/GSFC/Wallops Flight Facility
Wallops Island, Virginia 23337 USA

It has been known for sometime that radiosonde measurements made using the white-coated rod thermistor flown in the United States does not provide a representative value of the ambient temperature. Daniels (1968) suggested a method of resolving a better temperature using coatings having different emissivity values. Talbot (1972) reported that the long-wave emission from this thermistor resulted in measurements that were too cold at night and also largely compensated the daytime effect of solar heating. Hemispheric chart analysts realized that the US radiosonde provided widely differing day/night values of temperature and geopotential. McInturff, et al (1979) reported on the day/night differences and, using a significant number of radiosonde reports provided tables that were used to adjust daytime values to nighttime values. Although not a correction. This study did provide adjustments that enabled consistent hemispheric upper-air chart analysis.

In spite of the known effects of radiation on the rod thermistor little has been done to produce suitable thermistor corrections. Temperatures retrieved from satellites and other studies requiring radiosonde temperature data prompted NASA to review the question of radiosonde accuracy (Schmidlin, et al, 1986). Using a combination of white, aluminum, and black thermistor coatings it looked feasible to obtain the needed correction. Daytime radiosonde flights require all three thermistors while nighttime flights require two (white and aluminum). The values of the thermistors' emissivities and absorptivities were obtained from laboratory measurements. The correction is then obtained using these values and the thermistors' measured temperatures to solve three heat transfer equations solved simultaneously.

Figure 1a contains an example of the three thermistor profiles obtained from Crawley, England, on 21 February 1992 at 1116UTC. The separation of the temperature profiles is obvious, the black thermistor being warmest and the white coldest. These profiles were obtained on an cloudless day. The calculated correction for the white-coated thermistor, shown as temperature error, is seen in Figure 1b. The magnitude of the error grows until it reaches 1.1°C near 27 km (~15 hPa); it decreases above this level. This same temperature error-profile shape was found in the measurements acquired at all of the observation locations.

The three thermistor radiosonde approach has been found to be effective in accurately estimating corrections for the US radiosonde. Once the radiosonde temperature measurements have been corrected the resulting data can be effectively used to derived errors measured by other radiosonde types. Ideally, the process can be adopted at operational observing stations to provide correct temperature reports for use by the meteorological and climatological communities. Alternatively, it was considered that the thermistor error could also be obtained using a model (Luers, 1990; McMillin, et al, 1992). Information consisting of atmospheric radiances and transmission coupled with knowledge of environmental parameters such as ozone, water vapor, carbon dioxide, along with other observables such as clouds, skin temperature, etc. are used. Combining this information with the standard (white) thermistor's geometry, temperature, emissivity and absorptivity can provide an reasonably good estimate of the thermistor error.

Once measurement and NASA model methods provide corrections that coincide each must be examined for its potential as an operational procedure. We discuss three thermistor data for Wallops Island and Crawley, UK in concert with model results of the same radiosonde observations. Because the measurement method has been used to obtain data over a range of environmental conditions it is instructive to perturb the model's inputs to estimate the effect of various environmental conditions.

Figure 1a shows the temperature measurements of white, aluminum, and black thermistors on February 21, 1992 at 1116 UTC. The test flight was made at Crawley, England, as part of test flights conducted to evaluate potential reference radiosondes. The temperature of the dewpoint indicates high relative humidity up to about 2 km height, but no clouds were present. The separation between the white and black thermistors is a nominal value and is seen to increase with altitude. Figure 1b gives the temperature error of the white thermistor derived from solving three heat transfer equations simultaneously (solid line). At about 33 km the error becomes negative. This characteristic, to a larger or smaller degree, is found in all profiles of this type. The temperature error of the thermistor calculated by the model approach is also shown (dashed line). The agreement between the model and measurements are good. The model also predicts that the temperature error becomes negative near 33 km.

Figure 2a shows measurements made during night at Wallops Island, Va. during September 2, 1992. White and aluminum thermistors were used. As can be seen the temperature measurements are nearly identical up to near 23 km after which the qaluminum thermistor reads warmer than the white. The dewpoint curve indicates that a number of moisture levels, if not clouds, were present. A cirrus overcast was present with a base near 8 km. The solid line in Figure 2b is a representation of the error determined from the two thermistors. The dashed line is the model prediction, and as is evident the two curves, once again, agree. The negative temperature error at night is believed to come from the large emissivity of the white coating used on the rod thermistor.

Not shown in this paper are the occassions when the model and measurements disagree. Normally, this comes about from some factor not being included in the model, mostly a true representation of cirrus clouds because of a low overcast. Cirrus overcast when very thick tend to cause a very large negative error. There are examples when the error reaches as musch as -4°C.

The presentation covers more examples.

REFERENCES

Daniels, G. E., 1968: Errors of radiosonde and rocketsonde temperature sensors. Bull. Amer. Meteor. Soc., 49. 16-18.

Luers, J. K., 1990: Estimating the temperature error of the radiosonde rod thermistor under different environments. J. Atmos. Oceanic Tech. 7, 882-895.

McMillin, L., M. Uddstrom, and A. Coletti, 1992: A procedure for correcting radiosonde reports for radiation errors. J. Atmos. Oceanic Tech., 9, 801-811.

McInturff, R. M., F. G. Finger, K. W. Johnson, and J. D. Laver. 1979: Day-night differences in radiosonde observations of the stratosphere and troposphere. NOAA Tech. Memo. NWS NM<C 63. 47 pp.

Schmidlin, F. J., J. K. Luers, and P. D. Hoffman, 1986: Preliminary estimates of radiosonde thermistor errors. NASA Tech. Paper 2637. 15pp.

Talbot, J. E., 1972: Radiation influences on a white-coated thermistor temperature sensor in a radiosonde. Aust. Meteor. Mag., 20, 22-33.

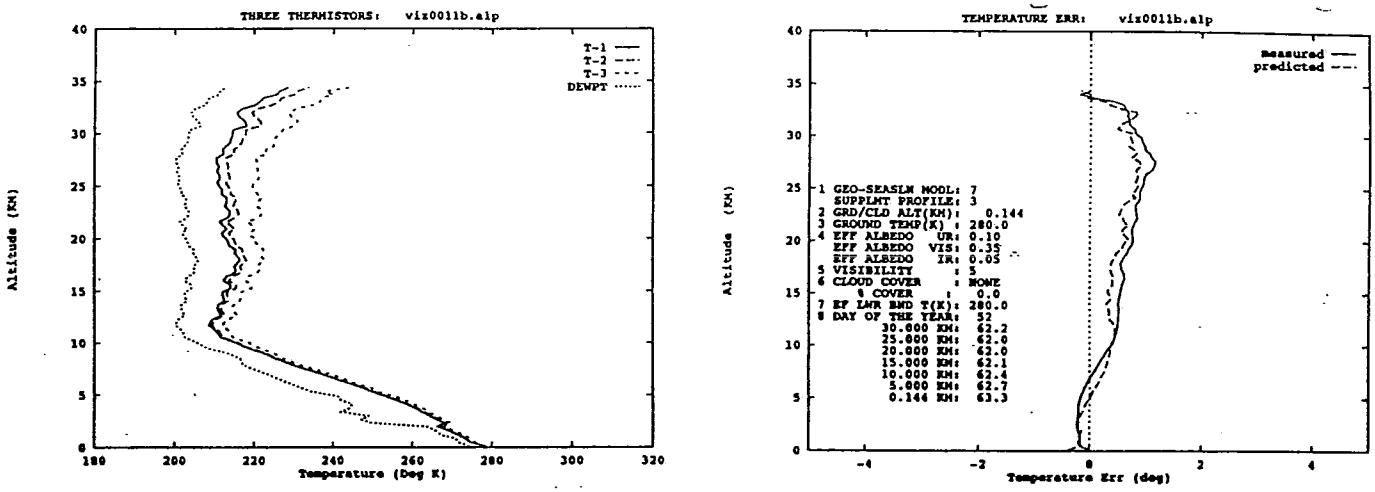

Figure 1 a) and b) See text for details.

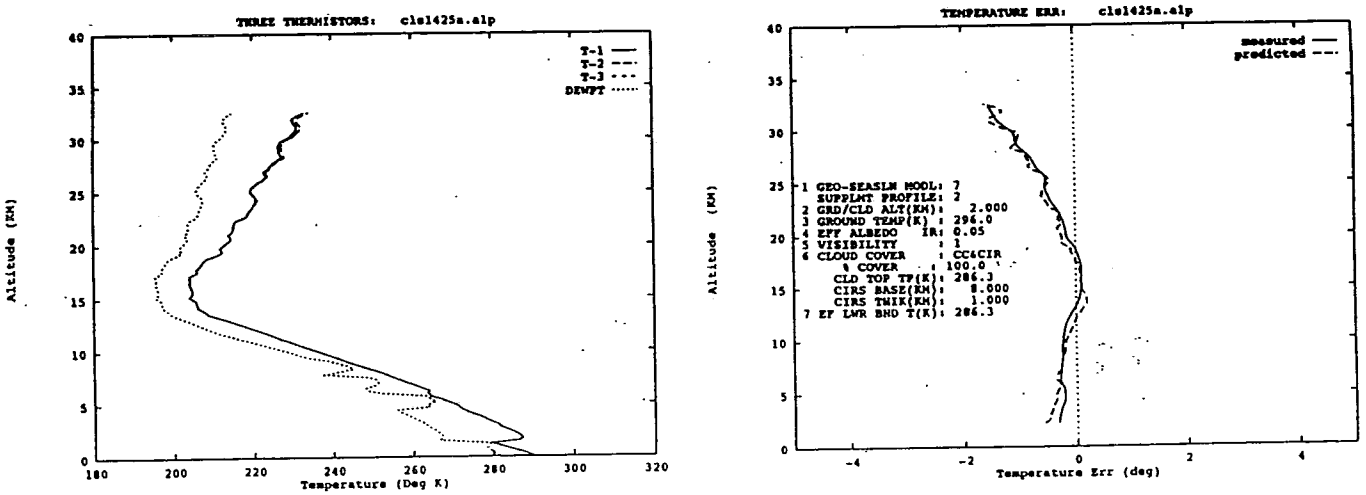

Figure 2 a) and b) See text for details.

DEVELOPMENT OF A REFERENCE RADIOSONDE

Walter F. Dabberdt
National Center for Atmospheric Research*
Boulder, Colorado 80307-3000 U.S.A.

Abstract. Significant errors can occur in vertical profiles obtained by *in situ* radiosonde measurements, including both upsondes and dropsondes. Presently there is not a capability available to assess both the absolute performance of particular radiosondes and specific sensors. Work currently underway is aimed at the development of a "reference radiosonde," a reusable device incorporating highly accurate, redundant wind and thermodynamic sensors. The reference radiosonde will significantly enhance the characterization of radiosonde- and sensor-performance, and will facilitate the assessment and improvement of existing devices and development of new sensors (*in situ* and remote sensors).

1. The Reference Radiosonde Concept

The radiosonde may be the single most important instrument for measurement of atmospheric variables required for determination of thermodynamic profiles and subsequent diagnostic and prognostic applications. It also provides benchmark data for determining the accuracy of various indirect and satellite-based measurements. As newer technologies are introduced which complement and may eventually replace the radiosonde, the absolute accuracy of current sonde measurements comes increasingly in question.

A reference radiosonde can provide the atmospheric science community with an accepted standard of accuracy that will serve the requirements for evaluation of operational radiosondes as well as other *in situ* (e.g. aircraft) and active and passive remote sensing techniques (e.g. DIAL and Raman lidar, and microwave radiometry and infrared interferometry). Such a reference system will be capable of extending the present consensus radiosonde intercomparison technique by providing an accepted ambient transfer standard. It can be used as a reference for the performance of new sensing systems, and also serve as a standard for benchmark global climate stations.

2. Examples of Measurement Uncertainties

To illustrate some of the measurement uncertainties and variations of operational radiosondes, examples are given of temperature and humidity errors introduced at launch as well as limitations in height-resolved wind structure due to the characteristics of the wind processing software algorithm and radiosonde tracking system. Both types of uncertainties can be resolved, although conventional operational practices do not. Systematic intercomparisons of various commercial radiosondes have been conducted by the World Meteorological Organization, yielding absolute uncertainties of wind measurements and relative uncertainties of thermodynamic variables.

Errors in low-level thermodynamic measurements obtained during the recent TOGA Coupled Ocean-Atmosphere Response Experiment (COARE) were presented by Cole (1994) along with a procedure to retrieve the true ambient profile. The problem arises due to the difference at launch between the indicated sonde temperature and relative humidity and the true ambient values. These differences arise either from ambient radiational heating of the sensors or the effects of air-conditioned (or heated) balloon inflation and launch shelters. Cole adjusted the indicated low-level thermodynamic profile to account for various surface launch ambiguities by

using independent unbiased surface measurements of temperature and humidity. Knowing the difference in the indicated surface values and the surface reference value, he determined the amount of heat associated with either the warming or cooling of the sonde sensor arm and then transferred the excess heat between the sonde and the ambient air (or vice versa) through consideration of the sensor ventilation rate after launch and the thermal properties of the sensor mount. The 06Z (16LT), 8 February 1993, sounding at Kavieng, New Ireland,Papua New Guinea (Lat 02°34'S, Lo 150°39'E) is an illustrative case. At launch, the indicated sonde temperature and relative humidity are 32.7C and 59.0%, while the actual ambient surface values are 30.1C and 72.2%, respectively. The sonde values equate to an indicated surface mixing ratio of 15.1 g kg^{-1}, while the actual surface value is 19.0 g kg^{-1}.

Williams, Wade and Morel (WWM, 1993) have explored the implications of the windfinding techniques used with the National Weather Service's Micro computer-based Automatic Radio Theodolite (Micro-ART) system with those used in the NAVAID-based CLASS sounding system developed at NCAR. Uncertainties associated with Micro-ART winds are the result of limitations in the radio theodolite tracking system and in the algorithms used to compute wind speed and direction. The accuracy of CLASS-derived winds is a function of the number, location and signal strength of time-of-arrival LORAN (or Omega) signals received and translated by the sonde. WWM compared standard Micro-ART and CLASS winds along with refined, non-standard Micro-ART winds for 30 co-located soundings made in the contiguous U.S. CLASS winds were computed at 6-s intervals using TOA data smoothed over 60-s periods. Standard Micro-ART winds are computed using the difference in the averages of three successive 6-s elevation (λ) and azimuth (α) angles obtained at 60-s intervals. Refined (6-s) Micro-ART winds were obtained in a similar but continuous manner. In neither case are outlier angles identified or removed. Lastly, WWM computed so-called STORM winds from Micro-ART observations using a three-step procedure. First, successive 6-s radiosonde positions (elevation and azimuth, pressure-altitude) were calculated using standard techniques. Second, outliers in position data were removed using a least-squares polynomial fit over a time interval determined by elevation angle (1 min for $\lambda > 15°$ increasing to 4 min as $\lambda \rightarrow 0°$). Third, position data were smoothed using a polynomial fit after removal of outlier data in step two.

Vertical profiles of wind speed using the four methods were compared by WWM for a high wind-speed sounding from 12Z, 17 June 1992, taken at Salt Lake City, Utah. The overall structure of the standard Micro-ART sounding is very consistent with the inherently higher resolution CLASS sounding. The refined 6-c Micro-ART sounding indicates additional structure though less than the CLASS sounding. The *edited* STORM sounding has additional structure very consistent with CLASS. The dropouts in all Micro-ART-based soundings result from exceedances of elevation criteria for the radio theodolite. While the two Micro-ART soundings are likely adequate for synoptic and prognostic applications, the CLASS and STORM soundings may be important to various mesoscale studies.

Schmidlin (1988) presents the results of the second phase of the WMO international radiosonde intercomparison conducted February-March 1985, at Wallops Island, Virginia. Five commercial radiosondes were flown simultaneously on each of 100 balloon flights tracked by FPQ-6 C-band radar. Wind estimates by GMD were found to be good at heights below 10 km, but large errors were reported at long ranges and low elevation angles. Daytime differences in temperature at standard pressure levels were $<0.5°K$, while the range of mean nighttime temperatures was $-1.0°K$. However, lapse rates indicated on exiting cloud tops frequently were superadiabatic for the rod thermistors and inversion for the capacitive sensor (note that the latter sensor has been superseded by an improved sensor). The indicated temperature differences at given pressure levels reflect both the performance of the temperature and pressure transducers. The study determined that all relative humidity measurements (carbon, lithium, and capacitance thin-film sensors) were in good agreement ($<2\%$) below the first cloud layer. At higher levels, the agreement was poor. Subsequent WMO intercomparisons provide additional insight into the

relative performance of various radiosondes, and indicate differences in performance as a result of sensor changes.

3. Initial Design of the Reference Radiosonde

The NCAR reference radiosonde system consists of a ground station, reference sonde data acquisition and telemetry platform (the 'sonde'), and atmospheric sensors. The initial design is based on a microprocessor-controlled digital sonde with a suite of high-quality sensors and redundant, lower-cost alternative sensors. The sonde is designed to be capable of using sensors with capacitive, resistive, voltage and frequency outputs, and to provide power and reference inputs to the sensors. The ground station is a modified version of the NCAR dropwindsonde data system. (Lally et al, 1989). Laboratory calibration facilities include: Two computer-controlled temperature/pressure chambers covering a range of -40° to +60°C and 20 to 1100 hPa; a portable humidity chamber capable of humidities over 10 to 95% RH; a "two pressure" humidity/temperature chamber with a range of 10 to 95% RH and -20° to + 50°C; and an open loop wind tunnel with a maximum speed of 25 ms^{-1}. In addition, primary standards, traceable to the National Institute of Standards and Technology (NIST), are used to calibrate the reference standards used in the systems described above. Dynamic pTH chambers are coming into use in Germany and Russia, and collaborative efforts are being explored.

Sonde. The sonde gondola is an insulated box 15x20x30 cm, containing the sonde electronic systems, a GPS engine, pressure sensor, lithium batteries and a duct for housing humidity sensors. Wands for holding temperature sensors are mounted on opposite corners of the gondola with lightweight booms extending from the other two corners to hold additional sensors or complete sondes. Total mass will vary from 800 to 1500 g depending on the mass of add-on sensors. A GPS antenna is mounted on the top of the sonde with a 400-MHz telemetry antenna on the bottom. Figure 1 illustrates the mechanical configuration of the prototype sonde.

Sensor Requirements. Sensors are being identified and evaluated in terms of their ability to meet the performance specifications as well as in consideration of their size, weight, availability, and cost. Performance specifications have been proposed, but are in the process of being refined through interaction with modelers, researchers, and operational groups. Accordingly, the sensor requirements found in Table 1 should be viewed as preliminary.

Candidate Pressure Sensors. Pressure is both measured and computed. The primary candidate is an oven-controlled temperature-compensated piezoresistive sensor. Oven-control facilitates calibration of the sensor with improved accuracy and reduced overall costs. Hypsometers provide improved accuracy at the lower pressure ranges, but this accuracy is not required since pressures can be computed from GPS derived altitude, and virtual temperature. At the lower pressures, pressure can be computed using the hydrostatic equation to accuracies of better than 0.1 hPa.

Candidate Temperature Sensors. Four types of temperature sensors are under consideration: a small (~10 mil) aluminized bead thermistor; a triad of moderate-sized (~35 mil) flake thermistors each with different radiative characteristics; a thin platinum wire; and a very small thermocouple with a thermally insulated reference junction.

Candidate Humidity Sensors. Humidity is the most difficult of the atmospheric variables to be measured. Candidate sensors include: dew/frost-point hygrometer (e.g. Oltmans, 1985); thin-film capacitance sensor (possibly heated); and a heated carbon hygristor.

Candidate Wind Sensors. Windfinding will be based on the Global Positioning System (GPS). A number of techniques are under development to provide a low-cost GPS radiosonde. AIR Inc. (Boulder, CO) has demonstrated a codeless receiver technique that requires minimum bandwidth

but measures winds only with no altitude capability. NAVSYS Corp. (Monument, CO) is developing a digital translation approach (TIDGET) that balances bandwidth and sampling rate. Vaisala Oy (Helsinki, Finland) has announced that it will have an operational GPS radiosonde in 1994.

It is essential that an accepted reference standard be available to determine the performance of these competing low-cost technologies, as well as other systems relying on the LORAN and OMEGA navigation-aids. Fortunately complete five- and six-channel GPS engines are now available at costs which are acceptable for an expendable reference radiosonde. When these proven commercial engines are combined with a ground-based receiver operating in the differential mode, wind accuracies of 0.1 ms^{-1} for 1-s averages are obtainable. Differential operation also provides absolute altitude accuracy of 5 m at all altitudes, permitting reference-quality pressure calculations using the hydrostatic equation.

4. Summary

The reference radiosonde serves a dual role. First, it is an instrumentation device that provides reference-quality *in situ* transfer standards, as well as a platform that can be used to test and evaluate the performance of various operational *in situ* sensors. Second, it can serve the international community as part of an ongoing collaborative program to assess and develop new radiosonde sensors or sensor configurations. Initial flight tests of the prototype reference radiosonde will be conducted early 1994.

Acknowledgments

NCAR is sponsored by the National Science Foundation. Development of the first-generation reference radiosonde is proceeding under the joint sponsorship of NSF/NCAR and the Department of Energy's Atmospheric Radiation Measurement program.

References

Dabberdt, W.F. and V.E. Lally, 1994: Uncertainties in radiosonde measurements and the development of a reference radiosonde, Proceedings, *Fifth Conference on Global Change Studies,* American Meteorological Society, Nashville, TN (January 24-28).

Lally, V. E., D. Lauritsen, T. Hock and K. Norris, 1989: Wind Measurements over the North Atlantic Using a Loran-C Dropwindsonde, NAVIGATION: *Journal of Institute of Navigation*, Vol. 36, No. 4, Winter 1989-1990.

Lally, V.E., 1991: A reference radiosonde. Proceedings, *Seventh Symposium of Meteorological Observations and Instrumentation*, American Meteorological Society, New Orleans, LA (January 14-18), pp. 217-220.

Oltmans, S.J., 1985: Measurements of water vapor in the stratosphere with a front-point hygrometer. Proceedings, *1985 International Symposium on Moisture and Humidity.* Washington, D.C. (April 15-18), pp. 251-258. Instrument Society of America, Research Triangle Park, NC.

Schmidlin, F.J., 1988: Instruments and observing methods. Report No. 29, WMO/TD-No.312, World Meteorological Organization, Geneva, pp.113.

Table 1. Preliminary Reference Radiosonde Specifications

Variable	Range	Accuracy	Precision
• Pressure	1060 - 10 hPa	<0.5 hPa	~0.1hPa
• Temperature	185 - 320 K	0.15 K	0.1 K
• Humidity, Td	210 - 320 K	Ta > 273 K:	
		1.0 K	0.2 K
		Ta = 210 K:	
		2.0 K	0.5 K
• Vector winds (10-s or 50-m ave.)	0 - 150 m/s	0.5 m/s	0.1 m/s

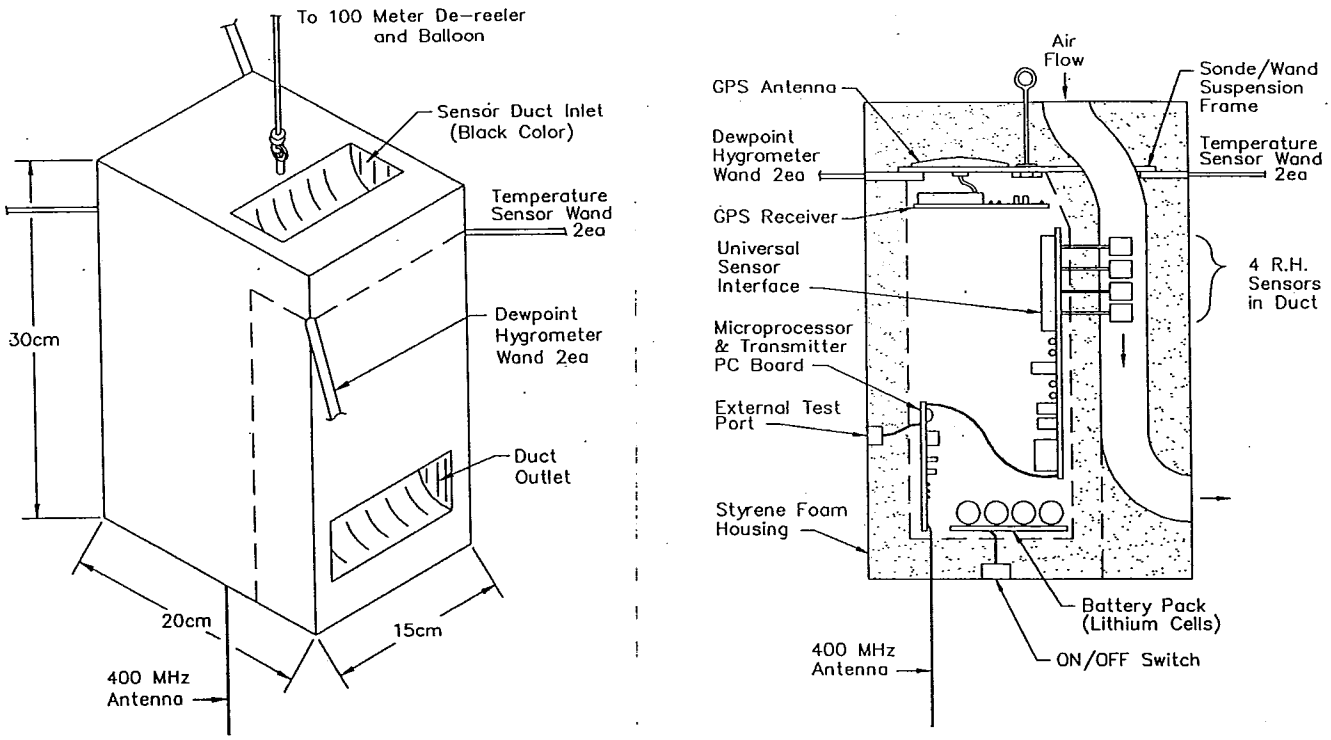

Figure 1. Reference Radiosonde: External view (left) and section view (right)

WINDFINDING IN RADIOSONDE USING GPS

K. Kaisti, T. Saarnimo and V. Karttunen
Vaisala Oy, Upper Air Division
Box 26, 00421 Helsinki, Finland

1. Introduction

The accuracy of traditional windfinding solutions (Omega, Loran etc) is not sufficient for all meteorological applications. There is also lack of global windfinding coverage with current navigational networks. The existing navaids are also susceptible to atmospheric electrical interference due to the long antenna required in radiosonde. Vaisala is therefore developing a new windfinding solution based on GPS that will improve the accuracy and give a global 24h coverage. The vertical resolution of windfinding will also greatly improve since no long integration times are needed. Table 1 summarises the accuracy of current navaid solutions and the accuracy of differential GPS as well.

Windfinding network	Wind vector [m/s]	Height [m]
Loran-C	0.5	-
Omega	1.0	-
Diff. GPS	0.1	10

Table 1. Comparison of different windfinding solutions.

GPS (Global Positioning System) is a satellite navigational system designed for extreme accuracy and world-wide coverage. The present satellite constellation consists of 25 working satellites. The satellites transmit a digitally modulated spread spectrum signal on carrier frequencies of 1.226 GHz and 1.575 GHz with a power level of -130 dBm i.e. well below thermal background noise. The 1.575 GHz carrier is modulated by a satellite specific pseudo random noise (PRN) code (C/A-code) with a chipping rate of 1.023 MHz. This spreads the spectrum effectively to 2 MHz. A satellite can be identified and tracked based on the PRN code that it uses. This is done by generating a local replica of the PRN code and using a correlation technique to lock onto the satellites. Four satellites are required for accurate 3-dimensional positioning.

2. Differential GPS

Since the radiosonde is a one time product the cost of the GPS receiver in sonde has to be kept as low a possible. The GPS windfinding system for the radiosonde is therefore based on differential GPS. The idea is to use two GPS receivers and a communication network between them. The dataprocessing of the GPS-signal is left to minimum in the radiosonde and the actual calculation of the wind solution is done at the ground station and thus a very low cost GPS sonde can be achieved.

The low cost GPS receiver in the radiosonde tracks four satellites and extracts the pseudo ranges to these satellites by using a code correlation technique. This technique removes the spread spectrum modulation of the GPS-signal and thus a narrow band signal results. The narrow band signal (1200 baud) that contains the pseudo range data can then be transmitted to the ground station by using the 403 MHz FM-transmitter in the radiosonde. The basic view of differential GPS for radiosonde use is presented in figure 1.

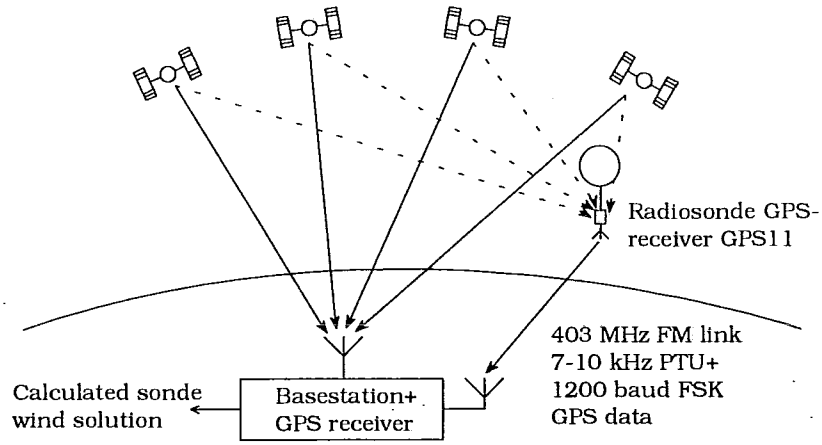

Figure 1. Implementation of differential GPS

The ground station receives the pseudo ranges and makes differential corrections to them. The windfinding calculation is done at the ground station based on the corrected pseudo ranges. The accuracy is even better than a complete GPS receiver can achieve since many of the errors are common to the receivers and thus a mathematical compensation can be made.

The GPS signal is 2 MHz wide which means that the sonde receiver cannot relay the signal as it is to the base station since this would occupy too much transmitting bandwidth. This means that the spread spectrum signal has to be removed in some way before the GPS signal can be sent to the base station using existing narrow band telemetry channels.

There are basically four ways of 'de spreading' the GPS signal:

1 using a code correlation technique
2 using a squaring receiver topology
3 using a code phase receiver topology
4 using a translator

2.1 Code correlation

Each satellite has its own unique Pseudo Random Noise (PRN) code that spreads the spectrum and makes a CDMA technique possible. A satellite can be acquired and tracked based on its PRN code it uses. This is done by creating a local copy of the satellite code and correlating the two signals. The code correlation technique gives the pseudo range to the satellite in question. For 3-dimensional navigation we need the pseudo ranges to four satellites to eliminate clock errors etc. The pseudo ranges differ slightly from true ranges since there are some small errors due to incorrect clocks, propagation delays, SA etc. The errors can, however, be mathematically compensated by using differential GPS since they are common to the receivers. This improves the accuracy of GPS to 10 meters in relative positioning and 0.1 m/s in relative speed. The benefits from a code correlating approach are that the pseudo ranges are eventually unambiguous and that the re acquisition of the satellite is fast if the satellite signal is lost. The pseudo ranges can be sent to the base station using a very narrow bandwidth (1200 baud). This is an important aspect in radiosonde use.

2.2 Squaring

The GPS signal can be received by using a squaring approach as well. Here the BPSK modulated GPS signal is squared (multiplied by itself). This generates a DC component plus a signal twice the frequency of the original signal. The BPSK modulated satellite code is lost in the squaring operation. The squared signal is, however, quite narrow banded (approximately 8 kHz) since it contains basically only the Doppler shifts (±4 kHz) of all the satellites in view due to their motion. To track the satellites the receiver has to know the Doppler shifts and directions of the satellites because the tracking filters have to be very narrow (~10 Hz) in order to find the satellite signals buried in the noise. The squaring approach requires some degree of 'intelligence' in order to find the satellite quickly if the signal is lost. Otherwise the re-

acquisition takes a considerable amount of time since the tracking filters are very narrow. Since the GPS signal has a power level of -130 dBm i.e. 20 dB below thermal noise there is a negative S/N-ratio. The power level of the signal drops to ¼ with the squaring operation which means that there is an conversion loss of 9 dB in the system. The negative S/N-ratio is also doubled. There is even a patent for a squaring GPS receiver for radiosonde use [Pat. U.S. 1988, p. 1] but no real products with this approach exist, however, for radiosonde use. The base station can calculate the sonde movements based on the Doppler shifts when the elevation angels to the satellites are known with respect to time.

2.3 Code phase receiver

The code phase receiver is the second type of codeless GPS receiver. The basic idea is to delay the received GPS signal with exactly half a C/A-code chip i.e. 487 ns and to cross correlate the delayed and the direct signal [Wells et. al, 1986, p. 7-10]. This method doesn't require knowledge of the code itself only its chipping rate. When the cross correlated signal is filtered the phase of the code sequence can be solved. This receiver suffers from code phase ambiguity whereas the squaring receiver suffers from carrier phase ambiguity. The code phase information contains the Doppler shifts of the satellites since all GPS signals are derived from the same GPS clock (=10.23 MHz) and are thus coherent. The BPSK modulated satellite signal is lost as well.

2.4 Translator

The true translator approach that relays the GPS spread spectrum signal to the base station is not feasible in radiosonde use because it occupies too much bandwidth. [Nordwall 1993, p. 71] presents, however, an approach where the 2 MHz GPS signal is digitized and compressed reducing the bandwidth to approx. 100 kHz. This is not a true low bandwidth solution and the accuracy of this differential GPS solution (0.2 m/s) is not as good as with code correlation approach.

3. Radiosonde GPS receiver GPS11

Vaisala's approach to the GPS receiver in radiosonde is based on the code correlation technique. This results in a low cost receiver and the complexity being in the base station unit.
The radiosonde GPS receiver GPS11 consists of the following building blocks (figure 2):

- GPS antenna
- Low Noise Amplifier (LNA)
- GPS radio
- Correlator

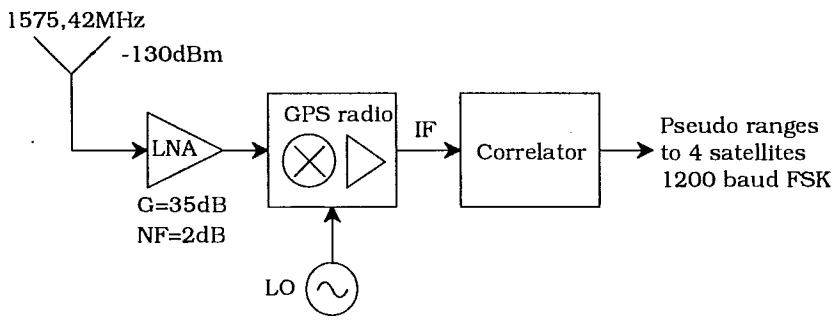

Figure 2. Block diagram of GPS11

The antenna has a gain pattern such that the pendulum effect (30° maximum) of the sonde doesn't loose the satellites. This means that there is antenna gain below horizon as well. The antenna has to maintain the right hand circularly polarized GPS signal on the total antenna beam as well. The Noise Figure (NF) of the receiver has to be kept as low as possible (<3dB). This is done by

using an LNA with adequate gain (35 dB) and a low NF (2 dB).

The GPS radio down converts the 1.5 GHz spread spectrum signal to a much lower Intermediate Frequency (IF) using direct conversion. It provides also more gain (100 db overall) to bring the noise signal to a more manageable level. The LNA and the radio are built on the same low cost 2-sided board to keep the cost down. The size of the radio is 70x80 mm^2 and it is screened to prevent interference.

The correlator acquires and tracks four satellites in order to make the continuous pseudo range measurements. New pseudo ranges to four satellites are sent to ground every second by using 1200 baud FSK modulation. The FSK signal can directly modulate the 400 MHz transmitter in the radiosonde resulting in a very cheap interface to the existing hardware. The size of the correlator module is nearly the same as the radio (70x70 mm^2) and it is a two layer board for cost reasons. In this way the two boards can be mounted on top of each other and thereby making a compact receiver, approximately 40 mm high. The GPS11 module is an add-on module to the existing radiosonde.

4. Base station GPS receiver

The existing ground equipment (DigiCora/Marwin) routes the detected 403 MHz FM-signal to the base station GPS receiver where the FSK signal is demodulated and the radiosonde wind solution is calculated. The GPS receiver will be available as an add-on-module to existing Vaisala ground equipment. The base station GPS receiver is a complete receiver that can handle differential GPS as well. The general view of the receiver is shown in figure 3.

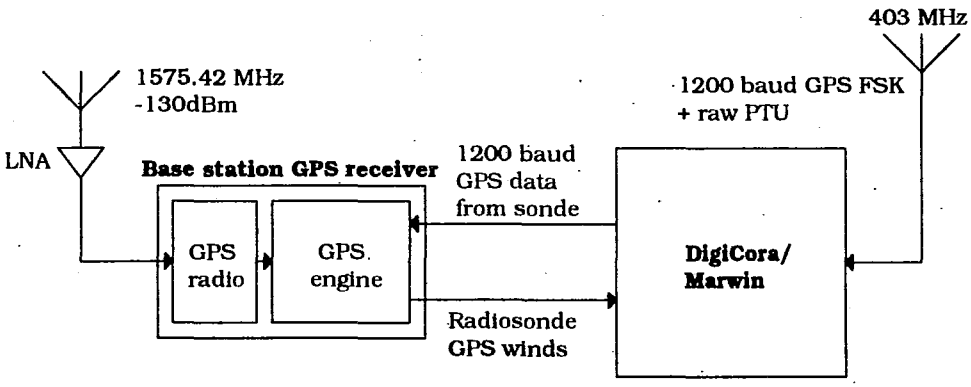

Figure 3. Base station GPS receiver.

The GPS antenna and the LNA can be e.g. a commercial patch antenna with adequate gain and a low NF. The gain of the antenna must exceed the coax cable losses if the antenna is mounted far from the receiver.

The GPS signal is down converted and amplified before it is passed to the GPS engine for further processing. The GPS engine performs data downloading from the satellites and local pseudo range measurements. The base station GPS receiver tracks the same four satellites as the sonde in order to get two sets of pseudo ranges that are used for differential positioning. The pseudo ranges from sonde are differentially corrected and the sonde wind solution is calculated based on the corrected pseudo ranges to give the accuracy listed in Table 1.

The calculated radiosonde wind solution is re-routed back to DigiCora/Marwin where it is combined with the normal meteorological data.

5. Preliminary test results

Thorough ground tests are being done at Vaisala at the moment. Preliminary test results on ground show that the theoretical accuracy of differential GPS can be achieved.

REFERENCES

Nordwall, Bruce D. 1993. GPS could improve sonobuoys, radiosondes. Aviation Week & Space Technology 18, 11, p- 71-72.

Pat. U.S. 4754 283. Codeless GPS Sonde. Tracor Aerospace Austin, Inc., Austin , Texas, USA. (Fowler, Clarence W., Tex, Elgin). Appl 875102, 28.6.1988. 8 p.

Wells, David E., Beck, N., Delikaraoglou, D., Klausberg, A., Krawisky, E.J., Lachapelle, G., Langley, R.B., Nakiboglu, M., Schwarz, K.P., Tranquilla, J.M., Vanícek, P. 1986. Guide To GPS Positioning. Canadian GPS Associates, Fredericton, N.B., Canada. 15.7 S.

A NEW GPS RAWINSONDE SYSTEM

David B. Call
Atmospheric Instrumentation Research, Inc.
8401 Baseline Road
Boulder, Colorado 80303 U.S.A.

INTRODUCTION

A new rawinsonde system, the GPS-700, measures atmospheric pressure, temperature, humidity (MET data) and wind velocity. The GPSonde[tm] (radiosonde) uses translated GPS (Global Positioning System) signals to produce wind velocity. The application of GPS technology to a low cost radiosonde is unique. This system provides the operator with a fully automatic, operational, upper air rawin station.

GPS TECHNOLOGY

The Global Positioning System constellation consists of 24 satellites, orbiting once every twelve (12) hours at an altitude of 20,000 kilometers. The orbital track of the satellites is such that four to eight appear above the horizon at all times. Each satellite contains a very stable rubidium frequency standard that is used to precisely synchronize the transmission of a uniquely coded signal. The signals are transmitted simultaneously at the same frequency using digital spread spectrum technology. By comparing the time of arrival of signals from 3 or more satellites, the position and velocity of a GPS receiver can accurately be determined. Commercial GPS receivers contain sophisticated digital signal processing circuitry that "code-correlates" or synchronizes with each satellite's unique "C/A" (Course Acquisition) code. The complexity and cost of even the simplest code-correlating receiver is prohibitive when considered for expendable radiosonde use.

THE GPSsonde

The GPSsonde (Figure 1) utilizes unique signal compression technology to reduce the cost, bandwidth and power of the disposable radiosonde receiver. The sonde receiver (Figure 2) compresses and combines the signals from all GPS satellites above the horizon and strong enough to be detected into a narrow frequency bandwidth (less than 500 Hz). The compressed GPS signal is then combined with sensor data from the digital MET Data Encoder and applied to the Frequency Modulation (FM) input of a transmitter tuned to 400-406 MHz and transmitted to the ground station for further processing. Since the GPS receiver's position and velocity are computed in the ground station, the cost of the radiosonde remains low. The GPS receiver power requirement is about one-tenth the power required for commercial C/A receivers. Table 1 lists GPS sonde receiver performance specifications.

The accuracy, response time, and resolution of the pressure, temperature, and relative humidity sensors approaches that of high quality laboratory instruments. Pressure is measured by a patented, dual diaphragm aneroid capacitance transducer. The pressure sensor's small temperature dependance is compensated for by a temperature- sensitive capacitor mounted near the sensor. The pressure sensor is insensitive to shock, vibration, acceleration, and orientation.

A small NTC (Negative Temperature Coefficient) bead thermistor is used for temperature measurement providing high sensitivity, fast response, and long-term stability. The sensor is coated with a water-proof, reflective material which reduces the effects of solar radiation.

Relative humidity is measured by AIR, Inc.'s, patented HUMAIR[tm] capacitive sensor with an accuracy of better than 3% over the range 0 to 100% RH. Hysteresis and linearity are less than 1% and exposure to 100% RH for long periods has little effect on stability. It provides accurate measurements in clouds, as well as above the troposphere where the atmosphere is very cold and dry. HUMAIR has a unique construction. The sensing polymer is 2 microns thick and is exposed to air flow on both surfaces. This thinness makes the HUMAIR time constant response to humidity fluctuations typically less than 1 second. Figure 3 depicts the relationship of sensor capacitance to relative humidity in ten percent (10%) steps from 5% to 95%. GPSonde sensor performance specifications are given in Table 2.

A microprocessor within the GPSonde measures pressure, temperature, and relative humidity (PTH) each second using RC oscillators and frequency counting circuitry. PTH sensor calibration coefficients are stored in the sonde's memory and transmitted along with measured sensor data, identification number, and CRC error detection code in serial "Manchester" format. Manchester encoded data and a sophisticated detection system at the ground station allows error-free telemetry reception even with very noisy signals. The sonde identification number insures that interfering radiosonde signals are not decoded in error. Automatic transmission of all sensor calibration coefficients eliminates the need for punched paper tape or manual entry of calibration data.

The crystal-controlled, narrow band, 400-406 MHz, GPSonde transmitter has frequency stability of better than $\pm$ 5KHz, and when used with the Model IS-5A-RCR receiver provides a range of 160 Km. The combined GPS and MET signal bandwidth (less than 10 KHz) easily fits within the 20 KHz channel spacing limitation imposed in some European countries.

The GPSonde is housed in a thermally insulated, light weight, small volume, styrofoam package. All printed circuit boards utilize SMD technology. It is powered by two (2) standard, 9 volt batteries which provide sufficient energy for a two (2) to three (3) hour flight. An easily accessible external switch activates the power. Temperature and HUMAIR sensors are mounted on an external boom with a protective rain shroud.

GPS-700 GROUND STATION

The ground station, Model GPS-700, consists of three major subsystems: UHF receiver/PTH processor, GPS winds processor, and an IBM-compatible 486 personal computer.

The UHF FM receiver was specifically designed for radiosonde telemetry reception. The receiver may be controlled through either an RS-232 port or the front panel keypad. The remote control feature enables the ground station computer to scan the meteorological frequency band and warn an operator of potentially interfering signals within the band. The receiver's digitally synthesized tuning range is 395 to 410 MHz and the AFC feature automatically adjusts the receiver tuning for best signal reception. Receiver IF bandwidth is 30 KHz and synthesizer step size is 2.5 KHz.

The PTH processor within the UHF receiver has two (2) microcomputers that receive and process telemetry data continuously. One (68HC11) converts the Manchester-encoded telemetry signal into standard binary data. The second (80186) calculates pressure, temperature, relative humidity and elapsed time in standard scientific units. The PTH processor is a data concentrator and coordinates serial communication between several RS-232 ports. One port supports remote control of the UHF receiver. A second port provides an interface to the winds processor. Receiver specifications are summarized in Table 3.

The GPS winds processor, Model 70, utilizes a dedicated 486 microcomputer, as well as custom circuitry for digital signal processing. It contains a commercial C/A code correlating GPS receiver that is used to derive UTC time, geodetic position, and the GPS constellation almanac.

A GPS receiver, essentially identical to that on the GPSonde, is installed in the Model 70 GPS Windfinder.

The digital processing circuitry was designed with hardware capacity to process up to four separate GPS signal inputs simultaneously. One input is used to process the translated GPS signals from the radiosonde. A second input processes base reference signals from a GPS receiver. Selective Availability/Anti-Spoof (SA/AS) are modifications made to GPS signals by the U.S. Department of Defense in order to degrade their performance so an unauthorized user cannot achieve GPS precision guidance capability. The apparent velocity of the ground station caused by SA/AS is subtracted, "differenced", to calculate the true GPSonde velocity. Using differential GPS tracking, sonde velocity can be measured to an accuracy of 0.25 m/s.

If the base station is moving at an unknown velocity, the system will use only the GPSonde signal for wind calculations. Under these conditions, the effects of SA/AS degrade performance to about 1 m/s wind accuracy.

The PC used with the system is a standard 486 personal computer with internal hard drive, 3.5 inch floppy, mouse, and super VGA color monitor. Table 4 provides Ground station specifications.

SYSTEM SOFTWARE

The operating system is IBM OS-2. Development of application software under OS-2 is significantly more challenging than Microsoft Inc.'s Windows running under DOS, but provides the reliability and capability to handle real time processes involving multiple interrupts and multi-tasking. Its reliability and "crash resistance" are important in scientific and operational applications. OS-2 is a multi-windowed operating environment that is powerful, flexible, and easy to learn. Multi-tasking capabilities of OS-2 are utilized in a number of ways in real time. Sounding data is presented in tabular and graphical format during the flight. All raw data is stored on hard disk.

WMO mandatory and significant levels, as well as the WMO messages, are automatically produced. Editing capability is provided to allow the operator to modify significant point selections and regenerate the message. The message can be sent automatically.

FLIGHT COMPARISONS

A.I.R., Inc., has tested the performance of GPS windfinding by simultaneously tracking, using separate ground stations, two radiosondes that are carried aloft on the same balloon. Figure 4 shows dual flight data comparing the Model GPS-700 to the A.I.R., Inc., Model IS-4C-MET NAVAIR System using cross chain LORAN. This data shows both the very good agreement between two totally unrelated windfinding techniques, and also the structure and detail that is not normally seen with conventional systems that heavily smooth wind data. Figure 5 is a plot of GPSonde data available in real time with the OS-2 windowed operating system.

CONCLUSIONS

The GPS-700 Rawinsonde System is the first practical, commercial application of the Global Positioning System for an upper air windfinding system. Worldwide availability of GPS and the small, compact size of the ground station make the GPS-700 a universal upper air sounding system.

Table 1
GPS SONDE RECEIVER SPECIFICATIONS

GPS Signal	L1 (1575.42 MHz)
Antenna	1/4 Wave RHCP Volute
Noise Figure	1.5 dB
Velocity Accuracy	0.25 m/s

Table 2
SENSOR PERFORMANCE SPECIFICATIONS

PRESSURE SENSOR

Type	Aneroid capacitance
Pressure Range	1050 to 5 hPa
Accuracy	1 hPa
Resolution	0.1 hPa
Response time	< 0.1 second

TEMPERATURE SENSOR

Type	Bead thermistor
Temperature Range	-90° to 50° C
Accuracy	0.3° C
Resolution	0.01° C
Coating	White
Nominal Resistance	10 K Ohm @ 25° C
Response time	< 1 second

HUMIDITY SENSOR

Type	Capacitance Polymer
Humidity Range	0 to 100% RH
Accuracy	3% RH
Hysteresis	<1% RH (0 to 100% RH)
Resolution	O.1% RH
Response time	< 1 second

Table 3
TELEMETRY PERFORMANCE SPECIFICATIONS

TRANSMITTER

Power Output	100 mW
Frequency Range	400 to 406 MHZ (Crystal selected)
Modulation	FM
Antenna	1/4 wave monopole
Frequency Stability	+/- 5 KHz
Deviation	5 KHz
Range	160 km

SIGNAL FORMAT

MET Data	Manchester, 1000 baud (Typ.)
MET Sample Rate	1 Hz
Error Detection	32 bit CRC
GPS Signal	500 Hz bandwidth

Table 4
GROUND STATION SPECIFICATION

COMPUTER

IBM Compatible PC	80486
RAM	16 MB
Hard Disc	210 MB
Floppy Disc	3.5", 1.44 MB
Display	VGA

UHF RECEIVER/PTH PROCESSOR

IF bandwidth	30 KHz
Detection	FM
AFC	Automatic
Preamp NF	1.0 dB
Sensitivity	0.5 microvolts
Synthesizer	2.5 KHz steps
Antenna	1/4 monopole
PTH Processor	400 to 2200 baud
PTH input	50 mV to 1.0 Vpp
PTH output	RS-232, ASCII or Binary

ATMOSPHERIC DATA PROCESSOR, MODEL 70

Input Channels	4
Processor	80486 SLC

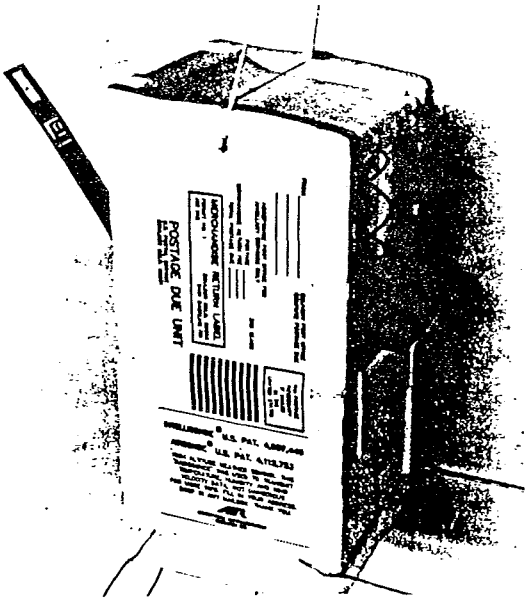

Figure 1: GPSonde

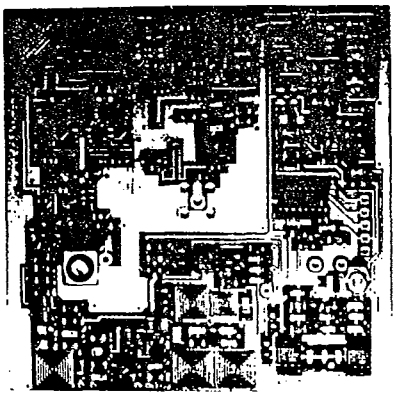

Figure 2: GPS Receiver Circuit Card

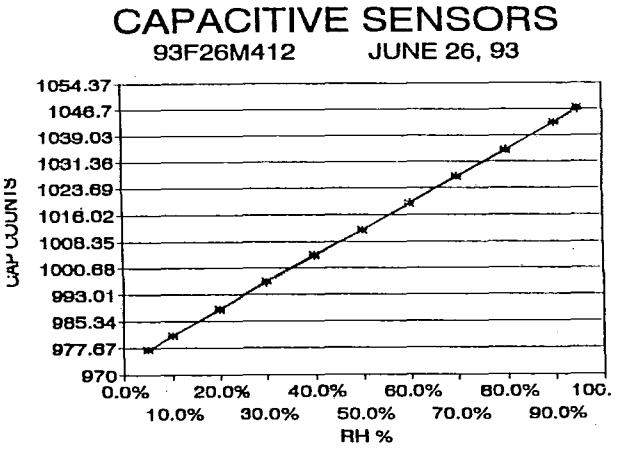

Figure 3: HUMAIR Hysteresis Plot

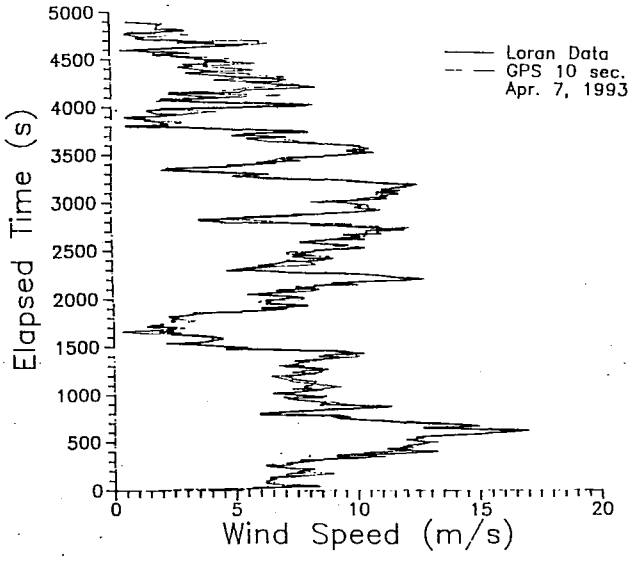

Figure 4: GPS/LORAN Dual Flight Comparison

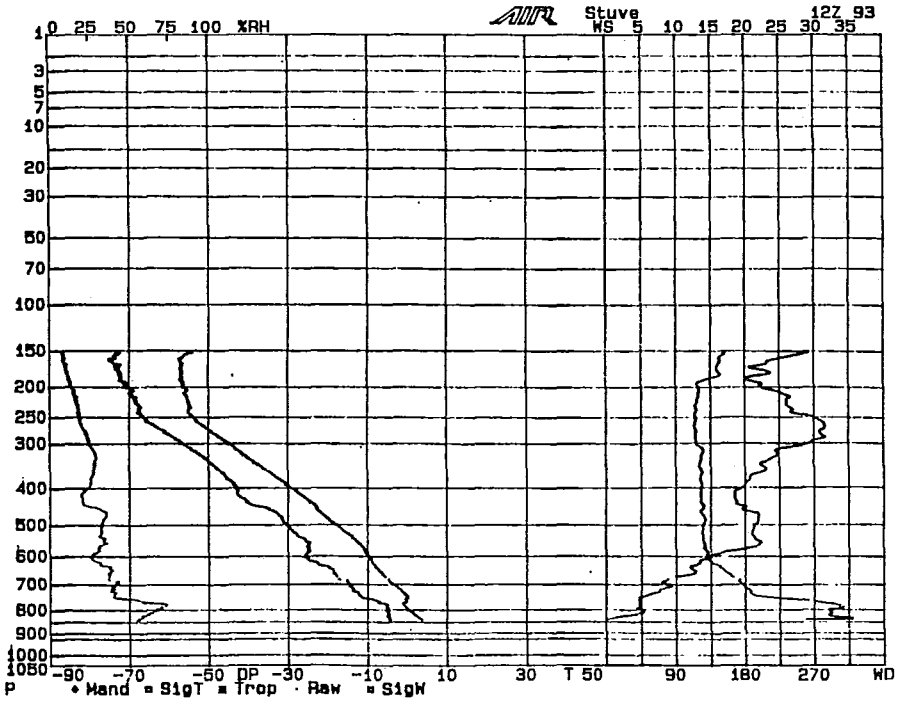

Figure 5: OS-2 GPSonde Graphic Display

TEST OF AN AUTOMATIC BALLOON FILLING AND LAUNCHING SYSTEM IN AN OPERATIONAL ENVIRONMENT

Ture Hovberg

Swedish Meteorological and Hydrological Institute, Sweden

1 Introduction

SMHI has tested a prototype of an automatic ballon filling and launching system in an operational environment at the Radiosonde Station at Sundsvall/Härnösand Airport (62°31N, 17°26E). The service at this radiosonde station is an integrated part of the meteorological routines at the Regional Meteorological Office at the airport. Normally, 3300 hours per year is used for the upper-air service at this station. Ten persons are educated in sonde operations.

The purpose of this test was to get a better basis for strategic planning of the future radiosonde stations network, in order to make further cost reduction. Of a special interest is the possibility to make the launchings automatized at the sonde stations, and remotely controlled from a common manned central. Another purpose of the test was to evaluate the utility of automatic balloon filling and launching technology, especially during winter conditions.

During the test period from February 18 to April 22 1993, 252 remotely controlled soundings was performed. Upper-air infomation from the test period was used operationally. A manual back-up routine was organized in order to guarantee the data availability. Notes concerning weather conditions, technical function etc was made during the test. The system was normally loaded with six radio sondes and balloons during the test.

2 Test object

The test object was an early prototype of an Autosonde System from Vaisala, designed for loading of maximum six balloons and sondes.

At the test site an Vaisala Marwin Radisonde System is used for routine upper-air operations. The Marwin System has Loran-C and Omega equipment for wind measurement.

The test equipment was not connected to the Marwin equipment during the test, and there was no control computer connected to the Autosonde and Marwin systems. A remote control for the Autosonde was situated indoors at the Radiosonde Station, close to the Marwin equipment. The key-pad of the remote control made it possible for the operator to initiate hydrogene filling and balloon launching remotely.

3 Test performance

The test was integrated in the routine service. Ten persons from the staff got one day of education in Autosonde handling, and four of them further one day of education in corrective maintenance.

During the test four daily soundings were made wind soundings at 0600 and 1800 UTC, and wind-, temperature- and humidity soundings at 0000 and 1800 UTC.

As the test system not included a control computer, a special routine was developed for manual handling of sound data tapes between groundcheck and launching. The sonde groundcheck and calibration as well as the Autosonde loading was made daytime. The launching was remotely controlled from the Marwin room in the office building. Manual launching was made only when the automatic launching failed, or if the Autosonde equipment was out of order. Notes concerning weather conditions, technical function etc during the test was made in a log book.

4 Weather during the test period

Some climate data from Sundsvall Airport during the test:

- Monthly mean temperature: February -2.8°C, Mars -0.6°C and April +2.9°C
- Lowest minimum temperature during the test: -18.0°C February 24
- Monthly precipitation amount: February 13.7 mm, Mars 7.8 mm and April 6.0 mm
- Maximum daily precipitation amount during the test: 8.6 mm February 18
- Maximum snow depth during the test: 11 cm February 20
- Maximum wind speed during the test (10 minutes average): 12 m/s Mars 9, 1800 UTC. At that moment wind gusts of 20 m/s was registered.

5 Result and discussion

Th information in the log book is analysed. All soundings from February 18. 1800 UTC are included, and have been divided into six classes. The result is given in Table 1.

Tabell 1: Autosonde statistics. Sundsvall, Febr. 18 - April 21, 1993.

Class	Number	%
1 Sounding accepted	240	95,2
2 Ballon burst	1	0,4
3 Sonde fail	3	1,2
4 Autosonde failure	1	0,4
5 Operator fail	4	1,6
6 Autosonde not used	3	1,2
SUM	252	100

The event with balloon burst took place at February 9, 1800 UTC, when wind gusts of 20 m/s was registered. The broken balloon blocked the Autosonde mechanism, and made it impossible to step forward to a new sonde, and manual launching had to be used. Manual sounding had to be used also at 0000 and 0600, as no operator with education in corrective maintenace was avaliable at that moment. The reason of the balloon burst is not quite clear, but it could have been caused by the relatively high wind gusts at the moment.

The three occasions with sonde fail has not been able to analyse in detail. One occasion could have been caused by the operator in the loading procedure, and the two other could have been damages of the sonde in the launching moment, caused by wind.

The Autosonde failure occurred Mars 9, 0000 UTC. At that event no answer from the Autosonde appeared when the launching was initiated, and manual sounding had to be used.Manual sounding had to be used also 0600, as no operator with education in corrective maintenace was avaliable at that moment. After manual reset in the Autosonde cabinet the equipment was working again.

The four cases that have been classified as operator fail are due to the manual routine for handling of sound data tapes between groundcheck and launching, and could probably have been avoided if an automatic routine in a control computer have been used.

When studying the log book it is easy to see, that the frequency of failure events has decreased in the later part of the test, when the routines have been more practiced

During the test, time studies have been performed. The result is given in Table 2.

Tabell 2: Time study. Sundsvall, Febr. 18 - April 21, 1993.

Working moment	Time in minutes
Groundcheck and calibration of 4 sondes and 4 balloons	34
Loading of 4 sondes and balloons in Autosonde	25
Preparation of 1 sonde for Autosonde	10
Supplementary work, launching etc	3
Average time for 1 sounding	28

6 Conclusion

The test has shown, that the average working time will be maximum two hour per day at a sounding frequency of four soundings per day, provided that the launchings are remotely controlled from a manned control central. The two hours work can be made daytime.

The Autosonde operators need no qualified technical education. Normal education for sounding operators, completed with an education in Autosonde operations is probably enough.

The weather during the test period has not offered extreme winds and temperatures or heavy snowfall. With reservation for the events of balloon burst and sonde damage, wich possibly was caused by strong wind, the Autosonde has worked very well.

The test has produced good basic information for specification of functions for remote control of Autosonde operation.

The test has produced good basic data for cost/benefit analysis. The level of costs for operator time and other management will make it easy to prove profitability for Autosonde.

The Autosonde operators' experience is very good. The tasks are much simplier, and there is no need of nighttime work outdoors. The automated hydrogene balloon filling is a substantial safety factor.

References

Vaisala, 1992. Vaisala Autosonde, A Fully Automatic Upper-air Sounding System. *Ref. No SR0583. Date 92-12-17*

NEXT GENERATION NAVAID WINDFINDING

Juhana Jaatinen

Vaisala Oy, Upper Air Division
Box 26, 00421 Helsinki, Finland

Abstract

This paper describes a new generation of precision NAVAID windfinding systems. The proposed system introduces both technical improvements and new concepts in windfinding. The power and versatility is achieved by using state-of-the-art Digital Signal Processing (DSP) techniques.

Several new features characterize the new system. Firstly, temporal resolution is one second instead of the previously common ten seconds. This is a decisive step towards fine vertical resolution in the order of 100 meters. The first layer is simultaneously lowered from the usual 500 - 600 meters to about 50 - 100 meters.

Secondly, the use of multifrequency composite NAVAID windfinding in the VLF frequency band gives practically complete coverage of the globe. This makes the system fairly immune to the loss of one or more transmitters, and expands the system life time especially in the case, that some Omega or other transmitters would be phased out. The overwhelming redundancy in the number of received stations also improves the possibility to detect and correct signal path propagation errors, which leads to better accuracy compared to the previous systems.

The new system provides improved windfinding performance with all NAVAID windfinding options on a single, small, multiprocessor subsystem. This includes the present three station and the new five station Alpha, and differential cross-chain Loran-C with the same hardware. The user can select windfinding mode simply by selecting radiosonde, either VLF-sonde or Loran-C sonde.

1. Introduction

NAVAID systems are designed to be used for navigational purposes, that is, determining the receiver absolute position. However, the accuracy of absolute position does not directly reflect the accuracy achieved in windfinding. More accurate wind estimate can be obtained by determining relative movement of the radiosonde compared to the transmitting NAVAID stations.

NAVAID windfinding systems are based on the reception of navigational signals by a radiosonde and processing these signals on a ground-based station. Determining wind velocity (speed and direction) contains the following steps:

- Signal detection and phase (time difference for Loran-C) component determination for each transmitter.
- Solving the wind vector from an overdetermined set of equations.
- Filtering noise from the wind profile (smoothing).

1.1. History

Vaisala was among the first companies to introduce NAVAID based windfinding systems in the early 70's. In these first generation systems position fix was done using signals of only three different stations, which the operator had to select prior to the balloon launch. Only one frequency of Omega, 13.6 kHz, was used. This three-station-method, as used in Vaisala's CORA, was not very successful, but gave encouraging results in good conditions.

A study on mathematical methods and programming algorithms combined with a new sounding computer, lead to a considerably improved product: the MicroCORA. The major advances in the second generation were: all eight Omega transmitters were used, a quality factor for each signal was computed, this factor was used for weighting when composing the wind vector, and the operator had the possibility to exclude bad stations instead of having to select the three supposedly best ones. MicroCORA uses polar correlator to determine the wind vector from one Omega frequency.

Further improvements were introduced in the new DigiCORA/Marwin -family in 1984. In the third generation sounding equipment the sounding process was automated, and several Omega frequencies were used together with one Alpha (Russian VLF) frequency making a total of eleven transmitters. All available signals contributed to the wind computation with automatic consistency checking, providing computed winds at 10 second intervals.

The DigiCORA/Marwin -family was upgraded with cross-chain Loran-C in 1987, and in 1991 with an option for six Communications VLF transmitters simultaneously with Omega and Alpha making a total of 17 available transmitters. Today the present DigiCORA/Marwin is widely accepted within the meteorological community.

2. Problem Definition

Several major improvements are expected from the new fourth generation sounding equipment. This paper focuses on the windfinding subsystem, the Navaid Processor, that handles signal detection and wind phase determination. The design goal is a Digital Signal Processing (DSP) based multiprocessor system in a single unit, that would replace all existing Vaisala NAVAID boards, including analog filter boards.

To improve windfinding performance there are several topics that should be taken into account in the proposed new system: all of the available dynamic range of the incoming signal should be used, steeper filters for improved noise rejection, more stations for better coverage, the new Alpha five station regime, differential calculation for all NAVAID options, and improved time (vertical) resolution.

System flexibility is also an important factor that should be taken into account in all phases of the design; not only for the Navaid Processor, but for the whole fourth generation sounding system.

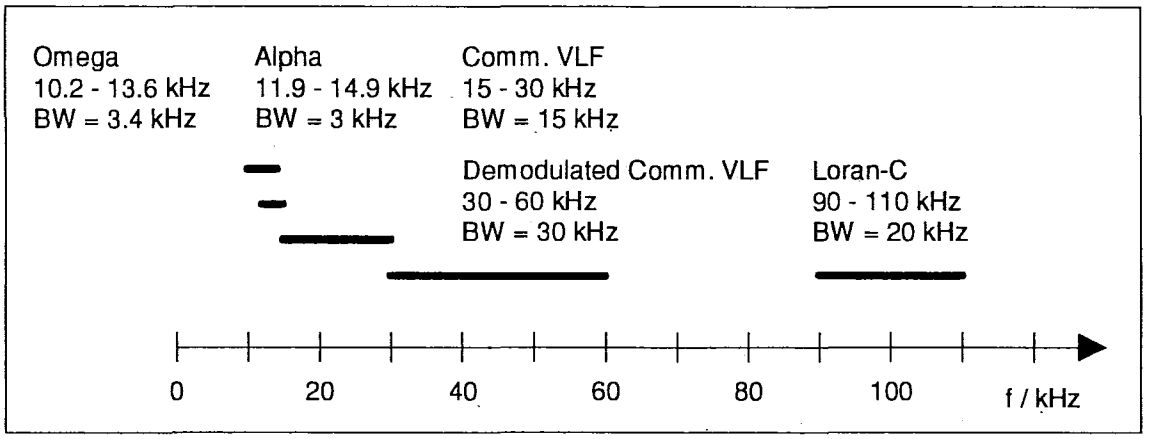

Figure 1. NAVAID frequency ranges

The large variety of NAVAID signals and frequency ranges, see Fig. 2, combined with the expected performance level leads to the use of state-of-the-art Digital Signal Processing (DSP) techniques.

3. Next Generation NAVAID Windfinding

Basis of the next generation NAVAID windfinding is the Navaid Processor subsystem, that handles signal detection and phase component determination. This data is then used for solving the wind vector and wind profile.

The Navaid Processor will be an integral part of future fourth generation Vaisala Sounding systems, but an option for connecting it to existing systems will be developed. A single Navaid Processor will implement Loran-C, Omega, Alpha, and Communications VLF sounding options.

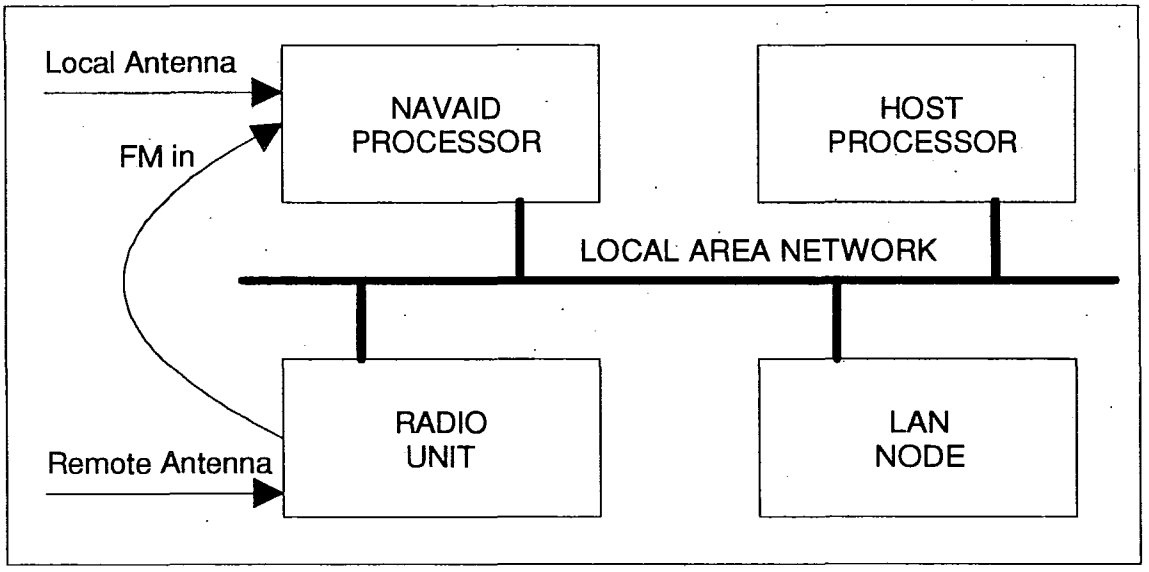

Figure 2. Next generation sounding system

In the next generation sounding system all units are connected with a Local Area Network (LAN), that serves as a communication path for sounding data and commands, and as a means for downloading program upgrades. This setup provides great flexibility in process load sharing in the multitasking multiprocessor system. A serial communication path will be used for connecting the Navaid Processor to existing systems with adequate processing capability.

3.1. Sounding Modes

Navaid Processor will implement cross-chain Loran-C, all Omega frequencies, the present multifrequency three station Alpha, the new multifrequency five station Alpha, and Communications VLF sounding options. There are two sounding modes:

- VLF NAVAID: Omega, Alpha, and Communications VLF simultaneously, and
- Cross-chain Loran-C.

Both sounding modes are implemented with a single Navaid Processor subsystem. Any combination of the VLF NAVAID mode can be used, and all stations contribute to a single one-second wind vector value.

3.2. Improved Wind Velocity Data

Since the system is designed for sounding purposes, dedicated algorithms can be used to improve wind vector accuracy. Output of the sounding system is wind velocity (speed and direction), not the absolute geographical position, although this can be computed from the wind velocity. Improved performance is expected from the new system because of advances in the algorithms, software and hardware.

Powerful Digital Signal Processing allows the generation of dense measurement data, once per second wind vectors, for all stations and for all frequencies. This has a considerable effect on vertical resolution of the wind profile, and the size of fine details that can be detected. There are ten times as many measurement points as before, which leads to smoothing filter lengths of $\frac{1}{5}$ or even $\frac{1}{10}$ of the present ones.

High resolution, high speed, analog to digital conversion can use the whole dynamic range available from the radio. Ultimate performance in poor conditions is to be expected, limited only by physical realities.

Differential phase calculation will be available for all NAVAID options, also for cross-chain Loran-C. This operation eliminates climatic disturbance in the signal propagation path, and local oscillator induced frequency drift from the resulting wind components.

Digital filters used in the preprocessing stages provide exact characteristics, steep roll-of rates, and very high stopband attenuation that is hard or impossible to match with their analog counterparts.

Floating-point numbers are used in all calculations. The better resolution and dynamic range guarantees, that there will be practically no over- or underflows in the digital signal processing and wind component determination.

3.3. Improved Tolerance for Absent Stations

The Navaid Processor uses more NAVAID stations and frequencies simultaneously than the existing systems. This includes the new Alpha multifrequency five station regime, and the use of all Omega frequencies. Hence, practically total windfinding coverage of the globe with improved station geometry will be available. One the other hand, the large number of VLF NAVAID stations used makes the system fairly immune to the loss of one or more transmitters.

3.4. Benefits of Digital Signal Processing

The proposed Navaid Processor implements all signal processing and filtering with a Digital Signal Processor, except the compulsory analog anti-aliasing filters. This technology brings several advantages compared to analog signal processing. The expected performance level and small size would not be feasible with conventional analog signal processing.

Digital Signal Processing brings several advantages compared to analog implementation. Since there are no tolerance problems of analog components, reliable system performance is achieved as stated in the specifications. Performance is stable also in the long run, because aging of digital components does not change their processing parameters.

Filters with exact characteristics, steeper roll-of rates, and very high stopband attenuation can be designed, with the only limiting factor being the available processing power. All analog filters have a digital implementation, but there are also digital filters that have no analog counterparts.

3.5. System Flexibility

All signal processing algorithms can be expressed mathematically. These can be implemented either with fixed hardware or software. Both approaches have their benefits and application fields.

If the analog-to-digital sampling rate allows the use of software implementation, this is the correct approach. Software implementation allows major modifications being made in the processing algorithms, which would not be possible with a fixed hardware implementation.

3.6. System Upgrading

Basically all programs will be downloaded to the Navaid Processor and other units of the new sounding system via Local Area Network, and stored into permanent FLASH-memory. System upgrade is a matter of inserting a storage media (3.5" disk, FLASH-card, etc.) to the system and performing program download.

3.7. Multiprocessor System

The proposed fourth generation sounding system is a true multitasking multiprocessor system. The Navaid Processor subsystem uses a floating-point Digital Signal Processor (DSP) for signal processing and a general purpose processor for communicating with the rest of the system.

4. Summary

A new and revolutionary NAVAID based sounding equipment generation is proposed. Windfinding performance is improved in several fields. Some of the benefits are one-second wind vectors, an improvement by one order of magnitude, practically total NAVAID coverage of the globe, and improved performance in poor conditions. Heart of the windfinding system is a new Digital Signal Processing (DSP) based Navaid Processor subsystem.

A SURFACE-BASED HYBRID UPPER-AIR SOUNDING SYSTEM

Antti A. Lange

Finnish Meteorological Institute (FMI)
P. O. Box 503, 00101 Helsinki 10, Finland

ABSTRACT

The selection of upper-air observing systems for a cost-effective upper-air sounding network of a national meteorological service (FMI) depends on the configuration, operating characteristics, capital and all running costs of equipment. Advancing microprocessor technology and effective computational methods make it possible to visualize and combine data in an optimal way from the various sources: weather balloons, radiosondes and the remote sensing systems like Doppler sodars, wind profilers, Radio-Acoustic Sounders (RASS), Doppler weather radars, lidars and microwave/infrared radiometers.

It is straightforward how the NAVAID-based upper-air windfinding can make use of the newest findings in Navigation Technology where so-called "hybrid" navigation is used for improved reliability and accuracy. These sophisticated computations are known as Kalman Filter. It also constitutes the theoretical (Optimal Control Theory) basis for integration of all sorts of observations. However, a conventional Kalman Filter of the Global Observing System calls for computational speeds of a thousand Crays (see "Report of the Critical Review Panel - Lower Tropospheric Profiling Symposium: Needs and Technologies", 1990). Recent developments in Meteorology are known as the 3- or 4-dimensional variational data assimilation (Thepaut and Courtier, 1991) and the real-time Optimum Calibration by Kalman Filtering (Lange, 1990).

Prospects for a procurement of the national hybrid network are reported with an emphasize on the quality assurance aspects.

1. Introduction

A national "hybrid" observing system network will be assembled. The newly purchased new-generation upper-air sounding systems will be integrated into the Finnish weather radar network and the satellite receiving and processing systems (METEOSAT and NOAA). The processing network will include a number of data visualization terminals based on low-cost microcomputers for the use of meteorologists, technicians, supervisory staff and customers. The objectives of the integrated network are as follows:

1) to provide synoptic TEMP and/or PILOT and other asynoptic upper-air observations and CLIMAT TEMP reports as well as ground weather radar observations from Finland for the national and international uses as specified in the WMO Manual on the Global Observing System;

2) to improve short-term weather forecasting, particularly for periods of up to 12 hours ahead, by rapidly obtaining and displaying remotely sensed data from possible wind profilers, acoustic- and radio-acoustic sounders, microwave and infrared radiometers, sferics receivers, lidars, etc.;

3) to collect and display data from environmental upper-air observing instruments for monitoring radio-activity, aerosols and chemical constituents of the atmosphere;

4) to accumulate climatological information for provision to FMI, WMO and other interested users; and,

5) to collect and assimilate data for research into the meteorological processes of national scale and advanced applications of satellite, weather radar and other remote sensing data in combination with in situ measurements.

2. The Meteorological Work Station (MWS)

The MWS workstation has been designed and programmed in-house at FMI. It will play a significant role in the advanced visualization of all observations and derived products. The data is currently available 24 hours backwards and numerical forecasts 10 days onwards. For trajectory calculation, forecasts for the last 10 days are also stored. The screen is automatically updated when new data arrive. The full data base will include:

- surface SYNOP and AWS observations
- upper-air soundings, also predicted ones from ECMWF and FMI's HIRLAM
- METEOSAT and NOAA images
- weather radar images from the NORDRAD radar stations
- numerical forecasts from ECMWF, Bracknell, Offenbach, Washington, and HIRLAM (FMI's own High Resolution Limited Area Model)
- interpreted products (cloudiness, significant weather, etc).

The integrated system will also incorporate the SMS (Supervisor Monitor Scheduler) that was developed at ECMWF. It will allow an automatic control of the national observing network and the dissemination of all weather data and forecast products to individual workstations at FMI and customer locations. The MWS application software is now being made independent of hardware by using Object Oriented Programming so that a variety of low-cost workstations based on UNIX, Windows NT, etc. can be supported.

3. The quality assurance

The planned integration will be based on the general principles of Kalman Filtering because of the following five reasons:

1) Kalman Filter is the only way of specifying the prediction and data assimilation problem that is mathematically rigorous;

2) It provides the objective accuracy estimates of weather analysis and forecasting;

3) Consequently, an optimum allocation of resources can be performed between computing power and observing instruments;

4) Control Theory provides the *observability* and *controllability* conditions for the feedback stability of a Kalman Filter system; and

5) The Kalman Filter system can be made to adapt to new circumstances i.e. the processing system learns from the mistakes it makes.

4. The integration

4.1 Upper-air winds

The main deficiency of the Omega/VLF-based windfinding has been a poor vertical resolution near the earth's surface. This problem is now being solved by adding an automatic radio-theodolite to the windfinding system so that it becomes a "hybrid" one. For the best possible results as regards accuracy and operational reliability, the data from the different sources will be combined at signal level i.e. the NAVAID phases, direction-finding angles and, possibly later, distance measurements obtained by some transponder means. The required Kalman Filter technology is from standard navigation literature.

4.2 The thermodynamic and other parameters

The prospective integration of observing instruments that are aiming at measuring such atmospheric parameters as pressure, temperature, humidity (PTU) and up- or downwelling infrared radiation, etc... calls for much more complex Kalman Filtering than that for NAVAID windfinding. This is because, firstly, their physical relationships in the atmosphere are governed by a complicated Partial Differential Equation (PDE) system instead of an ordinary simple one. Secondly, the conventional way of solving Kalman Filters has been the famous Kalman Recursions and they call for an immense computational capacity when the number of incoming signals is as large as it is in a practical atmospheric or environmental application.

5. Concluding remark

The fast ways of solving Kalman Filters and new-breed microprocessors like Pentium will make it possible to combine data reliably and visualize it effectively from windfinding devices, radiosondes as well as from surface- and satellite-based remote sensing systems.

REFERENCES

(1) Kalman, R. E. (1960): "A new approach to linear filtering and prediction problems". Trans. ASME J. of Basic Eng. 82:35-45.

(2) Lange, A. A. (1984):"Integration, calibration and intercomparison of windfinding devices". WMO Instruments and Observing Methods Report No. 15.

(3) Lange, A. A. (1988a): "A high-pass filter for optimum calibration of observing systems with applications". Simulation and Optimization of Large Systems, edited by A. J. Osiadacz, Oxford University Press/ Clarendon Press, Oxford, 1988, 311-327.

(4) Lange. A. A. (1988b): "Determination of the radiosonde biases by using satellite radiance measurements". WMO Instruments and Observing Methods Report No. 33, 201-206.

(5) Lange, A. A. (1990): "Real-time Optimum Calibration of large sensor systems by Kalman Filtering". IEEE PLANS '90 - Position Location and Navigation Symposium Record, March 1990, 146-149.

ACCURATE AND COST EFFECTIVE DESIGN OF RADIOSONDE WITH RESPECT OF CALIBRATION

Huang Bingxun Zhang Yongkuan

Chinese Academy of Meteorological Sciences(CAMS), China

1. Introduction

The weather analysis, especially the research of climate variance requires more accurate upper-air observing data. On the other hand, due to the rising of the consumable cost, the observing times and even the number of the stations of the upper-air network are decreasing recent years. The GOS is facing a critical situation. Therefore, how to reduce the cost as well as to improve the accuracy of the radiosonde is a vital problem to which close attention be paid by many meteorological services on the world.

It is clear that the radiosonde calibration accuracy is a important part of the radiosonde observation accuracy. Usually the achivement of high accuracy and long-tern stable calibration results in high cost of the sonde. Fortunately, now we have achieved a great step forward on the accurate and cost effective design of the radiosonde with respect of calibration. This article is intended to introduce some useful experiences in this matter.

2. Developing or Using Sensing Elements with Simple and Very Stable Calibration

Temperature element calibration is one of the main expense in the sonde production. For example, in order to obtain a accurate temperature calibration more than 6 calibration points are required for the old Chinese radiosonde. However, the effective period of the calibration is only one year and one year later, the sonde has to be recalibrated again. So to reduce the calibration points implies to reduce the production cost and to improve the long-tern stability of the calibration implies to decrease the operation cost of the upper-air stations.

Now we have developed a new ceramic thermistor temperature element with a diameter of 0.5mm[1]. According to the tests by using a high performance calibration system with an accuracy of $\pm 0.02^{\circ}C$, this thermistor obeys very exactly a rather simple calibration function:

$$R = aT^{c}e^{\frac{b}{T}} \qquad (1)$$

where R is resistance and T is temperature of the thermistor and a,b,c are constants. This function seems not as simple as a second order polynomial, but it also has only three constants. So only three accurate calibration points (e.g. $40^{\circ}C$, $-20^{\circ}C$, $-80^{\circ}C$) are required to obtain the values of a,b,c. The tests indicated that at any other temperature, the biases between interpolated and calibrated values are within $\pm 0.1^{\circ}C$.

However, in practice, it is difficult to directly calculate T from R by using (1). Therefore, when once we have determined the

values of a,b,c for each thermistor, we calculate 6 pairs of T,R values which uniformly distribute in the range of 50°C - -100°C with a increment of 30°C. By using these values then we can calculate the coefficients A,B,C,D,E of a fifth polynomial:

$$T=A+BR+CR^2+DR^3+ER^4+FR^5 \qquad (2)$$

The calculating tests indicated that calibration (2) is equivalent to (1) within ± 0.01 °C. Due to the using of computer all the calculations mentioned are very easy. In this way, we have achieved an accuracy temperature calibration for the thermistor by using only three accurate calibration points.

The second feature of the thermistor developed by CAMS is the good long-term stability of the calibration. Laboratory tests by using the method of water triple state point have shown that the resistance value of the thermistor at the temperature of water triple state point is very stable. The annual drift of the equivalent temperature is about 0.01°C. That is to say, the recalibration in the meteorological services is unnecessary for the thermistor even 3-5 years later.

Therefore, developing or using a sensing element with a simple and very stable calibration is very effective to achieve both accuracy and cost improvements.

3. Designing a Solid Measuring Circuit with High Linear Calibration and two reference channels

Any kinds of output of the sensing elements must be changed into a parameter which is suitable to be transmitted to the ground receiver. In the case of the new Chinese sonde, for example, the output of the measuring circuit is repeated period of the transmitted pulse series. Any devices used in the circuit subject to the effects of the surrounding temperature and the fed voltages and these effects result in a large drift of the calibration of the measuring circuit. Some times, the equivalent temperature drift may reach to several degrees.

In order to maintain the sonde in a low cost, any sophisticated methods of temperature and voltage stabilization are not acceptable. However, if we can develop a measuring circuit with high linear calibration and this performance is kept regardless of the large drift of the calibration, we will achieve both accuracy and cost effective goal by use of two reference channels of high accurate resistances. That means any calibration drift of the circuit can be corrected by the outputs of two reference channels as follows:

$$R=R_1+(R_2-R_1)\frac{(t-t_1)}{(t_2-t_1)} \qquad (3)$$

where t, t_1, t_2 are the repeated period outputs of the sensing element and reference resistances R, R_1, R_2 separately.

By use of solid devices, we do have developed a measuring circuit with high linear calibration. The laboratory and flight tests

using two high accurate fixed resistances to take the places of the temperature and humidity elements indicated that the transformation accuracy of the measuring circuit is within $\pm 0.1^{\circ}C$.

Due to the using of solid devices, the circuit of the radiosonde is very sturdy. Usually the circuit of the reclaimed sonde is in good condition. So after checking, the circuit can be used again.

4. Separately Using of the Calibrations of Elements and Measuring Circuit

Traditionally, especially in the manual or semi-automate system, the radiosonde factory provides only a composite calibration in a graph form for each element. For example, the temperature calibration is in a following overall form:

$$T=f(t) \tag{4}$$

Although we can directly obtain T from t, usually this is a complex function of t and more than 6 calibration points are required to reach high accuracy. However, it is difficult to reach a accuracy of $\pm 0.1^{\circ}C$ in the case of graphic form.

Now computer is widely used in the upper-air observation system. So we decided to maintain the formulas (3) and (2) and successively use them to calculate T from t. The advantage of this measure is very clear. When any sensing element is damaged, we need not to scrap the whole sonde like usually did for the old sonde. The only thing that should be done is to replace the element by new one and input the new coefficients of (2). Furthermore, due to the sturdiness of the solid circuit, when a released sonde is reclaimed, we can release the sonde again after replacing the elements and battery and checking the circuit. According to our experience, about 40% released radiosondes can be collected and used again. Therefore, the separately using of the calibrations of the elements and circuit is very useful for cutting down the operation cost of the upper-air observation network.

5, Conclusion

In order to improve the accuracy and reduce the cost of the radiosonde and its operational expense in the aspect of calibration, our useful experiences are: developing or using sensing elements with simple and very stable calibration; designing a sturdy solid measuring circuit with high linear calibration feature and two reference channels; separately using of the element calibrations and the measuring circuit calibration. In this way, the new designed Chinese radiosonde has the features of both high accuracy and low producing and operational cost.

References:

(1), Wang Jiulian, Huang Bingxun, A new Thermistor for Temperature Measurement, Meteorological Monthly, 9, (1986), 22

AN EXAMINATION OF NEW TECHNIQUE FOR TEMPERATURE AND HUMIDITY MEASUREMENTS CORRECTION EVALUATION USING DZHAMBOOL RADIOSONDE INTERCOMPARISON DATA

A.M. Balagurov, M.B. Fridzon, A.P. Kats
Central Aerological Observatory
Dolgoprudny, Moscow Reg.,Russia

The conventional radiation correction scheme for the Russian radiosondes MARZ-2 and MRZ-3 presented in [1] was obtained by analysing the differences between day- and nighttime measurements. Besides neglecting diurnal temperature variations, this method does not take into account some important factors, such as: infrared radiation, emissivity of the sensor, heat exchange, etc., which noticeable affect the measurements. This results in a certain over-estimation of the corrections, of an order of night-time radiation error.

A new method [2] of radiation corrections estimation has been developed in Russia , based on the solution of the radiation balance equation. It takes into consideration both external and internal sources of heat, which determine the difference between the temperature of the sensor in a radiation balance state and that of the ambient air. The influencing factors are direct and reflected solar radiation, heat radiation of the Earth and atmosphere, emissivity of the sensor itself, heat transfer to/from lead wires and electrical heating by the measurement current. The resulting radiation error can be written as follow:

$$(1)\qquad \Delta T_r = T_s - T_a = \frac{Q_{rh} - \varepsilon \times \sigma_0 \times T_s^4}{\alpha_s} - \frac{U^2}{R_s \times S_s \times \alpha_s} + \frac{2 \times \pi \times k}{S_s \times \alpha_s} \sqrt{2 \times \lambda_1 \times r_1^3 \times (\alpha_1 + 4 \times \varepsilon_1 \times \sigma_0 \times T_a^3)} \left[(T_s - T_a) - \frac{Q_{r1}}{\pi \times (\alpha_1 + 4 \times \varepsilon_1 \times \sigma_0 \times T_a^3)} \right]$$

Here, T_a is the actual air temperature; α_s - is the coefficient of convective heat exchange of the thermistor; $Q_{rh}=F_s*(1-A_d)*\varphi_{df}+[F_{re}*(1-A_{re})+F_{1e}*(1-A_{1e})+F_{1a}*(1-A_{1a})]*\varphi_{1a}$ is the radiation heat flow absorbed by a unit surface of the thermistor; F_s, F_{re}, F_{1e},F_{1a} are, respectively, the flows of direct solar radiation, radiation reflected from the underlying surface, and long-wave radiation of the Earth and atmosphere; A_d,A_{re},A_{1e} and A_{1a} are respectively the integral albedo of the thermistor surface for direct and reflected solar radiation and long wave radiation of the Earth and atmosphere; φ_{df} and φ_{1a} are the coefficients of irradiation of the thermistor; ε is the

emissivity of the thermistor; σ_0 is Stefan-Boltzmann constant; U is the voltage of the measuring electrical current in the thermistor, S_s is the electrical resistance of the thermistor; r_1, λ_1, α_1 and ε_{1r} are, respectively, the radius, coefficients of heat conductivity, convective heat exchange and emissivity of the lead wires; Q_{r1} is the radiation heat flow absorbed by a unit surface of the lead wires of the thermistor. similar to Q_{rh}.

The thermophysical and optical parameters of the thermistor were determined experimentally; atmospheric parameters were taken from thermodynamic and radiation atmospheric models. The radiation errors for the temperature sensor MMT-1 used in radiosondes MRZ and MARZ, calculated from equation (1) for average atmospheric conditions are presented in Fig. 1. This figure shows also the experimental estimates of radiation errors obtained with a thin-wire platinum thermometer (for sun elevation about 50 °), and "day minus night" operational radiation corrections, taken with reverse sign (for the same sun elevation). Also presented are the extreme values of radiation errors, calculated for 'warm' and 'cold' atmospheres.

The differences between the conventional radiation correction scheme and the one calculated from formula (1) were tabulated versus pressure, sun elevation and measured temperature proper as one of the major environmental parameter influencing on radiation errors. These tables were applied to Dzhambool Radiosonde Intercomparisons' [1] MRZ data. First, temperature and pressure from simultaneous data set were recalculated and then data for constant pressure levels were obtained. Several results had been supplied to Dr. J.Nash, as project coordinator, immediately in Dzhambool.

Figures 2.a and 2.b present the mean differences of simultaneous temperature measurements relative to FIN at nighttime (18 GMT) and day-time (06 GMT) conditions. The new MRZ data are marked as RRZ; other sondes are indicated as in [1]. It can be seen that in the daytime, RRZ deviation from FIN is small and, for all levels, it does not exceed 1 °C. At nighttime, RRZ data at upper levels show much better agreement with FIN, comparing with other radiosondes.

The relative humidity measurements' compatibility for the Russian radiosondes MRZ and MARZ [1] reveals its strong degradation at upper levels caused by the temperature influence and lag errors. The gold-beater skin sensors used in those radiosondes were comprehensively investigated in the 80's, using a wide spectrum of reference equipment. The estimates for temperature influence and response time were derived as follows:

2) $U_a=87*(0.0115*U_m)^{(1.284*\exp(-0.0125*t))}$

Here U_a, U_m are the actual and measured relative humidities in %RH, t is ambient temperature in ^{o}C.

(3) $\lambda_s=[4.99+170\times(|U^{1.25}-0.45|)^3]\times(8.3195\times e^{-0.0885t}+3.5)\times$
$\times(0.1567\times\sqrt{P}+0.045)\times(10.67/\sqrt{v}-1.084)/125.5$

(3) $\lambda_d=[4.99+220\times(|U^{1.25}-0.41|)^4]\times(8.3195\times e^{-0.0885t}+3.5)\times$
$\times(0.1567\times\sqrt{P}+0.045)\times(10.67/\sqrt{v}-1.084)/125.5$

Here λ_s,λ_d are the time constants for sorption and desorption, U is humidity in %RH, P is pressure in hPa, v is the ventilation speed in m/s, t is ambient temperature in ^{o}C.

References.

1. A.A.Ivanov,1989,WMO Instruments and Obs. Methods,Report No.40.
2. M.B.Fridzon, B.P.Zaichikov, N.V.Chromova,1988, Radiation Corrections in Radiosonde Measurement of Temperature. Meteorologia and Gydrologia[Soviet Meteorology and Hydrology], 1988, No. 6.
3. M.B.Fridzon,1989, Estimation of Temperature and Humidity Radiosonde Measurements Errors on the USSR Upper-air Network. Meteorologia and Gydrologia[Soviet Meteorology and Hydrology], No. 5.

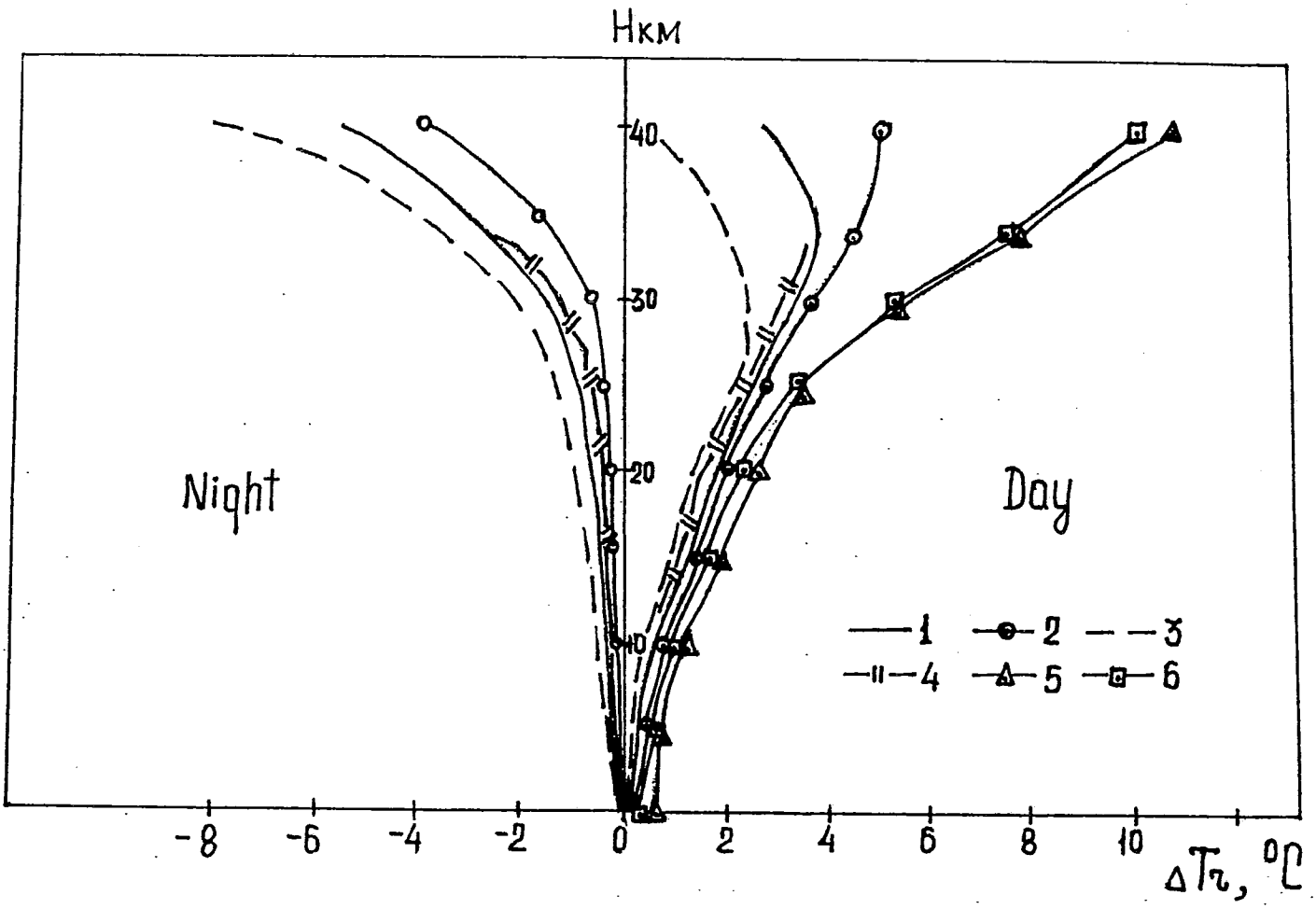

Fig.1. Radiation errors for MRZ and MARZ temperature sensors: derived from equation (1) for stanadard(1),'cold'(2) and 'warm'(3) atmosphere for day- ($h_{\odot}$=50°) and nighttime; experimantal estimates by thin-wire platinum thermometer(4); from conventional radiation correction scheme; estimated from (1) 'day-night' differences.

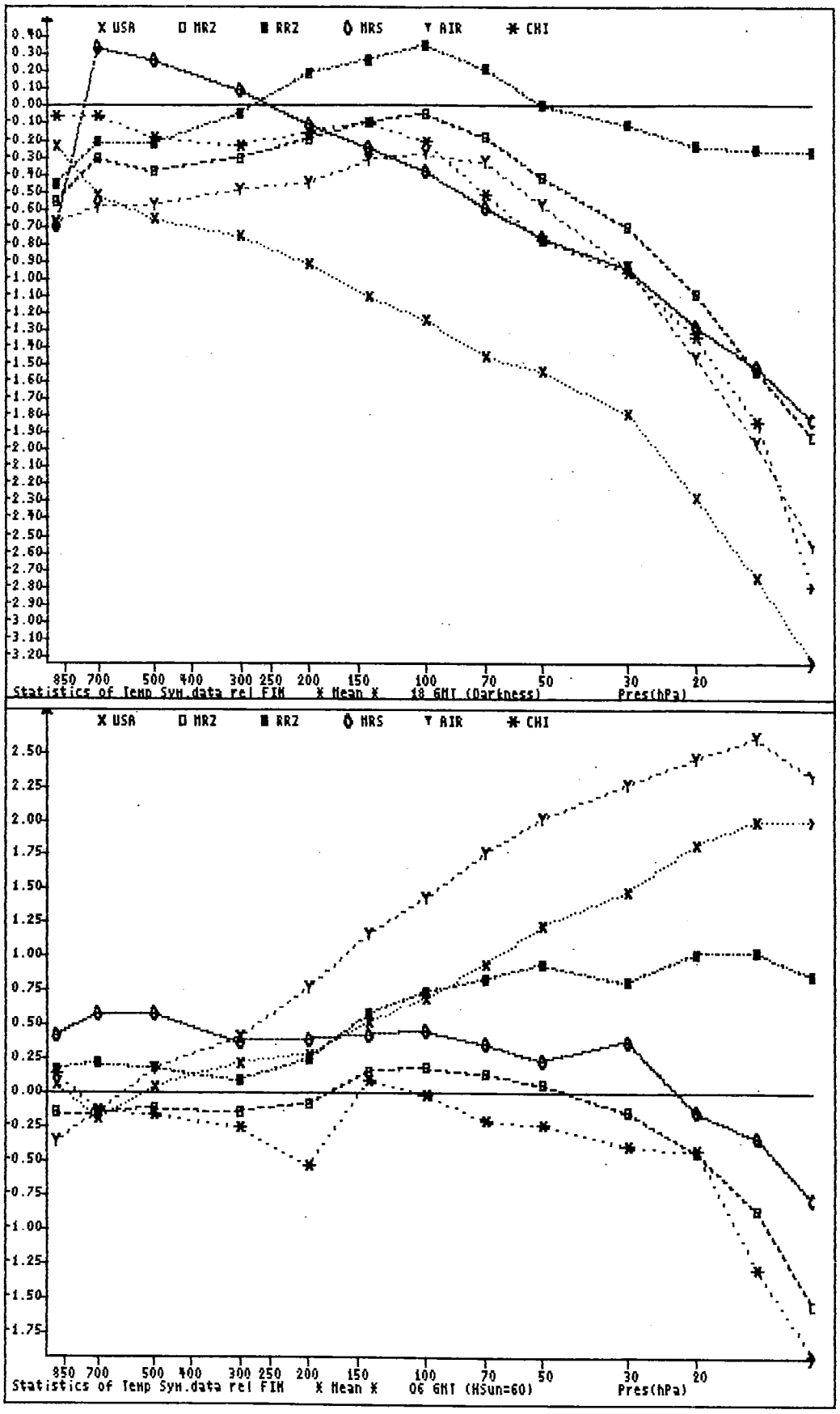

Fig.2. Mean differences of simultaneous temperature measruments in Dzhambool against RS-80 for night(a) and daytime(b) conditions

AN IMPROVEMENT OF TEMPERATURE AND HUMIDITY MEASUREMENTS ACCURACY ON THE RUSSIAN AEROLOGICAL NETWORK

A.M. Balagurov, M.B. Fridzon, S.P. Yessiak
Central Aerological Observatory
Dolgoprudny, Russia

In the 80's the Soviet radiosounding system has been re-equipped with the new solid-state, small-sized radiosondes MARZ (with the radar station "Meteorite") and MRZ (with computerized radar system AVK-1). At the same time obsolete temperature and humidity sensors were used in these radiosondes. As it is shown in [1], the major contribution to the total errors of radiosounding temperature and humidity measurements is made by sensors. Thus, the old Soviet temperature sensor MMT-1 has radiation and dynamic errors from 2 to 3 times larger than those of temperature sensors of the best world radiosondes (e.g., of the USA and Finland). Old Soviet humidity gold-bitter skin sensor is inferior to modern sensors in accuracy, temperature interval, and dynamic parameters.

Recently the development of modern temperature and humidity sensors has been completed1 in Russia. In 1990-91 based on these sensors a new radiosonde, MRZ-6, was created, to match the ground system AVK-1.

Sensors.

The sensitive element in the type ADTV-1 temperature sensor of MRZ-6 radiosonde is a thin nickel foil strip, made by fotolithografy method on a thin non-conducting film. It is constructed as a cylinder of twisted film, 1,5 mm in diameter and 10 mm in length, with rigid leads fixed on the frame. This sensor has passed the State approval tests and is included in the Gosstandart list of certified measuring instruments. The sensor's maximum error is within $\pm$ 0.5 °C in temperature interval from -90 to 60 °C, with 0 and 100 °C calibration points. Calibration function is given by the 4-th order polynomial.

The sensitivity to temperature changes is defined by the ratio of sensor resistances at 100 and 0 °C temperatures and is about 1.620. The sensor is covered with antiradiative enamel, similar to MRZ and MARZ. The nominal response time of the sensor is 5 s under normal conditions (pressure of 1000 hPa and blowing velocity of 5 m/s).

The DVR type humidity sensor of the radiosonde MRZ-6 consists of a sensitive element, similar in construction to Vaisala sensor, and capacity-to-frequency transformer. The sensitive element is a capacitor with 3 electrodes, two of which (lower) are arranged on a dielectric plate and the third, water-leaking electrode is placed over the humidity sensing layer, above the others two and is not connected with them. It is designed as a 8 x 6 x 0,6 mm plate installed on semi-rigid leads, connected with the lower electrodes. The capacity of the sensitive element changes within a 160 to 210 pF range, the mean sensitivity being 0.35 pF/%RH. The sensitive element is incorporated in a 30 x 40 mm plate on which the capacity-to-frequency transformer is assembled.

The DVR sensor has passed the State approval tests and is included in the Gosstandart list of certified measuring instruments. The sensor's maximum error of 20 °C is within $\pm$ 5 %RH in 0 to 100 %RH humidity interval from with 33 and 78 %RH

calibration points. The calibration function is given by the 3-th order polynomial.

The DVR response time under normal conditions and ventilation of 5 m/s does not exceed 3 s; the maximum error under operational conditions (temperature within -60 to 50 °C) is not more than 10 %RH (temperature influence on sensor readings is practically absent).

Block Diagram and operational Principles.

Block diagram of MRZ-6 is presented in Fig.1. The basic radiosonde parts are:

- a temperature sensor (TS) providing transformation of the ambient air temperature of -90 to 60 °C to electrical resistance varying in the range from 250 to 700 Ohm;
- a humidity sensor (transducer) (HT) providing transformation of the ambient air relative humidity of 0 to 100 %RH to electrical pulse repetition period of 5 to 15 ms;
- a radioblock providing transformation of the temperature sensor resistance as well as the reference and calibration resistance to electrical pulse repetition period; forming telemetry channels (including humidity channel); transmitting telemetry signals by a radio-frequency carrier of 1780 MHz to the ground station; providing of distance echo-signal in response to the ground station interrogation, transmitted by a radio-frequency carrier of 1780 MHz;
- water-activated battery for power supply with voltages of 9.5 and 28 V.

The main elements of the radioblock are:

- a measuring transducer (MT) providing the transformation of the temperature sensor resistance and a possibility of a transforming error's correction , through employing the reference and calibration channels; the transducer consists of a calibration circuit (CC), two analogue keys (AK), a measuring circuit (MC), a "voltage-to-frequency" converter (VFC) and a logical element (LE);
- a multiplexor switch (MS) providing the coupling of measuring transducer and humidity sensor outputs with the modulating input of the transponder;
- telemetry signals former of control signals for a successive cycle of telemetry signals transmission;
- a superregenerative transponder (ST) consisting of a 800 kHz quenching oscillator (QO), a 1780 MHz VHF master selfoscillator (VHF SO), a voltage stabilizer (VS) and a stabilizer of DC component of VHF current (CS);
- an antenna system (An) providing emission and reception of 1780 MHz signals.

Information on air temperature and humidity is transmitted by MRZ-6 as frequency signals, consecutively, through four telemetry channels: temperature, humidity, reference and calibration. The last two ones are introduced to minimize errors of temperature sensor resistance transformation.

An output informative parameter for temperature is the so called Y-parameter:

$$Y = \frac{Tt - To}{Tc - To}$$

here Tt is the period of pulse repetition for the temperature channel; To is the period of pulse repetition for the reference channel; Tc is the period of pulse repetition for the

calibration channel.

The absolute value of the pulse repetition period for the humidity channel is a measure of air humidity. To avoid the loss of information, the radiosonde MRZ-6 employs a twinned telemetry cycle with the transmission of the reference channel during the first semi-cycle and the calibration channel during the second one. Information on temperature and humidity is transmitted twice and once ,respectively, during each semi-cycle.

The duration of channels transmission is 5.1-5.4 s. For the channels' separation, the period of the reference channel pulse repetition is shorter and that of the calibration channel is longer than the other channels' by more than 200 mks. on-off time ratio of all the channels is within 1.8 to 2.2 and doesn't depend on their repetition period.

Construction.

The radioblock is arranged in rectangular polyfoam casing together with the battery ensuring the necessary thermal conditions during the flight. The casing consists of a frame and a cover matched together in the vertical plane, the dimension of the casing being 110 x 110 x 225 mm. The radioblock is assembled on a single-ended printed-circuit card. The antenna system of the radiosonde is made as quarter wave whip aerial with a flat square counterpoise, placed normal to the radioblock plate. The humidity sensor is situated in the upper part of the radiosonde casing so that the sensitive element is in the centre of the air inlet. The temperature sensor is positioned on connecting rods arranged on the external holder, placed at 45° to the radiosonde vertical axis so that the sensitive element is by more than 95 mm aside from and 45 mm above the radiosonde casing. The radiosonde is attached to suspension by a ribbon, fastening the radiosonde frame to the cover over the generatrix and providing their reliable fixture.

Trial results.

Complex trials were carried out involving radiosonde MRZ-6, which included both separate tests of the sensors and radioblock, and trials of the whole radiosonde under laboratory and field conditions. As it is impossible to comprehensively simulate in the the whole complex of physical factors, affecting radiosonde measurements under real flight conditions, a combined theoretic and experimental approach of measurement error investigation was used. So, the influence of some factors was evaluated primarily by means of theory and then coefficients of the theoretical dependences were experimentally tested in several points of the variability interval of a given factor. For example, by this method, the estimates of radiation and dynamic measurement errors for temperature and humidity have been received.

Figure 2 illustrates the results of launching the radiosonde MRZ-6 on a special aerostat, also carrying temperature (TR) and humidity (HR) reference gauges [1]. One can see, that the ADTV-1 results practically coincide with the ones of temperature reference. Deviations from humidity reference for DVR as well as for the gold-beater skin sensor(OHS) are insignificant at heights up to 6 km. However, the latter become essential at temperatures below -20 °C, while DVR readings are still close to reference and slightly differ from it due to the different response time.

The radiosonde has passed the State approval tests and is

included in the Gosstandart list of certified measuring instruments. The approval test has revealed the temperature and humidity maximum error of is 0.7 °C and 10 %RH respectively. Since 1992, MRZ-6 has underwent field test at Dolgoprudny upper-air station. Figure 3 presents the results of an MRZ-6 ascent between two operational ascents of MRZ-3. A good agreement of measured temperatures can be seen. The differences observed may be accounted for by the atmospheric variability. The humidities are compatible up to 8 km, but at upper levels, MRZ-6 shows much lower humidity than MRZ-3.

THE RADIOSONDE BLOCK DIAGRAM

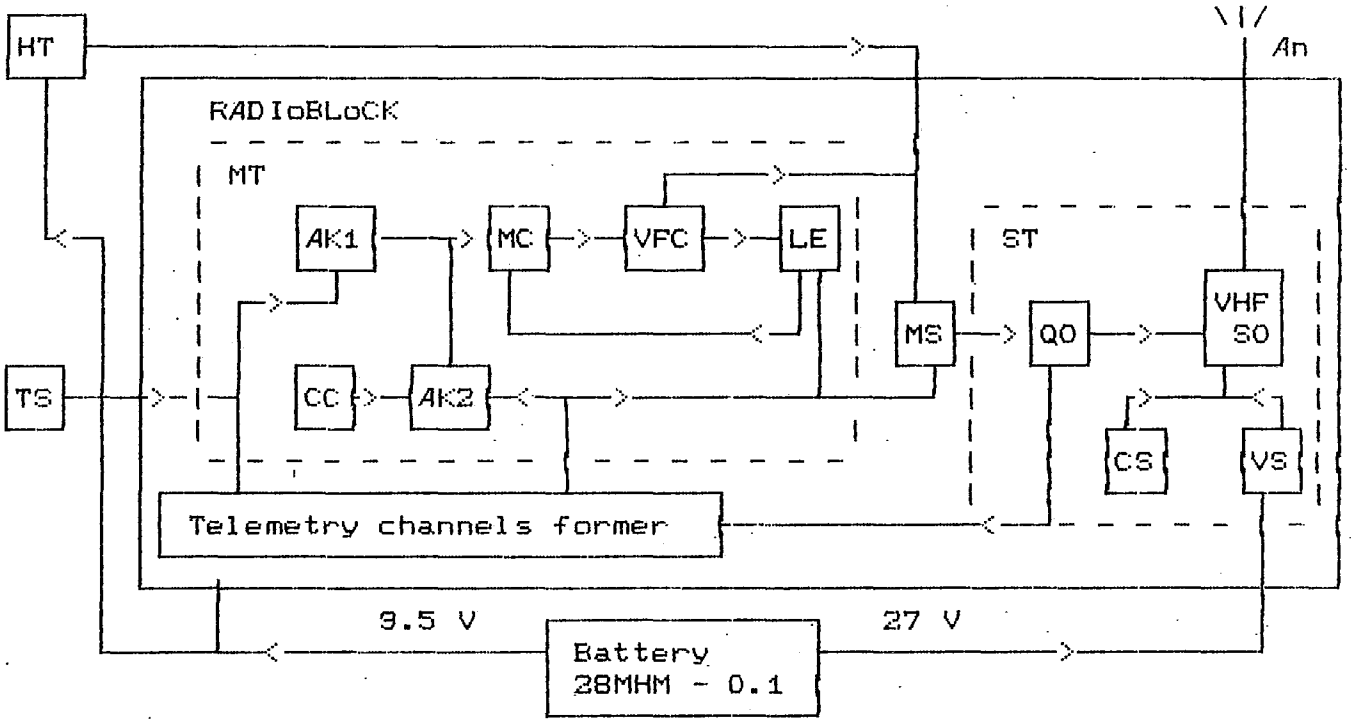

Fig.1

References.

1. M.B.Fridzon,1989, Estimation of Temperature and Humidity Radiosonde Measurements Errors on the USSR Upper-air Network. Meteorologia and Gydrologia[Soviet Meteorology and Hydrology], No. 5.

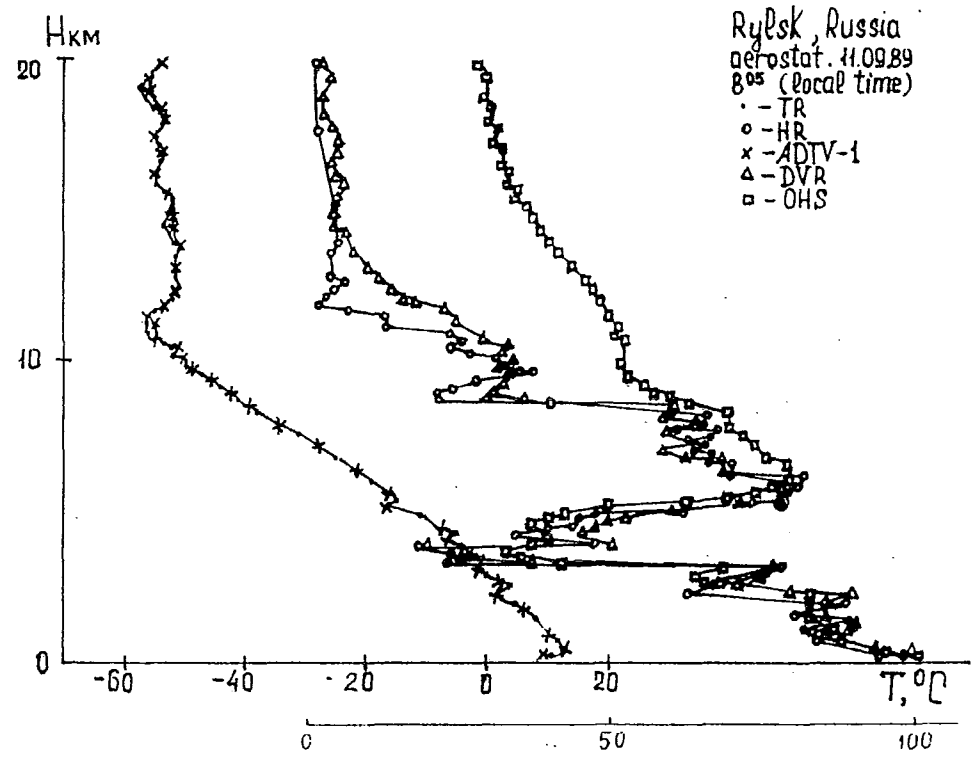

Fig.2. Temperature and humidity profiles.

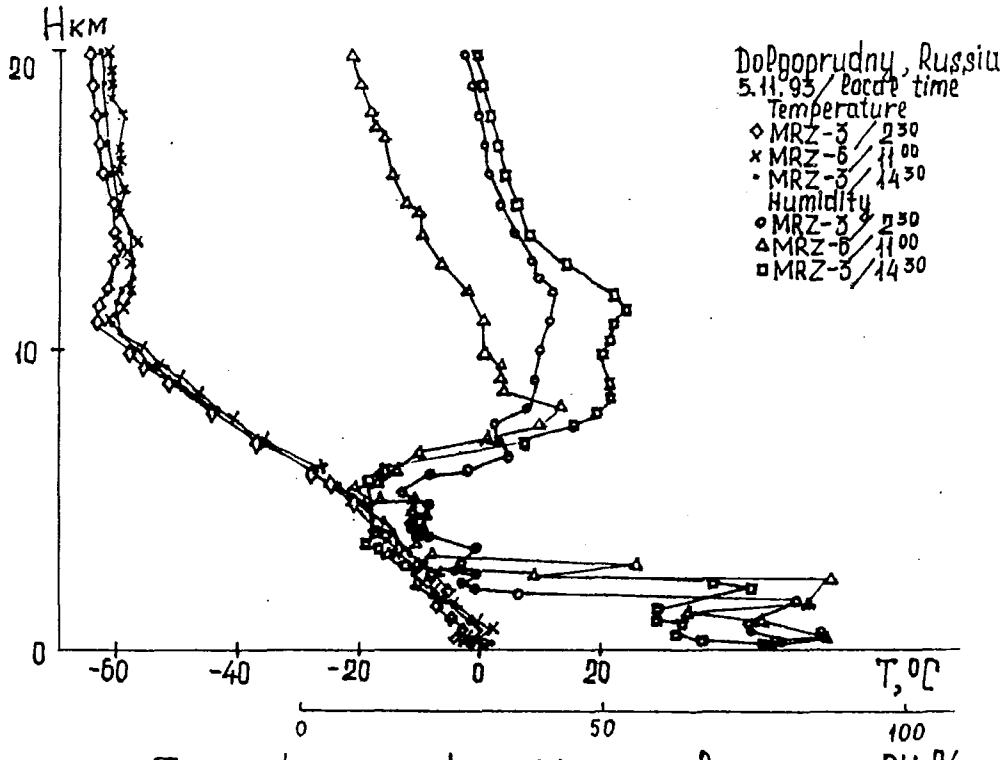

Fig.3. Temperature and humidity profiles.

VERIFICATION TECHNIQUE FOR AUTOMATED RADIOSOUNDING SYSTEM

A.M. Balagurov, A.P.Kats, Yu.V. Neiman, S.G. Osipova
Central Aerological Observatory
Dolgoprudny, Russia

The wide introduction of the automated radiosounding system during the last decade highly improved the quality of upper-air measurements. Monitoring of upper-air data quality, carried out by NWP centres [1], has demonstrated this improvement for constant pressure level data. Recent series of the WMO radiosonde intercomparisons [2,3] have shown better compatibility in simultaneous data, too. However, for many users and applications of upper-air information it is the full profile of the vertical distribution of temperature, humidity and wind (usually vs pressure) that is considered as the main radiosounding result. Due to GTS restrictions, this information is distributed in a reduced form via so called 'significant points' best representing the underlying profile. The selection criteria established in the Manual on Codes are poorly formalized and intended primarily for manual processing. So, they are applied in automated radiosounding systems differently and, possibly, inconsistently. Therefore, proper coding of aerological messages is one of the main problems in the development and testing of these systems. For those that utilize mini-computers with standard I/O devices or PC, this task is not very complicated - it may be solved by creating raw-data files with arbitrary distributions and then running the corresponding software for flight simulation.

This is not the case for ground systems equipped with mini-computers using firmware algorithms. Such algorithmic errors are possible that may show under a specific complex of weather conditions. Therefore, a sufficiently long period of time is needed for the field tests to detect these errors.

That is why for solving this and other problems of ensuring high data quality a hard- and software complex is under development in Russia for testing of the Russian radiosounding system AVK through simulating ascents with controlled profiles of meteorological variables. The main objective of this complex is to provide on-line reproducing, with controlled properties, the telemetry and radiotracking measuring signals, received by AVK during ascents under real conditions. An experimental model of the proposed device is available and in current use, making it possible to check the automatic selection of temperature and humidity significant levels under different conditions.

The model consists of personal computer equipped with a programmable controller, plugged into a standard expansion slot,

which simulates the operation of radiosonde measuring generator and is able to produce, for a given period, rectangular pulses with controlled frequency and duration. The output of the controller is connected with the modulator of the VHF generator of the conventional radiosonde MRZ (or MARZ for Meteorite-OKTAVA system testing; in principle, the controller may be used with any analog radiosonde after necessary adjustment of electrical parameters). The sonde runs of stationary power supply and generates VHF signals in conventional way. Available software makes it possible to simulate telemetry signals for arbitrary profiles of temperature and humidity. Conventional AVK facilities permit us to set the slant range increasing with a constant increment, and also constant elevation and azimuth, and thus simulate balloon flight with a constant ascent rate. Data processing is fulfilled automatically by AVK mini-computer as during conventional radiosonde ascent. The results of data processing are available for constant pressure levels and significant points from TEMP message and standard printout, and may be compared with predefined profile.

Fig. 1 presents the results of AVK processing for temperature and humidity profile simulated from flight 26 DigiCORA - RS-80 minute data of Dzhambool Radiosonde Intercomparisons (original DigiCORA selection of significant points is not presented due to incompatibility in vertical ascent rate). It shows a certain peculiarity of AVK-1 algorithms, consisting in the selection of significant points at heights multiple of 200 m below 3 km, 400 m within 3 to 6 km layer, 500 m within 6 to 10 layer, and 1 km above 10 km level.

The device described was utilised for AVK-1 firmware examination, software development for processing data from the new Russian radiosonde MRZ-6, other research tasks, e.g. for the determination of the timing delay of AVK-1 printout to eliminate timing errors in Dzhambool Radiosonde Intercomparisons MRZ data set.

At the moment, a full version of this complex is being developed which will also allow the simulation of co-ordinate measurements as well as the introduction of perturbations to measuring signals, their scale corresponding to real noise and measurement errors. Direct input into AVK mini-computer is being designed too. It is planned to utilize several complexes of the kind for AVK verifying under real operational conditions on the Russian upper-air network.

References.

1. M.Kitchen,1989,WMO Instruments and Obs. Methods,Report No.36.
2. J.Nash and F.J. Shmidlin,1987,WMO Instruments and Obs.Methods, Report No.30.
3. A.A.Ivanov,1989,,WMO Instruments and Obs. Methods,Report No.40.

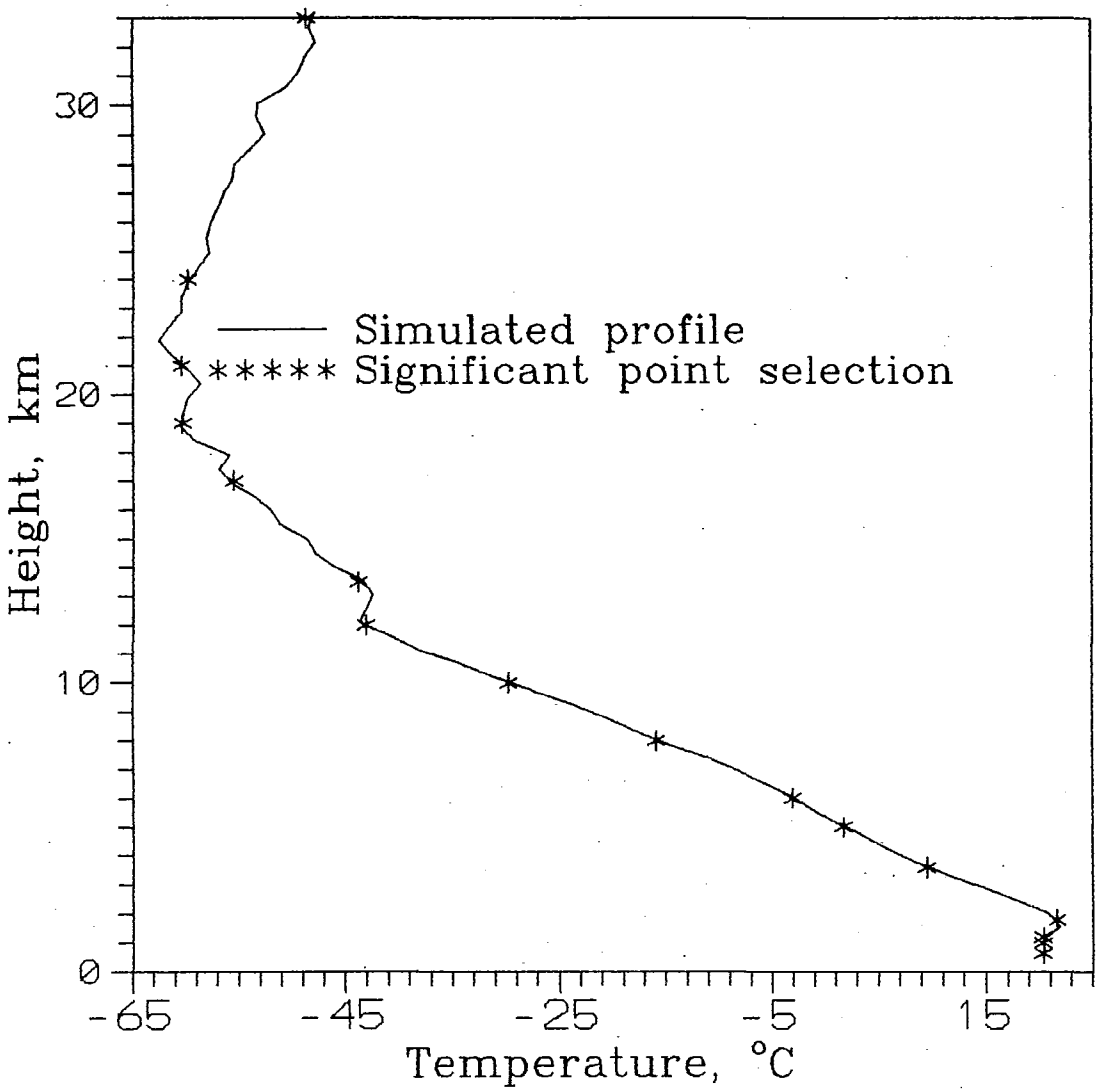

Fig.1. AVK significant point selection for simulated profile.

Session III

ENVIRONMENTAL MEASUREMENTS

Quality Assurance of Aerosol Optical Thickness Monitoring for the Lindenberg Sunphotometer Types BAS and ABAS

U. Leiterer; M. Weller; J. Urban; T. Naebert
Deutscher Wetterdienst, Meteorologisches Observatorium,
15864 Lindenberg, Germany

1. Introduction

The main problems of the spectral aerosol optical thickness monitoring (0,38-1,1 µm) are the stability of the sensitivity and the evaluation of the voltages generated by the extraterrestrial irradiance in the spectral channels at the top of the atmosphere. It will be reported on a new method of calibration and recalibration of sunphotometers used in Lindenberg. The main idea is to transfer the known extraterrestrial spectral solar radiometric scala to radiance- and irradiance etalons in a laboratory and to control the stability of the sunphotometers in the laboratory afterwards.
One essential feature of the Lindenberg sunphotometer objectives is the known effective solid angle ω which will be used to transfer the irradiances of the solar disk to radiances of a white etalon in the laboratory. The Lindenberg sunphotometer types distinguish from the WMO recommended sunphotometers by
- small viewing angle of about 1°,
- the use of an objective with a focus of about 80 mm,
- a high dynamic range of about 10^6; 6 sensitivity ranges and a resolution of 10^4.

Some results will be shown of radiance- and irradiance comparisons with substandards based on calibration of the Meteorological Observatory Lindenberg (MOL), Labs & Neckel-data (L&N), National Institute of Standards and Technology USA (NIST), Labsphere INC. USA (LAB) and Physikalisch-Technische Bundesanstalt FRG (PTB).

2. The radiometric transfer

Scheme 1 shows the method to find the extraterrestrial voltages U_{OP} for each wavelength of the sun-photometer. U_{OP} is the fundamental quantity to compute the aerosol optical thickness δ_A. The physical basis is the Bouger-Lambert'law

$$(1) \quad U_P = U_{OP}\ e^{-\delta_T \cdot m}$$

with U_P : photometer signal
δ_T : total optical thickness
m : air mass

Unfortunately the preconditions for the application of the Bouger-Lambert'law are not fulfilled under real atmospheric conditions and for filter-half-widths between 8 - 16 nm (as we used for the MOL-sunphotometer BAS 11). The application of the Bouger-Lambert'law is only a compromise, for 22 of the 33 used wavelengths. Here we get the extraterrestrial voltages U_O within ± 7 % accuracy. For the other 11 wavelengths there are higher deviations caused by Fraunhofer lines, atmospheric water vapour and oxygen lines and by some optical problems of the sunphotometer. Therfore one should provide the Bouger-Lambert'law with a correction function $\Theta(m)$ in the form

$$(2) \quad U_P = U_{OP} \cdot \Theta(m) \cdot e^{-\delta_T \cdot m} = U_{OP}(pre) \cdot \Theta_1 \cdot \Theta_2(m) \cdot e^{-\delta_T \cdot m}$$

with $U_{OP}(pre) \cdot \Theta_1 = U_{OP}$ for $m = 0$
$\Theta_2(m) \dashrightarrow 1$ for $m \dashrightarrow 0$

$U_{OP}(pre)$: preliminary result of the Langley-Plot
Θ_1 : constant part of the correction function $\Theta(m)$
$\Theta_2(m)$: variable part of the correction function $\Theta(m)$

The procedure to determine the constant and variable part of the correction function $\Theta(m)$ is described in [1].

The right side of scheme 1 illustrates the way of the extraterrestrial irradiance transfer to irradiance and radiance calibration factors and their applications to a irradiance - and radiance etalon in the laboratory. More details about

Quality Assurance

of extraterrestrial voltages U_{OP} for each wavelength

photometer signal

$$U_P = U_{OP}\, e^{-\delta_T \cdot m} \quad [1)]$$

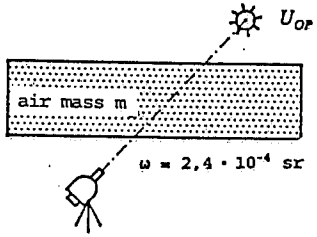

$$\delta_T = -\, m \cdot \ln \frac{U_P}{U_{OP}}$$

$\delta_T = \delta_A$ aerosol optical thickness

$+\delta_{Ray}$ Rayleigh optical thickness

$+\delta_{H2O}$ water vapor optical thickness

$+\delta_{O3}$ ozone optical thickness

$+\delta_{NO2}$ nitrogen dioxide optical thickness

$+\delta_{O2}$ oxygen optical thickness

$\} \; \delta_{RES}$

Aerosol Optical Thickness

$$\delta_A = \underbrace{-\, m \cdot \ln \frac{U_P}{U_{OP}}}_{\delta_T} - \underbrace{[\delta_{Ray} + \delta_{H2O} + \delta_{O3} + \delta_{NO2} + \delta_{O2}]}_{\delta_{RES}}$$

extraterrestrial signal

$U_{OP} \longrightarrow E_O$ extraterrestrial irradiance MOL, L & N {for wavelength of the BAS 11 and the data of Neckel & Labs 1984}

$K_{EP} = \frac{E_O}{U_{OP}}$ irradiance [E] calibr.factor

$K_{LP} = \frac{E_O}{U_{OP}} \cdot \frac{1}{\omega \cdot d}$ radiance [L] calibr.factor; ω: effective solide angle e.g. $\omega = 2{,}4 \cdot 10^{-4}$ sr; d: gain factor = 5400

natur terrestrial irradiance after transmission of the atmosphere

$U_P \longrightarrow E_P = K_{EP} \cdot U_P$ irradiance measured with the 1°-objectiv

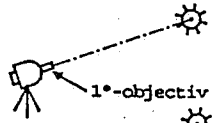

$U_{S\perp} \longrightarrow E_S = K_{ES} \cdot U_{S\perp}$ irradiance measured with the 2π-diffusor

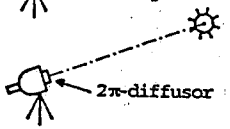

$U_{S\perp} = U_{SG\perp}$ (global radiation) $- U_{SD\perp}$ (diffuse part of global radiation without sun)

$E_S = E_P$ irradiance transfer of E_P (objective) to E_S (diffusor) or U_P to $U_{S\perp}$

$$K_{ES} \cdot U_{S\perp} = K_{EP} \cdot U_P$$

$$K_{ES} = K_{EP} \cdot \frac{U_P}{U_{S\perp}} = \frac{E_O}{U_{OP}} \cdot \frac{U_P}{U_{S\perp}}$$

labor

radiance

$$U_{WP} \longrightarrow L_{WP}(MOL, L\,\&\,N) = K_{LP} \cdot U_{WP} = \frac{E_O}{U_{OP}} \cdot \frac{1}{\omega \cdot d} \cdot U_{WP}$$

$$U_{OP} = \frac{U_{WP}\ (MOL, L\,\&\,N)}{L_{WP}\ (MOL, L\,\&\,N)} \cdot \frac{1}{\omega \cdot d} \cdot E_O\ (MOL, L\,\&\,N)$$

$$L_{WP}\ (MOL, L\,\&\,N) = \frac{\rho\,(BaSO_4) \cdot E_{HS}\ (MOL, L\,\&\,N)}{\pi}$$

irradiance

$$U_{HS} \longrightarrow E_{HS}(MOL, L\,\&\,N) = K_{ES} \cdot U_{HS}$$

for control of L_{WP}

$$\rho\,(BaSO_4) = \frac{L_{WP}(MOL, L\,\&\,N) \cdot \pi}{E_{HS}(MOL, L\,\&\,N)} \equiv const\ (> 10\ years)$$

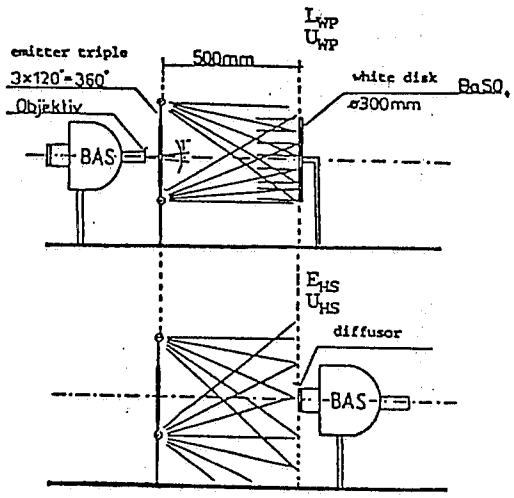

scheme 1

this method to transfer a known radiometric scale of the extraterrestrial solar spectrum [3] to a radiance- and irradiance etalon in the laboratory are published in [2].

The fundamental quantities are the
extraterrestrial irradiances E_O [L & N] related to Labs and Neckel and the
extraterrestrial voltages U_{OP} [MOL] of the sunphotometers of the Meteorological Observatory Lindenberg

We used the sunphotometer BAS 11 with 33 spectral channels, half-widths 8 - 16 nm for the transfer and neglected the correction-function $\Theta(m)$; see eq. (1). The result are more or less accurate calibration factors for radiances and irradiances. The deviations of the "correct" calibration factors of standards [LAB, NIST, PTB, MOL] to the calibration factors on the basis of the extraterrestrial irradiances E_O or voltages U_{OP} are reflected in the correction-function $\Theta(m)$; see eq. (2).

In the result of the radiometric transfer procedure (right side of scheme 1) one gets the derived
labor radiances
labor irradiances
labor spectral reflectance
} of irradiance-radiance etalon [MOL, L& N]

From this irradiance-radiance etalon [MOL, L & N] the fundamental quantity U_{OP} can be computed by

$$(3)\quad U_{OP} = \frac{U_{WP}\,(MOL,\ L\ \&\ N)}{L_{WP}\,(MOL,\ L\ \&\ N)} \cdot \frac{1}{\omega \cdot d}\ E_O\,(MOL,\ L\ \&\ N)$$

and may be used for laboratory control and quality assurance of U_{OP} of the sunphotometers.

Of course the radiometric basis of Labs & Neckel data can be replaced also by standards on the basis of NIST, LABSPHERE-NIST and PTB. The main point and main difficulty is to use only one type of standard for E_O and L_{WP}. That means one has to create new extraterrestrial E_O irradiances also if one uses radiances L_{WP} in the laboratory which are not related to E_O [MOL, L & N].

3. Results of radiance- and irradiance comparisons

Fig. 1, 2, 3, 4, 5, 6, 7 show comparisons between different irradiance- and radiance substandards offered by different companies. All these substandards are for sale and use for everybody. The comparisons won't to say anything about the absolute accuracy of there basis calibrations of the bureau of standards. We have also to taken into account some uncertainties of our transferradiometer (sunphotometer BAS 11).

Fig. 1 shows the relative deviations of the irradiance calibration factors K_E. The curve PTB/NIST represents the differences of K_E based on the same FEL-1000 W quartz-halogen- lamp type traceable to PTB [4] or NIST [5]. The deviations are small (2-5 %). The curve MOL/NIST describes the deviations of K_E based on the Lindenberg method [2, 3] to the NIST-standard related calibration factors.

Fig. 2 presents the relative deviations of the radiance calibration factors K_L. The NIST related radiance calibration factors K_L(NIST) have been computed by applying the known reflectance calibration standard ϱ(SPEC) [7] and the NIST related irradiance E(NIST) of the known FEL-lamp [5]:

$$(4)\quad L(NIST) = \frac{E(NIST) \cdot \pi}{\varrho(SPEC)} \qquad \text{with } K_L(NIST = \frac{L(NIST)}{U_P}$$

U_P : photometer signal
ϱ(SPEC) = 0.988 in the region 400...1100 nm

The radiance calibration factors K_L(LAB) are derived by means of the integrating (Ulbricht) sphere of LABSPHERE INC. [6]. The calibration factors of MOL and LAB are 8 to 15 % higher than the "NIST related" factors. A better correspondence has been found for the MOL and LAB calibration factors within ± 7 % for 22 of 33 wavelengths. Therefore the LABSPHERE radiance data could be included in the procedure of quality assurance of the MOL-sunphotometers.

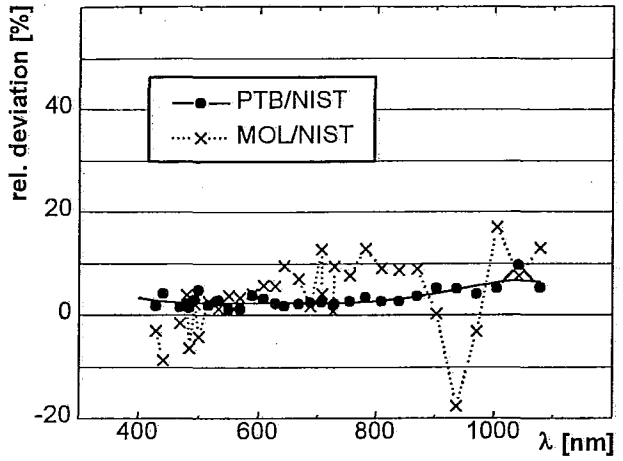

Fig.1 rel. deviation of irradiance calibration factors K_E

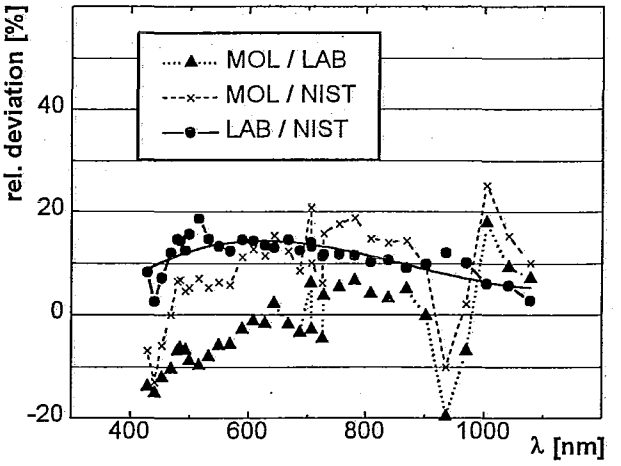

Fig.2 rel. deviation of radiance calibration factors K_L

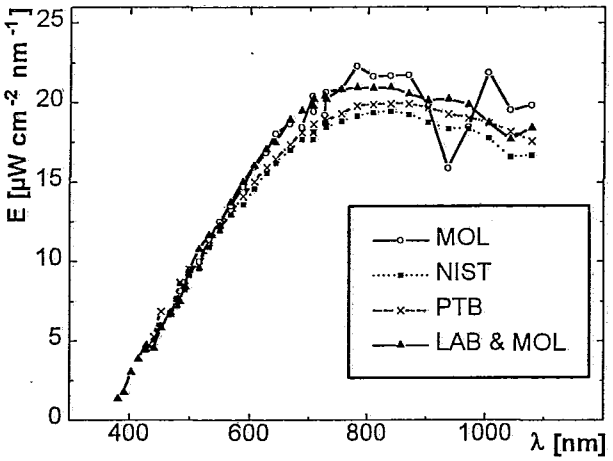

Fig.3 irradiances E of MOL- (3x240W) emitter-tripel computed with different irradiance calibration factors (MOL-extraterrestrial, NIST, PTB, LAB and MOL Reflectance Standard - see eq. (5))

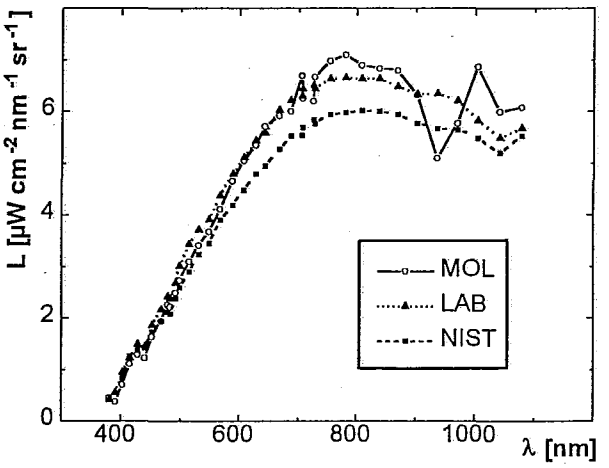

Fig.4 radiances L of MOL- (3x240W) emitter-tripel computed with different irradiance calibration factors (MOL-extraterrestrial, LAB, E NIST and Spectralon Reflectance Standard - see eq.(4))

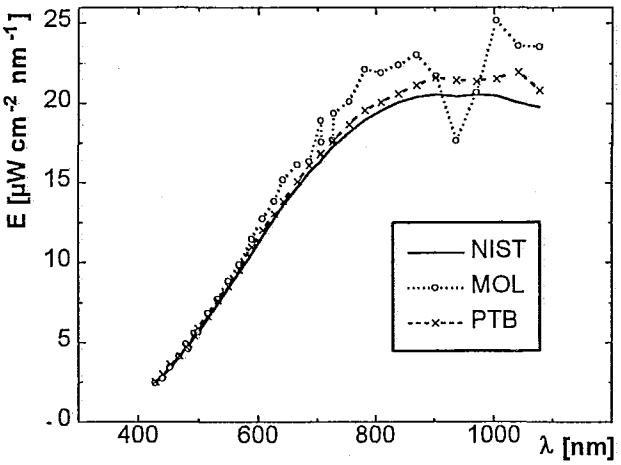

Fig.5 irradiances E of 1 kW FEL NIST lamp computed with different calibration factors (MOL, PTB)

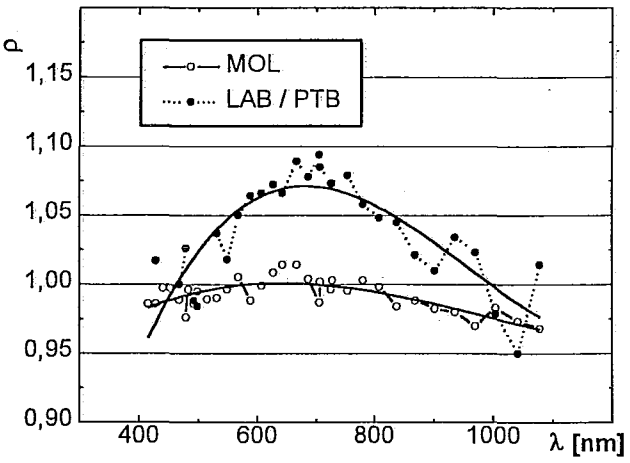

Fig.6 spectral reflectance ρ of the white disk type "MOL-$BaSO_4$" on the basis of the

—o— extraterrestrial radiance and irradiance transfer by the Lindenberg method (MOL-Reflectance-Standard)

····•···· LABSPHERE- radiance and PTB-irradiance calibration factors

All Figures are relevant for BAS 11

Fig. 3 and Fig. 4 show the irradiances **E** and the radiances **L** of the MOL-etalon (halogen emitter-triple combined with the $BaSO_4$-white disk, see scheme 1) computed with different calibration factors:

MOL irradiance - by the Lindenberg method, scheme 1, [2, 3]
radiance

LAB radiance - by means of integrating (Ulbricht) sphere of LABSPHERE, [6]

LAB irradiance - by use of the known spectral reflectance ϱ(MOL) of the MOL-Reflectance-Standard (Fig. 6 and scheme 1) and the eq. (5)

$$E(LAB) = \frac{K_L(LAB) \cdot U_{WP} \cdot \pi}{\varrho(MOL)} = \frac{L(LAB) \cdot \pi}{\varrho(MOL)} \qquad (5)$$

and U_{WP} : photometer signal

NIST radiance - by use of the known spectral reflectance ϱ(SPEC) of the LABSPHERE white target [7] and E(NIST) according to eq. (4)

NIST irradiance - by use of the NIST related calibration factors [5].

PTB irradiance - by use of the PTB related calibration factors [4].

Fig. 5 illustrates the irradiance E of the NIST related FEL 1000 W quartz-halogen-lamp No. 211 from EG & G, GAMMA SCIENTIFIC, compared with MOL - and PTB related calibration factors. A similar but not the same behavior is obvious as shown in Fig. 3 for the MOL - and PTB curves.

Fig. 6 shows the spectral hemispherical reflectance ϱ of the white disk type "MOL-$BaSO_4$". The light-incident angles of the 3 halogen lamps of the emitter-triple are 26° with respect to the normal through the center of the white disk. The curve ϱ(MOL) is related to the Lindenberg method as described in scheme 1 using the extraterrestrial irradiance data of Neckel & Labs [3] and the effective solid angle for each wavelength. It is a proven fact that the spectral reflectance ϱ(MOL) is very stable over many years (>10).

The curve ϱ(LAB/PTB) demonstrates the effect occuring when the radiance calibration factors of LABSPHERE INC. [6] and irradiance calibration factors related to a PTB-standard lamp [4] are used. We see that ϱ(LAB/PTB) coincides with ϱ(MOL) near 400 and 1000 nm but in the range 550 to 800 nm the LAB/PTB related calibration factors are 5...7 % higher. The reasons are unclear up to now.

4. Conclusions

The best results for maintenance and estimation of the extraterrestrial values U_O in the laboratory can be achieved by use of the more than 10 year old reflectance standard "MOL-$BaSO_4$" (Fig. 7b). We have found the best coincidence between the extraterrestrial irradiance of the Labs & Neckel-data [3] and the radiance of the LABSPHERE INC.-data [6] in order of ±7 %. Applying irradiance substandards related to PTB and NIST 1000 W-lamps the results are more contradictory especially in the spectral region between 550 and 800 nm. Therefore we use the irradiance and radiance data of the MOL-standard as shown in Fig. 7a also in the future.

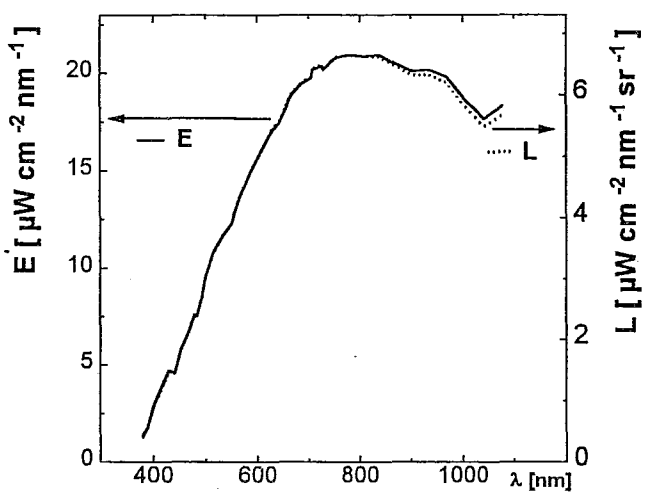

Fig. 7a irradiance E and radiance L of the MOL-standard

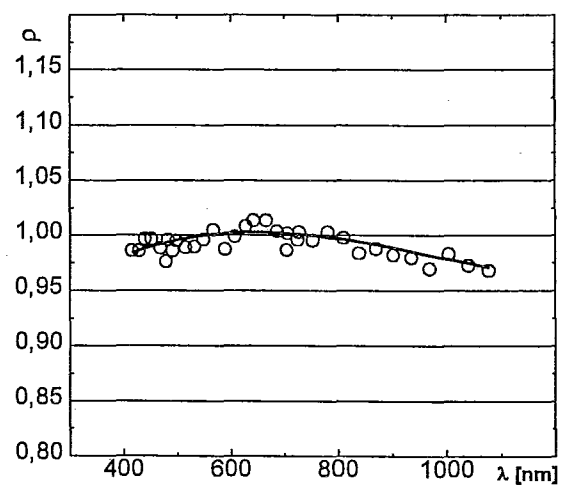

Fig. 7b spectral reflectance ρ of the MOL-standard

References:

[1] Leiterer, U.; Weller, M.; 1989: Zur Anwendung des Bouger-Lambert'schen Schwächungsgesetzes in einer realen Atmosphäre, unpublished paper, Meteorologisches Observatorium, 15864 Lindenberg, Germany, pp. 1-18

[2] Leiterer, U.; Weller, M.; 1993: Verfahren zur Bestrahlungsstärke- und Strahldichtekalibrierung von Spektrometern und Sonnenphotometern des Typs BAS, Meteorol. Zeitschrift, N.F.2, 108-115

[3] Neckel, H.; Labs, D.; 1984: The solar radiation between 330 and 12500 Å, Solar Physics 90, 205 - 258 and private communication of spectral solar data (tape) 1992.

[4] Physikalisch-Technische Bundesanstalt Braunschweig, BRD; 1993: Quarzhalogen-Glühlampe FEL Q 1000 / 4 CL, 1000 W, 120 V, Kalibrier-Nr. 41330-PTB-93 vom 26.05.93

[5] EG & G GAMMA SCIENTIFIC San Diego, CA, USA; 1992: Quarzhalogen lamp FEL, 1000 W, model: 5000-16 C, serial-no. GS 0889, certification date Sept. 25, 1992; traceable to NIST standard detector DR-11 (APR 1992) No. 844/248783-92 and NIST spectral irradiance NIST TEST No. 211 334

[6] LABSPHERE, INC., North Sutton, NH, USA; 1992: Uniform Source System USS-1200, calibration certificate Rep.No. 8890 A, B, C of Dec. 23, 1992; calibrated with equipment and methods traceable to NIST

[7] LABSPHERE, INC., North Sutton, NH, USA; 1992: Reflectance Calibration Standard, 8° / Hemispherical Reflectance Factor, calibration certificate target No. SRT-99-100-1882-A of Apr. 23, 1992; calibrated with equipment and methods traceable to NIST

Results of an Absorption Corrected Aerosol Optical Thickness Monitoring

M. Weller and U. Leiterer/Deutscher Wetterdienst
Meteorologisches Observatorium 15864 Lindenberg

METHODS

Multi-channel VIS/NIR sunphotometers developed by the authors [1] and calibrated with regard to the WMO recommended irradiance standard [2] are used for aerosol optical thickness (AOT) monitoring in the polar regions (background) and in Central Europe at the Meteorological Observatory Lindenberg (52° N; 14° E). The radiometric constancy of the devices is continually checked with regard to the Lindenberg laboratory standard. The procedures relating to this are given in the preceding paper and are based on the work represented in the TECO-report [3]. To derive the AOT, the spectral transmission τ of the atmosphere has to be measured. This is the reduction in solar intensity due to scattering and absorption. τ can be estimated using the Beer-Lambert law accordingly

(1) $$\tau(\lambda)=\frac{U(\lambda)}{U_o(\lambda)}=e^{-\delta(\lambda).m}$$

In (1) U_o (λ) is the spectrometer output for the extraterrestrial light intensity at a given wavelength incident at the top of the atmosphere, U (λ) is the intensity of the light transmitted to the earth's surface; m is the air mass defined as the length of path of direct solar radiation through the atmosphere as compared to the length of the vertical path through the atmosphere.

δ_T (λ), the so-called optical thickness represents a combination of light scattering and absorption by gases and particles (aerosols).

Bearing in mind the spectrometer filter's half-width of 8 - 16 nm, δ (λ) is actually the sum of 6 provable components:

δ_{RAY} (λ) — the optical thickness due to light scattering by molecules (Rayleigh scattering) given by the WMO recommended formula (2)

(2) $$\delta_{RAY}(\lambda) = P/1013{,}25 \times 0.00838\ \lambda^{-(3.9164 + 0.074\lambda + 0.5/\lambda)}$$ λ in μm; p in hPa

$\delta_{O2}(\lambda)$ — the O_2 caused light attenuation of approximately 760 nm

δ_{O3} (λ) — the optical thickness caused by O_3 absorption in the Chappius band

δ_{NO2} (λ) — the NO_2 caused absorption (maximum approximately 390 nm, extending to the VIS and overlapping with the O_3-Chappius band)

$\delta_{H2O(D)}$ — the absorption due to water vapour predominantly occurring in the $\varrho\sigma\tau$-band and

δ_{Ae} (λ) — the light extinction (mainly by scattering) due to particles, the so-called AOT

Since the absorption coefficients of O_3 and NO_2 are reasonably well established a variant of the Beer-Lambert law can be applied to determine how much of the solar light is absorbed by these gases if their concentrations are known.

The more or less narrow-banded unknown O_2 and H_2O (D) absorption can be eliminated fitting the AOT values with the help of the absorption free channels outside these bands.

So the determination of reliable O_3 and NO_2 concentrations remains (beside the mentioned radiometric problems) to separate the AOT measured at a rural site. Here the low NO_2 concentration was neglected until now. Concerning O_3 the Potsdam Dobson ozon values are used, which have been established 80 km from the AOT monitoring site. Nowadays a Brewer Mark 4 at the Lindenberg observatory allows the NO_2 and O_3 determination to be undertaken at the same site. So δ_{Ae} (λ) can finally be deduced from (1).

RESULTS

Beginning in February 1986 AOT has been derived in about 35 channels between 0.38 and 1.1 μm in the morning at sun heights between 10° and 15° (stable boundary layer conditions).

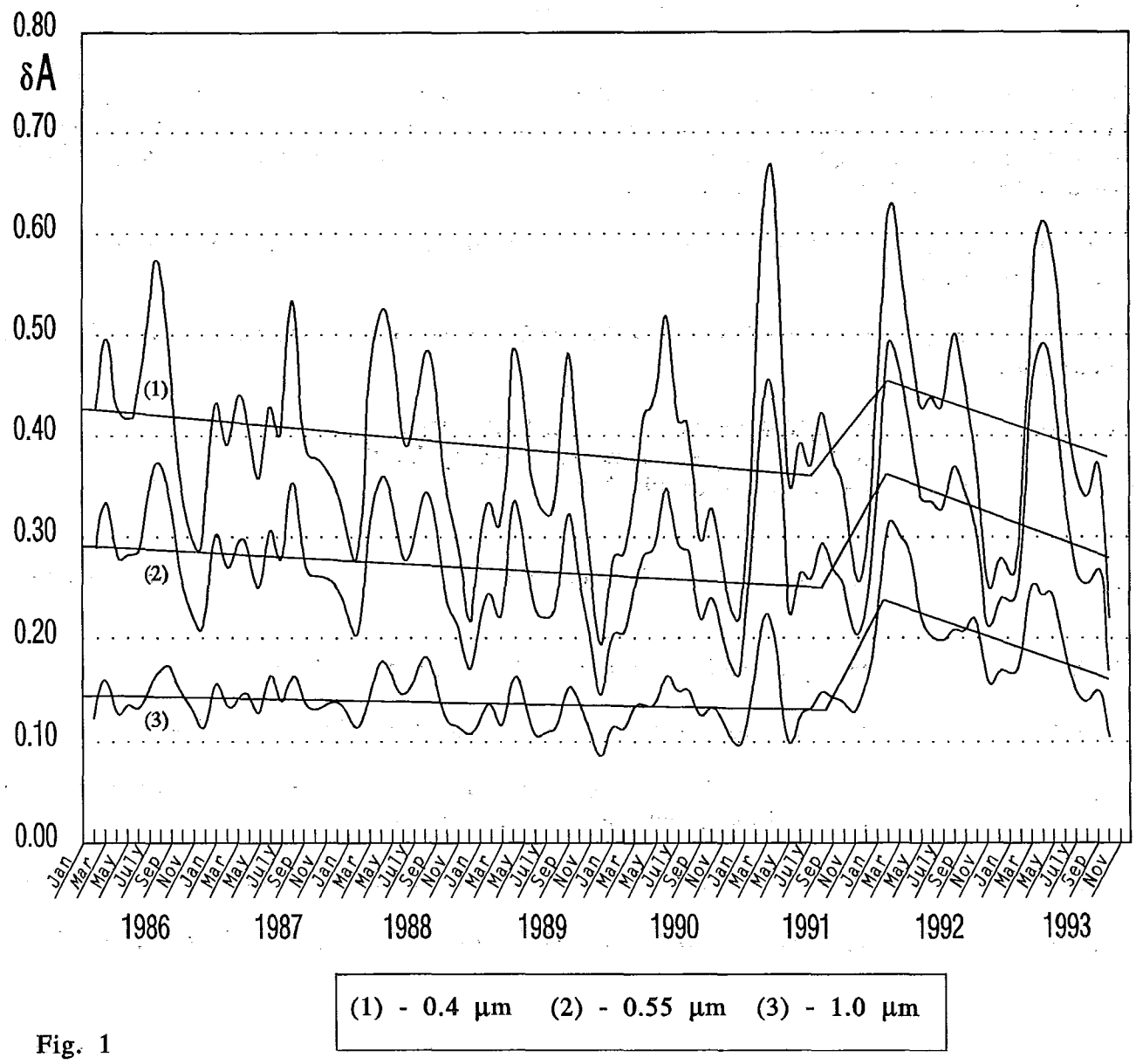

Fig. 1

Fig. 1 represents the temporal behaviour of the AOT for 0,4; 0,55 and 1,0 μm within the period of Feb. 1986 to August 1993. The AOT within the volcanic undisturbed period of Feb. 1986 to the end of July 1991 can be characterized as a postvolcanic one. A decrease of AOT occurred in all VIS and NIR channels. This is due to the dying-down of the El-Chicon perturbation in April 1982. The higher AOT-values in Feb./March 1992 seem to be caused by the transport of soot to Central Europe possibly from the Golf region and/or an accumulation of dust from the Sahara.

Numbering the days of monitoring with n ($0 \leq n \leq 1996$) the temporal behaviour of the AOT spectra for 0.4; 0.55 and 1.0 μm can be expressed by equations 1a to 1c.

(1a) δ_A (0.4 μm) = 0.426 - 3.336 . 10^{-5} n

(1b) δ_A (0.55 μm) = 0.291 - 2.058 . 10^{-5} n

(1c) δ_A (1,0 μm) = 0.145 - 7.150 . 10^{-6} n

The perturbation to the stratospheric aerosol by the eruptions of the Pinatubo stands out against this level and is clearly seen as a strong AOT increase from August 1991 to February 1992. This increase expressed by the equations 2a to 2c ($0 \leq n \leq 213$) was traced through the troposphere and differs significantly (Wilcoxon test) from the ground-based measurements of volcanic undisturbed monthly means for the period Nov. 1991 to July 1992.

(2a) δ_A (0.4 μm) = 0.359 + 4.770 . 10^{-4} n

(2b) δ_A (0.55 μm) = 0.250 + 5.600 . 10^{-4} n

(2c) δ_A (1.0 μm) = 0.131 + 5.690 . 10^{-4} n

After attaining the highest level, the AOT decrease is constantly similar to the dying-down of the El-Chicon perturbation 10 years ago. For the temporal behaviour from March 1992 to November 1993 ($0 \leq n \leq 610$) the following equations apply:

(3a) δ_A (0.4 μm) = 0.460 - 1.21 . 10^{-4} n

(3b) δ_A (0.55 μm) = 0.369 - 1.40 . 10^{-4} n

(3c) δ_A (1.0 μm) = 0.252 - 1.46 . 10^{-4} n

The O_3, $H_2O_{(D)}$ and recently NO_2 corrected spectra of AOT obeying Angströms potential law

(4) $\delta_A(\lambda) = \beta\lambda^{-\alpha}$; λ: wavelength in μm

$\beta = \delta_A$ (1.0 μm)

are classified with regard to the six most common air mass types.

Tab. 1 shows the mean values of the corresponding coefficients α and β together with the mean height of the homogeneous dust layer H_D.

In Tab. 2 those air mass types differing significantly from each other in α, β and H_D are marked.

Table 1

air mass type	α	β	H_D
arctic	1.04	0.107	3.0
subpolar	1.11	0.122	2.6
warmed subpolar	1.16	0.144	2.5
middle latitudes	1.20	0.159	2.5
subtropic	1.18	0.197	3.6
frontal mixing air	1.02	0.133	2.9

Table 2

air mass types to be compared	significant differences in α	β	H_D
arctic/subpolar	-	-	-
arctic/warmed subpolar	-	x	x
arctic/middle latitudes	x	x	-
arctic/subtropic	-	x	-
arctic/frontal	-	x	-
subpolar/warmed subpolar	-	x	-
subpolar/middle latitudes	-	x	-
subpolar/subtropic	-	x	x
subpolar/frontal	x	-	-
warmed subpolar/middle latidudes	-	-	-
warmed subpolar/subtropic	-	x	x
warmed subpolar/frontal	x	-	-
middle latitudes/subtropic	-	x	-
middle latitudes/frontal	x	-	-
subtropic/frontal	x	x	-

- no x yes

With our instruments handed over to the Russian Arctic and Antarctic Research Institute the AOT monitoring at the Antarctic Mirny station was continued. This allowed us to compare evaluated changes in reflectances R and transmittances T (global radiation) of the earth-atmosphere system and of the atmospheric absorption a all three of which are dependent on stratospheric volcanic aerosols over Antarctica and Central Europe. Above the Antarctic plateau with its high surface albedo the volcanic caused increase of the AOT leads to a decreasing albedo R of the earth-atmosphere system in the VIS and NIR. The Pinatubo/Cerro-Hudson aerosol acts over the adjacent "black" south polar ocean in the opposite direction. Here the system albedo R generally increases. Just as over the ocean the Pinatubo aerosol also causes an increase of R in Central Europe although this effect is not so pronounced because the spectral surface albedo exceeds the albedo of ocean water.

The consequences for the radiation absorbed by the earth's surface are almost the exact opposite of R. According to the balance equation

(5) $$R(\lambda) + [1 - A(\lambda)]\, T(\lambda) + a(\lambda) = 1$$

(A (λ) stands for the surface albedo) the first two summands of (5) changes in an exactly opposite way if a (λ) remains constant. This is not completely true because even aged volcanic aerosols increase the atmospheric absorption. So especially in the Antarctic the entrainment of volcanic aerosol increases the absorption rate, and the surface can not absorb the total quantity of the reduced radiation reflected into space. In detail R, T, A and a depend on the assumed models, wavelengths and sun heights.

Some recent papers [4] [5] [6] deal with the influence of natural and anthropogenic aerosols on climate change.
We restrict ourselves here to layer related heating rates resulting from radiative transfer calculations for different scenes of natural aerosol changes in a mid latitude winter. The natural climate forcings that seem to be most significant, based on systematic comparison of radiative effects, are changes of stratospheric aerosols owing to large volcanic eruptions. Comparisons of heating rates for 1) an aerosol-unburdened atmoshere (contr.), 2) a clean continental atmosphere (cc) and 3) a clean continental atmosphere influenced by stratospheric volcanic aerosol with different absorption properties (cc+volc) were made in association with the Max-Planck-Institute of Meteorology in Hamburg. It is obvious that the volcanic aerosols increase stratospheric heating rates [k/d] dependent on its absorbing components at the expense of the tropospheric heating caused by clean continental aerosols [Fig. 2a - 2 c].

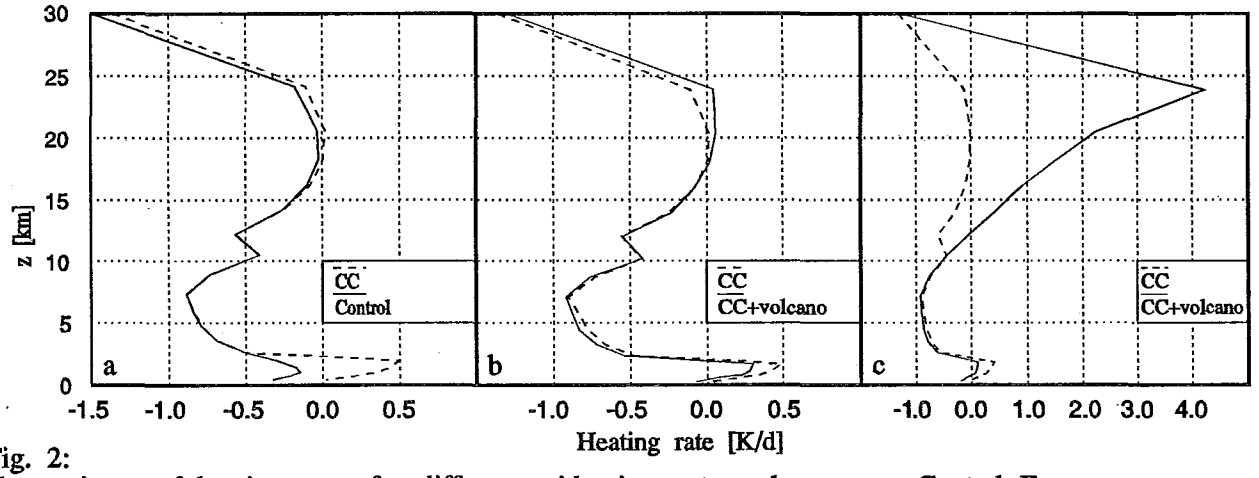

Fig. 2:
Comparisons of heating rates for different mid winter atmospheres over Central Europe
a: aerosol-unburdened atmosphere (control) compared with an atmosphere of clean continental aerosol (cc)
b: "cc-atmosphere" compared with "cc-atmosphere" influenced by non absorbing volcanic aerosols (cc+volcano)
c: "cc-atmosphere" compared with a "cc-atmosphere" influenced by absorbing volcanic aerosols (cc+volcano)

References

[1] Leiterer, U.; Weller, M., 1985: BAS - the project of an earth-atmosphere spectrophotometer for basic research, Acta Astronautica 12, No. 6, 419-429

[2] Neckel, H.; Labs, D., 1984: The solar radiation between 330 and 12500 A, Solar Physics, 90, 205-208

[3] Leiterer, U.; Weller, M., 1992: Method - fit for radiance - and irrandiance calibration of spectrometers and sunphotometers, WMO/TD No. 462, 191-194

[4] Charlson, R.J.; et. al. 1992: Climate forcing by anthropogenic aerosols, Science, Vol. 255, 423-430

[5] Graf, H.-F.; Schult, I., 1992: Globale Klimaeffekte von Vulkanaerosol, Umweltwissenschaften und Schadstoff-Forschung, Z. Umweltchem. Ökotox. 4 (6), 368-374

[6] Kiehl, J.T.; Briegleb, B.P., 1993: The relative roles of sulfate aerosols and greenhouse gases in climate forcing, Science, Vol. 260, 311-314

THE USE OF PRIMARY AND TRANSFER STANDARDS IN CALIBRATING MONITORS OF AIR POLLUTION

W. Rudolf, Federal Environmental Agency, Pilotstation Frankfurt/M

INTRODUCTION

Air Pollution is nowadays worldwide regarded to be one of the most important dangers to the total ecosystem of our world. National and international networks are operated to observe levels and trends of those components which are considered to act as guide substances for the quality of the atmosphere.

Within the member countries of the European Communities air pollutions such as sulphur dixide, nitrogen dioxide, carbon monoxide, ozone and suspended particulates have to be measured on a regular base. The measured values have to be reported to the Commission and, if the defined threshoulds are exceeded, measures to reduce these imissions have to be taken./1,2,3/

Because of the consequences which may be caused by those measurements, quality assurance programmes must confirm correct and true or at least harmonized and therefore comparable measurements.

Quality and comparability is given by a set of parameters, which at least consists of:

-- siting
-- quality of instruments
-- composition of the air under investigation
-- calibration
-- service
-- data acquisition
-- data managment

Each of these issues contains such an amount of philosophical and practical aspects, that it is not possible to discuss them within the frame of that paper, which restricts itself mainly to the issue *"calibration"*.
But one has to bare in mind, that each issue of those mentioned above contributes to the total quality of monitoring. Therefore it is not worthwhile to undertake sophisticated work into only some of them while leaving out the others.
Nevertheless one of the most important tasks in the quality assurarance chain for air pollutions is the necessity to trace the measurements back to true values.
Because nobody realy knows the truth, only accepted practices to relate measurements to a save base can be described here.

REFERENCE MEASURING METHODS; PRIMARY STANDARDS AND TRANSFER STANDARDS

The most important tools to do quality assurance are primary calibration gases, reference measuring methods and the combination of both.
The German guideline named *"Definition of Reference Methods, the Choice of Equivalence Methods and the Application of Calibration Procedures /4/ defines as follows":*

Reference Method:
A reference method consists of a reference measuring method and it's calibration with a primary standard.

Reference Measuring Method:
Methods whith which the complete determination of immissions is possible. Sophisticated experiences for years and widespread use of that method is a further necessity.

Primary Standards (primary calibration gases):
Primary Standards (primary calibration gases) are substances ore mixtures of substances with known properties (concentrations). These properties are determined (calculated) by basic physical or chemical measurements (length, mass, time) and those which can be calculated out of these basic measurements (molecular weight, molvolume)

The best known reference measuring methods are:

For SO_2 : TCM-method
For NO_2 : Saltzman-method
For O_3 : KJ-Method
For CO : Measurement by the Non-Dispersive Infra-Red-Method and calibration by calibration gases tracable back to primary gases.

The best known procedures for the preparation of primary calibration gases are.

- gravimetric determination
- permeation with regulare scaling
- volumetric dynamic mixing
- volumetric static mixing

These methods are described together with others in VDI- and ISO guidelines.
The main problem of the reference measuring methods when only internally *"calibrated"* by substances as disulfite, nitrite and iodide is, that the sampling line is not included and the substances taken for calibration are not identical with the substances to be measured.
The problem with primary calibration gases is, that the blending process may be in line with the accepted definition described above, but that quality may be lost with time.
In discussing these pro and cons within Germany, the chairmen of the appropriate groups of VDI decided, that the method a measurement has to be traced back to should be the primary standard, if there is one.
With respect to SO_2 comparisons between the TCM-method and primary SO_2-calibration gases, as an example blended by permeation devices or the static volumetric method, show differences which not exceed $\pm 3\%$ when exercised technicians are involved in the experiment.
Comparisons between the Saltzman method and primary NO_2-calibration gases produced by the permeation method or the oxidation of primary NO-calibration gases by gas phase titration show larger differences between 0 and about 10%.
An explanation for that differences and the variations of them may be given by possible impurities of the permeation systems
Therfore some German scientists tend to the statement. *"up to now no NO_2-calibration gases excist"*. On the other hand experiments within the Joint Research Centre of CEC, comparing NO_2-calibration gases prepared by permeation and static injection found a good agreement between these two methods. Additional infrared spetroscopic analyses of the used *"pure"* NO and NO_2 showed only neglectable inpurities.
In 1994 VDI working groups will, in close cooperation with CEC, reinvestigate that phenomena by sophisticated comparisons of the Saltzman method , primary NO-and NO_2-calibration gases, the KJ-method and UV-basic method (for ozone) via gas phase titration.

Whatever the result of that study may be, the determination of the purity of the used substances both for the preparation of calibration gases and the chemicals for the internal calibration of the above mentioned reference measuring methods must be brought to a saver base.

REFERENCE METHODS AND TRANSFER STANDARDS APPLIED IN GERMANY

In accordance to German and European legislation up to now 15 networks for the measurement of air pollutions are operated in Germany by the Federal Envoronmental Agency, Umweltbundesamt (UBA) and the German Bundesländer.
The standard equipment consists of continously working instruments for SO_2 NO, NO_2, particulates and ozone. In some traffic related stations instruments for the measurement of CO, benzene and soot are added.
Calibration, or more precisely, the check of the calibration curves of the instruments are carried out by:

- calibration gases stored in pressure cylinders (immission range or premixtures in the ppm range with appropriate dilution systems)
- permeation systems
- foil for the simulation of particulate concentrations
- ozone generators

These systems produce as a rule secondary standards. The concentrations are determined in the laboratory at the beginning and later on by regular comparison against a transfer standard.
"Secondary standard" doesn't mean *"minor quality"* but that the concentrations can't or arn't calculated directly and therefor have to be determined by parallel measurements against a transfer standard.
Transfer standards are more or less the same as mentioned above as secondary standards.In addition wet chemical methods as TCM, Saltzman, and the KJ-method are used.
For ozone it is recommended to use a transportable UV-instrument being calibrated against the reference UV-instrument in the laboratory, or to take the KJ-method.
The use of normal monitors as transfer standards is also possible for SO_2, NO_2 and CO if these monitors are selected especially for sufficient and well known stability.
In table 1 the results of a questionnaire send to the German networks are presented. It was asked, which reference, which transfer and which secondary standards for calibration purposes are used on a routine base.
Looking into the table it is obvious that reference methods in the strict sence of the definition mentioned obove is not obeyed in each laboratory and for each component, but that high attention is given to quality assurance, using reference measuring methods or primary standards. The combination of both is carried out on a regular base (about every 2 years) by ring analyses at Landesanstalt für Immissionsschutz in North Rhine Westfalia, or at UBA, Pilotstation in Frankfurt/M.
At UBA Pilotstation the static volumetric method for the preparation of primary standards is used for years. More recently Warren Spring Laboratory, UK, and the Joint Research Centre of CEC in Ispra confirmed that method as to be easy to handle and as to be of high accuracy and precision ($\pm 1\%$ can be achieved)
The main advantage is given by going down from 100 % SO_2 or NO into the sub - ppm - range (immission range) by a simple one step dilution.
Because this can be done with a transportable 100 l glas vessel and a stability better 1% is given for days, this is a method to blend a primary standard directly at the measuring station, avoiding the addition of errors as it occurs when using transfer standards.

COOPERATION WITH CEC

Round robins in Germany as described above are mostly carried out in close cooperation with CEC. The Joint Research Centre is now carriing out the third QA-programme for SO_2 and NO_2. While during the first and second ones mainly calibration gases were send around, the programme which has been started in 1993 exemplarely in Switzerland, France and Germany is designed to include the whole measuring place (sampling line, monitor and data acquisition) by the use of a calibration gas generator with high air flow capacity at randomly chosen measuring sites.
This is a very important step to get a better imagination of the total error which may occur in practicing air pollution measurements on a routine base.

References:

/1/ Council Directive of 15 July 1980 on air quality limit values and guide values for sulphur dioxide and suspended particulates (80/779/EWG). Official Journal of the European Communities 23 (1980), No. L 229, pp. 30/48.
Revised: (89/427/EWG). Ibid. 32 (1989), No. L 201, pp. 53/55.

/2/ Council Directive of 7 March 1985 on air quality standards for nitrogen dioxide (85/203/EGW). Official Journal of the European Communities (28 (1985), No. L 87, pp. 1/7.

/3/ Council Directive of 21 September 1992 on air pollution by ozone (92/72/EWG). Official Journal of thje European Communities 23, No. L 297/1.

/4/ Definition of Reference Procedures, choice of Equivalence Measuring Procedures and the Application of Calibration Procedures, Gemeinsames Ministerialblatt 1988, 191 f.

Table 1

METHOD OF REFERENCE (METHOD AND/OR STANDARD):

Summary of answers (10 German networks)

	1	2	3	4	5	6	7	8	9	10
SO_2 :	Sp, TCM	Sp, TCM	Pg	TCM	TCM, Sp	TCM	TCM, Ss	TCM	TCM/Perm	TCM
NO :	Sp	Sp	Pg(NO_2)	Sal	Sp	Sal	Sal	Sal/Pg(NO_2)	-	Sal
NO_2 :	Sp	Sp	Pg	Sal	Sal	Sal	Sal	Sal/Pg	Sal/Perm	Sal
CO :	Sp	Sp	Ss	Sp	Ss	Ss	Ss	Sp	Ss	Ss
O_3 :	UV	UV	KJ	KJ, UV	KJ	GPT, UV	KJ	KJ/UV	KJ+Ss	GPT
TSP :	G	-	F	G	F	F	F/P	G	G	G
HC :	Sp	-	Pg C_3H_8	Sp CH_4	Sp	Ss	Ss	-	-	Ss

remarks, abbreviations

-Sp-	primary standard	-G-	gravimetric	-KJ-	Kaliumjodid-method
-TCM-	TCM	-Pg-	gravimetric determination of the permeation rate	-F-	foil
-UV-	UV-absorption, basic procedure	-Ss-	secundary standard	-Sal-	Saltzman-method
-GPT-	gas phase titration	-TSP-	total suspended particulates	-P-	pin
---	no declaration			-HC-	hydrocarbons

TRANSFER OF STANDARDS FROM LABORATORY INTO FIELD (PERMEATION, SECOND INSTUMENT, IMMISSION CYLINDER, DILUTION):

Summary of answers (10 German networks)

	1	2	3	4	5	6	7	8	9	10
SO_2 :	Ss	Ss	Perm	D, Perm	D, Perm	Ss	Ss, Perm	Perm	D	Ss
NO :	Ss	Ss	Perm+R	D	D	Ss	Ss, Perm	Ss	D	Ss
NO_2 :	Ss, Conv	Ss, Konv	Perm	Ss	D, Perm	Ss, Conv	Ss, Perm	Perm	D	Ss
CO :	Ss	-	Ss	Ss	Ss	Ss	Ss	Ss	Ss	Ss
O_3 :	Gen	Gen	Mg	Gen ext	Gen	I	Gen, KJ	Gen	Gen	-
TSP :	F	-	F	F	F	F	F	F	F	-
HC :	TiL	-	Perm	-	Perm	-	Ss	Ss	-	-

remarks, abbreviation

-Ss-	secundary standard	-TiL-	transport of instrument into laboratory
-Conv-	control of converter efficiency	-Gen-	O_3-generator
-F-	foil for particulate density simulation	-i-	instrument
-Perm+R-	NO_2-permeation and reduction to NO with ext converter	-KJ-	Kaliumjodid
-D-	delution of pure mixtures	---	no measure of component

ADD-ON ENVIRONMENTAL MEASUREMENTS AT SYNOPTIC STATIONS

Kai Torp, PPM Systems Oy, Finland
Hannu Kokko and Mats Wiljander, Vaisala Oy, Finland

1. INTRODUCTION

The Meteorological Services are facing the requirements for increased automations, cost efficiency, revenue earning, improved end-user products etc.

One solution for these and future measuring needs is a versatile and flexible multipurpose data collection, processing and reporting device like the MILOS 500. The MILOS 500 can be connected to a wide range of different types of sensors, analysers and communication networks and be configured to meet a wide variety of existing and future measuring and reporting needs. An example of this kind of solution is combined automatic air quality and meteorological observations at synoptic stations.

The creation and implementation of such multipurpose measuring stations and networks will offer significant cost savings, both during the implementation phase as well as during the whole life time by reducing operation, telecommunication and maintenance costs of such a network. Therefore, organisations planning the implementation of new synoptical stations should also take into consideration their future measuring needs when deciding what instruments and measuring devices to use.

The MILOS 500 system can be interfaced with almost any kind of sensor or analyser. The user specific calculations and reports can be generated in real-time or on demand basis. The data distribution can be arranged so that it serves the individual end-user groups' requirements, supplying only the necessary data sets. Data services can be sold for example via direct phone lines or by providing the required reports or data sets.

2. TOMORROW'S MEASURING SYSTEMS ARE ALREADY IN USE TODAY

Tomorrow's measuring and reporting needs can already be solved today by choosing the right instruments. The MILOS 500 offers hardware and software flexibility, modern Bi-directional digital communication, high processing capacity, operation in extreme environmental conditions and low power

consumption. With the MILOS 500 it is possible to avoid measuring and reporting solutions which will be obsolete within the next 2 - 3 years.

The following are some examples of existing air-quality measuring systems comprising modern digital technology and Bi-directional communication.

3. BUILDING UP A MODERN AMBIENT-AIR MONITORING STATION

Let us imagine that we have on our desk a PC and a mouse. There are a few graphs on the display. First, without touching anything, we can check that there are no faults in the measurement system nor in the telephone lines. The curves in the graphs are not broken and they look similar to yesterday's curves. The rush hours have raised the CO- and NOx concentrations, at midnight there has been a peak of SO_2-emission in the neighboring factory.

Also the status window is empty - there are no computer detected problems. By clicking the mouse button we can see from the event-log that there has been a three hours' break of telephone-lines, but no loss of data. Just now there is another SO2-peak in the measurement station which is far from the factory. With these wind direction and wind speed conditions this is unusual ! By clicking the mouse button twice we can check the condition of the SO2-analyser; temperatures are normal such as the flows. It must be a true SO_2-concentration. How about a wind direction history of all measurement stations ? A little look at the graphs and it is clear - the wind has carried the same emission to the other stations, too.

The above mentioned introduction is not science-fiction. In about 25 towns in Finland it is an everyday job for the authorities. And most of them have used less than 100 000 USD to build up the whole system network.

MONITORING NETWORK

A typical Ambient Air Monitoring Network consists of:
* Measurement stations at selected locations
* Central PC with DILTA acquisition, collecting and reporting software
* Monitoring PCs or printers for the interested official authorities (or their customers)
* A data transmission network, typically a public telephone network with dial-up modems

MEASUREMENT STATION

A modern measurement station includes:
* Meteorological sensors; wind direction and speed, temperature and humidity which are the minimum requirement for air quality measurements.
* SO2 and NOx analysers
* In some cases CO and / or O3 analysers
* Dust analysers

Sensors and analysers are connected to the MILOS 500 data collection and processing unit. The analysers are connected to the MILOS 500 via Bi-

directional RS-232 serial lines. Thus the MILOS 500 can act either as a datalogger or as a multiplexer. This enables the central computer to communicate directly with the analysers.

Meteorological sensors

At least one station has to be equipped with meteorological sensors, typically wind direction and wind speed, temperature and humidity. If there is a possibility that meteorological conditions vary significantly from one measuring station to another, every station should be equipped with basic meteorological sensors. These sensors can be connected directly to the MILOS 500.

In addition, the whole range of sensors required for coding SYNOP messages and for collecting the climatological archives may be used. These include for example pressure, radiation, Present Weather, precipitation and ground temperature sensors at several levels.

Analysers

The most common air-quality analysers are SO_2, NOx, O3, CO and TRS (Total Reduced Sulphur). Modern SO_2 analysers use the UV fluorescence method. A zero-check is typically performed once a day and a span check once per month. NOx analysers use chemilumenence method and also a zero check is performed once a day, with a NO2-span check once per month. O3 analysis is performed by UV-absorption and does not need frequent calibration. CO analysers use IR absorption method and a once a day zeroing is typically done. For TRS-measuring there is a thermal converter with SO_2 scrubber and SO_2 analyser. There is a possibility to use the same SO_2 analyser for both TRS and SO_2 analysis by switching sampling techniques. Dust is measured by Beta absorption method and it needs a manual calibration only after changing the collector belt.

Calibration

Calibration is done by internal filters and permeation tubes. Modern analysers do the calibration independently at predetermined intervals. The older versions without a microprocessor need external relay contacts and a timing system. It is important to distinguish the calibration data from measured data and it is very useful to transfer the calibration results to the central computer.

Sampling

Analysers need a stable, not too humid sample flow. This is done using a probe with a heated inlet filter and usually a bypass flow pump which guarantees a stable flow. The analyser's inlets are connected to the probe. Humidity does not effect the measurements as long as the temperature remains above dewpoint temperature. A bypass flow pump is necessary when there are over four analysers at the station.

Other

There are also demands concerning the cabin. It should be easily transportable, electricity must be well designed to avoid electrical disturbances. Air-conditioning is definitely necessary. If telephone lines are a problem, then the use of cellular telephones and networks could be reasonable solutions.

Computers at Central Data Gathering Station

Central PC is 386sx or 486sc including;
* 4MB RAM, 100-200MB hard-disk, 14" - 20" sVGA display and mouse
* serial port and parallel port
* Windows 3.x
* DILTA acquisition software

Also there is a need for a proper modem and a printer.

Monitoring PC is typically a 386sx with 2 - 4 MB RAM, 40 - 200MB hard disk, SVGA display, a mouse, Windows 3.x and DILTA monitor software.

The central PC communicates with measurement stations via RS-232. This lets us choose the transmission techniques from a wide variety of communication means, such as:
* direct leased lines with or without modems
* public telephone networks with up to 9600 baud dial-up modems
* cellular telephone networks such as NMT, GSM
* private VHF or UHF radio links / networks

Graphs

To see the latest results in one sight on the display of the central PC, the user typically creates a graph window for each type of component. One for wind directions, another for SO_2, etc. We can put two different scales to one graph, for example both SO_2 and NO_2 to same graph with different scales in order to be able to compare these two easily. There are ten screens where we can create different layouts where the first ones could be of general type, with more accurate graphs in the following screens.

Calibrations

The meteorological components are easy to measure and save, but the air-quality components are a little more complicated because the analysers need regular calibration. Modern analysers can calibrate themselves automatically and with DILTA software we can easily control how the analyser calibration is performed. After each calibration the results are gathered by DILTA and will help us to ensure the quality of measurement results.

Diagnostics

Analysers communicate with DILTA via serial line, this means that commands can be given from DILTA for:
* changing settings of analysers
* perform diagnostics concerning sample flow, temperatures, etc..
The analysers can of course control themselves, and if a fault is detected, DILTA would get a warning via the MILOS 500.
DILTA also keeps a log of such events like connection problems, analyser warnings, unreasonable results, etc..

Handling of data

Especially with older types of analysers there is a need to edit the measured data. Sometimes a piece of data must be flagged as discarded, because of malfunction, test-conditions or some other reasons. Sometimes, depending on the calibration, the measured values must be increased or decreased. For these kind of purposes there is in DILTA an Archive handling application which allows us to do the prementioned actions very easily.

Reporting

DILTA calculates and prints out in the table form or in the graphical form all the common statistical values that are used in air-quality reports. It is possible to order more facilities to the report application or transfer the data to some other statistical applications.

While gathering the necessary data for air quality applications for DILTA system, the MILOS 500 can be simultaneously used for coding hourly or 3-hourly SYNOP messages, which are them automatically sent to the users. The data transmission can occur together with air quality data to reduce telecommunication costs. Also SPECI messages can be initiated to report and warn of some special weather phenomena.

Climatological as well as air quality data can be stored at the MILOS 500 station where it can be collected via serial or modem line or by using a PCMCIA/JEIDA standard memory cards.

DILTA software and the MILOS 500 data collection system offer flexibility in connecting the existing analysers and meteorological sensors for building a compact and cost-effective environmental station to serve multiple purposes.

MEASUREMENTS OF VERTICAL OZONE PROFILES WITH ECC-CAO SONDES DEVELOPED IN RUSSIA

A. M. Zvyagintsev
Central Aerological Observatory (CAO),
Pervomayskaya, 3, Dolgoprudny, Moscow Reg., 141700, Russia

There are various ozonesonde types (ECC, Brewer-Mast, Indian, Japanese et al.) that are currently in operational use in the WMO Global Ozone Observing System. Their qualities can be estimated from the analysis of routine measurements (e.g., published in WMO's "Ozone Data for the World"), some special publications, and international ozonesonde intercomparisons [1]. It may be concluded from all these sources that now Komhyr's electrochemical concentration cell (ECC) ozonesonde is the most prevalent one. Its advantages are as follows: 1) yielding absolute ozone concentration, which provides high accuracy in the 10-25 km region and 2) enabling an unskilled operator to achieve good results after a short training. The most important characteristic of the ozonesonde is the total ozone normalization factor, K, - the ratio of spectrophotometer (usually Dobson or Brewer) total ozone to ozonesonde one. In the recent balloon ozone intercomparison campaign [1], the average normalization factors for ECC ozonesonde and their standard deviation obtained by different operators were from 0.96 to 1.01 and about 0.032, respectively. For routine measurements these values are much larger: e.g., in 1983-1987 for NASA station in Natal, Brasil, they make about 1.02 and 0.11, respectively [2]. The shortcomings of ECC sondes are: 1) a relatively high cost (specifically, for us) and 2) general shortcomings that are inherent in electrochemical ozonesondes, namely: a) the relatively long timeresponse (about 30 s near the surface and more during ascent); b) sharp and non-controlled drop in precision above a 25-km level (measurement results are doubtful for heights more than 32 km); c) inconvenience due to using of "wet chemistry" during pre-flight preparation. In an attempt to eliminate some of these shortcomings, CAO undertook the development of its own ozonesonde.

An experimental electrochemical (ECC-CAO) ozonesonde has been developed and manufactured at CAO, using its own materials and technology. In its main features, the ECC-CAO sonde is similar to the well-known ECC-5a sonde, but cheaper. Using CAO sondes together with modified commercial MARZ or MRZ type radiosondes (which are combined with the Russian C-radar "Meteorit" or AVK, respectively) we obtain information about temperature, humidity and ozone concentration during ascent. Also, we have developed a chemiluminescent (CL-CAO) ozonesonde which has some advantages over ECC-CAO one (a time-response, a possibility to measure at any height, and an simple pre-flight preparation). However, ECC-CAO sonde has an advantage in precision because of the simplicity of its calibration and stability of its sensor during the flight.

The first tests of ECC-CAO ozonesondes were carried out at Rylsk (51 'N, 34 'E) in autumn 1989. More comprehensive investigations of our ozonesondes were carried out at Rylsk in summer 1990, jointly with specialists from Lindenberg Aerological Observatory (Germany) [3]. Three different electrochemical ozonesondes (ECC-5, OSE-4 and ECC-CAO) and chemiluminescent one (CL-CAO) were intercompared. The experiments included 2 launches of a multiple-instruments gondola and 6 balloon flights (3

triplets, 2 doublets and 1 singlet). In case of gondola flights, all the information was obtained directly from the microcomputer; in case of balloon flights, the results were derived from the diagram tape of the C-band radar "Meteorite-R". Absolute differences between ECC-5a and ECC-CAO data (corrected by the factor K) are as large as 10 nbars at all heights below 30 km. A relatively high normalization factor of 1.237 and its standard deviation of 0.212 for ECC-CAO sonde were obtained; apparently, it was caused mainly by the drawbacks in manufacturing and/or pre-flight preparation of a pump and partly by an error in measuring total ozone with the filter ozonometer M-124 (improved model of M-83), which made about 8 %. This was taken into account in improving the ozonesonde design.

In 1991-1992, we used modified ECC-CAO sondes in 20 balloon flights for measuring ozone profiles in Volgograd, Tashkent, Dushanbe, Khorog, and Dolgoprudny (see Table). Five different operators launched the ozonesondes. The results were calculated at CAO, using information from the radar tapes. Total ozone was measured in Volgograd with the ozonometer M-124; TOMS/METEOR-3 data were used for Central Asian sites; at Dolgoprudny, both kinds of data were used. The average normalization factor and its standard deviation (1.053 and 0.079, respectively), obtained in these measurements, are quite satisfactory and consistent with the routine ECC sonde measurements.

TABLE

Total Ozone Normalization Factors for ECC-CAO Ozonesonde in 1991-92

Station	'N	'W	Year	Month	Flight number	K	St. deviation
Volgograd	49	44	1991	Jun, Jul	6	1.102	0.079
Tashkent	41	69	1991	May, Nov	5	1.056	0.080
Dushanbe	38	68	1991	Nov	4	1.012	0.082
Khorog	37	71	1991	Nov	2	1.115	0.092
Dolgoprudny	56	38	1992	Nov	3	0.963	0.058
Average			1991-92		20	1.053	0.079

Some examples of modified ECC-CAO sonde's profiles, showing the ozonesonde efficiency are given in Figs. 1-3.

Fig.1 shows that both temperature and ozone profiles testify the replacement of air masses, the latter looking more sensitive.

In Fig.2 one can see a good agreement of ozone profiles obtained simultaneously at sites 300 km apart.

On 11-12 November 1992, when one of the lowest total ozone values ever registered in Moscow region was observed (240 D.U.), we performed three launches of ozonesonde payload. The payload consisted of an ECC-5a ozonesonde with a Vaisala RS-80 radiosonde (Finland) and of ECC-CAO ozonesonde with a MARZ-2-2 radiosonde. Each sonde had fully independent data acquisition, processing and transmission systems on the ground. The ozone vertical profiles obtained with the two ozonesondes were similar for all altitudes; for altitudes above 20 km they coincided with the CAO's empirical profile [4] for this time period (Fig.3).

The results obtained in these experiments prove that ECC-CAO ozonesonde can be used on a routine balloon network. The date of the beginning of regular ozonesonde soundings will strongly depend on the financial possibilities of Russia and other countries of the former Soviet Union.

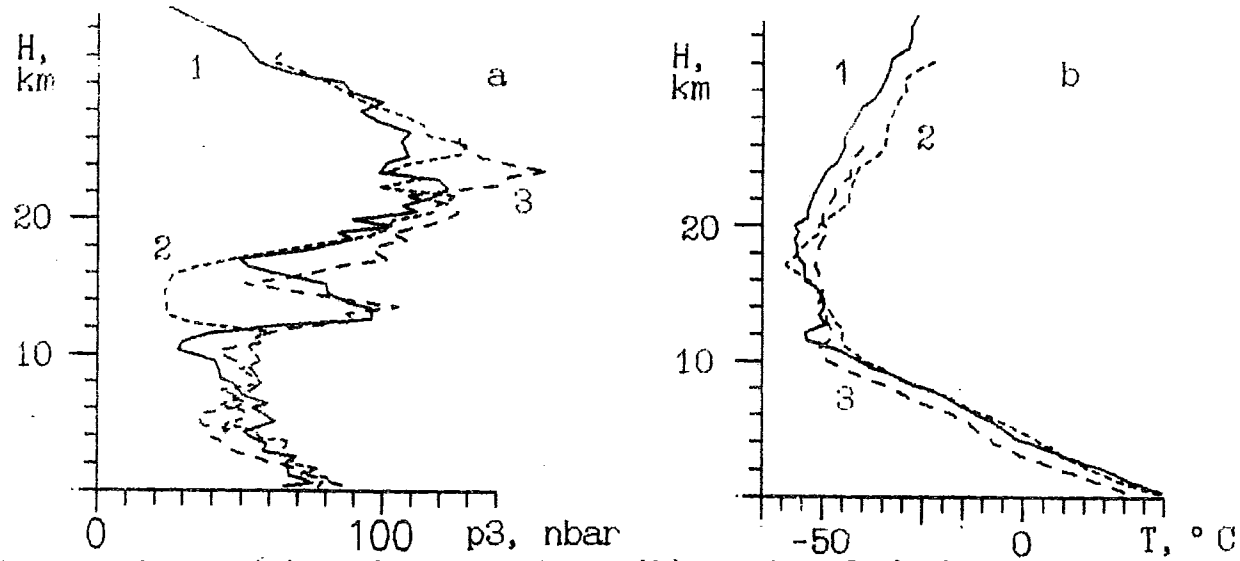

Fig. 1. Ozone (a) and temperature (b) vertical distribution measured on June 28 (1), July 1 (2), and 4 (3), 1991, at Volgograd.

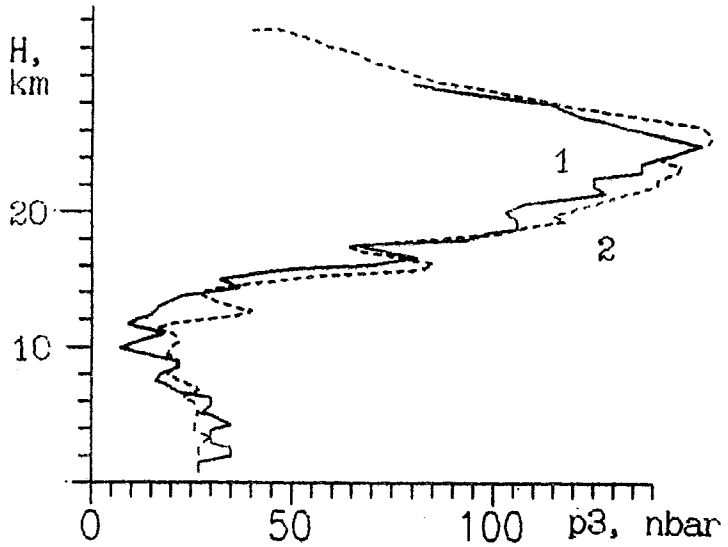

Fig. 2. Ozone vertical distribution measured on November 7, 1991, at Dushanbe (1) and Khorog (2).

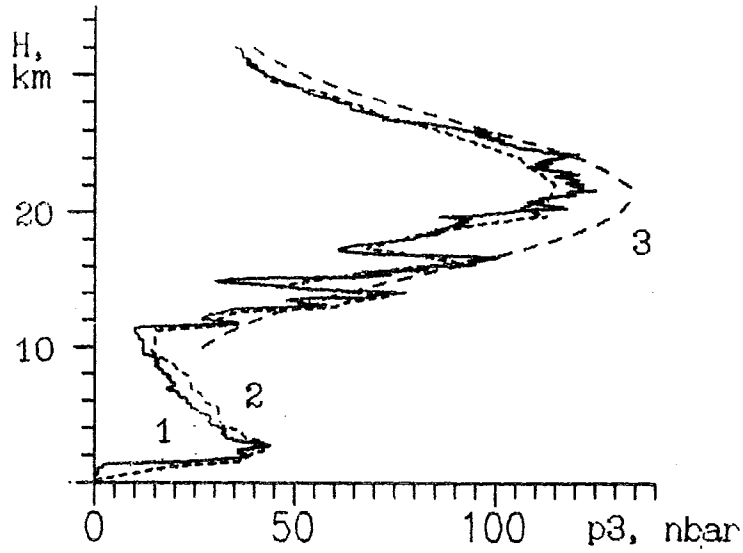

Fig. 3. Ozone vertical distribution measured on November 12, 1992, at Dolgoprudny by ECC-5a (1), ECC-CAO (2) sondes and empirical CAO-model profile (3).

REFERENCES

1. Kerr J.B., C.T. McElroy, H. Fast, S.J. Oltmans, J.A. Lathrop, E. Kyro, A. Paukkunen, H. Claude, U. Koehler, C.R. Sreedharan, T. Takao and Y. Tsukagoshi. The 1991 WMO ozonesonde intercomparison. - Proc. 1992 Quadrennial Ozone Symp., Virginia, 1992.

2. Kirchhoff V.W.J.H., Barnes R.A., Torres A.L. Ozone climatology at Natal, Brasil, from in situ ozonesonde data. - J. Geophys. Res., 1991, v. 96, No. D6, p. 10899-10909.

3. Albrecht H.-J., G. Peters, A.M. Zvyagintsev. Erste Ergebnisse eines Ozonsondenvergleichs in Rylsk (UdSSR). - Z. Meteorol., 1991, Bd. 41, H. 4, S. 309-310 (in German).

4. Bekoryukov V.I., V.N. Glazkov, V.V. Fyodorov. Empirical model of the ozone vertical distribution in the North Hemisphere. - Meteorology and Hydrology, 1990, No. 2, p. 53-57 (in Russian).

QUALITY ASSURANCE PLAN FOR THE WMO GLOBAL ATMOSPHERE WATCH (GAW)

Volker A. Mohnen, Wolfgang Seiler and Franz Slemr

Fraunhofer Institute for Environmental Research (IFU)
Garmisch-Partenkirchen, Germany

1. OVERVIEW

The issues of global change and man's influence on the quality of the natural environment are complex. The chemistry of the atmosphere is changing: a global warming is expected due to increasing concentrations of greenhouse gases (CH_4, CO_2, N_2O. CFCs and ozone) and altered amounts of clouds and particles in the atmosphere; the stratospheric ozone layer and consequently the surface solar flux of ultraviolet radiation are being modified; the integrated oxidation rate, loosely referred to as the oxidation efficiency or oxidation capacity ot the atmosphere is changing and the abundance of trace gases including those with significant greenhouse warming potential are perturbed. Assessment of the problems, their impacts and the responses to them occupy a prominent position of the international agenda today. Finding an ecologically effective and economically efficient solution to these problems confronts all countries of the world with a challenge of global dimensions.

The Global Atmosphere Watch (GAW) program of WMO is an integral part of the Global Climate Observing System (GCOS) established by WMO, UNESCO/IOC, UNEP and ICSU. GAW is devoted to the investigation of changing chemical composition and related physical characteristics of the global atmosphere. GAW is a coordinated network of observing stations, associated facilities and infrastructure encompassing measurement and related scientific assessment activities. The overall role of GAW is to supply basic information of known quality indicative of the atmospheric environment that transcends specific issues.

The GAW measurement responsibilities include:

- greenhouse gases
- ozone (surface, total and profile)
- radiation (including UV-B) and optical depth
- precipitation chemistry
- chemical and physical properties of aerosols
- reactive gases
- radionuclides
- related meteorological parameters.

The data obtained by GAW initially provide:

- integrated monitoring
- scientific assessments
- early warnings.

The GAW-structure calls for (1) up to 30 GLOBAL STATIONS located at remote pristine locations; (2) over 100 REGIONAL STATIONS for characterizing the regional environmental quality away from direct pollution sources; and (3) a mechanism/system of activities for producing measurements of known quality and of value for making environmental policy decisions (quality assurance/quality control).

2. IMPLEMENTATION

WMO's strategy for implementing total quality assurance is built around Quality Assurance/Science Activity (QA/SACs); following the recommendations of a meeting of experts assembled by WMO (March 26-30, 1992, Garmisch-Partenkirchen, Germany) and charged with the development of a quality assurance plan for GAW (WMO/GAW Report No. 80, 1992; "Report of the WMO Meeting of Experts on the Quality Assurance Plan for the Global Atmosphere Watch".) In June of 1992, the Executive Council of WMO, recalling previous concerns of data reliability and recognizing the importance of quality assured data, fully supported the actions taken by the Secretary-General and the EC Plan of Experts/CAS Working Group and endorsed the structure and establishment of QA/SACs within GAW. The Executive Council requested that the Secretary-General proceed with this development.

Accordingly, the WMO arranged a second meeting of experts (December 7-11, 1992, Garmisch-Partenkirchen, Germany) to develop guidelines for the implementation of these QA/SACs (WMO/GAW Report 1993 "Report of the WMO Meeting of Experts on the Implementation of Quality Assurance/Science Activity Centres for GAW"). The essential functions of these QA/SACs include the preparation and execution of (1) the comprehensive GAW Quality Assurance Programme for all measurement components, and (2) a plan for education and capacity building within the countries that have committed to maintain and operate GAW sites. Building the indigenous technical and scientific capabilities and infrastructure (particularly in developing countries) is an integral part of an effective QA programme.

The spread of QA/SAC activities will be broad, but first steps in their implementation need to be carefully directed. Contemporary concerns over possible chemical and climatic effects of the observed increases and decreases, respectively, in tropospheric and stratospheric ozone have resulted in selection of this issue as an example for describing the first detailed QA/SAC activity.

The overall function of the Quality Assurance/Science Activity Centres (QA/SACs) has been discussed in detail in WMO/GAW/Report Nos. 80 and 92. The QA/SACs provide to WMO the communications and constructive assistance necessary for maintaining consistent and known data quality in the Global Atmosphere Watch Programme so that it can achieve its monitoring goals. They are an essential and integral part of the GAW network and the operational mechanism for harmonization and coordination of GAW activities. All GAW participants will abide by the WMO policies and the QA/SAC procedures and methodologies to produce data bases of consistent and known quality. Although the country supporting the GAW site remains the primary owner of its site's data and may release it as agreed with WMO, the data can only be accepted as GAW data after completing the QA/QC procedures for GAW.

The QA/SACs will facilitate transfer of knowledge, experience and expertise within the network to ensure common practices. While the QA/SACs perform a network-wide quality review, the site Principal Scientist (PI) has primary responsibility for the quality of the data generated at his/her site. The QA/SACs will help establish and foster research ties among site PIs and with users of GAW data bases to ensure relevance to international scientific and policy concerns.

The QA/SACs will be advised by a policy advisory panel of neutral experts and by technical advisory panels which include site PIs. The effectiveness of the QA programme and QA/SAC procedures will be reviewed by WMO on a regular basis, e.g., after three to five years of operation.

3. QA/QC ACTIVITIES

The specific duties of QA/SACs include:

- Management of the preparation of the QA plans for environmental variables

– ensure the production of specifications to Data Quality Objectives (DQOs), Quality Assurance Project Plans (QAPjPs), lists of supporting information to be supplied and the corresponding protocols for flags

– perform pilot studies to test QC procedures on a limited scale before full implementation

– coordinate activities among all QA/SACs.

- Quality assurance support

– design and lead QC tests in consultation with sites to resolve performance questions

– prepare (or identify existing) QA/QC and data transfer protocols (For many environmental variables, QA procedures are already well established, and recognized authorities exist within the regions who are likely to be willing consultants.)

– prepare QC activity schedule, site-visits, expert consultations (performance and systems audits), calibrations, and intercomparisons

– promote twinning arrangements between sites

– identify sources of standards and instructions of usage (provide if necessary)

– periodically review site adequacy (in specific situations, QA activities may be delegated to appropriate expert groups outside the GAW network)

- Management review of data and QC products

– perform quality checks on data streams and QA products (primary quality checks must be performed by the site PI)

- transmit data, metadata, and flags to data centre following review within the specified period

- if review has not occurred within specified time, transmit data, metadata, and flags to Data Centre with a flag indicating that review has been delayed

- until QA procedures are fully implemented, all data, metadata and flags will pass through the QA/SAC with flags where appropriate, indicating that the QA/SAC has not reviewed a part of the data because the QA procedure for that part has not been elaborated

- allocate station performance categories.

  • Training

- develop an ongoing, network-specific educational programme (training courses, seminars, etc.)

- prepare (temporary appointments, etc.) and certification procedures to ensure that only trained personnel are involved in station operations

  • Communication and dissemination of information

- establish a communications network (e.g. e-mail, newsletter, bulletin boards, clearing house for urgent operational and other information etc.)

- promote awareness of technological **changes (workshops, training,** information)

- arrange periodic review meetings (including scientists, technicians and operators from GAW and other scientists whose work is of relevance to GAW) to present scientific results, exchange technical information, and facilitate coordination of QA procedures

- cooperate with international scientific programs involved in atmospheric research such as IGBP-IGAC.

The flows of data metadata, and flags, as well as the linkages between the sites, SAC, and data centers are shown in Figure 1.

Figure 2 provides a pictorial description of the general approach to be applied for quality-**assurance and measurement system** development. Here it is important to note the hierarchical decendency of elements from top of bottom, with each function fulfulling the needs of the function immediately above. Thus the scientific objectives associated with the measurement of a given parameter (Box 2) are chosen to resolve the issues identified by the GAW administration in consultation with The Panel. These scientific objectives are chosen so as to most effectively contribute to resolution of these issues within the practical constraints of current scientific knowledge and resource limitations. Initial assignments of required measurement uncertainty levels are established at this point to guide operations in succeeding boxes.

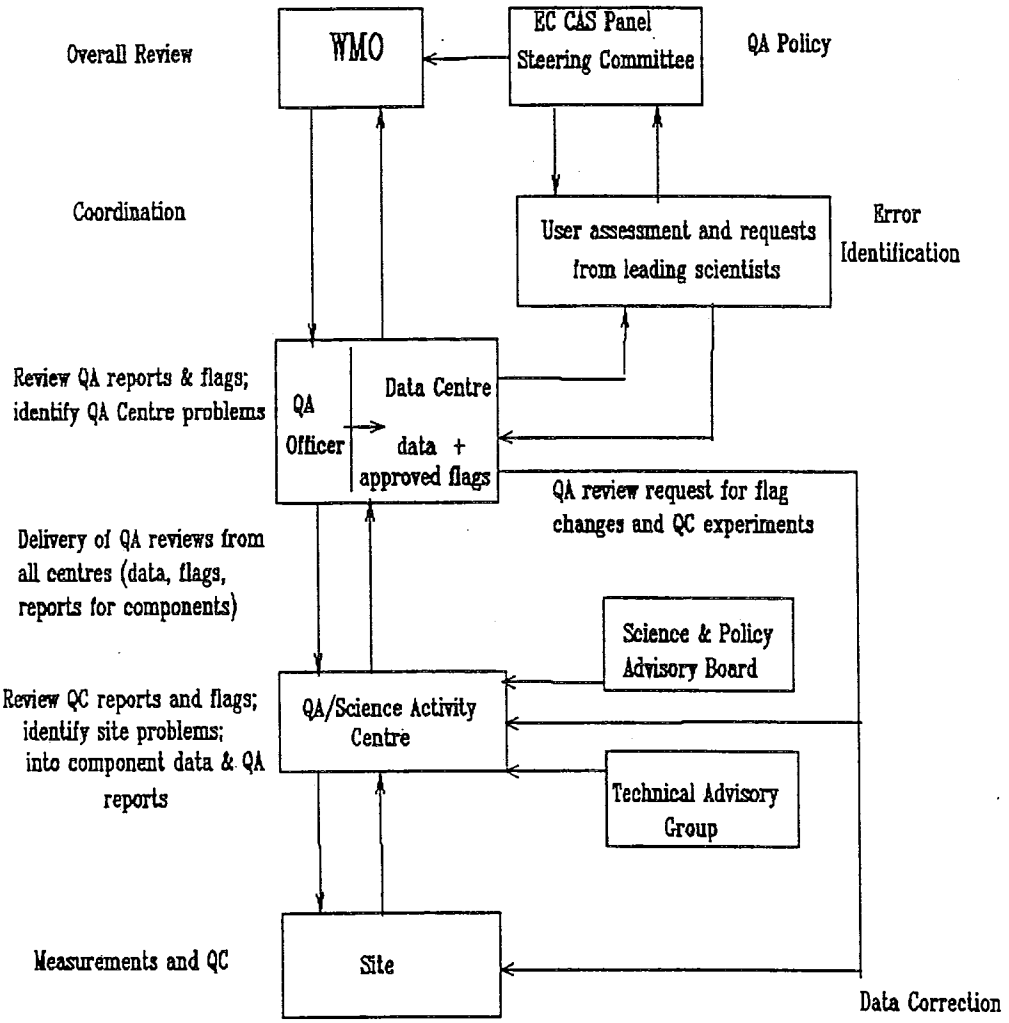

Figure 1: Flows of data and flags as well as the linkages between the sites, QA-SAC and data centers

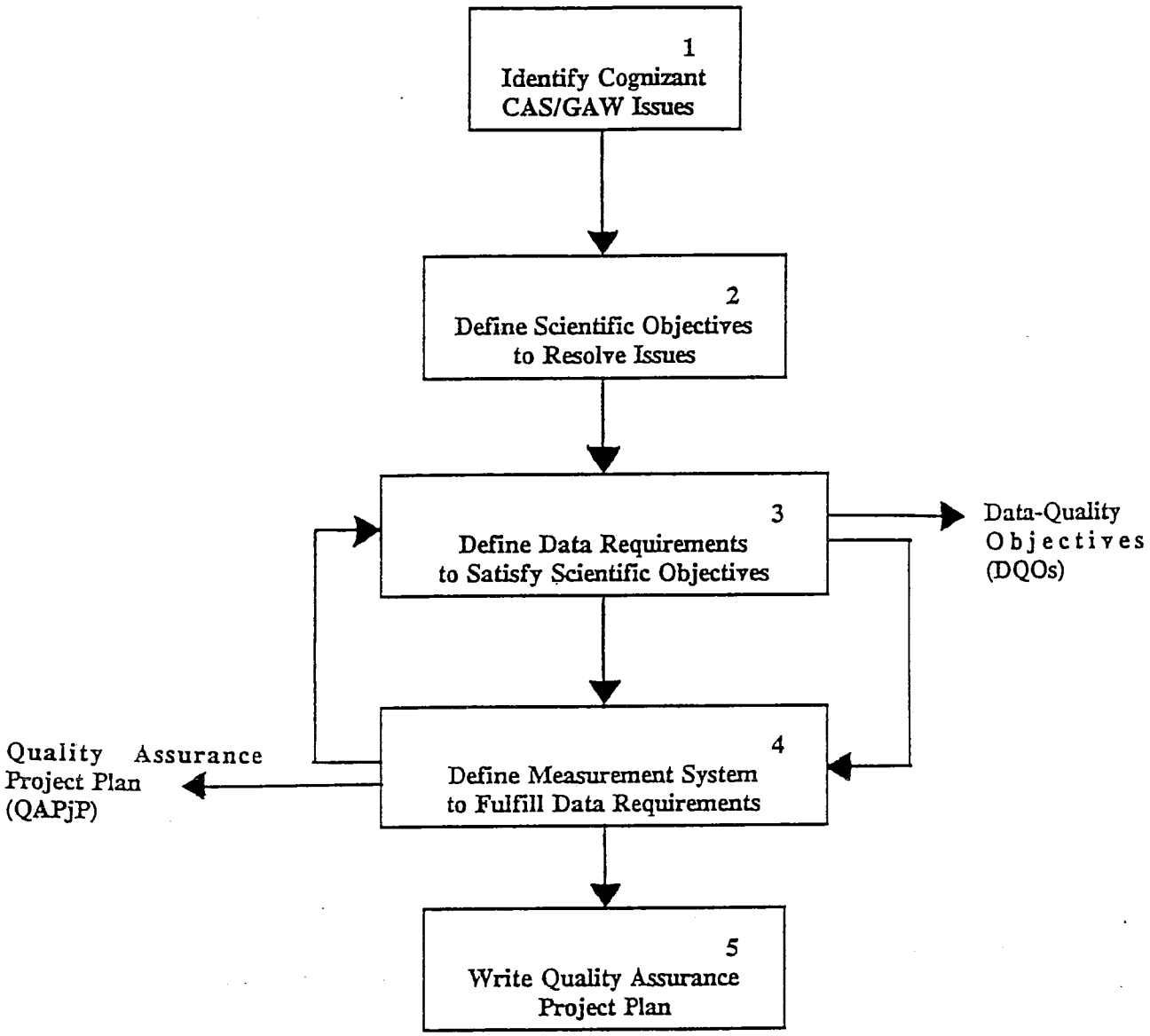

Figure 2. Road map for quality-assurance and measurement system development.

Box 3-4 addresses design of the scientific measurement system to fulfill the scientific objectives, in combination with the quality-assurance program associated with these measurements. These are closely coupled because their design is necessarily a joint, iterative process: the initial scientific design is challenged by the initial data-quality requirements, with resulting modifications, and the process continues until an acceptable convergence is attained. Typically the scientific design is conducted by posing a series of specific questions regarding the appropriateness of the measurement system to satisfy the scientific objectives.

These usually include (but are not restricted to) questions pertaining to required spatial resolution, temporal resolution, instrument accuracy, redundance, and ancillary measurements.

4. CONCLUSION

The scientific input to the debate on environmental issues must derive from an adequate knowledge base. This can only be achieved through high quality, strategically oriented observations, and research related to the particular issues. This necessitates the establishment of proper global environmental observation systems. It is the only effective way to ensure systematic gathering of data world-wide according to comparable and clearly defined measuring criteria, to enable coordinated data processing and quality assurance, and to facilitate the distribution and provision of available information to the widely varied group of users. This complex international task must be tackled jointly by international organizations and the scientific community.

5. ACKNOWLEDGEMENT

The QA/SAC activities are supported by the World Meteorological Organization (WMO), the German Ministry for Research and Technology (BMFT) and by the National Oceanic and Atmospheric Administration (NOAA).

PROCEDURES FOR RELIABLE EDDY COVARIANCE MEASUREMENTS OF ATMOSPHERIC HEAT AND CO_2 FLUXES

Bert Heusinkveld, Henk de Bruin, Anne Verhoef, Frits Antonysen, Willy Hillen

Wageningen Agricultural University, Department of Meteorology, Duivendaal 2, NL-6701 AP Wageningen, The Netherlands

INTRODUCTION

In energy balance studies at the earth's surface, the eddy covariance technique has proved to be the most reliable. This technique can also be used to measure CO_2 fluxes. The used set-up applies a 'Solent' Sonic anemometer and a 'Licor' closed path infrared gas analyzer. This paper describes the measurement, calibration and correction techniques used during the HAPEX-Sahel measurement campaign in Niger, 1992.
The HAPEX/Sahel project studies the semi-arid regions on the southern side of the Sahara desert. The overall aim is to characterise the energy and CO_2 exchanges at the earth's surface for global climate models. Inside the experimental area, a grid of 100 x 100 km square around Niamey, the capital of Niger, many research groups worked together on different sites. To improve intercomparison, many research groups used the same set-up to measure the energy balance with the eddy covariance technique. This technique requirers fast response sensors for windspeed, humidity and temperature. A new 'Licor' closed path gas analyzer gives the opportunity to measure carbon dioxide and water vapour fluxes simultaneously. The system has been tested during a measurement campaign in Niger (August..October 1992).
The set-up uses a Solent ultrasonic anemometer, a Licor gas analyzer and a computer, see figure 1.

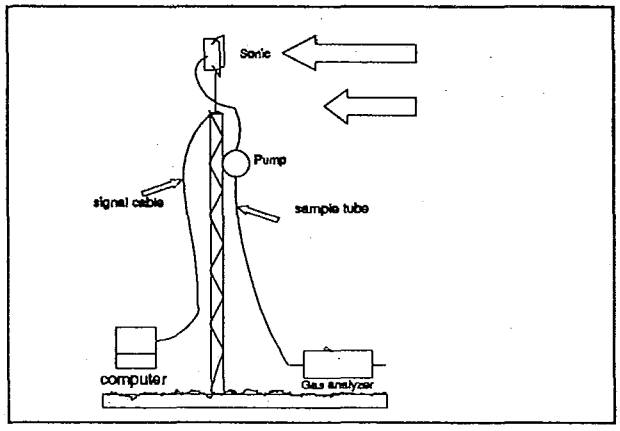

Figure 1 Basic set-up of flux station used during the HAPEX Sahel measurement campaign.

The set-up will be described in more detail.

ULTRASONIC ANEMOMETER

The ultrasonic anemometer, made by Solent, measures the 3 windcomponents at a rate of 20 Hz. The advantage of this sonic is that it can simultaneously measure up to 5 analog inputs (like a datalogger). The resolution of the built in analog to digital converter is limited to 11 bits. It will digitize any signal between 0 and 5 voltage. The gas analyzer will be connected to these input channels of the sonic. The noise of the analyzer is less than 0.2 ppm for CO_2. This means that the CO_2 signal must be scaled in such a way that there is no loss in resolution. Eleven bits resolution means a digitization into 2048 steps, because the noise of the analyzer is 0.2 ppm and we want to have a safety margin of at least a factor 4 (noise), the CO_2 signal must be scaled in such a way that 100 ppm 'fits' on this 0..5 voltage input range of the Sonic. For example 0 volts equals 300 ppm and 5 volts equals 400 ppm CO_2. Care must be taken to keep the signal inside this range.
The sonic outputs every 1 second a data record with 20 measurements of the u,v,w and speed of

sound, and the measurements of the analog channels, 20 numbers per channel. Looking at the records, it seems as if the analog channels are being measured at a rate of 20 Hz, but this is not the case, the numbers are 2 by 2 equal.
The sonic must be set perfectly vertical. When a sonic has been set vertical, still corrections are necessary. McMillen (1986) has found that even for a horizontal terrain, axis rotation is still necessary to calculate reliable covariances.
The set-up in Niger has used solar energy to generate power for all computers and instruments. The solar panels (type M55) were made by Siemens. These panels can produce 55 Watt at maximum each, efficiency reduces when panel temperature increases. The panels were positioned in a fixed angle. On average, 9.5 Watt/panel power consumption (day and night) is possible. Remember that HAPEX measurements started during the rainy season.
When connecting instruments together, ground loops can occur. The sonic relates its analog channels towards ground, the same ground as power ground. To solve this problem, differential instrumentation amplifiers powered by an isolated power supply (DC/DC converter) were used between sonic and instruments.

GAS ANALYZER

The gas analyzer is a Licor LI-6262 differential, infrared gas analyzer. The CO_2 and H_2O measurements are based on the difference in absorption of infrared radiation passing through two gas sampling cells. Due to dependency of concentration on pressure, the pressure inside the sample cell must be kept constant. To achieve this, the flowrate must be kept constant during measurements and the measurements must be corrected for atmospheric pressure.
Calibrating the analyzer with a calibration gas means that the pressure inside the sample cell must be kept the same as during the measurements. Maintaining the airflow during calibration the same as during measurements, will consume a lot of calibration gas. To avoid high calibration flowrates, one can make use of the automatic pressure correction of the analyzer. It is still advisable to shortly increase airflow and see what the difference is. The gas analyzer was equipped with a pressure sensor at the inlet of the gas chamber. It was not possible to measure pressure inside the sample cell.
Two gasses were used for calibration, a zero calibration gas and a dry gas with a concentration close to average ambient concentration (360 ppm). In eddy correlation applications it is not so important if there is a small zero shift in concentration, sensitivity must be kept constant. As a zero concentration gas, dry nitrogen can be used, with this gas, also the watervapour channel can be adjusted to zero.
The gas analyzer was working under extreme conditions, operating temperatures varying from 20 till 50 degrees celsius. The analyzer was placed in a radiation shielded box. Pumps and other power consuming devices, were placed outside this box. It is advisable to thermostrate the box with the gas analyzer, but this requires more energy.
The offset drifts with temperature, drift in sensitivity was negligible. To measure CO_2 fluxes, the covariance between the CO_2 signal with the vertical windspeed was calculated with the help of a program of the Edinbrough University. The gas analyzer must have a high enough sensitivity to be able to see the small fluctuations. The noise is typical 0.2 ppm CO_2 concentration (0.01 .. 2 Hz). Temperature changes have an effect on the offset but not on the span. The temperature effect is a slow process, this does not effect the covariance (over 15 min.). Detrending the signal can eliminate any low frequency (<0.005Hz) noise.
This closed path CO_2 measurement technique has advantages over open path systems. Fluctuation in temperature means density fluctuations, this effects the signal (span). The Licor gas analyzer corrects for slow temperature fluctuations. Short term temperature fluctuations, caused by the sensible heat flux, are damped out inside the tube. This means that there is no correction necessary for sensible heat flux on the CO_2 flux. The gas analyzer has build in correction routines for H_2O/CO_2 mixing ratios. The correction routines inside the gas analyzer will make the CO2 flux measurement not dependent on latent heat flux.

PUMP AND TUBING

The tube material should not interact with CO_2 or with water vapour. Polyethylene tubing is most suitable. The length and diameter of the tube must be kept small enough to prevent smearing of the signal. Smearing of the signal damps the higher frequency components.

The pump should not contaminate the gas sample, therefore a membrane pump was selected. The pump was driven by a DC-engine. To maintain a constant airflow, the pump must be kept at a constant voltage.

According to Leuning and King (1992), the airflow inside the sample tube should be turbulent. Turbulence prevents flowrate gradients over tube diameter and improves mixing. To achieve this, Reynolds number should at least be 2300, see figure 2.

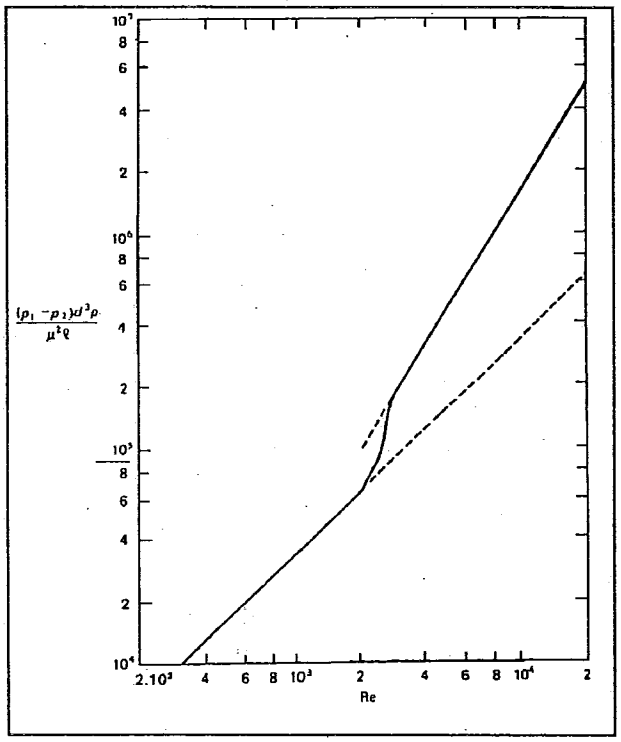

Figure 2 Variation of non-dimensional average pressure gradient with Reynolds number for pipe flow. Dotted lines: wholly laminar flow and wholly turbulent flow. Full line: example of actual case. Tritton, D.J. (1977) *Physical Fluid Dynamics*, p.17

From this figure it is clear that from a certain range the flow becomes turbulent inside a tube. Looking at figure 2, the flow becomes turbulent when:

$$\frac{(p_1-p_2)d^3\rho}{\mu^2 l}=1.7\bullet 10^5 \qquad (1)$$

Where p1-p2 is the pressure drop in the tube (N m^{-2}), d is diameter of tube (m), μ is dynamic viscosity of air (kg m^{-1} s^{-1}), ρ density of air (kg m^{-3}), l length of tube (m).

The pressure drop can be calculated, this information helps to select the right pump. The airflow can be calculated according to function 2, when assuming that the airflow becomes turbulent at Re=3000.

$$Re_{pipe}=\frac{\rho u_{av} d}{\mu} \qquad (2)$$

Where u_{av} is the average airspeed inside the tube (m s^{-1}). Table 1 uses these functions to calculate minimal flowrate and pressuredrop for turbulence in a tube.

d (mm)	l (m)	(p1-p2) (kPa)	u (m/s)	V (liter/min.)	timelag (s)
2.5	8	23.2	18	5.2	0.46
3.0	8	13.3	15	6.2	0.55
4.0	8	56.0	11	8.3	0.73
5.0	8	30.5	8.8	10.3	0.91
6.0	8	17.0	7.3	12.4	1.1

Table 1 Useful combinations for selecting sample tube and minimal flowrate

The pump was placed near the inlet, in the top of the mast. The advantage over a set-up with the pump downstream is the pressure. The gas analyzer will operate just above atmospheric pressure, the advantage is that sensitivity will be better, more CO_2 molecules per volume, and pressure will be less dependant on flowrate. Another thing which still can not be explained is that the analyzer should not work with pressures greater than 17kPa. Below this pressure, the automatic pressure correction does not seem to work for water vapour. Correcting this by hand, i.e. using the measurement of the pressure sensor and correcting the signal ($P_0/P_{analyzer}$), still gave the correct result.
The conclusion is that the automatic pressure correction is limited within a range of +/- 17kPa over or underpressure. Using the pump at the inlet prevents large pressures inside the analyzer. Pressure fluctuations of the pump are sufficiently damped by the volume of the tubes.

SENSIBLE HEAT FLUX CALCULATION

In eddy correlation techniques it is convenient to use the sonic speed of sound to calculate temperature fluctuations. This technique does not require delicate instruments like thin wire thermocouples. The advantage of the sonic temperature is that it is not dependant on radiation. According to Jacobs and McNaughton (1993), radiation loads on a thermocouple causes errors in the covariance w'T' calculation, because of the fluctuating windload on the sensor, causing a fluctuating radiation error.
The ultrasonic anemometer measures the speed of sound 20 times a second. This signal can be used to calculate temperature. Speed of sound depends on temperature and density of the air.

$$T_v = \frac{V_s^2 M}{\gamma R} \qquad (3)$$

Where: T_s Sonic anemometer temperature output (K), V_s Speed of sound in air(m s^{-1}), M Molecular weight (kg mol^{-1}), γ Ratio of heat capacities C_p (at constant pressure) and C_v (at constant volume) (J kg^{-1} K^{-1}), R Universal gas constant (J $mol^{-1}K^{-1}$).

When calculating heat fluxes by calculating covariances between T' and w' (eddy correlation), only temperature fluctuations are important. If the water vapour concentration is not taken into account, the sonic temperature, T_v, may differ from the absolute temperature, depending on the water vapour content in the air. This difference reaches up to ±0.7°C at 20°C and increases as temperature increases.

$$\sigma_{T_v}^2 = \sigma_T^2 + 1.02\ T\ \overline{q'T'} \qquad (4)$$

Using sonic temperature without latent heat flux correction will influence the sigma T and sensible heat flux calculation, because q' is correlated to T'. The explanation is that soundwaves travel faster in humid air, so this gives an over estimation of the heat flux and sigma T calculation. With equation 4 and 5 these effects can be corrected.

$$\overline{w'T_s}=\overline{w'T'}+0.51T\ \overline{w'q'} \tag{5}$$

A more detailed description is given by Schotanus (1983).
The sensible heat flux (Q_H) can be calculated by equation 6.

$$Q_H=\overline{\rho}C_{pd}(\overline{w'T'}+0.84T\ \overline{w'q'}) \tag{6}$$

Especially in semi-arid area's during the rainy season, the dependency of the specific heat (Cp) on humidity can not be neglected. According to Stull (1988), errors caused by specific heat changes can give up to 10% error in sensible heat flux calculation.

RESULTS

Figure 3 shows the CO_2 flux measurements over several days, just after the rainy season ended. It is clear that the CO_2 flux, or the plant activity, is decreasing in time, because the water content decreases. During the night the plants are dissimilating.

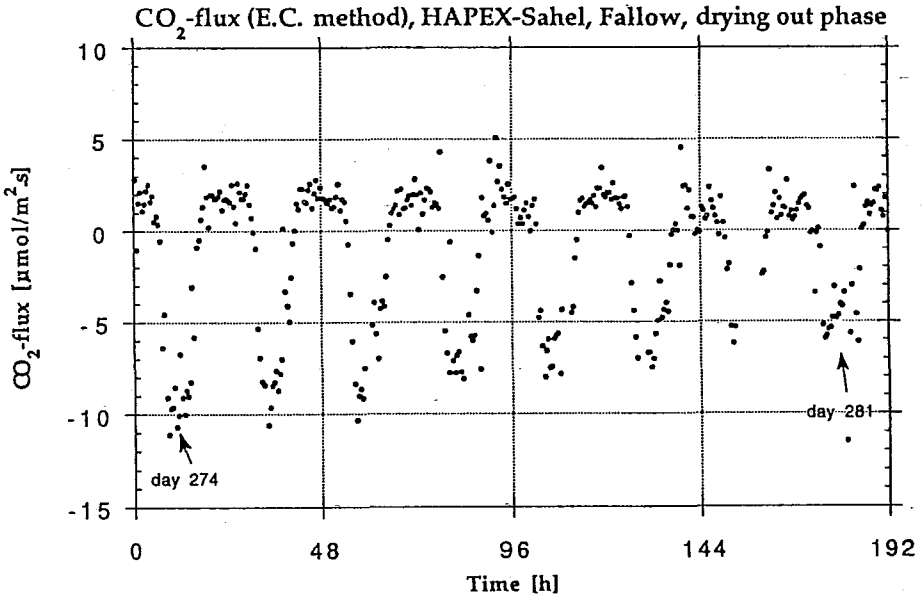

Figure 3 Graph of CO_2 flux in HAPEX Niger

REFERENCES

Jacobs and McNaughton:1993, 'The excess temperature of a rigid fast-response thermometer and its effects on measured heat flux', to be published in *Journal of Atmospheric and Oceanic Technology*

Leuning and King:1991, 'Comparison of eddy-covariance measurements of CO_2 fluxes by open- and closed-path CO_2 analyzers', *Boundary-Layer Meteorology*, October 1991

Willian J. Massman:August 20, 1991, 'The Attenuation of Concentration Fluctuations in Turbulent Flow Through a Tube', *J. of Geophysical Research* **96**, D8, p. 15, 269-15,273

McMillen R.T.:June 1986, 'A Basic Program For Eddy Correlation In Non-Simple Terrain', N.O.A.A. Technical Memo ERL ARL-147

Schotanus P.:May 1983, 'Temperature Measurements with a Sonic Anemometer and its application to Heat and Moisture Fluxes', *Boundary Layer Meteorology* **26** No.1, page 81

Stull Roland B., *Boundary Layer Meteorology*, 1988, ISBN 90-277-2769-6

Session IV

RADIATION MEASUREMENTS

SCAPP, a Compact Scanning Pyrheliometer/Pyranometer System for Direct, Diffuse and Global Solar Radiation

Bergholter, U., Dehne, K.
Meteorological Observatory Hamburg, Deutscher Wetterdienst, Germany

1. Introduction

The automatic sunshine sensor SONIe was developed by the Instrumentenamt Hamburg of Deutscher Wetterdienst to replace the Campbell Stokes sunshine recorder. The SONIe is produced since 1985 by a manufacturer of meteorological instruments, Siggelkow, in Hamburg. The principle of measurement is based on continuous scanning of narrow sectors of the sky stretching from zenith to the horizon. This is materialized by a rotating diaphragm head with a vertically oriented parallel slit (1,2). Radiant fluxes passing the slit are directed to a photo sensor by a special beam guide. The electrical signals generated by diffuse solar fluxes are measurable but, as intended, always very low. Fluxes from direct solar radiation, however, produce distinct signal peaks indicating sunshine, if they exceed a threshold corresponding to 120 Wm^{-2}.

From this starting point a feasibility study was performed (3) which will be reported here. It was the objective to find out whether the SONIe can be remodeled as a scanning sensor for the simultaneous measurement of diffuse and direct solar radiation, as these two are the main components, allowing to derive global radiation and sunshine duration by simple mathematical operations. Although the abbreviation 'SCAPP' is inspired by the idea of substituting at least one pyrheliometer and one pyranometer by one scanning instrument, it will hardly be possible to achieve the same overall accuracy as precision radiometers. In spite of some limitations SCAPP might become a very attractive system for tasks, where a small 'intelligent' sensor is needed with only little requirements for installation and alignment.

2. The SCAPP Concept

As the efforts necessary to develop a two-axis-scanner would be considerable, it was decided to maintain the basic construction of the SONIe with its one vertical axis, allowing azimuthal scanning only. It was a primary objective of the new design to find the optimal configuration for the diaphragms and the diffuser/filter/detector-combination, so that the measurement errors of both diffuse and direct solar radiation would be as small as possible. As far as remaining errors could be specified, an automatic software correction for the instantaneous values had to be provided within the system. For the statistical evaluation of correction functions it was necessary to measure and record simultaneously reference data from 'classical' radiometers.

Fig.1 shows the scheme of the scanning sensor head. The receiving plane is represented by a horizontally oriented diffuser disc in the center of rotation. The width (B) of the slit diaphragms, which are shown enlarged for better recognition, is manufactured to follow $B = B_0 \cdot \cos\gamma$ for rays reaching the center of the diffuser under the elevation angle γ. B_0 is the width at the horizon. The two inner diaphragms are made for stray light suppression within the sensor head. This configuration is the most favorable one for the measurement of diffuse radiation, if combinations of different shapes of diaphragms (parallel slit, spherical sector) and receiver types (horizontal plane, normal incidence) are compared. For homogeneous diffuse sky radiance the chosen diaphragm type with an ideal 'lambertian' diffuser will produce the angular responsivity curve 'C' in Fig.2 which exhibits nearly the same proportionality with $\sin\gamma \cdot \cos\gamma$ as pyranometers. For the direct solar radiation it is possible to correct by software the expected errors which depend on the solar elevation angle (see Fig.7).

A basic property of SCAPP is full computer controlled operation, especially including automatic detection and delimiting of a solar peak (signal maximum from direct radiation I), automatic separation and integration of solar peak and background diffuse radiation D (see Fig.3), automatic calculation of radiation fluxes and application of correction algorithms.

3. Setup, Measuring Properties, Operation

SCAPP consists of the sensor module to be mounted outside and the laboratory equipment for data acquisition, sensor control and power supply.

The **casing** of the sensor module as well as the glass dome (crown glass 70mm dia.) are original SONIe components. An additional protection against solar heating of the casing was added outside. The casing contains the newly designed rotating sensor head with original SONIe motor, gear and heater. The silicon sensor and the preamplifier replace the original parts.

The **sector-slit-diaphragm** is 1.4mm wide at the horizon, corresponding to a central field-of-view of 3.0 degrees, which decreases with increasing elevation angle and is half as much at 60 deg of elevation. As a **diffuser** a solid PTFE (Teflon) cylinder of 5mm dia. and 3mm thickness is used, which extends beyond the optical horizon by 0.2mm. This was the best result so far from many experiments to minimize cosine-errors with other shapes, sizes and positions of PTFE diffusers. The spectral stray coefficient of PTFE decreases strongly towards longer wavelength and causes an increased spectral dependence of the response (see Fig.5). The straight **beam-guide** of 3.0mm dia. between diffuser and detector is made from clear acrylic glass. It is fixed in the hollow shaft which drives the rotating head.

The SONIe **driving system** uses an unregulated DC-motor with reducing gear to drive an 180-degree-shutter directly, whereas the rotating head is driven by an additional 1:2 gear-drive. This way a scan is divided into a 'light' and a 'darkness' phase of 360 degrees each, the latter being used for zero offset compensation. The period of rotation is about 2 seconds. The 1:2 step-up-gear caused unexpected problems, as the angular velocity of driven toothed wheels is variable, oscillating with a constant mean value only. So the rotating head passes the solar peak at different positions with slightly different speed. As the data acquisition is operating at constant time intervals, varying integral values of I result. This can be seen in Fig.4 from the relative errors of I on a clear day, even so in Fig.7, where the values of several days are displayed versus the solar elevation. A set of data like this was used to derive the correction function for I by regression approximation.

As a **photodetector** the UV-enhanced type SD-172 UV ($3.2 \cdot 4.7 mm^2$) of SDC was chosen. The resulting relative spectral response of the combination with the abovementioned diffuser is shown in Fig.5, together with attractive alternatives. The detector output is preamplified by a two-stage-amplifier recommended for sunphotometry by WRCP/Davos.

In consideration of the high dynamic range of the sensor output between low diffuse and high direct radiation the **data acquisition** was performed using a combination of two 10-bit A/D converters with different input ranges. Data acquisition at 1000 samples per second (and the rest of the work) was performed by an Atari 1040ST, giving an angular resolution of 0.18 degrees of azimuth. This means that the transition of a solar peak is recorded by somewhat less than 30 samples. The software was written in assembler for the time-sensitive parts running interrupt-controlled in the background, whereas for the main programme Omikron-BASIC was successfully used. The computer software was designed to support the experimental work during the development of SCAPP (different modes of operation, a large number of online-adjustable parameters, protocols, etc.). One of the screens works like a two-channel sampling oscilloscope, showing operational parameters at the same time (see Fig.6 showing a solar peak).

From the single scans starting every 4 seconds and from the reference sensors means over 2, 4, 10 or 60 minutes were archived on floppy disc, while the daily printouts contain tables of hourly sums and daily graphs and error curves derived from the reference sensors.

4. Examples of Results, Accuracy

The overall uncertainty of the SCAPP results can be shown by comparison with reference data from well maintained pyrheliometers and pyranometers (with shade ring for diffuse radiation). The SCAPP raw data are subject to errors from spectral selectivity, receiver geometry, gear drive and temperature dependence. The final values of I_{scapp} are corrected using the regression versus solar elevation shown in Fig.7, the values of Dscapp are corrected for compensation of a temperature dependent influence from the old SONIe drive electronics.

Typical relative and absolute deviations of corrected SCAPP values from reference values are shown for **clear days** in Fig.8-10, where the time scale is true local time.

- The hourly sums of D_{scapp} deviate within +/-7%, if early morning and late evening hours are excluded, which exhibit rather large asymmetry. The daily sum deviates by -3%.
- The hourly sums of I_{scapp} deviate within +/-3%, excluding the first morning hour. The daily sum deviates by +0.3%.
- For the hourly sums of G_{scapp} which are calculated from D and I the hourly deviations are generally less than 3%, for the daily sum the deviation is almost zero. Errors in the morning and evening hours are partially compensated, pointing towards possibilities of further improvements.

For an **overcast day** (see Fig.11) I_{scapp} is practically zero. Hourly deviations of D_{scapp} range up to 10% but are averaged to zero in the daily total. The absolute errors of the morning and evening hours are negligible.

5. Conclusions

a) According to the comparison results the accuracy achieved by the experimental version of SCAPP described here corresponds to that of a second class pyranometer (after ISO 9060).
b) In 1994 a prototype for later commercial production will be designed with several improvements elaborated by this study (step motor drive, specially filtered silicon detector, quartz or PMMA diffuser, thermostat, etc.).
c) SCAPP is a multisensor (D,I,G,S) the use of which should be of special interest for applications requiring relatively small sensors, for instance agrometeorological tasks. Due to one-axis-scanning the use of SCAPP is impeded in latitudes lower than 30 degrees N or S, if the sun comes near to the zenith.
d) Due to its multisensor properties SCAPP should evidently be a cost-effective device if the costs of 'classical' radiometers for the same number of radiation quantities are considered.

6. Literature

- Lindner, P.; A new sunshine duration sensor in: Papers presented at the TECEMO, Noordwijkerhout, The Netherlands , 24-28 Sept. 1984
  WMO, Instruments and Observing Methods, Report No.15, 1984
- Dehne, K., Bergholter, U.; WMO Sunshine Duration Measurement Comparison 1988/89 in Hamburg in: International Pyrheliometer Comparisons IPC VII, 24 Sept.-12 Oct. 1990: Results and Symposium. Swiss Met.Inst. Working Report No.162 Davos and Zürich, 1991
- Bergholter, U., Dehne, K.; Messung von direkter und diffuser Sonnenstrahlung mittels SONIe-Sonnenscheinsensor. Abschlußbericht zum Forschungsvorhaben MOH/14, Deutscher Wetterdienst, Meteorologisches Observatorium Hamburg, August 1992

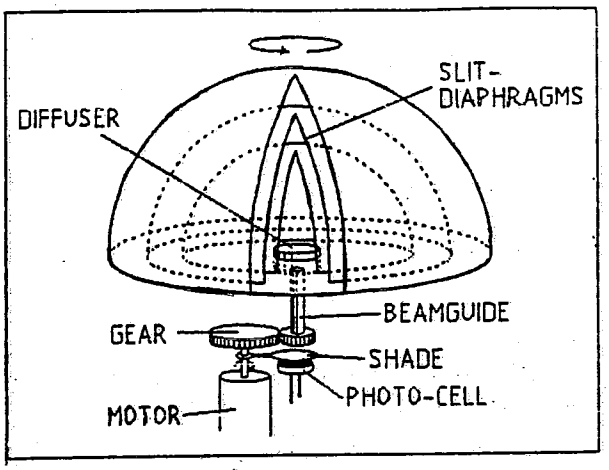

Fig. 1: Scanning device of SCAPP (schematic)

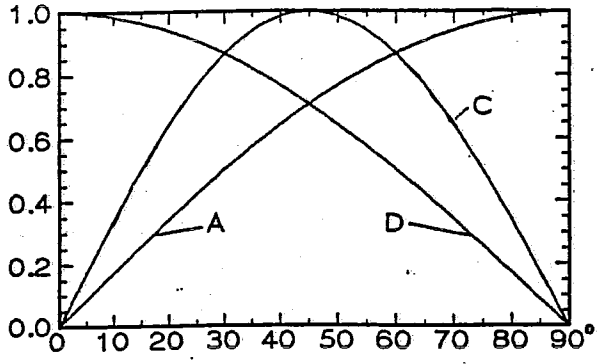

Fig. 2: Dependency of the relative responsivity on the solar elevation for different combinations of sensor / slit diaphragms

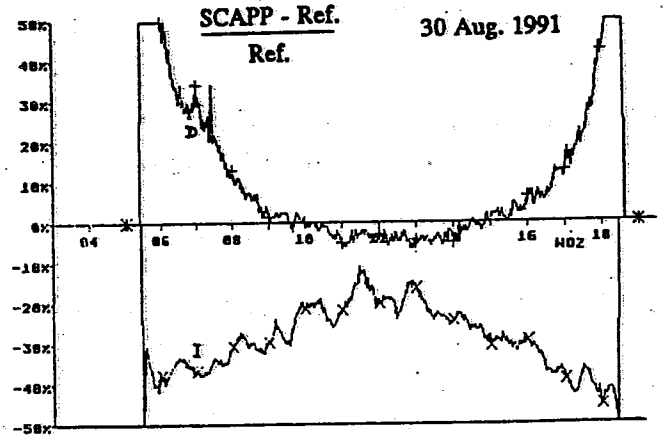

Fig. 4: Daily course of typical percentage deviations of the diffuse (D) and direct (I) solar radiation (clear sky)

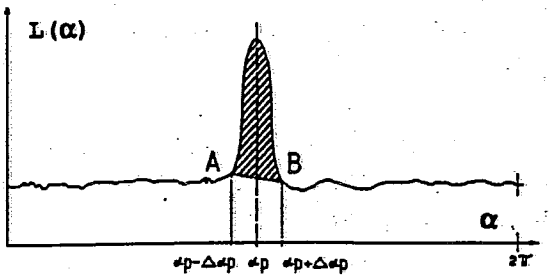

Fig. 3: Separation of the direct solar output from the diffuse solar signal (α: scanned azimuth angle, schematic)

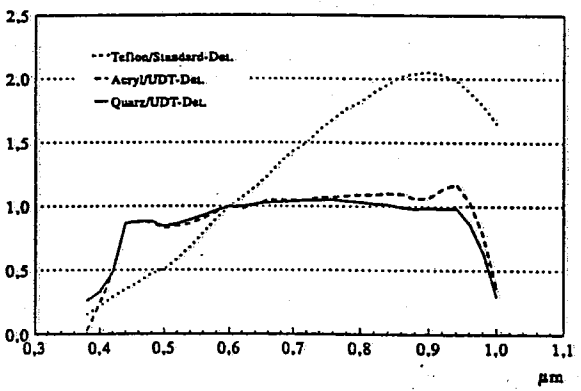

Fig. 5: Relative spectral response of different diffuser / sensor combinations (related to the response at 0,6 µm)

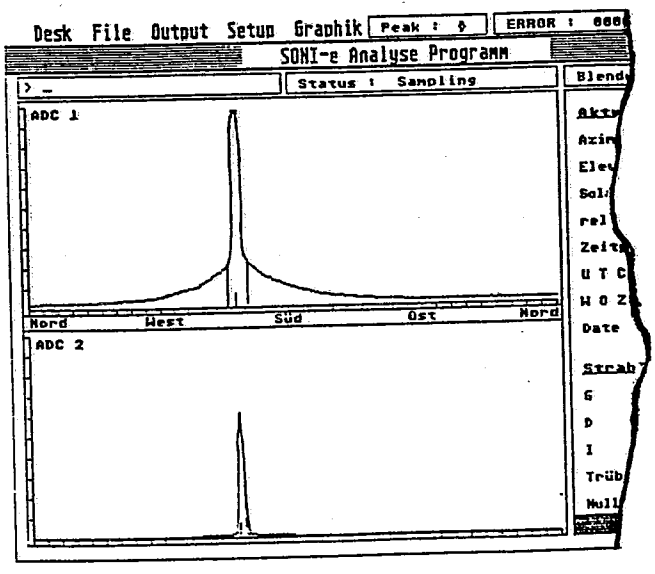

Fig. 6: Display of the scanned signals (cutting of a hardcopy of the screen)

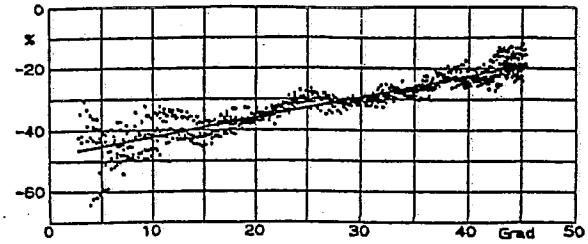

Fig. 7: Percentage deviation from the reference of the solar output (I) as function of the solar elevation

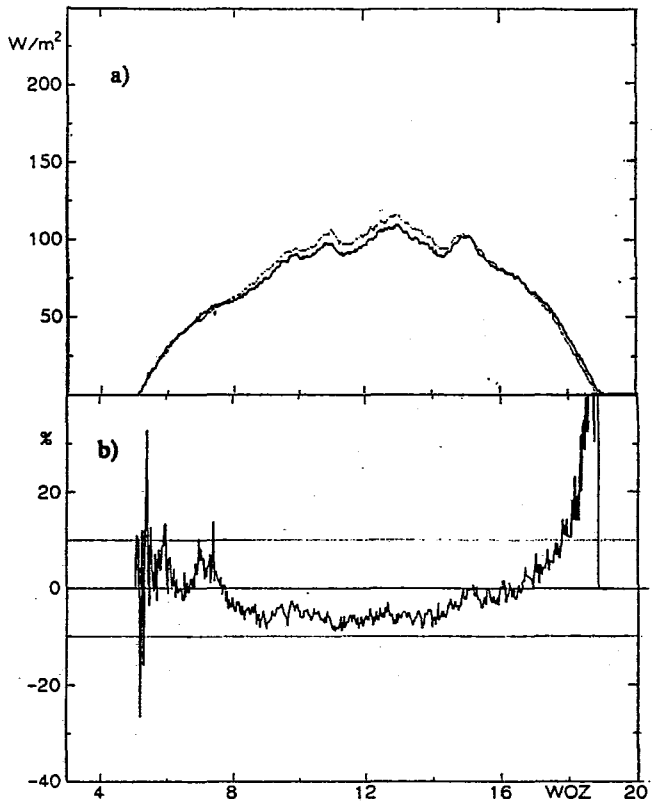

Fig. 8: a) Daily course of D-SCAPP and D-reference on clear 30 Aug. 1991
b) Percentage deviations derived from a)

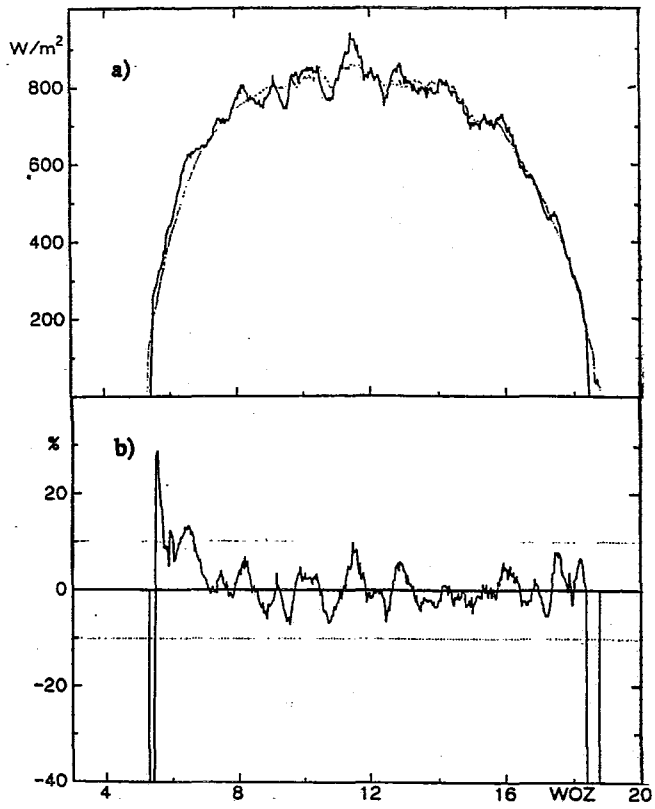

Fig. 9: a) Daily course of I-SCAPP and I-reference on 30 Aug. 1991
b) Percentage deviations derived from a)

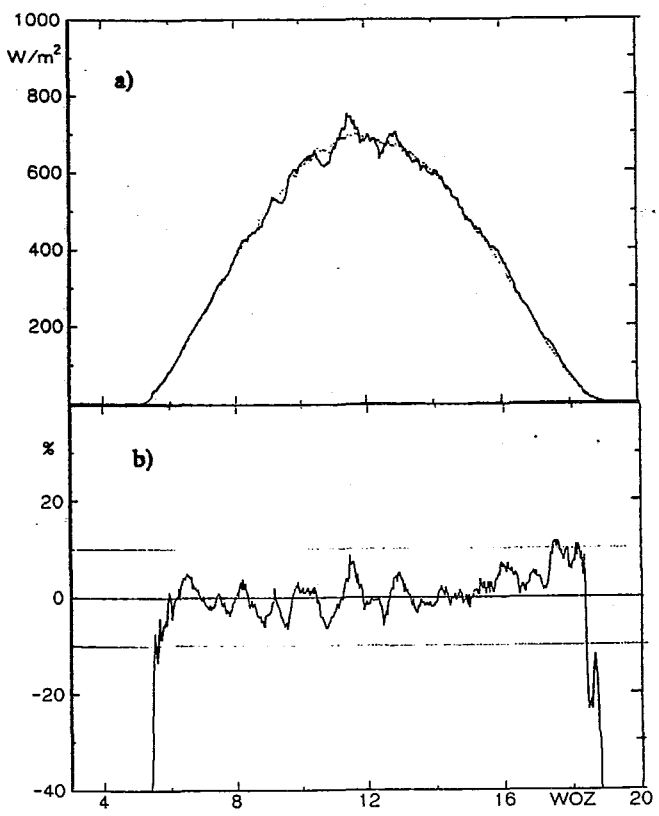

Fig. 10: a) Daily course of G-SCAPP and G-reference on 30 Aug. 1991
b) Percentage deviations derived from a)

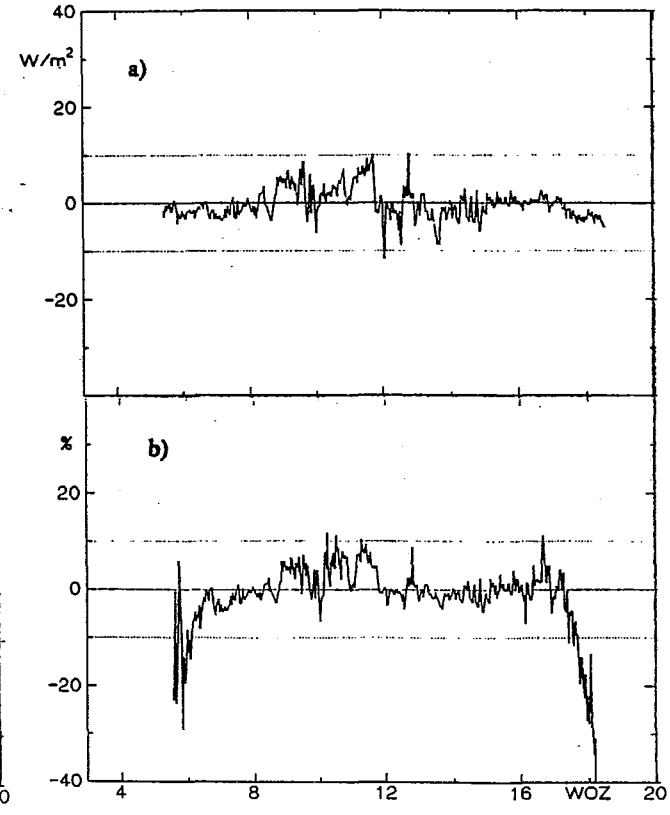

Fig. 11: Daily course of a) the absolute and b) the relative deviation of D-SCAPP from D-reference on the overcast 9 Sept. 1991

MAINTENANCE OF RADIATION STANDARDS IN INDIA

V.V. Abhyankar, V.V. Kanade and S.V. Prabhu
Instruments Division, Meteorological Office,
Pune, India.

1 A network of 45 radiation measuring stations is being maintained in India. Various parameters like global solar radiant exposure, diffuse solar radiant exposure, direct solar irradiance and net total radiant energy are measured in this network. The maintenance of this network is carried out at Pune by the Central Radiation Laboratory of the Instruments Division of Meteorological Department. This Laboratory is designated as the National Radiation Centre. WMO has also designated the Laboratory as one of the Regional Radiation Centres for the RA-II(Asia) Region. To meet this responsibility, the Laboratory maintains a series of standard pyrheliometers and pyranometers. Three cavity Radiometers serve as the primary standards and a series of Ångström pyrheliometers and NIPs serve as secondary and transfer standards. Table I lists the standards maintained by the Laboratory.

2. The maintenance of the standards involve periodical and regular intercomparisons. In view of the heavy clouding that prevail at Pune for more than 6 months in a year, the intercomparisons are carried out over a limited period only. Within the existing facility 4 cavity Radiometers and two Ångström pyrheliometers can be intercompared simultaneously. The standard pyranometers are calibrated with reference to one of the standard cavity radiometers by shade and unshade method only.

3. Of the primary standards, EPAC and PMO-6 have participated in IPCs at Davos, Switzerland. Ångström Pyrheliometer No. 508 had participated in IPC II and IPC III. EPAC had also participated as RA - II standard in the first RA-II/RA-V comparisons held at Tokyo.

More than 1320 comparative measurements were made during 1993 with the four absolute radiometers. Simultaneous measurements were made by experienced personnel, one individual managing only one instrument. The comparisons were carried out only when the sky was reasonably stable as seen from the diffuse irradiance records. In analysing the comparison data only EPAC, PMO-6 and HF were used as the standard group and TMI was not included in the group as its characterisation data could not be obtained from TMI despite our best efforts (obviously because TMI had not carried out the mandatory characterisation). The TMI instrument also does not give the direct solar irradiance correct even to first decimal. The data analysis shows (Fig 1) that the standards are maintaining their calibrations. EPAC has a tendency to read more by 0.31 per cent and HF lower by 0.35 per cent. PMO-6 is very close to the mean values of the irradiances ($\pm$0.04 per cent).

TMI shows much larger deviation, 0.85 per cent. Fig 1 also indicates that the standard deviations for all the four absolute radiometers are significant, HF having the lowest, viz ± 0.20 per cent. The performance history of EPAC in Pyrheliometer Comparisons is given in table II.

Ångström pyrheliometer No.8418 (Eppley make) had shown a 2.4 per cent decrease in its calibration factor after a minor repair in 1984. The shift has been stable till 1993 when it has again shown a sharp increase by about 2.4 per cent. Further calibrations are needed to confirm this change.

4 Among the pyranometers CM-5 No. 1039 and No. 1154 have a long history and they had shown excellent stability. CM-11 (two numbers) and the PSP serve as reference standards. The results of 1993 comparisons are shown in Fig 2. The stability of the calibration factors of all the instruments, even of CM-5, is within 1 per cent of the accepted values. Fig 3 shows the cosine response of different types of pyranometers as experimentally measured in the Laboratory at Pune. Most of the instruments respond well except at very large angles of incidence. PSP, CM-11 and strangely CM-5 instruments show very small deviations. Fig 4 shows the tilt effect on the pyranometers as experimentally determined at Pune. CM-11 instrument does not show any significant tilt effect while PSP has a very small effect. CM-5 shows a moderate effect. The studies being carried out at Pune show that the cosine response and tilt effect are quite individualistic. Hence where a serious study of the radiation data is desirable, the particular pyranometers should be characterised individually before the data collection starts.

TABLE - I

RADIATION STANDARDS AT PUNE

NAME	IDENTIFICATION NUMBER	MAKE
PYRHELIOMETER		
1. PACRAD	13219	Eppley
2. HF	18742	Eppley
3. PMO-6	811106	C.I.R.
4. TMI	68634	TMI
5. Ångström	8418	Eppley
6. - do -	508	Stockholm
7. - do -	501	- do -
8. - do -	507	- do -
9. - do -	520	- do -
10. - do -	540	- do -
11. - do -	145	- do -
12. - do -	249	- do -
13. - do -	72	- do -
14. - do -	SI-T-27	Smithsonian
15. Silver disk	SI - 51	- do -
16. - do -	SI - 91	- do -
17. Linke - Feussner	723225	Kipp & Zonen
18. NIP	5489	Eppley
19. NIP	5799A	- do -
PYRANOMETER		
1. PSP	11919F3	Eppley
2. CM-11	871776	Kipp & Zonen
3. CM-11	871777	- do -
4. CM-5	1039	- do -
5. CM-5	1154	- do -
6. CM-5	2299	- do -

TABLE - II

RESULTS ON EPAC PERFORMANCE

COMPARISONS	YEAR	RATIOS WITH STD GROUP	STANDARD DEVIATION %
IPC V	1980	0.99532	0.12
IPC VI	1985	1.00545	0.19
I RA-II/RA-V	1989	0.99955	-
IPC VII	1990	1.00088	0.54
NATIONAL	1993	1.00310	0.27

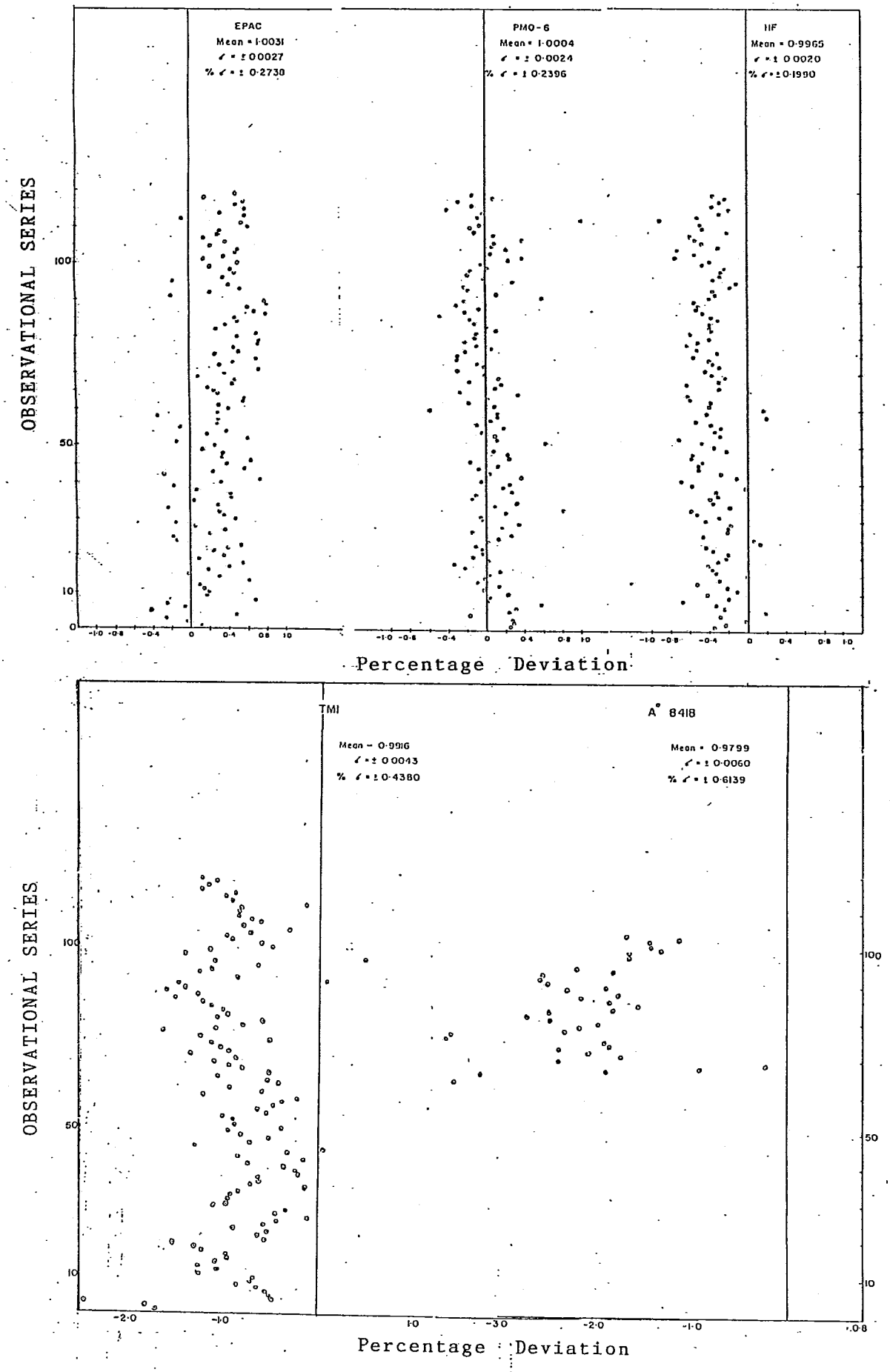

FIG. 1 COMPARISON OF PYRHELIOMETERS

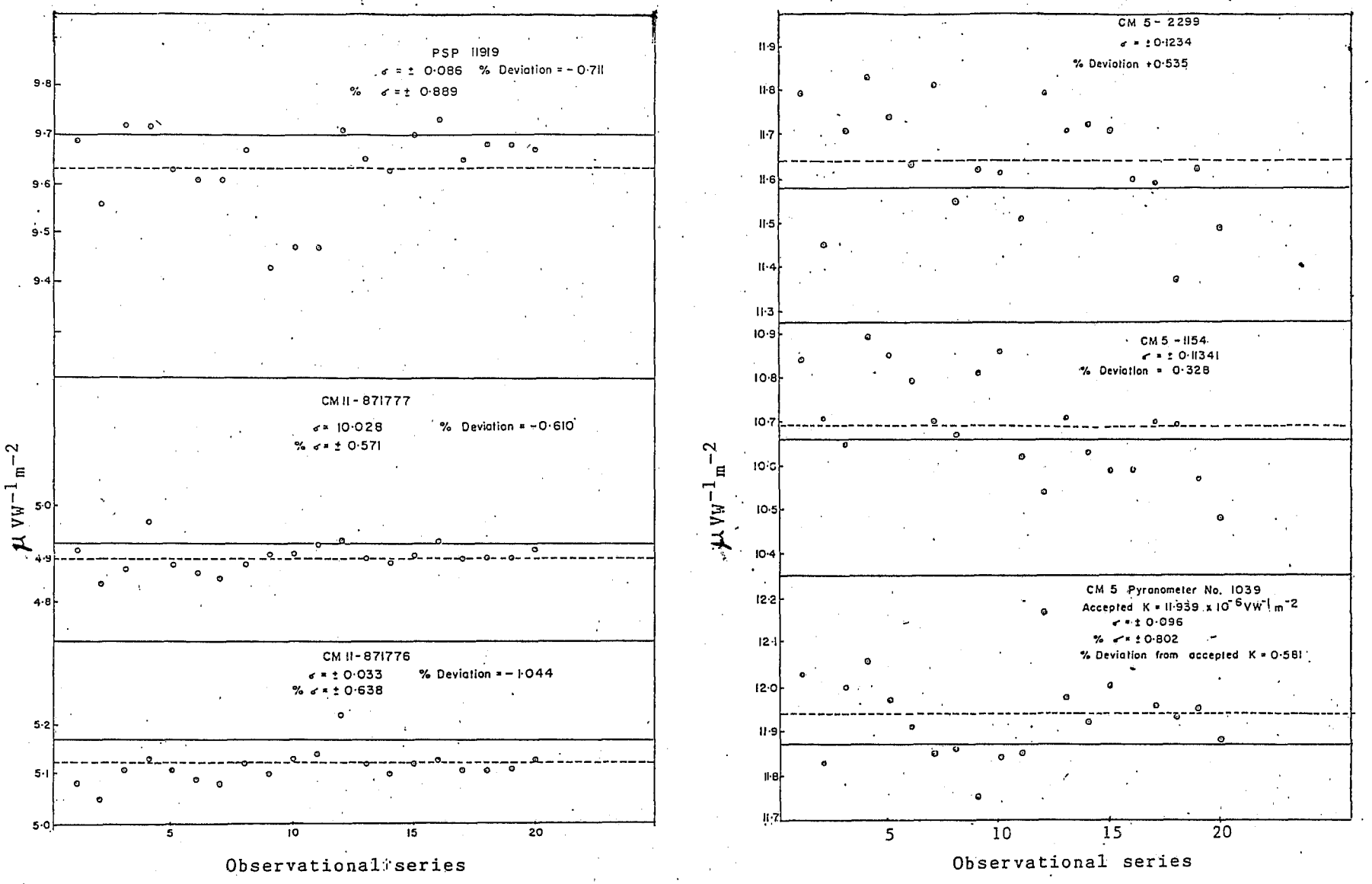

FIG. 2 CALIBRATION OF PYRANOMETERS

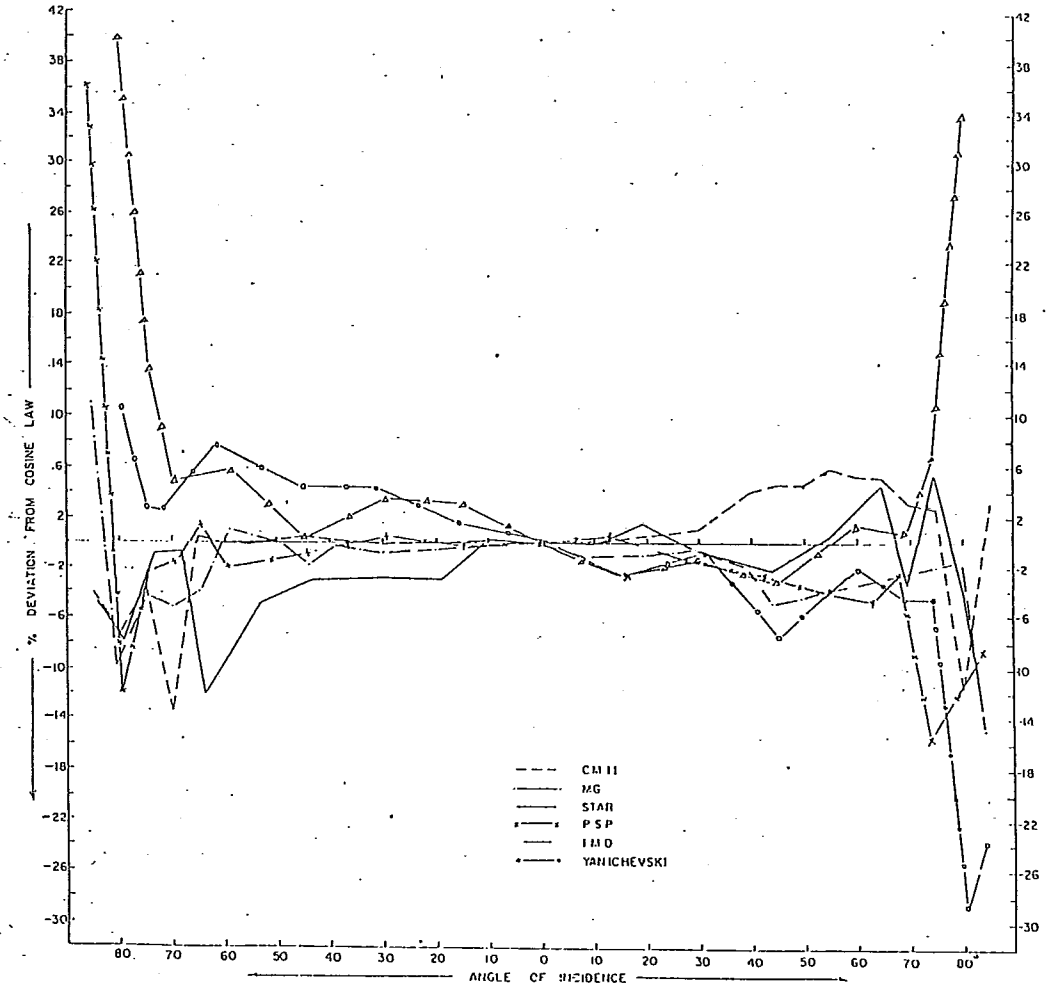

FIG. 3 COSINE RESPONSE OF PYRANOMETERS

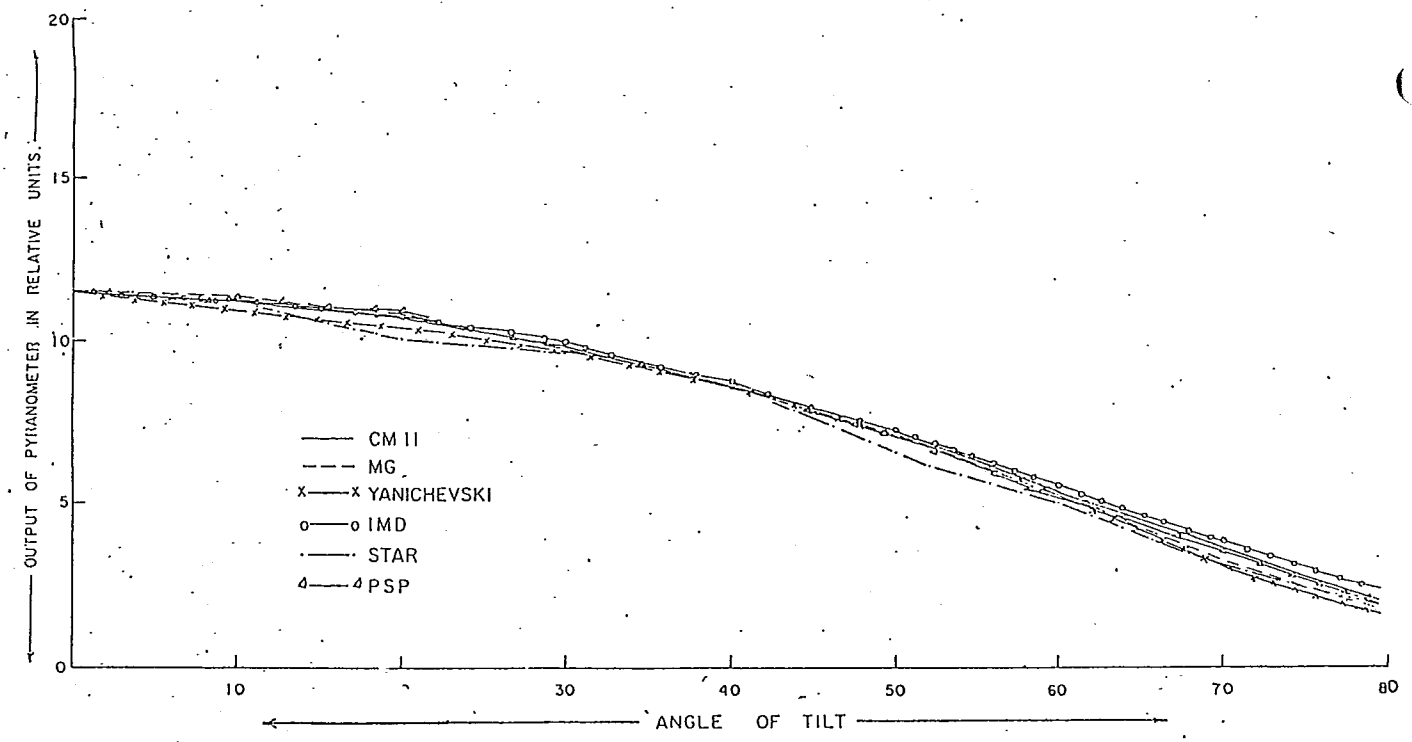

FIG. 4 TILT EFFECT ON PYRANOMETERS

A new Approach to Calibrate Eppley PIR Pyrgeometers

R. Philipona and C. Fröhlich

Physikalisch-Meteorologisches Observatorium Davos, World Radiation Center,

CH-7260 Davos Dorf, Switzerland.

1. Introduction

A growing demand of reliable measurements of the surface radiation budget more and more emphasizes the need for improving instruments measuring the terrestrial and atmospheric radiation. At present, in this long-wave spectral range, commercially available instruments allow an estimate of the infrared radiative flux with an accuracy of no better than ±10 Wm^{-2}. The Eppley Laboratory's pyrgeometer, which has been introduced in 1970, is an instrument designed to measure hemispheric radiation in the 4-50 μm spectral range, and it has ever since been one of the most investigated and used instrument besides the classical pyrradiometers.

The Precision Infrared Radiometer PIR (pyrgeometer) is a development from the Eppley Precision Spectral Pyranometer and was first described by Drummond et al (1970). The blackened thermopile originally was enveloped by a KRS-5 dome with an interference filter, vacuum deposited on the inside of the hemisphere. Early deterioration of KRS-5 under long periods of exposure caused Eppley Laboratories in 1976 to introduce the pyrgeometer with silicon dome. Transmissivity of silicon domes, with deposited low pass interference filters, undergoes a sharp transition from opaque to maximal transmission between 3 and 4 μm, and within the region of 4 - 50 μm it varies between 0.25 and 0.40. Albrecht et al. (1974) found that temperature differences between body and dome of the pyrgeometer produced perturbing additional thermal radiation and described the thermal balance of pyrgeometers based on the body temperature T_b (measured at the cold junction of the thermopile) and the dome temperature T_d of the pyrgeometer. PIR's have since then been equipped with a thermistor mounted at the lower rim of the silicon dome. Enz et al. (1975) reported that dome ventilation minimizes thermal effects due to differential heating between dome and cold junction. Albrecht and Cox (1977) identified additional systematic errors due to battery voltage uncertainties and nonlinearity of circuitry at extreme temperatures. Since air borne measurements, with extreme temperatures involved, were the principle concern in their paper, nonlinearity of circuitry was of much higher importance compared to earth-bound surface measurements. The battery voltage problem can easily be overcome by taking it out and instead measuring the temperature-compensated thermopile output and the temperature T_b at the cold junction of the thermopile in order to calculate the radiation losses.

This paper presents results of further investigations of PIR pyrgeometers, in regard to their calibration and to their performance in shaded and unshaded field measurements, including above mentioned suggestions and improvements. Since movable parts of shading apparatuses are difficult to handle in remote regions with harsh climatic conditions, it is the aim of our investigation to demonstrate that PIR pyrgeometers can be used in unshaded mode of operation and measure infrared irradiance with an uncertainty of ±2 Wm^{-2}.

2. Calibration apparatus

The newly developed calibration apparatus is a black body radiation source which consists of a cylindrical enclosure with L/d = 3.4 containing a bottom plate with a central entrance hole and a convex shaped cover (see Figure 1). A helical grove is machined into the cylindrical aluminum body as well as in the bottom and top plate and acts as a conduit for the conditioning fluid. A powerful fluid circulation system allows to keep

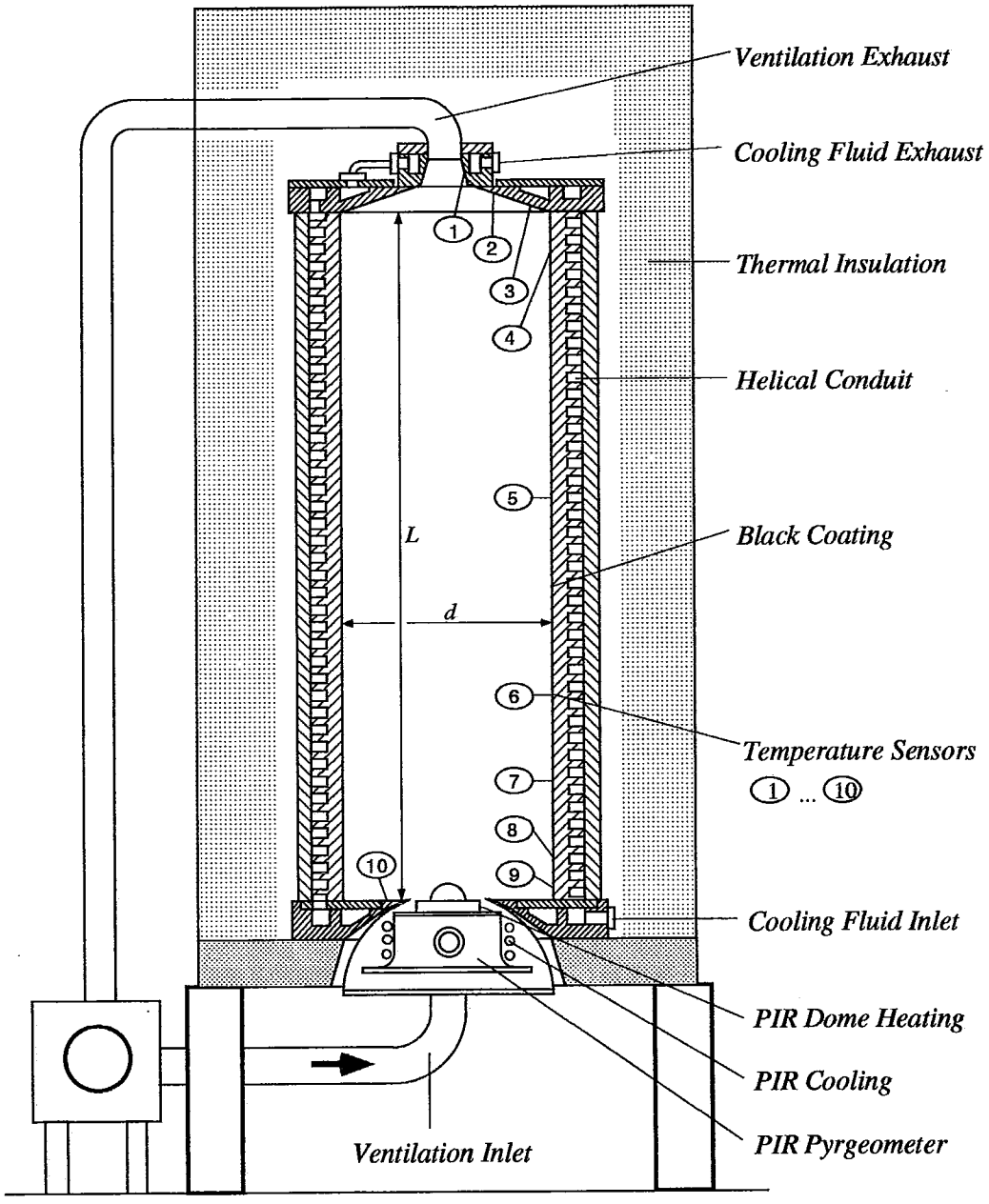

Figure 1: Calibration apparatus which consists of a cylindrical black body radiation source (L = 610 mm, d = 180 mm) and the housing for the pyrgeometer providing thermal conditioning and an air flow system.

the enclosure at homogeneous temperatures in the range of -30° to +60° C. Ten previously calibrated thermistors are fixed to the inside wall of the cavity which is painted with Chemglaze Z306 black coating. Total emissivity of the cylindrical cavity has been analyzed by applying radiant flux balances to infinitesimal elements of surface which finally led to the over-all heat flux at the detector to be calibrated. With an emissivity value of 0.96 of the black coating of the inside wall and the given geometry of the enclosure, a total emissivity value of 0.9985 has been determined for this source. With the cavity cooled to 0°C a uniform temperature within 0.1°C is measured at the inside wall. The ten thermistors are furthermore weighted in respect to their location and their bearing to the flux at the detector.

The calibration apparatus is also equipped with a housing for the pyrgeometer which is positioned underneath the cylindrical cavity. Air flow around the instrument and its hemispherical dome is provided as well as individual cooling and heating of the pyrgeometer body and dome. This additional cooling and heating systems allows PIRs to be calibrated at various body temperatures and to hold the instrument at thermal equilibrium for extended time periods. The sensitivity C of the instrument can also be determined with the sensor temperature T_s equal to the dome temperature T_d, and hence avoid the problem of differential heating and related corrections of thermal effects. A Campbell Scientific Ltd. CR10 datalogger and a personal computer are used to record the temperatures and the signal values from the calibration apparatus and the instrument to be calibrated.

3. Calibration and field measurements

Ice cavities and the newly developed calibration apparatus have been used to characterize and to calibrate PIRs. Ice cavities rely on one single reference temperature, and were found to be difficult to handle during long term experiments which makes measurements at thermal equilibrium almost impossible. However, dynamic effects due to thermal unbalance are not negligible during calibration. These problems are easily overcome with the calibration apparatus with homogeneous black body radiation, and which provides body and dome temperature control of the pyrgeometer. Important temperature gradients have been measured on the silicon dome using additional temperature probes. Similar gradients were also observed in field measurements, particularly in unshaded operation. Hence, inadequate dome temperature measurements and related incorrect dome emission corrections make accurate pyrgeometer calibration and measurements impossible. A new dome temperature probing has been installed on PIR pyrgeometers in order to measure a representative mean temperature of the silicon dome. Dome ventilation is also used during calibration but was found to be of minor importance, since first, ventilation was inadequate to provide a homogeneous temperature distribution of the hemisphere and second, it became irrelevant with the new dome temperature probing system which correctly measures the mean temperature of the silicon dome. In the thermal balance equation the temperature of the sensor surface T_s is the relevant temperature and not the temperature of the body T_b which is measured and normally used in the equation. However the equation can be rearranged for T_b but a temperature dependent sensitivity factor C has to be introduced. Neglecting this temperature dependence means that C is only valid at and close to the temperature at which the calibration has been performed. In order to take care of the differential heating of the dome Albrecht et al. (1974) introduced a factor K to correct the outgoing radiation. This factor is directly related to the physical characteristics of the dome. However, if the temperature of the dome is not measured correctly the K has no longer a true physical meaning. If the dome temperature is correctly measured the K factor indeed corresponds to the physical characteristics of the dome.

Experiments have shown that although appropriate ventilation has been applied, cooling of the hemispherical dome during calibration is as pronounced as during field measurements. Accurate dome temperature measurement is therefore crucial not only in field measurements but also during calibration. On the Eppley pyrgeometer, the dome temperature is measured with a thermistor mounted at the inside lower rim of the

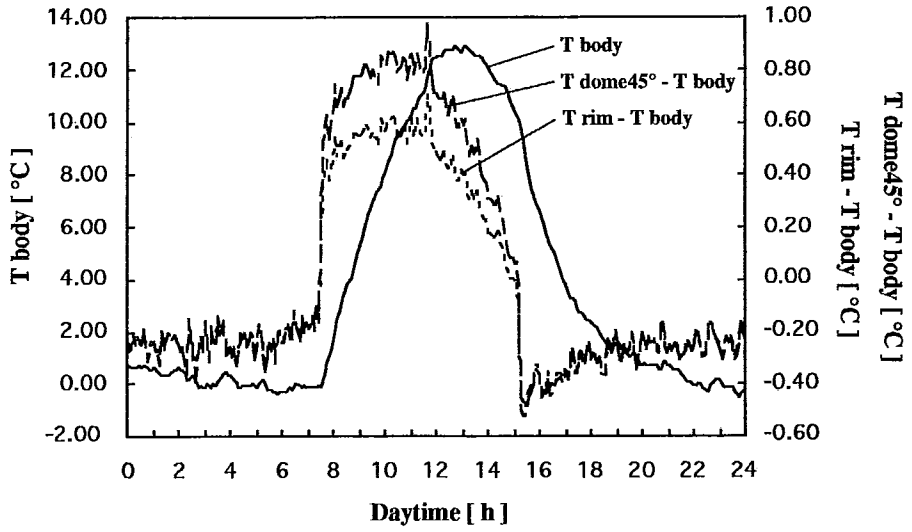

Figure 2: Daily evolution of the pyrgeometers body temperature and Tdom - Tbody from measurements at 45° and the rim of the silicon dome.

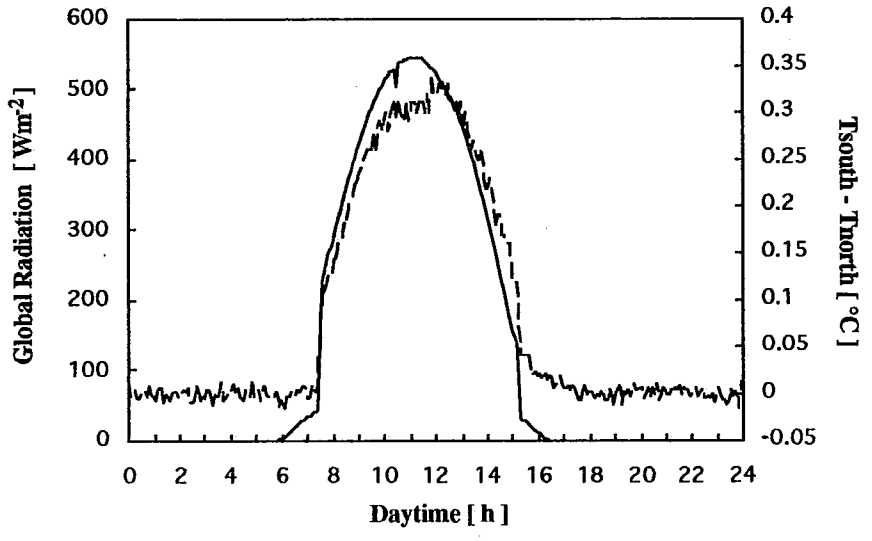

Figure 3: Daily evolution of the global radiation and the dome temperature difference between south and north of the hemisphere.

silicon dome. Tests with thermistors fixed on the outside of the dome during calibration showed important temperature gradients between the lower rim and the apex of the hemisphere. Numerical calculations of the thermal radiation balance between dome and sensor surface showed that even with gradients of up to 1°C between rim and apex, measurements at 45° zenith angle are in good agreement with the mean value of the dome temperature. To account also for azimuthal gradients during unshaded field measurements, three thermistors are fixed at 120° intervals.

Three PIRs have been modified accordingly. Field measurements comparing the new and the old dome temperature sensing system are shown in Figure 2. The daily evolution of the pyrgeometers body temperature is shown, as well as two plots of the evolution of the difference of the dome temperature minus the body temperature, one plot showing the dome temperature as the mean value of the three measurements at 45°, and the other plot representing the old measurement at the rim of the dome.

An additional problem of unshaded instruments consists of the fact that a small part of the infrared radiation of the Sun is included in the measurement. However, pyranometers measuring global short-wave radiation are calibrated in such a way that the IR part of the Sun is already included. Since the transition of the low pass filter of PIR domes lies somewhere between 3 and 4 μm, the direct solar radiation to be subtracted needs to be determined. By comparing unshaded and shaded pyrgeometers, a direct sun factor F is determined for each pyrgeometer. The three thermistors at 45° allow to determine the temperature difference between the Sun faced and the northern part of the hemisphere. Figure 3 shows the evolution of the global radiation and the temperature difference between north and south for the same day as shown in figure 2. This temperature difference following the evolution of the global radiation, multiplied with the direct sun factor F, can be used as a measure to correct for the direct infrared solar part which has to be subtracted from the measurement. The same correction could also be made by using the short wave global radiation measurement. Remotely located instruments will further be equipped with a fixed shadow bar mounted in the south of the instrument. This shadow bar allows at solar noon to check the reading of the instrument under shaded conditions and to redetermine the direct sun factor F.

4. Conclusions

The aim of our investigation is to demonstrate that Epply pyrgeometers can be characterized in a way that also in unshaded operation very accurate measurements can be obtained. During calibration a wide range of source and body temperature has to be covered to allow accurate determination of C and K. In order to get a representative average temperature of the dome at least three evenly distributed sensors have to be used. Field test measurements demonstrate that the problem of differential heating can be overcome by correctly measuring the dome temperature with three thermistors fixed at 45°. Moreover the difference between the three thermometers can be used as a measure for solar irradiance and to correct for the infrared part (> 3-4 μm) of this irradiance.

References:

-Drummond, A.J., W.J. Scholes and J.H. Brown, 1970: A new approach to the measurement of terrestrial long-wave radiation. WMO Tech. Note No. **104**, 383-387.

-Albrecht, B., M. Peollet and S.K. Cox, 1974: Pyrgeometer measurements from aircraft. Rev. Sci. Instr., **45**, 33-38.

-Enz, J.W., J.C. Klink and D.G. Baker, 1975: Solar radiation effects on pyrgeometer performance. J. Appl. Meteor., **14**, 1297-1302.

-Albrecht, B., and S.K. Cox, 1977: Procedures for improving pyrgeometer performance. J. Appl. Meteor., **46**, 188-197.

BROADBAND INFRARED INSTRUMENTATION PERFORMANCE EVALUATION

by

John J. DeLuisi

NOAA Environmental Research Laboratory

Boulder, Colorado 80303

FOREWORD

The Baseline Surface Radiation Network (BSRN) is a function of the World Climate Research Program (WCRP) dedicated to monitoring the surface radiation budget at nearly 30 sites located around the globe. Uniform operation of instrumentation, including their calibrations has been a main concern of the network station managers. The performance of broadband IR sensors such as pyrgeometers and pyrradiometers has been an issue with the BSRN scientists becaouse of conflicting information found in the literature and by opinions circulating within the scientific community. The BSRN has conducted two field tests, one at the Coffeyville First ISCCP Regional Experiment (FIRE) and the other at Boulder, Colorado to evaluate the performance of IR instruments. In addition, because of differences seen between different calibration devices, a Round-Robin test of unique calibration apparatus at nine laboratories is currently underway. This presentation will describe the results of the field experiments and the progress thus far achieved in the Round-Robin test.

INTRODUCTION

During 13 November to 7 December, 1991, NOAA hosted a broadband IR radiometer intercomparison and also participated in the First ISCCP Regional Experiment (FIRE II) held at Coffeyville, Kansas. The IR experiment was conducted in accordance with plans that were developed at the end of the BSRN meeting at Davos in August 1991 (see WMO/TD-No. 453, November 1991). The primary objective was to determine the best method for measurement of broadband IR irradiance for application in the BSRN network. The approach was by intercomparison of the various instruments used among participating BSRN labs and by comparison with "official" estimates of the downwelling IR irradiance that would be provided by the SPECTral Radiation Experiment (SPECTRE) which also participated prominently in FIRE II as an adjunct experiment. A secondary objective was to assist SPECTRE with trace gas measurements of CO_2, CH_4, NO_2, CFCs 11 and 12 and vertical profiles of O_3 to improve the accuracy of the SPECTRE radiative transfer calculations.

As the hosts of the BSRN experiment, NOAA provided a trailer, data acquisition system, data loggers, many instrument mounts, and a computer. NOAA also provided personnel to conduct field operations. Seventeen IR instruments, provided by eight countries participated in the experiment. Table 1 lists the instruments, whether they were shaded and ventilated, and the participants. Solar radiometers were provided to supply data for the pyrradiometers which measure all wave (shortwave + longwave) radiation. The experiment was successfully completed. Pyrradiometers were involved in the experiment but are not considered in this report.

RESULTS OF THE COFFEYVILLE EXPERIMENT

An analysis of the FIRE II pyrgeometer intercomparison data has yielded a reasonably good picture of the performance of shaded and ventilated Eppley pyrgeometers viz. that under most circumstances, when compared to a reference instrument of the same type, agreement near the two percent level (6-8 $W \cdot m^{-2}$) occurred most of the time. Effects of dome solar heating and possible solar radiation leakage by the dome filter were seen during daytime with the unshaded and unventilated instruments. During periods of sunshine, the dome heating (and possibly filter leakage) introduced additional noise on the order of two percent (6-8 $W \cdot m^{-2}$) to the signals from the unshaded and unventilated instruments.

Additional analyses are expected from other scientists for a consensus of opinion that will be given at a topical BSRN meeting, being scheduled for the spring of 1994. The conclusions of the Coffeyville experiment will be finalized at this meeting. The absolute irradiance values of SPECTRE were supplied by the University of Maryland this past November. These values were derived from IR interferometer measurements for clear skies with the use of radiative transfer calculations to convert radiance to irradiance. A preliminary analysis using the SPECTRE results indicates agreement with a shaded and ventilated pyrgeometer on the order of 5 $W \cdot m^{-2}$ which is rather remarkable considering that an estimate of 30 $W \cdot m^{-2}$ was suggested at a BSRN meeting in Washington, D.C., 1-5 December, 1990 (see WMO KD-No. 406, March 1991).

A paper describing preliminary results of the Coffeyville experiment (DeLuisi et al., 1992). A formal report describing the efforts of the BSRN will eventually be prepared for publication, bearing a full complement of participant authorship.

HIGH HEAT STRESS PYRGEOMETER INTERCOMPARISON

During August and September of 1992, NOAA conducted a follow-up experiment of broadband radiometers similar to the FIRE II experiment. The objective was to determine effects of elevated solar heating of Eppley Pyrgeometer domes because the Coffeyville experiment was conducted during the cool period of November and December. Eight Eppley pyrgeometers were used in this experiment. The first phase of the experiment was to have all instruments deployed without shading or ventilating. This was done to check the behavior of the instruments during nighttime when they are essentially in thermal equilibrium and subjected to the same atmospheric conditions. At nighttime the domes are not being heated by the sun and, therefore, the dome correction term is minimized (it may still not be quite 0, however). A preliminary analysis suggests results similar to those of FIRE II (i.e. 12-16 $W \cdot m^{-2}$). However, it was noted that when the calibration constants of all instruments were adjusted to agree with a common value (our choice was the mean), the disagreement among instruments was further reduced to the level of a few percent, or approximately 8 $W \cdot m^{-2}$ even during daytime. Since all instruments were freshly calibrated with the same blackbody source, the cause for the differences seen among the unadjusted calibrations is not clear and will require further investigation.

Additional analyses were performed to determine the effects of dome heating during sunshine hours. Two instruments were shaded and ventilated, two were ventilated, two were shaded and two were neither shaded nor ventilated. The two shaded and ventilated instruments were used as reference instruments to compare with the unshaded and unventilated instruments. The results were essentially the same as those in Coffeyville. The problem with the treatment of dome heating is determining

the "correct" constant for the dome heating term in the pyrgeometer reduction equation. There is some indication from this experiment that filter solar leakage may be involved and this would compound the problem with the dome heating term. An attempt should be made to quantify the magnitude of the solar leakage problem.

A special comment is in order here. Whereas the BSRN is currently working on improving the accuracy of the presently available broadband instrumentation by rather simple means, this is considered to be a temporary solution to a longstanding problem. That is, the present class of broadband instrumentation is seriously outdated, and improved instrumentation is urgently needed to meet the new demands for climate research measurements. The BSRN constituency is dedicated to finding ways to improve the situation. Switzerland is developing a broadband radiance detector that should be ready for testing this summer. Eppley Lab tested a new pyrgeometer design at the Coffeyville intercomparison, and English scientists have been working with their own improved version of the Eppley pyrgeometer that performs quite well on aircraft.

ROUND ROBIN CALIBRATION EXPERIMENT

BSRN scientists recently organized and initiated an important Round-Robin calibration experiment which has been in progress since March 1993. The variations in calibrations that were noted in the Coffeyville intercomparison motivated BSRN scientists to initiate a Round-Robin comparison of calibration devices, all being of different design since no standard exists. A data logger and computer apparatus were assembled to accompany 5 pyrgeometers that were supplied by NOAA, Switzerland, NASA, Canada, and Australia. Nine labs are participating. The labs are located in the U.S., Australia, Japan, Canada, Switzerland, Germany, and England. From this experiment, the BSRN scientists hope to derive some insight into the cause(s) for the differences in calibrations that were encountered in the Coffeyville experiment (i.e. up to 7%). It is also hoped that this work will lead the BSRN scientists toward a best choice for calibration equipment that may be used by all BSRN laboratories. A status update of the Round Robin intercomparison is given in Appendix 1.

SUMMARY

By performing field intercomparisons of radiometric instrumentation, problems of accuracy, calibration, and even malfunctioning instruments can be uncovered. A considerable amount of new information on the field performance of pyrgeometers and the uncertainties in the calibrations of pyrgeometers has been derived from two field intercomparisons. It appears that a well maintained, shaded and ventilated, and carefully calibrated pyrgeometer can provide accurate measurements on the order of a few percent, approaching 5 $W \bullet m^{-2}$ for clear sky conditions. These results should not be misinterpreted with the belief that the measurement of IR irradiance is without need of further improvement. There still exist a number of questions to be answered regarding the performance of such instruments during transient atmospheric conditions and the behavior of the instrument in a non-equilibrium thermal state. Also in need of further study is the leakage of solar radiation by the dome. Calibration of IR radiometers is done with custom built devices at the various laboratories of countries participating in the BSRN. A comparison of these devices is presently in progress, and it is hoped that a superior method of calibration will evolve from the effort.

REFERENCES

DeLuisi, K. Dehne, R. Vogt, T. Konzelmann, and A. Ohmura, First results of the BSRN broadband IR radiometer intercomparison at FIRE II, "Current Problems in Atmospheric Radiation 1992, Proceedings of the IRS," Tallinn, Estonia, pp. 559-564, A. Deepak Publishing, 1992.

APPENDIX 1
PYRGEOMETER ROUND ROBIN CALIBRATION STATUS

1. Pyrgeometer Round Robin calibration were scheduled to start in March, 1993. Instruments were shipped to *Site 1* Bruce Forgan (March 2, 1993)@ Bureau of Meteorology, Melbourne, AUSTRALIA. Pyrgeometers were returned to NOAA after calibration and received July 10, 1993.
   Problem identified: Logistics for international Shipment
   Remedy: Use of a custom shipping agent at each country entry point.

2. Instruments were shipped to *Site 2* John Hickey (July 22, 1993)@ Eppley Laboratories, Newport, Rhode Island. U.S.A. Pyrgeometers were returned to NOAA after calibration and received August 9, 1993.
   Problem identified: erratic thermopile, temperature drifts with time
   Remedy: Ground was disconnected on instrument.

3. Instruments were shipped to *Site 3* Bruce McArthur (September 8, 1993)@ Atmospheric Environmental Service, Downsview, Ontario, CANADA. Pyrgeometers were returned to NOAA after calibration and received October 18, 1993.

4. Instruments were shipped to *Site 4* Masataka Shiobara (October 18, 1993)@ Meteorological Research Institute, Tsukuba, JAPAN. Pyrgeometers were returned to NOAA after calibration and received November 11, 1993.
   Problem identified: all computer files deleted
   Remedy: Program installation from back up disk.

5. Instruments were shipped to *Site 5* Klaus Dehne (November 30, 1993)@ Deutscher Wetterdienst, Meteorologishes Observatorium, Hamburg, GERMANY. Pyrgeometers are in the process of being calibrated.

Locations Remaining on Calibration Circuit with tentative dates.
1. Atsumu Ohmura (Zurich, SWITZERLAND) January 1994
2. John Seymour (Farnborough, ENGLAND) February 1994
3. Francisco Valero (Moffet Field, California, USA) March 1994
4. Steven Bender (Los Alamos, NM, USA) April 1994

Tab. 1: Participating broadband infrared radiometers

radio-meters	type	no.	shaded dome	ventilated dome	institution	P.I.
pyrgeom.	PIR	12001 F3	•	•	IMS/Israel	Manes
	"	13678 F3	•	•	AWS/Australia	Forgan
	"	20468 F3	—	—	Univ. Maryland/USA	Pinker
	"	26181 F3	—	—	NASA/USA	Whitlock
	"	26802 F3	•	•	SMA/Switzerland	Heimo
	"	27594 F3	•	•	Met.Nat./France	Olivieri
	"	27701 F3	•	•	DWD/Germany	Dehne
	"	28146 F3	•	•	AES/Canada	McArthur
	"	28630 F3	•	•	NOAA/CMDL/USA	Dutton
	DS	9674	—	—	NOAA/NAVY/USA	Nelson
	"	9682	—	—	-"-	-"-
	SIR, PIR	8-48	•	•	Eppley/USA	Hickey
	PG	001	—	•	Kipp & Zonen/Netherland	van den Bos
	"	002	—	—	-"-	-"-
pyrradiom.	ST-25	136	•	•	ETH Zürich/Switzerland	Ohmura
	"Schulze "	310 269 (Basel)	—	•	GIB/Switzerland	Vogt
	"	310 279 (Berlin)	•	•	-"-	-"-

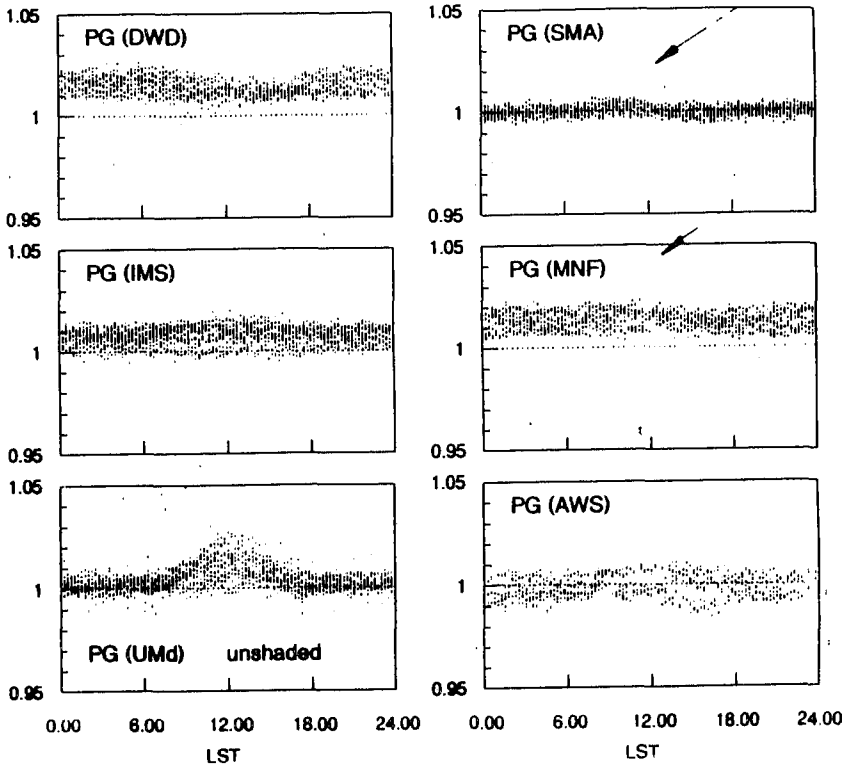

Fig. 1. The ratio of test pyrgeometer data to the reference pyrgeometer data (ordinate) vs time (abscissa) for several days. The reference pyrgeometer data was was from the NOAA pyrgeometer.
DWD: German Meteorological Service
SMA: Swiss Meterological Service
IMS: Israeli Meteorological Service
MNF: French Meteorological Network
UMD: University of Maryland
AWS: Australian Weather Service
* Note the dome breaking effect of the unshaded pyrgeometer in the UMD plot.

DETERMINATION OF GENUINE DIRECTIONAL CHARACTERISTICS OF PYRANOMETER

HIROSE Yasuo
Observations Division
Obsevations Department of Japan Meteorological Agency, Tokyo

1. Introduction

The calibration of pyranometer in the Japan Meteorological Agency has been carried out by outdoor comparison with reference pyranometer for several weeks under various sky conditions. This method has many practical advantages, but an annoying problem arises along with it.

It was the late 1970's when we became aware that the measured values by two pyranometers of the same type calibrated during different seasons did not necessarily agree with each other under the same measuring condition. By many comparisons and examinations we soon realized on a quantitative basis that the sensitivity of reference pyranometer changed through seasons and affected the calibration factors of calibrated instruments significantly. It was due result because the sensitivity of pyranometer takes different values for different conditions in general, but no serious attention had been paid to this problem before those times. The lack of reliable testing devices might be one of the reasons.

Increasing demands for more accurate solar radiation measurements stimulated us to endeavour to eliminate the biases caused by the characteristics of reference pyranometer from the calibration factors. It eventually led us back to reexamination of the shading disk method which was used to determine the sensitivity of reference pyranometer by comparison with standard pyrheliometer. The conclusion was that the systematic methods and the testing apparatuses should be developed in order to obtain the accurate characteristics of pyranometer and incorporate them into the sensitivity fuction in an appropriate manner.

In this paper, the procedures to obtain the sensitivity function of pyranometer, brief descriptions of the testing apparatuses for this purpose, and some outcomes of our methods are presented. Here we introduced a directional function free of non-linearity in place of cosine response, and dealt with the static characteristics other than the spectral response because that might be sufficient for meteorological purposes.

2. Theoretical Bases

The directional nonuniformity of the sensitivity of pyranometer arises from the refraction and the concentration of incident radiation by the glassdome(s), the directional dependence of the absorptance of the radiation receiver, etc. Those optical factors are combined to make a function that gives the relation between the incident irradiance to be measured and the absorbed irradiance at the receiver. The output voltage of pyranometer in turn is basically proportional to the absorbed irradiance, and the ratio may depend on the thermal state of pyranometer. Thus, on condition that pyranometer is placed horizontally and exposed to global solar radiation, we obtain a pair of pyranometer equations expressed as follows:

$$V = K_0 \cdot H(t,A) \cdot A \qquad (1)$$

$$A = S \cdot \cos z \cdot G(z,\phi) + \int D(z',\phi') \cdot \cos z' \cdot G(z',\phi') \cdot d\Omega \qquad (2)$$

where

(z,ϕ) : zenith angle and azimuth of incident radiation
S : direct solar irradiance, $D(z',\phi')$: sky radiance by diffuse solar radiation
A : absorbed irradiance, V : output voltage, t : body temperature, K_0 : constant
$H(t,A)$: thermal function, $G(z,\phi)$: optical function, Ω : solid angle of sky

By normalizing as $g(z,\phi) \equiv G(z,\phi)/G(0,*)$ and $a \equiv A/G(0,*)$, the forms (1) and (2) can be rewriten

$$V = k_0 \cdot h(t,a) \cdot a \tag{3}$$

$$a = g(z,\phi) \cdot S \cdot \cos z + U \cdot Ed$$

$$= g(z,\phi) \cdot \{1 + F \cdot (U / g(z,\phi) - 1)\} \cdot Eg \tag{4}$$

where

$$Eg = S \cdot \cos z + Ed \tag{5}$$

$$U = \int_\Omega D(z',\phi') \cdot \cos z' \cdot g(z',\phi') \cdot d\Omega \; / \; Ed \tag{6}$$

$$F = Ed / Eg \tag{7}$$

Eg : global solar irradiance, Ed : diffuse solar irradiance
$h(t,a)$: thermal function normalized as $h(t_0,a_0) = 1$, k_0 : constant

It is clear that the quantity a coincides with the irradiance of parallel beam when it comes from zenith, and then the constant k_0 is the sensitivity of pyranometer under the fixed measuring condition of $(t=t_0, a=a_0)$. The ratio F is an index of sky condition, that is, $F=1$ for overcast sky. The normalized function $g(z,\phi)$ represents the genuine directional characteristics of pyranometer. The weighted mean U depends on the distribution of sky radiance. For simplicity and practical reason, let us assume that sky radiance $D(z',\phi')$ is uniform throughout the entire hemisphere, then U becomes again a characteristic value of pyranometer. The thermal function $h(t,a)$ expresses temperature response or non-linearity depending on the parameter taken as variable. Actual sensitivity V/Eg under various measuring conditions can be calculated by determining k_0, $h(t,a)$, $g(z,\phi)$, and U.

3. Procedures

Step 1) Collimation Tube

Prior to other tests, absolute sensitivity of pyranometer under a measuring condition should be known. It is done by comparing pyranometer attached to collimation tube with absolute pyrheliometer using the direct sun as radiation source (Fig.1). The tube is 1.0 m long and has the opening half angle of 2.8° which is close to that of absolute pyrheliometer, for example, Eppley HF. The outer wall is painted white and equipped with carefully aligned diopters. The inner wall is furnished with thirty-nine diaphragms and coated with matting black paint. The tube is mounted on sun tracker and continuously driven during the comparison. About thirty sets of comparison data are obtained in a relatively short time of, say, one hour under clear and steady sky.

$$V(t_i,S_i) = k_0 \cdot h(t_i,S_i) \cdot S_i \tag{8}$$

where

S_i : direct solar irradiance, t_i : body temperature of pyranometer

Body temperature is measured with thermopile sheet (Philips PR6452A) attached to pyranometer and covered by aluminum foil to shade it from the sun.

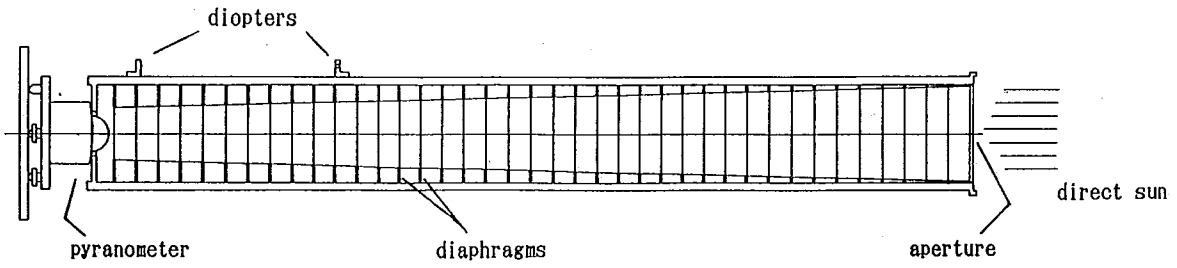

Fig.1 Collimation tube.

Step 2) Thermal characteristics

As $h(t, a)$ is two dimensional function, the testing apparatus has the facilities to change t and a simultaneously (Fig.2). Ambient temperatures and the changing rates can be arranged arbitrarily by programmable controller. The incident radiation is dimmed by a set of rotating sectors. Each sector, having the radius of 175 mm, has four fan-shaped windows opened regularly and rotates at 1,200 RPM. The transmittance of rotating sector is calibrated accurately by using compensation pyrheliometer and absolute pyrheliometer. The radiation source is 300 W xenon lamp which generates the irradiance of about 1 kW/m^2. The infrared part of the radiation is cut well. High stability under 0.1 % of irradiance is attained by optoelectronic servomechanism. In our case four points for temperature and five points for transmittance are chosen, namely $t_j \fallingdotseq +50, +25, 0, -25$ ℃ and $\rho_m = 1.0000, 0.8898, 0.6667, 0.4440, 0.2212$ which are normalized by 90 %-sector in order to eliminate the fringe effect of rotating sector. Accurate body temperature is measured with thermopile sheet in the same way as mentioned in step 1). It takes about ten hours to complete the whole test.

$$V(t_j, \rho_m \cdot S_0) = k_0 \cdot h(t_j, \rho_m \cdot S_0) \cdot \rho_m \cdot S_0 \qquad (9)$$

where

S_0 : irradiance dimmed by 90 %-sector

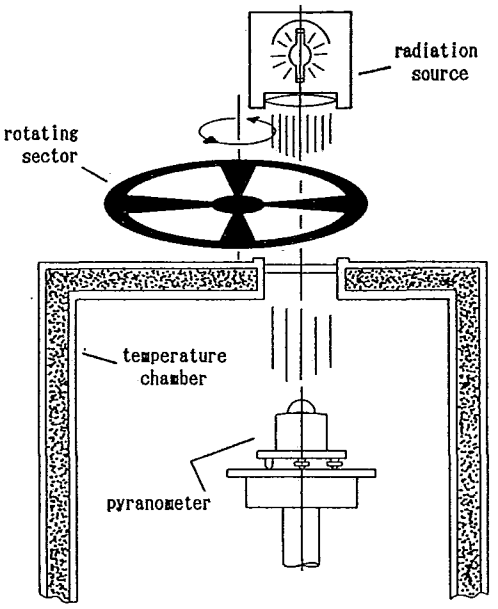

Fig.2 Thermal test.

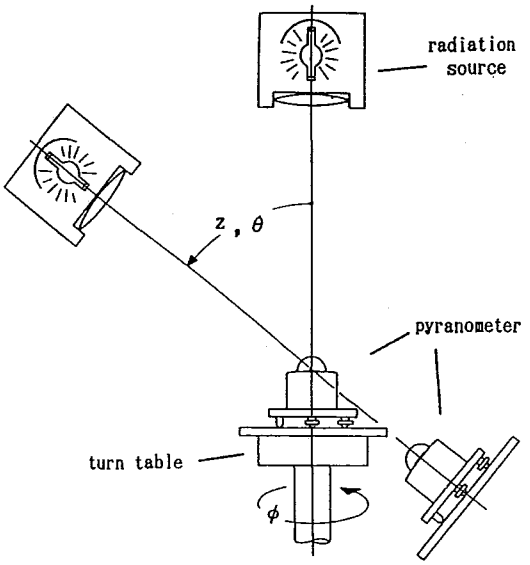

Fig.3 Directional and tilting test.

Step 3) Directional characteristics

The test comprises obtaining the cosine responses at various azimuthal angles (Fig.3). The radiation source is the same as used in the thermal test. Parallelized and spatially uniform radiation beam is obtained by parabolic reflector and collective lens. The whole optical system in the lamp house is fixed tightly to prevent the distortion by tilting which tends to cause the variation of the spatial distribution of irradiance. The change of the irradiance at the center of the turn table is kept under 0.1 % during the test. The angles are selected as follows: z_j= 0, 10, 20, 30, 40, 50, 60, 70, 75, 80, 85° ; ϕ_m= -180, -150, ···, 0, +30, +60, ···, +150, +180° (= -180°).

$$\frac{V(t_c, S_0, z_j, \phi_m)}{V(t_c, S_0, 0, *)} \Big/ \cos z_j = \frac{h\,[t_c,\ g(z_j, \phi_m) \cdot S_0 \cdot \cos z_j] \cdot g(z_j, \phi_m)}{h\,[t_c,\ S_0]} \qquad (10)$$

where

S_0 : irradiance for $z = 0°$, t_c : body temperature of pyranometer

The left side of (10) is the definition of cosine response for $\phi = \phi_m$.

Step 4) Tilt effect

The tilt effect of pyranometer is tested by using the same apparatus as used in **step 3)**. The turn table is united to the rotating axis of radiation source rigidly by a coupling rod. Every 10° of tilt angle from horizontal to vertical the output of pyranometer are measured for the two azimuthal angles of ϕ=0° and ϕ=+90° . The tilt effect $\tau(\theta)$ is defined as follows:

$$\tau(\theta) = V(\theta) \,/\, V(0) \tag{11}$$

where

θ : tilt angle

Step 5) Calculations

On the results obtained through the preceding steps, we can determine all the quantities necessary to establish the sensitivity function of pyranometer. From **(8)**,**(9)**,and **(11)** it follows that

$$S_0 = \frac{V(t_1, S_0)}{V(t_i, S_i)/\tau_i} \cdot h^*(t_i, S_i) \cdot S_i \tag{12}$$

where

$h^*(t, a)$: tentative thermal function normalized as $h^*(t_1, S_0) = 1$

τ_i : tilt effect for the comparison data of collimation tube

From **(9)** we have

$$h^*(t_j, \rho_m \cdot S_0) = \frac{V(t_j, \rho_m \cdot S_0)}{V(t_1, S_0)} \cdot \frac{1}{\rho_m} \tag{13}$$

Assuming that S_0 = 0.9 kW/m^2 we obtain the first approximations of $h^*(t_j, \rho_m \cdot S_0)$ at 4×5 grid points by **(13)**. Linear interpolations or extrapolations make $h^*(t_i, S_i)$, and by substituting them into **(12)** S_{0i} can be obtained for each data of collimation tube. They are averaged over i and substituted again in **(13)** as the second approximation of S_0. By repeating these procedures S_0 and $h^*(t_j, \rho_m \cdot S_0)$ converge to fixed values. Thus $h(t, a)$ normalized as h(+20℃, 1kW/m^2)=1 can be determined at 4×5 grid points. The sensitivity k_{0i} is calculated by **(8)** for each data of collimation tube. By averaging them over i we obtain the final value of k_0 with the standard deviation of 0.2~0.4 % depending on the sky condition.

Next, we determine S_0 for the test of directional characteristics using the same procedures as mentioned above, and calculate the values of $g(z_j, \phi_m)$ in **(10)** by iterative method, then obtain the directional function $g(z, \phi)$ at 11×12 grid points. Finally, U can be calculated by **(6)** assuming that $D(z', \phi')$ is constant.

4. Applications

Once the sensitivity function of pyranometer is established with sufficient accuracy, following applications become possible: (1) accurate measurement of diffuse solar radiation by a shading pyranometer (2) accurate measurement of direct/ diffuse/ global solar radiaion by using a pyranometer and a pyrheliometer (3) calculation of the sensitivities of pyranometer through seasons at a fixed measuring site. As our purpose was to determine unbiased global solar irradiances for calibration, we take up the examples of the application (3) mentioned above. In Fig.4 the sensitivity curves of three actual pyranometers, namely two of **EKO MS801** now used as calibration reference and an **EPPLEY PSP** used as calibration reference before 1984, are shown. They are the six-hour daytime means calculated under the typical temperatures and irradiances at the calibration site (**TSUKUBA(TATENO), +36° 03′ N, +140° 08′ E, 21 m MSL**). The seasonal change and the F-dependence of the sensitivity of **EPPLEY PSP** are chiefly due to the strong directional dependence of the sensitivity. In our case the average of the sensitivities for F=0.3, 0.5, and 0.7 is adopted as the sensitivity of the calibration reference and changed everyday through seasons along the sensitivity curve, thus eliminating the biases of the reference values caused by the characteristics of reference pyranometer.

The availability of our methods, including the accuracy of the determined characteristics, is verified fairly well by comparing the global solar irradiances obtained by different characterized pyranometers under various measuring conditions.

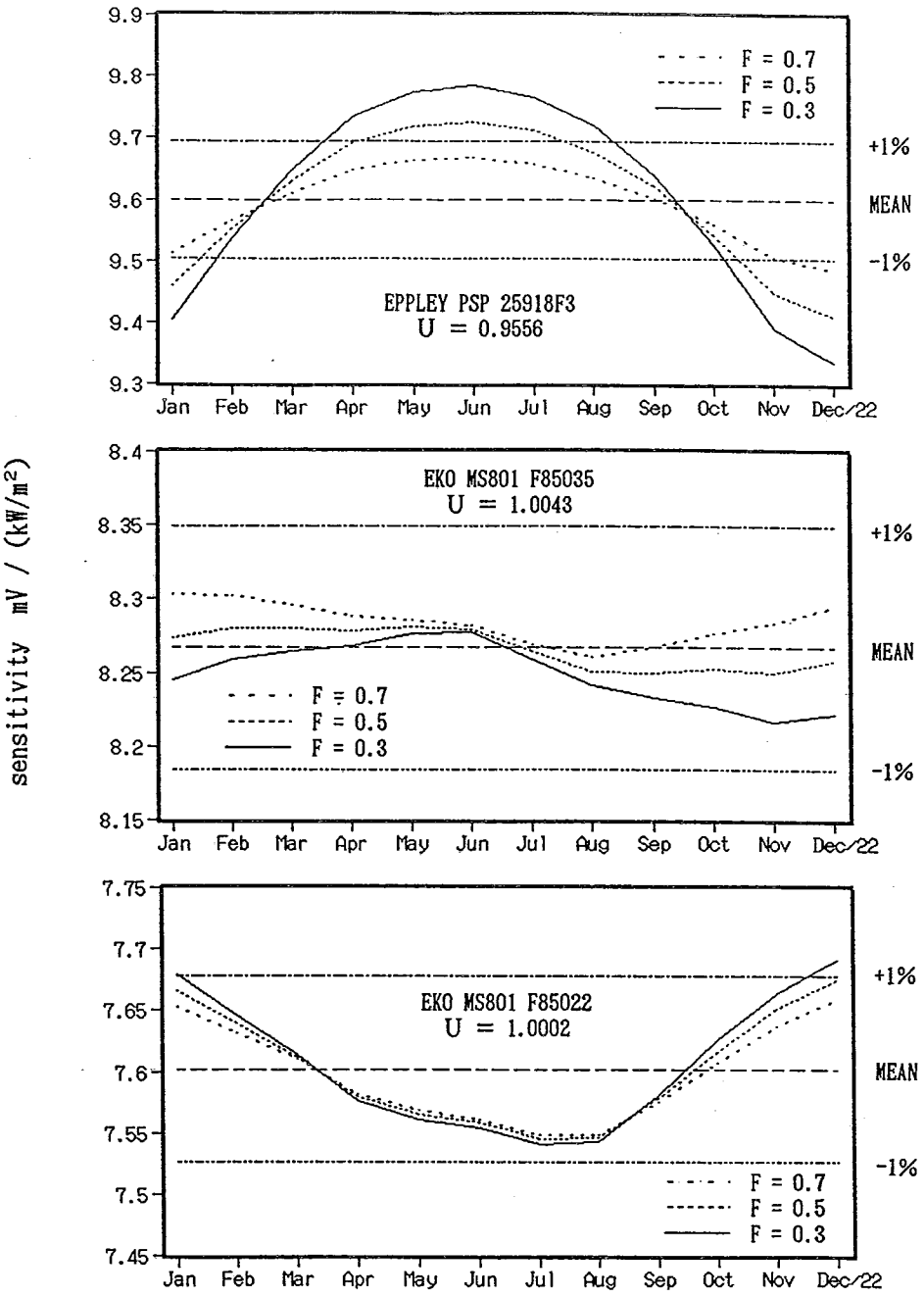

Fig.4 Sensitivity curves through seasons at the calibration site (TSUKUBA).

5. References

(1) Bahm, R.J. & Nakos, J.C. (1979), FINAL REPORT, THE CALIBRATION OF SOLAR RADIATION MEASURING INSTRUMENTS, The Bureau of Engineering Research, The University of New Mexico.
(2) INTERNATIONAL ENERGY AGENCY, task III, performance testing of solar collectors, results of a pyranometer comparison, Davos, March 5 and 6 1980.
(3) WMO-No.8 (1983), GUIDE TO METEOROLOGICAL INSTRUMENTS AND METHODS OF OBSERVATION, Chap.9.
(4) Hirose, Y. (1986), On the Trial of Calculating Global Solar Irradiance in Consideration of the Characteristic Functions of Pyranometer, Japan J.Met.Res.,Vol.38,No.3.
(5) ISO 9847 (1992), Solar energy - Calibration of field pyranometers by comparison to a reference pyranometer.

* * *

THERMAL DELAY OF PYRANOMETERS

Bingzhong Wang
(Chinese Academy of Meteorological Sciences, Beijing, 100081, China)
Guoquan Qiu & Shensheng Li
(Department of Physics, Capital Normal University, Beijing 100037, China)

1. INTRODUCTION

In accurate determination of solar radiation, it is often necessary to take the "zero reading" at first, and then take the normal reading of output. It is only the difference of these two readings corresponds to the actual radiation output. For example, it is customary to do this during caliberation of a pyranometer or determination of its performance parameters, such as cosine response and azimuth response. In general cases, the pyranometer has a cover, the problem is how long time should be waited to take the readings. We find in our experiments that if we take readings according to conventional "time of response" of pyranometers, even if as long as 99.5% of the response time, it is still not enough for sufficient response of the pyranometers. Of course, this phenomenon is occured because there has no unified method for determining the actual response time of pyranometers.

According to the conventional understanding of response time of pyranometers, it is assumed that the variation of its output with time is following the simple exponential laws of charging and discharging of a RC circuit. But the experimental results showed that this understanding is oversimplified. Hence some attentions were paid by several scientists, [1, 2] and some of them have proposed the idea that there would be two time constants of pyranometers. [3] They were concentrated in the error of determinations caused by the rapid variation of irradiation and the time delay of response of sensors. We have performed some experimental studies about the effect of pyranometer output under constant irradiation with different time since 1990, [4] and several new results were obtained which is the main content to be considered in this paper.

2. EXPERIMENTAL DEVICE

The experimental device for measuring the response time of different models of pyranometers is shown in Fig. 1.

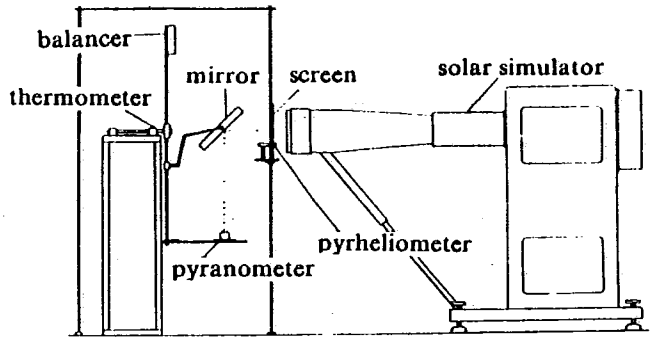

Fig. 1. Experimental device for measuring the response time of pyranometers

Light Source System

A solar simulator of Model TM-3000A is used as the light source, its irradiation is variable between 0.7 and 1.5 solar constant, and its stability can be maintained as $<\pm 1.5\%$/hr. A metallic reflective mirror tilted at an angle 45° in front of the solar simulator can assure the incident light reaching the surface of pyranometers perpendicularly with almost constant intensity during the experiment.

Because it can not be made sure absolutely that the intensity of the light source remains stable during the whole process of measurement, so a pyrheliometer facing directly the simulator is used to monitor the small variation of the light source. Both outputs of the pyrheliometer and the pyranometer under mersurement are in voltage signals, and two digital voltmeters with high accuracy ($6\frac{1}{2}$ digits) and IEEE-488 interface are used and controlled automatically by a micro-computer to take the readings simultaneously. All data are stored automatically in the diskettes.

Screening System

To avoid or reduce the interference of other diffused lights, the door and windows of the lab are screened, the device is put in a small dark cabinet of area $4m^2$, with double-layer black cloths surrounding it. Hence, there is no other light source except the solar simulator.

Temperature Controlling System

To reduce the effect of environmental temperature to the measuring results, an air-conditioner is used. To avoid the temperature rise in the small dark cabinet due to long time irradiation, a fan is used at the lower corner of the light source side to make forced ventilation, and an exhaust gap is set at the upper corner of other side. The temperature in the small dark cabinet is read by

a digital thermomter made of platinum resistance. The temperature control is man -made, and the range of the temperature variation is within ±0.5℃ during a day.

3. PROCEDURE OF MEASUREMENT AND TREATMENT OF EXPERIMENTAL DATA

At the same time to start the irradiation source, the cover of monitoring pyranometer (A) is taken off to preheat and all the electric instruments are switched on. Put the pyranometer under test (B) on a horizontal table and its face of sensor is placed at the center of luminous disk to assure the uniformity of irradiance. But the cover of B is not taken off yet, so it is not exposed to irradiation. Take off the cover of B after 30 min. and start the program of a microcomputer to assure the collection of output voltages of A and B continuously and simultaneously. The number of collected data are 800 pairs in total for single test. The time interval of successive data collection is about 2s, so the time needed to achieve a complete set of measurement is about 30 min.. The collected data are automatically input into diskettes.

Then pick out experimental data in order, and take 5 pairs as a subset, so there are 160 subsets in a complete set. The average value of every subset is c alculated by following formulas:

$$\bar{A}_n=\frac{1}{5}\sum_{i=1}^{5} A_{i,n} \tag{1}$$

and

$$\bar{B}_n=\frac{1}{5}\sum_{i=1}^{5} B_{i,n} \tag{2}$$

At the beginning of data collection, A is sufficiently exposed to irradiation and preheated, while B is just subjected to irradiation. The thermal aspects of A and B are different, it is the main factor that produces the difference of their outputs. As the time duration is elongated, the difference between the two outputs decreases gradually and approaches the same value finally. We take the data of last 40 subsets (i. e. from 121st to 160th subsets) as basic data to determine the quantitative relation between the outputs of A and B, and to calculate the proportionality ratios according to conventional method:

$$\frac{\bar{B}_{121}}{\bar{A}_{121}}=K_{121},\quad \frac{\bar{B}_{122}}{\bar{A}_{122}}=K_{122},\cdots\cdots,\quad \frac{\bar{B}_{160}}{\bar{A}_{160}}=K_{160}. \tag{3}$$

and

$$\frac{1}{40}(K_{121}+K_{122}+\cdots\cdots+K_{160})=K \tag{4}$$

Hence the following relation can be obtained:

$$\hat{B}_n = K \bar{A}_n \tag{5}$$

Substitute the measured values of A_1, A_2, ···, A_{120} in formula (5), then the corresponding accurate outputs of B, i.e., $\hat{B}_1$, $\hat{B}_2$, ···, $\hat{B}_{120}$ can be obtained. By comparing $\hat{B}_n$ and $\bar{B}_n$ (n=1, 2, ···, 120) one by one respectively, then the relative error of measurement of every subset R_n can be calculated from following equation:

$$R_n = \frac{\hat{B}_n - \bar{B}_n}{\hat{B}_n} \times 100\% \tag{6}$$

4. RESULTS AND DISCUSSIONS

Fig. 2 (a) represents the experimental result of one TBQ-2 pyranometer and the imitative curve of experimental data. The time interval between two adjacent points on the curve is 10s. Fig. 2 (b) represents the experimental results of three TBQ-2 pyranometers by several measurements and their corresponding imitative curves. We can obtain following conclusions from the figures:

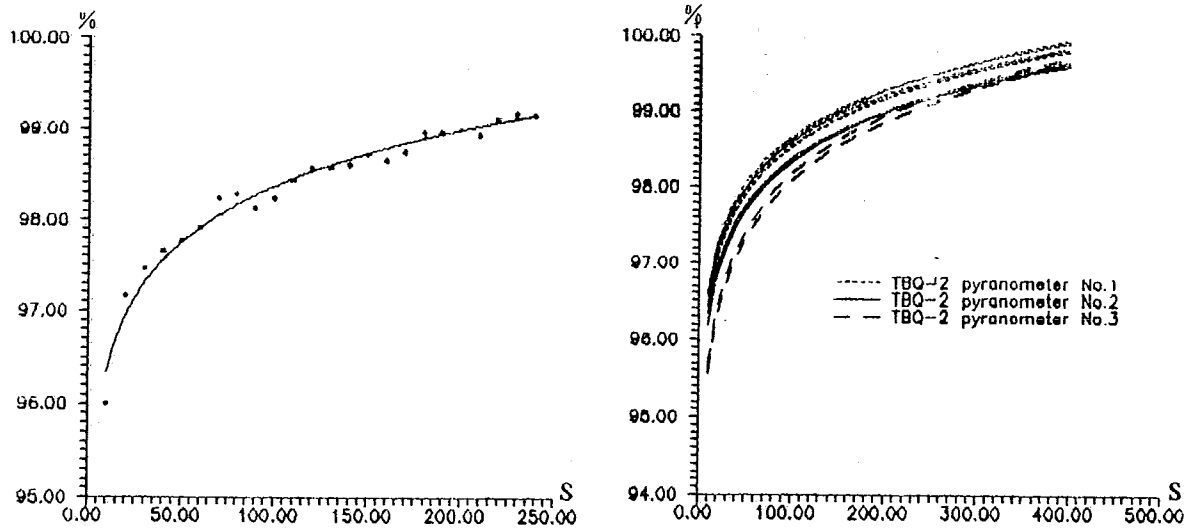

(a) One TBQ-2 pyranometer (b) Three TBQ-2 pyranometers

Fig. 2 Experimental results of TBQ-2 pyranometers and their corresponding imitative curves

(1)For pyranometers of same model, there are definite differences between different individuals, but the tendencies of variation of their outputs with time are almost the same in general.

(2) For the same pyranometer, there are only very small differences between different measurements, and these differences are apparently smaller than that of

different individuals.

(3) For practical applications, if experimental error of the order less than 1% is considered to be corresponding the calibrated error and the intrinsic accuracy of the instruments used and can be neglected, then for TBQ-2 pyranometer, at least 3 min. must be waited after the covers are taken off, and then the output readings can be considered as creditable. But the 99.5% response time of this model is only 10-20s conventionally.

The above phenomenon is not only for pyranometers of TBQ-2 model. We have performed several measurements with same procedure for pyranometers of different types and models, and the results are listed in Tab. 1. The data show that above phenomenon is not accidental but existing generally. The reason of this is that pyranometers have not been exposed sufficiently to irradiation and have not enough time to establish stable thermel eguilibrium. We propose to call this phenomenon as "thermal delay" of pyranometers.

Tab. 1. Thermal stable time of six conventional pyranometers

Type	All black			Black and White		
Model	TBQ-2	DFY-4	Eppley PSP	TBQ-2	DFY-2	Eppley 848
Manufacturer	China	China	USA	China	China	USA
Thermal stable time (s)	180	19	23	9	38	90

Although this phenomenon would not occur in case that pyranometers are exposed continuously to irradiation, thus the output data would not be affected. But the thermal stable time should be certainly one of the essential indices for international standardization of pyranometers, and in some special cases would cause significaut error if we do not take it into cinsideration. Therefore, attention must be paid to it if accurate measurements and creditable experimental data are required.

REFERENCES

1. Brinkworth, B. J. and D. R. Hughes, A method of obtaining fast response in solar pyranometers, *J. Phys. (E), Sci. Instrum.*, 8, 902-903 (1975).
2. Brinkworth, B. J. and D. R. Hughes, Accelerated response of thermopile pyranometer, *Solar Energy*, 18, 403-404 (1976).
3. Shen, B. and A. M. Robinson, Measurement and analysis of the step respnose of pyranometers requiring second-order correction, *Solar Energy*, 49, 309-313 (1992).
4. Wang Bingzhong, Ge Hongchuan, Di Naili and Li Shensheng, The thermal stable time of pyranometers, *Quart. J. of Appl. Meteor.* 3 (Suppl.), 124-128 (1992), (in Chinese).

Session V

QUALITY ASSURANCE

Calibration Procedures for Relative Humidity Sensors

Jitze P. van der Meulen and André van Londen
Royal Netherlands Meteorological Institute,
de Bilt, Netherlands

Abstract

Frequent calibrations of relative humidity measuring instruments is a strong constraint to fulfil the stated accuracy requirements. As a consequence the procedures to calibrate these instruments should be well defined and reliable. It is a common experience that calibration of humidity sensors needs special care and quality control to ensure appropriate adjustments of the transmitters.
This paper will describe and discuss in some detail the recommended procedures and with respect to other, more commonly accepted procedures.

1. Introduction.

Since 1987 KNMI uses polymer based sensors to measure relative humidity. These types of sensors have the advantage that the dielectric constant is linear with RH but rather independent of temperature. Alternatives like psychrometers or dew point mirror based systems need frequent maintenance, which makes them unsuitable for automatic remote measurements.
However, experiences with these types of polymer sensors are not completely satisfactory until today. It is found for a number of types that the low term stability and the temperature independency does not meet the stated accuracy requirements within a calibration interval of half a year. Moreover, frequent appropriate calibration and adjustment is a basic requirement for operational use.

2. Use of filters

In a previous paper [1] attention was drawn to the appropriate use of filters. Two types of filters may be distinguished:

Type I : Hydrophillic depth-filters (e.g. sintered bronze).
Type II: Hydrophobic membrane filters (e.g. PTFE layers, manufactured by Gore & Co. or Schleicher & Schüll).

It is demonstrated that both types of filters does not influence significantly the response times of the sensors (see ref. [1]). Both types of filters have their own advantages and disadvantages. In summary the following aspects are relevant:

Type I:

— Aerosols and spray are captured by the filter. In case of pollution by salt, etc., the vapour pressure will be influenced, reducing the measured RH.
— The filter may collect an amount of water during period with 100% RH, which will take time to evaporate when RH drops.
\+ When t drops to t_{dew}, vapour will condense on the filter and not on the polymer sensor.

Type II:

\+ Membrane filters do not capture (polluted) condensed vapour; it rejects water droplets and aerosols
\- When t drops to t_{dew}, vapour will condense inside the filter tube and on the polymer sensor. The condensed

---

[1] Van der Meulen, J.P. (1988): "On the Need of Appropriate Filter Techniques to be Considered using Electrical Humidity Sensors", in: Instruments and Observing Methods Report No 33 (WMO/TD-No 222), pp. 55.

water may contain polluted gasses: The sensor may be contaminated and an offset may be introduced.
- After a period of condensation, it will take much time for the condensed water to evaporate and pass through the filter, leaving behind any contamination inside the polymer sensor.

In summary we may state that type I filters introduce micro-climates, due to pollution of the filter, whereas type II filters do trap water vapour, catching chemical aggressive gasses which will deposit in the sensor material. As a consequence, calibration and maintenance procedures should include appropriate care for the filters.

3. Temperature dependency

Polymer sensors are more or less independent of temperature. However to meet the WMO accuracy requirement within a temperature range from -30°C to +40°C temperature compensation is necessary. Some manufacturers provide their transmitters with temperature sensors for compensation purposes. An advantage of transmitters producing both temperature and RH is the possibility to calculate t_{dew}.
However, temperature tests on RH-transmitters has demonstrated significant temperature dependencies for a number of instruments.
It was found that the same temperature dependency holds for sensors manufactured from polymer material from the same batch. As a consequence manufacturers should test the temperature in dependency of the material first before producing any RH sensor. Fig. 1 shows a typical example of the results we have found. Note that these results are

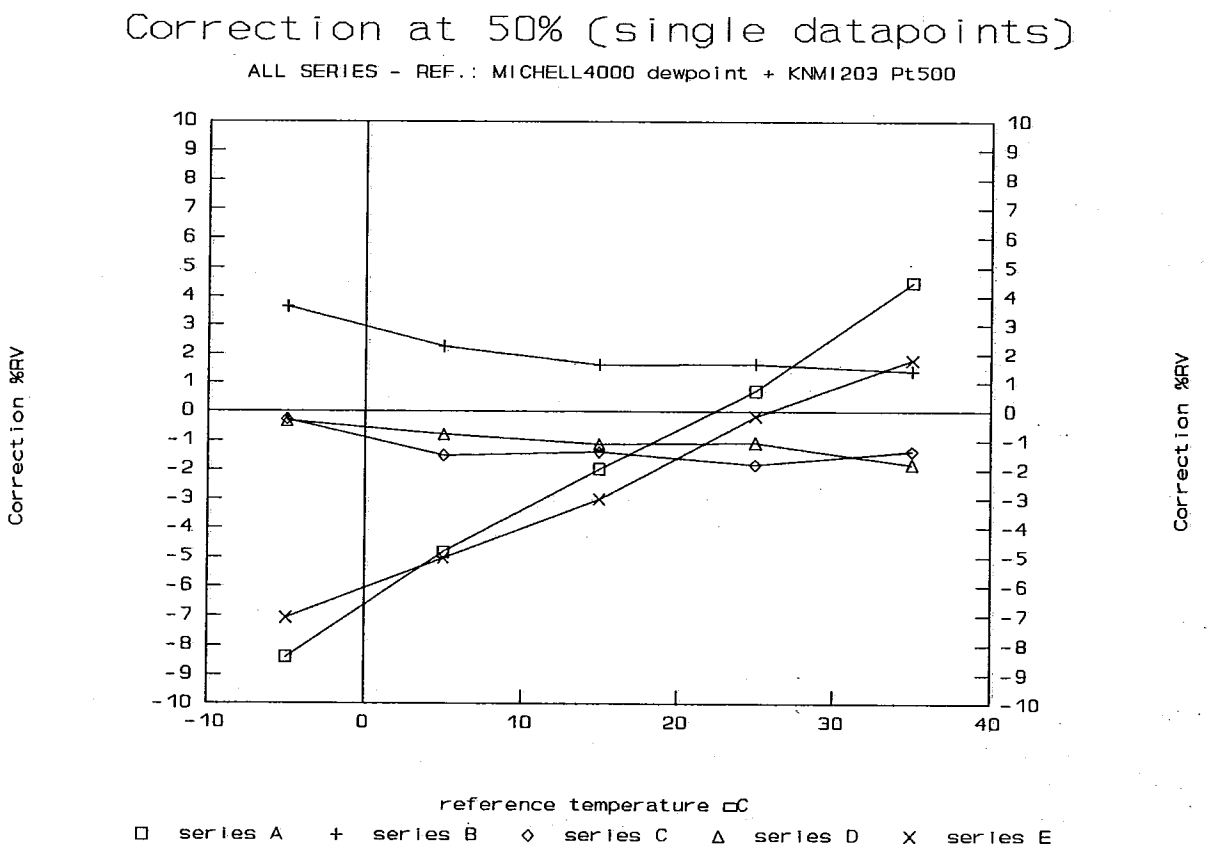

Fig. 1, Calibration curves for 5 series of transmitters.

based on calibrations of series, just arrived from the manufacturers. Due to this experience it is recommended to perform a temperature dependency test first before declaring a transmitter to be suitable for operational measurements.

4. Calibration procedures

The most popular method to calibrate polymer based sensors is by using the so-called LiCl method: Inside a small box a tissue is placed and wetted by a solution of LiCl in water. Above this tissue and in this box a well defined vapour saturation pressure will arise. Then the sensor is screwn into this box, but without the filter. Although this method is quite efficient, a number of disadvantages should be noted:

1) Before and after use, the box should be cleaned thoroughly. Residues of LiCl after use may influence following calibrations. Neatness is a first requirement.

2) The stated RH is defined for a certain temperature (22°C). Temperature measurements are necessary to be aware of a correct temperature, or for use of correction tables.

3) The transmitter is calibrated without its filter and no experience will be gained concerning contamination.

4) There is no direct control on the quality of the LiCl solution and consequently on the reference RH.

5) Screwing and unscrewing of box and filter may damage the sensor by touching it.

Because of the disadvantages and the need for fully automatic calibration and adjustment procedures at the calibration facility of KNMI, we have developed an automatic calibration and adjustment system based on clear procedures. To be able to perform automatic adjustments KNMI has chosen for the Vaisala type 233 programmable humidity transmitter. This transmitter has an RS 232 interface for computer communications and a "flash eprom", in which calibration parameters may be stored and kept even if the power supply will be cut off. For analog output of data also two programmable channels are available (e.g. for RH and for temperature). A brief overview of the system is presented in fig. 2.

Use is made of a Weiss climate chamber (type 500 ABT/30J4), controlled automatically by a computer. Even the flow over the cooling baths are controlled by the computer with stepping motors. With this climate chamber any RH can be stabilized within -20°C to +40°C.

As references use is made of a Pt500 temperature sensor, calibrated with a WECC certified temperature needle (accuracy: 0.01 °C). The dew point temperature is measured with a Michell type 4000 dew point mirror system (also WECC certified). This system is mounted inside the climate chamber on such a way that with the help of an ocular it is possible to control the mirror from outside. Since pollution will affect the measured t_{dew}, use is made of two back-up sensors (Vaisala 233) for real-time control purposes.

With the help of the computerized system it is possible to calibrate and re-program the humidity transmitters on a uniform manner and with only minor human effort. Moreover a whole series can be calibrated together in the climate chamber. A major advantage is the possibility to test the temperature independency of the transmitters as part of the total procedure.

A standard procedure for calibration and adjustment of humidity transmitters (Vaisala 233) is as follows:

1) Instalment of the humidity transmitters in the climate chamber (maximum: 6).

2) Control (visually) of the dew point mirror; cleaning if necessary.

3) Start computer programme by entry of sensor identification number and other information.

4) Computer system orders the climate chamber to install at 20°C and 17%RH and waits until stabilization. By automatic fine tuning of air flow, the RH inside the chamber will keep stable within ± 0.25% RH.

5) If the system is found to be stable during 2 minutes within ± 0,25%RH, data is collected from references, sub-references and RH transmitters. (Sub-references are used for contamination control purposes, tolerance: 0,5 %RH). RH is calculated from t and t_{dew} using the formula recommended by CIMO-X.

6) actions 4) and 5) are repeated for 8 other values of RH (27%, 37% ... 97% RH) providing 9 calibration data points.

7) If one of the nine data points differs more than 0,5 %RH from the reference values a fourth order polynome fit is calculated through the correction data points $C_i \equiv U_{i,\,ref} - U_i$ (i = 1 ..9). The resulting parameters of this fit are programmed into the flash eprom of the transmitter.

8) For control purposes actions 4) and 5) are repeated for U = 97% and 67% (accepted tolerance: 0,5 % RH).

9) After acceptance, parameters and data are stored in the database of the computer system to be able to evaluate the long term behaviour of the transmitter.

If, after control, any transmitter does not meet the stated tolerances it will be redrawn from the total collection of operational instruments.

New instruments are controlled for temperature independency (-10°C, 0°C, ... 40°C).
The calibration interval is chosen to be 6 months during which an accuracy of ± 3,5 %RH is guaranteed.
A benefit of this procedure is the ability to calibrate sensors with and without filters. As a consequence it is possible to distinguish drifting phenomena caused by degradation of the sensor or by contamination of the filter.

5. Summary

Use of PTFE membrane filters may cause degradation of the polymer sensor during periods with strong condensation caused by temperature drop and in regions with polluted air.
For calibration purposes, the use of an computerized automatic climate chamber has great advantages above the LiCl-method. To gain optimal benefit, references should be WECC certified and careful maintained.

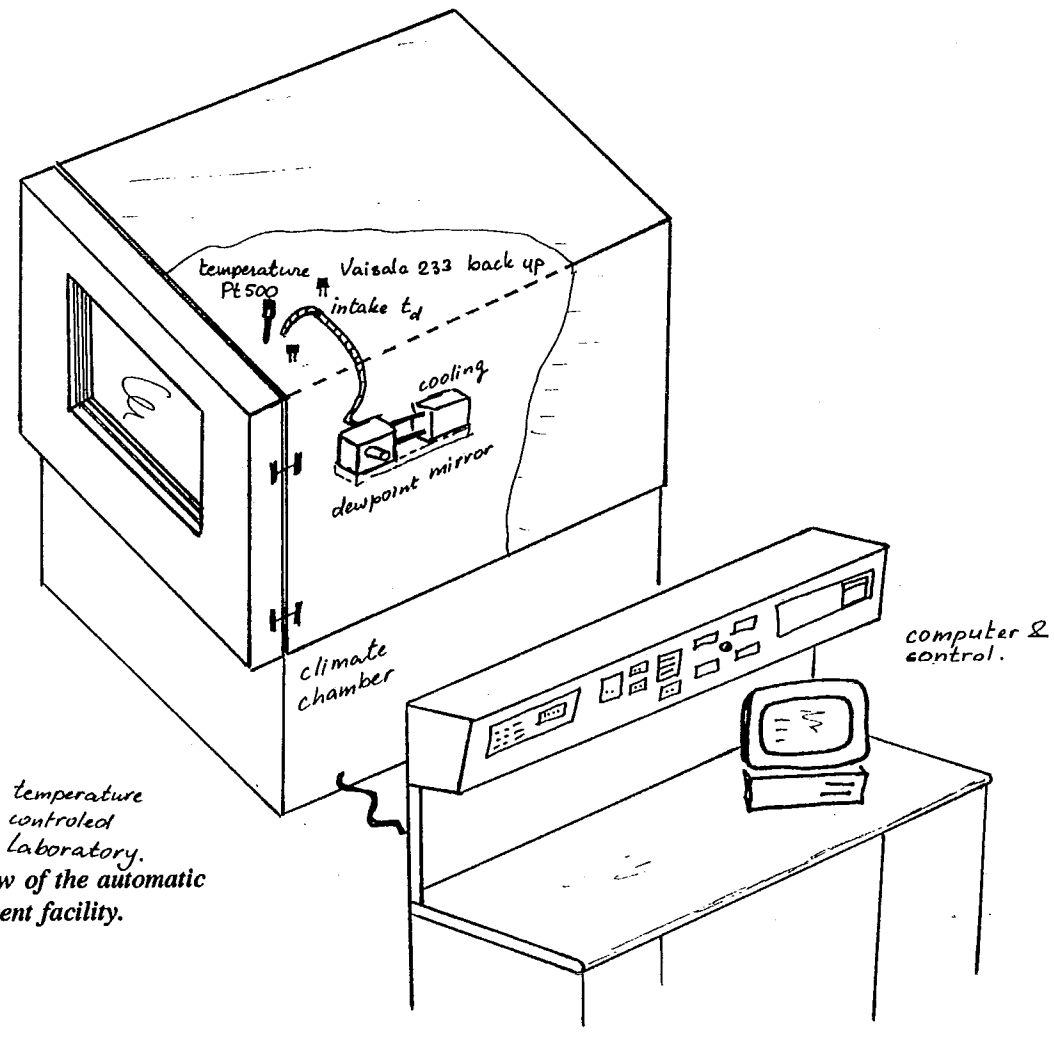

Fig. 2, General overview of the automatic calibration and adjustment facility.

CALIBRATION OF FIELD BAROMETERS THERMOHYGROGRAPHS, RAIN GAUGES AND LIQUID IN GLASS THERMOMETERS

G. M. MUCHEMI

KENYA

1.0 INTRODUCTION

Calibration is a process of ascertaining that an instrument indicates measured values as close as possible to Internationally agreed true values for the quantity or parameter being measured.

2.0. FUNDAMENTAL UNITS AND STANDARDS OF MEASUREMENT

2.2.1. The International System of units (S.I.) recognises unit of Length as the metre (m), unit of time as the Second(s), unit of Mass as the Kilogram (kg) and unit of temperature as the kelvin(k). The Considines, Ref(1) and The Guilde Ref(2) define these units as follows:

2.2. The metre (m) is the Length of a path travelled by light in vacuum during a time interval of 1/299 792 458 of a second. The time of flight is measured by frequency comparison with laser radiation of krypton 86 as the Standard. 1m = 1000 millimeter (mm)

2.3. The second (s) is the duration of 919 263 1770 cycles of the radiation associated with a specific transmission of the cesium atom.

2.4. The Kilogram (k) is the mass of Plantinum Iridium alloy cylinder (Standard) that attains a speed of 1 metre per second when acted upon for one second by a force of 1 Newton(N). Pressure is defined as Newton per square metre and the S.I unit is the pascal (pa). A hectopascal (hpa) is now the unit of pressure in meteorology. 1 hpa = 100pa

2.5. The Kelvin (k) is the fraction 1/273.16 of the Thermodynamic temperature of the triple point of water under 1013.25 hpa pressure. The degree celsius is equal to the kelvin. The kelvin scale has zero temperature at absolute zero, while celsius scale has 273.16°k as its zero.

2.6. These are some of base units whose Standards of measurement are kept at National bureau of standards and must be traced to as a requirement.

3.0 TERMS AND CHARACTERISTICS

3.1. The curve traced by an instrument pointer from zero to maximum indication and back to zero is known as the instrument characteristic.

3.2. The terms range and span describe the region over which an instrument is to measure the variable. Instrument accuracy,

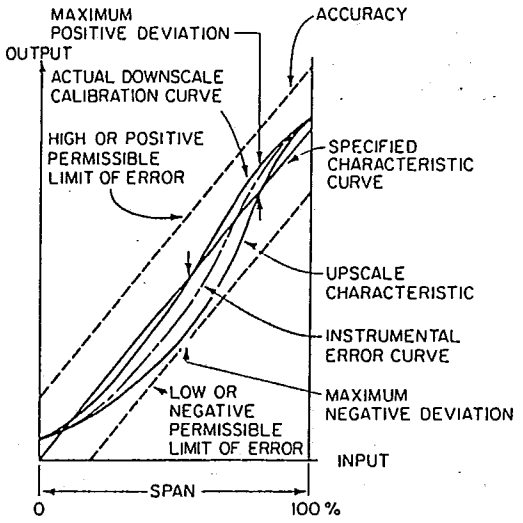

Accuracy rating.

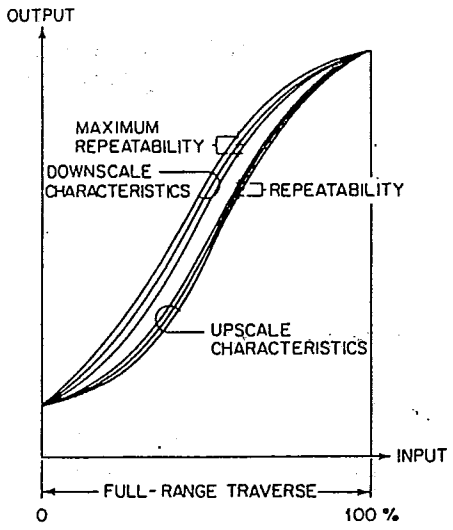

Repeatability.

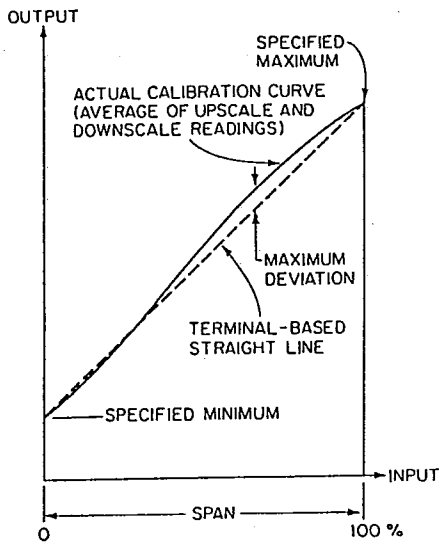

Terminal-based linearity.

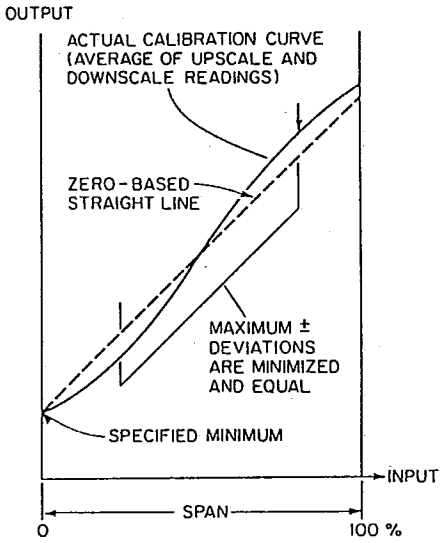

Zero-based linearity.

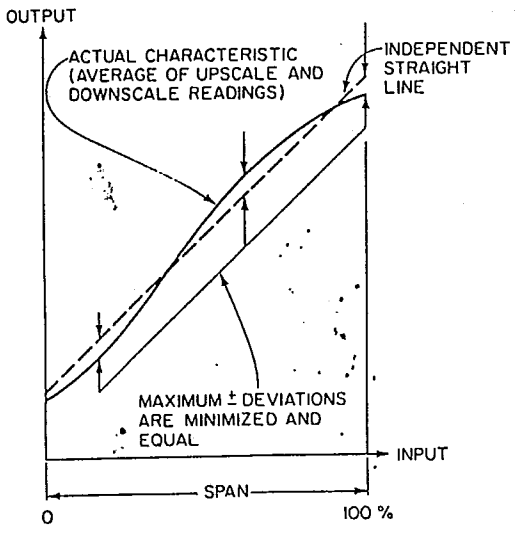

Independent linearity.

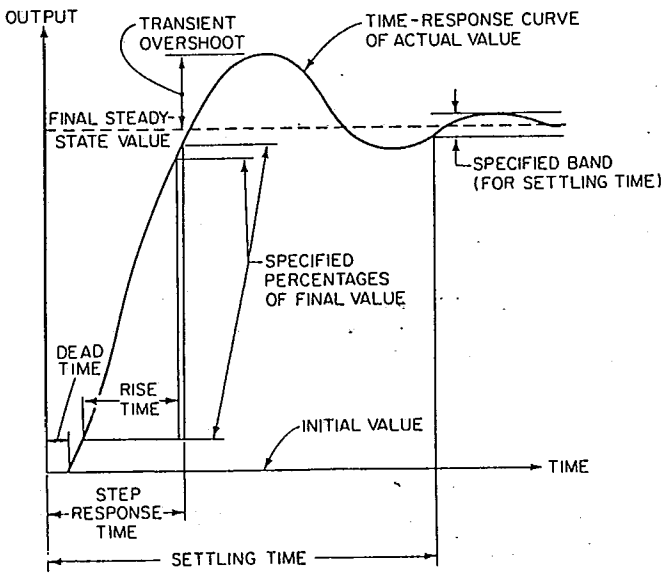

Typical time response of a system to a step increase in input.

readability and repeatability depend on these two terms.

3.3. Accuracy is either rated against span, or range or reading e.g. 0.01% of span or ±0.01 mm of reading.

3.4. The difference between Instrument Indication and the Ideal Value is known as Instrument Error.
Error = Indication - Ideal value.

2.3.5. The correction is the quantity added to the Instrument Indication to get Ideal Value.
Correction = Ideal Value - Indicated Value.

3.6. Damping is a progressive reduction of oscillation in a measuring Instrument. The response to an abrupt change in the measurand is: **critically damped,** if the response is fast and without overshoot; **under damped,** if overshoot occurs; and **over damped** if response is slower than critical. These terms are specified under **Damping factor** on a specific Instrument.

3.7. Rise time is time required for an Instrument to indicate 90 to 95% of a known steady state increment.

2.3.8. Settling time is time required for an instrument to indicate and remain within a specified narrow band centred on the steady state value after initialisation of a step change.

3.9. Time constant (T) is the time required by an instrument to register 63.2% of the total rise for a step change.

2.3.10 Generally, all types of instruments should have very short time constant, but some are deliberately given long time constant (e.g. Symon type earth thermometer) to allow for reading.

4.0. BACKGROUND INFORMATION

4.1. Barometers used at Meteorological Stations are either mercury or aneroid types. The principle of a mercury barometer is that atmospheric pressure balances against the weight of a column of mercury. Aneroid barometers consist of a closed metal chamber (capsule), completely or partially evacuated and a strong spring system to prevent chamaber from collapsing due to atmospheric pressure. The spring force is at equilibrium with atmospheric pressure force, thus affording the measurement of the later. Mercury Barometers read true pressure only under standard conditions. Methods of reducing read pressures to standard conditions are outlined in reference (2) paragraph 3.2.6.

4.2. Thermhygrographs record both temperature and relative humidity (R.H.) against a time scale provided by a mechanical clock. A bimetallic element moves temperature recording pen with changes of temperature while a hair strand control R.H. pen with changes of humidity.

4.3. Rainfall recorders in use here are of tilting siphon or Natural siphon or tipping bucket type. Recording charts are diven by mechanical clocks. Tipping bucket types found here are accumulative type.

4.4. Percentage R.H., vapour pressure, Dew point temperature, maximum and minimum temperatures are measured with Liquid in glass thermometers. Minimum thermometer is filled with alcohol and all others are filled with mercury.

5.0. CALIBRATION PROCEDURES AND FIELD CHECKS

5.1.0 Calibration Equipment

5.1.1. Hass Instrument company Primary and Secondary Barometer Mark II, scale 0 ±1050 hpa is a laboratory standard against which kew barometers and Aneroid Barometers are compared. An automatic gravity correcting scale is incooperated. Pressure is controllable from zero to 1050 hpa within the calibrating system.

5.1.2. Froilab temperature and Humidity Chamber with relative humidity controllable from 0 to ±00% and temperatures controllable from below 0°c to over 50°c calibrates Lambrecht, Joules Richard and Casella Thermohygrographs.

5.1.3. Raingauges are calibrated with a standard camdem rain measure and a standardised dispenser. The dispenser calibrates the tipping bucket raingauges.

5.1.4. A Vibrograf Timer establishes correct timing for all mechanical instrument clocks.

5.1.5. Liquid in glass thermometers are compared with Platinum Resistance (pt) thermometer Bendix PT - 1m-8-8p in a constant temperature oil bath under full Immersion conditions. A standard bridge model 9801 - T with mirror galvanometer model 9462A from Guildline Instrument Company reads the resistance of pt at null point or at balance.

5.2.0 Calibration Procedures

5.2.1 Barometers

Two aneroid barometers are used for field checks of barometers. The barometers are calibrated against the Hass barometer in the range 800hpa to 1020 hpa for both increasing and decreasing pressures at 10 hpa intervals. From the average of up and down scale readings at each set pressure, a correction factor is established. This method checks the instrument against hysteresis error.

Mercury barometers of kew type are calibrated to establish Index errors at 50 hpa Intervals for both up-and down scale set pressures. When gravity and temperature correction are subtracted from set pressures as read from Hass barometer, the remainder constitute an Index error.

The computation of gravity and temperature corrections is done in conformity with instructions in reference (2) page 3.6 paragraph 3.2.6 and respective smithsonian tables-reference (3).

The two aneroid barometers are taken around meteorological stations by a qualified Meteorologist to compare field barometers at 2 years interval. After the field inspection a check is carried again.

5.2.2. Thermohygrographs

The instrument clock is adjusted with the help of vibrograf against gain or loss of time. During assembling process a check is made on pen pivots and all lubricable points and adjustment carried to reduce friction as much as possible. The pen moving elements are adjusted so that the pens indicates ambient temperature and 50% relative Humidity respecitvely. The pen pressure on the chart is also adjusted. The instrument is forced to draw a short horizontal line, then put in the chamber and chamber is tightly closed. The chamber temperatures and Humidities are varied from ambient to minimum and maximum chart indications at 10°c and 10% R.H. intervals. About 30 minutes are allowed for each setting. Average results obtained for up and down scale settings are plotted against those of setting. These should lie within 5°c and 10% R.H. tolerance as shown on diagram (8). The results will show whether range and span are to be adjusted or the instrument requires zero adjustment or its good, and subsequent remedial measures are carried.

5.2.3 Raingauges

Raingauge calibrating measures are matched with catch area of each type of gauge. The rain recorders check points are zero, maximum point on chart, time of siphoning and the actual 5 mm interval accurcay as shown on diargram (9).

5.2.4 Liquid in Glass Thermometers

Maximum temperature indicating thermometers are calibrated or read against standard pt when the bath temperature is rising, and the corrections established for all set points.

Minimum temperature indicating thermometers are compared during falling temperatures. Hence the bath is heated to 40°c. There after cooling is done at interval of 10°c.

Ordinary temperature thermometers are read for set temperatures in both rising and decreasing temperatures. The average of the two reading constitute an error and corrections are computed from these values. A zero correction curve is drawn as shown on drawing (10).

6.0 Conformity Requirements.

6.1. Both mercury and Aneroid barometters accuracy is ±0.3 hpa. Reference 2.P.3.3.

6.2 Thermohygrographs tolerances are ±5% R.H. and ±2.5°c for temperature.

6.3 Rainfall recorders accuracy must remain at ±0.1 mm at all calibration intervals.

6.4 Thermometers accuracy requirement are explained in reference (2) P.4.7, but at Kenya Meteorological services, we prefer ±0.1°c, because experience show that corrections are sometimes ignored.

THERMOHYGROGRAPH CALIBRATION drg-8

TYPE _____

SERIAL NO. _____

DATE _____

SIGNED _____

TYPE _____

SERIAL NO. _____

DATE _____

SIGNED _____

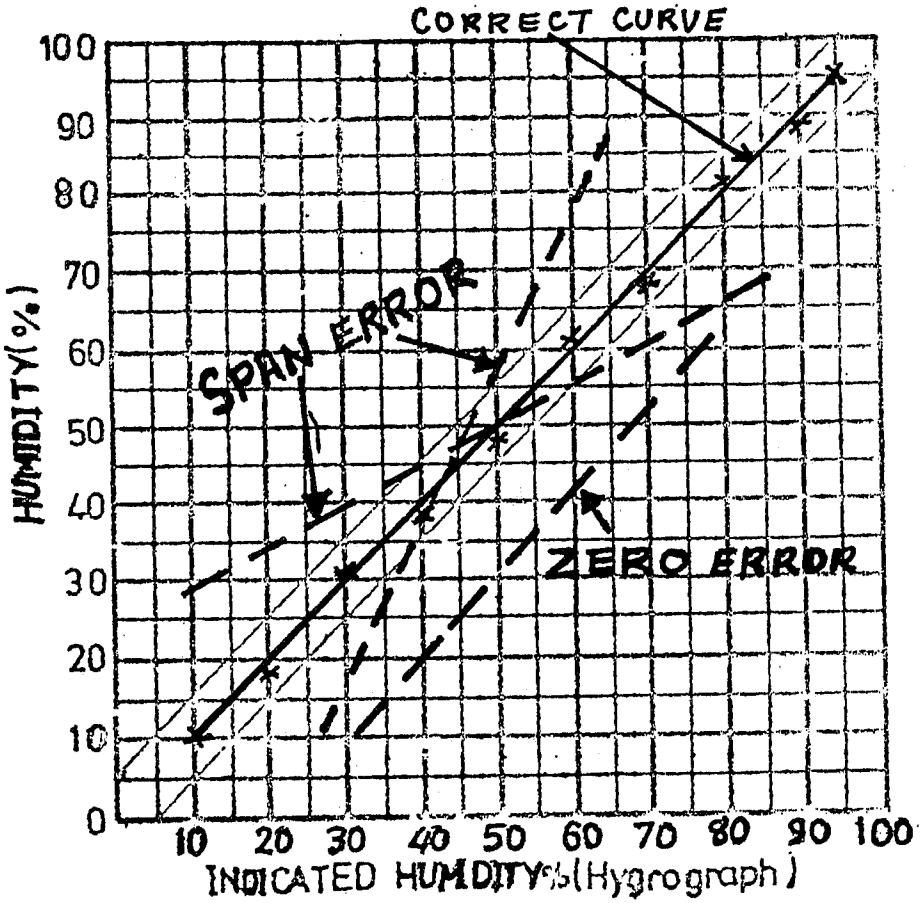

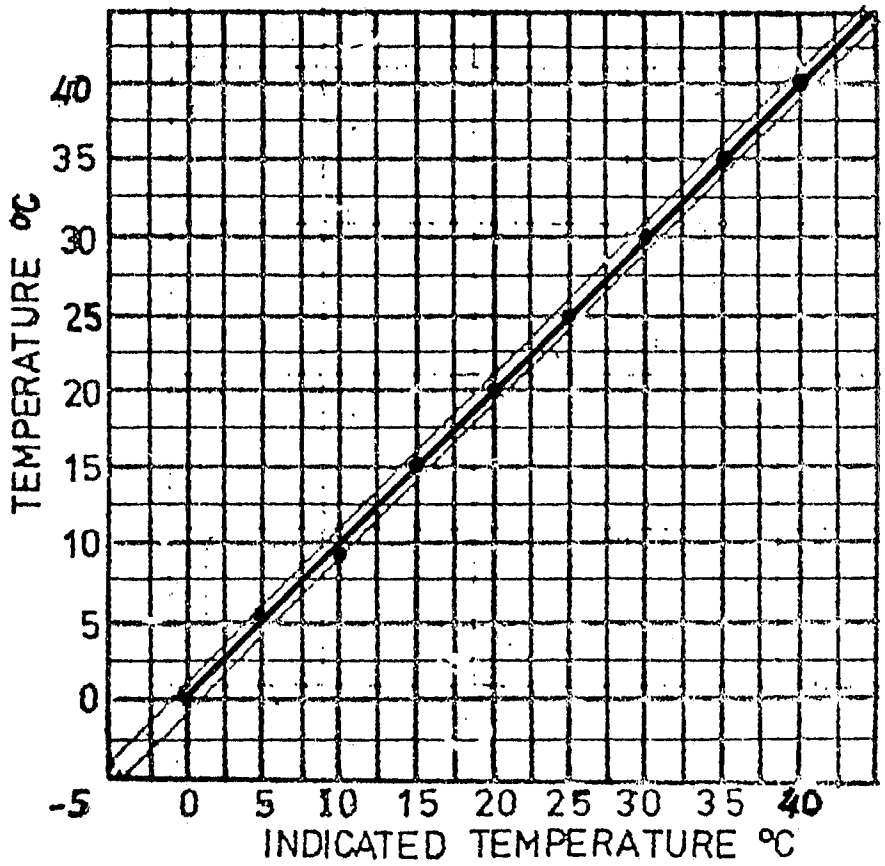

1322M-002-002 jd

drg- 9

DINES' TROPICAL
RECORDING RAIN GAUGE

Date.....19.....

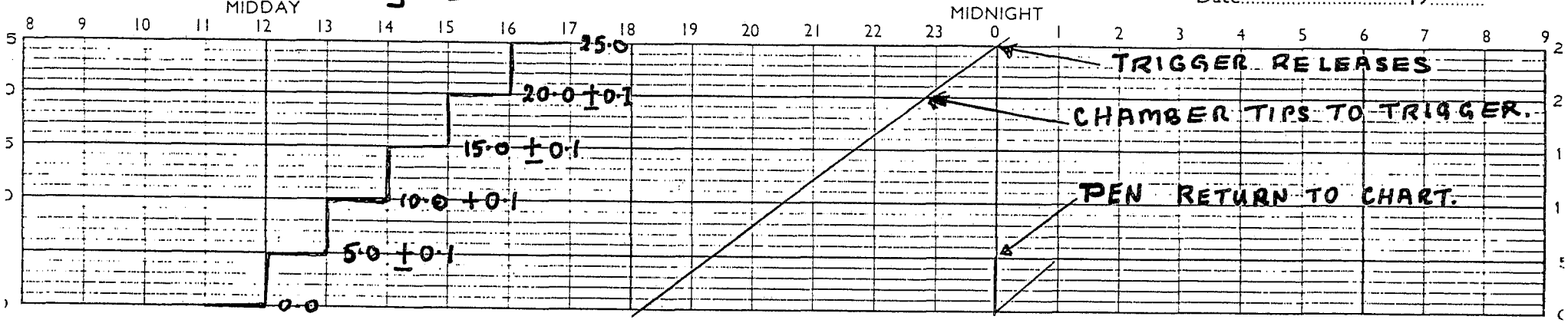

DURATION OF RAINFALL.....h. TOTAL BY RAIN RECORDER.....mm TOTAL BY CHECK GAUGE 9h to 9h.....mm

Scales:- 25mm of rain = 50mm 1 hr = 11·4mm CHART No. W3311/1

THOMAS HAYWOOD & SONS LTD. NEW ELTHAM. LONDON S.E.9. 2BW

drg-10

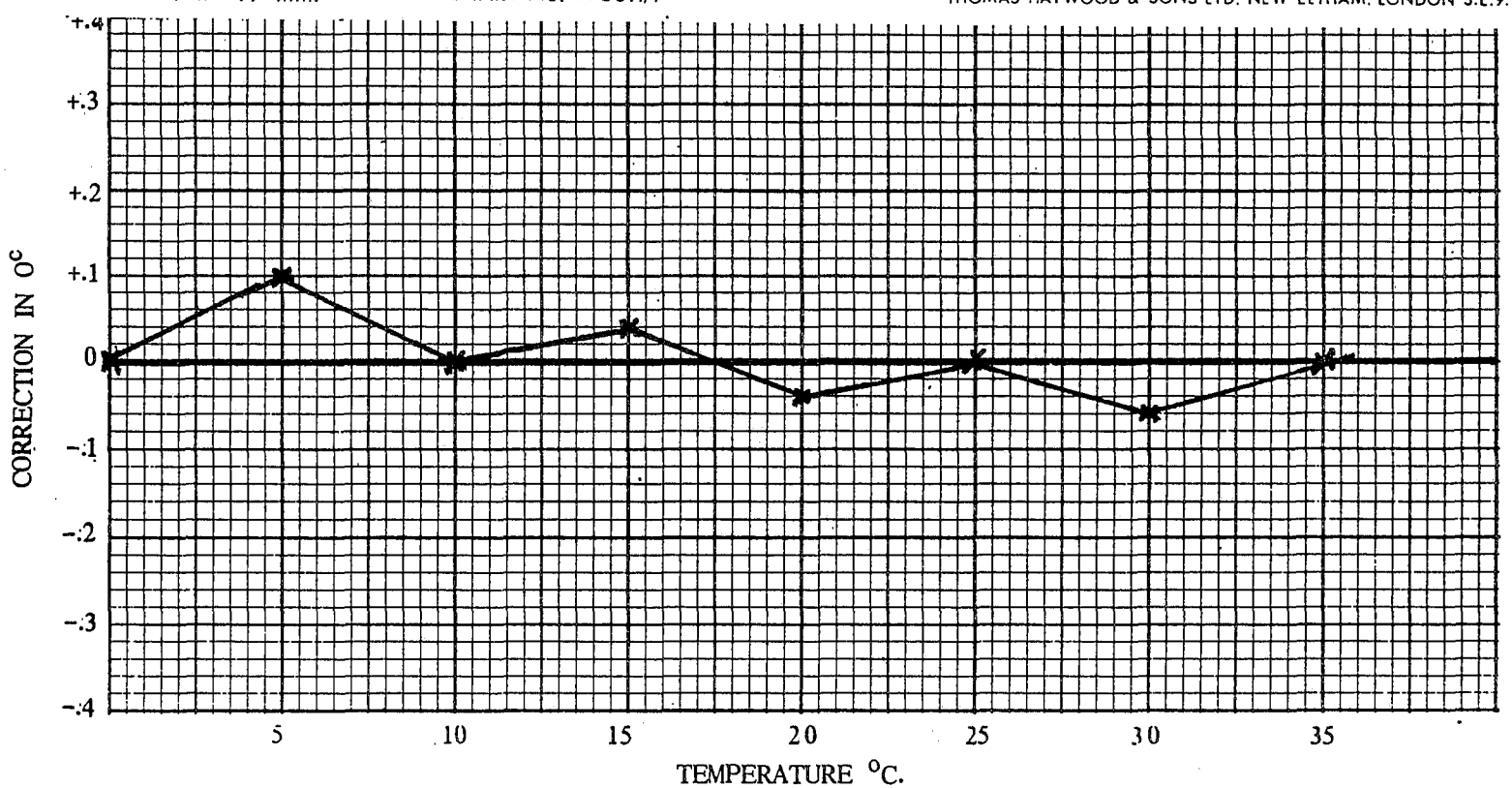

DINES' TROPICAL
RECORDING RAIN GAUGE

Date.....19.....

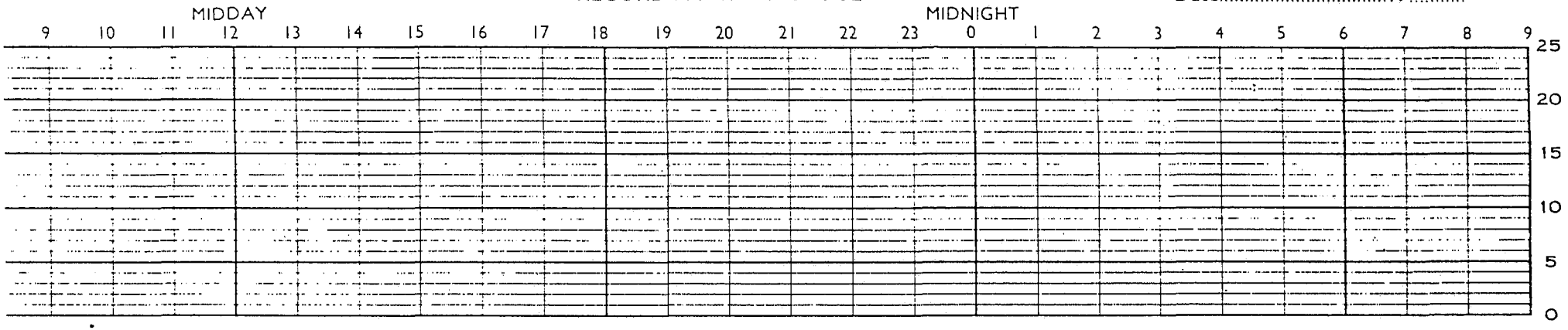

DURATION OF RAINFALL.....h. TOTAL BY RAIN RECORDER.....mm TOTAL BY CHECK GAUGE 9h to 9h.....mm

Scales:- 25mm of rain = 50mm 1 hr = 11·4mm CHART No. W3311/1

THOMAS HAYWOOD & SONS LTD. NEW ELTHAM. LONDON S.E.9. 2BW

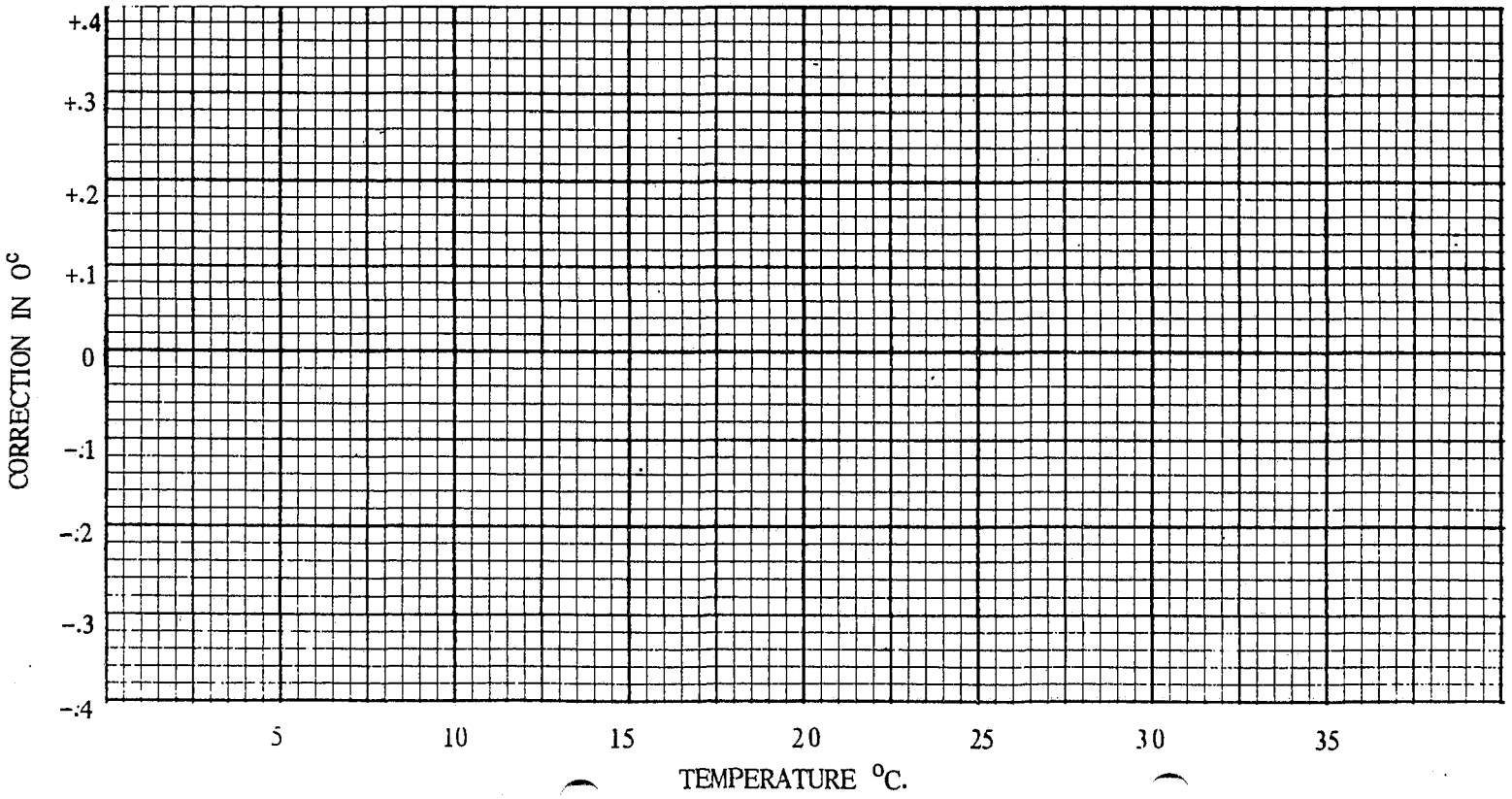

Reference:

1. Process instruments and controls Handbook; 3rd Edition; Douglas M. Considine and Glenn D. considine.

2. Guide to meteorological instruments and methods of observation, 5th Edition, WMO - No. 8.

3. Smithsonian meteorological Tables 6th Edition: Robert J. List. U.S. Weather Bureau.

Calibration of electrical Sensors for Temperature, Pressure, Humidity and Wind

Olbrück, G.

Deutscher Wetterdienst
Instrumentenamt Hamburg
Frahmredder 95, D-22361 Hamburg 65

1.0 Introduction

The increasing use of electrical sensors in automatic meteorological weather stations brings about that the calibration procedures are carried out with an electronic equipment which has to allow for the connection of different types of sensors with different kinds of signals and data formats. Besides, routine and environmental measurements have opened a wide market which is served by manufacturers with a wide-ranging offer of different sensor types.

Therefore, the user is facing an extensive offer of meteorological sensors from which he has to lay down a standard if he will not fall a victim to this diversity. The Instrumentenamt of the German Weather Service in Hamburg accepted this challenge by mounting a programmable system for short- and long-term tests of individual adapted meteorological sensors.

2.0 System for short- and long-term tests of individual adapted meteorological sensors

2.1 System design

The METEOROS-System serves for the calibration and testing of meteorological sensors using reference sensors for each parameter. These references are secondary references which in most cases have been calibrated with locally available primary standards described in the following chapters.

An essential characteristic of the METEOSROS-System is a multi-purpose software for data acquisition, processing, analyzing and displaying. As can be seen from figure 1 the master station serves two slave stations, the laboratory places for pressure and humidity tests as well as sensor calibration. The whole system consists of three IBM PS/2 stations, the cabling and the signal boxes with special interfaces for the connection of different sensor types.

2.1.1 Hardware structure

According to this structure the system provides the user with a multitude of connection facilities.

Analog inputs/outputs -
Today the system has 16 analog inputs and additional 7 inputs for Pt 100; the number of analog inputs can be increased up to 64 inputs, those of the Pt 100 up to 16. Besides, there are two analog outputs for recording purposes controlled by the user software. The input amplifier is programmable between a gain of 1 to 500 according to the specific channel.

Digital inputs -
There are two serial inputs for different pulse sequences, 12 serial inputs RS 232 and 4 serial inputs RS 422.

Data processing -
An IBM PS/2 extended by a 486 DX 33 microprocessor used as a master station serves two slave stations by a duplex RS 422 data line each. The data are stored on a 240 MByte fixed-disk.

To overcome the problem of multi-tasking when using DOS as an operating system the product family of the IBM Realtime Interface Coprocessors (RIC) was installed. The RIC-product allows multitasking, real-time processing and communication with different controllers and instruments. The RIC-card installed in the IBM PS/2 uses the INTEL 80186 micro-processor; so, configuration corresponds to a processor in a processor.

2.1.2 Software structure

Data processing runs with the operating system DOS 6.0 and WINDOWS 3.1; therefore, a mouse can be used to pick out all functions, even those of the IMC-Software FAMOS which is used for the **F**ast **A**nalysis and **M**onitoring **O**f **S**ignals. The data acquisition is carried out with the MS-C/C++ user software which allows for the connection of different types of sensors to the system.

The analog data acquisition is executed with a maximal accuracy of 12 bit binary corresponding to 0.025% of the final deflection and the digital data acquisition guarantees a 32-bit floating-point accuracy. The normal measuring frequency is 0,1 Hz, whereas an analog signal transfer can be operated with a maximal scan of 1 kHz. Up to 6 groups of measuring data can be processed each containing the signals of 8 analog/digital - pure and mixed - sensors. The transfer rate ranges from 50 to 19.200 Baud using the serial data channels (RS 232/422).

Data processing is carried out in this way that all digital signals collected faster than 0,1 Hz are averaged over 10 seconds automatically. The conversion of the raw data from sensors for different parameters in physical mks-units is also done automatically. The running data of a special sensor can be displayed on-line.

2.2 Reference sensors

2.2.1 Pressure

The main reference for the calibration of pressure sensors is the regional standard mercury barometer which shows an accuracy of +/- 0,02 hPa. A secondary reference is the SPERRY Air Data Pressure Standard type ADT-321 with a pulse output. The integration time for each value is 10 s and its accuracy +/- 0,002 hPa. Besides, the DRUCK, Precision Digital Barometer type DPI 141 is used as a secondary standard with an accuracy of +/- 0,025 hPa. 10 seconds averages are processed and transferred via the serial output.

2.2.2 Temperature

The calibration of reference thermometers is carried out with the ISOTECH Triple-Point Calibrator which uses water (Triple-Point: 0,01 °C, accuracy: +/- 0,0001 K), Diphenyl-Ether (Triple-Point: 26,869 °C, Accuracy: 0,002 K) and Ethylene-Carbonate (Triple-Point: 36,315 °C, Accuracy: 0,001 K) for the appointment of three fix-points in the positiv temperature scale. Triple-points are ideal fix-points for the calibration of thermometers, because they can be produced precisely and maintained over a long time.

2.2.3 Humidity

The calibration of humidity sensors in the climatic chamber is done with an ASSMANN-Aspirator using quartz sensor QUAT 200 from HERAEUS as dry and wet thermometer with an accuracy of +/- 0,03 K. Additional, especially for the negativ temperature area, a dew point mirror type S 3000-Special from MICHELL is used in the range -30 °C to +40 °C with an accuracy of +/- 0,15 K

2.2.4 Wind

The Instrumentenamt Hamburg operates a return-flow wind-tunnel with an elliptical cross-section (a: 1.03 m, b: 0,66 m). A wind velocity of 0,2 m/s to 50 m/s can be generated which is made available on a test section of 1,28 m. The horizontal air flow in this section is defined by a TSI type 8530-1/8470 in the range 0,05 to 5,0 m/s and by a Betz-Microanemometer in the range 5 m/s to 50 m/s.

In the past no primary reference systems for the calibration of wind sensors have been available. Therefore, the calibration of wind sensors in the wind-tunnel was only sufficient for network sensors. Today, a Laser-Doppler Anemometer (LDA) is a suitable instrument to carry out a highly exact determination of the velocity of flow using liquid particels generated by an aerosol generator and sprayed into the flow as a tracer. A calibration of the LDA is not necessary, because the system can be explained by physical constants and system parameters like the wave length of the laser light and the optical geometry of the laser beams. The measuring-range extends from -40 m/s to 200 m/s subdivided in smaller ranges specific for the system. Therefore, a resolution of 3 mm/s is available in the lower ranges - for instance: - 0,2 m/s to + 0,6 m/s.

3.0 Conclusion

The above METEOROS-System represents a solution how to use analysis software developed for the DOS operating system in a multitasking environment. As it was not possible to buy such a system on the market a lot of user software had to be written to make the system as universal as it works today.

The high resolution in the data acquisition brings about that the phases of icing and deicing in the climatic chamber as well as the behaviour of sensors especially in the negativ temperature range can be displayed in detail. Thus, the quality of meteorological sensors is to be increased in close cooperation between the user and the manufacturer. This is one of the main tasks in quality controlling since the national meteorological service has decided not to develop sensors by itself.

At a time of strong business there is hardly time to read large articles, therefore, the presentation of measuring results on a monitor or as a hard-copy from a colour printer is the quickest and sometimes most impressive way of information. In this regard the FAMOS analysis software provides the user with an extensive parcel of tools especially for editing in a natural science vocabulary with the use of mathematical functions. In this respect the conversion from DOS to UNIX is not a question of the hardware but has to be answered if these powerfull analysis software modules will be provided for a multitasking operational software.

4.0 Recommendation

With an extension of the 1-dimensional LDA-System one will be able to make more accurate and efficient flow measurements. With an advanced flow measuring equipment there is the possibility to analyse the quality of the velocity distribution in a special cross-section of flow over the entire measuring range without affecting the actual conditions of the measurement. On the other side, one will be able to measure the turbulence in the distinct environment of a mechanical or electrical wind sensor or different kinds of meteorological screens.

A further extension with a phase Doppler opens the possibility to detect the distribution of particel sizes and numbers which are passing a special measuring volume, that means calibration of rain gauges and particel collecting instruments. Particel concentrations are analized with a data rate about 100.000 particels per second.

In this regard the laser technique provides the user with a powerful tool for the calibration of wind sensors as well as particle collectors. A disadvantage of the system is the high capital expenditure which forces the services to decide on the cost effectiveness of such an investment.

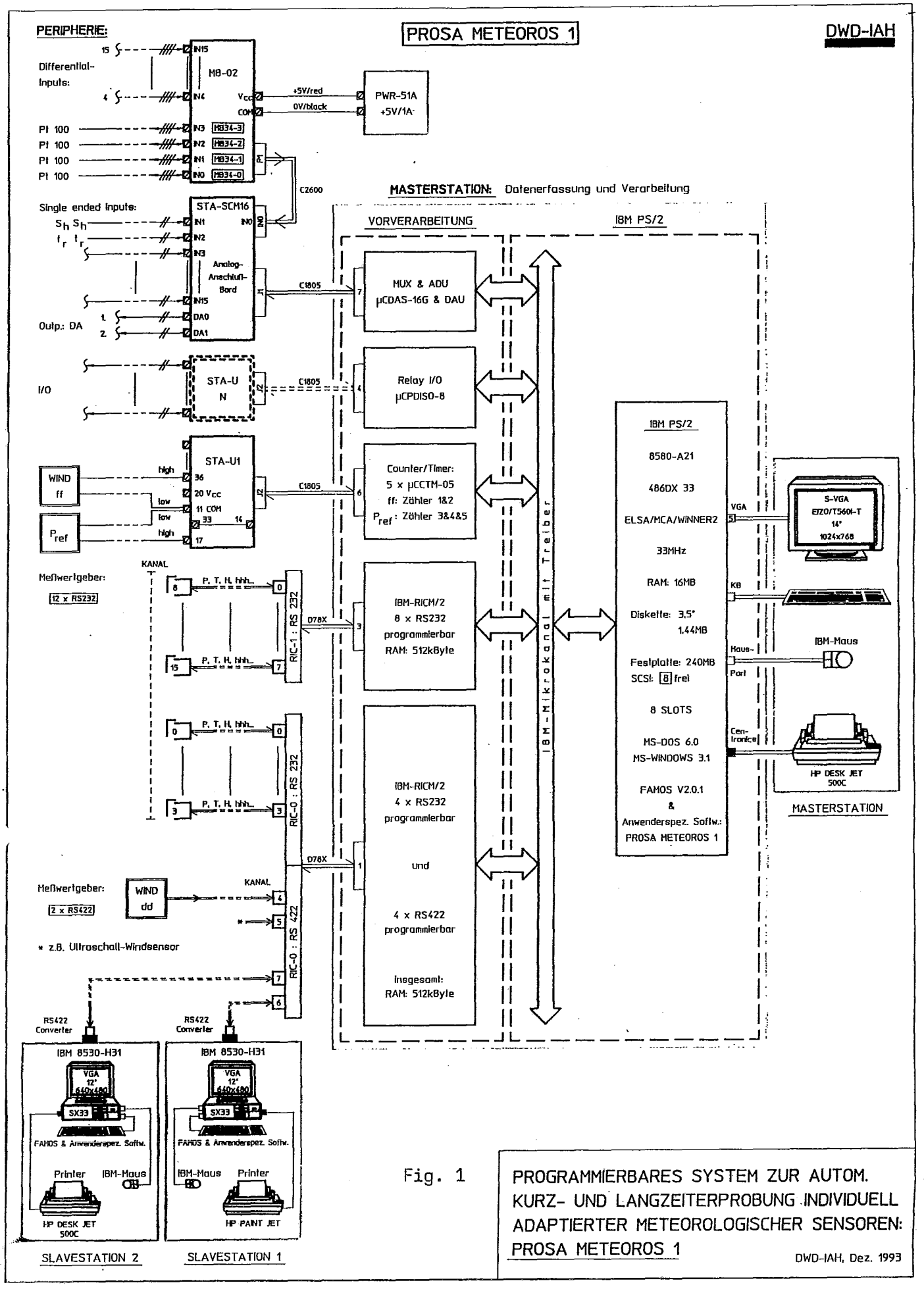

Fig. 1

PROGRAMMIERBARES SYSTEM ZUR AUTOM. KURZ- UND LANGZEITERPROBUNG INDIVIDUELL ADAPTIERTER METEOROLOGISCHER SENSOREN: PROSA METEOROS 1

DWD-IAH, Dez. 1993

FIELD EXPERIENCES IN UNMANNED METEOROLOGICAL DATA COLLECTION

by

R.D. Vashistha, M.S. Rawat and R. Pratap
Meteorological Office, Pune. India

1. INTRODUCTION

The Indian Peninsula has varied weather conditions over an year. It has its own peculiar phenomena of summer and winter monsoons. Quite a few cyclonic storms frequent the region each year resulting in enormous loss to life and property. Collection, processing and dissemination of real time meteorological data pertaining to disturbed weather conditions in the Indian Peninsula is therefore of paramount importance for disaster warning and cyclone havoc mitigation. The availability of the Indian National Satellite System has opened up a very high potential for the continuous monitoring of the meteorological conditions over the land and surrounding ocean environment.

2. INSAT - DATA COLLECTION SYSTEM CONCEPT

As part of the overall meteorological application programme under the INSAT project, India Meteorological Department (IMD) has established 100 weather data collection systems, in different parts of India, in remote and inaccessible places. The system consists of the following components.

(i) Sensors and signal conditioning unit.

(ii) The electronics package consisting of Data Conversion, Storage and Transmission System (DCSTS).

(iii) Antenna.

(iv) The power supply system.

(v) Weather proof housing for enclosing the electronics and power supply.

(vi) The onboard DCP transponder (DRT).

(vii) Ground receiving and data processing system.

3. PERFORMANCE OF DCP SYSTEMS.

Transmission of real time meteorological data through satellite was started in India with the launch of INSAT-1B in 1982. The electronics package like DCSTS and signal conditioning units of DCP system have been designed and fabricated by using high quality components. Both these units have worked upto the required levels of expectation. The technical characteristics of the various components of the systems are given in Table 1. The performance of power supply

system has been of prime concern in operating and maintaining these systems in India. Most of the breakdowns were due to battery rundown caused by the frequent failures in the commercial ac supply on which these systems were operating in the initial phase. To overcome this, photovoltaic charging sources are being provided at most of the DCP sites in a phased manner.

4. DATA QUALITY

The evaluation of DCP data with ground truth from co-located observatories have been carried out. Intercomparison of data from three co-located DCPs have also been carried out. The overall accuracy of the data from the DCPs was found to be mostly within the required limits specified by WMO for acceptance of data from automatic type of weather reporting systems.

With uninterrupted power supply by using solar panels, it is observed that 19 of these stations have given troublefree operation without a single failure for more than 400 days of continuous operation. The one failure was due to antenna connector/cable shorting. The quality of DCP data from these stations has been within the specified limits on most of the occasions. Fig 1 presents the deviation of DCP temperature, pressure and dew point from the surface observatory data for a typical month at a typical unattended site. It is observed that temperature and pressure values agree within $1^{o}C$ and 1 hPa for more than 95% of the observations. Dew point, however, agrees within $1^{o}C$ for 65% of the observations only.

5. Every effort is being made to bring all the 100 stations to the high level performance of the presently 20 stations. Continuous experimental studies are being made to achieve a better performance level and repeatability for the dew point measurements.

The present system reports only the instantaneous wind as against the averaged wind needed for the synoptic purposes. Hence the relative performances could not be compared. However, an identical wind system used in aeronautical meteorological observing stations has given an excellent performance. Rainfall data are not compared here for want of enough comparative measurements.

TABLE - I

Technical Characteristics of Data Collection

PARAMETER	SENSOR USED	MEASUREMENT LIMIT	BASIC ACCURACY
1.Air temperature	Thermistor	0-50°C or (-20 to +30°C)	0.20°C
2.Wet bulb temperature	Thermistor	0-50°C or (-20 to +30°C)	0.20°C
3.System Housing temp.	Thermistor	0-50°C or (-20 to +30°C)	0.20°C
4.Wind speed	Cup Generator Anemometer	0-100 KNOTS	1KNOT
5.Wind direction	Potentiometric wind - vane	0-360°	1°
6.Atmospheric pressure	Potentiometric aneroid capsule	0-100 hPa above a fixed datum	0.3hPa
7.Relative humidity	Humicap	0-100%	10%
8.Rainfall	Tipping bucket raingauge	0-10239 mm	1 mm

DATA TELEMETRY LINK CHARACTERISTICS

(a)	Carrier Frequency	402.75 MHz
(b)	Data Coding	PCM-NRZ
(c)	Data rate	4.8 kHz
(d)	Data Band width	6 kHz
(e)	Frequency stability	±1 ppm/year max
(f)	Antenna	Left hand circularly polarised tapered helix having a 12db gain and 40° beam width
(g)	Transmitted Power	3W to 10W variable
(h)	EIRP	16.5 dbW.

POWER SUPPLY SYSTEM

(a) Lead acid batteries of + 24V/100AH with an automatic arrangement for charging by ac main chargers.

(b) Maintenance free batteries of ±24V (100AH) with an arrangement of automatic charging by employing photovoltaic modules of 30 W capacity.

TOTAL SYSTEM POWER CONSUMPTION

(i) Total power consumption (+ve) = 50 W

(ii) Total power consumption (-ve) = 15 W

DATA TRANSMISSION TECHNIQUE

Pseudo Random Burst Sequence (PRBS) mode of transmission giving three messages every hour.

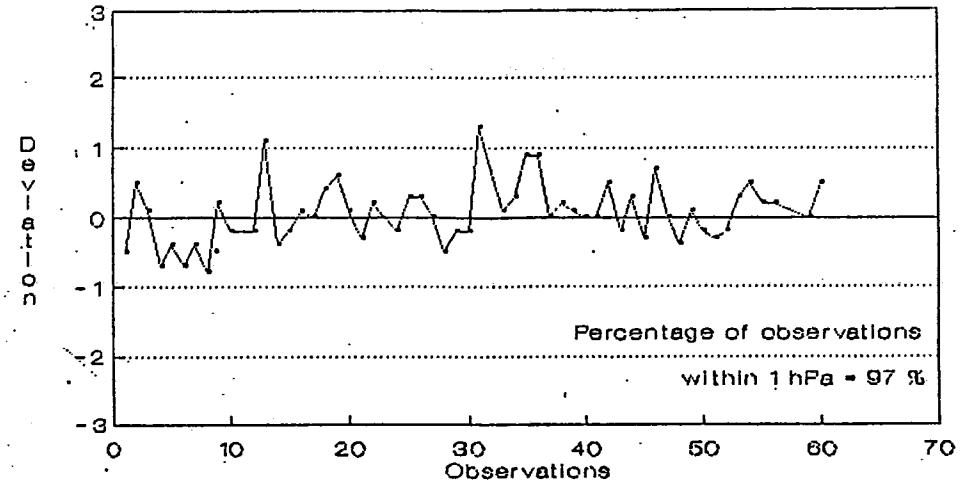

Pressure

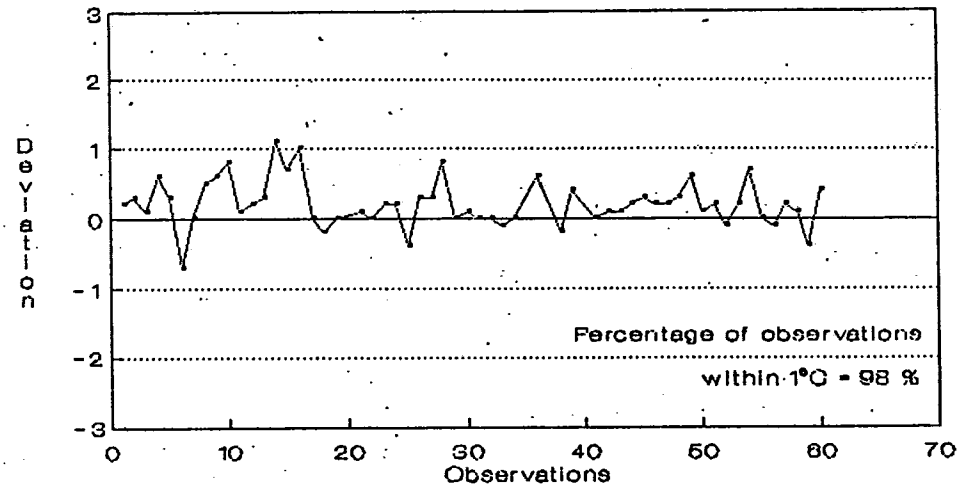

Dry bulb Temp.

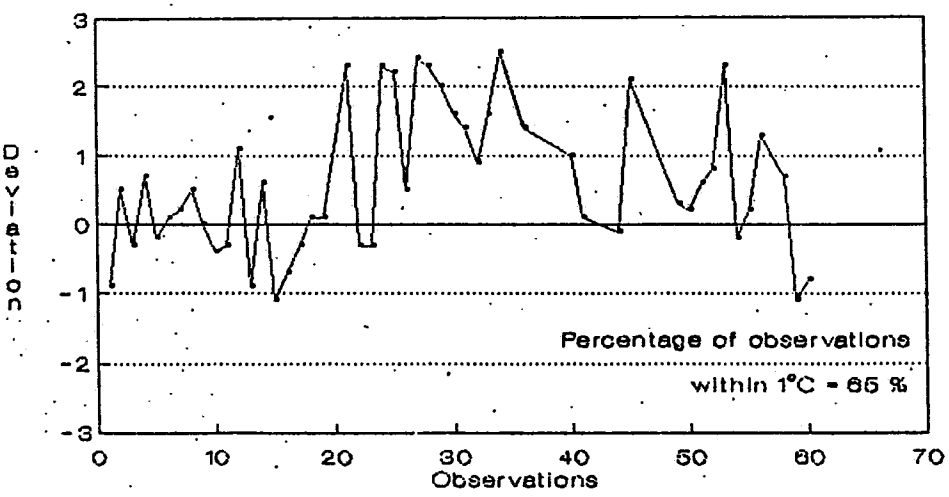

Dew point Temp.

Performance of DCP system at Pune w.r.t. synoptic observations
Month : June 93

ОБЗОР КАЧЕСТВА НАЗЕМНЫХ МЕТЕОРОЛОГИЧЕСКИХ ПРИБОРОВ И МЕТОДОВ НАБЛЮДЕНИЯ ВО ВЬЕТНАМЕ

Чан Ван Шап
Управление сети Гидрометеорологической службы Вьетнама.

OVERVIEW OF SURFACE METEOROLOGICAL INSTRUMENT QUALITY AND METHODS OF OBSERVATION IN VIETNAM

Tran Van Sap
Network operation Department of HMS of Vietnam

The meteorological network in Vietnam was mainly established in the years 60-70 of this century. In Southern part of the country, before 1975, the network was supplied with " West " meteorological instruments and methods of observation (MIMO), while the Northern part mainly used the former Soviet and European ones.

Nowadays, MIMO in Vietnam has changed very slowly. Most of instruments are absolete . The calibration system has not been improved. So the quality of some instruments has not been of international level and not met the WMO requirement.

Vietnam is hoping to cooperate with all country-members of WMO and to be helped by the WMO/CIMO in the field of instrument development, so that in near future, it can attain the regional and international level.

This 's first time an expert of Vietnam attends the CIMO/TECO with the hope to exchange views and experiences with other delegates and through the METEOREX-94 he 'll get more usefull information on recent development of MIMO and find opportunities of cooperation and development.

Сеть метеорологических станции в Вьетнаме в настоящее время имеет 160 станции, расположенных на не большой территории, но растянутой на 16 градусах северной широты. Имеются и станции на равнинах, на высоких горах, на берегах моря и также на отдаленных островах восточного моря.

Вьетнам находится в тропическом мусоном районе. Здесь имеются два сухого и дождевого сезонов, и также являются ярко отличающими холодным и теплым сезонами. Вьетнамский берег моря растянут на более чем 3000 КМ со севера на юг и находящийся в районах активных действии тайфунов, тропических циклонов и других возмущении, вызывающих ежегодные опасные явления погоды.

Поэтому метеорологическая работа в Вьетнаме встречает большую трудность в выборе сщрта инструментов и методов наблюдения для обеспечения качества наблюдения и измерении.

Сеть метеорологических станции в Вьетнаме в основном была основана в период 60-70ых годов этого столетия. Некоторые станции в важных репрезентативных центрах были основаны французскими метеорологами в начале 20 -ого столетия и продолжают действовать в настоящее время. На юге страны метеорологические станции почти были основаны только после освобождения Мая 1975 года.

Поэтому метеорологические инструменты и методы наблюдения в Вьетнаме имеются следующие особенности :

- На Юге страны до 1975 года, пользовались в основном инструментами и методами наблюдения страны - запада, как Америка и Франция.

- На Севере со дня образования и на Юге после 1975 года пользовались инструментами и методами наблюдения бывшего Советского Союза и других стран восточной Европы.

Такое положение дел приводит к определенной трудности во обработке и сравнении данных и определения качества наблюдения.

Кроме того, под влиянием 30-летней войны и из-за нынешних изменении международных экономических отношении, обеспечение и переобеспечение метеорологических интрументов

по современному направлению в Вьетнаме медленно осуществлено.

Можно указать следующие специфики в области инструментов и методов наблюдения :

1. Метеорологические приборы измерения основаны со дня образования станций, во основном с 25-30 лет тому назад. В том числе и имеются приборы, действующие до настоящего времени. Сорт приборов многообразен и приведен от многих источников и из различных стран. Чуствительность приборов, вобщем, не велика.

Состояние качества некоторых основных приборов для наземного наблюдения, следующее :

+ Приборы для измерения ветра :

Наболее чем 90% станций используются традиционные флюгеры Вильда. На набережных и островых станциях, флюгеры Вильда очень быстро выходят из строя, скорости ветра не достаточно определены, особенно в диапазоне высоких скоростей. В случае ураганых ветров выше 40 м/с, наблюдение методом Бофорта является основным.

В неданнее время, мы внедряли и успешно пользовались некоторыми современными приборами измерения ветра, такими как приборы в комплесе автоматической метеорологической станции фирмы ВАЙШАЛА / Финляндии / , приборы ТАВИД-87 / Франции /, дистанионные приборы ЕЛ и ЕУ - 1 /Китая/. Результаты пользования показывают, что эти приборы являются современными, с высокой точностю и большими диапазонами измерения скорости. Они удовлетворяются требованиям измерений скорости ураганых ветров. Однако существуют и проблемы, которые требуют дальнейщего решения, например источники питания для отдаленых станции, устранение шума радиопередачи на измеряемую скорость, жравчина элементов прибора из-за соленного воздуха на островых и набережных станциях и.т.п.

В следующем 2-летнем плане было запланировано полностю изменение всех флюгеров Вильда более новыми современыми приборами Китая, Франции и Англии, по

...

направлению самозаписи и дистационного измерения.

+ Самозаписцы для регистраций осадков включают в себя 121 штуку симфоного типа, были сделанные в бывшем советском союза и пользованы, по крайней мере, уже 20 лет. Плювиографы симфоного типа, как извесно, точно регистрируют количество осадков в случае слабого и умеренного дождей. В случае сильных дождей, что часто встречается в 6-месячном дождевом сезоне в Вьетнаме, они проявляют небольщую эффективность. Линия записи на ленте, в таком случае, обычно прямолинейны из-за неслива воды из сосуда прибора. Кроме того, следующие сливы, как обычно отступаются от 10-ой точки.

Простые дождемеры /площадь сечения 200 см2 / являются распространенным прибором на более 760 станциях и постах сети. Однако результаты измерения по этому прибору уверены и сравнимы с результатами других приборов.

+ Для измерения атмосферного давления на 58 станции, применяются ртутные барометры типа КЮУ /49 штук/ и Фортения /9 штук/. 60% этих барометров было сделано в бывщем Советском Союзе, остальные были сделаны в Китая, Франции и Польше. Около 70% действующих барометрав имеет поправки межьше чем / 0,3/нра, 30% оставщих имеет поправки выше чем допустимого предела. Калибровка действующих барометров в нашей стране так же встречает большие трудности из-за отдаленности местонахождения станций, низкого уровня развития транспорта в горных районах.

Барографы / а так же и термографы и гигрографы / пользуемые на сети, были сделаны так же в Советском Союзе 20 лет тому назад, но еще не плохо работают. Особенностью этих приборов является механическая устойчивость, точность и удобство пользования.

Основным недостатком традиционных метеорологических самопйпев является бумажная лента. В условиях высокой влажности /больше 90%/ и в дождевое время, линия записи обычно сливается, что приводит к трудности в обработке лент с требуемой точностю.

+ Сеть радиационных станции в Вьетнаме не велика. Приборы для измерения - советские. Однако за длительный период эксплуатации, они уже стали малоустойчивыми, низкокачественными и

...

они стоят перемене новыми современными приборами.

+ Приборами измерения испарения с поверхности водоема являются советские ГГИ-3000 и американские КЛАСС-А. Оба этих приборов дают хорошие и сопоставляемые результаты измерения.

+ Для измерения других параметров, такие как температура воздуха и почвы, влажности воздуча... применяются обычные популярные ртутные и спиртные термометры и они всегда дают уверенные результаты.

На некоторых метеорологических и агрометеорологических станциях, были применяемы приборы дистанционного измерения температуры почвы, произведенные нашими специалистами, тоже дают удовлетворяемые результаты. В настоящее время, такое направление развития у нас заслуживает особое внимание и является перспективным.

2. Второй особенностью является то, что система калибровки не достаточно и комплесно построена. Гидрометслужба Вьетнама в настоящее время может калибровать только приборы для измерения температуры, влажности воздуха и атмосферного давления. Был запланирован проект построения системы калибровки приборов измерения ветра и солнячной радиации за период 1994-1995 гг. Важной проблемой сейчас является выбор сответствующих и удовлетворяющих техническим требованием, приборов и методов калибровки.

Исходя из вышесказанного, можно сказать, что приборы измерения и соответственные с ними методы наблюдения в Вьетнаме еще слабые, осталые и низкокачественные и пока не отвечают международные требования и стандарты.

Мы желаем и решительно стараемся так, чтобы за не далегкое время метео инструменты и методы наблюдения достигают регионального и международного уровня.

Для достижения этой цели, мы считаем, одним из важных условии является сотрудничество между Вьетнамом и всеми другими странами членами ВМО. Мы желаем также получить всестороную помощь КИМН во области инструментов и методов наблюдения. Основной целю нашего прибывания на этом совещании КИМН, в том числе на этой конференший является обмена опытами и через МЕТЕОРЕХ-94, изучение новых достижении других членов во области инструментов и методов наблюдения и искание возможности сотрудничества и развития.

THE ELECTROMECHANICAL MACHINE SHOP AT STRA OF THE NATIONAL HYDROLOGICAL AND MARIGRAPHICAL SERVICE OF ITALY

ANTONIO RUSCONI
NATIONAL HYDROLOGICAL AND MARIGRAPHICAL SERVICE, ROME, ITALY

ABSTRACT

In Italy the Hydrological and Marigraphical Service has used its own Electromechanical Machine Shop at Stra (Venice) since 1908 for the construction, the repair and the calibration of the main measuring instruments which the Service itself and numerous other users need. This paper illustrates the main instruments constructed and their evolution over the years thanks to the experience gained and the gradual transformation from the electric to the electronic field.

1) INTRODUCTION - The first Hydrological Office, in the modern sense of the word, was established in 1908; it had become necessary in the Veneto regions where the "Magistrato alle Acque" with an ancient and famous tradition dating back to the times of the Venetian Republic, had just been reconstituted with the principle task of managing and regulating the waters of the rivers and of the sea around the Venice Lagoon.

The Hydrological Office, having the responsibility, on behalf of the Magistrato alle Acque, to deal with the orderly and methodical collection of the hydrological and meteorological observations regarding the rivers and their mountain basins, the Lagoon and the sea of Venice, began to install several monitoring networks opportunely located in the Department. At first these were equipped with measuring instruments acquired from abroad, seeing that, at that time, there were no specialised firms in Italy for the construction of hydrological instruments.

Later, the increase in number of the observation stations showed up the need for an autonomous organism able to take care of the maintenance, the management and repair of the ever more numerous meterological and hydrological instruments installed, so that in 1911 a precision mechanical Machine Shop, directly responsible to the Hydrological Office, was established and located initially in some of the premises of the famous National Villa "Pisani" at Stra, an important and active town not far from Venice, on the way to Padua, along the famous "Riviera del Brenta". At the same time an agreement was stipulated with the Hydrological Institute of Padua University aimed at scientific co-operation in the hydrotechnical field through an optimal use of the installations of the Machine Shop.

In 1915, with the acquisition of new premises and special machine tools, the Machine Shop began the study and the construction of its own instruments needed by the Hydrological Office; in 1919 it began to mass produce hydrometrographs and

current meters for all the Italian Hydrological Service, established in 1917, and for the other offices of the Civil Engineers, for the Land Reclamation Consortium and for other public and private agencies.

At a distance of almost 80 years from the establishment of the Machine Shop, a recent State Law (n.183 of 1989) has forseen the re-organisation and the strengthening of the National Hydrological and Marigraphical Service (S.I.M.N.). The new regulations, forseeing the re-organisation of the complex sector of soil defence in Italy, has re-organised the Natioanl Technical Services making them responsible to the President of the Council of Ministers, thus renewing the need for the State Machine Shop at Stra, currently being strengthened and re-organised, taking particular care of the transition from an exclusively electromechanical sector to one which is also electronic.

This indicates the importance attributed to the role and the tasks of the Machine Shop for the calibration, the control, the validation and homologation of the hydrological instrumentation produced both in Italy and abroad, either by public bodies or private companies, acording to the criteria laid down by the World Meteorological Organisation.

2) BRIEF DESCRIPTION OF THE MACHINE SHOP - The Machine Shop at Stra, currently situated in Via Nazionale, is formed of a group of premises of about 800sq.m. as well as about 1600sq.m. of open area and 300 sq.m. of terrace. It includes an entrance; fundamental services; two laboratories, one mechanical and one electronic; a room for the permanent display of the instrumentation; the office; store-rooms for material, samples and stamping molds; store-rooms for new instruments, those repaired, to be repaired, to be tested, etc. There is also the laboratory for the assembly and testing of clock mechanisms and the calibration of instruments; the premises dedicated to sanding work; painting and, finally, welding either oxyacetylene, arc, tin or soldering and the tack welding machine. The instruments are tested in the external space and on the terrace.

At present the main machine tools installed, which are used for the working of the materials and for the construction of all the components of various dimensions which make up the instruments, include four precision lathes; an assembly table; two prisms; two mini-drills; a precision angular drill; a milling cutter for gears; a heavy-duty drill; a cutting-off saw; a hack-saw; a cutting-off machine of large dimensions; a press for stamping; a manual guillotine; a fly press; two lathes of large dimensions; a tapping machine; a pantograph; a medium-size drill; three springs for sharpening; two electric belts for cleaning the materials, and lastly, various electric and electronic material such as an oscilloscope; a frequency gauge, etc.

For the calibration of current meters, the Hydrological Office once used the pool in the park of "Villa Pisani", opportunely equipped with a mobile trolley. Some years ago, the pool which was constructed in the XVII century was reintegrated into the monumental complex and therefore the calibration of

current meters is now carried out at the Hydraulics Laboratory of Padua University.

3) THE TRADITIONAL PRODUCTION OF THE MACHINE SHOP - The main instruments constructed by the Machine Shop at Stra are:

- PRECIPITATION GAUGE C.10 which constitutes the simple, exact, classical instrument for measuring the depth of precipitation, and comprises a cylindrical recipient of terneplate, mounted on a special stand, whose upper rim is a brass ring with a sharp edge bounding an area of 0.1 sq.m. The bottom of the recipient is a reversed cone so as to reduce loss by evaporation and also for this reason a cone-shaped lid is placed at 10 cm. from the upper rim, with a small central hole for the passage of the rainwater.

- SOUNDING LINES F.10 and G.20 are generally used for measuring the level of water in wells for the altimetric survey of subterranean waters, that is to determine the level in the shafts of hydrometrographic installations. The two instruments are substantially similar, for example, sounding line F.10 has a measuring tape with a cylindrical brass weight at the end, hollow inside and constructed in such a way that on meeting the surface of the water the air inside is forced to hiss out.

- WINCH M.40 facilitates volume measurements in fluvial sections where it is not possible to use the customary current meter mounted on shafts. The headpiece is furnished with a meter-counting device and can also be used as a simple sounding-line for direct depth readings. The functions of this winch can be compared to those of a cable-way since, in the case of flow measurements, a weight of about 25 kg with a rudder ensuring constant countercurrent orientation is applied. The drum of the winch can hold up to 40 m of bearing cable inside which electric wires trasmit the impulses of either the current meter or of the bed-sweeping device.

-TURBIDIMETER - BORE C.M.1 is a simple and practical instrument for sampling water to measure turbidity, salinity, etc. It can be used with both a rigid system fixed to lenticular rods like those used for the current meters, or with a suspension system fixed to a light steel cable. The bore is immerged open and horizontal often with a weighted direction rudder, and a few seconds are sufficient to activate a regular flow through the cylindrical body of the bore which is closed by a slip hook system operated by the fall of a weight running along the suspension cable.

- HYDROMETROGRAPHS NT 225 and G 440 for the automatic recording of the level in a basin or water-course or the sea on graph paper around a revolving cylinder by means of a clockwork mechanism at a daily or weekly speed. In particular, G 440 has a cylinder 44 cm high, twice that of NT 225, and with a level excursion from 0.45 m to 9 m. G 440 has been used for more than 80 years to measure the sea level at Punta Salute, Venice.

- CURRENT METERS U.25/50, A.100, A.50 to be applied to the winches or the river cable-ways, to be used either forded or on a stand, each furnished with one or more propellers of different

weights for different speeds. The electrical impulses of the propeller rotations can be varied as desired every 10 or 20 rotations for model U.25/50 and every 25, 50 or 100 rotations for the other types. A.100 is very sensitive and, thanks to the particular care given to the profile and the propeller so as to obtain the maximum quality and the minimum inertia of the rotating system, responds well at speeds from 0.05 to 4.00 m/s

-PLUVIOGRAPH M.20 is of the balance type and represents the most well known product of the Machine Shop. It consents the recording of the depth of rain on the soil, tracing the relative diagram in time on a specially prepared chart around a rotating cylinder. Every impulse of the writing point corresponds to 0.2mm of rainfall, but lesser depths of precipitation are not lost because they are retained by the instrument until the next rainfall. The rotation of the cylinder can be weekly or daily but,in any case, the winding of the clock mechanism lasts 8 days. The instrument is subjected to scrupulous calibration with a water jet corresponding to precipitation of 50 mm/hr; for much stronger or much weaker intensities the instrument makes an error in deficit or in excess respectively which, however, is not greater than 1%.

Other instruments traditionally produced by the Machine Shop are, for instance: - THE FLUVIAL CABLE-WAY BE/80, THE TOTALISING PRECIPITATION GAUGE and the SNOW WEIGHING INSTRUMENT C.N.1.

4) NEW PRODUCTS - Recently the remarkable experience and skill acquired by the staff of the Machine Shop has made possible the design, experimentation and construction for use of a new type of instrumentation which, although maintaining the traditional format, thanks to several new improvements, often extremely clever, makes them more precise and to be preferred even to those designed with completely more "modern" criteria.

This is the case, for example, of the PLUVIOGRAPH P.E. in which the recording of the snow-rain precipitation is the same as the classical mechanical pluviographs, that is, by means of a tracing on a weekly chart. Whilst, however, in the traditional method the tracing is in the circumferance arc, instead in the Pluviograph P.E. the tracing is a straight line because the writing point is connected to a trolley moving on a vertical threaded rod which, rotating, causes straight vertical movements of the trolley and, therefore, of the writing point. The advantage is a greater legibility of the pluviographs. The recordings of the precipitations is done traditionally on weekly graphs but in this case the recorder is located inside the observer's house: therefore, he can check the correct working of the instrument more frequently and more easily. Lastly, as the instrument is indoors where the temperature and the humidity are subject to weaker variations than outside the electromechanical equipment guarantees a more regular function, the tracing by the writing point is no longer on a damp or dry chart but one with constant humidity and thus the tracing is clearer. Finally, a refined evolution of the balance results in an increased precision compared to model M.20 in the cases of heavy rainfall allowing the recovery of the very small quantities of water which

continue to fall into the full cup of the descending balance before it is intercepted by the rising empty cup.

Other important instrumentation of the new type are, for instance, the BORE FOR THE SAMPLING OF WATER AT ANY DEPTH formed of a cylindrical brass tube 6 cm diameter and 50 cm long composed internally of movable piston-type sections closed by special load-and-hold mechanisms, always full of water in descent because communicating with the exterior. At the pre-establsihed point, by means of a trigger command, the movement of one section expels the water which was above and, at the same time, loads through holes the water to be analysed; THE CURRENT METER FOR VERTICAL FLOWS IN WELLS, for the measurement in artesean wells of possible intakes of water between one water bearing stratum and another with possible measurement of volume, supplied with an extremely sensitive propeller and an internal electronic water-proof apparatus which, on the surface, allows the visualisation of the direction and number of rotations in a pre-established time; the ELECTRONIC CURRENT METER WITH WATER-PROOF LIQUID CHRYSTAL LED and finally the TIDE GAUGE ME 1 installed in several points of the Venice Lagoon for the reading of the tide, also by the general public (in St. Mark's Square, near Rialto Bridge, etc.), in which the parts for measuring and recording sea level and those for tracing the weekly chart on a scaled index so as to be understood by the general public (written in several languages) are 1000 m apart; the instrument is also furnished with an alarm which turns on a flashing red light in conditions of "acqua alta".

VALIDATION AUTOMATIQUE LOCALE DES INFORMATIONS D'UNE STATION METEOROLOGIQUE

J. Pilon
Météo-France

"Il est possible d'exiger des observations exactes d'instruments météorologiques tels que baromètres, thermomètres, hygromètres, anémomètres, mais, dès qu'il s'agit de l'état du ciel, des apparences du temps, des appréciations correctes et partout comparables sont presque impossibles à réaliser, et l'on ne peut pas compter que les observations locales seront faites partout de la même façon. Pourtant cette appréciation locale des caractères du temps, en ce qui concerne la prévision à courte échéance, a, sinon autant, mais presque autant d'importance que la carte synoptique."

Jean Rouch - Les méthodes de prévision du temps, 1924.

Introduction

Météo-France a lancé il y a quatre ans le projet SOLFEGE, destiné à compléter le programme d'automatisation de l'observation de surface par la caractérisation du "temps présent".

Dans ce cadre, plusieurs systèmes spécifiques ont été définis puis développés et industrialisés. Ils viennent compléter la panoplie des équipements classiques sur les sites d'observation. Chacun de ces nouveaux instruments prend en charge un aspect du temps présent et établit un diagnostic primaire qui est transmis à la station automatique.

Cette dernière, dotée d'une puissance de traitement renforcée et d'une capacité de mémorisation adéquate, élabore à partir de l'ensemble des informations dont elle dispose, les différents diagnostics du temps présent utilisés pour le codage de l'information météorologique des messages réguliers ou de signalisation.

Cette élaboration repose sur la possibilité -nouvelle- de combiner les mesures des capteurs traditionnels et les diagnostics primaires issus des équipements observant le temps présent ; en même temps, elle accrédite l'ensemble des informations disponibles et fournit des estimations sur la qualité de leur contenu.

Contenu de l'observation automatique locale

L'automatisation de l'observation locale, même au terme de développements instrumentaux importants, ne permet pas d'appréhender *tous* les phénomènes météorologiques, tels qu'ils sont décrits par exemple dans l'Atlas international des nuages. Il serait d'ailleurs inutile qu'il en soit ainsi : l'observation des nuages depuis la surface et le codage précis de leurs différents types, genres, particularités, etc. , sont moins nécessaires que par le passé, du fait de la mise en place des moyens d'observation à large couverture spatiale que sont les radars et les satellites. Il serait irréaliste de chercher à détecter, par voie automatique, certains phénomènes très particuliers tels l'arc en ciel ou le rayon vert ; cette détection serait d'ailleurs sans grand intérêt dans la pratique quotidienne de l'exploitation météorologique.

D'autres éléments, comme la trombe, se soustrairont sans doute longtemps à toute velléité d'observation automatisée ; il est vrai que celle-ci, à cause de son caractère très localisé, échappe souvent à l'observation humaine.

Enfin il semble difficile d'appréhender par voie automatique des événements (autres que les orages) se produisant au voisinage de la station, mais non sur son site lui-même.

Pour quels phénomènes est-il absolument nécessaire de maintenir -grâce à des systèmes automatiques- une observation locale depuis la surface ?

Si l'on s'en tient à des besoins de type météorologie générale : renseignement, prévision immédiate, et pour des conditions climatiques qui sont celles de l'Europe occidentale, on estime qu'il est impératif de savoir restituer les éléments suivants :

- précipitations convectives ou stratiformes : nature, caractéristiques et intensité qualitative
- altérations de la visibilité : cause, importance
- présence et nature de dépôts d'hydrométéores sur le sol
- nébulosité totale et hauteur du plafond nuageux
- évolution convective orageuse, occurrence d'orage avec ou sans précipitation

D'autres phénomènes du temps présent, comme le transport de particules (chasse-sable, chasse-neige,...) présentent un intérêt certain pour la compréhension d'une situation météorologique, mais ont été jugés moins prioritaires et n'ont pas fait l'objet de développements instrumentaux spécifiques.

Choix instrumentaux ; informations restituées par les capteurs temps présent

Plusieurs dispositifs instrumentaux ont été étudiés. Certains ont été définis et développés par Météo-France, d'autres ont été choisis parmi des équipements commercialement disponibles.

De façon générale, ces nouveaux équipements délivrent leurs informations à la station automatique une fois par minute. Ces informations sont constituées d'un diagnostic primaire relatif à l'aspect du temps présent exploré par l'équipement (par exemple, l'identifieur de précipitations fournit : "Pluie", "Bruine", "Neige", "Grêle",...). Ce diagnostic primaire est parfois accompagné d'un indicateur sur sa plausibilité (de "très crédible" à "très douteux"), et d'informations quantitatives spécifiques.

Le tableau suivant précise pour chaque équipement, le principe de mesure mis en oeuvre, le diagnostic primaire qu'il fournit et son statut (commercialisé, prototype industriel ou recherche).

Equipement	**Principe mis en oeuvre**	**Diagnostic primaire (1mn)**	**Statut**
Identifieur de précipitations	Diffusion latérale micro-onde Mesure Doppler des vitesses de chute des précipitations par radar à 25 GHz	Occurrence d'une précipitation, nature des hydrométéores présents et intensité qualitative	Prototype industriel
Estimateur d'état du sol	Diffusion et réflexion d'un signal lumineux sur une cible au sol	Nature du dépôt d'hydrométéores sur le sol [Hauteur de neige]	Prototype industriel [Rech. et dévelop.]
Visibilimètre	Diffusion d'un signal lumineux sur les suspensions d'hydrométéores	Occurrence de brouillard ou de brume - visibilité	Système commercial
Estimateur de nébulosité	Séparation ciel bleu / nuages sur images vidéo de la voûte céleste	Nébulosité totale qualitative ou par octas. [Nébulosité des différentes couches]	Rech. et dévelop. [Rech. et dévelop.]
Détecteur d'orage	Suivi du champ électrostatique local par moulin à champ (si capteur local) ou localisation des éclairs par interférométrie (si réseau à large couverture spatiale)	Occurrence d'orage et intensité qualitative. [Risque d'orage].	Système commercial [Rech. et dévelop.]

Equipé de ces capteurs complémentaires observant les phénomènes du temps présent, un site d'observation et de mesures météorologiques possède un système d'informations disponibles en permanence. L'exploitation judicieuse de ces informations permet de restituer la plus grande variété des situations météorologiques, d'affermir la qualité de cette restitution, et en même temps, de surveiller le fonctionnement des capteurs eux-mêmes.

Détermination initiale du temps présent

La simple juxtaposition des informations produites capteurs ci-dessus n'est pas suffisante pour délivrer des messages ayant un sens météorologique.
Une première raison est que ces capteurs n'ont, individuellement, qu'une "vue" partielle des différents phénomènes et de leurs manifestations.
En second lieu, les diagnostics qu'ils délivrent portent sur des durées d'analyse relativement courtes, d'environune minute.

Pour nombre de phénomènes du temps présent, tels qu'ils sont présentés par exemple dans le manuel des codes de l'O.M.M, il est nécessaire de pouvoir associer des diagnostics primaires issus de capteurs distincts ; c'est le cas par exemple des temps présents : "Pluie se congelant, modérée" ou "Orage fort, avec averses de pluie et/ou de neige".

Par ailleurs, il faut souvent avoir recours aux diagnostics antérieurs (de quelques minutes à plusieurs dizaines de minutes) pour pouvoir caractériser tel ou tel phénomène ; par exemple : "Brouillard devenant plus dense" ou "Pluie intermittente".

Enfin, les messages météorologiques synoptiques sont diffusés à un rythme bien plus lent que la cadence de production des systèmes d'observation automatiques ; il y a donc lieu de synthétiser ces données trop abondantes, de façon à ne pas encombrer les réseaux de transmissions météorologiques d'informations souvent largement redondantes. Dans le même temps, l'évaluation continue du temps présent est nécessaire, de façon à pouvoir délivrer en temps voulu des messages de signalisation de phénomènes particuliers ou dangereux (première chute de neige de la journée, orage...).

La détermination automatique du code décrivant le temps présent repose sur un algorithme qui, supposant que les diagnostics primaires et les mesures sont dignes de confiance, explore la table des codes temps présent à la recherche de la ou des entrée(s) candidate(s). Au cours de cette exploration, on utilise d'abord les indications fournies pour la minute courante, quand celles-ci expriment une détection positive d'événement (par exemple : "Chute de neige"). On examine ensuite les diagnostics des minutes écoulées, qui ont été enregistrés. Ils permettront soit d'apporter une précision sur le caractère du phénomène courant (précipitation continue ou intermittente, brouillard s'épaississant), soit de déterminer le temps caractéristique au cours de l'heure précédente, si aucun phénomène particulier n'est en cours.

Ce processus est déclenché dans la station automatique à chaque minute ; il conduit à la fourniture d'un ou plusieurs codes candidats. On sélectionne alors en général celui dont le code est le plus élevé. C'est le diagnostic initial du temps-présent.

Ce mécanisme repose donc sur deux hypothèses : les informations en entrée doivent être suffisamment nombreuses et diversifiées pour permettre la distinction entre tous les types de temps possibles ; ces informations doivent être exactes. Or aucun système n'étant totalement fiable, il y a lieu de se prémunir contre l'éventualité d'informations erronées en entrée. Pour les systèmes de temps présent, cela signifie que l'on doit contrôler le bien-fondé des diagnostics primaires.

Contrôles et validation

Dans le cas -de plus en plus fréquent- où un contrôle humain ne peut être effectué au niveau de la station automatique, on utilise la base d'informations disponibles localement.

Cette base d'informations contient, outre les mesures et diagnostics primaires provenant des différents capteurs et instruments constituant la configuration de la station, les éléments suivants :
- des informations de fonctionnement ("correct", "hors service", "dégradé"...) fournies par certains équipements,
- des valeurs de précision de mesures et de conditions nominales de fonctionnement,
- des indications sur la plausibilité de leur diagnostic primaire, délivrées certains systèmes de temps présent.

S'y ajoutent également :

- les valeurs des variations temporelles de certains paramètres, calculées sur diverses périodes de temps (5 mn, 30 mn, 60 mn...),
- les données climatologiques du site : normales saisonnières, extrema, fréquences d'occurrence des phénomènes,
- des repères temporels (heure dans la journée, heures de lever et coucher du soleil, jour dans l'année, saison, date de la dernière intervention d'entretien sur le site),
- les valeurs prévues de certains paramètres, calculées à partir des données antérieures par des formules empiriques ou des modèles numériques locaux, activables dans certaines situations spécifiques, tels certains modèles d'évolution nocturne de la température de l'air en l'absence de nébulosité et par vent calme (par exemple : [Cellier, 1993]).

A tout instant -à chaque pas de temps d'une minute-, l'ensemble de ces informations doit posséder une certaine *cohérence*, dans la mesure ou elles sont représentatives de la situation météorologique en cours. Ainsi, en été, à l'arrivée d'une perturbation non orageuse, il sera "logique" d'observer de la pluie, et en même temps des quantités de précipitation non nulles, un sol mouillé, un ciel totalement couvert, une insolation nulle, une température de l'air positive, pas d'orage, etc. Un diagnostic initial tel que : "Pluie continue modérée au moment de l'observation", aura pu être formé à partir des diagnostics primaires suivants :

-(identifieur de précipitations)- "Chute modérée de pluie ininterrompue depuis plusieurs minutes" /1/
-(estimateur de l'état du sol)- "Sol mouillé depuis plusieurs minutes" /2/
-(détecteur d'orage)- "Pas d'orage en cours ni dans l'heure précédente". /3/

Chacun des diagnostics primaires intervenant dans le diagnostic initial est confronté au reste de la base d'informations. Cette confrontation s'exprime par des règles d'évaluation associées au diagnostic initial, dans lesquelles on exprime le degré de renforcement (ou d'affaiblissement) d'un diagnostic primaire en fonction d'une partie -pertinente- des autres paramètres. Pour poursuivre avec l'exemple ci-dessus, on peut extraire les quelques règles suivantes :

-(nébulosité)- le ciel est totalement couvert depuis le début de la précipitation (renforcement de /1/, moyen) ; le ciel n'est pas totalement couvert depuis plusieurs minutes (affaiblissement de /1/ et /3/, moyen) ; la nébulosité est nulle ou très faible (affaiblissement de /1/, important)
-(visibilité)- la visibilité a modérément baissé et reste à une valeur stable depuis le début de la précipitation (renforcement de /1/, moyen) ; la visibilité a beaucoup baissé ou subit des variations erratiques (affaiblissement de /1/, important)
-(pluviomètrie)- aucun basculement d'auget n'a eu lieu depuis le début de la "précipitation" (affaiblissement de /1/, important, affaiblissement de /2/, moyen)
-(pression)-: la pression est très élevée (affaiblissement de /1/, moyen) ; elle vient de subir une baisse ou une baisse suivie d'une hausse (renforcement de /1/, important)

Le fait de disposer des diagnostics primaires provenant des capteurs de temps présent permet d'aller plus loin que les quelques vérifications formelles en vigueur sur les stations automatiques actuellement en exploitation (du type "$T_d \leq T$", etc.) [Acheson, 1987] et de s'appuyer sur une "approche physique qualitative adaptée au raisonnement temporel multi-variables" [Chavaux, 1991].

Après confrontation aux autres éléments de la base d'information par le biais des règles associées au diagnostic initial, un diagnostic primaire peut subir un affaiblissement ; la cause en est au dysfonctionnement soit du capteur de temps présent à l'origine du diagnostic primaire, et dans ce cas l'affaiblissement sera très important, soit d'un autre capteur, auquel cas seul un nombre limité de règles sera concerné.

Le dysfonctionnement d'un capteur peut avoir une cause interne : panne subite (par exemple : blocage de l'identifieur de précipitation sur "Pluie") ou progressive (dégradation de la mesure de pression), ou bien une cause externe, avec l'intervention d'éléments non météorologiques, qui vont altérer le milieu dans lequel sont réalisées les mesures et observations : chute de feuilles mortes, système d'arrosage automatique à proximité d'un parc à instruments, présence d'oiseaux et d'insectes, pollution radioélectrique, etc.

La validation repose sur le mécanisme suivant : à partir du diagnostic initial , on détermine par application des règles d'évaluation si les diagnostics primaires sont renforcés ou affaiblis.

Si, au terme de cette application, on a obtenu uniquement des renforcements de cohérence, le diagnostic initial est retenu et sera fourni aux utilisateurs comme diagnostic définitif.

Si, en revanche, il y a affaiblissement, il y a lieu d'en déterminer la cause, de déclarer invalide la source d'information et les valeurs qui en découlent, de ne plus explorer (provisoirement) les règles qui les mentionnent, puis de recommencer la détermination du diagnostic. Il y a alors *révision* du diagnostic. A son terme, ce processus permet de conclure en faveur soit d'un diagnostic définitif, soit d'une absence de diagnostic parce que les informations des divers capteurs sont trop contradictoires.

L'utilisation d'une base de règles dans la station automatique permet de prendre en compte facilement l'ajout ou le retrait de règles, à la suite d'un apprentissage sur des situations météorologiques de plus en plus variées ; elle autorise l'existence de variantes dans les configurations de capteurs entre différents sites d'observation ; enfin, cette base de règle reflète aisément l'évolution de l'état de fonctionnement des capteurs présents sur un site.

Cette approche a suggéré d'articuler le mécanisme de validation autour d'un système expert, inspiré de systèmes à vocation prédictive ([Brion, 1992]).

La nécessaire gestion de l'incertain y sera assurée par la mise en oeuvre du calcul flou et de la logique floue (voir par exemple [Bouchon-Meunier, 1993]), techniques qui permettent de traiter des prémisses, des règles et des conclusions "non précises", de la forme :

> "Dans le contexte de tel diagnostic initial,
> le renforcement/affaiblissement de tel diagnostic primaire est : limité/moyen/important
> si telle valeur est : très-peu/peu/moyennement/beaucoup/très élevée/faible"

Par exemple, on acceptera des conditions comme : "la force du vent est modérée à forte", "la température est très basse", etc.

La réalisation d'un tel système de contrôle et de validation est en cours.

Conclusion

Avec l'apparition de nouveaux capteurs météorologiques, dédiés à l'observation du temps présent, il devient possible à Météo-France d'envisager l'automatisation intégrale de l'observation depuis la surface.

Ces systèmes, pour être véritablement intégrés aux réseaux opérationnels, doivent être accompagnés, au niveau des stations automatiques, de la mise en place d'un logiciel de contrôle et de validation fiable.

L'emploi de techniques comme la logique floue et les systèmes experts, permettant de raisonner sur des informations non absolument certaines, autorise la réalisation d'une telle application.

Références

Acheson D., 1987 : Some general considerations and specific examples in the design of algorithms for synoptic automatic weather stations. *Instruments and observing methods - Report No 19. WMO.*

Bouchon-Meunier B., 1993 : La logique floue. *Presses universitaires de France.*

Brion D., 1992 : Etude de la prévision du brouillard à Tours. Méthode statistique et mise en oeuvre d'un système expert *Note du SMIRIC n°1. Météo-France.*

Cellier P., 1993 : An operational model for predicting minimum temperatures near the soil surface under clear sky conditions. *J. Appl. Meteor.* ,**32,** 871-883

Chavaux F., 1991 : Proposition de contribution au projet SOLFEGE. *(Communication personnelle).Météo-France.*

SUIVI QUALITE DES MESURES DANS LES RESEAUX DE METEO-FRANCE

M. LEROY, METEO-FRANCE/SETIM

FRANCE

1 - INTRODUCTION

L'amélioration et la connaissance de la qualité des mesures météorologiques nécessitent un travail permanent de suivi. La réalité des mesures sur le terrain est souvent très différente des recommandations d'implantation et de précision requises par les utilisateurs et exprimées en particulier dans le guide CIMO.
Météo-France redéfinit les procédures du suivi qualité de son réseau de mesure : documentation de l'exposition des mesures, connaissance des caractéristiques des instruments utilisés, recette technique de ces instruments, étalonnage et mise en oeuvre des contrôles métrologiques réguliers, formation des observateurs.
Après quelques considérations générales, nous donnerons quelques exemples appliqués à des mesures de base en météorologie.

2 - CONSIDERATIONS GENERALES

2.1. EXPOSITION DES INSTRUMENTS

Sauf cas particuliers, les mesures météorologiques ont généralement une vocation synoptique, l'implantation d'une station de mesure et de ses capteurs doit donc suivre certaines règles garantissant leur représentativité vis-à-vis de cette échelle synoptique.
Ces règles idéales d'implantation sont bien connues des services météorologiques et pratiquement identiques d'un service à l'autre. Certaine d'entre elles, l'implantation de la mesure du vent par exemple, sont malheureusement difficiles à suivre et la réalité peut s'écarter notablement de la théorie. Dans ce cas, fréquent, il serait intéressant de corriger les mesures des effets perturbateurs d'implantation. Ceci impose déjà de documenter le site, de connaître les effets perturbateurs théoriques et d'appliquer des méthodes connues de correction. Une enquête récente a été conduite par Mr J. EHINGER pour la CIMO. Cette enquête montre l'homogénéité des règles d'implantation, l'absence quasi-générale de corrections opérationnelles de mesures et la rareté même d'une documentation précise et codifiée d'un site, permettant à l'utilisateur final de connaître la validité de la mesure.
Ainsi un premier pas vers l'amélioration de la qualité des mesures vis-à-vis de leur exposition, serait de définir une classification d'un site en fonction des règles idéales d'implantation et des écarts à ces règles, quantifiées en terme d'effet si possible.
Pour sa part, Météo-France n'en est qu'à ses débuts vis-à-vis de cette documentation. Un rôle normalisateur de la CIMO dans ce domaine est fortement souhaitable.

2.2. CARACTERISTIQUES METROLOGIQUES DES INSTRUMENTS

2.2.1. Connaissance des caractéristiques

Les diverses commissions de l'OMM se sont réunies les années passées pour aboutir en 91 à des tableaux unifiés, vis-à-vis des diverses utilisations, des précisions requises pour les mesures météorologiques. Ces spécifications sont nécessaires aux "instrumentalistes" et aux gestionnaires des réseaux

météorologiques. Elles sont malheureusement souvent fort éloignées des réalités et de l'état de l'art dans le domaine instrumental. Ainsi, elles courent le risque d'être considérées comme utopiques et donc inutilisables. Pour limiter ce risque, il convient d'entamer un dialogue entre les utilisateurs et les responsables des réseaux de mesure de façon à établir le meilleur compromis entre le besoin et les possibilités techniques, sans négliger l'aspect économique, qui en final est un élément déterminant de choix. Cette démarche est en fait une analyse de la valeur. Elle nécessite d'abord une connaissance précise des caractéristiques réelles des instruments météorologiques. Les caractéristiques annoncées par les fournisseurs sont souvent très optimistes et demandent à être contrôlées. Une difficulté réside dans le fait que pour certaines mesures, il n'existe pas de référence métrologique (la visibilité par exemple). Cela rend donc la "vraie" valeur inconnue. Les intercomparaisons internationales d'instruments organisées par la CIMO ou les divers services météorologiques sont un moyen privilégié de connaître les caractéristiques des instruments et de s'approcher de cette "vraie" valeur.

2.2.2. Cahier des charges

Les cahiers des charges destinés à l'approvisionnement des instruments de mesure doivent bien sûr être réalistes et contrôlables. Si les performances requises d'un instrument ne sont pas contrôlables, elles sont théoriques et éventuellement sans intérêt. La connaissance ou l'estimation de la "vraie" valeur est donc nécessaire pour qualifier un instrument.
Certains capteurs (mesures de pression, température, humidité,..) offrent l'avantage de pouvoir être reliés à des références métrologiques et testés dans un environnement contrôlé de laboratoire. Les spécifications sont alors relativement faciles à exprimer.
Il faut tenir compte des facteurs d'influence intervenant lors des mesures opérationnelles, effectuées dans des conditions extérieures souvent fort éloignées des conditions de laboratoire. Un moyen de contourner la difficulté est de tenter d'identifier à priori les facteurs d'influence possible et donc de spécifier l'influence individuelle de ces facteurs, qui deviennent alors parfois vérifiables en laboratoire.
La connaissance des caractéristiques des instruments est évidemment une grande aide à la rédaction de cahier des charges réalistes et contrôlables. Elle peut être insuffisante, par exemple vis-à-vis de nouveaux instruments de mesure, de caractéristiques éventuelles inconnues.
Dans l'absolu, un cahier des charges ne devrait être que fonctionnel, sans imposer de contraintes techniques particulières. C'est généralement le cas des cahiers des charges d'équipements nouveaux pour lesquels il n'est pas souhaitable d'imposer des solutions techniques qui pourraient s'avérer restrictives. A l'issue d'une phase de test et après le choix de l'instrument retenu pour une application donnée, il est hautement souhaitable de rédiger un "cahier de spécifications techniques" décrivant des caractéristiques techniques et métrologiques vérifiables.

2.3. ETALONNAGE ET METROLOGIE

Les instruments météorologiques sont des instruments de mesure pour lesquels l'aspect métrologique est primordial. Il existe donc généralement dans les services météorologiques une chaîne métrologique plus ou moins bien organisée, permettant de "garantir" (ou tenter de garantir) la qualité métrologique des données sur le terrain. Ceci nécessite des références métrologiques de laboratoire, des étalons de travail transportables sur site, des méthodes bien définies.
Météo-France, pour ses besoins propres et dans le cadre du Centre Régional d'Instrument de l'AR VI, a fait un gros effort d'investissement et d'organisation dans ce domaine. Ainsi, pour son réseau de mesure, tous les

instruments classiques tels que thermomètres, baromètres, hygromètres subissent des étalonnages en laboratoire.

2.4. RECETTE TECHNIQUE DES INSTRUMENTS

La disponibilité de cahiers des charges réalistes et contrôlables, ainsi qu'un service technique et un laboratoire de métrologie, permettent d'effectuer des recettes techniques des matériels approvisionnés. Météo-France travaille à formaliser ces contrôles par des documents appelés "cahier de recette technique". L'expérience montre que ces recettes sont indispensables et sont un facteur essentiel de la qualité des instruments de mesure. Elles sont une contrainte pour le fournisseur et doivent donc être acceptées et négociées avec celui-ci. Elles peuvent s'avérer un facteur d'accroîssement de la qualité des prestations du fournisseur, grâce à des contrôles indépendants.

2.5. PROCEDURES REGULIERES DE CONTROLE

Les caractéristiques d'un instrument ne sont malheureusement pas stables dans le temps. Elles peuvent aussi être dégradées par le transport, l'installation, des erreurs humaines.
Pour certaines mesures, des contrôles de cohérence spatiaux-temporels peuvent être appliqués. Les écarts par rapport à l'analyse ou au "first guess" des modèles numériques sont parfois utilisables, bien qu'assez peu adaptés pour les mesures au sol, fortement influencées par des phénomènes géographiques de petite échelle, encore mal appréhendés par les modèles.
Des contrôles croisés de capteurs sont souhaitables pour détecter d'éventuelles dérives ou anomalies. Il faut toutefois être prudent dans l'interprétation de tels contrôles, la référence exacte de la mesure n'étant pas connue ; mais cela permet d'alerter les services de maintenance sur des anomalies.
Des étalonnages réguliers, soit sur site, soit en laboratoire, sont nécessaires pour contrôler la stabilité des capteurs dans le temps. La tendance actuelle de Météo-France est d'effectuer ces étalonnages en laboratoire par permutation de capteurs. Enfin, des procédures de maintenance préventive doivent être définies et appliquées.

2.6. FORMATION, DOCUMENTATION

L'automatisation des mesures dans les réseaux météorologiques ne nécessite plus l'intervention régulière d'un observateur. La surveillance des capteurs doit donc être organisée car elle n'est plus indispensable au travail quotidien de l'observateur.
Dans une station météorologique de Météo-France, les postes d'observateur à plein temps sont de plus en plus rares. Le temps est partagé entre observation, climatologie, renseignement et si l'on y prend garde, le contrôle des mesures automatisées peut être négligé. Il est donc important de fournir à la station une documentation sur les caractéristiques des instruments, leurs problèmes potentiels et les procédures de contrôle et d'entretien. Cette documentation est indispensable à la bonne motivation de l'observateur.

3 - EXEMPLES DE SUIVI

3.1. HUMIDITE

Météo-France vient de renouveler les hygromètres de son réseau à la suite d'un appel d'offres et de tests de longue durée en extérieur. Un des problèmes majeurs des capteurs d'humidité est leur comportement à saturation. Ces conditions sont difficilement contrôlables en laboratoire et la plupart des capteurs d'humidité utilisés dans l'industrie ne fonctionnent pas sur une gamme aussi étendue qu'en météorologie, d'où l'importance des tests en extérieur.

A l'heure actuelle, tous les hygromètres de notre réseau ont été recettés individuellement par Météo-France (SETIM, laboratoire de métrologie) : contrôle fonctionnel et métrologique. Les limites de rejet fixées sont de ±4 % sur la gamme de mesure de 10 à 90 %, à température ambiante. Les capteurs sont changés annuellement pour ajustage éventuel chez le fournisseur, le SETIM se contentant de contrôler ses prestations. La bonne qualité de ces prestations conduit le SETIM à pratiquer une procédure de contrôle sur échantillonnage.
Sur le terrain, des comparaisons sont effectuées avec les psychromètres équipant encore les stations de mesure. En France, les psychromètres sont installés dans des abris à ventilation naturelle qui peuvent donc conduire à une nette surévaluation de l'hygromètre calculée à partir du psychromètre, lorsque la vitesse de ventilation est faible (la vitesse de ventilation à l'intérieur de l'abri est voisine du dixième de celle à l'extérieur). Les observateurs ayant par habitude tendance à considérer le psychromètre comme une référence, une large campagne d'information (exposés oraux et documentation) a été menée auprès des stations d'observation pour informer les observateurs et les utilisateurs des incertitudes de mesure liées à chaque instrument. Les utilisateurs sont particulièrement sensibles aux performances des instruments au voisinage de la saturation, comme cela apparaît d'ailleurs dans les souhaits de précision requis par l'OMM (1% au voisinage de la saturation). Or, l'incertitude de mesure des capteurs de type capacitif est plus grande au voisinage de la saturation et par ailleurs les humidités très fortes sont difficilement contrôlables en laboratoire. Là aussi, l'adéquation entre l'état de l'art et les performances requises reste à faire.
Dans un proche avenir, Météo-France va supprimer les psychromètres et thermo-hygrographes de secours de station. Une Station Automatique de Secours va être installée avec acquisition directe de la température et de l'humidité. Ce doublement des capteurs va autoriser leur contrôle et la détection d'éventuelles dérives.
Le changement des capteurs utilisés, les nouvelles procédures de contrôles et de renouvellement des capteurs ont conduit à une amélioration significative des mesures d'humidité dans le réseau. Ces mesures restent délicates et génèrent des coûts de fonctionnement relativement élevés mais nécessaires. Ces coûts de fonctionnement sont une cause potentielle de non qualité, la tentation de faire des économies est grande : il est toujours plus facile d'investir pour la première installation que pour le fonctionnement courant.

3.2. PRESSION

Ce paramètre est un exemple typique de l'inadéquation entre les souhaits annoncés des utilisateurs (0.1 hPa pour les besoins synoptiques !) et les performances obtenues en opérationnel. Une telle précision ne peut-être obtenue qu'en laboratoire.
Les performances requises par Météo-France sont une incertitude inférieure à 0.5 hPa sur une période d'un an. Le problème principal des baromètres numériques de réseau est la dérive dans le temps qui doit rester inférieure à 0.2 hPa/an.
Tous les capteurs sont recettés individuellement au SETIM. Sur la gamme de température 5 à 40°C, les limites de rejet ont été fixées à ±0.4 hPa. Ces limites sont théoriquement en-deçà des performances annoncées par plusieurs fournisseurs et ne devraient donc pas poser problème. L'expérience a montré le contraire et renforce la nécessité du contrôle métrologique.
La nouvelle procédure mise en place par Météo-France impose un changement et un étalonnage (avec ajustable éventuel) annuel. Profitant des moyens de mesure de son laboratoire de métrologie, ces étalonnages sont effectués au SETIM.
Les services régionaux disposent d'un étalon de laboratoire, d'un générateur de pression/dépression et d'un baromètre de transfert permettant de contrôler les capteurs avant leur mise en place et d'étalonner localement les baromètres holostériques de moindre précision.
Le laboratoire de métrologie du SETIM dispose d'un étalon primaire (balance de force Desgranges et Huot) permettant l'étalonnage des capteurs du réseau (via

l'utilisation de baromètres numériques de travail) et l'étalonnage d'étalons nationaux d'autres services météorologiques. Ce laboratoire n'est pas encore reconnu par les laboratoires métrologiques internationaux. Notre objectif est de le devenir dans les prochaines années ; nos méthodes, notre personnel et notre équipement devraient le permettre ; le processus formel d'habilitation est long.
Un contrôle spatial basé sur le monitoring du modèle de prévision est en cours d'expérimentation. La pression est un des rares paramètres mesuré au sol qui devrait pouvoir être contrôlé par ce moyen. La qualité du monitoring pour les radiosondages a fait ses preuves et a déjà permis de mettre en évidence des anomalies ou des erreurs d'exploitation sur les baromètres de stations de radiosondage.
Certains sites de mesure fort ventés peuvent être perturbés par les effets dynamiques du vent. Par ailleurs, de nombreuses stations du Sud de la France (et Outre-Mer) sont climatisées. Un soin tout particulier doit donc être apporté aux prises de pression, soin qui n'a pas toujours été apporté dans le passé.

3.3. MESURE DU VENT

La mesure du vent est celle pour laquelle les contraintes de dégagement sont les plus difficiles à respecter (10 fois la hauteur des obstacles environnants). Ainsi, l'expérience montre que de nombreux points de mesure ne respectent pas ces contraintes. Il est souvent difficile, voire impossible de trouver le point d'implantation idéal. Souvent, sur aérodrome, les lieux dégagés tombent dans les zones de servitudes de l'aéroport et ne sont donc pas utilisables. Par ailleurs, un lieu dégagé est souvent situé à grande distance de la station météorologique. Le terrain n'appartient plus alors au service météorologique, la distance conduit à des coûts d'installation très élevés. La tendance est alors grande et malheureusement souvent suivie, de privilégier l'aspect économique à la représentativité de la mesure. Toutes ces raisons conduisent souvent à une implantation fort perturbée. Il est donc important de veiller, tant que faire se peut, au respect de règles minimales d'implantation. L'expérience de Météo-France montre que ce processus est difficile, puisqu'il se confronte à des problèmes de logistique et de coût ; la tendance des gestionnaires est de minimiser ces coûts.
Un moyen de contourner cette difficulté, sans la résoudre, est de caractériser le site de façon à informer les utilisateurs des données de sa représentativité. Les codes internationaux actuels ne permettent pas cette caractérisation et devraient conduire à interdire la diffusion de certaines mesures du vent sur les canaux internationaux. Là aussi, une telle proposition se heurte au désir général de disposer d'un maximum de mesures.
Une classification des sites de mesure du vent est proposée dans les normes de l'ASTM et mériterait d'être discutée et normalisée par la CIMO. Cela autoriserait une documentation internationale des sites.
Aux effets d'environnement immédiat se rajoutent les effets orographiques. Un exemple typique en France est la mesure du vent dans un sémaphore, station de surveillance marine aux bords des côtes. Ces stations de part leur situation sont souvent les premières stations d'observation des perturbations venant de l'ouest. Elles sont souvent en bord de falaise et subissent une accélération du vent pouvant atteindre un facteur 1.7 d'après les diverses études sur le terrain et en veine hydraulique. Un déport du pylône vers l'intérieur des terres s'avère souvent impraticable et est rejeté pour des questions financières. Des formules de correction pourraient être apportées après une étude détaillée du site en veine hydraulique. Mais, de façon opérationnelle, aucune correction n'est appliquée en France. Est-ce le cas ailleurs ?
L'aspect étalonnage des anémomètres pose moins de problèmes. Les caractéristiques des capteurs sont généralement déterminés par construction et peuvent sans trop de difficulté suivre les recommandations de la CIMO. La récente intercomparaison anémométrique montre que dans des conditions courantes (hors givrage sévère) les informations issues des capteurs différents sont

souvent très proches entre elles, du moins pour les capteurs "classiques" à moulinet ou hélice.
Un point à surveiller est le seuil de démarrage, susceptible d'augmenter dans le temps à cause de contraintes mécaniques. Une vérification bi-annuelle est donc recommandée. Cette vérification n'est pas aisée, les souffleries classiques ne sont pas adaptées aux basses vitesses, inférieures à 5 m/s. L'utilisation d'un mesureur de couple est possible. Il doit préalablement être étalonné avec les anémomètres utilisés pour établir la correspondance couple-seuil de démarrage. Le SETIM vient de réaliser une petite soufflerie permettant de générer de faibles vitesses de 0.1 à 3 m/s. Le seuil de démarrage peut être déterminé avec une incertitude de 0.1 m/s.
Les moulinets d'anémomètres, en matière plastique, vieillissent et doivent être remplacés tous les 2 ans, sous peine de devenir cassants et donc fragiles aux fortes vitesses.
Par leur situation élevée sur un pylône généralement métallique, les appareils de mesure du vent sont aussi particulièrement sujets aux surtensions générées par la foudre. Ces surtensions peuvent provenir des câbles de mesure et d'alimentation. Il est donc fortement recommandé d'utiliser des capteurs modernes dont la conception autorise une transmission numérique des informations et donc un isolement galvanique grâce à des modems. Météo-France met en place des capteurs entièrement numériques (DEOLIA 92) qui possèdent même leur propre alimentation par panneau solaire pour disposer d'un isolement complet.

CONCLUSION

L'amélioration de la qualité des mesures météorologiques passe d'abord par une adéquation réelle entre les performances des appareils (et donc l'état de l'art) et les précisions requises. Cette adéquation doit être formalisée par des cahiers des charges réalistes et contrôlables.
De plus, les conditions réelles d'implantation des mesures sont souvent éloignées des recommandations. Une classification normalisées des sites est donc souhaitable.
Sur ces deux points, une coordination de la CIMO paraît nécessaire. Le SETIM, en tant que Centre Régional d'Instrument pour l'AR VI, espère amener une contribution utile dans les prochaines années.

Bibliographie

J. EHINGER, rapporteur CIMO pour "Siting and exposure of meteorological instruments".

Final report of the meeting of experts on operational accuracy requirements (June 1991).

AN ALGORITHM FOR REAL-TIME DATA QUALITY CONTROL AT THE AUTOMATIC METEOROLOGICAL STATION NETWORK (AMSN) IN ISRAEL

by

A. Manes and Sarah Rubin

Israel Meteorological Service (IMS)
Bet Dagan 50250, P.O.Box 25, Israel

1. INTRODUCTION.

The Israel Meteorological Service (IMS) is operating presently an Automatic Meteorological Station Network (ASMN) consisting of about 40 stations. The synoptic and special purpose stations (e.g. air quality control, agrometeorological etc.) are interrogated every hour, or more frequently upon request, by a central computer facility located at the Central Meteorological Institute in Bet Dagan. Online data quality control is carried out by running an "Interactive Verification, Administration and Correction" (INVAC) programme, developed at the IMS for a 486 IBM PC. The algorithm of the INVAC programme is presented. Suspected data are screened out and flagged. The INVAC reports are used as feedback for maintenance and fast troubleshooting at the stations. The preliminary checked data are available in real time also for the Forecasting Center, for the issue of adverse weather conditions warnings, intermittent control of emissions of pollutants from major pollution sources, forest fire warnings, frost risk warnings, etc.

2. DATA QUALITY CONTROL - THEORY.

Data quality control procedures are based on physical consistency, as well as on the sequential and statistical features of the various meteorological parameters.
For given geographic location, climatic region, month and hour of the day, each parameter can be assigned certain acceptance limits on both sides of a central tendency typical for most meteorological parameters. These limits can be deterministic on one side, both sides, or can be determined in statistical terms only, e.g. as the predetermined lowest and highest percentiles of the actual distribution (not necessarily normal).

3. DETECTION OF COARSE ERRORS - GROSS LIMITS ACCEPTANCE TEST.

This is a simple and fast screening procedure aimed to detect coarse measurement errors in the process of station interrogation. For each station and each parameter some simple and deterministic, gross limits are determined, based on physical and climatic consistency of the measured data. In table 1 an example of such "Gross Acceptance Limits" is given.

Table 1. Example of deterministic acceptance limits.

Parameter	Acceptance limits
Temperature (T)	-10 - +50
Precipitation (PPT)	PPT $\geq$ 0 mm
Global radiation	0 - 1350 W/M2
Sunshine duration	n $\leq$ N (max possible)
Relative Humidity	0% - 100%
Dew point (DP)	DP $<$ T
Wind speed	0 - 200 kt
Wind direction	0° - 360°

4. STATISTICAL LIMITS ACCEPTANCE TEST.

Let Xp be the value of a parameter measured at a given station, hour and given month of the year.
Let F(p) be the actual frequency distribution of the parameter for the given hour and month, showing some central tendency.
As the probability that Xp will be at the tails of the distribution is small, the tails can be used as statistical acceptance limits.
The 1st and 99th percentiles of the distribution can be used:

$$\text{1st percentile} \leq X_p \leq \text{99th percentile}$$

Data outside these limits will be flagged for further exploration and subjective judgement.

5. SEQUENTIAL QUALITY CONTROL TEST (SQCT).

The basic assumption underlying SQCT is that a time sequence of observed values of a parameter is expected to exhibit a certain measure of persistence (coherence), depending on the value of the standard deviation and the autocorrelation function:

The following "Threshold Equation" is tested:

$$[X_T - X_{T-1}] \leq a\sigma\sqrt{2(1-r)}$$

Where:
- X_T - parameter value measured at time T
- X_{T-1} - parameter value measured at time T-1
- σ - standard deviation of the parameter X
- r - autocorrelation coefficient of X with lag 1
- a - a constant selected empirically.

6. Z-SCORE RUNNING SUM TEST.

This test is used to detect systematic, relatively small errors caused by calibration offset of measuring instruments, or zero drifts.

For a given hour and month of the year it is assumed that the parametr value, exhibiting a distribution with a central tendency, should move randomly around the median value, and given enough time, the algebraic sum of these deviations should be zero, or at least not deviate strongly from zero (should remain within several st. dev.):

$$[\Sigma(X_i - \overline{X})/\sigma] \leq 3$$

If a tendency shows up for the Z-Score Running Sum to increase steadily, an offset error should be suspected.

REFERENCES

1. Policy on Services for Communication and Archiving of Data from Automatic Stations. Environment canada, 1983.

2. Ponting, J.F. and M.A. Sarson (1984): Operational Quality Evaluation of Surface Observations. WMO Report No. 15: Instruments and Observing Methods, p. 239-243. Geneva, 1984.

3. Acheson, D.T. (1987): Some General Considerations and Specific Examples in the Design of Algorithms for Synoptic Automatic Weather Stations. Instruments and Observing Methods, Report No. 19, WMO/TD - No. 230, Geneva, 1987.

4. Painting, D. (1991): Guidance on the Establishment of Algorithms for Use in Synoptic Automatic Weather Stations. WMO/TD-No. 452. Instruments and Observing Methods, Report No. 47.

ISO STANDARDS FOR METEOROLOGICAL MEASUREMENTS

Thomas J. Lockhart, CCM

Meteorological Standards Institute
Fox Island, Washington 98333, USA

BACKGROUND

There were eighteen participants at TECO-92 who expressed an interest in the formation of a committee or subcommittee within ISO to consider international standards on meteorological instrumentation. This was in response to a paper (Ref. 1, 1992) describing the proposed process by which such a subcommittee was being formed. Another five names were added by the author to make a mailing list of twenty three.

Letters were sent to this mailing list in March of last year describing the application to ISO/TC 146, Air Quality, to form a subcommittee on meteorology. Since TC 146 was meeting in Philadelphia, PA, USA, at ASTM (American Society for Testing and Materials) headquarters during October 4-8, 1993, an organizational meeting for the proposed new subcommittee was scheduled.

The application was sent to the 22 participating countries and 30 observer countries of TC 146 by Dr. Klaus Grefen, Secretariat, Kommission Reinhaltung der Luft, im VDI und DIN, Postfach 1139, D-4000 Dusseldorf 1. It is necessary for five member countries to agree to an active role in the new subcommittee for the formation process to proceed. This requirement was satisfied with the responses from France (AFNOR), Germany (DIN), Poland (PKNMiJ), Turkey (TSE) and USA (ANSI).

ORGANIZATIONAL MEETING

The minutes of the organizational meeting of October 4-5, 1993, show the following persons present:

Canada	Lou Shenfeld, P.Eng.	The MEP Company
France	Michel Leroy	METRO FRANCE
Germany	Harald Brunger	VDI DIN
	Ernst Dittmann	DWD (Nat. Wea. Ser.)
	Klaus Grefen	VDI DIN, Sect. TC 146
	Rolf Kordecki	VDI DIN
	Werner Rudolf	Fed. Enviro. Agency
Netherlands	Cornelis A. Aronds	Chairman, TC 146
UK	W.G. Cummings	
	D.D.B.H. Munns	Inspectorate of Poll.
USA	Carlton O. Hommel	ASTM D-22
	S.D. Allen Iske	ASTM D-22
	Thomas J. Lockhart, secretary	Meteor. Standards Inst.
	Clayt Matthews	USA TAG for TC 146
	Harry L. Rook	NIST, ASTM D-22
	John T. Snow, chairman	Purdue University
	Richard Thomas	NOAA/NWS
WMO	Klaus Schulze	World Weather Watch

Examples of meteorological standards were distributed to those present. It was stated that the German standards would soon be translated into English.

Copies of ASTM D-22.11 standards were distributed.

Standard Test Method for Determining the Performance of a Cup Anemometer or Propeller Anemometer (D 5096-90)

Standard Test Method for Determining the Dynamic Performance of a Wind Vane (D 5366-93)

Standard Practice for Measuring Surface Wind and Temperature by Acoustic Means (draft 9, 8/24/93)

Copies of the cover page of three VDI standards were distributed.

Meteorological Measurements Concerning Questions of Air Pollution (VDI 3786, Part 2)

Determination of the vertical wind profile by Doppler SODAR systems (VDI 3786, Part 11)

Turbulence measurements with sonic anemometers (VDI 3786, Part 12)

The title "Meteorology" was chosen for the subcommittee after a discussion which included the suggested title "Environmental Meteorology." This suggestion, with its implication that there was some sort of meteorology that was not associated with the environment, was not accepted.

The scope of the sub-committee was defined. It is:

"The subcommittee is concerned with the standardization of the definition, measurement and application (for example models) of meteorological variables with respect to air quality and other environmental purposes."

The example of models was used because it is an important application for air quality measurements. It was acknowledged that, while a "standard model" would be difficult to define, the effort to do so may suggest model elements or attributes worthy of standardization. Model validation methods would be an example.

The purpose and justification for establishing a subcommittee on meteorology was discussed at length. A consensus was reached for the following:

"There is a need for extension of existing meteorological guidelines into international standards. A strong relationship exists between air quality and meteorological variables. There is, therefore, a need for standardization of the definition, measurement and application of meteorological variables with respect to air quality and other environmental purposes. ISO is the proper body to establish international standards because of the nature and methodology of this organization. A new subcommittee, SC5, is proposed because the subject is not covered in the scopes of the existing subcommittees of TC 146, and expansion of their scopes is not practical because of the nature of the subject."

There was considerable discussion of the role of the World Meteorological Organization (WMO) and its Commission for Instruments and Methods of Observation (CIMO) in establishing meteorological standards. The value of the Guide to Meteorological Instrument and Observing Practices (WMO No. 8, 1983) was acknowledged. Differences in the structures of ISO and WMO were discussed.

ISO abides by the traditional values of a standards organization. Its members, some 90 countries, consist of national standards bodies (ANSI, the American National Standards Institute, is the member body from the United States). Membership is open to all interested parties who may wish to volunteer their expertise toward a consensus standard. Due process is applied through balloting draft standards. Negative votes must be acknowledged and satisfied by one of several acceptable methods. Memberships are balanced so that no one organization, be it governmental, industrial or societal, is able to dominate the process for any purpose. All recognized standards-writing organizations apply these practices.

WMO is a body of government meteorological services. It provides advice to member countries through reports, instrument intercomparisons, guide documents and meetings for the purpose of standard meteorological practice. It was recognized that a close relationship between WMO/CIMO and ISO/TC146/SC5 will be to the advantage of both organizations. It is hoped that ISO standards will strengthen WMO documents and practices through reference.

The program of work listed general areas of meteorological measurement. It will be the first task of the new subcommittee to make this list specific with work groups and their leaders identified. The initial list was:

Surface wind
Air temperature
Humidity
Solar and terrestrial radiation
Precipitation
Atmospheric Pressure
Surface Characteristics

A list of some existing standards was compiled. A more comprehensive list is in order before the "harmonizing" processes of finding international consensus begins. The initial list follows:

AS 2923 Ambient Air - Guide for Measurement of Horizontal Wind for Air Quality
ASTM D 5096 Standard Test Method for Determining the Performance of a Cup Anemometer or Propeller Anemometer
ASTM D 5366 Standard Test Method for Determining the Dynamic Performance of a Wind Vane
BS 185 Meteorology
BS 692 Specification for meteorological thermometers
BS 2520 Specification for barometer conventions and tables, their application and use
BS 3883 Specification for drum chart mechanisms for meteorological recorders
BS 5284 Specification for aspirated hygrometer
BS 7527, Part 1 Environmental parameters and their severities
BS 7527, Part 2 Environmental conditions appearing in nature
BS 8104 Code of practice for assessing exposure of walls to wind-driven rain
VDI 3786, Part 11 Determination of the vertical wind profile by Doppler SODAR systems
VDI 3786, Part 2 Wind, Meteorological Measurements Concerning Questions of Air Pollution
VDI 3786, Part 12, Turbulence measurements with sonic anemometers

The initial membership list for TC 146/SC 5 shows five participating "P" members and seven observing "O" members. Some countries expect to become active members after the subcommittee is formally created.

P-Members	O-Members
ANSI (USA)	BSI (United Kingdom)
DIN (Germany)	ON (Austria)
TSE (Turkey)	SCC (Canada)
PKNMiJ (Poland)	SABS (South Africa)
AFNOR (France)	NSAI (Ireland)
	Inst. o. Environm. Health?/New Zealand
	Uni Leuven/Louvain?/Belgium

A letter from Steven P. Cornish, Program Administrator, Standards Technology for the USA Member Body of ISO, dated October 5, 1993, was received and reviewed. It requests that the secretariat of the proposed ISO/TC 146 subcommittee on meteorology be allocated to ANSI. It also nominates Dr. John Snow of Purdue University to serve as Chairman of this subcommittee.

It was considered important for an official liaison be established with WMO. The fact that a request for WMO liaison already exists was noted.

FUTURE ACTIVITIES

There is a continuing need for unambiguous consensus standard methods and definitions for most meteorological variables. Whenever an instrument, sensor or system is accompanied by a set of specifications, there needs to be a recognized method by which it can be determined whether or not the specifications are met, as advertised. The measurement process is largely independent of the application of the data. Siting and summarization methods are often designed for specific applications. The work of ISO/TC146/SC5 will concentrate on the measurement process.

For the goals of this new subcommittee to be reached and to be valuable to air quality and other applications, a membership of experienced meteorologists and engineers is essential. We encourage all who feel they can make a contribution to this process to contact the leader of the delegation to TC 146 from the member organization in your country. In the United States the process would be as follows.

Contact the Chairman of ASTM D-22.09, the Technical Advisory Group (TAG) to TC146, and ask to join this TAG. The contact should be made through

Mr. George A. Luciw, Staff Manager for D-22
ASTM
1916 Race Street
Philadelphia, PA 19103-1187, USA
(215-299-5571) or (fax 215-299-2630)

It is not necessary to be a member of ASTM to be a member of the TAG, but it is customary to be a member of D-22.11 on meteorology to participate in the standards writing activities of ASTM.

Meetings of ISO/TC146/SC5 will be called by the Chairman, Professor John T. Snow. US delegates to the meeting will be designated by ANSI upon recommendation from the US TAG. Only delegates from member countries may attend and vote at meetings. Most of the business of a subcommittee is conducted by mail.

A parallel process will exist for all member countries. What the process is can be learned from the leader of the TC 146 delegation. Members of delegations to ISO-/TC146/SC5 need not be expert in air quality applications. They should be expert in the field of meteorological measurement.

It takes a minimum of four months to call a meeting for a subcommittee. An informal meeting of "friends of ISO/TC146/SC5" is planned for March 1, 1994, from 14.00 to 17.30 in the vicinity of METROEX-94. If you are interested in learning about this standards program or participating in it, please attend or send a representative. All of the attendees of the organizing meeting in Philadelphia will also be invited to attend.

For any further information or help in joining the ISO/TC146/SC5 activity, contact:

Thomas J. Lockhart, CCM
Secretary, ISO/TC146/SC5
Meteorological Standards Institute
P. O. Box 26
Fox Island, WA 98333-0026, USA
(206-549-2179) or (fax 206-549-2758)

REFERENCES

Ref. 1 Lockhart, T.J., 1992: International Instrument Standards for Comparability. WMO Technical Conference on Instruments and Methods of Observation (TECO-92), Vienna, Austria, 11-15 May. WMO/TD-No. 462, pages 208-211.

Session VI

REMOTE SENSING

A NEW CLOUD HEIGHT INDICATOR USING A SINGLE PULSE EYE -SAFE ERBIUM GLASS LASER

J.L.GAUMET, O.PEYRAT, M.CLUZEAU
METEO-FRANCE
7 rue Teiserenc de Bort
78190 TRAPPES FRANCE

P. PIERRARD, J. PRIEUR
SOPELEM/SOFRETEC
53 rue Casimir Perier
95872 BEZONS FRANCE

I - INTRODUCTION

The French aeronautical station network is still equipped with spark flash lamp ceilometers. New instruments derived from LIDAR technologies with Gallium Arsenide laser transmitter are progressively remplacing these old equipments.
These laser ceilometers, also called cloud height indicators, however, provide good measurements but do not present sufficient eye-safe protection for maintenance operations.
For these reasons, the SOPELEM-SOFRETEC, in association with METEO-FRANCE, has decided to develop a new cloud height indicator using a solid-state Erbium Glass laser which offers absolute eye-safety.
Moreover, this company has a great experience in military laser range-finders and can propose high quality and low cost equipments.

II - METHODOLOGY.

1°) LIDAR principles.

The monostatic LIDAR principles are similar to those of conventional RADAR. The transmitted beam is attenuated on its path, backscattered at range R and again attenuated on its return path to the receiver. The power P(R) arriving at the receiver is given by :

$$P(R) = \frac{K_o \, \beta(R) \, e^{-2\int_o^R \alpha(r)\,dr}}{R^2}$$

Where $\beta(R)$ is the backscatter coefficient at range R.
$\alpha(R)$ is the extinction coefficient which is range dependent.
K_o the apparatus constant.

The two unknowns in the lidar equation are $\beta(R)$ and $\alpha(R)$ and both are dependent on the nature of the scattering particles. They are related according to a power law of the form:

$$\beta = k \alpha^n$$

where k depends on wavelength and size distribution of particles.
and $n \sim 1$.

2°) LIDAR inversion.

KLETT has developed the backward inversion method using the analytical solution of the LIDAR equation. The solution is written as :

$$\alpha(R) = \frac{P(R).R^2}{\left(P(R_o)\,R_o^2\right)/\alpha_o - 2\int_{R_o}^{R} P(r)\,r^2\,dr}$$

where α_o, the extinction coefficient at a reference range Ro is the integration constant.
This equation is known to become unstable with increasing range because the denominator is a small difference between two increasingly large numbers.
KLETT avoided these instabilities by choosing the boundary value at the far end Rm of the range interval, thus inverting the equation in the backward instead of the forward direction. The new solution becomes :

$$\alpha(R) = \frac{P(R).R^2}{\left(P(R_m)\,R_m^2\right)/\alpha_m + 2\int_R^{R_m} P(r)\,r^2\,dr}$$

3°) Principle of the ceilometer.

The cloud base can be defined as rapid transition within few tenth meter between a clear atmosphere and a dense droplet medium. The cloudbase is then identified by a sharp increase of backscattering signal when the laser beam penetrates inside the cloud.
In order to become independent of the high signal contribution from the near-range part of the lidar return which can mask cloud peaks, the range-finding will be performed by processing profiles of the extinction coefficient calculated by KLETT's inversion method. As with the backscattering signal, the cloud base will be identified by detection of a sharp increase on the extinction profile.
Cloud height is then determined by measuring the time of flight of a single laser pulse to reach the cloud and return to the ground.
Moreover, clouds frequently display variations in the height of the bottom in time and space. These variations are commonly observable by eye from the surface as texture in the appearance of cloud bottom. Consequently, for low ceiling , the pulse repetition rate must be relatively high, around 4 pulses per minute.

III - DESCRIPTION OF THE CEILOMETER.

1°) - Laboratory and prototype equipment.

The transmitter is a highly reliable Q-Switched optically pumped solid-state laser. The laser amplifier media is a glass rod doped with Erbium generating a stimulated emission at a wavelength of 1,54 µm. Due to the wavelength and the high power laser, the receiver head is greatly simplified.
The infrared range also has the advantage of being in the wavelength where sun noise radiation is lower.
A low cost InGaAs PIN photodiode with a sunlight filter gives good performances of the equipment. The signal collected by the photodiode is then amplified, digitized and processed via a specific software.

	EXPERIMENTAL CEILOMETER	**PROTOTYPE CEILOMETER**
TRANSMITTER	Er:Glass LASER	**Er:Glass LASER**
WAVELENGTH	1.54 µm	**1.54 µm**
OUTPUT ENERGY	12 mJ	**8 mJ**
PULSE WIDTH	30 ns	**30 ns**
LASER SAFETY CLASS	CLASS 3A	**CLASS 1**
PEAK POWER	400 kW	**260 kW**
DIVERGENCE	4 mrd	**1.5 mrd**
RECEIVER		
LENS DIAMETER	30 mm	**65 mm**
FIELD OF VIEW	5 mrd	**3.5 mrd**
PHOTODIODE	PIN (InGaAs)	**PIN (InGaAs)**
MINIMAL DETECTABLE POWER	100 nW	**60 nW**
PROCESSING UNIT	PERSONAL COMPUTER	**SINGLE BOARD**
SAMPLE FREQUENCY	50 MHz	**14.98 MHz**
PROCESSOR	i 386 - 33 MHz	**M 68302**

Table 1 : **Technical characteristics of the experimental and the prototype ceilometers**

The basic element of the experimental equipment is a modified SOPELEM-SOFRETEC range-finder used for artillery. There are no changes in the Erbium : Glass single pulse laser head and the receiver and transmitter optics. A very low noise logarithmic amplifier is used to compress the received signal. A fast digital oscilloscope remote-controlled by a personal computer is used to record and memorise backscattering.. This experimental equipment has been used to collect the data of one or several layers of clouds over a range of 1500m. The prototype has enhanced technical characteristics (Table 1) and can measure clouds up to 3000m. It is a self-contained compact ceilometer comprising a single board with a microprocessor. The figure 1 represents maximum range versus visibility for the experimental and the prototype ceilometers.

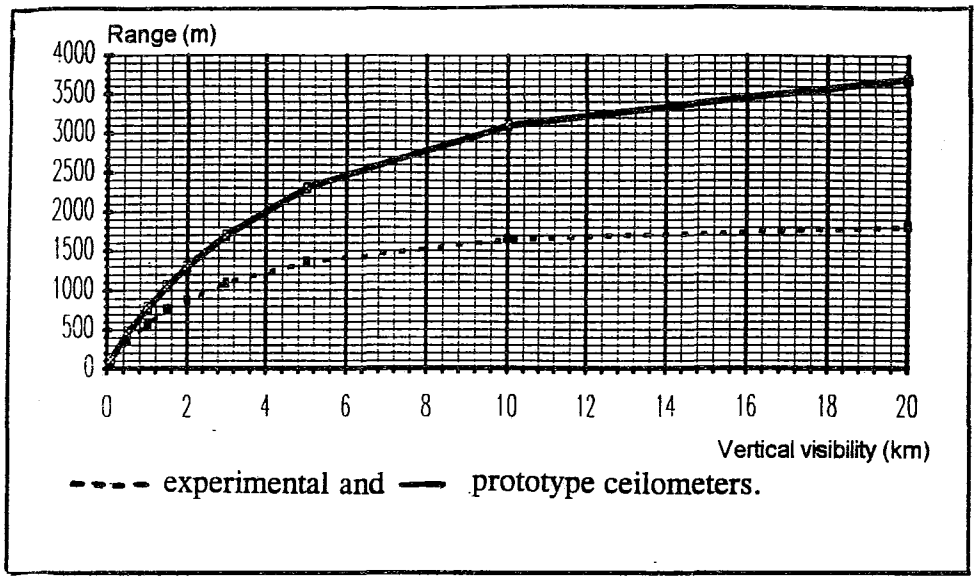

Figure 1 : Range versus visibility for experimental and prototype ceilometers

2°) Eye-safety principle.

Laser equipment with full eye-safety is now available for installation, operation and maintenance phases. In the Infra-red band, the wavelengths between 700 and 1400 nm are transmitted through the ocular media, as shown in figure 2.
This range can cause maximum retina injury. The diameter of the spot, formed by the few milliradian divergence of the collimated laser beam is a few tenth of a micrometer, therefore the retina destruction threshold is reached with very low input energy.
Beyond 1400 nm laser energy is absorbed by the internal media : cornea, vitreous humor, lens. The retina is no longer a critical factor for the acceptable input energy. The Maximal Permissive Exposure (MPE), specified by the laser standards at each w avelength, can be used to calculate the Nominal Optical Hazard Distance (NOHD) at which exposure to a laser beam begins to be safe. The NOHD for a Neodyme : YAG, a Er : Glass and AsGa diode laser are described in Table 2.

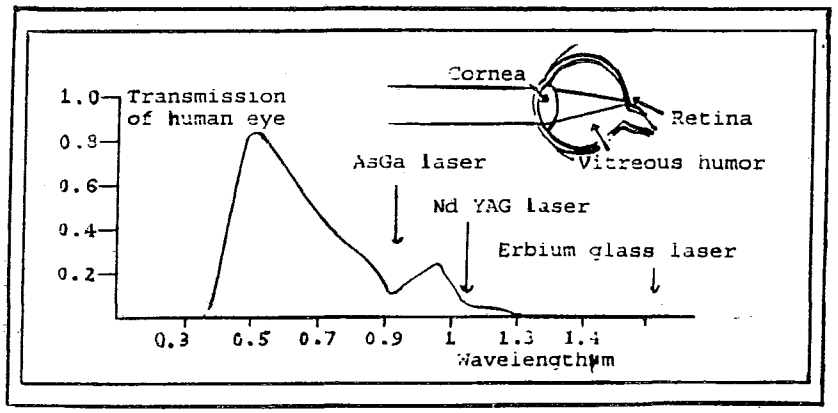

Figure 2 : Eye transmission versus wavelength

	NACKED EYE NOHD	MAGNIFYING OPTICS X 10 NOHD	CHARACTERISTICS USED DIAM. BEAM (cm) OUTPUT	ENERGY/ PULSE (mJ)	MPE */ PULSE (J/cm^2)	REPETITION RATE (Hz)
LASER DIODE AsGa (0.9 µm) (class 3)	160 m	2500 m	5	$1.5\ 10^{-3}$	$5\ 10^{-7}$	2000
Nd YAG (1.06µm) (class 3)	1400 m	> 10000 m	1.5	20	$5\ 10^{-6}$	1
Er :Glass (1.54µm) (class 1)	**0 m**	**0 m**	**1.5**	**8**	**1.0**	**1**

Table 2 NOHD for Nd : YAG, Er : Glass and AsGa diode laser

* Freq < 10 Hz, Θ = 0.5 mrd, Δt < 100 ns.
Data standard : ANSI-Z-136.1 and IEC 825.

IV - FIRST EXPERIMENTAL RESULTS.

1°) Backscatter and extinction profiles from cloudy atmosphere.

The backscattering signal P(r) is obtained by direct measurement of the light which reaches the detector.
The extinction profile $\alpha(R)$ is determined by a signal inversion using the KLETT method. The cloudbase can be identified on the direct or inverse signal, indifferently. The inversion eliminates the strong part of the signal backscattered by low atmospheric layers and consequently improves the cloud height determination in this part the of atmosphere. However, the inversion method needs significant signal to noise ratios and the knowledge of a boundary value in altitude of the extinction coefficient α_m.Difficulties may exist to evaluate this boundary. The figure 3 shows an example of basckatter and klett 's inversion profiles.

2°) Cloud base height comparisons.

The figure 4 represents cloudbase height comparisons between the laboratory equipment and the spark flash lamp ceilometer of the French meteorological network (TNA). These measurements show a good correlation of 787 points (r = 0.82) between the two ceilometers, despite the very different techniques. Moreover, these cloud base heights are obtained from the backscattered signal without application of the inversion method.

V - CONCLUSION

The laboratory equipments do not provide optimum characteristics to obtain high signal to noise ratios. These first results will be improved by the characteristics of the prototype and the new laser range-finder algorithm with better signal to noise ratios.
SOPELEM-SOFRETEC, a french optronic company, has long been deeply involved in the designing and the manufacturing of range-finders based on the technology of laser ceilometers. This long acquired experience and know-how has now been applied to design a new ceilometer.
The main advantages of such Erbium : Glass ceilometer are :

- Always eyesafe even for maintenance.
- Modular design offers easy and low cost maintenance.
- Enhanced performances despite smoke and dust.
- Production of low cost effective equipment.
- Possibility to design a compact and low weight equipment.

The next work of METEO-FRANCE is the improvement of the inversion algorithm for a better cloud detection.

VI - REFERENCES

KLETT J.D. stable analytical inversion solution for processing LIDAR returns. J. of applied optics vol 20 n°2 15 Jan. 1981.
CARNUTH W. and REITER R. cloud extinction profile measurements by LIDAR using klett 's inversion method vol 25 n°17 1 Sept. 1986.

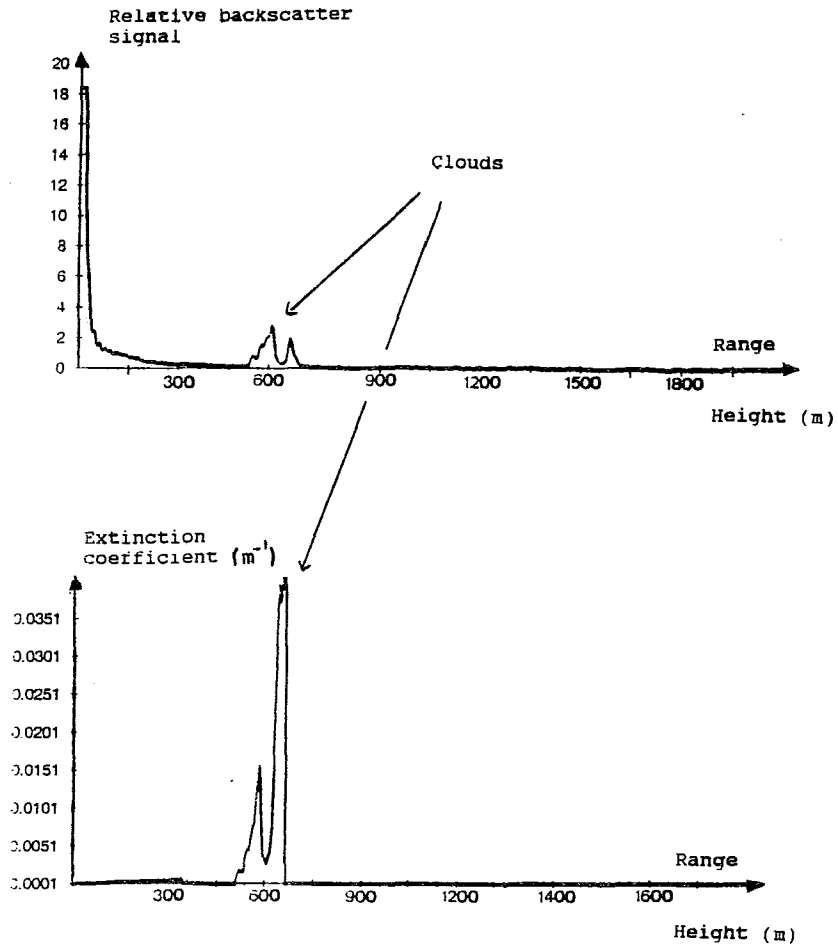

Figure 3 : Backscatter and klett 's inversion profiles

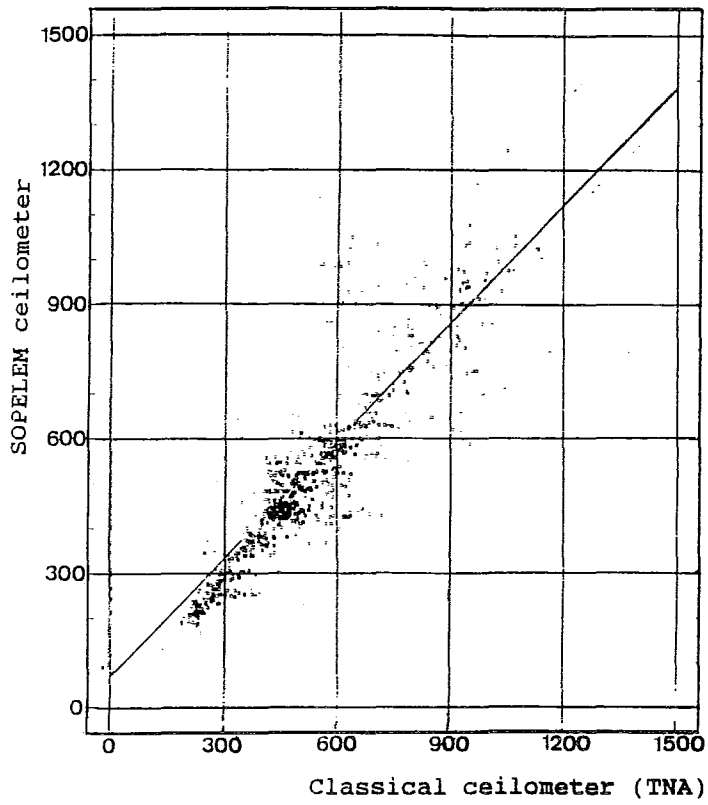

Figure 4 : Cloud height comparisons between classical (TNA) and Erbium Laser ceilometers

Comparison of windprofiler and rawinsonde measurements

Neisser,J.; U. Görsdorf; H. Steinhagen; Deutscher Wetterdienst,

Meteorologisches Observatorium Lindenberg, Germany

1 Introduction

Routine balloon soundings from several hundred location around the globe provide a very important part of the meteorological data input into the analysis and the forecast models. This network of radiosonde stations is able to resolve the synoptic-scale structure of the wind and temperature fields with a temporal resolution of 6 to 12 h. But an other measuring technology is necessary for the better understanding of mesoscale processes and with it of the improvement of weather forecasts.
Therefore during the last 20 years a large progress has been made in the development of wind-profiling technology using clear-air Doppler radar techniques. These wind profilers are appropriate tools to measure the vertical profiles of the three-dimensional velocity vector with high temporal ($\leq$1 h) and vertical ($\approx$300 m) resolution into the troposphere and the lower stratosphere (Röttger and Larsen, 1990, for a review). The installation of the NOAA 30-stations Wind Profiler Demonstration Network in the central United States was a first step to incorporate the high time-resolution radar-derived wind data in operational meteorology (Serafin, Dabberdt, 1990). This network provides improved horizontal and temporal resolution in comparison with the rawinsonde network.
Before wind profiler data can be used in operational service as a matter of routine, however, comparisons with standard rawinsonde data should be conducted in order to assure that wind profilers will constitute a consistent and reliable addition to the existing array of observational technologies used to provide data for model input (Weber and Wuertz, 1990). These comparisons may be based upon field campaigns, or on long-term observation programs if feasible.
A number of comparisons of wind profiler and rawinsonde data have been carried out to date in a variety of locations, including Arecibo (Fukao, 1982), Poker Flat (Larsen, 1983), Denver (Weber and Wuertz, 1990), and Saipan (May, 1993). In Europe, comparisons between wind profiler and rawinsonde measurements have been generally succesful but limited in excent (Czechowsky et al., 1984; Rüster et al., 1986, Yoe et al., 1993).
The purpose of the present paper is to compare wind profiler data with corresponding rawinsonde measurements as a preliminary step toward the eventual operational use of profilers by the German Weather Service and as a representative example for Central Europe. For this purpose a field campaign has been carried out from 26 Oct. to the 7 Nov. 1992 using the SOUSY-VHF-Radar of the Max-Planck-Institut für Aeronomie and a mobile rawinsonde station of the German Weather Service deployed in the Harz Mountains near Bad Lauterberg.

2 Measuring program

Continuous measurements of the wind field were made over a period of 12 days during the field campaign with the SOUSY-VHF-Radar. The main parameters of this system are listed in Table 1:

SOUSY - VHF - Radar	
Operational frequency	53.5 MHz
Pulse peak power	600 kW
Effective antenna area	3150 m^2
Altitude range	2 to 25 km
Range resolution	300 m
One way beam width	5°
Number of beams	5
Zenith distance	7°
Minimum time resolution for one wind profile	1 minute
Incoherent averaging time	20 minutes

The backscattered power was measured in the altitude range from 2 to 25 km with a range resolution of 300 m. The radar beam directed first vertically, then was tilted away from vertical at an angle of 7° toward the north, east, south and west. The coherent averaging time was approximately 1/6 s and 64-point complex time series were measured for every range gate along each beam. Thus a complete profile of 5 radial velocities at a given height was obtained about every minute. To eliminate outliers and reduce the data volume to manageable amount, the raw radial velocities have been averaged for a period of 20 minutes. From these, complete averaged wind profiles have been calculated.
An important factor for the comparison of radar and rawinsonde data are differences arising from the actual spatial variation of the wind field. Therefore, a mobile rawinsonde station was deployed and operated only 5 km from the radar site at the place called Stöberhai. The wind measurements were accomplished using a wind finder radar which tracked balloon-borne and targets. The wind data were determinated for 300 m height intervals. The other meteorological parameters (P, T, H) have been received from the Vaisala Radiosonde system RS 80 / PC-Cora. Rawinsonde launches were performed every 12 hours (12 and 00 LT). During some special measuring periods the launch interval was decreased to 2 and 3 hours. The local rawinsonde data have been supplemented with the standard measurements of the aerological station Hannover.

3 Comparison of windprofiler and rawinsonde measurements

3.1 Methods of comparison

To make the comparison of wind profiler and rawinsonde data as meaningful as possible, differences in their respective measurement principles must be considered. The rawinsondes data are got at various heights at different times and locations due to finite ascent time and advection of the target, whereas the wind profiler provide wind velocities over a single site while probing all ranges quasi-simultaneously. Furthermore, the two systems sample on different spatial and temporal scales. Therefore, it is expected that the differences between wind profiler and rawinsondes results Δv are produced not only by measurement errors of both systems Δv_e, but also by the spatial Δv_s and temporal Δv_t variations of the wind field:

$$\Delta v = \Delta v_t + \Delta v_s + \Delta v_e$$

The random terms of these differences can be neglected by averaging over a large number of measurements. The temporal and spatial separations of the measurements respectivly the instruments were small by special adaptation procedures of the data sets of the different kinds

of wind measurements. Under this conditions Δv depends on Δv_e only.

3.2 Results

During the campaign a total of 36 rawinsonde balloons were launched successfully. The comparison were made for a height interval from 2 to 20 km. In contrast to the standard analysis a modified algorithm for the calculation of wind data was used. Based on the raw rawinsonde data measured every 10 sec, the wind velocity was calculated for the same 300 m height intervals as for the SOUSY-VHF-Radar. Therefore the time averaging interval depended on the ascent rate.
The time averaging interval of the wind profiler data was centered on the middle time of a rawinsonde flight. The mean differences of all 36 soundings are presented in Figures 1 a, b. No editing of the data has been performed. It is readily seen that the rawinsonde measures 0.5 to 2.0 m/s larger values than SOUSY-VHF-Radar throughout most of the troposphere. In the region of the wind maximum near 10 km, these differences increase to about 2 to 4 ms^{-1}. These large differences correspond to larger wind speeds, those in excess of about 30 ms^{-1}. In the lower stratosphere the differences tend to be scattered about around zero with maximum absolute values of 3 ms^{-1} (Fig. 1a). The standard deviation is 1.5 to 3.5 m/s in the troposphere, 4 to 6.5 ms^{-1} at heights between 10 and 13 km and 2 to 5 ms^{-1} above 13 km.
The wind direction differences (Fig. 1b) are small with a maximum of 5° in the troposphere and 12° in the stratosphere, although the rawinsonde values in the troposphere show a systematic clockwise shift relative to the profiler data. The corresponding standard deviation is 17° at a height of about 3 km, decreases to 4° at 5 km and increase gradually to a mean value of 12° at 20 km. Similar mean differences were found between the radar wind measurement and the rawinsonde data of the station Hannover, but the standard deviations are even found to be even larger.
The rms-differences of wind speed in dependence on the temporal separation between the two kinds of measurements show for the lower and middle troposphere a marked minimum for small temporal differences whereas for the higher levels no dependence was found. A temporal seperation up to 60 minutes have no significant influence on the rms-differences for all hight levels (Fig. 2)
Considerating the spatial separation of the measurements the horizontal wind gradient was estimated as well from profiler beams pair as from the gradient between the measurement of several neighbouring rawinsonde stations. For both methods the spatial adaptation shows no clear improvement in the statistical characteristics of the comparison as can be seen in following Table 2:

	"temporal adaptation"			"temporal and spatial adaptation"		
Height level [m]	BIAS [m/s]	STD [m/s]	RMS [m/s]	BIAS [m/s]	STD [m/s]	RMS [m/s]
5000	0,4	1,8	1,8	0,5	1,7	1,7
10000	2,9	5,4	6,0	2,9	5,3	5,8
16000	-1,2	4,4	4,3	-1,3	4,4	4,3

The possible reasons for this result are the different scales and the random errors of the measurement systems (s. following Table 3).

Height level [m]	Large scale gradient calculated from estimated wind gradient and the distance between windprofiler site and rawinsonde position [m/s]	Mean random measurement error of rawinsonde [m/s]	Variation of 5 minutes averaging wind speed measured by SOUSY-VHF-Radar [m/s]
5000	0,19	1,35	3,47
10000	0,57	3,31	6,06
16000	0,19	4,08	4,22

The result of the statistics of the comparison of the wind profiler data and the data of collocated rawinsondes indicate a good agreement as well for the wind speed and as for the direction. The differences are statistically not significant when the relatively large standard deviation are considered.

References

Czechowsky, P., G. Schmidt, and R. Rüster, The mobile SOUSY Doppler radar: Technical design and first results, *Radio Sci.*, **19,** 441-450, 1984.

Fukao, S., T. Sato, N. Yamasaki, R.N. Harper, and S. Kato, Wind measurement by a UHF Doppler radar and rawinsondes: Comparison made on 26 days (August-September 1977) at Arecibo, Puerto Rico, *J. Appl. Meteorol.*, **21,** 1357-1363, 1982.

Larsen, M.F., Can a VHF Doppler radar provide synoptic wind data? A comparison of 30 days of radar and radiosonde data, *Mon. Wea. Rev.*, **111,** 2047-2057, 1983.

May, T., Comparison of wind Profiler and radiosonde measurements in the Tropics, *J. Atmos. Oceanic Technol.*, 122-127, 1993.

Röttger, J. and M.F. Larsen, UHF/VHF Radar Techniques for Atmospheric Research and Wind Profiler Applications in Radar in Meteorology, (ed. D. Atlas), *American Meteorol. Soc.*, Boston, 235-281, 1990.

Rüster,R., J. Klostermeyer, and J. Röttger, SOUSY VHF Radar Measurements in the lower and middle atmosphere, *IEEE Transactions on Geoscience and Remote sensing*, GE-24, **6**, 966-974, Nov. 1986.

Serafin, R.J., and W.F. Dabberdt, Profiling networks and developments in the United States, *Meteorol. Rdsch. 42*, 70-83, 1990.

Weber, B.L., and D.B. Wuertz, Comparison of Rawinsonde and Wind Profiler Radar Measurements, *J. Atm. Oceanic Technol.*, **7**, 157-174, 1990.

Yoe, J.G., R. Roth, R. Rüster, H. Voigt, O. Danne, A. Muschinski, and M. Schlüter, Vertical velocities over Central Germany during a TOASTE campaign: Comparison of SOUSY-VHF-Radar Observations and BKN-Modeled results, *Submitted to Meteorol. Zeitschr.*, 1993.

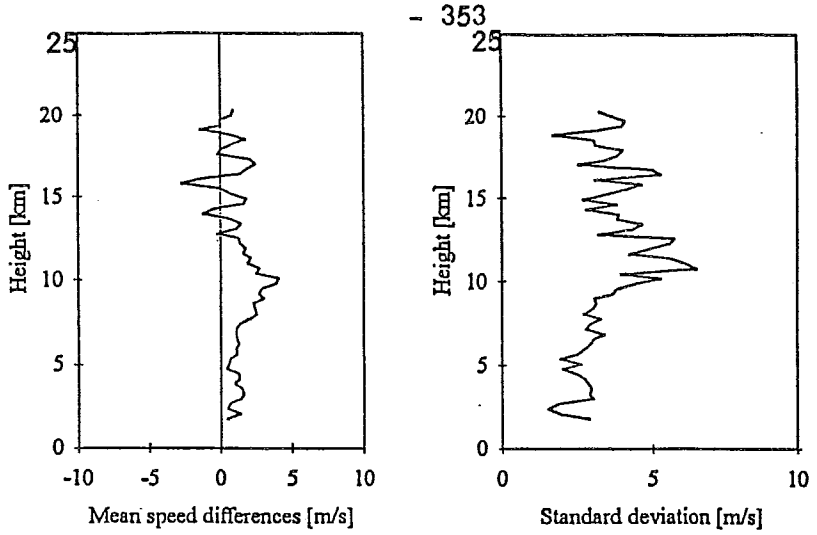

Fig.1a Mean wind speed differences between Stöberhai rawinsonde and SOUSY-VHF-Radar data, and the corresponding standard deviations as functions of height

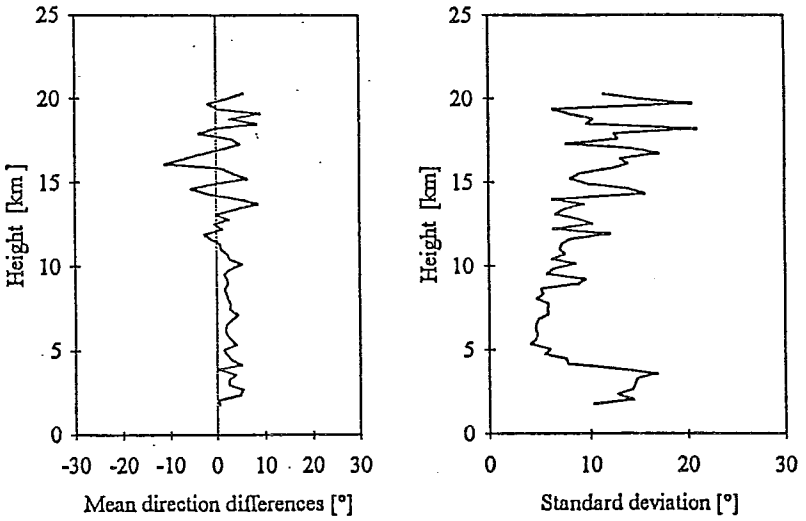

Fig.1b As in Figure 11, but for the wind direction data

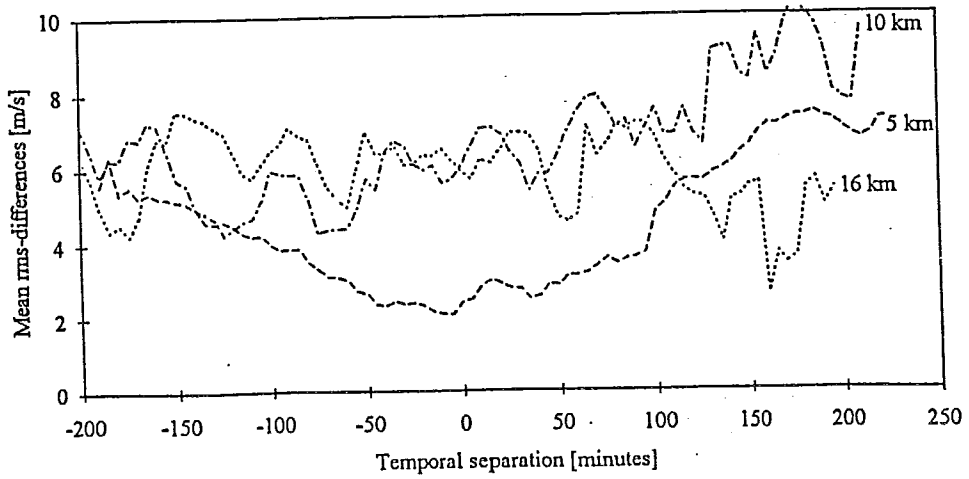

Fig.2 Dependence of rms wind speed differences on the temporal separation of the SOUSY-VHF-Radar measurements and the rawinsonde measurements for 36 cases

A UHF Wind Profiler with RASS for the Boundary Layer: System description and preliminary results

H. Steinhagen, A. Christoph, W. Christoph, U. Görsdorf, J. Lippmann, J. Neisser, Deutscher Wetterdienst, Meteorologisches Observatorium Lindenberg, Germany
J. W. Neuschaefer, K.R. Peterman, G. Pratt, C. Schneider, Radian Corporation, Boulder, USA

1. Introduction

The measurement of vertical windprofiles by the use of pulsed Doppler radars (wind profilers) is well established for meteorological research as well as for operational applications in the field of meteorology (Röttger and Larsen, 1990; Gage, 1990). The three main types of wind profilers operate typically at frequencies in the region of 50, 400 and 1000 MHz. Depending on these operating frequencies the wind profilers can measure the wind in different stories of the atmosphere. With the 50 MHz wind profiler it is possible to measure from 2 to 30 km. The 400 MHz wind profilers can acquire data from 500 meter to 16 km (Martner et. al. 1992). But these wind profilers do not allow to measure wind data in the first 2000 m of the atmosphere with the necessary height resolution of 50 to 100 m. The mesoscale forecasting models as one of the most important user of the new data sources require however height resoluted data, especially at the lowest 2000 m, since one-third of the model layers typically are located below 2500 m. Therefore the boundary layer wind profilers play an important part in the meteorological research as well as in the operational use of corresponding wind data.
The solution of the frequency allocation problem is a chief prerequisite for using wind profilers owing to the dense occupancy of the frequency bands especially in Europe. For the boundary layer wind profilers there exists not one homogeneous solution all over the world. In the USA the boundary layer wind profilers operate at a frequency of 915 MHz (Ecklund et al. 1988, 1990). In France a frequency of 961 MHz is used (Petitdidier et al. 1990). In German as well as in other european countries it was not possible to obtain a frequency allocation for one of these frequencies. After profound investigations the most european countries have decided, that boundary layer wind profilers ought to work at 1290 MHz. On the basis of this decision the German Weather Service began its research program by means of a boundary layer wind profiler at the Meteorological Observatory Lindenberg. The purpose of this research program is the long-term and profound preparation to use remote sensing methods in the field of the operational meteorology. In this paper it is described the new wind profiler at 1290 MHz and initial results. One importent question is, whether the higher operating frequency is suitable likewise for the acquisition of boundary layer wind data. Beyond it the research program of the Meteorological Observatory Lindenberg required some special features of the wind profiler.

2. Special features of the wind profiler

The main points of the first phase of the research program are:

1. The determination of the accuracy and the reliability of the wind data.
2. The estimation of meteorological and other influences of the wind data and their correction
3. The estimation of the real measuring limits (for example height coverage) depending on the meteorological conditions, which predominate in Middle Europe.

These main points lead to requirements of an universal and flexible boundary layer wind profiler, which go beyond an operational system. With such an extended system the possibility is given to optimize the prototype of an operational wind profiler, which will be used in the future for wind profiler networks.
These requirements are:

1. The complement of the boundary layer wind profiler with a Radio-Acoustic Sounding System (RASS) to measure also the temperature profile,
2. The arrangement of the wind profiler antenna and the acoustical source on a turntable to optimize the RASS,
3. The acquisition of the meteorological surface measurements near the profiler,
4. An extensive and well planned quality control and data evaluation,
5. The flexible variation of the system parameters.

The position of this wind profiler at the site of the Meteorological Observatory Lindenberg was decisive, because being an operational rawinsonde station with four ascends per day. By it the possibility is given to compare the different measurements over a long period during different meteorological conditions.

The wind profiler with RASS was developed by the Radian Corporation on the basis of the requirements of the German Weather Service.For it a lot of research results of the National Oceanic and Atmospheric Administration and the National Center of Atmospheric Research and also Sonoma Technology was used. The turntable, the turntable control and the surface measurements were the design of the German Weather Service.

3. System description

3.1 Block diagram

A block diagram of the boundary layer wind profiler is shown in Fig. 1 The antenna of the profiler and the acoustical source of RASS are erected on a turntable being controlled by the turntable processor. The transmit/receive unit convert the 1290 MHz transmitted and received signal to an intermediate frequency of 60 MHz. In this way the transmission cable losses on the 60 m cables between the antenna and the shelter containing the radar processor and the transmit/receive interface can be kept small. The transmit/-receive interface is controlled by the radar processor, which also makes available the signals for the acoustical source by an acoustical amplifier. The radar processor calculates the spectral, moment, wind and temperature data. The wind and temperature data are transmitted by an optical cable with a length of 800m

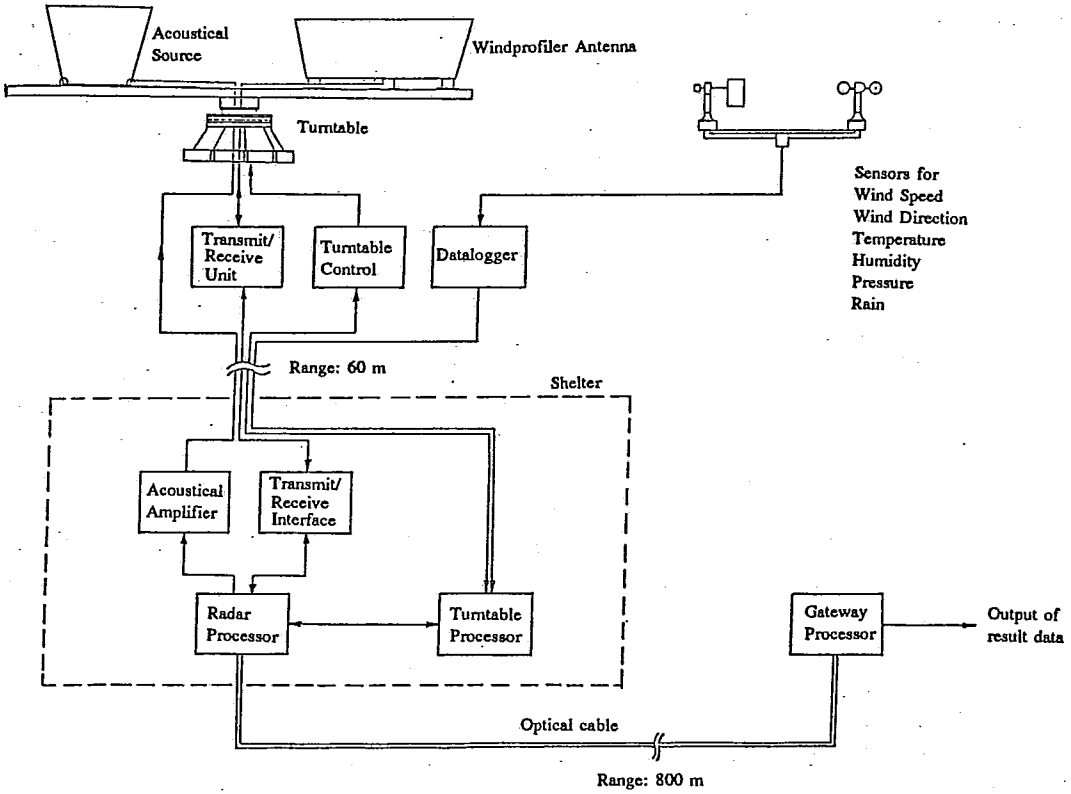

Fig. 1: Block diagram of the 1290 MHz Boundary Layer Wind Profiler

to the gateway processor, which performs the quality control, the data presentation and output.
The sensors of the meteorological surface measurements are situated near the profiler and connected with a datalogger. The surface data are transmitted from the datalogger to the turntable processor and from here to the radar processor. There the wind and temperature profiles measured by the profiler are complemented by the corresponding surface measurement.

3.2 Wind profiler

The wind profiler LAP-3000a can operate unattended and provide continous real-time atmospheric wind data with different vertical resolution of 50, 100, 200 or 400 m, reliably to 3 km. The microstrip antenna of the wind profiler consists of nine panels, each with 36 antenna "patches" (Ecklund et al. 1988). The microstrip antenna pointing direction is controlled by phase into five beam directions, one vertical and four 15,5° oblique beams. The size of the whole microstrip antenna is 2,7 m x 2,7 m (Effective antenna area: 6,8 m^2). Around the antenna a clutter fence is arranged to minimize the sidelobe level of the antenna radiation.
The backscatter signals are received by the transmit/receive unit and interface to the radar processor. The operator can select on the radar processor all the different parameters of the data processing. The most

important are the height resolution (50, 100, 200, 400), the number of range gates (maximum 40), the inter-pulse period(minimum 20 μs), the number of coherent and spectral averages, the number of points of the Fast Fourier Transform (maximum 2048), the number of pulse code cells (0 - 16) and the beam sequence. The calculation of the wind data is carried out based on the consensus average algorithm (Brewster, 1989), which is very useful by the processing of disturbed data. This algorithm allows to select the size of a window including the further processed data and also a percentage set of data which must fall in this window. With all these possibilities the operator can optimize the wind profiler for different applications.

3.3 RASS

May et al. (1990) showed, that the use of a RASS in combination with a wind profiler is very favourable. To measure simultaneously the vertical velocity and the speed of sound the radar processor has the possibility to realize the power spectral analysis with 2048 complex time series points and a Nyquist velocity of about 350 m/s. In this way, both the clear-air signal near zero velocity and the RASS signal near the speed of sound (330 m/s) can be measured during the same time. Therefore the RASS temperature measurement can be corrected for the influence of vertical wind. For a good RASS measurement it is crucial, that the wavelength of the acoustical signal is matched to half of the wind profiler wavelength (Bragg condition) and that the backscattered signal is focused onto the wind profiler antenna (May et al. 1988). For the first requirement a frequency modulated continuous wave (FM-CW) as a linear sweep or as a pseudo random signal is generated. Since the wind leads to a drift of the acoustical wave the backscattered spot must be focused onto wind profiler antenna depending on the wind speed and direction. For it the profiler antenna and the acoustical sources are arranged on the turntable. In this way the RASS can be optimize by rotation of the turntable corresponding to the wind direction and by moving the acoustical source on the turntable corresponding to the wind speed.

3.4 Data evaluation by the user

The user can carry out the evaluation of wind and temperature data with the so called gateway processor located 800 meters away from the radar processor. The gateway processor can perform four separate tasks.

1. Remote control of the wind profiler. This includes turning the profiler on and off, checking the status of the profiler, changing the parameters using the profiler and retrieving wind and temperature data.
2. Converting wind and temperature data into a user-friendly format written in daily and hourly files for each sampling parameter set with unique filenames.
3. Creating of screen and paper displays of the horizontal and vertical wind components, temperature and also refractive index structure constant C_n^2. This allows the user the fast access to the data and also the editing of the data files. Wind speed and direction are displayed in time-height cross-section using the standard wind barb convention or color contours. Vertical profiles of virtual temperature data are displayed in line profiles or color contours.
4. The Quality Control algorithms developed by Weber and Wuertz (1989) check the data consistency in a time-height-window by comparison of each datum with his neighbouring data in the time and height scales. If the differences between one data point and his neighbouring points is greater than a definable value this point is recognize as suspect. Depending on the difference each data point is flagged up operationally with one of three identities: valid, suspect or invalid.

4. Preliminary results

The wind profiler was put into operation on 07/10/93. Since then the normal operating procedure is determining by incoherent averages of the wind for 50 min periods at each of four azimuth beams separated by 90°, and the vertical beam, and of the temperature for the remaining 10 min. of each hour at the vertical beam. The first results ought to presented by measurements of the 15/11/93.

During the measuring period a low pressure area extending to high levels moved over North Germany from west to east connected with a large precipitation area. The centre of the cyclone passed the measurement site during the morning of the 15/11/93 as it can be seen on of wind shift of 180° in Fig. 2. On the backside of the low pressure area colder and more dry air streamed from Scandinavian to Germany demonstrated with the hourly temperature profiles in Fig. 3. The high time resolution allows a detailed analysis of such mesoscale processes.

The comparison of the profiler measurements with the operational rawinsonding shows a good agreement by the wind data as well as the temperature data (Fig. 4). The differences are lower than 2 m/s (wind speed), 10° (wind direction), and 1,1 °C (virtual temperature) respectivly. This differences can be explained

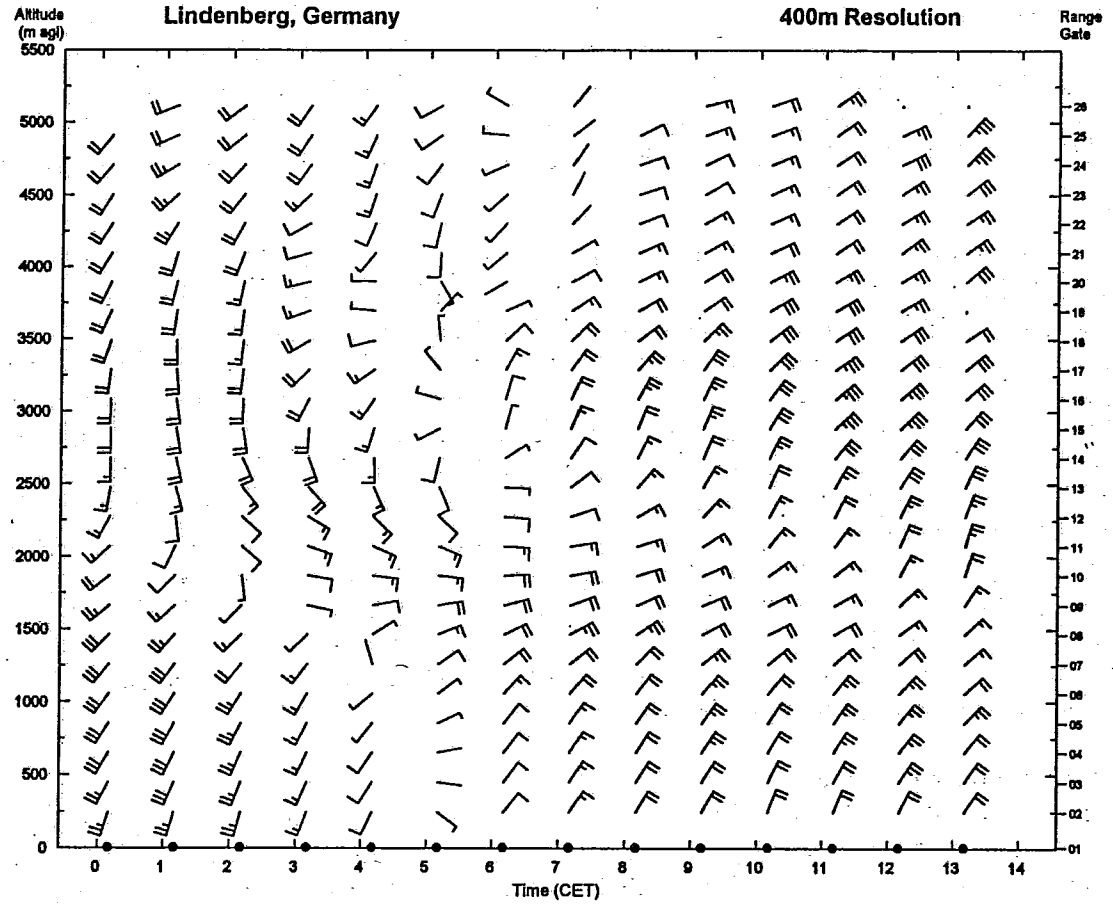

Fig. 2: Time-height cross section measured in Lindenberg on 15/11/93 in a sampling period of 49 minutes with a height resolution of 405 m and a vertical spacing of 202 m.

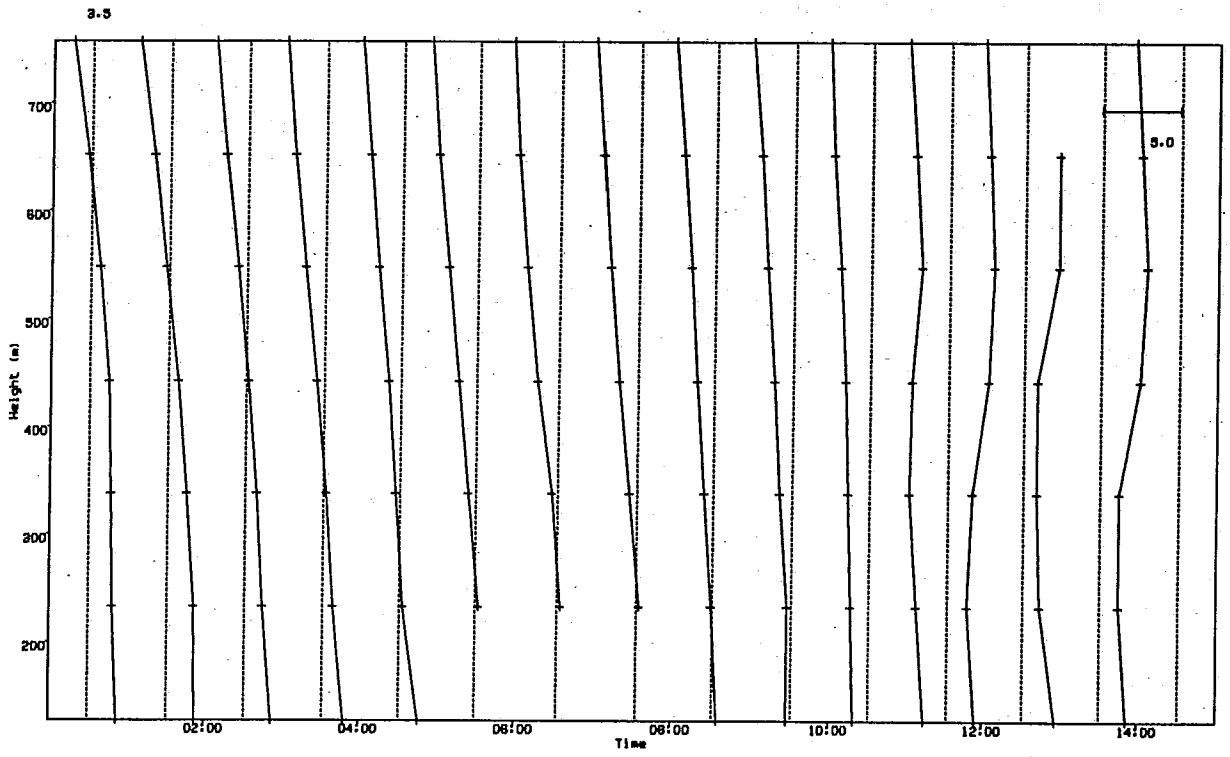

Fig. 3.: Hourly profiles of virtual temperature measured in Lindenberg on 15/11/93 in a sampling period of 10 minutes with a height resolution and vertical spacing of 100 m (The vertical dashed lines correspond to 3,5 °C, the difference between the vertical dashed lines is 5,0 °C)

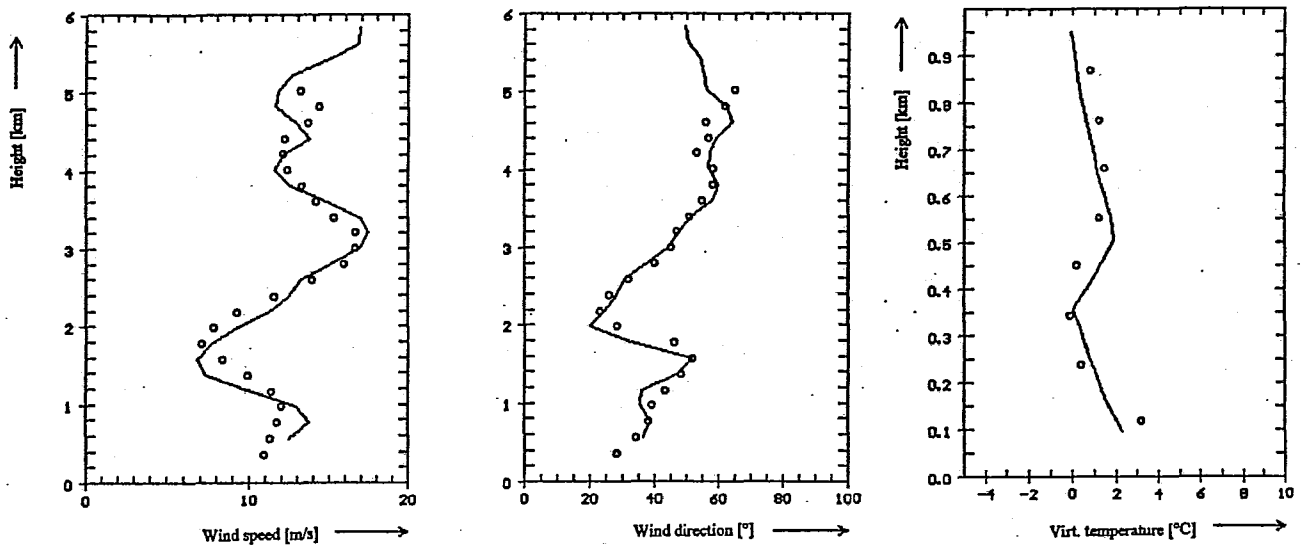

Fig. 4: Comparison of vertical wind speed, wind direction and virtual temperature profiles measured by wind profiler (circles) and rawinsonde (solid lines) on 15/11/93 12°° CET.

with the accuracy and with the different averaging time of the both measuring systems.

5. Conclusion

It was described the components and the properties of a boundary layer wind profiler at 1290 MHz with RASS in an operational application of the German Weather Service. This wind profiler installed at the Meteorological Observatory Lindenberg provides wind and temperature measurements in the first few kilometers of the atmosphere with a minimal height resolution of 50 meters and a time resolution of about 1 to 60 minutes. The properties and capabilities of the system are demonstrated by some first wind and temperature measurements. The comparison with rawinsonde masurements shows a good agreement.
In the future it is planned to compare operationally the wind profiler data with other data (rawinsonde, tethersonde, SODAR), to test the different measuring possibilities of the profiler, to optimize the system for the use in Middle Europe and to find an optimal system configuration for futher operational applications.

6. References

Brewster, K. A., 1989: Quality Control of Wind Profiler Data, Training manual number 2, NOAA

Ecklund, W. l:, D.A. Carter and B. B. Balsley, 1988: A UHF Wind Profiler for the Boundary Layer: Brief Description and Initial Results, Journal of Atmospheric and Oceanic Technology, vol. 5, p. 432-441

Ecklund, W. L., D.A. Carter, B.B. Balsley, P. E. Currier, J. L. Green, B. L. Weber, K. S. Gage, 1990: Field tests of a lower tropospheric wind profiler, Radio science, vol. 25, Nr. 5, p. 899-906

Gage, K. S., 1990: Radar Observations of the Free Atmosphere: Structure and Dynamics in D. Atlas: Radar in Meteorology American Meteorological Society, Boston, p. 534-565

Martner, B.E., D.B. Wuertz, B.B. Stankov, R.G. Strauch, E.R. Westwater, K.S. Gage, W.L. Ecklund, C.L. Martin and W.F. Dabberdt, 1992: An Evaluation of Wind Profiler, RASS and Microwave Radiometer Performance; submissed to the Bulletin of the American Meteorological Society

May, P. T., R. G. Strauch and K. P. Moran, 1988: The Altitude Coverage of Temperature Measurements using RASS with Wind Profiler Radars Geophysical Research Letters, vol 15, Nr. 12, p. 1381-1384

May, P.T., R. G. Strauch, K.P. Moran and W.L. Ecklund, 1990: Temperature Sounding by RASS with Wind Profiler Radars, A preliminary study, IEEE Transactions on Geoscience and Remote Sensing, vol 28, Nr. 1, January, p. 19-27

Petitdidier, M., V. Klaus, F. Baudin, C. Bourdier, M. Chrochet, A. Desautez, C. Guerin, R. Ney, G. Penazzi and P. Quinty, 1990: The 961/45 MHz bifrequency INSU/METEO Stratospheric radar, Meteorolog. Rundschau 42, p. 142-151

Röttger, J. and M.F. Larsen, 1990: UHF, VHF Radar Techniques for Atmospheric Research and Wind Profiler Applications in D.Atlas: Radar in Meteorology, American Meteorol. Society, Boston, p. 235-281

Wuertz, D.B. and B.L. Weber, 1989: Editing Wind Profiler Measurements, NOAA Technical Report, ERL 438-WPL 62

INTERCOMPARISON OF REMOTE AND BALLOON-BORNE SENSORS

Robert O. Olsen
Battlefield Environment Directorate
U.S. Army Research Laboratory
White Sands Missile Range, NM, USA

Richard J. Okrasinski and Greg J. Cook
Physical Science Laboratory
New Mexico State University
Las Cruces, NM, USA

INTRODUCTION

The Joint Acoustic Propagation Experiment (JAPE-91) was conducted at White Sands Missile Range, New Mexico during July 11-28 and August 19-29 of 1991. Two Doppler sodars, a 924 MHz wind profiler, and a Radio Acoustic Sounding System (RASS) were deployed by the U.S. Army Research Laboratory to collect boundary layer wind and temperature data in support of the experiment. Upper-air wind, temperature, and humidity data were also collected by periodically released rawinsondes.

This information was later analyzed to evaluate the capabilities of the four remote sensors. Wind data from the UHF profiler and temperature data collected by the RASS were statistically compared with concurrent rawinsonde measurements. Similarly, simultaneous measurements from the two sodars were compared with each other and with concurrent wind profiler data. The percent of the time that data were successfully measured at each sampling height was also calculated to determine the functional vertical range of each remote sensor.

INSTRUMENT DESCRIPTION

The sodars transmit one vertical and two tilted acoustic beams. Changes in the acoustic refractive index caused by temperature fluctuations scatter some of the transmitted energy back to the antennas. Doppler shifts in these backscattered signals are used to derive the wind velocities along the three beam paths. Horizontal wind speeds and directions are then computed from the radial velocities. The sodars are used to measure winds between 50 m and 750 m above the surface.

Both sodars were manufactured by REMTECH, Inc. The older A0 model uses a trailer-mounted array of three acoustic antennas, two of which are tilted 18° from the vertical, and the newer PA2 uses a single phased array antenna with three electronically steered beams, two of which are directed 30° from the vertical and 90° from each other. Frequency coded transmissions are propagated at frequencies centered at 1600 Hz with an acoustic power of 60 W by the A0 and at 2100 Hz with an acoustic power of 140 W by the PA2.

The wind profiler transmits three 924 MHz beams, one vertical and two tilted 15° from vertical, from 3 antennas. Doppler shifts in the backscattered signals are used to derive the wind velocities along the beam paths. One-hour averaged horizontal wind data was computed from the radial velocities using a random sample consensus technique. The maximum measurement height is a function of the intensity of the backscattering and the vertical resolution of the wind data, but is usually between 2 and 4 km. Peak pulse power is 500 W.

The vertical radar antenna is also used to track 2000 Hz acoustic beams transmitted by the conjunctive RASS. Doppler shifts in the backscattered energy determine the speed of the acoustic signal which is proportional to the virtual temperature of the medium. Maximum measurement height is about

1 km. Both the wind profiler and the RASS were developed by the NOAA Wave Propagation Laboratory.

Different radiosonde systems were deployed for the July and August phases of JAPE-91. In July, a system manufactured by Atmospheric Instrument Research, Inc. (AIR) was used, consisting of a 1680 MHz sonde tracked by an automatic radio theodolite using a phase array antenna. Height, temperature, humidity, and balloon-to-ground azimuth and elevation angles were recorded for every 4-5 seconds of flight. In August, a Omega Navaid system using equipment manufactured by Vaisala Oy was substituted to collect data at greater heights. Vaisala RS-80 radiosondes tracked by a Vaisala Digicora ground station provided measurements for every 10 seconds of flight.

DATA COLLECTION

JAPE-91 was conducted in the extreme southeast corner of White Sands Missile Range in south central New Mexico, USA. This is an arid region situated in a broad basin between two mountain ranges. The nearest significant feature is the 300-m high Jarilla Mountains which are approximately 4 km to the east. The test area slopes from an elevation of 1275 m to 1254 m above sea level from south to north.

The A0 sodar, the wind profiler and RASS, and the radiosonde station were located at the same site. The PA2 sodar was situated approximately 4.5 km to the south next to a 40-m hill. Other than the hill, there were no significant terrain features in the vicinity of the two locations.

Fifteen-minute averaged wind data were collected by the two sodars every 50 m above the surface between July 21-29. PA2 data were collected at 15 heights between 50 m and 750 m. Concurrent A0 winds were measured at 15 levels between 50 m and 750 m from 0245 on July 21 to 2115 on July 27 GMT and at 12 levels between 50 m and 600 m the rest of the time.

Two sets of 1-hour averaged UHF wind profiler data were collected. Winds with a vertical resolution of 101 m were measured at 25 levels between 167 and 2601 m, and 203-m resolution winds were measured at 24 levels between 246 and 4911 m. The profiler was turned off during several testing periods to avoid interfering with other instrumentation. A total of 84 hours of data were collected in July.

Five-minute averaged virtual temperatures were collected hourly by the RASS between 127 m and 1283 m above the ground at 12 equally spaced heights. Forty-five hours of data were collected in July, and 144 hours were collected in August.

Thirty-three AIR radiosondes were flown during July and tracked to 5 km above the surface. Seven Vaisala sondes, tracked to 15-20 km, were released during August.

DATA COMPARISONS

UHF Wind Profiler

In most cases, the wind profiler does not successfully collect data at all of its programmed altitudes. The strength of the returned signal is a function of the intensity of the turbulent scattering in the region being probed and is often too weak to be interpreted. Lower resolution winds are measured with greater success since longer pulse lengths and more energy is transmitted. The profiler height range, therefore, is dependent on both the state of the atmosphere and the resolution of the measurement. The percent of the time that 1-hour wind profiler measurements were successfully collected in July were computed for each interrogation height and plotted in Figure 1. At 2 km, for example, 101-m and 203-m resolution winds were collected about 55% and 90% of the time, respectively.

To investigate the accuracy of these measurements, low-resolution (203-m) wind profiler data collected in July was statistically compared with data from 20 rawinsonde soundings that were launched

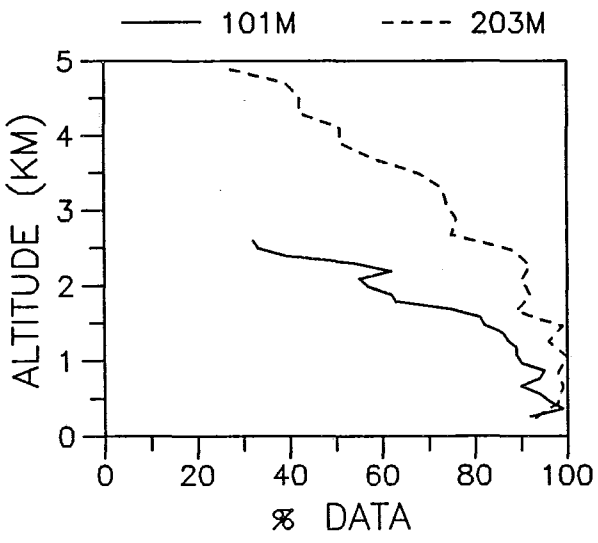

Figure 1. Percent of the time that horizontal wind data were successfully collected by the UHF wind profiler at 101-m (solid line) and 203-m (dashed line) resolutions.

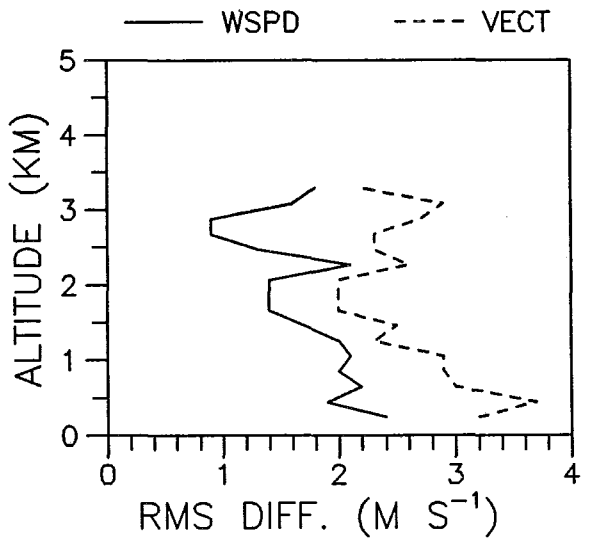

Figure 2. Rms wind speed differences (solid line) and vector wind differences (dashed line) of concurrent UHF wind profiler and rawinsonde data.

within 30 minutes of one of the profiler interrogation times. The rawinsonde winds were calculated for 200-m layers and interpolated to the profiler heights so that both data sets had approximately the same vertical scale. There is still a rather large temporal difference, however, since the profiler winds are averaged over 1 hour and the rawinsonde winds were computed for approximately 40 seconds of flight. In addition, the balloon drifts away from the site as it rises. Nevertheless, the agreement between the rawinsondes and profiler was fairly good as shown in Figure 2 where the rms wind speed and vector wind differences are plotted versus height. The latter were calculated by taking the square root of the sum of the mean square differences in the east-west and north-south component winds and are, therefore, a function of the differences in both wind speed and direction. Most of the rms vector differences were close to 2.5 m s^{-1}. This is not much larger than the 1.5-2.0 m s^{-1} vector differences that were found between the same radiosonde system and a reference high-precision radar during a radiosonde intercomparison experiment (Olsen et al., 1991). These statistics also compare favorably with the results of a study by Weber and Wuertz (1990) in which the standard deviation of the differences in the east-west and north-south wind velocities measured by a wind profiler and rawinsondes were found to be about 2.5 m s^{-1}.

Sodars

Since the strength of the backscattered sodar signal is largely a function of the intensity and scale of the temperature fluctuations in the region being probed, the sodar height ranges vary greatly with atmospheric conditions. Using 15-minute averaged wind data collected by the A0 and PA2 sodars between July 21-29, the success rate of data collection was computed as a function of altitude and is shown in Figure 3. The PA2, as expected, had a greater range. At 600 m, for example, the A0 and PA2 sodars obtained a measurement approximately 40% and 85% of the time, respectively.

Using this same data set, the comparability of the two sensors was studied by calculating statistics of the differences between their simultaneous measurements. The number of concurrent data points ranged from 616 at 100 m to 300 at 600 m. The rms wind speed and vector wind differences, plotted in Figure 4, were close to 2 and 3 m s^{-1}, respectively, at all altitudes. Means and standard deviations of the differences in wind speed and direction were also calculated for comparison with the results of an earlier analysis of 20-minute averaged wind data collected by two collocated A0 sodars (Chintawongvanich et al., 1989). The standard deviations of the differences were 1.7-1.8 m s^{-1} and 41-54° at JAPE-91 and 1.1-1.4 m s^{-1} and 22-32° in the earlier study. Mean differences were about a tenth as large. The poorer JAPE-91 statistics may be partially due to the 4.5 km separation of the two sodars.

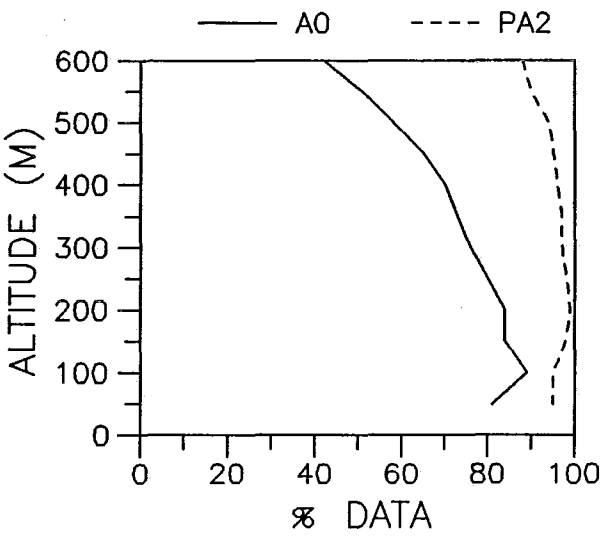

Figure 3. Percent of the time that horizontal wind data were successfully collected by the A0 (solid line) and PA2 (dashed line) sodar.

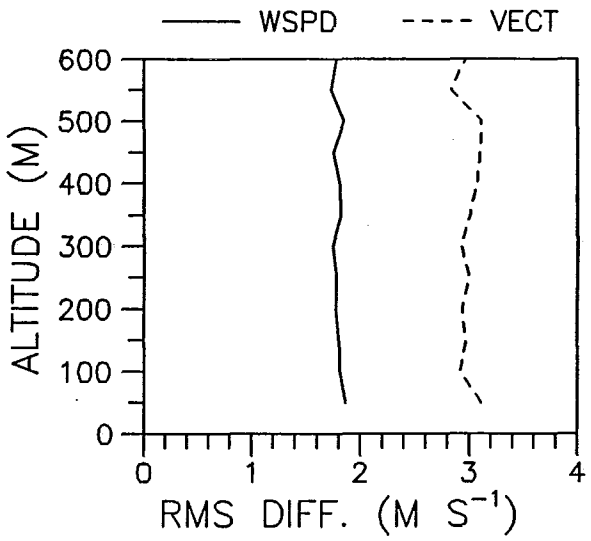

Figure 4. Rms wind speed differences (solid line) and vector wind differences (dashed line) of concurrent A0 and PA2 sodar wind data.

Table 1. Sodar-UHF Profiler Rms Differences

ALT (m)	WIND SPEED A0-UHF (m s^{-1})	WIND SPEED PA2-UHF (m s^{-1})	VECTOR WIND A0-UHF (m s^{-1})	VECTOR WIND PA2-UHF (m s^{-1})	NPTS
268	1.5	2.0	1.9	2.5	25
369	1.5	2.0	1.9	2.5	15
471	1.4	1.9	1.7	2.5	13

Both sodars were similarly compared with concurrent wind profiler measurements. The sodar data were first averaged over 1-hour periods and vertically interpolated to the profiler heights. Statistics of the differences between simultaneous 1-hour sodar and profiler data were then calculated using only those periods when data were available from all three sensors. The rms wind speed and vector wind differences are shown in Table 1. The A0 sodar, which was at the same site as the wind profiler, was found to be in better agreement with the profiler than the more distant PA2.

Radio Acoustic Sounding System (RASS)

The height range of the RASS, which consists of a sodar and a radar, also varies with atmospheric conditions. The data collection success rate, calculated with measurements from both the July and August phase of JAPE-91, is shown in Figure 5. Almost no data were obtained above 652 m. Measurements up to this level were statistically compared with virtual temperatures computed from 22 radiosonde soundings which were released within 30 minutes of one of the RASS interrogation times. Means, standard deviations, and root-mean-squares of the differences are printed in Table 2. The rms differences of .7-.9 °C are comparable with those found by May et al. (1989).

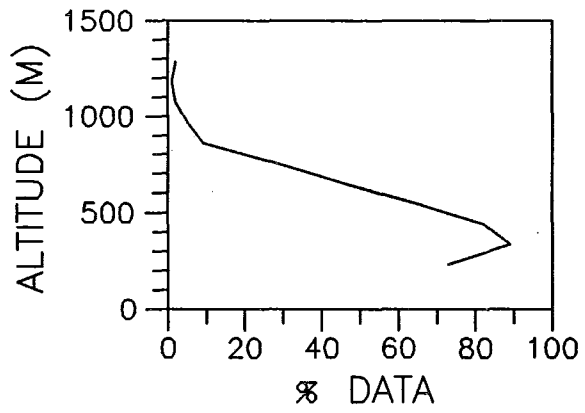

Figure 5. Percent of the time that temperature data were successfully collected by the RASS.

Table 2. RASS-Radiosonde Differences in Virtual Temperature

ALT (m)	MEAN	SDEV (°C)	RMS	NPTS
233	.0	.7	.7	20
338	.3	.7	.8	22
442	.6	.7	.9	21
548	.5	.6	.8	17
652	.4	.7	.8	12

CONCLUSIONS

Statistical agreement between the radiosonde data and the wind profiler and RASS measurements collected at JAPE-91 was comparable with the results of other similar studies. The rms temperature and vector wind differences between concurrent measurements were approximately .8 °C and 2.5 m s^{-1}, respectively. Standard deviations of the differences in the sodar wind speeds and directions were somewhat greater than those that were found between two collocated sodars in a previous study, however. This may be partially due to the 4.5 km separation of the two sensors. The sodar rms vector wind differences were about 3 m s^{-1}.

Data were successfully collected at least 50% of the time at all heights below 600 m by the A0 sodar, below 652 m by the RASS, and below 2.3 and 4.3 km by the UHF wind profiler at 101-m and 203-m vertical resolutions, respectively. More than 85% of the PA2 data were collected at all altitudes up to 600 m.

REFERENCES

Chintawongvanich, P., R. O. Olsen, and C. A. Biltoff, 1989: Intercomparison of wind measurements from two acoustic Doppler sodars, a laser Doppler lidar, and in situ sensors. *J. Atmos. Oceanic Technol.*, **6**, 785-797.

May, P. T., K. P. Moran, and R. G. Strauch, 1989: The accuracy of RASS temperature measurements. *J Appl. Meteor.*, **28**, 1329-1335.

Olsen, R. O., R. J. Okrasinski, and F. J. Schmidlin, 1991: Intercomparison of upper air data derived from various radiosonde systems. Preprints, *7th Symp. on Meteor. Observations and Instrumentation*, New Orleans, Amer. Meteor. Soc., 232-236.

Weber, B. L., and D. B. Wuertz, 1990: Comparison of rawinsonde and wind profiler radar measurements. *J. Atmos. Oceanic Technol.*, **7**, 157-174.

DISCLAIMERS

The citation of trade names and names of manufacturers in this paper is not to be construed as official Government endorsement or approval of commercial products or services referenced herein.

MOBILE PROFILER SYSTEM: REPLACING BALLOON-BORNE METEOROLOGICAL SYSTEMS

Robert E. McPeek[1] and Mary Ann Seagraves
U.S. Army Research Laboratory
White Sands Missile Range, NM, USA

1. INTRODUCTION

Marksmen through the ages have known that they have to account for "windage" to hit their targets. However today's artillerymen know that they need more information about the atmosphere than just windage to accurately fire their cannons. The range of artillery fires has steadily increased during the last 50 years, with current estimates that the range of cannon artillery will exceed 40 km in the near future. Deep attack weapons are being planned that will be launched into the enemy's territory, called the target area, as deep as 500 km. Wind, particularly at the projectile apogee, is the major meteorological (met) factor in artillery aiming accuracy. Temperature, pressure and humidity also affect the ability to hit the target. Vertical profiles of met data to apogee are required to adjust the direction of fire so that the target will be hit. Current requirements are for vertical spacing of data points, or resolution, that varies from 500 m near the ground to 2 km at 20 km altitude.

To collect the needed met data profiles the artillery has developed several systems over the last 50 years that are based on instruments measuring met profile data carried aloft by helium-filled balloons. These instruments, called radiosondes, collect the met data and radio it to the ground as they ascend. Typically, over 2 hr are needed for an instrument to ascend to the required 20 km altitude, with a new balloon being launched, on average, about every 4 hr. The Army Materiel Systems Analysis Activity has conducted studies that correlate the artillery aiming accuracy in terms of miss distance from the target to the time between when the met data was taken and when it was used. These studies have shown that, in general, the miss distance of an artillery shell increases exponentially as the met data get older.

A potential solution to this met data timeliness problem that holds great promise is a data-merging concept that combines data from state-of-the-art sensors based on the ground and on meteorological satellites. This solution takes advantage of the real-time capability of the ground-based sensors to measure met profile data, while the extended areal coverage of the met satellite provides met data profiles deep into the target area. This concept is being implemented in the Army's Mobile Profiler System (MPS), which is planned to be a product improvement to the AN TMQ-41 Met Measuring Set.

The U.S. Army Research Lab Battlefield Environment Directorate at White Sands Missile Range, NM, and the National Oceanic and Atmospheric Administration (NOAA) Environment Technology Laboratory in Boulder, CO, are developing the MPS as illustrated in figure 1. The MPS is designed to satisfy Army target area met data requirements for vertical met profiles to an altitude of 30 km across a front 100 km wide and out a distance of 500 km. Profiles will be spaced approximately 40 km apart over a complete satellite swath, about 1800 km wide. The Army Program Executive Office for Intelligence and Electronic Warfare through the Program Manager for Electronic Warfare/Reconnaissance Surveillance and Target Acquisition (PM EW/RSTA) is sponsoring the MPS development as a product improvement to the balloon-based systems now in use.

2. METHODS

2.1 MPS Sensors

The MPS uses satellite-borne and ground-based state-of-the-art remote sensors as shown in figure 2 to derive the required met profiles. The satellite-borne sensors include infrared and microwave sounders flown on the NOAA TIROS and Defense Meteorological Satellite Program polar-orbiting met satellites. Not to be confused with the more familiar satellite imagery, these sensors measure radiometric data in many channels of the visible, infrared and microwave bands of the electromagnetic spectrum. The data are converted using radiative transfer inversion algorithms to wind, temperature, pressure and humidity data for the region from approximately 3 to 30 km altitude. Data are measured at 400 meters vertical resolution.

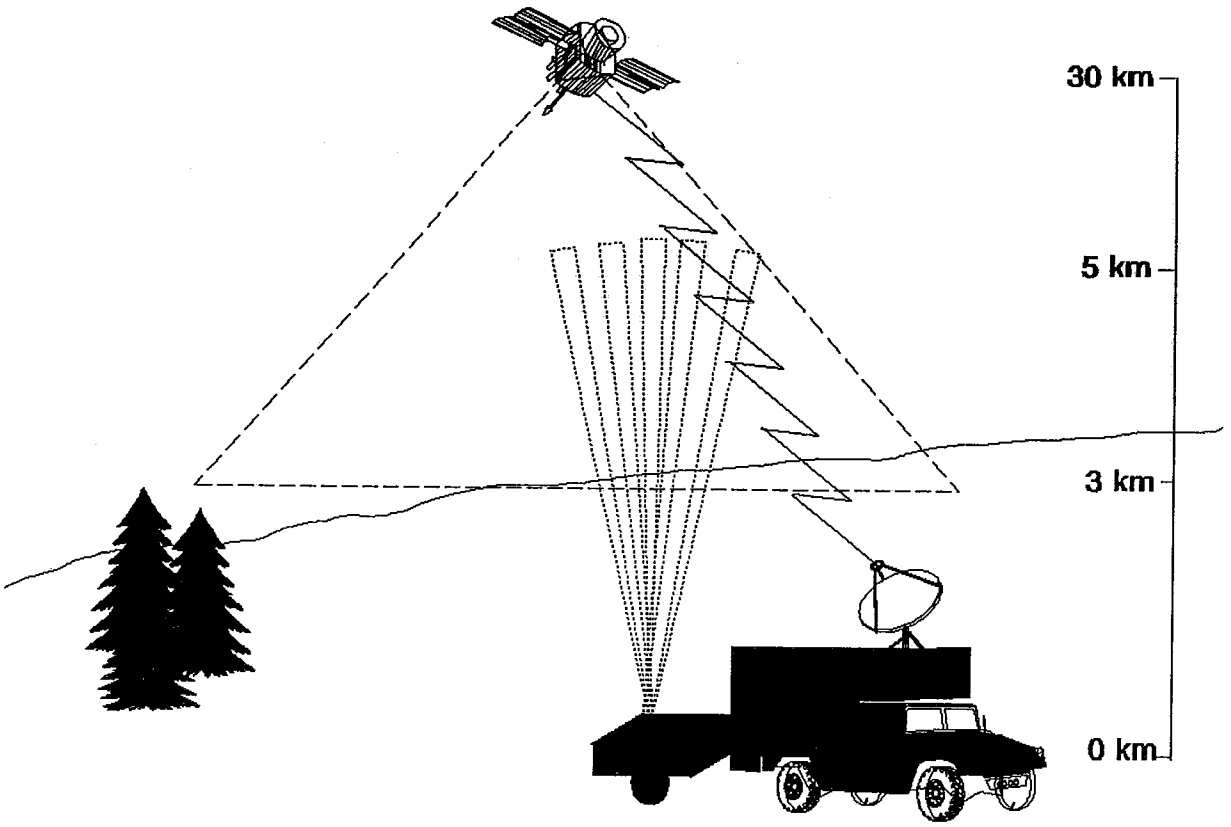

FIGURE 1. The Mobile Profiler System

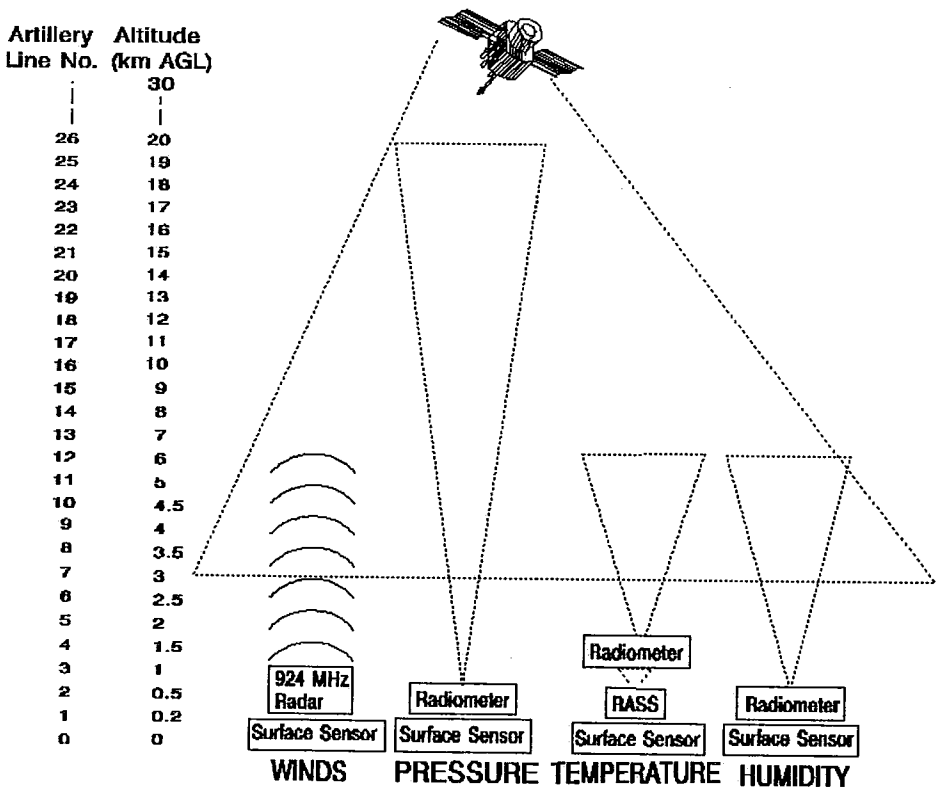

FIGURE 2. The MPS uses a variety of state-of-the-art sensors.

The ground-based sensors are organized around a 924 Mhz phased-array wind-profiling radar that measures winds to approximately 6 km altitude. Winds are measured every 100 m vertically. Temperatures are profiled at 100 meters resolution from the surface to 1 km altitude using a Radio Acoustic Sounding System (RASS) and from 1 km to 6 km every 400 m using a 4-channel passive microwave temperature profiler. Pressure is also profiled using this sensor from the surface to 6 km or more at the same resolution as temperature. Humidity profiles are provided with a 2-channel water vapor radiometer. Surface wind, temperature, pressure and humidity are measured using standard surface met sensors. Also, the MPS uses an on-board Global Positioning System (GPS) receiver to provide highly accurate position location information.

2.2 Data Merging Algorithm

The concept of merging satellite and ground-based sensor sounding data to produce combined atmospheric profiles is at the heart of the MPS. Ground-based sensors provide atmospheric profiles every 2.5 minutes to 6 km altitude. However, they are limited in areal coverage (i.e., point measurements) and altitude range. On the other hand, satellite sounder instruments in both the infrared and microwave frequencies provide profiles with wide areal coverage (the full 1800 km swath width) from about 3 km to 30 km altitude. The atmospheric profiles are of low temporal resolution (a pass approximately every 3 hr) and lose required accuracy below 3 km. The MPS merged satellite and ground-based sensors sounding concept[2] provides integrated atmospheric profiles by synergistically combining the best capabilities of each system while avoiding their negative consequences. The resulting combined atmospheric profiles, as shown in figure 3, are of high resolution and accuracy, extend from the surface to an altitude of 30 km or more, and can be derived over the full width of a satellite pass.

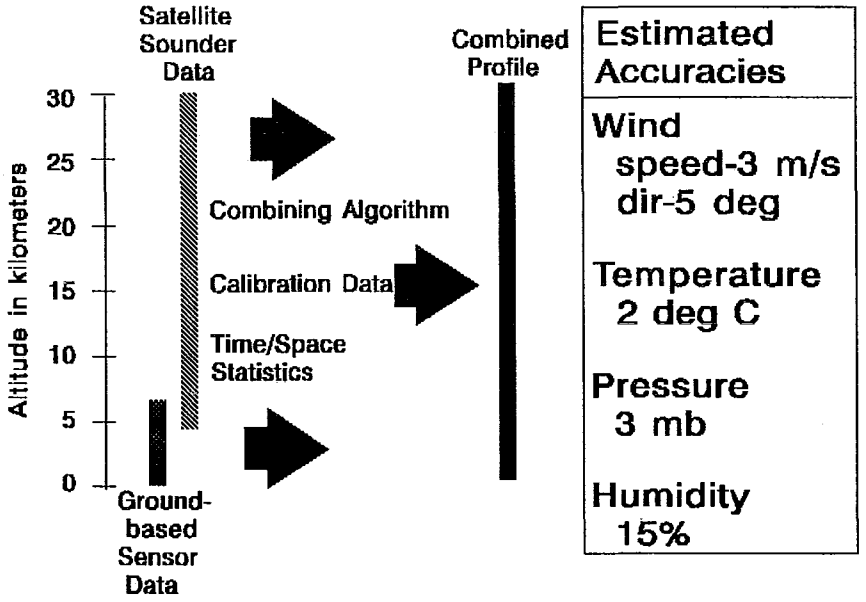

FIGURE 3. Data accuracies expected from MPS combined profiles.

2.3 Computers/Nowcast Met Model

The MPS is built on Army Command and Control System (ACCS) Common Hardware and Software (CHS) computer equipment. Two Hewlett Packard 700 series workstations (a primary and a backup) along with a single 80486-based PC are used in the system. All functions, including sensor operation, integration and control, data base management, product generation and display, and external communications are handled

by the computers. The workstations are used to derive wind, temperature, pressure and humidity data from satellite data. Also, they are used to run a regional-size area nowcast model that is used to adjust the upper level (3 km and above) met fields between satellite passes. In this way 3-dimensional profile fields are made for the entire target area every 15 minutes.

3. DISCUSSION

The feasibility of the MPS has been established by continuously operating the system in a laboratory mode since February 1993. While the MPS is operating full-time, the sensor integration and control program has been the subject of on-going software modifications and upgrades to make it computer hardware independent. The MPS has under-gone shake-down testing in the Los Angeles, CA, basin as part of a South Coast Air Quality Management District air quality study. An example of wind data collected during this period may be seen in figure 4, where the wind direction is indicated by the direction of the shaft of the wind barb and speed is shown by the indicators attached to the shaft, the longer lines indicating 10 m/s each and the shorter ones 5 m/s of wind speed.

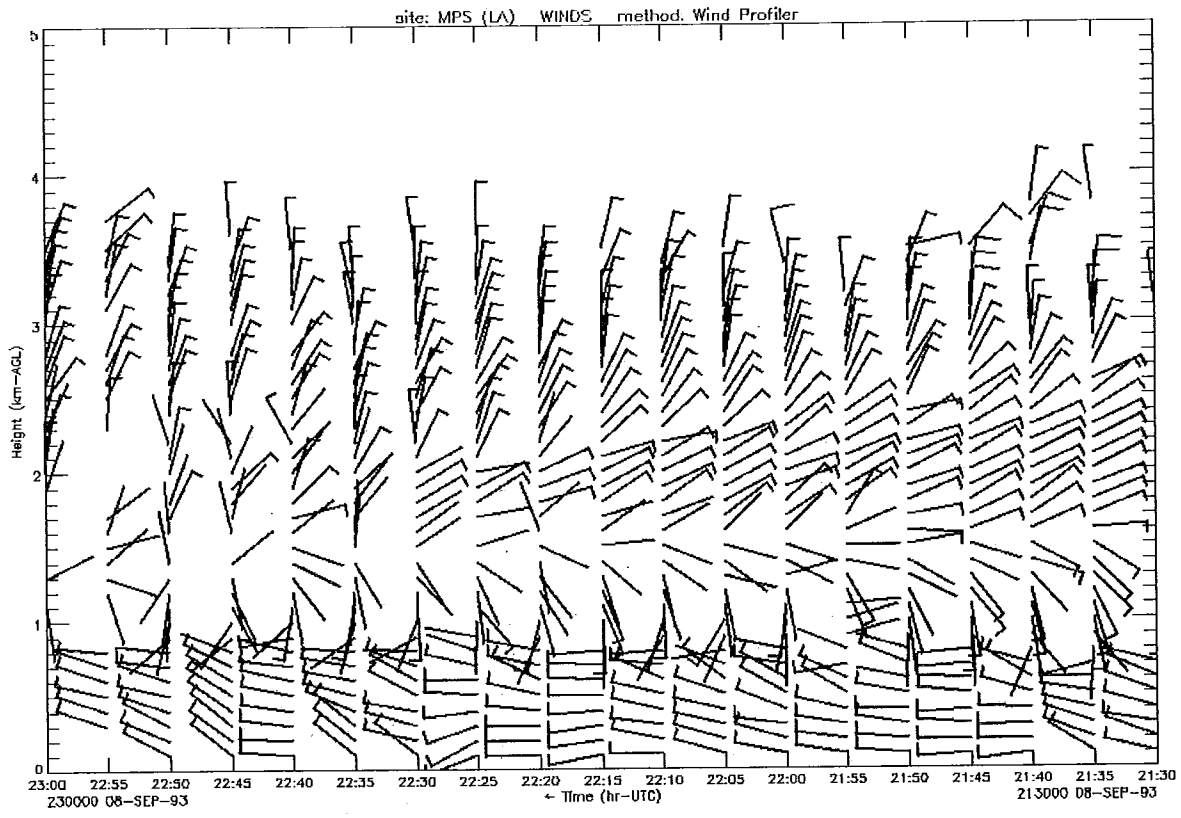

FIGURE 4. MPS wind data

The MPS will undergo additional testing at White Sands Missile Range, NM, to collect data for determining reliability, availability, and maintainability baseline metrics. A formal technical demonstration is scheduled for April 1994. The technical demonstration will be fully documented, along with the complete system hardware and software specifications. These documents will be transitioned to the PM EW/RSTA by the end of FY94.

The MPS provides real-time vertical and 3-dimensional met profiles to satisfy deep attack target area meteorology applications. It uses state-of-the-art satellite and ground-based sensors to profile the target area atmosphere from the surface to 30 km across a 100 km front out to a distance of 500 km to provide data needed to successfully execute the Army's cannon artillery and deep attack missions. A data merging algorithm that uses all available data is at the heart of the system. The use of ACCS CHS and a computer nowcast model rounds out the formidable capabilities of the MPS. The fielding of the MPS will solve many of the data timeliness problems of the balloon-based systems, while reducing the total

amount of equipment needed to make vertical profile measurements on the battlefield.

In addition to the artillery applications, the MPS is an ideal platform for monitoring the atmosphere for air quality regulatory compliance and emergency pollution episodes. With the addition of appropriate particulate and gaseous pollution sensors the MPS role can be expanded to include both civilian and military environmental cleanup and pollution monitoring functions. The MPS can also provide essential met data for war-time use of chemical agents and support to aviation units.

Real-time met vertical profile data is needed by both the Army and civilian communities. The MPS is being developed to satisfy these many needs well beyond the turn of the century.

REFERENCES

1. Mr. McPeek is currently affiliated with Air Weather Service, Scott AFB, Il.

2. Cogan, J. and A. Izaguirre, 1993, A Preliminary Method for Atmospheric Soundings in Near Real Time Using Satellite and Ground-Based Remotely Sensed Data, ARL-TR-240, U.S. Army Research Laboratory, White Sands Missile Range, NM.

The Operation of the DWD Weather-Radar-Network

Mammen, T.

Deutscher Wetterdienst
Instrumentenamt Hamburg
Frahmredder 95, D-22361 Hamburg 65

1.0 Introduction

Weatherradars are employed in DWD since several tens of years. During the continuous evolution some major steps can be marked. The first generation of Weatherradars was completely analog. The antenna could be positioned by hand or be put into continuous azimuthal revolution. The display was an analog RHI, PPI and A-Scope. The development of fast digital circuits lead in the 70es to the 2nd generation of Weatherradars: the analog signals from the receiver are digitized and processed by computers. These computers also control the antenna and submit the radarproducts to lots of users at any distance from the radar. A computer-controlled automatic radar is prerequisite for the 3rd generation of weatherradar: the Weather-Radar-Network. In a well shaped network the distance between the radars is so small, i.e. the coverage is so good, that the products can be computed independent from the radar-sites.
At present the stage of the DWD-Weather-Radar-Network is between the 2nd and 3rd generation. It consists of 5 operational systems (intensity only) and one research-system. Until spring of 1995 five more systems (with doppler) will be installed. The final number will be about 15. The locations are given in Figure 1. The systems on site produce 2D and 3D products witch are distributed to the users. At the DWD-center a 2D Composite is created and spread.

2.0 Recommendations and system-design

The recommendations for the Weather-Radar-Network are derivable from requirements from the users. At the moment the users can be divided into two groups: forecasting personnel and hydrologists. The first group is interested to get a 3D radar-picture with a high resolution in space and time. The hydrologists need the precipitation at the ground over the whole area with a maximum accuracy. All users ask for a continuous availability, homogeneity and optimum cluttersuppression.
The use of radar-data as input for numerical models is in Germany still under development.
A sufficient coverage is achieved by installing enough systems and by choosing optimum sites for the radars.This should also take into account the fade-out of the radar-beam by obstacles and the raise of the radar-beam with distance due to earth-curvature. Here should be noted, that a radar-beam with .5-degree elevation points at a height of approx. 1.5 km. So the siting of the radars is important especially for hydrological use of the data.

The other recommendations lead to radar systems as shown systematically in figure 2. The computer-controlled C-Band radar consists mainly of the analog parts transmitter/receiver and Servo and the digital part signal-processor and radar-computer. To get a considerable time resolution the antenna is able to run at up to 6 rpm and the signal-processor can compute up to 2048 data per pulse (at 1200 Hz PRF). The systems runs automatically a 3D cycle every 15 minutes, i.e. data are taken with a range of 230 km at 19 elevation angles, and a 2D cycle every 5 minutes at the lowest possible elevation angle with a range of 100 km. On the way of data-processing between raw input data and user-disseminated-products the amount of data is continuously reduced, while keeping nearly all meteorological information for the special user.
Clutter suppression is done in different ways. All systems use cluttermaps, i.e. at a weather-free situation all elements with non-zero signal are marked in the data-volume. All these elements are disregarded at future computations. The new doppler-systems allow for clutter cancelation by filtering, i.e. elements with velocities near zero are disregarded. With the new signal-processor RVP-6 additionally a statistical clutterfilter can be employed. It removes all targets with a spectrum typical for clutter targets.
Homogeneity is very important for a network. In DWD this is achieved by running mostly identical systems and calibrate them in the same way. So the existing systems are upgraded with the same signal-processor and data processing as the new systems (as far as it is possible with intensity-only radars). In a network the homogeneity must be combined with an optimum accuracy. To reach the goal of an overall absolute accuracy of about 1 Db a combined service/calibration and monitoring system was introduced.

3.0 Maintenance and Monitoring

The technical staff for the weatherradar-service is situated at 5 locations in Germany to minimize traveltime, -expenses and stoppage of a system in case of failure. The coordination is at the operational center in Hamburg. At this point it should be noted that a great part of the radar-system-functionalism resides in the built-in computers. Therefore, radar engineers and computer-specialists work close together in the project. Without a strong teamwork it is impossible to keep a modern radar system at work.
There are several tools used to keep the systems in an optimal operational state.

3.1. Built-In-Test-Equipment (BITE)

At all important parts of the systems there are sensors which measure analog values or the status of components. These messages are collected by a small computer. It's reaction is twice: first, it checks wether there is danger for the hole or part of the system. In this case the endangered parts are shut down. Second, a message is send to the host-computer. So the service-staff gets soon knowledge on system-problems.

3.2. On-Line Calibration

In the past the drift of the analog parts of transmitter and receiver could only be taken into account by monthly checks and recalibration. The new systems have a built-in calibrated (better than .5 Db) test-signal-generator (TSG), whose output is feed into the receiver-system automatically by the software of the radarcomputer. The results are used to compute new calibration-constants. Because the drift of the TSG is much smaller than that of the very sensitive receiver system this procedure prevents from drifts in the receiversystem.

3.3. On-Site-Systemcheck and Repair

All systems are checked on-site at fixed time intervals by specially trained personnel. This is necessary though the systems are running automatically. Experience shows that the reliability of the radars is continuously improved so that the checking-intervals can be enlarged. Nevertheless, the systems should be checked and recalibrated if necessary at least every two weeks. Another aspect is the training-on-job of the staff. Especially when components fail the technicians need experience with the system. This can only be achieved when they work regularly with the system. We also got to know that every system tends to develop it's own life, i.e. it differs in some kinds from the other systems in it's behavior. Even if a lot of account is put on homogeneity this is a matter of fact. This has also a consequence for the participation of companies in the overhaul of the systems. In Germany the manufacturer is included in the repair of the systems at the weekend and in complicated situations. To make this possible over a longer time the company must be informed about any change of the system. For this reason it is connected to the Weather-Radar-Wide-Area-Network (WAN), so information can be easily send to everyone.

3.4. Monitoring / Operational Center

To achieve and keep a homogeneous network it is necessary to create one operational center. The center for the DWD is situated in Hamburg. It is responsible for:

- daily monitoring of all systems via remote access (Datex-P)
- keep the education of the whole DWD-technical-personnel at a high level
- help the local technicians with problems
- keep the systems at an actual state (see also 3.5)

At the operational center radar- and computerengineers work very close together. An optimum performance is only achievable if the radar is regarded as a system and not as a summary of components. A lot of attention has to be put on the well "co-operation" of the components.

3.5. Upgrading of the Systems

Experience has shown that it becomes very expensive to keep systems, especially data-processing systems, on a fixed release. The older the systems the more the firms increase their prices for spares and support. So it is absolutely necessary to keep all components at an efficient actual state. At the moment DWD is introducing a new type of weatherradar, please contact the author for more information.

4.0 Future Developments

The past has shown that the recommendations from the users changed significantly with their knowledge of the system. Up to now only DWD-forecasting-personnel and -hydrologists use the data operational. The next years will bring at least two steps: first, it must be assumed, that the radar products will become more popular and will be made available to more direct users. Second, the hydrological users will become more in the same way as the on-line calibration with ground-stations is improved. Research in the field of weatherradar is very active. New methods and algorithms will be available for operational use. They must be implemented into the systems as soon as they are fully tested. With respect to the european-radar-composite maintenance policies of the associated countries should be harmonized.
A modern weather-radar-system is very dynamic and of great value for meteorology and hydrology if it is kept on an actual state.

Reference:

Clift, G.A. 1985: Use of Radar in Meteorology; WMO Technical Note No. 181, 90p.

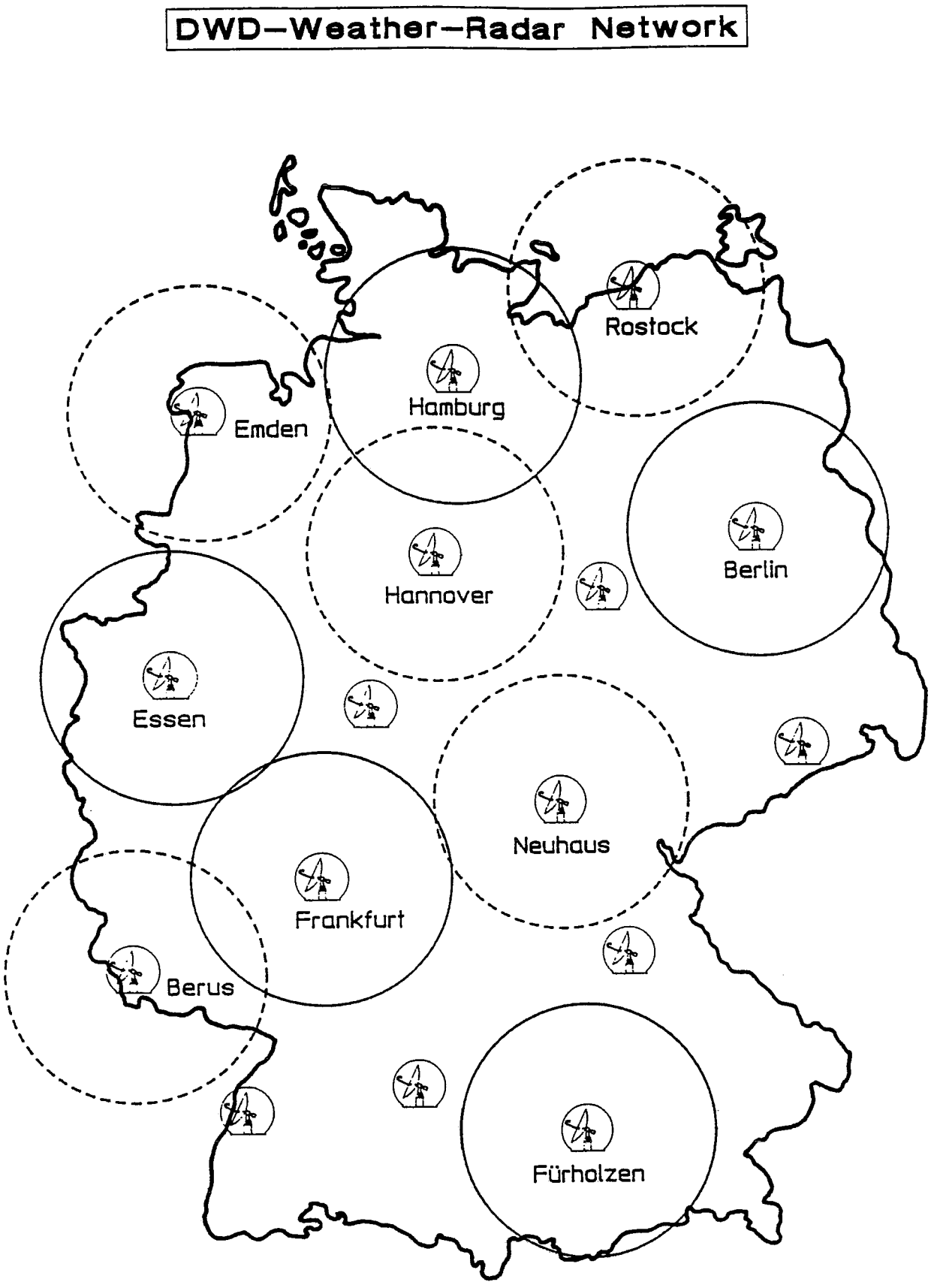

Figure 1: Locations of waetherradarsystems: solid - existing, dashed - until spring 1995, open - planned. The circles mark 100 km distance from the site.

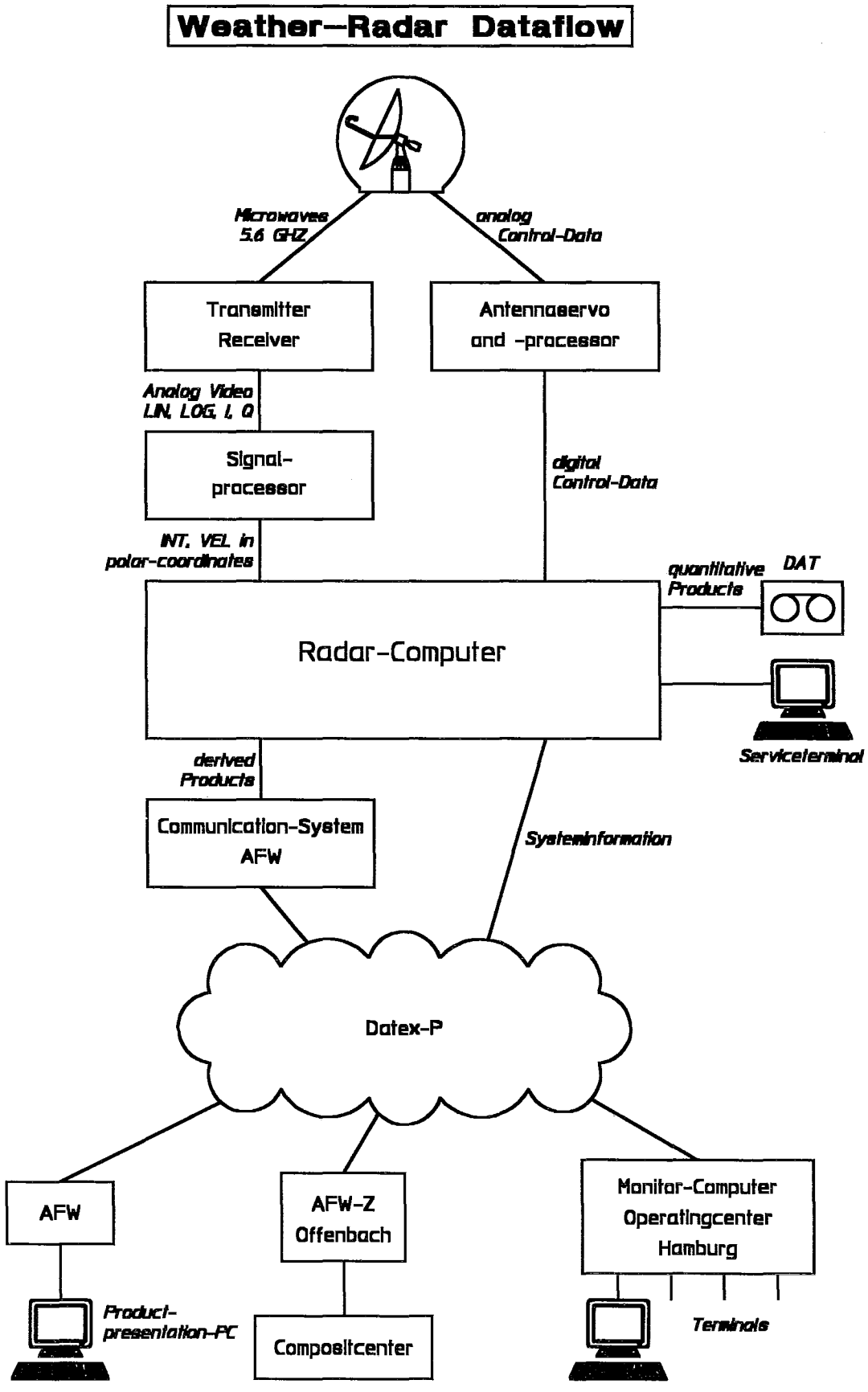

Figure 2: Data-flow in the DWD-Weather-Radar-Network. Supply of users is presented in the lower left. Monitoring equipment is shown at lower right.

DEVELOPMENT OF NEW SYSTEM FOR DETERMINING CENTER OF TYPHOON USING WEATHER RADAR DATA IN JMA

Tatsuo Yokoyama and Kota Nakai

Observations Department, Japan Meteorological Agency
1-3-4, Otemachi, Chiyoda-ku, Tokyo, 100 Japan

1. Introduction

Weather radar observation is indispensable for accurate detection of the location and the strength of a typhoon, which leads to improvement in the accuracy of typhoon forecasts and warnings. At the Meteorological Agency (JMA), the center and the moving direction and speed of a typhoon and developing/decaying process of radar echoes are determined on the PPI scope manually by an expert and the information is reported to neighboring countries with the code form of FM-20 RADOB through the GTS. The accuracy of the center of a typhoon depends on the experience of each expert.

The JMA has been operating the Radar Echo Digitizing and Disseminating System (REDIS) since 1983. The REDIS is similar to the DVIP (Digital Video Integrator and Processor). The digitized data obtained from the REDIS are shown on the color display.

The new system using the personal computer (PC) for determining the center of a typhoon from the REDIS imagery has been developed in the JMA. Fig. 1 shows the radar system of the JMA. This system reduces operation time and burden on experts determining the center of a typhoon.

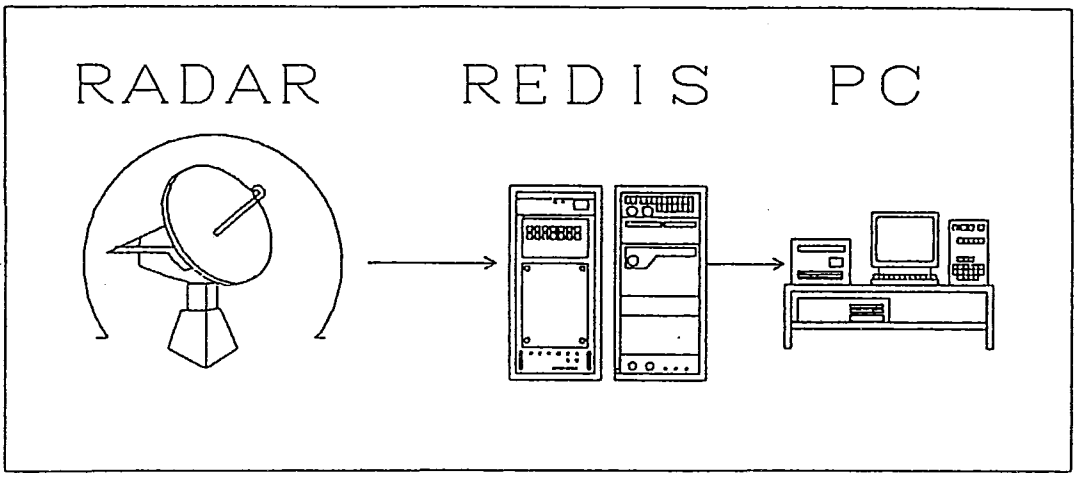

Fig.1 Radar system of the JMA

2. Algorithm for determining the center of a typhoon using the PC

2.1 Radar data used for determining the center of a typhoon

Reflectivity data, which are divided into six levels with 15 dBZ interval and are indicated on the color display, are used for determining the center of a typhoon. An example of displayed image is shown in Fig.2. The area of this image indication is 500km squared and the image is constituted from 2.5km squared grid data. The image is renewed every seven minutes.

2.2 Algorithm for determining the center of a typhoon

Radar echoes with a typhoon and a tropical cyclone vary according to their scale, stage of development, features of structure, topographical influence, etc. In case of a typical typhoon, precipitation echoes observed by weather radar are called, from outer of place, "precursor band", "outer band", "inner band" and "eye wall". In case of a decaying typhoon, the eye wall may not be observed clearly.

The center of a typhoon analyzed from radar data is usually the geometrical center of empty area surrounded with the eye wall echo or the inner band echo.

(1) Approximation to a logarithmic spiral

Inner bands are divided into two kinds, "spiral band" on the echo near the center and "rain shield" on the echo apart from the center. A typhoon has many band echoes from the eye wall to outer bands, which look like logarithmic spirals whose cross angles are ten degrees to twenty degrees. Therefore, the name of spiral band is generally used for expressing band echoes outside of eye wall.

The system for determining the center of a typhoon described here uses the property that band echoes outside of the center can be approximated to a logarithmic spiral.

The procedure for determining the center of a typhoon by man-machine interaction is as follows.

(i) The operator displays several kinds of logarithmic spiral on the radar echo imagery on the color screen of the PC.

(ii) He/she moves and rotates those logarithmic spirals in all directions with use of the mouse or from the key board of the PC.

(iii) A spiral best fitting to the band echoes outside of the eye wall is selected by the operator.

(iv) The PC recognizes the center of its spiral curve as the center of the typhoon and computes its geographical position.

In case of determining the center by man-machine interaction, the time required for determining a best fitting spiral and the accuracy of the typhoon center position depend on how much experience an operator has on typhoon observations by the weather radar. Therefore, the following algorithm for determining the center automatically was developed.

The procedure for automatic fitting is as follows.

(i) The operator specifies several points on a noteworthy band echo with a typhoon.

(ii) The PC decides the most suitable spiral using the least squares method and indicates the position of the typhoon center (see Fig.2).

The position of the typhoon center is estimated by this method in shorter time than by man-machine interaction.

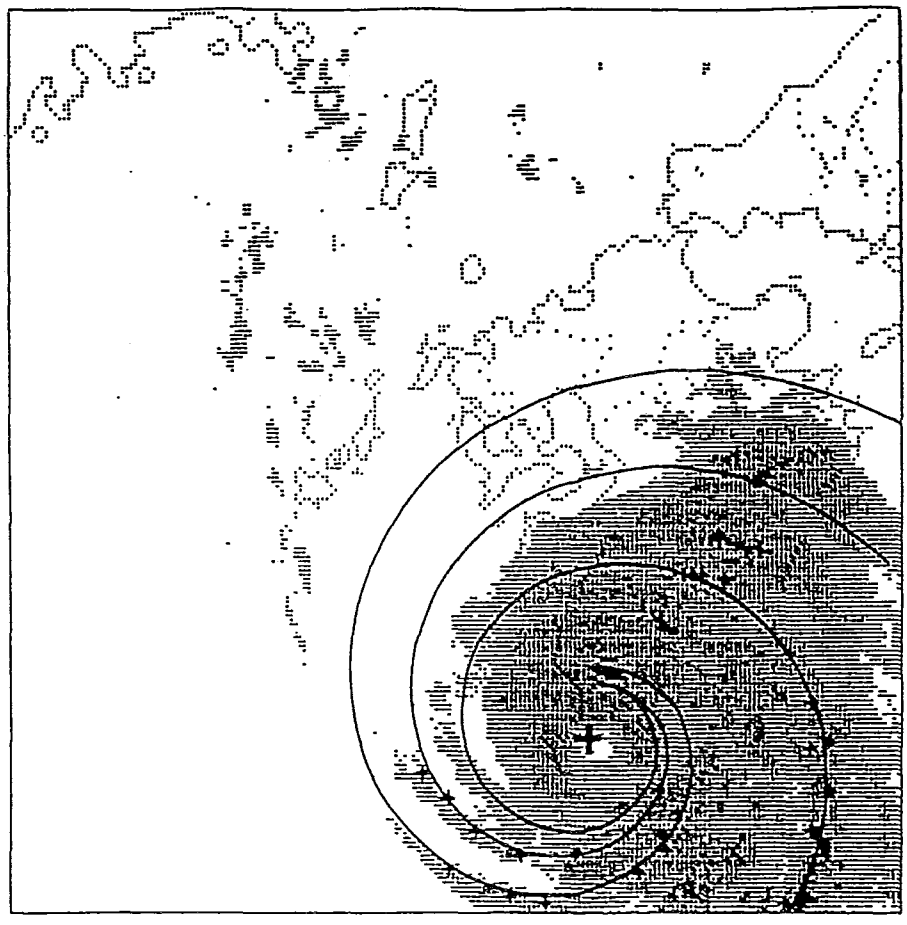

Fig.2 Reflectivity imagery of T8911 observed at 0200JST on 28 July 1989 by the weather radar and indication of the best fitting logarithmic spiral. Symbol +(small) is a point on the noteworthy band echo marked by an operator; +(large), the center of T8911 determined by the best fitting spiral.

(2) Approximation to a circle or a ellipse

In case that the echo of eye wall is shaped like a circle or a ellipse, the best fitting circle or ellipse is selected making use of man-machine interaction described above. The center of the circle or the ellipse is recognized as the center of a typhoon. In this case there is no great difference between in the accuracy of the center determined by different operators because they select the same circle or ellipse as the best fitting one.

3. Accuracy of determining by this system

To evaluate the accuracy of the center determined by the methods shown here, they are compared with positions of the center by the conventional method sketching PPI imageries with regard to several typhoons which passed through Kyusyu district of Japan from 1989 to 1991. And both of the two are compared with the best track positions which are synthetically analyzed using surface weather observations, marine weather observations, GMS imageries besides weather radar imageries by the JMA forecasting department. Results are shown in Table 1 and Table 2.

Table 1 shows positions determined by each of the three methods on TYPHOON 8911 JUDY (T8911) and Table 2 is on TYPHOON 9119 MIREILLE (T9119). In both cases, the logarithmic spiral approximation method is applied for determining the center.

Table 1 Positions of center of T8911 determined by each method

Time of observation	Center determined by PC method	Center determined by sketcing method	Center determined by synthetic analysis
27 July 1989 19JST	(30.6° N, 131.9° E)	(30.5° N, 131.8° E)	(30.6° N, 131.9° E)
20	(30.6° N, 131.6° E)	(30.6° N, 131.5° E)	(30.6° N, 131.7° E)
21	(30.7° N, 131.5° E)	(30.8° N, 131.4° E)	(30.7° N, 131.5° E)
22	(30.9° N, 131.2° E)	(30.9° N, 131.2° E)	(30.9° N, 131.2° E)
23	(31.0° N, 131.2° E)	(31.0° N, 131.0° E)	(31.0° N, 131.0° E)
28 July 1989 00JST	(31.1° N, 130.9° E)	(31.1° N, 130.8° E)	(31.1° N, 130.8° E)
01	(31.2° N, 130.7° E)	(31.2° N, 130.7° E)	(31.2° N, 130.6° E)
02	(31.4° N, 130.4° E)	(31.4° N, 130.4° E)	(31.4° N, 130.4° E)
03	(31.6° N, 130.3° E)	(31.5° N, 130.3° E)	(31.6° N, 130.2° E)
04	(31.7° N, 130.2° E)	(31.7° N, 130.2° E)	(31.7° N, 130.1° E)
05	(32.0° N, 130.0° E)	(31.9° N, 130.0° E)	(31.9° N, 130.0° E)
06	(32.1° N, 129.8° E)	(32.1° N, 129.8° E)	(32.1° N, 129.8° E)
07	(32.4° N, 129.7° E)	(32.3° N, 129.6° E)	(32.3° N, 129.6° E)
08	(32.6° N, 129.5° E)	(32.5° N, 129.4° E)	(32.5° N, 129.4° E)
09	(32.7° N, 129.2° E)	(32.6° N, 129.2° E)	(32.7° N, 129.2° E)

Table 2 Positions of center of T9119 determined by each method

Time of observation	Center determined by PC method	Center determined by sketcing method	Center determined by synthetic analysis
27 Sep. 1991 12JST	(31.1° N, 128.4° E)	(31.2° N, 128.2° E)	(31.2° N, 128.4° E)
13	(31.6° N, 128.6° E)	(31.6° N, 128.7° E)	(31.6° N, 128.7° E)
14	(32.0° N, 129.0° E)	(32.1° N, 128.9° E)	(32.0° N, 128.9° E)
15	(32.5° N, 129.3° E)	(32.4° N, 129.2° E)	(32.5° N, 129.3° E)
16	(32.8° N, 129.8° E)	(32.8° N, 129.7° E)	(33.0° N, 129.6° E)
17	(33.2° N, 130.3° E)	(33.2° N, 130.2° E)	(33.3° N, 130.1° E)
18	(33.6° N, 130.5° E)	(33.7° N, 130.3° E)	(33.9° N, 130.6° E)
19	(34.2° N, 131.0° E)	(34.2° N, 131.0° E)	(34.5° N, 131.2° E)
09	(32.7° N, 129.2° E)	(32.6° N, 129.2° E)	(32.7° N, 129.2° E)

There is no great difference between positions of center of T8911 at each time determined by three methods, namely the PC method, the sketching method and the synthetic analysis (best track). In case of T9119, the result is almost same as T8911.

The time required for determining the center of a typhoon by the PC method is less than ten minutes. On the other hand, the conventional sketching method requires at least fifteen minutes even if an expert of radar observations analyzes. Therefore, the PC method is more effective than the sketching one.

4. Concluding Remarks

The JMA Observations Department is improving the system for determining the center of a typhoon using the PC, especially the algorithm to determine the center of a typhoon which has neither a distinct eye wall nor strong spiral band echoes. And the programs for making the message with the code of FM-20 RADOB automatically after determining the center of a typhoon. The new system is planned to be put into operation in 1994.

Detailed information is available at the Observations Department of the JMA.

Acknowledgement. The authors would like to express their gratitude to colleagues at the radar observation stations in the JMA, who supported our work.

PROBLEMS OF METEORSAT IR IMAGE CALIBRATION FOR RAINFALL ESTIMATES IN KENYA

Stephen H. Mwandoto
Kenya meteorological Department
P.O. Box 30259
NAIROBI, KENYA

INTRODUCTION

Since 1960, the potential has existed for rain estimation from satellite imagery. Several schemes using visible and infrared imagery or a combination of both; from geo-synchronous or polar-orbiting satellites have been devised and these may be summarised in four broud groups:

(a) Cloud life history techniques; which are appropriate for severe storm forecasting (e.g scofield and oliver, 1977).

(b) Threshold techniques; which are appropriate for estimating daily rainfall in similar climatological regions (e.g. Negri et al. 1984) or for obtaining monthly rainfall over large regions of the globe (e.g. Motell and Weare, 1987).

(c) Cloud indexing techniques, which are appropirate for estimating rainfall in regions of agricultural interest or for use in water resources and stream flow prediction (e.g. Barrett and Martin 1981)

(d) Pattern recognition techniques; which are appropriate for delineating regions of rainfall within a cloud mass and for estimating instataneous rainfall rates (e.g. Lovejoy and Austin, 1979; Tsonis and Isaac 1985 and O'Sullivan et al 1990).

This paper gives results of an IR image cloud pattern recognition technique used to estimate rainfall using 3 images and 13 synoptic stations for ground truthing.

The pattern recognition techniques used in this study are preferable to the cloud indixing; cloud-life history; or thresholding techniques for the following reasons:

(i) Cloud indexing techniques require subjective interpretation of satellite images; thus the resulting rainfall; estimates are not available in real time.

(ii) Cloud-life history techniques require extensive computer time and multiple satellite images in order to make rainfall estimates; thereby making their use in real time analysis difficult; and

(iii) Threshold techniques are restricted to decision boundaries parallel to VIS and IR co-ordinate axes (Lovejoy and Austin, 1979); whereas the decision boundaries for pattern recognition techniques have no such restrictions.

DATA

SURFACE DATA

13 synoptic stations in Kenya giving hourly records of rainfall were used for ground-truthing for a period of two years, 1989-1990. The periods of interest were March-May and October-November, which represent the two rain seasons in Kenya, the long and short rains respectively.

Cloud observations (type, amount and height) were also obtained from the same period of time.

IR Image data

IR Satellite imagery was obtained from a primary Data User Meteosat receiver (PDUS) located in Nairobi. IR image statistics for 12 hours (1500 GMT to 02 GMT) formed a composite cold cloud duration image. The individual images used in this work were those obtained at 1600, 1800 and 2000GMT; and these were analysed using temperature thresholds -15 C, -35 C and -60 C.

The spatial resolution for each pixel of the IR image is 5 x 5 km at the point of Nadir. The pixel at each of the 13 stations used were sampled using a 20 x 20 pixel array defined here as a "Window". This represented an area of 100km on the ground. A total of 11,700 records of rainfall and IR image data were analysed.

Figure 1 shows the locations of the 13 synoptic stations in Kenya where the pixel arrays were sampled.

METHODLOGY

Analysis of IR image data

Two methods were used to analyse the data:

(a) Using simple contigency tables
(b) Using principal component analysis (PCA)

Analysis using contingency tables:

The IR image patterns defined as SMALL, MEDIUM, LARGHE CELL EDGE and UNIFORM; were classified into three rainfall categries of No rain, Rainfall (<10mm) and Heavy Rain (>10mm); according to the temperature thresholds of the cloud-top at -15 C, -35 C and -60 C.

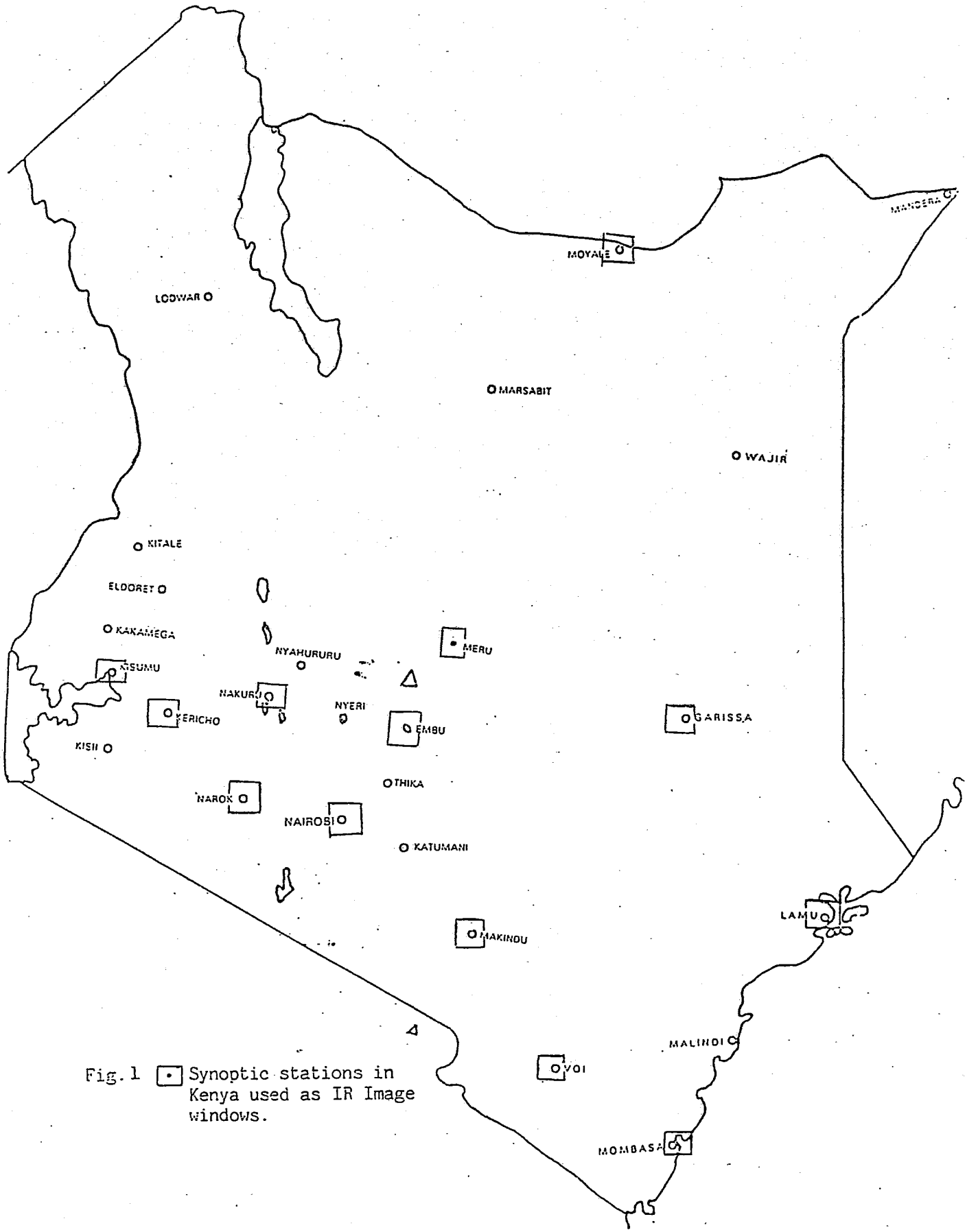

Fig. 1 ⊡ Synoptic stations in Kenya used as IR Image windows.

Results and Discussion

% Probability of rainfall occurence from IR image cloud patterns.

From the analysis of the data in table 1, it is clear that the medium and large cell edge patterns are the most frequent in all the rain seasons. These two storm cells also register the higher amount of rainfall irrespective of when this rainfall is recorded - before or after IR image time. It can also be observed from the same table that, more rainfall events are recorded at the temperature thresholds of < -15 C and <-35C. However, since most of Kenya, with the exception of a few places, particularly along the Coast; experience heavy thunderstorms at <-35 C, the later appears the better temperature threshold for rainfall estimates.

IR image cloud pattern Analysis using PCA.

Table 2a-b below gives FA results for the March-May rainfall season during 1989-1990:

From Table 2a, at temperature thresholds <-35 C to <-60 C, the five factors explain between 15 to 60% of the variance in the diurnal rainfall regime in Kenya for the two year period of the data analysed. The spatial cluster of the March to May rainfall variance is further depicted by the map patterns of the five (5) FA modes (table 3 and figure 2).

DISCUSSIONS

For the March-May rainfall season (1989), the eigen vector which best represents the diurnal rainfall characteristics is in the two temperature thresholds <-15 C and < -35 C used in the FA analysis of IR image cloud derived rainfall (table 2a) At the temperature threshold <-15 C the synoptic stations clustering at factor 1 lies within the region in the west of Kenya where significant rainfall is received from late afternoon through early evenin g and part of the night. Using the temperature threshold of < -15 C the south-eastern highlands of Kenya including Nairobi are included in the same category.

These results are replicated using data for 1990, although the variance which describes this rainfall character is lower (i.e. factor 2 instead of 1).

At the lower temperature threshold used in the FA (<-60C) only Nakuru and Kericho are shown to be grouped together under the same rainfall regime (Factor 1 - 1989 season, Factor 4, 1990 season) This shows that only in this region are precipitating storms able to develop at temperatures below <-60 C. These diurnal rainfall regimes at the various eigen vectors can be seen in figure 2a - b below.

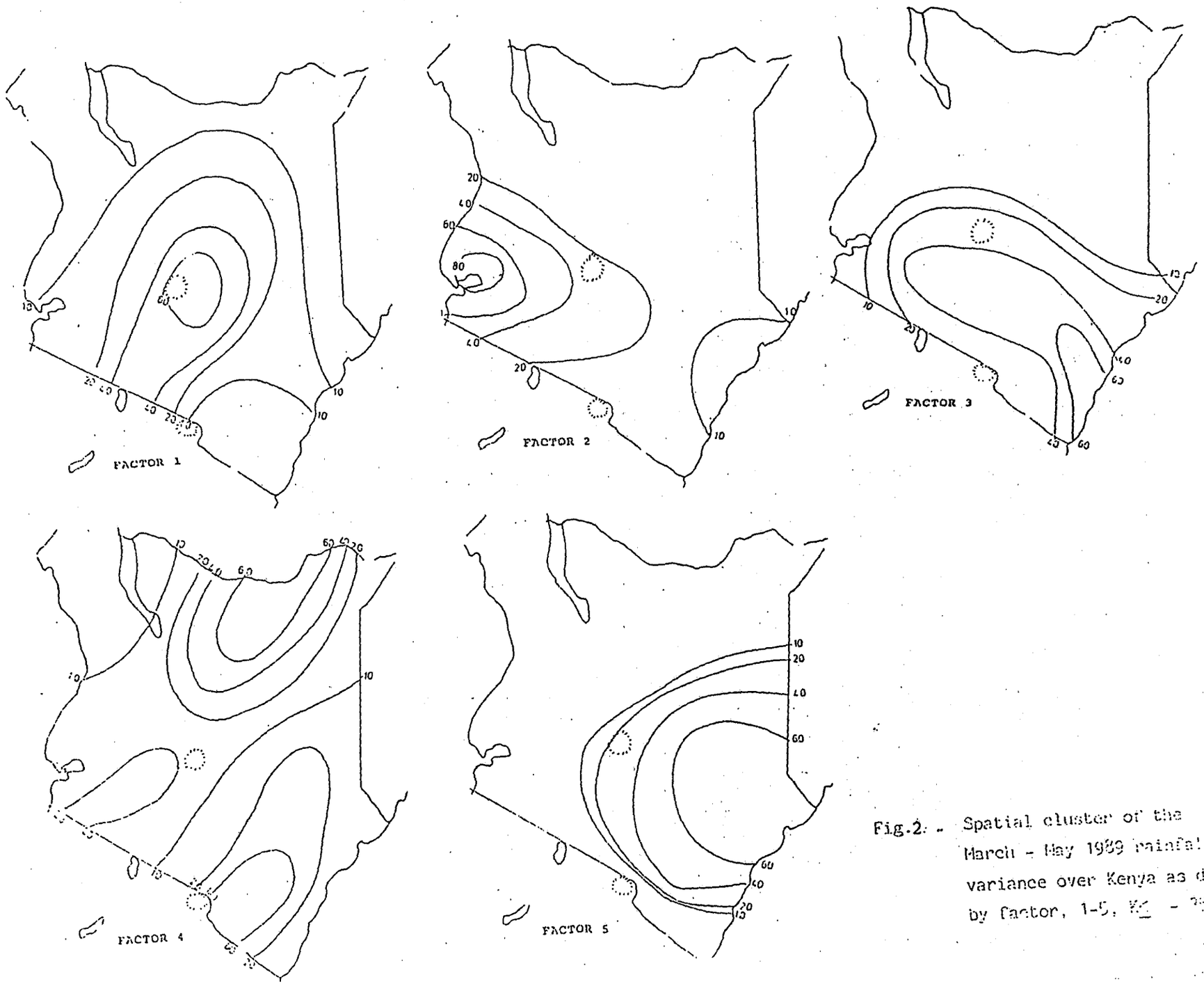

Fig.2. - Spatial cluster of the March - May 1989 rainfall variance over Kenya as depicted by factor, 1-5, [illegible].

From the IR image patterns obtained from the 1989 and 1990 data the associated rainfall 1-hour before and after IR image time was calculated from the rainfall record charts for each station, image, temperature threshold and each season. The rainfall was lagged for 1-hour centered on the IR image time to take into account the 'life-cycle' effect of a developing thunderstorm.

The 'life-cycle' effect generally causes the area covered by an individual cloud as detected by satellites to log its rainfall.

Table 1a+b.! shows the calculated probabilities of rainfall occurance for the analysed IR images for the two seasons in 1989. These % probabilies were calculated only from rain events.

Analysis of IR image Data Using principal component Analysis (PCA).

The principal component analysis (PCA) and Factor analysis (FA) are some of the models that can be derived from the empirical orthogonal solutions. The basic principles of such analyses are derived from the concept of variance.

The FA model can be represented mathematically as below:

$$Zi = ai1\ F1 + ai2\ F2 + aim\ Fm + dilli$$

$$i = 1,2,\ldots\ldots M;$$

where Zi is the variable i in the standardised form, Fi represents the factors, while ai1 is the standard multiple regression coefficient of the variable i; whereas di and Ui are the unique factor and regression loading of the unique factor respectively.

The loadings can be obtained from the correlation and covariance matrices of the variables (e.g Richman 1981).

The principal components (Factors) are always extracted in the descending order of eigen values. This means that only a few of the factors which explain the highest proportion of the variance are considered. Thus under PCA, variables or locations which are interelated cluster together on to similar vector spaces (factors).

In this paper, the data used to generate the spatial correlation metrix consisted of time series of rainfall for each season at 1600, 1800 and 2000GMT from storms derived using the 3 temperature thresholds -15 C, -35 C and -60 C.

Results from these analyses will be discussed next.

For the short rain season (October - November) the temperature threshold <-15 C and <-35 C similarly describes adequately the rainfall regimes in Kenya.
For the season in 1989 and 1990, the South-eastern highlands including Nairobi and the Central region are best characterised by factor 1 at the lower threshold(<-35). The western areas (mainly ares around Kericho, Narok, Nakuru and Kisumu) are still in the same grouping albeit at low variance (factors 5 and 6 (1989), 2 and 4 (1990))

Stability of PCA patterns:

The question of whether the patterns derived from PCA are physically realistic and climatologically stable has been raised by many researchers (e.g. Ogallo 1989, Barnston and Livezey (1987) etc.)

In this study, the stability of the PCA patterns was investigated by comparing the patterns of the PCA modes derived from the March-May IR image data and lagged rainfall with interstation correlations. Thus the correlation between this (highest loading) station and itself is taken as 1.0 and plotted at the station location. The correlation between this station and all other stations was then plotted. Figures 3a + b shows the interstation correlations for the dominant modes at the 3 temperature thresholds in the long rains and at 2 thresholds in the short rain season.

The spatial PCA patterns of the mapped correlations and those of loadings were found to be consistent.

It is important to note that the rainfall charactericed by the hormogenous zones discribed above is derived from the medium and large cell edges, which are prodominant in both the long and short rain season. It is also reasonable to suggest that the temperature threshold <-35 C effectively described the observed diurnal rainfall regime and also its spatial character in Kenya. Only a few stations in western Kenya (Kericho, Kisumu, Nakuru) have shown the precipitating storms colder that -60 C can be identified using meteosat IR Imagery; in both the long and short rain season.

Table 1a Infrared Image cloud patterns, mean could top temperature range and lagged rainfall

LONG RAINS: MARCH - MAY 1989

CLOUD PATTERN/RAINFALL CLOUD TOP TEMP $\leq -60^{\circ}$ - ALL 3 IR IMAGES

	1 HR BEFORE IR IMAGE TIME					1 HR AFTER IR IMAGE TIME				
CLOUD PATTERN	NO RAIN	RAINFALL <10MM	RAINFALL >10MM	Σ	*% PROB.	NO RAIN	RAINFALL <10MM	RAINFALL >10MM	Σ	*% PROB.
S	18	8	1	27	13	20	3	4	27	11
M	73	24	7	104	45	78	19	7	104	41
LCE	32	19	3	54	32	32	20	2	54	35
U	9	6	1	16	10	8	4	4	16	13
Σ	132	57	12	201		138	46	17	201	

CLOUD TOP TEMP $\leq -35^{\circ}$ TO $< -60^{\circ}$ - ALL 3 HRS

S	84	11	3	98	8	84	11	3	98	8
M	173	30	7	210	22	178	27	5	210	19
LCE	209	79	7	295	51	222	57	16	295	44
U	80	24	6	110	18	122	40	7	169	28
Σ	546	144	23	713		606	135	31	772	

CLOUD TOP TEMP. $\leq -15^{\circ}$ TO $< -35^{\circ}$ ALL 3 IR IMAGES

S	124	16	0	140	7	127	12	1	140	7
M	219	35	4	258	18	222	34	2	258	19
LCE	377	84	11	472	44	397	67	8	472	40
U	189	62	6	257	31	195	52	10	257	33
Σ	909	197	21	1127		941	165	21	1127	

TABLE % Probability of rainfall occurrence of IR image, cloud patterns and rainfall rates
(* % determined only from all rainfall events)

Table 1.b. Infrared image cloud patterns, mean cloud top temperature range and lagged rainfall.

SHORT RAINS: OCT-DEC 1989.

CLOUD PATTERN/RAINFALL CLOUD TOP TEMP -60°c ALL3 IR IMAGES

1 HR BEFORE IR IMAGE TIME

CLOUND PATTERN	NO RAIN	RAINFALL 10MM	10MM	≤	*% PROB.	NO RAIN	<10MM	<10MM		% PROB.
S	21	11	3	35	16	26	9	0	35	13
M	55	29	3	87	37	63	21	3	87	34
LCE	40	26	4	70	35	41	25	4	70	41
U	12	8	2	22	12	14	6	2	22	11
≤	128	74	12	214		144	61	9	214	
CLOUD TOP TEMP -35°C TO - 60°C ALL 3 HRS										
S	56	10	2	68	8	58	8	2	68	9
M	91	27	3	121	20	98	19	4	121	20
LCE	163	52	9	224	40	167	48	9	224	50
U	65	43	5	113	32	78	30	5	113	31
≤	375	132	19	526		402	105	8	526	
CLOUD TEMP ≤-15°C TO<-35°C ALL IR IMAGES										
S	105	16	3	124	10	111	10	3	124	8
M	150	17	5	172	11	151	16	5	172	13
LCE	241	73	7	321	41	257	57	7	321	40
U	152	68	8	228	39	164	56	8	228	40
≤	648	174	23	845		691	139	23	845	

TABLE % Probability of rainfall occurrence of IR image, cloud patterns and rainfall rates
(* % determined only from all rainfall events)

TABLE 2A Dominant Eigen Vector Obtained by PCA: March-May 1989.

TEMPERATURE THRESHOLD VARIANCE (%)	FACTOR	EIGEN VALUE	VARIANCE EXTRACTED(%)	COMMULATIVE VARIANCE (%)
T Less or Equal to -15 °C	1	2.9	22.2	22.2
	2	1.2	9.5	31.7
	3	1.19	9.2	40.9
T Less or Equal to -35 °C	1	2.09	16.1	16.1
	2	1.35	10.3	26.4
	3	1.15	8.9	35.3
	4	1.07	8.2	43.5
	5	1.03	7.9	51.4
T Less or Equal to -60°C	1	1.50	13.7	13.7
	2	1.36	12.4	26.1
	3	1.18	10.7	36.8
	4	1.12	10.2	47.0
	5	1.02	9.2	56.2

Table 2b Dominant Eigen Vector Obtained by PCA: March-May (1990)

TEMPERATURE THRESHOLD	FACTOR	EIGEN VALUE	VARIANCE EXTRACTED(%)	COMMULATIVE VARIANCE (%)
-15°C	1	2.07	16.0	16.0
	2	1.36	10.4	26.4
	3	1.16	7.0	35.4
	4	1.07	8.2	43.6
-35 °C	1	2.0	15.2	15.2
	2	1.23	9.5	24.7
	3	1.18	9.0	33.7
	4	1.09	8.4	42.1
	5	1.01	7.8	49.9
-60 °C	1	1.62	13.5	13.5
	2	1.36	11.3	24.9
	3	1.24	10.4	35.1
	4	1.17	9.7	44.8
	5	1.08	7.9	53.9

Table 3a. Station clustering - March - May 1989.

Temp.Threshold/Factor	1	2	3	4	5
-15 °C	Kericho Kisumu Narok Nakuru	Meru Embu Moyale	Mombasa Garissa Voi Lamu Nairobi Makindu	-	-

-35 °C	1	2	3	4	5
	Makindu Nairobi Kericho Narok Nakuru Kisumu	Kericho Kisumu Meru Embu	Voi Kisumu	Mombasa Garissa	Lamu

-60 °C	1	2	3	4	5
	Nakuru Kericho Moyale	Meru Kisumu Makindu	Embu Narok	Nairobi Makindu Voi	Garissa

Table 3b Station clustering - March -May 1990

T-Threshold/ Factor	1	2	3	4
-15 °C	Embu Makindu Nairobi Voi	Kisumu Kericho Nakuru Narok	Moyale Garissa Meru	Lamu Mombasa

-35 °C	1	2	3	4	5
	Mombasa Nairobi Voi	Meru Embu Narok	Moyale Garissa Nakuru	Makindu Lamu Kisumu	Kericho

-60 °C	1	2	3	4	5
	Mombasa Embu Nairobi	Narok Kisumu Voi	Meru Makindu	Kericho Nakuru	Moyale Garissa

CONCLUSION

The results from this study have indicated that meteosat IR image data can successfully be utilized for many purposes. In this particular instance the objective was to devise a simple and non-expensive methodology whereby rainfall estimates in near real time using infrared images could be done.

'To a great extent, the objective has been met. The temperature threshold of ,-35 C effectively describes the observed diurnal regime and also its spartial character in Kenya. Only a few stations in Western Kenya (Kericho, Kisumu and Nakuru) have shown precipitating storms colder than -60 C in both the rain seasons.
These results can further be confirmed using radar data as a comparison.

REFERENCES

Barrett, E.C. and D.W. Martin (1981): The use of satellite data in rainfall monitoring. Academic press, 340pp.

Lovejoy S. and G.L. Austin (1979): The delineation of rain areas from visible and infrared satellite data for GATE and latitude.
Atmos. Ocean, 17, 71-92.

Motell, C.M. and B.C. Weare (1987): Estimating tropical rainfall using digital satellite data. J. Climate Appl. Meteor. 26, 1436-1446.

Negri, A.J., R.F. Adler and P.J. Wetzel (1984): Rain estimation from satellites - an examination of the Griffith Woodley technique. J. Climate Appl. Meteor. 23, 102-116.

O'ISullivan et al (1990): Rain estimation from infrared and visible GOES satellite data. J. Appl. Meteor. 29, 209-223.

Richman, M.B. (1981): Obliquely rotated principal components. An improved meteorological typing technique. J. Appl. Meteor. 20, 1145-59.

Scofield, R.A. and V.J. Oliver (1977): A scheme for estimating convective rainfall from satellite imagery. NOAA Tech. Memo. NESS 86, 47pp. (NTIS PB - 270 762/891)

Tsonis, A.A. and G.A. Isaac (1985): On a new approach for instantaneous rain area delineation in the mid-latitudes using GOES data. J. Climate Appl. Meteor. 24, 1208-1218.

714CD DOPPLER WEATHER RADAR SYSTEM

Wang Shunsheng Cai Zuojin Gao Yuchun

Institute of Mesoscale Meteorology
Chinese Academy of Meteorological Sciences
46 Baishiqiao Road, Beijing 100081, PRC

1. GENERAL

The 714CD is 5cm wavelength doppler weather radar which is the first doppler weather radar made in China. It applies to the State Meteorological Administration and others.

The 714CD has the advantage of the earlier meteorological radar both in engineering technology and in meteorological measurement.As a coherent "Doppler" radar, It provides not only accurate reflectivity measurement, but also measurement of the radial component of motion of the targets. It requires high speed data processing for signal analysis and man-machine interface.

2. BASIC UNIT DESCRIPTION

For descriptive purposes the 714CD unit can be divided into three parts:

.Radar made up of antenna,transmitter,receiver and the associated support circuity.

.Singal processor gave reflectivity, velocity, data formatting and antenna control.

.Data processing terminal made up of proudcts generator and color display.

The radar is designed with a coherent "phaselock" technique. It is maintained by very stable-oscillator and reference signal sources which kept same phase as transimitted frequency. These sources are used as reference in extracting the doppler frequency shift of the return signal which is proportional to the radial motion of the target. The transmiter part adapts to the coaxial magnetron and phaselock technique. Transmitted peak power is 250 kilowatts. The antenna has a center feed parabolic reflector with a diameter of approximately 4 meters.The beam width (on one way 3 dB) is 1.0 degree. The diameter of radome is approximately 5.6 meters. The receiver uses two frequency mixers to down convert the received signal to video signal. The signal has an amplitude proportional to radar reflectivity and contains a frequence componet equal to doppler shift. The receiver outputs three signal: reflectivity, inphase(I) and quadrature (Q) having a phase difference of 90 degrees. The effective dynamic range of the linear receiver is controlled by AGC.

The signal processor extracts meteorological information from the returned signal. These are: the equivalent radar reflectivity, Ze, the radial velocity , i.e, the componet of motion of the reflecting particles toward or away from the radar. Reflectivity is estimated by a linear average and exponential integral of several return pulses.Velocity is estimated from several return pulses. The signal processor also outputs the time series of I,Q data on single bin. The data analysis and display are completed by a PC-386 computer.

The PC-386 computer controls the antenna through a single-board computer. The PC-386 processes echo data and displays products on VGA cardbase. Three scan modes are PPI, RHI and Volume scan. The products include PPI, RHI,CAPPI, ETPPI,VAD and storm tracking etc.. The products can be distributed to the users outside through a satellite and wireless communication system.

This radar has been working three years and supported our experiment in summer. The data are very useful to the mesoscale analyses.

714CD Dopple Radar Characteristics

Antenna Subsystem

Antenna	Paraboloid of Revolution
Polarization	Horizontal
Reflector diameter	4 meters
Gain	40dB
First sidelobe level	-25dB
Beam width	1.0 degree

Transmitter and Receiver Subsystem

Transmitter	
Frequency range	5420MHz to 5440 MHz
Peak power	250KW
Pulse width	1 us (coherent) , 2us
PRFs	1000Hz (coherent),200Hz
Receiver	
Dynamic range	80dB

Signal Processor Subsystem

Velocity calculation	Complex Covariance Argument
Algorithm	Pulse-Pair Processing
Estimate accuracy	1 m/s
Range increment	0.25KM ,0.5KM
Azimuth increment	1 degress
Intensity calculation	Return Power Average
Algorithm	Linear average and exponential integral
Estimate accuracy	1 dB
Range increment	0.25KM ,0.5KM,1.0KM,2.0KM
Azimuth increment	1 degress

Data processing Terminal

Computer	PC-386
Display resolution	640x480x4bit
Communication between signal processor and host	DMA, RS232C
Display range	400KM and 200KM (Reflectivity) 100KM,50KM (Reflectivity and Velocity)
Products	PPI,RHI,CAPPI,ETPPI,VAD,VCS etc.

DOPPLER WEATHER RADAR SYSTEMS IN SCREX

Ge Runsheng and Xu Baoxiang

Institute of Mesoscale Meteor.
Chinese Academy of Meteor.Sci.
46 Baishiqiao Road,Beijing 100081,PRC

1.SEVERE CONVECTIVE RAINSTORM EXPERIMENT(SCREX)

The main goal of a proposed coopperative project, SCREX, is to much improve our understanding about the nature of disastrous rainstorms by means of intensive observations based on an advanced mesoscale network with high resolution in temporal and spatial domains and further modeling studies in detail.

Beijing area is one of the main regions of summer storm in China. According to historically statistic meteorological data around Beijing, 75% of total precipitation amount of whole year was produced in the months from June to August, and about 50% rainfall of the storms, which participated more than 100mm rain one day had been fallen within six hours.It is clear that the heavy rainfall in Beijing is closely related to the development of severe convection. On the other hand, the topography around Beijing ("horn" like ground feature,facing sea towards east and surrounding by mountains from north and west sides) strongly affect the precipitation in the area.This greatly stimulated meteorologists for research on the phenomenon and its generality.

Since 1989 the Institute of Mesoscale Meteorology has organized a series of field experiments and theoretical studies for preparing the SCREX experiment. Upon these efforts we do gain more and more knowledge and are planning to conduct the SCREX experiment in Beijing area between 1994-1995 (Ge,1991).

2. OBSERVATIONAL NETWORK FOR SCREX

During the last decade an advanced mesoscale meteorological experiment base has been built in Beijing-Tianjin-Hebei region (Ge and Wang, 1991). The observational network consists of two Doppler weather radars, two digitized weather radars, one UHF wind profiler, one microwave radiometer,one LLP lightning location system (3 stations) one single station lightnig location system, 21 automatic meteorological surface stations and GMS satellite reception equipment. The conventional upper air sounding data and surface data are available, special, meteorological data can be sampled every hour, parts of them may be got continuously or at every 5 -minute period.

Among the facilities in the network, the two Doppler weather radars played very important rule.

For the planned SCREX, the observational network will be much improved. In addition to Intensive Operational Period (IOP) observational requirments,3 UHF wind profilers and one more Doppler weather radar are expected. The GMS-4 and possible FY-2 Satellite data will provide high quality background for SCREX. A brief description of the planned network is show in Figure 1.

3. DOPPLE WERTHER RADAR IN SCREX

There are two Doppler weather radars in the existed network. The basic radar performance presented in table 1 (Ge and Liu, 1989;Wang et al.1993)

Model	CAMS	714CD
Wavelength(cm)	10.7	5.6
Peak Power(kw)	500	250
Sensitivity(dBm)	-107	-106
Phase Noise(degree)	1.1	2.5
Beam Width(degree)	1.0	1.0
Manufacture	USA	PRC

Table 1. Doppler weather radar performance

Now, we are developing retrieval technique from single Doppler radar data and asking for a third Doppler radar for overcoming the difficulty, 100 km apart of the two Doppler radars, which is not favorable of dual Doppler radar analysis. Furthermore,we pay more attention to improve our radar software package and study how to put Doppler radar data into mesoscale model.

REFERENCES

Ge,R., 1991: Proposal to Severe Convective Rainstorm Experiment (SCREX). Special issue.

Ge,R.,and P. Wang, 1991: Beijing-Tianjin-Hebei experimental base of mesoscale meteorology-severe storm laboratory. Annual Report of AMS.

Ge,R.and E.Liu,1989: An estimate of detectivity of CAMS Doppler weather radar. J. AMS,4(2),133-140

Wang, S. et al.,1993: 714CD Doppler weather radar system.(ibid)

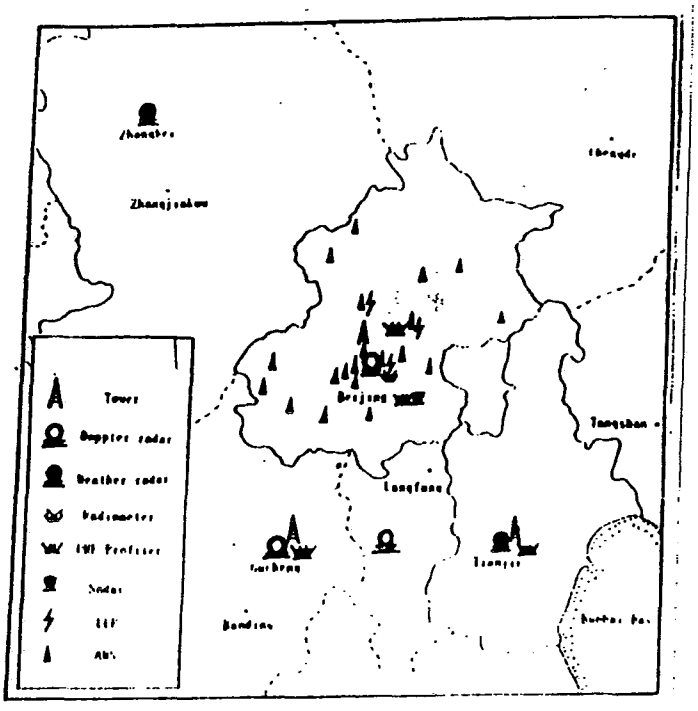

Fig1.Planned observational network for SCREX

G.Shchukin, N.Popova and I.Tarabukin
Main Geophysical Observatory, St.Petersburg, Russia

Passive-active method for radar evaluation of clouds water content's density and precipitation's intensity

ABSTRACT

Passive and active radar methods are applied succesfully in a number of cases connected with remote sensing of convective clouds and precipitation. But none of these methods used separately gives full information on physical conditions in clouds systems. Only complexing of different methods allows it, to eliminate this deficiency to a big extent. Such complexing can be optimally realized through development of radiotechnical instruments allowing synchronous measurements of reflected radar signals and cloudy atmosphere's own radiothermal emission coming from the same direction. By joint application of passive and active radars it is possible to determine the water content and precipitation's intensity distribution along the sounding path.

ПАССИВНО-АКТИВНЫЙ РАДИОЛОКАЦИОННЫЙ МЕТОД ДЛЯ ОЦЕНКИ ВЛАГОСОДЕРЖАНИЯ ОБЛАКОВ И ИНТЕНСИВНОСТИ ОСАДКОВ.

Г.Г.ЩУКИН, Н.Д.ПОПОВА, И.А.ТАРАБУКИН

Методы активной и пассивной радиолокации успешно применяются для решения целого ряда задач, связанных с дистанционным зондированием конвективных облаков и осадков. Ни один из этих методов в отдельности не позволяет получать достаточно полную информацию о физическом состоянии облачных систем. Лишь их комплексирование в значительной степени устраняет этот недостаток. В наиболее полном виде указанное комплексирование заключается в создании радиотехнических средств, позволяющих получать одновременно и из одних и тех же направлений отраженный радиолокационный сигнал и собственное радиотепловое излучение облачной атмосферы.

Совместное применение пассивно-активной радиолокации позволяет решать следующие задачи:

–определение водозапаса (интеграл от профиля подности) облаков и осадков,

–оценка средней водности по выбранному направлению,

–определение профиля коэффициента поглощения вдоль направления зондирования,

–получение оценок полного содержания жидкокапельной влаги в конвективных ячейках,

–определение профиля водности облаков в направлении визирования,

–оценка интенсивности жидких осадков,

–исследование изменения указанных характеристик во времени в процессе естественной эволюции конвективных облаков и при искусственных воздействиях на них.

Результаты совместных пассивно-активных радиолокационных измерений могут быть использованы при оценке условий возможного обледенения воздушных судов.

Для решения указанных выше задач в ГГО им.А.И.Воейкова был создан макет пассивно-активной радиолокационной станции (ПАРЛС) на базе подвижного варианта метеорологического радиолокатора МРЛ-2 и модуляционного СВЧ-радиометра на длину волны $\lambda = 3.2$ см

/I,2/. Для полного совмещения радиолокационной и радиотеплолокационной информации во времени и в пространстве необходима одновременная работа радиолокатора и радиометра на одну антенну. Для обеспечения электромагнитной совместимости этих устройств была предусмотрена развязка между ними, составляющая не менее I40 дБ.

Преимуществами ПАРЛС являются: простота конструкции, высокий уровень развязки радиометра и МРЛ, принципиальная возможность использования в комплексе любого радиометра трехсантиметрового диапазона. К недостаткам следует отнести большие потери в волноводном тракте МРЛ, приводящие к заметному падению реальной чувствительности радиометра, высокие требования к стабильности фазы опорного напряжения радиометра, снижение дальности действия МРЛ до 90 км.

Для функционирования комплекса был разработан ряд программ:
- программа ввода информации с активного и пассивного каналов,
- программа отображения информации на цветном экране,
- программа документирования и архивации получаемых данных,
- программа общения с оператором.

Кроме того созданы программы для различных задач исследования облаков и осадков.

Основной методикой наблюдений конвективных ячеек с помощью ПАРЛС является выполнение азимутальных (горизонтальных) разрезов с "выходом" на участки ясного неба, находящиеся рядом с исследуемыми ячейками. За ясное небо принимаются участки,которые не дают радиоэха. При использовании этой методики определяется непосредственно величина оптической толщины облака по формуле:

$$\tau(A,B) = -\ln \frac{U_{оп} - U(A,B)}{U_{оп} - U_{н}}$$

От оптической толщины облака с помощью соотношения:

$$\tau(A,B) = \psi(T_{э\,обл})\, W(A,B)$$

можно перейти к водозапасу W в направлении (A,B). Оценки показали, что относительная средняя квадратическая погрешность определения водозапаса составляет 20–30 %.

3.

Как уже отмечалось, результаты измерений, полученные при помощи ПАРЛС, могут быть использованы для решения обратных задач, т.е. восстановления профилей коэффициента поглощения и водности в зондируемом облачном слое, а также определения интенсивности дождя. Для решения этих задач разработаны методики, которые используются в алгоритмах программ пассивно-активных радиолокационных исследований облаков и осадков /3/. При оценке коэффициента поглощения и водности облаков и осадков радиолокационная отражаемость используется в качестве весовой характеристики при распределении оптической толщины или водозапаса по направлению зондирования. Основанием для такого подхода послужили результаты численного эксперимента, который показал, что, несмотря на значительное различие величин вклада q капель какого-либо участка спектра в радиолокационную отражаемость и водность (коэффициент поглощения), отмечается консервативность параметра q при изменении спектра капель. Это позволяет принять, что q_w/q_z и использовать радиолокационную отражаемость в качестве весовой характеристики при оценке α_n и w /3/.

Для определения коэффициента поглощения облачной атмосферы получено выражение:

$$\alpha_n(\ell) = \frac{\sqrt{Z(\ell)}}{\int_\ell \sqrt{Z(\ell)}\, d\ell}\, \tau ,$$

где τ – оптическая толщина в Нп, Z – радиолокационная отражаемость в мм^6/м^3, α – коэффициент поглощения в км$^{-1}$, ℓ – расстояние в км. По найденным значениям коэффициентов поглощения можно произвести оценку водности облаков и интенсивности осадков. Для λ =3 см соотношение для водности имеет вид:

$$w(\ell) = \frac{91.833}{B(t_{obл})}\, \alpha_n(\ell)$$

Здесь w(I) – водность в г/м^3, $t_{obл}$ – температура облачных капель. Температурный коэффициент $B(t_{obл})$ имеет следующие значения:

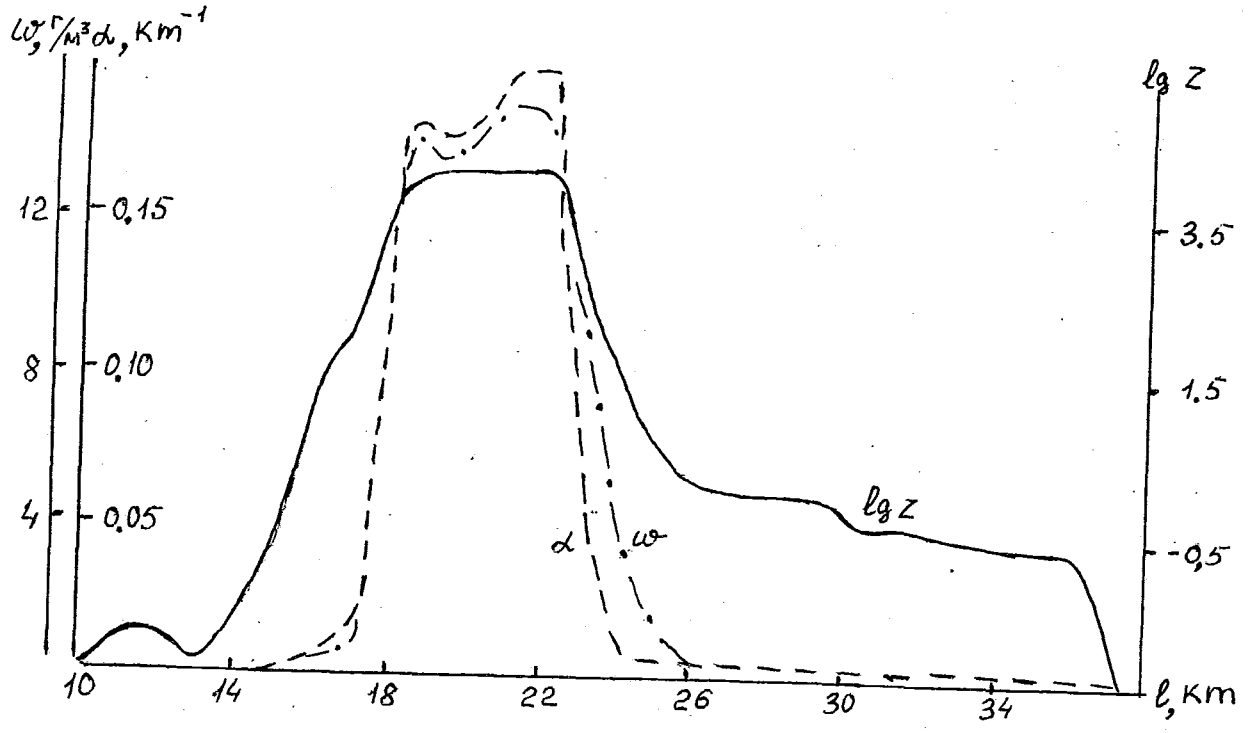

Рис. I. Распределение отражаемости $lg\,Z$, коэффициента поглощения α и водности ω вдоль направления зондирования конвективного облака при $\beta = 5.4^{0}$.

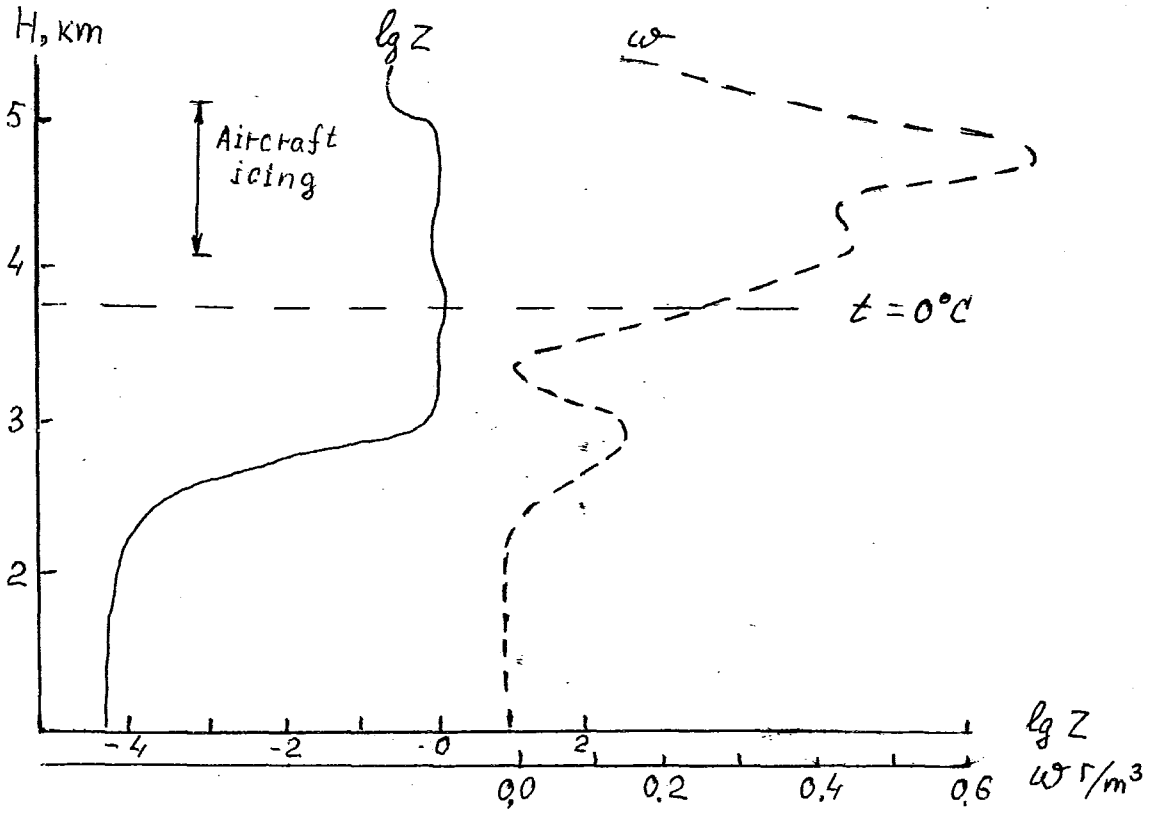

Рис. 2. Профили отражаемости $lg\,Z$ и водности ω в конвективном облаке на удалении 20 км от ПАРЛС.

4.

$t°C$	-10	0	10	20
$B(t)$	2.51	1.7	1.27	1.0

При исследовании осадков для перехода от водности дождя к интенсивности следует использовать соотношения / 3 /:

$$I = 3.4\, w^{1.33} \quad \text{при} \quad \leqslant \quad 0.32\ г/м^3$$
$$I = 2.8\, w^{1.17} \quad \text{при} \quad > \quad 0.32\ г/^3$$

На рис.1 изображено изменение радиолокационной отражаемости $lg\, z$ в одном из направлений (азимут 327.5°), полученное при зондировании под углом места $\beta = 5.4°$. Поскольку ДНА пересекала зондируемый слой ниже нулевой изотермы, то мы полагаем, что осуществлялось при этом зондирование слоя осадков. На этом рисунке представлены восстановленные профили коэффициента поглощения и водности вдоль направления визирования. Максимальные значения этих параметров получены на участках дальности 18–22 км, что соответствует высоте 1.7 – 2.1 км. Расчетное значение интенсивности осадков на этих высотах составило около 60 мм/ час.

Проведение серий азимутальных разрезов под разными углами места дает пространственное изменение параметров облачности. Разработанные программы позволяют построить вертикальные профили для интересующего нас удаления от ПАРЛС. В качестве примера на рис.2 изображены профили $lg\, z$ и водности в зондируемом облаке на удалении 20 км от пункта наблюдений. На этом же рисунке указан облачный слой, в котором существуют условия возможного обледенения.

Из анализа полученных результатов следует, что разрабатываемые пассивно-активный радиолокационные методы исследования облаков и осадков имеют перспективы дальнейшего развития.

Литература.

1. Щукин Г.Г., Бобылев Л.П. и др. Комплексное активно-пассивное зондирование облачности.–Труды ГГО, 1978, вып.411, с.3–12.
2. Попова Н.Д., Щукин Г.Г. Определение водности облаков и интенсивности осадков методами пассивно-активной радиолокации.–Метеорология и гидрология, 1989, №8, с.3–7.

THE METHOD AND TECHNIQUE FOR REMOTE MEASUREMENTS OF BOUNDARY LAYER TEMPERATURE PROFILE

A. Ivanov, E. Kadygrov
Central Aerological Observatory, Russia

1. INTRODUCTION

The atmospheric boundary layer plays an important role in the interactions between the atmosphere and the Earth surface. There are extremely wide variety of possible temperature profiles T(h) in the boundary layer-usual adiabatic, isothermal, with inversion, with elevated inversion. For measurements of the boundary layer temperature profile possible to use different methods: in situ measurements with radiosonde,tethered balloon meteorological tower, remote sensing measurements with SODAR, with microwave radiometers. In this report results of development of methods and equipment for remote sensing of the boundary layer temperature profile by using microwave radiometers with working frequency in molecular oxygen absorption band center at 60 GHz are described.

2. CONCEPT

There are some methods of remote troposphere temperature sensing, using the wing of the molecular oxygen absorption band at frequencies f=53-58 GHz [1,2]. But measurements of atmospheric boundary layer temperature profile had some particular difficulties. The variatians in radiation intensity of a boundary layer are small and the sensitivity of a microwave radiometer must be very high (better than 0,1K). And for this purpose the microwave radiometric measurements accurasy at low elevation angles become insufficient due to sidelobe effect so antenna must have sidelobe as less as possible [1-3]. The measurements must be not sensitive to air humidity and fog so neccesary to use frequency in the center of the molecular oxygen absorption band near 60 GHz.
The radiometer band width must be wide (about 2÷3 GHz) for receiving the high sensitivity. Boundary layer temperature dependence T(h) has fast dynamics so measurements can be done automatically earch 5÷10 minutes with automatically calibration by using internal noise generator. Also there are some difficulties in obtaining T(h) when solving the retrieval problem. Methods of statistical regularisation [1,2] difficult to use due to extraordinary spatial and time variety of T(h) from wich impossible practically to extract any representative statistical ensemble with a stable covariational bindings [4,5].

3. RETRIEVAL METHOD

The technique that we use for microwave remote sensing of the atmospheric boundary layer temperature is based on measuring thermal radiation of atmosphere in the center of the molecular oxygen absorption band near 60 GHz, where the skin depth is about 300 m [3÷5]. By definition the skin depth is equal to the height H_b where optical depth

$$\tau(H_b)=1/\cos\theta\int_0^{H_b}k_f(h)\,dh=1 \qquad (1)$$

where $k_f(h)$ - absorption coefficient [6].
Remote temperature sensing of the boundary layer is conducted by measurements of the radiobrightness temperature at different zenith angles $\theta=0^o\div90^o$ [3-5]. In this case depth of the contributing radiation layer changes in a range 0 to 300 m. The expression for the radiobrightness temperature T_b has the form [5]:

$$T_b(\theta)=1/\cos\theta\int_0^H T(h)k_f(h,T)\exp[-1/\cos\theta\int_0^h k_f(h',T)dh']dh=\int_0^H T(h)W(h,\theta)dh \qquad (2)$$

where $W(h,\theta)$ - weighting function; $H\approx 3$ km - upper limit of integration.

For retrieval processing we used itteraction method of Chahine with original algorithm. We made comparizon with radiosonde, than with recieving by radiosonde temperature profile count absorption coefficient [6] and weighting function. At the next step we used differential weighting function for different angles:

$$\Delta T_i=T(\theta_i)-T(\theta_{i-1})=\int_0^\infty T(h)[W(h,\theta_i)-W(h,\theta_{i-1})]dZ \qquad (3)$$

From equation (3) we received dependence θ_i with H_b. Iteraction algoritm:

$$dT_{n_i}^{(n+1)}=dT_{(h_i)}^{(h)} * \frac{\widetilde{dT_b}(\theta_i,\theta_{i-1})}{dT_b(\theta_i,\theta_{i-1})} \qquad (4)$$

Where $\widetilde{dT_b}(\theta_i,\theta_{i-1})=\widetilde{T_b}(\theta_i)-\widetilde{T_b}(\theta_{i-1})$ - measurement changing of radiobrightness temperature with angle θ_i and θ_{i-1}, $dT_b(\theta_i,\theta_{i-1})$ - from equation (3); $dT_{hi}^{(h)}$ - changing of atmosphere temperature at the heght h_i. For this type of retrieval processing it is sufficent 0,5 sec for 1 profile when we used computer IBM-PC/AT-286.

4. EQUIPMENT

A block diagram of the equipment for boundary layer temperature profile determination using microwave radiometric observation is shown at fig.1

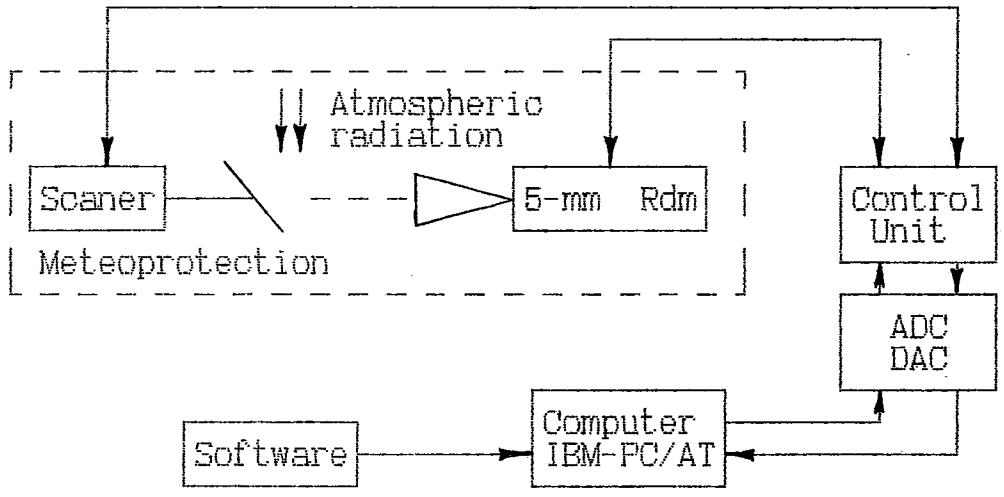

Fig. 1

The high-sensitivity all solid state superheterodyne receiver (radiometer) at the central frequency 60 GHz was developed in the Space Research Institute (Moscow) as by - product of the Relict-2 mission [7]. The sensitivity of this radiometer (without cooling) is 0,04K with an integration time 1 sec. The antenna is a scalar horn with beamwidth of about 4^o and has a small scattering coefficient outside the main lobe ($\beta\approx 1\%$). Input circuit of the radiometer consist of a waveguide isolator, reference noise sourse, DSB Schottky diode mixer with loss of 3dB. The local oscillator is an original InP Gunn-effect oscillator with low power consumption

of 0,8W and relatively high efficienty of 3%. Transistor IF amplifier has a power gain of 45 dB, noise temperature 70K and bandwidth about 2 GHz. The total equivalent noise of the receiver doesn't exceed 600K [3-5]. The calibration of the receiver was conducted by the internal noise generator. This noise generator produces the reference temperature step, which determine the scale of the instrument. For the absolute radiation measurements at least one additional point must be known. This known point was the radiation temperature at horizontal direction, which equals to the air temperature near the earth surface T_o. For beam scanning we used rotating mirror in discrete scanning mode with variable reflection angle (11 steps). The duration of temperature measurement cycle is about 3 minutes in complete automatic mode.

5. EXPERIMENTAL RESULTS

Several instruments was constructed for checking this methods and equipment in field conditions. The experiments was conducted in 1989-1993 in Moscow region (56N, 35E), in Kursk region (52N, 35E), near the lake Imandra (67N, 32E), in Iakutia (67N, 125E), in Heiss Island (81N, 58E). The radiobrightness temperature measurements at 10 fixed angles from horizon to zenith was repeated every 10 minute in wide range of outside temperature from 218K up to 308K. The contact measurements was carried out simultaneously in some selected times by radiosonde, tethered balloon, meteorological tower with temperature sensors. According to comparison it was shown the possibility to realice retrieval error of T(h) 0,2-0,3K for flat profile and 0,4-0.5K for profiles with temperature inversion in height from the ground up to 600 m. Differences between data of two simulteneonsly operating radiometers was less than 0,1K. For ecological tasks two set of equipment now is working more than one year in automatical mode in Iakutia and in Moscow. At Fig.2 is shown results of comparison radiometers data and radiosonde data which was made in the Central Aerological Observatory in September-October 1993 (71 set).

6. CONCLUSION

Developments method and equipment for remote sensing of atmospheric temperature at the center of molecular oxygen band at 60 GHz (5mm) allows:

- to carry out sounding of temperature profile up to 600 m with vertical resolution 30÷50 m;
- to realise a retrieval error of temperature profiles not greater than 0,5K;
- to record reliably the main features of temperature profiles and their dynamics;
- to carry out measurements in all weather conditions excluding strong rain.

7. ACKNOWLEDGMENT

The authors would like to express their appreciation to I.Strukov,A.Troitsky,M.Sorokin, M.Khajkin, A.Koldaev, S.Viazankin, E.Miller without whose assistance this work would not be possible.

8. REFERENCES

1. E.R. Westwater. Monthly Weather Rev., vol.100, pp. 12-22, 1972
2. A.V. Troitsky. Inv. Vuzov, Radiofisica, vol.20, pp. 198-211, 1977

3. K.P. Gajkovich, E.N. Kadygrov, A.V. Troitsky and A.N. Shaposhnikov. In: Proc. of all - USSS Conf. Applications of the Remote Radiophysical Technics to Environmental studies (Erevan, USSR). Apr, 1990, pp. 28-29 (in russian)
4. V.D. Gromov, E.N. Kadygrov, A.S. Kosov. In: Proc. Symp. Wave propagation and remote sensing, Ravenskar, United Kingdom, 8-12 June 1992, pp. 3.4.1 - 3.4.5
5. A.V. Troitsky, K.P. Gajkovich, V.D. Gromov, E.N. Kadygrov, A.S. Kosov. IEEE Trans. on Geoscience and Remote Sensing, vol. 31, N 1, 1993, pp. 116-120
6. P.W. Rosenkranz. IEEE Trans. Ant. Propagat, 1975, v.AP-23, N 4, p. 498-506
7. I.A. Strukov e.a. In: Proc. of the 29-th Liege International Astrophysical Colloquium, Liege, Belgium, July 3-5, 1990, pp. 99-104.

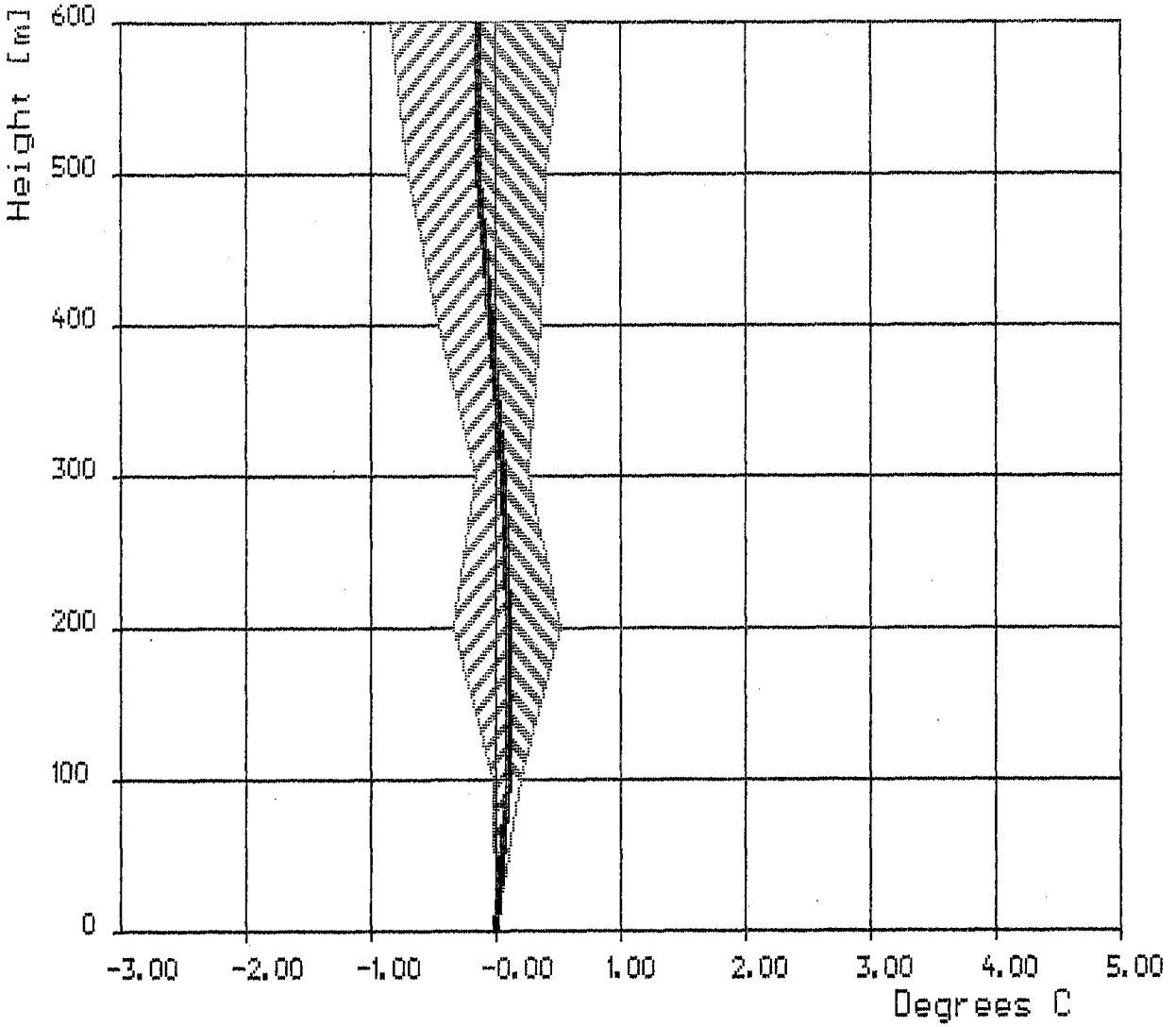

Hight M	M.S.D. C	R.M.S C
600	-0.1	0.6
500	-0.1	0.5
400	-0.0	0.4
300	0.1	0.2
200	0.1	0.4
100	0.1	0.1
0	0.0	0.0

Results of the comparison between radiosondes and microwave remote sensing temperature data. (71 set)

REMOTE SENSING OF AIRCRAFT ICING ZONES PARAMETERS

M.N. Haikin, A.V. Koldaev,
Central Aeerological Observatory, Russia

INTRODUCTION

The forecast of aircraft icing is very actually problem especialy due to great dangerose of the flights through such zones in clouds in start/landing regimes. It is well known, the presence of super cold liquid water in clouds is main reason of aircraft icing The remote measurements of liquid water drops temperature and liquid water content in clouds can give possibility to estimate a probability of aircraft icing risk.

The method and equipment described in this report is based on the simultaneous measurement of brightness temperature by means of two ground based microwave radiometers with wavelength 2.7 mm and 8.0 mm.

THE THEORY OF METHOD

The expression for brightness temperature of clear atmosphere measured by microwave radiometers is given by [1]

$$T_0(\lambda) = T_{ef}(\lambda)\cdot[1-\exp(-\tau_0(\lambda)] \qquad (1)$$

where $T_0(\lambda)$ - brightness temperature of clear sky on wavelengh λ; $\tau_0(\lambda)$ - opacity of clear atmosphere on wavelengh λ; $T_{ef}(\lambda)$ - effective temperature of clear atmosphere.

For cloud atmosphere brightness temperature T_w is given by

$$T_w(\lambda) = T_{ef}(\lambda)\cdot[1-\exp(-\tau(\lambda)] \qquad (2)$$

where $T_{ef}(\lambda)$ - effective temperature of cloud atmosphere. With small errores we may suppose $T_{ef}=T_{ef}$.

$$\tau(\lambda) = \tau_0(\lambda) + \tau_w(\lambda) \qquad (3)$$

where $\tau_w(\lambda)$ - opacity of cloud.

The clouds with drop size less than 100μ is possible to consider as pure absorption medium and, applying Rayleigh approximation we can write,

$$\tau_w(\lambda) = a(\lambda,T_{lw})\cdot W \qquad (4)$$

where W - Integrated Liquid Water (ILW) of cloud [kg/m^2]; $a(\lambda,T_{lw})$ - coefficient, depending from wavelength and temperature of liquid water drops in the cloud - T_{lw}

From Eqns. (3), (4) by substituting

$$R(T_{lw}) = a(\lambda_1,T_{lw})/a(\lambda_2,T_{lw}) \qquad (5)$$

we can receive

$$\tau(\lambda_1)=R(T_{lw})\cdot\tau_2(\lambda)+C(T_{lw}) \qquad (6)$$

where $C(T_{lw}) = \tau_0(\lambda_1)-R(T_{lw})\cdot\tau_0(\lambda_2)$ (7)

The calculation of $a(\lambda,T_{lw})$ for λ=2.7 mm and λ=8.0 mm in temperature diapason from -20^{0}C to +5^{0}C $R(T_{lw})$ allow to approximat $R(T_{lw})$ by expression:

$$R(T_{lw}) = 0.1 \cdot T_{lw} + 4.28 \qquad (8)$$

The coefficients $R(T_{lw})$ and $C(T_{lw})$ in (6) is calculated from regression tusk solution for a set of $\tau(\lambda)$ measurement in cloud zone in wich T_{lw}=const is supposed. After that we can receive temperature of liquid water drops in cloud from (8) and determine coefficient $a(\lambda, T_{lw})$ in (4). The calculation of $\tau_0(\lambda)$ for λ_1=2.7 mm and λ_2=8.0 mm, based on radiosond date received in Dolgoprudny, was made and it is shown, that the connection of these values can be approximated by expression:

$$\tau_0(8.0) = \alpha \cdot \tau_0(2.7) + b \qquad (9)$$

Where α=0.127; b=0.03. So, from (6) and (9) we can obtain

$$\tau_0(8.0) = [R(T_{lw}) \cdot b - C(T_{lw})]/[R(T_{lw}) - \alpha] \qquad (10)$$

$$\tau_0(2.7) = [b - C(T_{lw})]/[R(T_{lw}) - \alpha] \qquad (11)$$

From (4), using calculated $\tau_0(\lambda)$, we can obtain W:

$$W = \tau(\lambda) - \tau_0(\lambda)/a(\lambda, T_{lw}) \qquad (12)$$

MEASUREMENTS

The determination of integral liquid water (ILW) and temperature of liquid water drops (T_{lw}) in clouds were executed in July-August 1993 in Central Aerological Observatory (Dolgoprudny, Moscow region). The main parameters of microwave radiometers, used in this experiment, are shown in table 1.

Table 1

The main parameters of microwave radiometers

Wavelength [mm]	2.7	8.0
Frequency [GHz]	110.8	37.5
Measuring temperature [K]	1 - 300	5 - 400
Sensitivity (integr.time=1 s) [K]	0.05	0.05
Side lobe suppression [dB]	- 40	- 30
Antenna diagram width [grad]	1.5	1.5
Temperature stability [K/10_0C]	1.0	2.5
Modulation frequency [KHz]	1.0	1,2-1,6
Power feed [V]	+27	+27
Power consumption [Wt]	27	27
Weight [kg]	5	4

The radiometeric system was installed on the top of six-flo-

or building on height 22 m over the ground. The system operates as non-service equipment , appropriate for use under field conditions in temperature range -60C - +40C. The measurements were carred out in automatic operational mode. The data received were registrated by means of IBM PC/AT with special card.

Interactiv regim of express data processing is available in duration of measurements. Brightness temperature measured by each radiometer is drowed on the computer screen by two color line in time of measurements. Liquid water zone existance is detected visualy when brightness temperature is 0.3K more than clear sky one. Each zone is defined as a local for the part of brightness temperature record from one deep minimum to outher. Deep minimum means value of signal in the local minimum is more than two time less than in the local maximum. The local zone is marked immideately after registration and 4 steps express evoluation of the data is performed.

1. Production of the cloud trasfer velosity(from standart weather radar net) on the measured duration time of the zone is calculated. Result is equal to horizontal dimension of the zone.
2. Solution of regression task, as described above, is made to estimate mean temperature of cloud water drop.
3. Knowledge of hight profile of atmosphere temperature(obtaned from radiozond or aircraft data) allows to associate of liquid water zone with the concret hight.
4. By use of results of regression task solution, the Integral Liquid Water content is calculated.

The data obtaned by the above procedure can be very useful for duty meteorologist in an airport in case the same microwave system is installed near the start/landing track. In addition , on the base of this data it is possible to estimate thickness of liquid water layer by dividing of ILW on mean value of LWC for the observed type of clouds. Estimation of expected rate of ising for each type of aircrafts can be sufficiently improved by use of determined temperature of cloud drops.

RESULTS.

Examples of ILW and T_{lw} determination in clouds 27 July 1993 are shown in figures 1 and 2. The solid line in fig.1 indicate the change of ILW, received 08/27/93 from 10 to 11 GMT. In fig.1 is indicated three cloud zones in wich T_{lw} was calculated. These zones are drowed by horizontal dashed lines. Near them are shown the value of temperature and hight, wich was received from radiozond temperature profile. The mean T_{lw} in the first cloud zones, 10:15 to 10:18 is equal $-2^{0}C$. The mean value of ILW in this cloud was 0.18 kg/m^2 and horizontal size was about 2 km. In the second zone registrated from 10:28 to 10:34, we alsow observed cloud with $T_{lw}=-2^{0}C$. The mean ILW=0.16 kg/m^2 and horizontal size L was equaled about 1 km. In the third zone, registrated from 10:36 to 14:54 mean T_{lw} and temperature in separate clouds was the same and was equaled $+2^{0}C$.

A case of observation clouds on two levels is indicated in fig.2. In the first zone, registrated from 13:03 to 13:15, mean T_{lw} and T_{lw} in cloud (13:05-13:08) were equaled $+4^{0}C$ and $+3^{0}C$ respectively. In the second zone, (time 13:23-13:33) $T_{lw}=-3^{0}C$, ILW=0.18kg/m^2, L=4-5 km. In the third zone $T_{lw}=-4^{0}C$, ILW=0.12kg/m^2 and L=6-7 km.

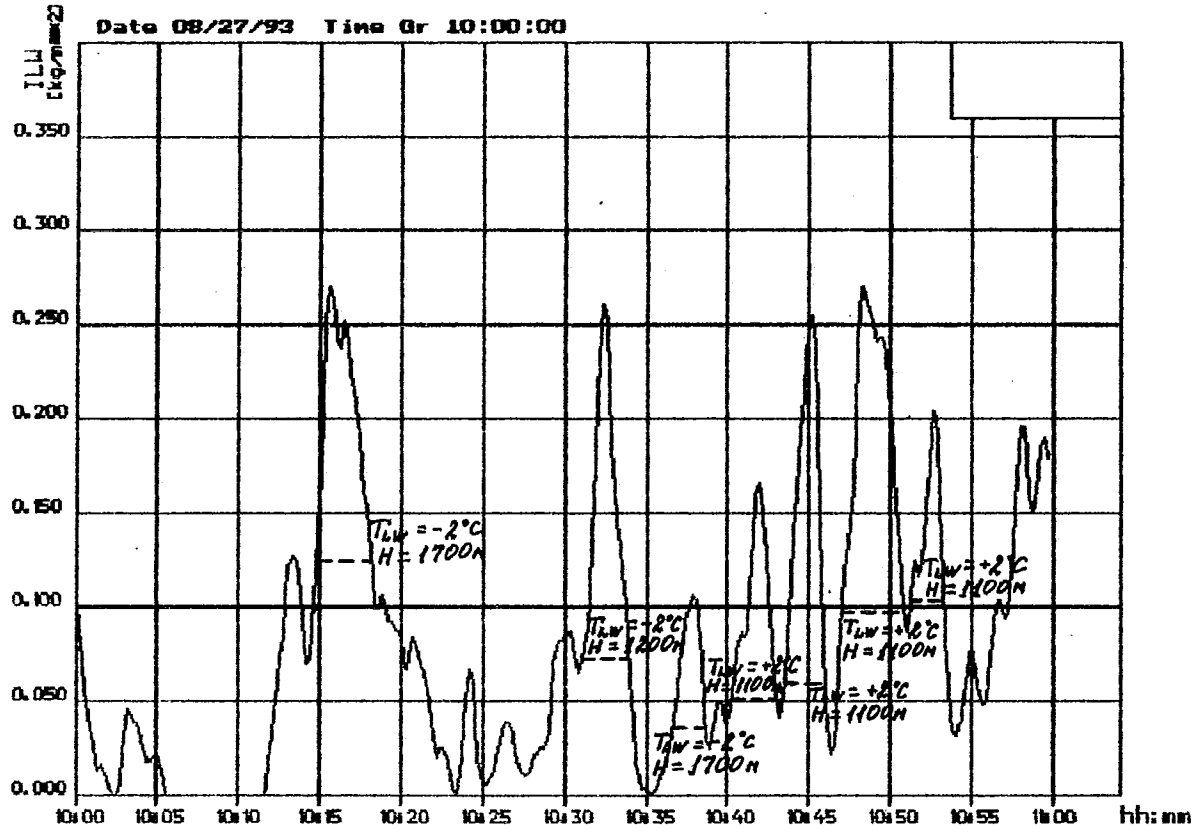

Fig.1 The solid line indicates ILW. The dashed lines indicate T_{lw} and height of cloud zone in wich these values vere measured

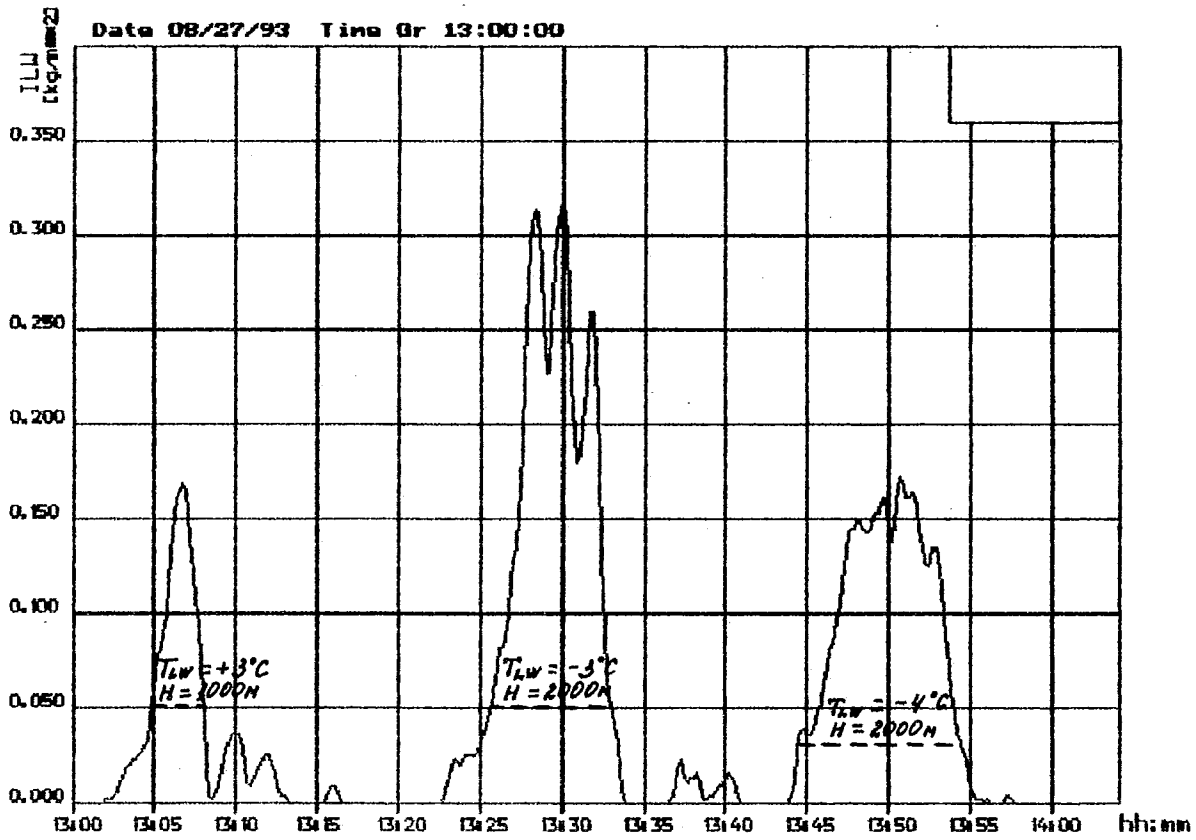

Fig.2 The same as in fig.1

The lidar measurements of bottom level of clouds, made in CAO 08/27/93, have showed, that there were presented two levels of clouds, one on hight 1-1.5 km, and the second on hight 1.8-2.5 km.

CONCLUSIONS

- Two-wavelength automaticaly operated radiomric system for simultaneous determination of Integral Liquid Water content and mean temperature of cloud drops was created.
- Two month experiment for determination of ILW and mean temperature into non-presipitable clouds was done. This work shown the usefulness of application of the radiometric system as a standart tool for airport meteorologocal service for use in aircraft ising forecusting.
- The procedure developed for data evoluation can be simply modified to perform data processing in comletely automatic mode.
- The theoretical method developed for radiometric data performance by means of regression task solution can take wide application in different part of remote sensing of atmosphere.

REFERENCE

[1] F.T. Ulaby, R.K. Moore and A.K.Fung 'Passive microwave sensing of the atmosphere /Microwave remote sensing. Active and Passive. 1985.

APPENDICES

LIST OF MEMBERS OF THE INTERNATIONAL ORGANIZING COMMITTEE FOR PREPARATION OF THE WMO TECHNICAL CONFERENCE ON INSTRUMENTS AND METHODS OF OBSERVATION

(TECO-94)

A. Van Gysegem	Scientific Director	Belgium
M. Rochas		France
K. Schulze	Co-ordinator of TECO-94	WMO Secretariat

LIST OF PUBLICATIONS
in the
INSTRUMENTS AND OBSERVING METHODS REPORTS SERIES

No. 1 Automated Meteorological Systems.
Papers presented at the Technical Conference on Evolution and Standardization of Observing Techniques in Light of Automation
(Norrköping, Sweden, 1980)

No. 2 Instrument Development Inquiry (Third Edition), 1980

No. 3 Lower Tropospheric Data Compatibility. Low-level Intercomparison Experiment (USA, 1979)

No. 4 WMO Equipment Survey - Meteorological Satellite Ground-based Receiving Equipment, 1980

No. 5 WMO Catalogue of Radiosondes in Use by Members, 1981
(out of print)

No. 6 Preliminary Analysis of a Questionnaire on Aerodrome Meteorological Measurements
By M. M. Etienne, 1981

No. 7 The Meteorological Use of Navaid Systems
- A brief technical assessment
By A. Lange, 1981

No. 8 Report on Meteorological Radars
By G. A. Clift, 1981

No. 9 Papers presented at the Second WMO Technical Conference on Instruments and Methods of Observation (TECIMO-II)
(Mexico City, 1981)

No. 10 Radiation Effects on the WMO Reference Psychrometer in the Field
By R. G. Wylie and T. Lalas, 1981

No. 11 WMO Catalogue of Radiosondes in Use by Members, 1982

No. 12 Meteorological Observations by Laser Indirect Sensing Techniques
By A. O. van Gysegem, 1982

No. 13 The Use of Hydrogen for Inflation of Meteorological Balloons, 1982

No. 14 Summary Results of a 1978 Survey of Calibration Facilities and of Tests and Evaluation of Instruments
(out of print)

No. 15 Papers presented at the WMO Technical Conference on Instruments and Cost-Effective Meteorological Observations (TECEMO),
(Noordwijkerhout, Netherlands, 1984)

No. 16 (TD 146) Comparison of Pyranometers and Electronic Sunshine Duration Recorders of RA VI (Budapest, 1984)
By G. Major, 1986

No. 17 (TD 38) International Comparison of National Precipitation Gauges with a Reference Pit Gauge,
By B. Sevruk and W. R. Hamon, 1984

No. 18 (TD 112) Guidance Material on Meteorological Instruments Suitable for Use in Developing Countries
By E. S. Engawi, 1986

No. 19 (TD 230) Some General Considerations and Specific Examples in the Design of Algorithms for Synoptic Automatic Weather Stations
By D. T. Acheson, 1987

No. 20 (TD 177) Stations Automatiques à Faible Coût
By P. Viton, 1986

No. 21 (TD 175) Algorithms for Automatic Aerological Soundings
By A. H. Hooper, 1986

No. 22 (TD 50) Papers presented at the WMO Technical Conference on Instruments and Methods of Observation (TECIMO-III) (Ottawa, 1985)

No. 23 (TD 51) Keynote papers presented at the Third WMO Technical Conference on Instruments and Methods of Observation (TECIMO-III) (Ottawa, 1985)

No. 24 (TD 231) Instruments Development Inquiry (Fourth Edition)
By E. Prokhorov, 1987

No. 25 (TD 104) Papers presented at the Workshop on the Correction of Precipitation Measurements (Zürich, Switzerland, 1985)

No. 26 Lectures presented at the Workshop for Instrument Specialists, (Buenos Aires 1984) (in Spanish) **(out of print)**

No. 27 (TD 176) WMO Catalogue of Radiosondes and Upper-Air Wind Systems in Use by Members, 1986

No. 28 (TD 174) WMO International Radiosonde Comparison, Phase I, (Beaufort Park, UK, 1984)
By A. H. Hooper, 1986

No. 29 (TD 312) WMO International Radiosonde Intercomparison, Phase II) (Wallops Island, USA, 1985)
By F. Schmidlin

No. 30 (TD 195) WMO International Radiosonde Comparison (UK, 1984 / USA, 1985)
By J. Nash and F. Schmidlin, 1987
(out of print)

No. 31 The Measurement of Gustiness at Routine Wind Stations - A Review
By A. C. M. Beljaars, 1987

No. 32 (TD 217) WMO International Ceilometer Intercomparison (UK, 1986)
By D. W. Jones, M. Ouldridge and D. J. Painting, 1988

No. 33 (TD 222) Papers presented at the WMO Technical Conference on Instruments and Methods of Observation (TECO-1988)
(Leipzig, German Democratic Republic, 1988)
(out of print)

No. 34 (TD 289) WMO Assmann Aspiration Psychrometer Intercomparison
(Potsdam, German Democratic Republic, 1987)
By D. Sonntag, 1989

No. 35 (TD 303) Papers presented at the Fourth WMO Technical Conference on Instruments and Methods of Observation (TECIMO-IV)
(Brussels, 1989)
(out of print)

No. 36 (TD 344) Compatibility of Radiosonde Geopotential Measurements
By M. Kitchen, 1988

No. 37 (TD 309) Information on Weather Radars used by WMO Members
By M. Gilet, 1989

No. 38 (TD 316) WMO International Hygrometer Intercomparison (Oslo, Norway, 1989)
By J. Skaar, K. Hegg, T. Moe, K. Smedstud
(out of print)

No. 39 (TD 313) Catalogue of National Standard Precipitation Gauges
By B. Sevruk and S. Klemm, 1989

No. 40 (TD 451) WMO International Radiosonde Comparison, Phase III (Dzhambul, USSR, 1989)
By A. Ivanov, A. Kats, S. Kurnosenko, J. Nash, and N. Zaitseva

No. 41 (TD 401) First WMO International Intercomparison of Visibility Measurements (UK, 1989)
By D. J. Griggs, D. W. Jones, M. Ouldridge, W. R. Sparks

No. 42 WMO Automatic Sunshine Duration Measurement Comparison
(Hamburg, Federal Republic of Germany, 1989)
(In preparation)

No. 43 (TD 308) First WMO Regional Pyrheliometer Comparison of RA II/RA V
(Tokyo, Japan, 1989)

No. 44 (TD 345) First WMO Regional Pyrheliometer Comparison of RA IV (Ensenada, Mexico, 1989)
By I. Galindo

No. 45 (TD 310) Analysis of Instrument Calibration Methods used by Members
By H. Döring, 1989

No. 46 (TD 474) WMO Digital Barometer Comparison (De Bilt, Netherlands, 1989)
By J.P. van der Meulen

No. 47 (TD 452) Reports of the CIMO Working Group on Surface Measurements
Guidance on the Establishment of Algorithms for Use in Synoptic Automatic Weather Stations - Processing of Surface Wind Data
By D. Painting, 1991

No. 48 (TD 328) International Workshop on Precipitation Measurements
(St. Moritz, Switzerland, 1989)

No. 49 (TD 462) Papers presented at the WMO Technical Conference on Instruments and Methods of Observation (TECO-92)
(Vienna, Austria, 1992)

No. 50 (TD 541) Historical Changes in Radiosonde Instruments and Practices
By D. J. Gaffen, 1993

No. 51 (TD 570) Overview of Real-time Lightning Detection Systems for use by Meteorological Services
By R.L. Holle and R.E. López, 1993

No. 52 (TD 571) Results of the Working Group on Weather Radars
Part I: Severe Weather Recognition, By G. G. Shchukin
Part II: Utilization of Doppler Radars for Monitoring Tropical Cyclones as one Element of the Global Monitoring System, By Hisao Ohno, 1993

No. 53 (TD 572) Segunda Compariación de la OMM de Pirheliómetros Patrones Nacionales AR III
(Buenos Aires, 1991)
By M. Ginzburg

No. 54 (TD 578) Instruments Development Inquiry
By J.P. van der Meulen, 1993

No. 55 (TD 589) Siting and Exposure of Meteorological Instruments
By J. Ehinger, 1993

No. 56 (TD 587) Report by the Rapporteur on Radiosonde Compatibility Monitoring
Part A - WMO Catalogue of Radiosondes and Upper-air Wind Systems in use by Members (1993)
Part B - Compatibility of Radiosonde Geopotential Measurements 1990, 1991 and 1992
By T. Oakley, 1993

****